



**Biochemical Characteristics and Antimicrobial  
Potential of Seed and Nut Oils Against  
*Staphylococcus aureus***

**Oluwapamilerin Damola Yangomodou**

**School of Environment and Life Sciences  
University of Salford, UK**

Submitted as partial fulfilment of the requirements of the  
Degree of Doctor of Philosophy, 2019.

## Table of Contents

<b>List of Tables .....</b>	<b>i</b>
<b>List of Figures.....</b>	<b>iv</b>
<b>Acknowledgments .....</b>	<b>xiii</b>
<b>Declaration.....</b>	<b>xiv</b>
<b>List of abbreviations .....</b>	<b>xv</b>
<b>Abstract.....</b>	<b>xvii</b>
<b>Chapter 1. Introduction to <i>Staphylococcus aureus</i> .....</b>	<b>1</b>
1.1 Brief historical perspective of staphylococci .....	1
1.2 Classification and status of staphylococcal species .....	2
1.3 <i>Staphylococcus aureus</i> .....	2
1.3.1 Morphology and biochemical characteristics of <i>S. aureus</i> .....	2
1.3.2 Epidemiology of <i>S. aureus</i> infections .....	3
1.3.3 Carriage of <i>S aureus</i> .....	6
1.3.4 Transmission and risk factors of colonization of human nose with <i>S. aureus</i> .....	6
1.4. <i>S. aureus</i> virulence and diseases .....	13
1.4.1 <i>S. aureus</i> virulence factors and pathogenesis of infections .....	13
1.4.2 Strategy of host colonization and diseases .....	16
1.5 Biofilms.....	21
1.5.1 <i>S. aureus</i> biofilm .....	21
1.5.2 The phases of <i>S. aureus</i> biofilm formation.....	22
1.5.3 Enzymatic dispersal mechanism in <i>S. aureus</i> .....	24
1.5.3.1 Serine proteases .....	24
1.5.3.2 Cysteine proteases .....	24
1.5.3.3 Metalloprotease .....	24
1.6 Biofilm formation and quorum sensing in <i>S. aureus</i> .....	25
1.6.1 The accessory gene regulator quorum sensing in <i>S. aureus</i> .....	25

1.6.2 Regulatory factors identified in <i>S. aureus</i> .....	27
1.6.3 The <i>agr</i> system in <i>S. aureus</i> .....	28
1.7 Antibiotic resistance and resistance mechanisms in <i>S. aureus</i> .....	29
1.7.1 Antibiotics commonly used in the treatment of <i>S. aureus</i> infections and their mode of action. ....	29
1.7.1.1 Inhibition of peptidoglycan synthesis.....	30
1.7.1.2 Creation of an alternate pathway .....	30
1.7.1.3 Inhibitors of protein synthesis .....	31
1.7.1.4 Inhibitors of topoisomerase synthesis .....	32
1.7.2 Development of antibiotic resistance in <i>S. aureus</i> . ....	32
1.7.2.1 Time line and brief history of antibiotic resistance in staphylococci.....	32
1.7.3. Resistant mechanisms exhibited by MRSA to selected clinically important drugs ...	33
1.7.3.1 Biochemical mechanism of resistance.....	33
1.7.3.2 Genetic mechanism of antibiotic resistance in <i>S. aureus</i> .....	35
1.7.4 MRSA 252 and antibiotic resistance.....	38
1.7.5 Some identified factors for the emergence and spread of resistance in <i>S. aureus</i> .....	39
1.8 Plant seed and nuts.....	41
1.8.1 Nuts and seed types and their ethnobotanical uses.....	41
1.9 Phytochemicals compound in nuts and antimicrobial activity of plant oils.....	44
1.9.1 Plant oils .....	44
1.9.2 Bioactive phytochemicals compounds in nuts and their classifications.....	45
1.9.3 Antibacterial activity of plant oils.....	48
<b>Chapter 2. Materials and Methods.....</b>	<b>51</b>
2.1 Materials.....	51
2.1.1 Collection of plant materials and identification .....	51
2.1.2 Solvents, chemicals and media used in this study .....	52
2.1.3 Bacterial strains used for antimicrobial susceptibility testing.....	53

2.1.4 Antibiotics discs .....	53
2.2 Methods.....	54
2.2.1 Extraction process of African walnut, cashew and pumpkin oils and their respective extracts.....	54
2.3 Preliminary phytochemicals analysis of African walnut, cashew and pumpkin oils with their respective extracts.....	57
2.3.1 Determination of Flavonoids .....	57
2.3.2 Determination of alkaloids .....	57
2.3.3 Determination of saponins.....	57
2.3.4 Determination of tannins .....	58
2.3.5 Determination of phenol.....	58
2.3.6 Determination of terpenoids .....	58
2.4 Identification and investigation of biofilm production in MRSA 252 and <i>S. aureus</i> ATCC 6538 .....	58
2.4.1 Identification of <i>S. aureus</i> isolates .....	58
2.5 Screening of oils and extracts for antimicrobial activity against MRSA 252 and ATCC 6538.....	61
2.5.1 Growth of <i>S. aureus</i> strains for analysis.....	61
2.5.2 Maintenance of test organisms .....	62
2.5.3 Antimicrobial susceptibility testing of seed and nut oils.....	63
2.6 Molecular study of MRSA 252 and <i>S. aureus</i> ATCC 6538 virulence genes.....	71
2.6.1 Scanning electron microscopy.....	71
2.6.2 RNA isolation from and MRSA 252 and <i>S. aureus</i> ATCC 6538.....	72
2.6.3 Reverse transcription polymerase chain reaction (RT-PCR) .....	73
2.6.4 Quantitative real time PCR (qRT-PCR).....	75
2.7 Screening of oils of African walnut, cashew and pumpkin oils for synergy, biofilm kill time and determining the efficacy of oils in the treatment of staphylococcal infections using <i>Galleria mellonella</i> as an <i>in-vivo</i> -model.....	80

2.7.1 Synergy test .....	80
2.7.2 Biofilm time-kill assay .....	81
2.7.3 Preliminary assessment of the pathogenicity of MRSA 252 and ATCC 6538 and efficacy of African walnut oil in treating staphylococcal infections .....	81
2.8 Identification of the most active oil.....	84
2.8.1 Analytical methods for identification of fatty acids in African walnut oil.....	84
2.8.2 Fractionation of the active African walnut oil.....	85
2.8.3 Molecular structure identification .....	86
2.8.4 Antimicrobial activity of fractions .....	88
<b>Chapter 3. Extraction of Plant Seed and Nut Oils and their Respective Extracts.....</b>	<b>89</b>
3.1 Introduction .....	89
3.2 Results .....	91
3.2.1 Extraction of African walnut, cashew and pumpkin oils.....	91
3.2.2 Physical characteristics of oils and extracts of African walnut, cashew and pumpkin .....	95
3.2.3 Phytochemical screening of oils of African walnut, cashew and pumpkin with their respective extracts.....	97
3.2.4 Ultraviolet absorption of plant oils and extracts.....	99
3.2.5 FTIR spectra analysis .....	102
3.3 Discussion .....	106
<b>Chapter 4. Establishing the Methodology for the Identification and Biofilm formation of Methicillin Resistant (MRSA 252) and Susceptible <i>S. aureus</i> (ATCC 6538) .....</b>	<b>109</b>
4.1 Introduction .....	109
4.2 Results .....	110
4.2.1 Confirmation of the strains .....	110
4.2.2 Antibiotic sensitivity test .....	112
4.2.3 Biofilm formation assay .....	112
4.2.4 Quantification of biofilm formation by microtiter plate (MTP) method .....	113

4.3 Discussion .....	118
<b>Chapter 5. Screening of Plant Seed and Nut Oils and their Respective Extracts for Antimicrobial Activity against MRSA 252 and <i>S. aureus</i> ATCC 6538.....</b>	<b>121</b>
5.1 Introduction .....	121
5.2. Results .....	125
5.2.1 Antibiotic sensitivity testing of seed and nut oils against MRSA 252 and <i>S. aureus</i> ATCC 6538 .....	125
5.2.2 Oil control plates and well diffusion results of African walnut, cashew and fluted pumpkin extracts .....	145
5.2.3 Minimum inhibitory concentration and minimum biofilm inhibitory concentration of oils against MRSA 252 and <i>S. aureus</i> ATCC 6538 planktonic and biofilms .....	148
5.2.4 MICs and MBICs of African walnut, cashew and fluted pumpkin.....	154
5.2.5 Minimum biofilm eradication concentration of African walnut, cashew fluted pumpkin oils against MRSA 252 and <i>S. aureus</i> ATCC 6538 biofilms.....	166
5.3 Discussion .....	179
<b>Chapter 6. Molecular study of MRSA 252 and <i>S. aureus</i> ATCC 6538 Virulence Gene.....</b>	<b>185</b>
6.1 Introduction .....	185
6.2 Results .....	187
6.2.1 Preparation of MRSA 252 and ATCC 6538 for SEM.....	187
6.2.2 Scanning electron microscopy (SEM).....	188
6.2.2.1 SEM of MRSA 252.....	189
6.2.2.2 SEM of ATCC 6538.....	190
6.2.3 RNA extraction and gel electrophoresis of the RNA extracted from MRSA 252 and <i>S. aureus</i> ATCC 6538 biofilms. ....	192
6.2.3.1 Agarose gel electrophoresis of RNA extracted from MRSA 252 and ATCC 6538 at 6, 12, 24 and 48 h .....	199
6.2.3.2 Agarose gel electrophoresis of RNA extracted from MRSA 252 biofilms after treatment with fluted pumpkin, African walnut and cashew oil .....	199

6.2.3.3 Agarose gel electrophoresis of RNA extracted from <i>S. aureus</i> ATCC 6538 biofilms after treatment with fluted pumpkin, African walnut and cashew oil .....	199
6.2.4 Reverse transcription PCR products from RNA extracted from ATCC 6538 and MRSA 252 biofilms. ....	195
6.2.4.1 RT-PCR products of selected reference genes.....	196
6.2.4.2 RT-PCR products of adhesion and biofilm genes in ATCC 6538 and MRSA 252 at different growth time points .....	199
6.2.5 RT-PCR products of selected antibiotic and food poisoning genes .....	215
6.2.6 RT-PCR products of selected quorum sensing genes.....	220
6.2.7 Analysis of the quantitative real time PCR results of selected reference genes ....	220
6.2.7.1 Amplification efficiency and determination of PCR efficiency of reference genes.....	221
6.2.7.2 Assessment of stability and validation of reference genes.....	222
6.2.7.3 Analysis of the qRT-PCR results of selected target genes.....	226
6.3 Discussion .....	250

**Chapter 7: Screening African Walnut, Cashew and Pumpkin Oils for Synergy, Kill Kinetics and Establishing the Efficacy of African Walnut Oil in the Treatment of Staphylococcal Infections using *Galleria mellonella* as an *in-vivo* model .....254**

7.1 Introduction .....	254
7.2 Result.....	257
7.2.1 Biofilm time-kill assay .....	257
7.2.2 Synergy activity of plant oils with antibiotics. ....	264
7.2.3 Assessing the efficacy of African walnut oil in the treatment of staphylococcal infections .....	268
7.3 Discussion .....	279

**Chapter 8. Identification of Active type of Components in African Walnut Oil .....282**

8.1 Introduction .....	282
8.2 Results .....	283

8.2.1 Identification of fatty acid methyl esters (FAMES) of Supelco 37 standards mix.....	283
8.2.1.1 Fatty acid profile of Supelco 37 standard FAME mix.....	284
8.2.1.2 Chromatograms of FAME mix (C8 - C24) standards.....	285
8.2.2 Fatty acid profile of African walnut oil.....	286
8.2.2.1 Chromatograms and spectra results of FAME of African walnut oil.....	293
8.2.3 Chemical and antimicrobial investigation of African walnut oil.....	291
8.2.3.1 Separation and purification of African walnut oil.....	297
8.2.3.2 Bioassay-guided fraction and antimicrobial activity of African walnut oil.....	292
8.2.4 Molecular structure identification.....	294
8.2.4.1 Fourier transform infra-red spectroscopy of African walnut oil fractions.....	294
8.2.4.2 Nuclear magnetic resonance of African walnut oil fractions.....	298
8.3 Discussion.....	304
<b>Chapter 9. General Discussion and Future Research.....</b>	<b>307</b>
9.1 Summary of main findings.....	307
9.2 Future Research.....	315
<b>References.....</b>	<b>316</b>
<b>Appendix 1. Hydrogen proton NMR (<sup>1</sup>H NMR) of fraction 2 of walnut oil.....</b>	<b>339</b>
<b>Appendix 2. Carbon NMR (<sup>13</sup>C NMR) of fraction 2 of walnut oil.....</b>	<b>343</b>
<b>Appendix 3. Attached proton test (APT) of fraction 2 of walnut oil.....</b>	<b>347</b>
<b>Appendix 4. <sup>1</sup>H NMR of linolenic acid.....</b>	<b>351</b>
<b>Appendix 5. <sup>13</sup>C NMR of linolenic acid.....</b>	<b>339</b>
<b>Appendix 6. APT of linolenic acid.....</b>	<b>343</b>
<b>Appendix 7. <sup>1</sup>H NMR of fraction 3 of walnut oil.....</b>	<b>347</b>
<b>Appendix 8. <sup>13</sup>C NMR of fraction 3 of walnut oil.....</b>	<b>351</b>
<b>Appendix 9. Attached proton test (APT) of fraction 3 of walnut oil.....</b>	<b>351</b>
<b>Appendix 10 &amp; 11. <sup>1</sup>H NMR of fraction 2 of walnut oil.....</b>	<b>353</b>

## List of Tables

Table 1. Ethnobotanical uses of African walnut, cashew and pumpkin seeds in Nigeria.....	44
Table 2. Plant materials used in this study.....	52
Table 3. Antibiotics used in the study.....	54
Table 4. Reverse transcription master mix components and volume used for the second step reaction of cDNA synthesis.....	74
Table 5. The RT-PCR reaction mixture for all the target genes analysed in <i>S. aureus</i> ATCC 6538.....	74
Table 6. The thermocycling temperatures and times used for RT-PCR amplification of each primer sets of adhesion and biofilm genes.....	75
Table 7. The thermocycling temperatures and times used for RT-PCR amplification of each primer sets of antibiotics and enterotoxins gene.....	75
Table 8. The qPCR reaction temperature for the reference and target genes.....	76
Table 9. Primer sequences used in this study.....	77
Table 10. Yield of oils obtained from screw press after each extraction.....	91
Table 11. Average yields and percentage yield of extracts of African walnut ( <i>Tetracarpidium conophorum</i> ).....	92
Table 12. Average yields and percentage yield of cashew ( <i>Anacardium occidentale</i> ).....	93
Table 13. Average yields and percentage yield of fluted pumpkin ( <i>Telfaira occidentalis</i> )....	93
Table 14. Physical appearances of screw pressed oils.....	95
Table 15. Physical appearances of solvent extracted African walnut ( <i>Tetracarpidium conophorum</i> ).....	96
Table 16. Physical appearances of solvent extracted cashew ( <i>Anacardium occidentale</i> ).....	96
Table 17. Physical appearances of solvent extracted pumpkin ( <i>Telfaira occidentalis</i> ).....	96
Table 18. Preliminary qualitative photochemical results of African walnut ( <i>Tetracarpidium conophorum</i> ).....	98
Table 19. Preliminary qualitative photochemical results of cashew ( <i>Anacardium occidentale</i> ).....	98
Table 20. Preliminary qualitative phytochemicals result of pumpkin ( <i>Telfaira occidentalis</i> ).....	98
Table 21. Infrared absorption of African walnut oil.....	103
Table 22. Infrared absorption of cashew oil.....	104
Table 23. Infrared absorption of pumpkin oil.....	105

Table 24. Colony and morphological characteristics of MRSA 252 and <i>S. aureus</i> ATCC 6538 after 24 hours of culturing on different growth media.....	110
Table 25. MRSA 252 and <i>S. aureus</i> ATCC 6538 counts in 12 h, 24 h and 48 h-biofilms, in growth recovery media expressed as log <sub>10</sub> cfu/mL, after exposure to different concentrations of African walnut oil.....	168
Table 26. MRSA 252 and <i>S. aureus</i> ATCC 6538 counts in 12 h, 24 h and 48 h-biofilms, in growth recovery media expressed as log <sub>10</sub> cfu/mL, after exposure to different concentrations of cashew oil.....	172
Table 27. MRSA 252 and <i>S. aureus</i> ATCC 6538 counts in 12 h, 24 h and 48 h-biofilms, in growth recovery media expressed as log <sub>10</sub> CFU/mL, after exposure to different concentrations of fluted pumpkin oil.....	175
Table 28. Reference and target genes efficiency, amplicon melting points and r <sup>2</sup> values for the curves.....	221
Table 29. Stability (M) value calculated using the GeNorm software.....	224
Table 30. Stability (M) values calculated using the NormFinder software.....	225
Table 31. Biofilm time-killing of African walnut oil against MRSA 252 and <i>S. aureus</i> ATCC 6538.....	258
Table 32. Biofilm time-killing of cashew oil against MRSA 252 and <i>S. aureus</i> ATCC 6538.....	260
Table 33. Biofilm time-killing of pumpkin oil against MRSA 252 and <i>S. aureus</i> ATCC 6538.....	263
Table 34. Fractional inhibitory concentration (FIC) indices of African walnut oil combined with antibiotics.....	266
Table 35. FIC and FIC index results from the combination of African walnut oil and antibiotics on MRSA 252 and ATCC 6538.....	267
Table 36. Fractional inhibitory concentration (FIC) and (FIC) indices (FICI) of pumpkin oil combined with antibiotics on MRSA 252 and ATCC 6538.....	267
Table 37. FIC and FICI data results from the combination of pumpkin oil with antibiotics.....	268
Table 38. CFU/Larvae per 10 µL injections of infecting doses of MRSA 252 and ATCC 6538 calculated from the original CFU counts.....	270
Table 39. Survivors and dead recorded between day 1 to 5 after infecting <i>G. mellonella</i> with MRSA 252 infecting doses.....	273
Table 40. Survivors and dead recorded between day 1 to 5 after infecting <i>G. mellonella</i> with ATCC 6538 infecting doses.....	275

Table 41. Survivors and dead recorded between day 1 to 5 after infecting <i>G. mellonella</i> with ATCC 6538 and MRSA 252 infecting dose ( $10^{-6}$ CFU/Larva) and treatment with antibiotic and African walnut oil.....	278
Table 42. Elution order and retention times of compounds observed in standard FAME mix (C8 - C24) from GC-MS analysis.....	283
Table 43. Fatty acid methyl ester profile of African walnut oil.....	286
Table 44. Data of fractions temperature range and the yield of each African walnut oil fraction.....	291
Table 45. Diameter of inhibitory zones produced by the four fractions.....	293
Table 46. Infrared absorption of fraction 1 (A) of African walnut oil.....	294
Table 47. Infrared absorption of fraction 2 (B) of African walnut oil.....	295
Table 48. Infrared absorption of fraction C of African walnut oil.....	296
Table 49. Chemical shifts and assignments of the characteristic resonances in the $^1\text{H}$ NMR spectra of fraction 2 (A) of African walnut oil and linolenic acid standard.....	301
Table 50. Chemical shifts and assignments of the characteristic resonances in the $^{13}\text{C}$ NMR and APT of fraction 2 (A).....	302
Table 51. Chemical shifts and assignments of the characteristic resonances in the $^1\text{H}$ NMR spectra of fraction 3 (B) of African walnut oil.....	303
Table 52. Chemical shifts and assignments of the characteristic resonances in the $^{13}\text{C}$ NMR and APT spectra of Fraction 3 (B).....	303

## List of Figures

Figure 1. Morphology of <i>S. aureus</i> in cluster, chains and single arrangements .....	1
Figure 2. Golden yellow colonies of <i>S. aureus</i> bacterium on agar plate .....	3
Figure 3. MRSA clonal complexes identified in Nigeria.. .....	5
Figure 4. Virulence factors of <i>S. aureus</i> with both cell wall associated proteins and secreted proteins playing roles as pathogenic determinants. ....	18
Figure 5. Schematic diagram of <i>S. aureus</i> accessory gene regulatory system (agr).....	29
Figure 6: African walnuts in Nigeria. ....	42
Figure 7. Cashew nut in Nigeria. ....	42
Figure 8. Pumpkin seeds in Nigeria. ....	43
Figure 9. Classes of phytochemicals of nuts.....	45
Figure 10. Alkaloids, phenol and carotenoids present in nuts .....	46
Figure 11. Plant seed and nuts used in this study .....	51
Figure 12. Example of separately prepared plates with oils for biofilm inhibitory concentration determined by broth microdilution method and safranin staining. ....	68
Figure 13: ATR-FTIR spectrophotometer .....	86
Figure 14: UV-visible spectrophotometer .....	87
Figure 15. A graphical representation of the average percentage yield of African walnut, cashew and pumpkin oils.....	92
Figure 16. Graphical representation of the percentage yield of African walnut, cashew and pumpkin extracts.....	94
Figure 17. Physical appearances of each oil sample as observed after extraction.....	95
Figure 18. Physical appearances of extracts of walnut, cashew and pumpkin .....	97
Figure 19. Ultra-violet absorption spectrum of walnut, cashew and pumpkin oils. ....	99
Figure 20. Ultra-violet absorption spectrum of African walnut, cashew and pumpkin chloroform extracts.....	100
Figure 21. Ultra-violet absorption spectrum of African walnut, cashew and pumpkin petroleum ether extracts.....	101
Figure 22. Ultra-violet absorption spectrum of African walnut, cashew and pumpkin hexane extracts.....	102
Figure 23. FTIR spectrum of African walnut oil. ....	103
Figure 24. FTIR spectrum of cashew oil. ....	104
Figure 25. FTIR spectrum of pumpkin oil.....	105

Figure 26. Appearance of ATCC6538 and MRSA 252 on TSA and Columbia blood base agar .....	111
Figure 27. Catalase test results of MRSA 252 and <i>S. aureus</i> ATCC 6538.....	111
Figure 28. Antibiotic confirmatory test of ATCC 6538 and MRSA 252 .....	112
Figure 29. Biofilm (slime) productions by ATCC 12228, ATCC 6538 and MRSA 252 on CRA plates.....	113
Figure 30. Biofilm formation of ATCC 6538 on 24-well tissue culture microtiter plate.....	114
Figure 31. Biofilm formation of MRSA 252 on 24-well tissue culture microtiter plate. ....	115
Figure 32. Quantification of ATCC 12228, ATCC 6538 and MRSA 252 biofilms formed on polystyrene microtiter plate after 12 h, 24 h and 48 hours at OD 595 nm. ....	116
Figure 33. Resistant pattern of MRSA 252 to commercial antibiotics and synergy effect of African walnut oil with antibiotics .....	126
Figure 34. Disk diffusion assay identifies African walnut oil and some selected commercial antibiotics with antimicrobial activity. ....	128
Figure 35. Resistant pattern of MRSA 252 to commercial antibiotics and synergy effect of cashew oil with antibiotics. ....	130
Figure 36. Disk diffusion assay identifies cashew oil and some selected commercial antibiotics with antimicrobial activity. ....	132
Figure 37. Resistant pattern of MRSA 252 to commercial antibiotics and synergy effect of fluted pumpkin oil with antibiotics.....	134
Figure 38. Disk diffusion assay identifies fluted pumpkin oil and selected commercial antibiotics with antimicrobial activity. ....	135
Figure 39. Resistant pattern of ATCC 6538 to commercial antibiotics and synergy effect of African walnut oil with antibiotics .....	137
Figure 40. Disk diffusion assay identifies walnut oil and selected commercial antibiotics with antimicrobial activity. ....	139
Figure 41. Resistant pattern of ATCC 6538 to commercial antibiotics and synergy effect of cashew oil with antibiotics .....	140
Figure 42. Disk diffusion assay identifies cashew oil and selected commercial antibiotics with antimicrobial activity.....	141
Figure 43. Resistant pattern of ATCC 6538 to commercial antibiotics and synergy effect of fluted pumpkin oil with antibiotics.....	143
Figure 44. Disk diffusion assay identifies fluted pumpkin oil and selected commercial antibiotics with antimicrobial activity. ....	144

Figure 45. Control plates of ATCC 6538 and MRSA 252 showing no zone of inhibitions with DMSO and mineral oil. ....	146
Figure 46. Representative plates for well diffusion of African walnut extracts against MRSA 252 and ATCC 6538.....	147
Figure 47. Representative plates for well diffusion of fluted pumpkin extracts against MRSA 252 and ATCC 6538.....	147
Figure 48. Minimum inhibitory concentration and minimum biofilm inhibitory concentration of African walnut oil tested against MRSA 252 and <i>S. aureus</i> ATCC 6538 planktonic cells and preformed biofilms after 24 hours of incubation at 37°C in 96-well tissue culture polystyrene plate.....	150
Figure 49. Minimum inhibitory concentration and minimum biofilm inhibitory concentration of cashew oil tested on MRSA 252 and <i>S. aureus</i> ATCC 6538 planktonic cells and preformed biofilms formed after 24 hours of incubation at 37°C in 96-well tissue culture polystyrene plates. ....	152
Figure 50. Minimum inhibitory concentration and minimum biofilm inhibitory concentration fluted pumpkin oil tested on MRSA 252 and <i>S. aureus</i> ATCC 6538 planktonic cells and preformed biofilms formed after 24 hours of incubation at 37°C in 96-well tissue culture plates.....	153
Figure 51. Minimum inhibitory concentration and minimum biofilm inhibitory concentration of hexane extract African walnut tested on <i>S. aureus</i> ATCC 6538 and MRSA 252 planktonic cells and biofilms formed after 24 hours of incubation at 37°C in 96-well tissue culture polystyrene plates .....	156
Figure 52. Minimum inhibitory concentration and minimum biofilm inhibitory concentration of African walnut petroleum ether extract tested on <i>S. aureus</i> ATCC 6538 and MRSA 252 planktonic cells and biofilms formed after 24 hours of incubation at 37°C in 96-well tissue culture polystyrene plate.....	158
Figure 53. Minimum inhibitory concentration and minimum biofilm inhibitory concentration of cashew hexane extract tested on <i>S. aureus</i> ATCC 6538 and MRSA 252 planktonic cells and biofilms formed after 24 hours of incubation at 37°C in 96-well tissue culture polystyrene plate.....	159
Figure 54. Minimum inhibitory concentration and minimum biofilm inhibitory concentration of cashew petroleum ether extract tested on <i>S. aureus</i> ATCC 6538 and MRSA 252 planktonic cells and biofilms formed after 24 hours of incubation at 37°C in 96-well microtiter polystyrene plate .....	161

Figure 55. Minimum inhibitory concentration and minimum biofilm inhibitory concentration of pumpkin hexane extract tested on <i>S. aureus</i> ATCC 6538 and MRSA 252 planktonic cells and biofilms formed after 24 hours of incubation at 37°C in 96-well tissue culture polystyrene plate.....	163
Figure 56. Minimum inhibitory concentration and minimum biofilm inhibitory concentration of pumpkin petroleum ether tested on <i>S. aureus</i> ATCC 6538 and MRSA 252 planktonic cells and biofilms formed after 24 hours of incubation at 37°C in 96-well tissue culture polystyrene plate.....	165
Figure 57. Preformed biofilms of ATCC 6538 on MBEC pegs. ....	167
Figure 58. Preformed biofilms of MRSA 252 on MBEC pegs.....	167
Figure 59. Reduction of MRSA 252 preformed biofilm on pegs following exposure to increasing concentrations of African walnut oil at 0.98-500 mg/mL after 6, 12, 24 and 48 h of incubation at 37°C. ....	169
Figure 60. Reduction of <i>S. aureus</i> ATCC 6538 preformed biofilm on pegs following exposure to increasing concentrations of African walnut oil at 0.98-500 mg/mL after 6, 12, 24 and 48 h of incubation at 37°C. ....	170
Figure 61. Reduction of MRSA 252 preformed biofilm on pegs following exposure to increasing concentrations of cashew oil at 0.98-500 mg/mL after 6, 12, 24 and 48 h of incubation at 37°C. ....	173
Figure 62. Reduction of <i>S. aureus</i> ATCC 6538 preformed biofilm on pegs following exposure to increasing concentrations of cashew oil at 0.98-500 mg/mL after 6, 12, 24 and 48 h of incubation at 37°C. ....	174
Figure 63. Reduction of MRSA 252 preformed biofilm on pegs following exposure to increasing concentrations of fluted pumpkin oil at 0.98-500 mg/mL after 6, 12, 24 and 48 h of incubation at 37°C. ....	176
Figure 64. Reduction of ATCC 6538 preformed biofilm on pegs following exposure to increasing concentrations of fluted pumpkin oil at 0.98-500 mg/mL after 6, 12, 24 and 48 h of incubation at 37°C. ....	177
Figure 65. Growth curve of MRSA 252 and ATCC 6538 grown in trypticase soy broth enriched with 1 % glucose at 37 °C for 48 h. ....	187
Figure 66. SEM images (A-D) of MRSA 252 grown in trypticase soy broth enriched with glucose for 6, 12, 24 and 48 h respectively, then imaged with FEI Quanta FEG 250 FESEM. ....	189

Figure 67. SEM images (A-D) of ATCC 6538 grown in trypticase soy broth enriched with glucose for 6, 12, 24 and 48 h 24 h respectively, then imaged with FEI Quanta FEG 250 FESEM .....	189
Figure 68. SEM images (A-D) of MRSA 252 grown in trypticase soy broth enriched with glucose for 6, 12, 24 and 48 h respectively, then imaged with FEI Quanta FEG 250 FESEM .....	190
Figure 69. SEM images (A-D) of ATCC 6538 grown in trypticase soy broth enriched with glucose for 6, 12, 24 and 48 h respectively, then imaged with FEI Quanta FEG 250 FESEM .....	191
Figure 70. Agarose gel electrophoresis of RNA extracted from MRSA 252 and <i>S. aureus</i> ATCC 6538 biofilms at 6 h. ....	192
Figure 71. Agarose gel electrophoresis of RNA extracted from MRSA 252 and <i>S. aureus</i> ATCC 6538 biofilms at 12 h, 24 h and 48 h.....	193
Figure 72. Agarose gel electrophoresis of RNA extracted from MRSA 252 biofilms after 12 h, 24 h and 48 h treatment with fluted pumpkin, African walnut and cashew oils. ....	193
Figure 73. Agarose gel electrophoresis of rna extracted from <i>S. aureus</i> atcc 6538 biofilms after 12 h, 24 h and 48 h treatment with African walnut, cashew and fluted pumpkin oils. ....	194
Figure 74. Agarose gels showing the RT-PCR products of the 16S rRNA, <i>gmk</i> , <i>gyrA</i> and <i>proC</i> genes of (A) <i>S. aureus</i> ATCC 6538 and (B) MRSA 252 biofilms at 12, 24 and 48 h. ....	196
Figure 75. Agarose gels showing the RT-PCR products of the <i>tpiA</i> , <i>glyA</i> , <i>pyk</i> and <i>gapdh</i> genes of (A) <i>S. aureus</i> ATCC 6538 and (B) MRSA 252 biofilms. ....	197
Figure 76. Agarose gels showing the RT-PCR products of the <i>rho</i> and <i>rpoD</i> genes of (a) <i>S. aureus</i> ATCC 6538 and (b) MRSA 252 biofilms.....	198
Figure 77. Agarose gel electrophoresis of RT-PCR products of <i>rrsc</i> gene for <i>S. aureus</i> ATCC 6538 and MRSA 252 biofilms.....	199
Agarose gel electrophoresis of RT-PCR amplification products of 16S rRNA, <i>gmk</i> , <i>gyrA</i> , <i>icaA</i> , <i>icaB</i> , <i>icaC</i> and <i>icaD</i> genes for (A) <i>S. aureus</i> ATCC 6538 and (B) MRSA 252 cultured for 6 h. ....	200
Agarose gel electrophoresis of RT-PCR amplification products of 16S rRNA, <i>gmk</i> , <i>gyrA</i> <i>fnbA</i> , <i>fnbB</i> , <i>fib</i> , <i>ebps</i> and <i>eno</i> for (A) ATCC 6538 and (B) MRSA 252 cells cultured for 6 h. ....	201

Figure 78. Agarose gel electrophoresis of RT-PCR amplification products of 16S rRNA, gmK, gyrA, clfA, clfB and cna of (a) MRSA 252 and (b) ATCC 6538 cells cultured at 6 h. ....	203
Figure 79. Agarose gel electrophoresis of RT-PCR amplification products of 16S RNA, gmK, gyrA, RNAlI, RNAlII, sea, and seb genes for (a) <i>S. aureus</i> ATCC 6538 and (b) MRSA 252 cells. ....	204
Figure 80. Agarose gel electrophoresis of RT-PCR amplification products of 16S rRNA, gmK, gyrA, mecA, emrA and blaZ genes for (a) <i>S. aureus</i> ATCC 6538 and (b) MRSA 252 cultured cells. ....	205
Figure 81. Agarose gel electrophoresis of RT-PCR amplification products of agrA gene for <i>S. aureus</i> ATCC 6538 and MRSA 252 biofilms. ....	206
Figure 82. Agarose gel electrophoresis of RT-PCR amplification products of 16S rRNA, gmK, gyrA, icaA and icaB genes for (a) <i>S. aureus</i> ATCC 6538 and (b) MRSA 252 biofilms. ....	207
Figure 83. Agarose gel electrophoresis of RT-PCR amplification products of 16S RNA, gmK, gyrA, icaC and icaD genes for (a) <i>S. aureus</i> ATCC 6538 and (b) MRSA 252 biofilms. ....	208
Figure 84. Agarose gel electrophoresis of RT-PCR amplification products of 16S RNA, gmK, gyrA, fnbA and fnbB genes for (a) <i>S. aureus</i> ATCC 6538 and (b) MRSA 252 biofilms. ....	210
Figure 85. Agarose gel electrophoresis of RT-PCR amplification products of 16S rRNA, gmK, gyrA, fib and cna genes for (a) <i>S. aureus</i> ATCC 6538 and (b) MRSA 252 biofilms. ....	211
Figure 86. Agarose gel electrophoresis of RT-PCR amplification products of 16S RNA, gmK, gyrA, clfA and clfB genes for (a) <i>S. aureus</i> ATCC 6538 and (b) MRSA 252 biofilms. ....	213
Figure 87. Agarose gel electrophoresis of RT-PCR amplification products of 16S rRNA, gmK, gyrA, ebps and eno genes for (a) <i>S. aureus</i> ATCC 6538 and (b) MRSA 252 biofilms. ....	214
Figure 88. Agarose gel electrophoresis of RT-PCR amplification products of 16S rRNA, gmK, gyrA, mecA and blaZ genes for (a) <i>S. aureus</i> ATCC 6538 and (b) MRSA 252 biofilms. ....	215
Figure 89. Agarose gel electrophoresis of RT-PCR amplification products of 16S rRNA, gmK, gyrA, sea and seb genes for (A) <i>S. aureus</i> ATCC 6538 and (B) MRSA 252 biofilms. ....	217

Figure 90. Agarose gel electrophoresis of RT-PCR amplification products of 16S rRNA, gmk, gyrA, RNAPII and RNAPIII genes for (a) <i>S. aureus</i> ATCC 6538 and (b) MRSA 252 biofilms.....	218
Figure 91. Agarose gel electrophoresis of RT-CR amplification products of agrA gene for <i>S. aureus</i> ATCC 6538 and MRSA 252 biofilms. ....	219
Figure 92. A. Mean Ct values obtained from RT-qPCR expression levels of nine reference genes in ATCC 6538. ....	222
Figure 93. Mean Ct values obtained from RT-qPCR expression levels of nine reference genes in MRSA 252. s .....	222
Figure 94. Stability value ranking of the reference genes in ATCC 6538, as determined by geNorm .....	223
Figure 95. The stability value ranking of the reference genes in MRSA 252, as determined by geNorm. ....	224
Figure 96. The expression of <i>icaA</i> gene in biofilms of MRSA 252 and <i>S. aureus</i> ATCC 6538 before and after treatment with African walnut and fluted pumpkin oils. ....	226
Figure 97. The expression of <i>icaB</i> gene in biofilms of MRSA 252 and <i>S. aureus</i> ATCC 6538 before and after treatment with African walnut and fluted pumpkin oils. ....	228
Figure 98. The expression of <i>icaC</i> gene in biofilms of MRSA 252 and <i>S. aureus</i> ATCC 6538 before and after treatment with African walnut and fluted pumpkin oils. ....	230
Figure 99. The expression of <i>icaD</i> gene in biofilms of MRSA 252 and <i>S. aureus</i> ATCC 6538 before and after treatment with African walnut and fluted pumpkin oils .....	232
Figure 100. The expression of <i>fnbA</i> gene in biofilms of MRSA 252 and <i>S. aureus</i> ATCC 6538 before and after treatment with African walnut and fluted pumpkin oils. ....	234
Figure 101. The expression of <i>fnbB</i> gene in biofilms of MRSA 252 and <i>S. aureus</i> ATCC 6538 before and after treatment with African walnut and fluted pumpkin oils. ....	236
Figure 102. The expression of <i>fib</i> gene in biofilms of MRSA 252 and <i>S. aureus</i> ATCC 6538 before and after treatment with African walnut and pumpkin oils.....	238
Figure 103. The expression of <i>clfA</i> gene in biofilms of MRSA 252 and <i>S. aureus</i> ATCC 6538 before and after treatment with African walnut and fluted pumpkin oils. ....	240
Figure 104. The expression of <i>clfB</i> gene in biofilms of MRSA 252 and <i>S. aureus</i> ATCC 6538 before and after treatment with African walnut and fluted pumpkin oils. ....	242
Figure 105. The expression of agrA gene in biofilms of MRSA 252 and <i>S. aureus</i> ATCC 6538 before and after treatment with African walnut and fluted pumpkin oils. ....	244

Figure 106. The expression of <i>eno</i> gene in biofilms of MRSA 252 and <i>S. aureus</i> ATCC 6538 before and after treatment with African walnut and fluted pumpkin oils. ....	246
Figure 107. The expression of <i>mecA</i> and <i>blaZ</i> gene in biofilms of MRSA 252 before and after treatment with African walnut and fluted pumpkin oils. ....	248
Figure 108. Time exposure viability curve (log <sub>10</sub> CFU/mL over 24 h) for mature MRSA 252 biofilm incubated with African walnut oil at MBEC (62.5 mg/mL) for 24 h at 37°C ...	258
Figure 109. Time exposure viability curve (log <sub>10</sub> CFU/mL over 24 h) for preformed ATCC 6538 biofilm incubated with African walnut oil at MBEC (31.25 mg/mL) for 24 h at 37°C. ....	259
Figure 110. Time exposure viability curves (log <sub>10</sub> CFU/mL over 24 h) for preformed MRSA 252 biofilm incubated with cashew oil at MBEC (500 mg/mL) at 37°C. ....	261
Figure 111. Time exposure viability curves (log <sub>10</sub> CFU/mL over 24 h) for preformed ATCC 6538 biofilm incubated with cashew oil at MBEC (500 mg/mL) at 37°C. ....	261
Figure 112. Time exposure viability curve (log <sub>10</sub> CFU/mL over 24 h) for preformed MRSA 252 biofilm incubated with pumpkin oil at MBEC (250 mg/mL) for 24 h at 37°C. ....	263
Figure 113. Time kill exposure viability curve (log <sub>10</sub> CFU/mL over 24 h) for preformed ATCC 6538 biofilm incubated with pumpkin oil at MBEC (125 mg/mL) for 24 h at 37°C. ....	264
Figure 114. Representative trial microtiter plate for the individual MIC determination trials. ....	265
Figure 115. Observed changes in <i>G. mellonella</i> before, after infection and with combinational treatment. ....	269
Figure 116. One day (24 h) post inoculation of <i>G. mellonella</i> larvae infected with 10 µL of 100 infecting doses of MRSA 252 and ATCC 6538 biofilm cultures (stationary phase cultures). ....	271
Figure 117. Representative photographs of petri-plates containing <i>G. mellonella</i> infected with MRSA 252 biofilm cultures. ....	272
Figure 118. The survival of <i>G. mellonella</i> larvae infected with MRSA 252. ....	273
Figure 119. Representative photographs of petri-plates containing <i>G. mellonella</i> infected with <i>S. aureus</i> ATCC 6538. ....	274
Figure 120. The survival of <i>G. mellonella</i> larvae infected with ATCC 6538. ....	275
Figure 121. Visual observation of <i>G. mellonella</i> before and after treatment with antibiotic and African walnut oil for 5 days. ....	276

Figure 122. Percentage survival from <i>G. mellonella</i> (n=15-20 per group) groups infected MRSA 252 and ATCC 6538 and treated with antibiotic and African walnut oil. ....	277
Figure 123. GC-MS chromatogram showing peaks of fatty acid methyl esters (C8:C17) and their retention times identified in Supelco standard FAME mix.....	284
Figure 124. GC-MS chromatogram showing peaks of fatty acid methyl esters (C18:C20) and their retention times identified in Supelco standard FAME mix.....	285
Figure 125. GC-MS chromatogram showing peaks of fatty acid methyl esters (C21:C24) and their retention times identified in Supelco standard FAME mix.....	285
Figure 126. Fatty acids methyl esters identified in African walnut oil and proportion through GC-MS results. ....	287
Figure 127. GC-MS chromatogram of major fatty acid methyl esters identified in African walnut oil with their retention times.....	287
Figure 128. Mass spectrum of linolenic acid methyl ester (C18:3) identified in African walnut oil.....	288
Figure 129. Mass spectrum of palmitic acid methyl esters (C16:0) identified in African walnut oil. ....	288
Figure 130. Mass spectrum of linoleic acid methyl esters (C18:2) identified in African walnut oil.....	289
Figure 131. Mass spectrum of stearic acid methyl esters (C18:0) identified in African walnut oil.....	289
Figure 132. GC-MS chromatogram and spectrum of eicosenoic acid methyl esters (C20:1) identified in African walnut oil .....	290
Figure 133. Scheme of bioassay guided-fractionation of African walnut oil and antimicrobial activity of the four fractions. ....	292
Figure 134. FTIR spectrum of fraction A obtained from fractional distillation of African walnut oil. ....	294
Figure 135. FTIR spectrum of fraction B obtained from fractional distillation of African walnut oil .....	295
Figure 136. FTIR spectrum of fraction C obtained from fractional distillation of African walnut oil. ....	296
Figure 137: Linolenic acid showing protons and assigned peak .....	300

## **Acknowledgments**

I would like to express my gratitude to my supervisor, Dr Natalie Ferry for her guidance, patience and support throughout this project and a special thanks to my co-supervisor Dr John Hadfield for all his help and support.

Thanks to the technicians at University of Salford who are helpful in the laboratory especially Helen Bradshaw, Tony Bodel, and Sally Shephard. Also, a special thanks to Abby and Dr Patricia Ragazzon for their help and advice on chemistry.

I would like to thank my employer, Olabisi Onabanjo University, Ago-Iwoye, Ogun State, College of Agricultural Sciences, Yewa, Aiyetoro, Ogun-state and the Tertiary Education Trust Fund for their financial support for this project.

I also worked with loving and kind colleagues and I would like to thank them for all of their support, including Kuburat, Grace, Arvind, Jessica, Segun, Graham and Amjed. A special thanks to Amjed, Stephen and Henry for their countless help in the project. To my late friend, Odio, thank you for being there for me when you were alive.

My deep and special thanks to my husband, Femi Fakile, and my beloved children for love and joys they share to me and for their patience and encouragements. Also, many thanks to all my sisters and brothers for their support and encouragement. I would like to thank Salewa, Jayden, Jerahmeel and mum Olunuga for their support and love throughout my study.

I would like to express my appreciation to my dear parents, who always give me prayer and blessing for my study. I would like to dedicate this thesis to the memory of my late mother whom we started the journey of this study together. I miss you mum.

Lastly to God be all the glory, great things he has done for me. I thank him for his love and grace to pursue and complete this project.

## **Declaration**

The work in this thesis was carried out at the University of Salford. All the work presented was conducted by me at the University of Salford, except where otherwise stated in the text. During the period of the PhD study, some of the contents and findings have been presented in local and international conferences prior to submission of the thesis. The researcher declares that no part of this work referred to in this thesis has been submitted for a degree or any other qualification within the University of Salford or any other institution.

Oluwapamilerin Damola Yangomodou

## List of abbreviations

Agr	Accessory gene regulator
AID/HIV	Autoimmune deficiency diseases
BF3	Boron trifluoride
BHI	Brain Heart Infusion
CC	Clonal complex
CFU	Colony forming units
CA-MRSA	Community- associated methicillin resistant <i>S. aureus</i>
CAPD	Continuous ambulatory peritoneal dialysis
FnBP	Fibrinogen binding protein
FTIR	Fourier-transform infrared spectroscopy
GC-MS	Gas chromatography mass spectrometry
HA-MRSA	Hospital-acquired methicillin resistant <i>S. aureus</i>
ICU	Intensive care unit
IcaADBC	Intercellular adhesion genes
mecA	Methicillin resistance gene
MRSA	Methicillin resistant <i>S. aureus</i>
MSSA	Methicillin Susceptible <i>S. aureus</i>
MRSA	Methicillin-resistant <i>Staphylococcus aureus</i>
MSCRAMM	Microbial surface components recognizing adhesive matrix molecules
MBIC	Minimum biofilm inhibitory Concentration
MBEC	Minimum biofilm inhibitory Concentration
MIC	Minimum Inhibitory Concentration
MHA	Mueller Hinton Agar
MHB	Mueller-Hinton broth
NMR	Nuclear magnetic resonance
ORF	Open reading frame
OD	Optical density
PVL	Panton-Valentine Leukocidin
PCR	Polymerase Chain Reaction
QT-PCR	Real-time quantitative PCR

RNA	Ribonucleic acid
SAB	<i>S. aureus</i> bacteraemia
SEM	Scanning electron microscopy
SCCmec	Staphylococcal chromosomal cassette mec
<i>S. aureus</i>	Staphylococcus aureus
TSST	toxic shock syndrome toxin
Tn	transposon
TSA	Tryptic Soy Agar
TSB	Tryptic Soy Broth
USA	United States of America
UTI	Urinary tract infection
VISA	Vancomycin intermediately susceptible <i>S. aureus</i>

## Abstract

The antibacterial activities of oils and extracts from walnut, cashew and pumpkin were investigated on methicillin resistant and susceptible strain MRSA 252 and *S. aureus* ATCC 6538 using the disc agar diffusion technique. Results revealed that the tested bacteria were sensitive to the three oils. Walnut and pumpkin oil showed better activity with clear zones of inhibitions. A combinational study of oils with conventional antibiotics shows that MRSA 252 and ATCC 6538 exhibited different reactions such as synergy, resistant, potentiation and indifference effects when combined with the oils. Minimum inhibitory concentration (MIC) and minimum biofilm inhibition concentration (MBIC) tests show that inhibitory effect of walnut oil against MRSA 252 and *S. aureus* ATCC 6538 biofilm formation was stronger compared to cashew and pumpkin oils. In addition, minimum biofilm eradication concentration (MBEC) test revealed that walnut and pumpkin oils were able to eradicate preformed biofilms of MRSA 252 and ATCC 6538 within 48 h of growth with eradication from 12 h with reduced viable counts. Preliminary investigation of the pathogenicity of the *S. aureus* strains showed that MRSA 252 biofilms were more virulent against *Galleria mellonella* than *S. aureus* ATCC 6538 biofilms. A test to determine whether walnut oil could treat infections caused by both strains shows that *G. mellonella* previously infected with MRSA 252 and *S. aureus* ATCC 6538 biofilms were able to survive in a 5-day study even though they developed brownish pellicles. Scanning electron microscopy (SEM) of *S. aureus* biofilms shows that MRSA 252 and ATCC 6538 biofilms produced different morphological structures and slime confirming the complexity of the biofilms. Using molecular methods, polymerase chain reaction (PCR) confirms the presence of numerous virulence genes such as adhesion, biofilm and antibiotic resistance genes in MRSA 252 and ATCC 6538, gene expression analysis results indicates that intercellular adhesion (*icaADBC*) genes were down-regulated between 6-12 h and only up-regulated at 24 h, the biofilm formation genes were up-regulated at 12, 24 and 48 h while the accessory regulatory gene (*agrA*) and methicillin resistant (*mecA*) gene were up-regulated at 12 and 24 h but down-regulated at 48 h in the strains. Preliminary chemical investigation of walnut oil indicates the presence of different compounds that could be responsible for its antimicrobial activity. Using gas chromatography–mass spectrometry (GC-MS), major and minor fatty acids were identified in walnut oil. Structural elucidation of the fractionated walnut oil sample conducted using hydrogen proton NMR ( $^1\text{H}$  NMR),  $^{13}\text{C}$  NMR, attached proton test (APT), confirmed linolenic acid and glyceric acid as the probable compounds responsible for its activity against MRSA 252 and *S. aureus* ATCC 6538 biofilms.

# Chapter 1. Introduction to *Staphylococcus aureus*

## 1.1 Brief historical perspective of staphylococci

The staphylococci are members of the family of Gram-positive cocci, Staphylococcaceae, which is in the order Bacillaceae (Kuroda *et al.*, 2001). The term Staphylococcus means bunch of grapes, for their ability to form clusters which are grape – like (Figure 1). Since many decades ago, *S. aureus* was the first bacterial human pathogen identified (Davies and Davies, 2010). In 1878, Koch was the first scientist to differentiate gram positive cocci from gram negative cocci strains and recognized that human infection such as abscesses is connected with the presence of clusters of gram-positive cocci. The author noted that different human diseases were caused by staphylococci depending on whether they formed cocci in pairs or clusters. In 1880, Sir Alexander Ogston, a Scottish surgeon conclusively established the causative role of the coccus in abscesses and other suppurative lesions. During Alexander Ogston research study, he discovered a cluster forming coccus was the cause of certain pyogenic abscesses in human beings when he injected the pus from the knee of a man containing staphylococci into mice, and it produced abscesses; however, when the pus was heated and treated with phenol no abscesses was produced. Therefore in 1882, Ogston named the bacteria staphylococcus. Similarly, Lious pasteur who worked on coagulase testing was able to classify staphylococci rather than pigment production, wherein a positive coagulase test was able to identify *S. aureus*. Thereafter, in 1884, Rosenbach succeeded in differentiating staphylococci species based on their colonial pigmentation, whereby the most pathogenic staphylococcal strain formed a golden pigment and less pathogenic strains produced white colonies. Based on this, Rosenbach called the pathogenic strain with golden pigments *S. aureus* and the less pathogenic strain with white colonies *S. albus* now known as *S. epidermidis*.

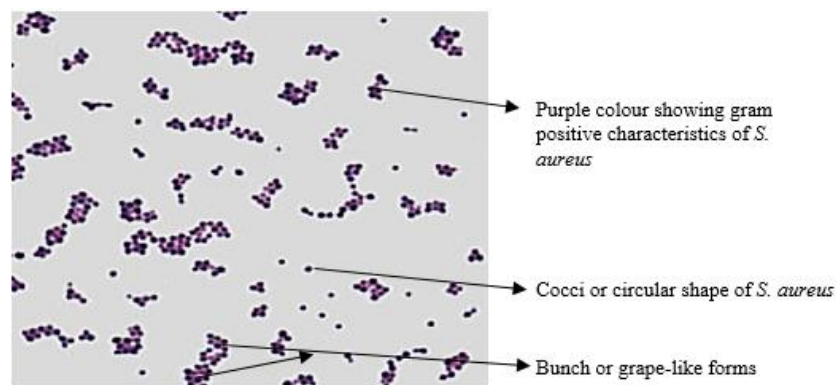


**Figure 1. Morphology of *S. aureus* in cluster, chains and single arrangements**

*S. aureus* stained by crystal violet and observed under the microscope using 10 x magnification lens

## 1.2 Classification and status of staphylococcal species

Historically the genera *Staphylococcus* and *Micrococcus* were placed together with the genera *Stomatococcus* and *Planococcus* in the same family, classified Micrococcaceae, but molecular test and chemotaxonomic analysis showed that the various catalase positive and gram-positive cocci differ (Plata *et al.*, 2009). Based on this, the family Staphylococcaceae and other families including Listeriaceae, Planococcaceae, Bacillaceae and Paenibacillaceae are all placed in the order Bacillales which belong to the class Bacilli (Vasconcelos and de Souza, 2010).

As of the year 2014, there are 41 known species and 24 subspecies in the *Staphylococcus* genus. About half of these staphylococcal species are endogenous to humans, including coagulase-negative species: *S. epidermidis*, *S. saprophyticus*, *S. cohnii*, *S. haemolyticus*, *S. xylosus*, *S. warneri*, *S. hominis*, *S. capitis*, *S. simulans*, *S. saccharolyticus*, *S. caprae*, *S. auricularis*, *S. lugdunensis*, and *S. schleiferi* and coagulase positive species: *S. aureus* (Vasconcelos and de Souza, 2010).

## 1.3 *Staphylococcus aureus*

### 1.3.1 Morphology and biochemical characteristics of *S. aureus*

*S. aureus* is a spherical and cluster forming coccus approximately 1µm in diameter (Plata *et al.*, 2009) (Figure 2). *S. aureus* is a non-motile, non-spore former and facultative anaerobe that grow by aerobic respiration or by fermentation of glucose that yields mainly lactic acid. *S. aureus* is oxidase negative (Okafor, 2011). The bacterium is catalase, coagulase and mannitol positive, a major distinguishing factor of *S. aureus* from *S. epidermidis*. *S. aureus* can grow between 15°C - 45°C and at sodium chloride (NaCl) concentrations as high as 15% (Bruins *et al.*, 2007). On solid medium, *S. aureus* form characteristic smooth and translucent golden yellow colonies on general purpose medium due to the secretion of carotenoids situated in their cell membrane (Trüper and Schleifer, 2006). This carotenoid pigment gives *S. aureus* its characteristic colour and protects the bacteria from the action of toxic oxidants from polymorphonuclear cells (PMN) and phagocytes (Samyuktha and Mahajan, 2016).



**Figure 2. Golden yellow colonies of *S. aureus* bacterium on agar plate**

Photograph of *S. aureus* on trypticase soy agar showing a growing pattern of spherical cocci.

### **1.3.2 Epidemiology of *S. aureus* infections**

#### **1.3.2.1 Global epidemiology of *S. aureus* and MRSA**

Healthcare-associated methicillin resistant *S. aureus* (HA-MRSA) otherwise referred to as hospital associated MRSA are clonal lineages that typically cause hospital-acquired infections, whereas community-associated methicillin resistant *S. aureus* (CA-MRSA) infections are composed of different lineages and occur in people with no previous history of hospitalisation (Chambers, 2001).

#### **1.3.2.2 HA-MRSA**

In majority of the hospitals across the world, hospital acquired (HA) types of MRSA are highly prevalent. Based on the LEADER Program, data obtained from 2004 and 2005 shows a prevalence of 54.3% and 58.2% in the USA (Tenover *et al.*, 2006; Chambers, 2001; Faria *et al.*, 2005). Although invasive MRSA infections in healthcare settings seem to be decreasing in the USA it is still a threat to patients. Between the year 2005 and 2011, the rates of invasive MRSA dropped by 31%; and the largest decrease (55%) was observed among hospital infections (CDC, Threat Report 2013). In 2008 and 2011 precisely, MRSA proportions observed in Canada and Australia were 27.1% and 30.4% (Potashman *et al.*, 2016; Hassoun, Linden & Friedman 2017). In Europe and Northern Europe, MRSA proportions are generally lower and higher in both South and South-Eastern countries. In 2012, the average proportion of MRSA isolated from invasive infection was 17.9% (EARSS Annual Report, 2012). Only two countries, Portugal and Romania reported proportions above 50%, which were 53.8% and 53.9 (Goossens *et al.*, 2005). Many countries, particularly African countries report a 10%-50% average proportion of MRSA isolated from invasive infection in healthcare settings while

lower proportions (3%) have been reported in 6 countries, including Denmark (1.3%), Iceland (1.7%), Finland (2.1%), the Netherlands (1.3%), Sweden (0.7%) and Norway (1.3%) (Larsen *et al.*, 2009; Tavares, 2014). Statistically significant decreasing trends which have been observed in some European countries, in recent years. Arguably, this has been caused by improved infection control as well as the restriction of some antibiotic classes in the hospitals globally (Harbarth *et al.*, 2015).

Currently, many *S. aureus* isolates (50%) now show resistance to methicillin in most countries in East Asian countries including Taiwan (65.1%), Hong Kong (56.9%), Korea (78.6%), Vietnam (75.1%), Sri Lanka (87.5%) and Thailand (57.0%) (Nickerson *et al.*, 2012; Chuang and Huang, 2013). Countries such as Iran, reported 44.5% *S. aureus* isolates as MRSA strains (Askari *et al.*, 2012). In contrast, lower prevalence was recorded in India and the Philippines (22.6%) and (38.1%) *S. aureus* isolates being MRSA (Mahmood *et al.*, 2010).

In African countries, the prevalence of MRSA has never been lower than 50% in most of the African countries, except for South Africa (19%) (Falagas *et al.*, 2013). Sporadic increase in resistant MRSA isolates have been reported in Tunisia, the prevalence of MRSA increased from 17% to 41% between 2003 and 2007 (Borg *et al.*, 2007), in Libya it was 32% in 2007. In Botswana, the prevalence was between 24–42% between 2001 and 2008. In Algeria and Egypt, the prevalence was 45% and 52% between 2003 and 2005, respectively. Ethiopia and Ivory Coast recorded a prevalence of 49% and 40%, respectively. In South Africa, the prevalence decreased from 37% in 2006 to 25% during 2007–2010 (Borg *et al.*, 2007).

### **1.3.2.3 Prevalence of MRSA in Nigeria and other African countries**

In a review conducted in Nigeria, the prevalence was higher in the Northern part than the Southern part. The prevalence was 30% and 28% between 2005 and 2010, respectively. Majority of the healthcare MRSA were found to be transmitted mostly from personnel infected with MRSA to patients. In a review study, conducted in 2013 by the Nnamdi Azikiwe University Teaching Hospital, Nnewi, health-care workers including medical doctors, nurses and laboratory scientists, accounted for 24%, 35% and 29% of personnel to patient transmission of MRSA (Akujobi *et al.*, 2013). Similarly, in 2018, Abdullahi and Iregbu, (2018) conducted a study at the National hospital Abuja, Nigeria, and suggested that the carriage rate of MRSA among health-care workers was 13.6% and higher prevalence was observed among the clinical healthcare workers than the non-clinical staff (10% vs. 3.6%). In 2013, Udobi, and co-workers conducted a study in intensive care unit at Ahmadu Bello hospital, Zaria and reported a

prevalence of MRSA colonization among healthcare and patients to be 11.83% and 2.1% and all MRSA isolates were highly resistant to antibiotics such as penicillin, erythromycin, and 17 (85.7%) were highly sensitive to vancomycin. Borg and colleagues (2007) reported a high prevalence of more than 50% of MRSA strains in countries including Jordan, Malta, Cyprus and Egypt. This high prevalence in Nigeria and the neighbouring countries was attributed to overcrowding, poor infection control facilities, lack of control of antibiotic usage and poor hand-hygiene facilities in the hospitals (Borg *et al.*, 2007).

Most of MRSA infections are caused by *S. aureus* strains belonging to a few clonal complexes (CC) in hospitals between 1962 and 2007 (Abdulgader *et al.*, 2015). The most prevalent are CC5 (USA100 a Japan clone, USA800 a pediatric clone, UK-EMRSA-3, Italian or Southern German clone, CC8 a Iberian clone or UK-EMRSA-5 a Rome clone, USA500 or UK-EMRSA-2 or 6 a Brazilian clone, CC22 or UK-EMRSA-15, CC30 or USA200, UK-EMRSA-16, USA1100, the Pacific Oceania clone), and CC45 or USA600, a Berlin clone (In summary, the two most abundant clones worldwide are the CC5 and CC8. Two pandemic HA-MRSA clones, namely multilocus sequence type (ST) 239 (CC8) and ST5 (CC5), have been spreading in many countries. In Nigeria, and her neighbouring countries, isolates of CC5, CC30, CC80 and CC152 (Figure 3) were non-cytotoxic, whereas isolates of CC22, CC8, CC15, CC45 and CC88 were very cytotoxic (Abdulgader *et al.*, 2015).

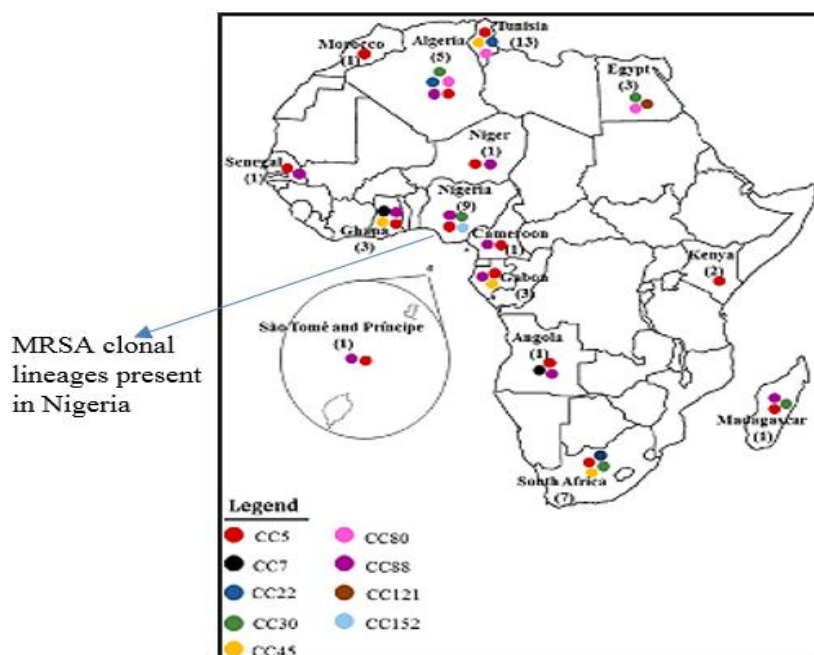


Figure 3. MRSA clonal complexes identified in Nigeria. Source: Abdulgader *et al.*, (2015).

### **1.3.3 Carriage of *S aureus***

*S. aureus* colonizes the human body without any clinical signs and symptoms and lives as a commensal in the human nose. its main habitat is the anterior of the nares (Krismer and Peschel, 2011). It infects the nasal vestibule, which is the anterior part of the nasal cavity, it resides on the small tiny hairs called vibrissae (Wertheim *et al.*, 2005). This organism can also be found transiently on the skin, respiratory tract, and intestines. Three main states of human nasal carriage patterns exist among healthy individuals in a population (Verhoeven *et al.*, 2014). About 20% of healthy individuals never carry *S. aureus* at all and are thus referred to as non-carriage individuals (Lamers *et al.*, 2011). Approx. 60% harbour *S. aureus* but not all the time and finally 20% of healthy individuals harbour *S. aureus* persistently without any clinical signs (Wertheim *et al.*, 2005). *S. aureus* isolates of major concern to the medical society are methicillin-sensitive and resistant strains, which are also persistent colonizers. The persistent and the intermittent carriers are regarded as being responsible for disseminating *S. aureus* into the hospital and community settings (Kuehnert, *et al.*, 2006). This is because they are carriers of *S. aureus*. The anterior of the nares are lined by epidermis that are fully keratinised with sebaceous glands, hairs and sweat glands. The nasal vestibule is enclosed by cartilages present in the nose and lined by the epithelium that lines the skin which becomes continuous with the nasal mucous membrane (Derycke *et al.*, 2010). Apparently *S aureus* flourishes here in absence of host defenses. For *S aureus* to adhere in the vestibule, it establishes interaction with host cell surfaces to prevent their rapid elimination by both physical and chemical means. To effectively colonize the host, it is thought that surface components of *S. aureus* cells interact with surface components such as glycoproteins and proteoglycans which are on the human cell membranes. Glycoproteins and proteoglycans are known to contribute to the adhesion of bacteria. Other vital surfaces to which *S. aureus* adheres include surfactant protein A which acts are surface receptors, mucin coated epithelial cells, secretory immunoglobulin A and glycolipids (Derycke *et al.*, 2010).

### **1.3.4 Transmission and risk factors of colonization of human nose with *S. aureus***

#### **1.3.4.1 Transmission of *S. aureus***

Since *S. aureus* is a normal human flora and is found in various body sites, infection can occur when the colonising strain gain access to a normally sterile site as a result of skin trauma or injury to mucosal surfaces (Ricciardi-Castagnoli & Granucci, 2002). Usually trauma incidents cause minor injuries to the skin or multiple layers of epithelial tissues. Skin traumas are caused

by cuts, abrasion, burns and other forms of injury (Ricciardi-Castagnoli & Granucci, 2002). Skin trauma incidents are acute wounds, which have a probability of becoming chronic wounds if not managed properly (Stone, 2013). In addition, *S. aureus* can also be transmitted from person to person via contaminated hands and objects or, less often, by inhalation of infected droplets dispersed by sneezing or coughing. Once the bacterium is transmitted, it may likely become established as the recipient flora and later gain access to a sterile body site (Ricciardi-Castagnoli and Granucci, 2002; Percival *et al.*, 2015). The spread of *S. aureus* through direct contact with an infected person possess a serious challenge in the hospital settings and community.

#### **1.3.4.2 Risk factors of colonization with *S. aureus***

*S. aureus* can infect anyone at any certain age, but certain people are more prone or are at increased risk of developing very serious staphylococcal infections. These include people who have a weak immune system or suffered chronic illnesses (Ricciardi-Castagnoli & Granucci, 2002). Generally, *S. aureus* infections occur when the immune system of the host is weakened and as such it cannot respond to external stimuli (Ricciardi-Castagnoli and Granucci, 2002). This means infections occur more in immunocompromised persons with weak immune systems (Ricciardi-Castagnoli and Granucci, 2002). Health conditions such as cancer, autoimmune deficiency diseases or have human immunodeficiency virus (AIDS/HIV) and diabetes reduces human immunity and increases the danger of hospital associated MRSA (Albertson *et al.*, 2015).

Current invasive medical tests such as catheterization, dialysis and surgery increase risk of infection because the processes require frequent use of catheters or insertion of needles to access the bloodstream (Percival *et al.*, 2015). Also, patients with serious health related problems admitted in hospital for long period of time in the intensive care unit are exposed to longer use of invasive devices and increased contact with healthcare workers. Therefore, length of stay and use of invasive procedures are possible risk factors of acquiring health care associated infections (HAI) such as urinary infections associated with catheter, surgical site infection and blood infections (Stone, 2013). Patients who undergone surgery continually or have implanted medical device such as an artificial joint are at higher risk of infection. This is because implants are foreign materials in the human body associated with risk of microbial infection (bacterial or fungal infections) overtime. Implant infections occur by inoculation of a few pathogen from the patient's skin or mucous membranes during implantation. At times, the

bacterium may be acquired from the hands of the surgical doctors, nurses or other clinical staff (Percival *et al.*, 2015).

Workers in health care centres (assistant physicians, nurses, cleaners, doctors) and people who come in contact with these set of workers are also at high risk of MRSA infections (Cohen *et al.*, 2012). Children especially new-born are also at high risk of infection because of their low immunity (PrabhuDas *et al.*, 2011). Major risk factors for new born includes premature birth and low weight A child is premature when born before 38 weeks and this means the infant have underdeveloped immune system, making them prone to increase infections (PrabhuDas *et al.*, 2011; Schaumburg *et al.*, 2014).

Involvement in matches (for example football, wrestling) (Grosset-Janin *et al.*, 2012) use of contaminated materials by many people (razors, towels) (Batabyal *et al.*, 2012; Miller and Diep, 2008), inadequate personal hygiene and poor sanitary conditions (Samuel *et al.*, 2010) are all community acquired MRSA infections risk factors.

Interestingly, another MRSA risk factor is companion animals (Cuny *et al.*, 2010). Studies have showed that it is very likely that people get infected from rabbits, dogs, pigs, horses, and cats, because they have been found to harbor *S. aureus* (Cohn and Middleton, 2010; Petinaki and Spiliopoulou, 2012; Labro and Bryskier, 2014).

#### **1.3.4.3 Colonization of *S. aureus* in human nasal carriage and increased risk of subsequent infections**

Colonization increases the risk for subsequent human infection. Previous reports have associated nasal carriage with increased infection danger in hospital victims after surgical operations. Colonization of the anterior nares provides a reservoir through which this pathogenic bacterium is disseminated to other body sites when host defenses are breached, whether by aspiration, shaving, insertion of catheter or surgery (Gordon and Lowy, 2008). Once an individual is colonized, there is an increased risk for *S. aureus* infection and development of subsequent of human infections. Majority of the studies carried out between 1990s to 2014 has clearly showed that nasal carriage of *S. aureus* increases the risk for the development of nosocomial infections in patients in hospital settings. These includes patients undergoing surgery (includes thoracic and orthopaedic surgery) (Jensen *et al.*, 1999; Kalmeijer *et al.*, 2000; Wertheim *et al.*, 2005), those on continuous ambulatory peritoneal dialysis (CAPD) or haemodialysis (Luzar *et al.*, 1990; Wanten *et al.*, 1996; Zimakoff *et al.*, 1996);

Nouwen *et al.*, 2005), those with AIDs and HIV (Nguyen *et al.*, 1999; Winke *et al.*, 1992), those with intravascular devices-related *S. aureus* bacteraemia (SAB) (Snydman *et al.*, (1990), those with liver cirrhosis and after liver transplantation (Lefranc *et al.*, 2005), patients admitted to intensive care units (ICU) (Corbella *et al.*, 1997; Pujol *et al.*, 1996; Keene *et al.*, 2005; Honda *et al.*, 2010), those with Wegener's granulomatosis (Stegeman *et al.*, 1994; Zycinska *et al.*, 2008), those colonized with MRSA and patients with diabetes mellitus (insulin-dependent) (Kluytmans *et al.*, 1997; Wertheim *et al.*, 2005; Datta *et al.*, 2014).

In surgical patients, the risk of developing *S. aureus* bacteraemia has been observed. Wertheim *et al.*, (2004) identified *S. aureus* as the most frequent cause of bacteraemia in hospital patients. They screened 14008 patients comprising of non-bacteraemia and non-surgical patients for *S. aureus* carriage and possibility of developing nosocomial bacteraemia. In this study, they observed that there was a 3-fold higher risk for non-surgical patients who were *S. aureus* nasal carriers 1.2% (40/3420), to acquire a nosocomial blood infection versus non-carriers 0.4% (41/10 588). A relative risk of 3.0 was also noted for the development of nosocomial bacteraemia. Furthermore, Jensen and his co-workers looked at nasal carriage in relation to surgery. Nasal cultures were performed in 61 (72%) of 85 hospital-acquired *S. aureus* bacteraemia (SAB) patients. They observed that nasal carriers among patients in surgery had significantly increased risk (OR 4.0) for nosocomial bacteraemia compared to patients without SAB (Jensen *et al.*, 1999).

In orthopaedic surgery, *S. aureus* has been identified as the main causative pathogen for surgical site infections. Kalmeijer *et al.*, (2000) observed a cohort of 272 patients in orthopaedic surgery with prosthetic implants for the risk of developing surgical site infections (SSI). Of these patients, 6.6% (18) of 272 patients had infections at the site, 11 had superficial infection and 7 patients had deep surgical site infections. *S. aureus* was seen as the main pathogen responsible for these three cases of surgical site infections. Kalmeijer *et al.*, (2000), suggested that high-level nasal carriage of *S. aureus* was the most crucial factor for developing surgical site infections with *S. aureus*.

In patients undergoing haemodialysis, *S. aureus* is the most frequently found bacterium in infections at the vascular access site causing bacteraemia. In a prospective study on 43 haemodialysis patients by Nielsen *et al.*, (1998), they found that the relative risk for *S. aureus* bacteraemia was 26.2 (6.1–113) when *S. aureus* was colonising the vascular insertion site, and 3.3 (0.74–15.1), in the case of *S. aureus* nasal carriage. They reasoned that haemodialysis

catheter-related *S. aureus* bacteraemia was highly unlikely if the patient had not been nasally colonized or at the insertion site during the time the catheter was inserted.

In patients on continuous ambulatory peritoneal dialysis (CAPD), *S. aureus* is the main cause of CAPD –related infections, often leading to catheter loss. Nasal carriage is a major risk factor for infections in patients on CAPD, mainly associated with exit site and tunnel infections. Luzar *et al.*, (1990) studied 140 patients just starting (CAPD) in an hospital in England to assess the relation of the nasal carriage of *S. aureus* to subsequent catheter-exit-site infection or peritonitis. In this study, 63 patients were nasally colonized with *S. aureus* and nasal carriage frequently reoccur among the patients having diabetes than among the 110 patients who were not undergoing CAPD. The nasal carriers of *S. aureus* had a significantly increased risk of exit-site infection than the non-carriers. Also risk of peritonitis was higher in nasally colonized patients. Luzar *et al.*, (1990), concluded that in patients starting CAPD, nasal carriage of *S. aureus* is associated with catheter-exit-site infection. Similarly, Wanten *et al.*, (1996) has established that nasal carriage of *S. aureus* increases the risk for subsequent infection in patients on CAPD. In a prospective study by Wanten *et al.*, (1996), 54 patients on CAPD were assessed and 31 (57%) patients were found to be nasal carriers of *S. aureus*, 6 of these 31 patients developed peritonitis as opposed to patients who were non-carriers. In a recent study, Nouwen *et al.*, (2005) investigated the risk of *S. aureus* nasal carriage among 52 patients on CAPD. The 52 patients tested comprised of persistent (20), intermittent (10) and non-carriers (22). In this study they found that only persistent and not intermittent *S. aureus* carriers were significantly at higher risk for all CPD-related infections.

In human immunodeficiency virus patients, nosocomial *S. aureus* bacteraemia, skin and soft tissue infections have been observed, which often reoccur. Even increased infection rates are found in patients with autoimmune diseases compared with HIV patients. Nguyen *et al.*, (1999) found that nasal carriage is a determinant for the development of *S. aureus* infection in this patient population. Other risk factors for infection such as low CD4 cell count, vascular catheter, and neutropenia were identified. The risk for developing an *S. aureus* infection was approximately ten percent for every six months in patients who were nasal carriers of *S. aureus* and had CD4 cell counts of less than 100 cells/L. Similarly, in HIV infected patients, *S. aureus* septicaemia have been identified. Winke *et al.*, (1992) investigated 136 HIV-infected patients for the *S. aureus* nasal carriage and development of subsequent *S. aureus* infection. They observed that 60 of 136 HIV-infected patients harboured *S. aureus* in their nose on culturing compared to 12 of 39 patients with chronic infections and 11 of 47 hospital staff that are

healthy. Another 12 HIV-infected patients were also identified to be *S. aureus* carriers on follow-up cultures. They also observed that AIDs patients had a higher carriage rate compared to HIV-positive patients indicating that *S. aureus* nasally colonized patients were more critically ill. Additionally, 8 patients with *S. aureus* septicaemia were observed, all of whom were nasal carriers; and no *S. aureus* septicaemia was observed in the non-colonized patients.

In liver transplant patients *S. aureus* is the prominent cause of bacterial infection. Nasal carriage of MRSA is associated with a high risk of infection in patients undergoing surgery. Lefranc *et al.*, (2005) carried out a prospective cohort study to identify the risk factors for *S. aureus* infection immediately after liver transplantation. Three hundred and twenty-three patients (323) were assessed. Of the 323 patients 19.5% (63) patients developed staphylococcal infection (36 MRSA) and (27 MSSA) within one month of surgical operation. Lefranc *et al.*, (2005) concluded that, preoperative nasal carriage of MSSA and MRSA is an independent risk factor for *S. aureus* infection in liver transplant patients.

Pujol *et al.*, (1996) looked at the development of bacteraemia in patients in an intensive care unit (ICU). Majority of *S. aureus* bacteraemia is caused by intravascular devices. In this cohort study, Pujol *et al.*, (1996) reported that 38 (7.7%) of 488 patients admitted to the ICU had *S. aureus* bacteraemia. Rates of bacteraemia determined in patients were 24 (38%) of the MRSA carriers, 8 (9.5%) of the MSSA carriers, and 6 (1.7%) of non-carriers. Carriers of *S. aureus* had a relative risk of 12.4 for the development of bacteraemia. The relative risk for *S. aureus* bacteraemia was 3.9 for MRSA carriers. They suggested that among ICU patients, nasal carriers of *S. aureus* are at increased risk for *S. aureus* bacteraemia. In a more recent study, colonization with *S. aureus* seem to pose serious risk for subsequent *S. aureus* infection. *S. aureus* is a significant cause of infection in ICU patients. Also, a prospective cohort study on 5,161 patients admitted in the ICU by Honda *et al.*, (2010) showed that approximately 1433 patients (27.8%) of 5,161 were nasally colonized by *S. aureus* at admission. Six hundred and seventy-four patients (47%) and 759 (53%) patients were colonized with MRSA and MSSA. They established that ICU patients colonized with *S. aureus* were at increased risk of developing a *S. aureus* infection in the care unit. Keene *et al.*, (2005) evaluated *S. aureus* nasal colonization and the risk of subsequent *S. aureus* infection in (ICU) patients. A cohort study of 208 patients admitted in ICU showed that 47 (23%) were nasally colonized with *S. aureus* and 24% of these patients developed *S. aureus* infections versus 2% of non-colonized patients. Keene *et al.*, (2005) believed *S. aureus* infection was significantly elevated in nasally colonized ICU patients. Furthermore, *S. aureus* nasal carriage has been linked with subsequent

staphylococcal infections in ICU patients. In 1994, 752 patients admitted to an ICU for more than 2 days were studied prospectively for *S. aureus* colonization and infection. At the ICU admission 166 (22.1%) patients carried *S. aureus* in their nose, while 586 patients were non-carriers. Of the 166 patients harbouring *S. aureus* in their nose, 163 harbored MSSA and 3 MRSA. During their stay in the ICU 24 of the 586 patients who were non-carriers became nasal carriers (eleven harbored MSSA and thirteen MRSA), and 1 patient initially colonized by MSSA was recolonized by methicillin resistant *S. aureus*. However, after 14 days, patients harbouring *S. aureus* in their nose was at greater risk of developing Staphylococcal infections at ICU admission than for patients found to be initially negative (Corbella *et al.*, 1997).

Also, regarding intravascular device-related bacteraemia, Snyderman *et al.*, (1990) reported on a cohort of 107 interleukin-2 treated patients. In their study they monitored patients undergoing the interleukin-2 +/- LAK cancer immunotherapy and control groups of patients in the surgical intensive care unit, patients receiving parenteral nutrition, and patients with tumors for the subsequent development of nosocomial bacteraemia. They identified *S. aureus* bacteraemia among the patients receiving parenteral nutrition (2.8%), in the surgical intensive care unit (4.1%) or having tumours (1.9%). *S. aureus* seems to be causative agent of the bacteraemia. Snyderman *et al.*, (1990) reasoned that colonization with *S. aureus* increased the risk of *S. aureus* bacteraemia 6.3-fold, they suggested that *S. aureus* colonization of both the nose and skin desquamation increased the risk of *S. aureus* bacteraemia 14.5-fold in patients receiving interleukin-2 treatment.

In MRSA carriers, increased risk of *S. aureus* infection has been suggested. Lye *et al.*, (1993) observed that among patients undergoing CAPD, nasal carriers were at increased risk for MRSA infection compared with non-carriers. In this study, they found an increased rate of exit site infection and peritonitis in MRSA nasal carriers. Moreover, in the MRSA carriers, there was a higher number of catheter losses and CAPD patient dropouts. In addition, MRSA nasal carriage is considered a main risk factor for subsequent endogenous infections. A prospective cohort study of 306 outpatients under maintenance haemodialysis from a dialysis centre in Taiwan conducted between March 2007 to December 2008 by Lai *et al.*, (2011) revealed that 29 MRSA carriers (9.48%) were identified at study start. After a period of 613 days of maintenance, significant survival differences between MRSA carriers and those who do not carry MRSA were observed. Compared with non-carriers, MRSA carriers had a 2.46-fold increased risk of subsequent infections. Recently, in a retrospective cohort study conducted by Datta *et al.*, (2013) on 1,140 patients who are MRSA-positive under between March 2008 and

June 2011 at a tertiary care teaching hospital in USA observed that there was a significant trend in infection risk with increasing nasal burden.

Lastly, chronic nasal carriage has been associated with high relapse of Wegener granulomatosis in hospital out patients. In this study, 57 out patients were observed. Among these patients, 36 were chronic nasal carriers of *S. aureus*, 22 of thirty-six patients who were either persistently or intermittently positive for antineutrophil cytoplasmic antibody (ANCA) had a relapse as opposed to 1 of twenty-one persistently negative patients This subgroup of patients was more prone to relapse of Wegener granulomatosis (Stegeman *et al.*, 1994). Wegener's granulomatosis is a necrotizing granulomatous inflammation of both the upper and lower respiratory tract and glomerulonephritis. Zycinska *et al.*, (2008) examined possible risk factors for relapse including refractory nasal carriage of *S. aureus* in patients with Wegener's granulomatosis. Swab cultures from the nose of 28 patients suffering from Wegener's granulomatosis were taken. In the study, Zycinska *et al.*, (2008) observed that the 28 patients were chronic nasal carriers of *S. aureus* and this was identified as an independent risk factor for relapse in patients with Wegener's granulomatosis.

#### **1.4. *S. aureus* virulence and diseases**

##### **1.4.1 *S. aureus* virulence factors and pathogenesis of infections**

The ability of *S. aureus* to cause infections depends on the numerous virulence factors expressed by the pathogen to aid its pathogenicity in human body (Foster, 2014; Deleo *et al.*, 2011). One of the virulence factors are cell surface proteins and extracellular proteins that promote colonization of the host tissues. Other types of virulence factors such as capsule and protein A helps the bacterium to inhibit phagocytosis and evasion of the immune system resulting in the persistence of bacteria in the host blood. Furthermore, other potential virulence factors such as toxins damage host tissues causing varying clinical symptoms (O'Riordian and Lee, 2004; Curtis, 2005). For most infections caused by *S. aureus*, pathogenesis is caused by many factors. Therefore, it is difficult to determine the role of any factor. Before an infection can be initiated by *S. aureus* it must first gain access into the body. It can enter in several ways; via the nose or mucosal surfaces, open wounds or sores, surgery sites or intravenous drug use (Foster, 2014; Curtis, 2005). Once it gains access, it establishes itself by attaching to the host tissues or cells. This it does by expressing cell surface proteins that promote their attachment to host proteins such as laminin and fibronectin that are part of the extracellular matrix (ECM) of the epithelial and endothelial cells. Fibronectin is found on both epithelial and endothelial

cell surfaces and a vital component of blood clots (Deleo *et al.*, 2011). Furthermore, majority of *S. aureus* strains are also known to express a fibrin or fibrinogen binding protein (fib) responsible for attachment of *S. aureus* to traumatized tissues and blood clots.

After attachment to host tissue, *S. aureus* further expresses many virulence factors that has the capability to subvert host defense mechanisms (Deleo *et al.*, 2011). To do this, *S. aureus* again expresses a capsular polysaccharide of either capsular polysaccharide 5 or capsular polysaccharide 8 that prevent the bacterium from being phagocytosed by the host neutrophils. Protein A is surface protein produced by *S. aureus*, which binds immunoglobulin G molecules by the Fc region. In blood, *S. aureus* bind to IgG molecules in a wrong orientation thus disrupting opsonophagocytic (Foster, 2014; Deleo *et al.*, 2011). *S. aureus* may also secrete chemotaxis inhibitory protein (CHIP) of staphylococci or the extracellular adherence protein (EAP), which interfere with neutrophil extravasation and chemotaxis to the site of infection (Foster, 2004). *S. aureus* produces many enzymes, that enable it to invade and destroy host tissues and spread to other sites. These includes proteases, lipases, and elastases (Foster, 2014).

Also, *S. aureus* is known to express several toxins that are potentially responsible for the development of symptoms during occurrence of an infection (Dinges *et al.*, 2000). Most of these are produced in the stationary phase of growth. For example, leucocidin toxin causes membrane damage to leukocytes; alpha-toxin ( $\alpha$ -toxin) is responsible for septic shock; enterotoxins and toxic shock syndrome toxin (TSST-1) is responsible for toxic shock, some toxins cause erythrocytes damage, causing hemolysis (Dinges *et al.*, 2000; Plata *et al.*, 2009). However, of all these toxins,  $\alpha$ -toxin is the most potent membrane-damaging toxin produced by *S. aureus*. Alpha-toxin is expressed as a monomer that binds to the membrane of susceptible host cells. After binding, the different subunits then oligomerize together forming hexameric rings with a central pore via which most cellular contents leak (Dinges *et al.*, 2000). Usually for successful binding, susceptible host cells have a receptor mainly for  $\alpha$ -toxin, which permits low concentrations of  $\alpha$ -toxin to bind, causing small pores through which monovalent cations can pass. But at high concentrations, non-specific reactions occur between the toxin with membrane lipids, causing larger pores through which small molecules and divalent ions can pass. Receptors such as platelets and monocytes present in susceptible hosts are sensitive to alpha-toxin. Both receptors have affinity sites that allow successful binding of toxin. After binding, many secondary reactions take place causing cytokines and eicosanoids release which inturn triggers the expression of some inflammatory mediators (DuMont *et al.*, 2013; Spaulding *et al.*, 2013). This reaction can cause the commonly known septic shock syndrome that occur

during chronic infections caused by *S. aureus*. Other toxins such as leucocidin and Gamma-toxin ( $\gamma$ -toxin) are two-component protein toxins that damage membranes of susceptible host cells. The two proteins are produced separately but act together to damage membranes. Gamma-toxin locus expresses three main protein components. Components A and B of  $\gamma$ -toxin are hemolytic and weakly leukotoxic. The classical Panton and Valentine (PV) leukocidin is different from leukotoxin which is expressed by the  $\gamma$ -toxin locus. It has potent leukotoxicity and, in contrast to  $\gamma$ -toxin, is nonhemolytic. Panton and valentine leukocidin cause dermonecrosis infection when injected subcutaneously in rabbits. In addition, at a low concentration the toxin releases inflammatory mediators from human neutrophils, leading to degranulation (Dinges *et al.*, 2000; DuMont *et al.*, 2013; Spaulding *et al.*, 2013).

Other toxins expressed by *S. aureus* are exotoxins. Exotoxins are toxins secreted by bacteria that can cause damage to the host by destroying cells or disrupting normal cellular metabolism. Exotoxins are referred to as superantigens or pyrogenic toxin superantigens because they provoke non-specific activation of the human immune system. Superantigens interact with antigen-presenting cells and T cells, by direct binding of the major histocompatibility complex (MHC) class II proteins and T-cell receptors, to induce T cells proliferation resulting in polyclonal T cell activation and massive cytokine release, thereby bypassing the normal antigen processing and presenting mechanism (Miljković-Selimović *et al.*, 2015). Examples of such exotoxins are toxic shock syndrome toxin (TSST-1) and enterotoxins toxins. These two toxins are secreted by *S. aureus* with several biological attributes like pyrogenicity and superantigenicity (Orwin *et al.*, 2002). Enterotoxin has six serotypes namely serotype A, B, C, D, E, and G. Enterotoxins are the common cause diarrhoea and vomiting when ingested in food and are responsible for staphylococcal food poisoning. When enterotoxin is produced systemically, it can cause TSS by stimulating T cells expressing V $\beta$  element in their T-cell receptor, leading to proliferation of T-cell and continuous release of proinflammatory cytokines for example TNF- $\alpha$ , interferon- $\gamma$ , interleukin (IL)-1 $\beta$  and IL-6 (Krakauer and Stiles, 2013). Toxic shock syndrome B and C cause 50% of non-menstrual TSS in women. TSST-1 is also responsible for 80% of TSS, including all women menstrual cases. TSS can occur as a consequence to any staphylococcal infection if an enterotoxin or TSST-1 is systemically expressed and the host does not have appropriate neutralizing antibodies. What it does is that it stimulates the production of increased number of interleukins (interleukin 1 and 2) and tumor necrosis factor (Massignani *et al.*, 2013).

## **1.4.2 Strategy of host colonization and diseases**

The pathogenicity of *S. aureus* is because of the production of a large variety of protein virulence factors including membrane cell wall interface protein, membrane proteins, cell wall-proteins and proteins actively secreted through different pathways into the extracellular milieu. All these virulence factors enable and determine the pathogenicity of *S. aureus* playing vital role in the colonization and invasion of host tissues, facilitate persistence help to evade the immune system of the host and mediate cytotoxicity. As such all these proteins constitute a reservoir of virulence factors (Ajayi, 2018).

*S. aureus* employ many strategies to be able to colonize and infect the host latter. These strategies are mediated by secretion of virulence factors (Gordon and Lowy, 2008). A primary event in *S. aureus* colonization is the adherence to host components mediated by binding of fibronectin, fibrinogen and cytokeratins usually within nasal epithelium. This binding is mediated by more than one adhesin proteins that mediate the initial attachment of bacteria to host tissue, providing a critical step to establish infection. These adhesins can be categorized into two: cell surface proteins of *S. aureus* called microbial surface components recognizing adhesive matrix molecules” (MSCRAMMs) and “secreted expanded repertoire adhesive molecules” (SERAMS) (Gordon and Lowy, 2008).

### **1.4.2.1 Microbial surface component recognising adhesive matrix molecule (MSCRAMMS)**

MSCRAMMs are cell surface proteins encoded on the bacterial chromosome and have single or multiple binding ligands (Foster *et al.*, 2016). In *S. aureus*, numerous MSCRAMMs are anchored to the cell peptidoglycan by a covalent bond through conserved mechanism. This mechanism involves a conserved protein structure with a N-terminal secretory signal peptide needed for the transport or translocation of protein from across the interior of *S. aureus* cell to its outer membrane (Sec-dependent secretion), and a positively charge tail –C-domain, which ensures that the protein is not produced. Close to the C-terminal is a transmembrane spanning terminal, which is itself preceded by a LPXTG motif that is essential for anchoring the cell proteins into the cell wall peptidoglycan. This process of anchoring involves a transpeptidation mechanism, which is brought about by sortase enzyme. Sortase enzyme is encoded by the gene *srtA* and it is a membrane enzyme that cleaves the MSCRAMMs between the threonine and the glycine of its LPXTG motif, and catalyzes the formation of an amide bond between carboxyl-group of threonine and the amino-group of peptidoglycans. Examples of

MSCRAMMs include protein A, clumping factors A and B (ClfA and ClfB) (Siboo *et al.*, 2001; O'Brien *et al.*, 2002; Hair *et al.*, 2010), fibronectin binding proteins A and B (FnbA and FnbB) (Fowler *et al.*, 2000; Wann, Gurusiddappa & Höök, 2000; Massey *et al.*, 2001), and collagen-binding protein (Cna) (Hienz *et al.*, 1996; Deivanayagam *et al.*, 2000; Que and Glauser 2005), fibronogen binding proteins (Fib) (Cho *et al.*, 2001; Ajayi, 2018) and elastin binding protein (Ebp) (Downer *et al.*, 2002) (Figure 4).

MSCRAMMs play important role in initiation of acute and severe human infections (Archer *et al.*, 2011). *S. aureus* strains possess different groups of MSCRAMMs and so may be inclined to causing different kinds of human infections (Gordon and Lowy, 2008). Once *S. aureus* can adhere to human tissues or medical prosthetic materials, it is able to grow and persist in various ways. It can form slime called biofilms on host tissues and surfaces of prosthetic materials enabling it to persevere by evading host defenses and antimicrobial agents (Gordon and Lowy, 2008). The ability of *S. aureus* to form biofilm and reside in it, is probably one major reason why medical device infections and other human diseases, are difficult to treat. For example, the infected prosthetic device can be so difficult to eradicate without removal of the device from the host body (Gordon and Lowy, 2008).

Acute or mild infections caused by the bacterium include skin and soft tissue infections (for example boils, impetigo, cellulitis and skin abscess) (Archer *et al.*, 2011). However, *S. aureus* infections becomes worse because of its ability to form biofilms which are slimy protective coverings. Chronic infections associated with biofilm includes (a) osteomyelitis (bone infection) (b) indwelling medical device infection (caused by the formation of *S. aureus* biofilm on orthopaedic implants including wires, external fixators, pins, mini-large fragment implants and nails). Other indwelling medical devices that are liable to staphylococcal biofilm infection include intravenous catheters, mechanical heart valves, invasive blood pressure units, stitch materials, cosmetic surgical implants, penile implants, infusion pumps, pacemakers and central nervous system shunts, (c) Chronic wound infections such as pressure sores, venous stasis ulcers and diabetic foot ulcers), (d) endocarditis (infection of the heart valve), (e) ocular infections which include conjunctivitis, keratitis and endophthalmitis, (f) periodontitis (inflammation and infection of the ligaments and bones that support the teeth and peri-implantitis), (g) chronic rhinosinusitis (inflammation of the nasal passages and sinus cavities) (Archer *et al.*, 2011) and (h) bacteraemia (blood stream infection) (Agarwal *et al.*, 2010).

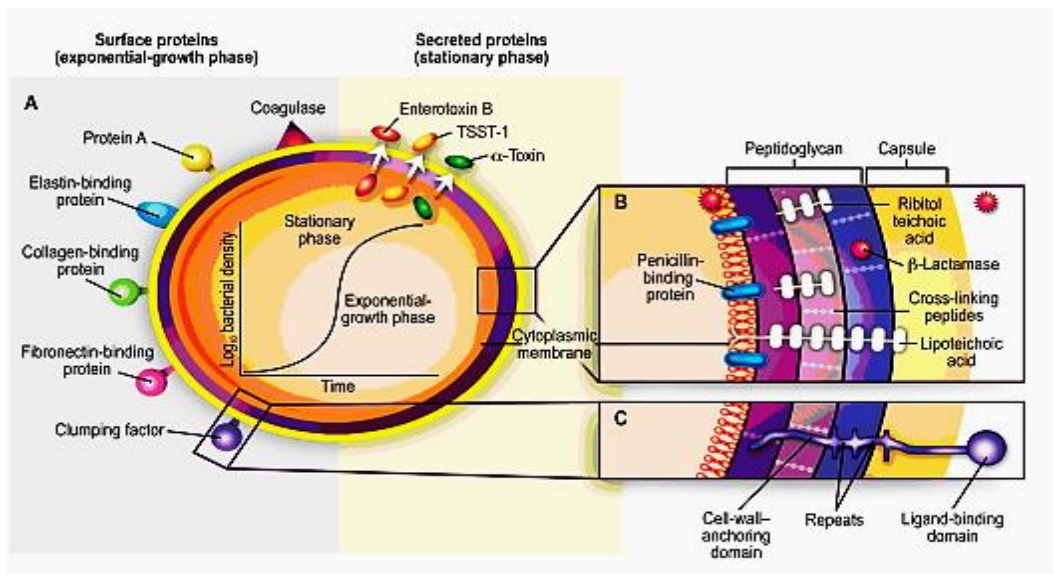


**Figure 4. Virulence factors of *S. aureus* with both cell wall associated proteins and secreted proteins playing roles as pathogenic determinants (Gordon and Lowy, 2008).**

From the image represented above, A, shows surface and secreted proteins, B and C, are cross-sections of the cell wall envelope.

### **Fibronectin binding proteins (Fnbps)**

Fibronectin binding protein (FnbA and FnbB) are *S. aureus* MSCRAMMs, encoded by fibronectin A and B (*fnbA* and *fnbB*) genes (Foster *et al.*, 2014; Foster, 2016). These two proteins are closely related but individually transcribed. Protein fibronectins of *S. aureus* are multifunctional adhesins which recognize fibrinogen, fibronectin as well as elastin. Both proteins have considerable organization and similar sequence and are comprised of a few well-defined domains. Binding proteins of FnbA and FnbB contain a secretory signal sequence at the N-terminal of the A domain and a C-terminal domain LPXTG motif necessary for sortase mediated anchoring of the fibronectins to the peptidoglycan. The N-terminal of the A domains of FnBPs are found on the cell surface and facilitates elastin and fibrinogen binding (Foster *et al.*, 2014; Foster, 2016).

The binding of FnbA and FnbB to host fibronectin enhances the adherence and invasion of *S. aureus* into the osteoblasts, epithelial, endothelial, fibroblastic cells which are not phagocytic. The invasion mediated by fibronectins takes place via the formation of a fibronectin bridge between the bacterium and the alpha 5 beta 1 integrin (Henderson *et al.*, 2011). This in-turn enhances the dissemination of *S. aureus* from the host blood stream to vital internal organs and

escape of immune responses and antimicrobials (Foster *et al.*, 2014). This was demonstrated in the study of the role of FnbA in endocarditis where binding to fibronectin and fibrinogen is considered vital in establishment of Staphylococcal endocarditis. Binding to fibronectin was required for the disease to spread and while binding of fibrinogen was essential for initial attachment on damaged valves (Burke *et al.*, 2010).

### **Clumping factors (Clfs)**

ClfA is *S. aureus* binding protein with two main domains designated as N2 and N3 that binds to the C-domain of the fg (fibrinogen) gamma chain resulting in platelet aggregation or bacterial clumping in human blood (Talay, 2004). The contribution of ClfA to *S. aureus* pathogenesis has been demonstrated in different animal models of infections. In an arthritis model, an *S. aureus* mutant lacking functional clfA couldn't cause arthritis when compared to the Newman wild type strain. In this study, mice were immunized with recombinantly produced ClfA domain which conferred some protection from subsequent infections by the induction of ClfA-specific antibodies (Lacey, *et al.*, 2016). ClfB also bind fibrinogen (Fg), a glycopeptide present in human blood responsible for blood clotting. Fg is the major human blood protein deposited on implanted medical devices (Deivanayagam *et al.*, 2002). ClfB is a bifunctional adhesin. In addition to Fg, clfB can bind to type I cytokeratin I0 present on the squamous of human nasal cells. Cytokeratin I0 is the main component of squamous cells and is a major factor determining the ability of the bacterium to adhere to squamous epithelial cells and to colonize the anterior nares of humans (Ganesh *et al.*, 2011).

### **Collagen adhesin protein (Cna)**

Cna is the collagen binding MSCRAMM of *S. aureus* (Zong *et al.*, 2005). Cna shares a common structural organization with other surface proteins, that includes (a) an N-terminal signal sequence, (b) a repetitive region (c) a non-repetitive region and (d) C-terminus anchoring domain that includes a hydrophobic membrane-spanning domain, an LPXTG anchoring motif, and an amino acid carboxy-terminal tail (Nallapareddy *et al.*, 2003). The repetitive region exhibits strain-dependent variability with respect to length while the non-repetitive region is often responsible for binding of the ECM protein. Though the *S. aureus* cna shares these structural attributes, it is unique by comparison to other surface proteins. For example, the gene encoding Cna is not available in all *S. aureus* isolates. In addition, although it has the LPXTG anchoring motif, Cna seems to be anchored to the *S. aureus* cell through its hydrophobic

membrane-spanning domain rather than a covalent linkage to the cell wall peptidoglycan (Snodgrass *et al.*, 1999).

### **Staphylococcal protein A (spa)**

Protein A is a crucial MSCRAMM of *S. aureus*. Protein A is coded by the spa gene and it has multifunctional roles (Kerrigan *et al.*, 2002). Firstly, spa can bind to the Fc portion of immunoglobulin G (IgG) antibody, resulting in the pathogen becoming coated with IgG in an inappropriate conformation not recognized by the Fc receptor on neutrophils resulting in evasion of phagocytosis. Secondly, spa can bind to the fab region of IgM (immunoglobulin M) antibody, on the surface of B lymphocyte cell receptors, leading to increased number of B cells (activation) and cell death (apoptosis) (Goodyear and Silverman, 2003). Thirdly, spa binds to TNFR1 (tumor-necrosis factor) on the air way epithelium and stimulate a 22-inflammatory response dominated by polymorphonuclear leukocytes in airway epithelial cells. This sort of interaction plays a key role in the pathogenesis of *S. aureus* pneumonia (Bien *et al.*, 2011).

### **Elastin binding protein (EbpS)**

Elastin binding protein Elastin, together with microfibrillar constituents, make up the elastic fiber extracellular matrix (Kielty *et al.*, 2002). Microfibrillars are fiber-like strands, consisting of glycoproteins and cellulose. The role of elastin is to maintain the structural integrity and function of tissues in which extensibility or deformability is necessary. Thus, elastic fibers and elastin are available in human tissues that require elasticity for example major blood vessels, skin and lungs (Downer *et al.*, 2002).

#### **1.4.2.2 Secreted expanded repertoire adhesive molecules (SERAMS)**

SERAMs are the second group of adhesins. SERAMs are secreted but partially bound to cell surface. SERAMs are not related in structure but share a common function. SERAMs include the extracellular fibrinogen binding protein (Efb), extracellular matrix protein (Emp) and extracellular adhesive protein (Eap) (Chavakis *et al.*, 2007). Eap appears to be the well-studied *S. aureus* adhesin. Eap enhances adherence of *S. aureus* to human components. Harraghy *et al.*, (2003) purified Eap from the supernatant of *S. aureus* and found that it was capable of binding to the surface of *S. aureus* and to at least seven human blood proteins for example fg, fn, vitronectin and prothrombin.

### **1.4.2.3 *S. aureus* intercellular adhesion genes**

The *icaA*, *icaB*, *icaC* and *icaD* operons have also been identified in *S. aureus*. They are the *icaADBC* operons which encodes the structural genes necessary for synthesis of PIA. The *ica* operon is composed of four open reading frames, (*icaA*, *icaD*, *icaB* and *icaC*) and a regulatory gene known as *icaR*. *IcaA* is responsible for N-acetylglucosaminyl transferase activity during PIA synthesis; *IcaD* is required for optimal transferase activity. *IcaB*, a deacetylase, is responsible for the deacetylation of the poly-N-acetylglucosamine molecule. *IcaC* is a transmembrane protein that plays a putative role in externalisation, elongation and translocation of the growing polysaccharide to the cell surface and is responsible for the production of the length of PIA molecule (McCann *et al.*, 2008).

## **1.5 Biofilms**

### **1.5.1 *S. aureus* biofilm**

Naturally, bacteria have two growth life styles termed planktonic or sessile. Planktonic growth means the growth of bacterial cells in liquid while the sessile growth refers to bacterial cells that are attached to a surface (Davey and O'Toole, 2000). Interestingly in biofilm formation, planktonic cells are the ones that form biofilms (Mancl *et al.*, 2013). In simple terms a biofilm is a collection of bacterial cells that is encased in an exopolymeric substance produced by them (Carr *et al.*, 2009).

The structure of *S. aureus* biofilm is complex and heterogeneous (Flemming and Wingender, 2010). Visualization of biofilm structures by some researchers under the microscope has described the structure of biofilm as mushroom-shaped and often formed by microcolonies (Flemming and Wingender, 2010). Biofilm structure contains interstitial voids through which essential nutrients flow into different microbial communities of the biofilm (Stewart and Franklin, 2008).

*S. aureus* has an extracellular matrix known as EPS that acts as slime or glue (Flemming and Wingender, 2010). The EPS encloses all microbial cells and allows the assemblage of *S. aureus* cells into biofilms (Vertes *et al.*, 2012). Major constituents of the extracellular matrix of most biofilm forming organisms that have frequently been reported include protein, DNA and polysaccharide intercellular adhesin (PIA). Although the constituents of the extracellular matrix of *S. aureus* are still not clear, varying reports have been given about the main constituent of the extracellular matrix of *S. aureus* (Flemming and Wingender, 2010). PIA is

comprised of 80-85% beta-1-6 linked –N-acetyl glucosamine and a small amount of residues that consists of 15-20% of ester linked succinate and phosphate (Rohde *et al.*, 2010). The *icaADBC* operon identified in majority of *S. aureus* species is responsible for PIA production (Beenken *et al.*, 2004). *S. aureus* biofilm matrix comprises extracellular DNA (eDNA), human factors and proteins that are secreted and obtained from lysis and PIA (Foulston *et al.*, 2014). eDNA is a product of autolysis of subpopulations (Bayles *et al.*, 2007).

*S. aureus* may form biofilms on biotic and abiotic or inert surfaces (Aparna and Yadav, 2008). Factors that have great influence on biofilm formation mechanism of *S. aureus* are: the bacterial species (strain characteristics), the substratum (physical and chemical properties) and environmental factors (Renner and Weibel, 2011). Other important vital factors affecting the adherence of microbes to different surfaces include: bacteria, suitable substrate and cellular recognition of attachment sites on a surface, composition of cell outer layer, exposure of planktonic cells to sub-inhibitory concentrations of antibiotics, nutrient availability, structure of cell surface, quorum sensing and regulatory network within the entire population (Paraje, 2011).

### **1.5.2 The phases of *S. aureus* biofilm formation**

A few studies in human pathogenic organisms forming biofilm have provided concise details of biofilm formation in *S. aureus*. The formation of biofilm in *S. aureus* is in three important phases attachment phase, fully matured phase and dispersal phase (Yarwood *et al.*, 2004).

Biofilms form by initial attachment to a surface, which can occur on tissues or after covering of an abiotic surface by host matrix proteins in the human body. The attachment of *S. aureus* to human extracellular matrix proteins is the first step of biofilm formation. *S. aureus* expresses numerous MSCRAMMs that can adhere to human matrix proteins (such as fibrinogen or fibronectin) deposited on implants (Otto, 2008). MSCRAMMs have three main regions or domains, a ligand binding region (that is exposed), a cell wall spanning domain which contain a repeat sequence and a sorting signal region containing a LPXTG motif (Foster *et al.*, 2014). The anchorage of MSCRAMMs to *S. aureus* cell wall is covalently initiated by the enzymes known as sortases that cleaves the C-terminal of LPXTG of the MSCRAMMs to cell wall. An important member of this family is Sortase A that has the capacity to recognize the C-terminal of the LPXTG motif of the MSCRAMMs (Tsompanidou *et al.*, 2012).

The attachment of *S. aureus* to abiotic surfaces (biomaterials) largely depends on the nature of the polymer material and on the cell surface characteristics of the bacteria. The initial interaction is believed to occur via nonspecific physicochemical forces such as charge, van der Waals forces, and hydrophobic interactions (Gross *et al.*, 2001). *S. aureus* colonization of abiotic surfaces depends on the charge of its teichoic acids. The role of teichoic acids in the first step of biofilm formation, however, has remained elusive. *S. aureus* teichoic acids are highly charged cell wall anionic polymers that are uniformly distributed over the entire *S. aureus* peptidoglycan wall, contributing a large amount of negative charge to the bacterial surface. There are two types of teichoic acids, wall teichoic acid (WTA) and lipoteichoic acid (LTA). *S. aureus* teichoic acids are composed of alternating phosphate and ribitol (wall teichoic acids) or glycerol (lipoteichoic acids) groups, which are replaced with d-alanine and *N*-acetylglucosamine. Research studies have shown that an *S. aureus dltA* mutant bearing a stronger negative charge due to the lack of D-alanine esters in its teichoic acid can no longer attach to polystyrene or glass. The much stronger net negative charge of the *dltA* mutant, however, probably leads to a pronounced increase in the repulsive forces, thereby disabling any adherence of the bacteria to polystyrene or glass (Gross *et al.*, 2001).

Maturation phase is the second phase of biofilm formation in *S. aureus* (Molin and Tolker-Nielsen, 2003). This phase is distinguished by intercellular aggregation resulting from gradual accumulation and structuring forces. Once *S. aureus* attaches to a surface, it proliferates facilitating the synthesis of (PIA) responsible for cell-cell adhesion (Heilmann, 2011). At the end of maturation phase, biofilm has a 3 dimensional structure (Garrett *et al.*, 2008).

The third phase is the detachment (or dispersal) phase. Biofilm detachment is crucial for the dissemination of *S. aureus* to other colonization sites. Dispersal may occur by the detachment of pair or cluster cells. Several factors may contribute to detachment (a) cessation of the production of biofilm building material, such as exopolysaccharide, and (b) detachment factors, such as secreted enzymes (proteases nuclease and dispersin B) and surfactants phenol-soluble modulins (PSMs) that degrade the matrix (Otto, 2008). The enzymatic dispersal mechanism that has been described in *S. aureus* is the protease dispersal mechanism (Lister and Horswill, 2014; Mukherji *et al.*, 2015).

### **1.5.3 Enzymatic dispersal mechanism in *S. aureus***

#### **(i) Extracellular proteases of *S. aureus***

There are over 10 proteases secreted by most *S. aureus* strains. The proteases encoded in the *S. aureus* genome are organized into four distinct operons mediating synthesis of a metalloprotease (Aur), seven serine proteases (SspA and SplA-F) (organized in two distinct operons), and two cysteine proteases (Staphopains ScpA and SspB). The six Spl enzymes coded by splA-F do not require proteolytic activation. The Aur, ScpA, SspA, and SspB proteases are produced as zymogens or pro-enzymes). The Aur and ScpA zymogens undergo auto-proteolytic cleavage outside the cell and SspA and SspB are activated in a subsequent proteolytic cascade which is initiated with cleavage of SspA by Aur which then activates SspB. The secreted extracellular proteases have a broad substrate specificity hence can degrade both surface proteins and secreted proteins (Mootz *et al.*, 2013).

#### **1.5.3.1 Serine proteases**

Serine proteases are enzymes that contain a histidine, serine, and/or an aspartate residue at their active site. The seven serine proteases secreted by *S. aureus* are all members of the trypsin family of enzymes. The SspA and SspB protease are encoded by a single polycistronic operon wherein SspA is a serine protease and SspB is a cysteine protease. The six Spl proteases (Spl $ABCDEF$ ) are encoded by a separate polycistronic operon and are active upon secretion. SspA, also known as V8 protease, is a glutamyl endopeptidase that has the distinction of being the first purified and characterized proteolytic enzyme of *S. aureus* (Mukherji *et al.*, 2015).

#### **1.5.3.2 Cysteine proteases**

Cysteine proteases are characterized by two nucleophilic cysteine residues joined together by a thiol bond. *S. aureus* secretes two cysteine proteases, ScpA and SspB, which have been termed Staphopain A and Staphopain B (Mukherji *et al.*, 2015).

#### **1.5.3.3 Metalloprotease**

Metalloprotease (Aur) is the only metalloprotease secreted by *S. aureus*. Aur is required to activate SspA by proteolytic cleavage and this initiates a proteolytic cascade of activation (Mukherji *et al.*, 2015).

## **(ii) Protease dispersal mechanism**

The ability of *S. aureus* proteases to disrupt proteinaceous matrix materials has been demonstrated in previous studies. It has been shown that V8 serine protease can degrade FnBPs and aureolysin can degrade ClfB to mediate biofilm disruption. While the staphopains can disrupt the biofilm matrix, no target proteins have yet been found. The underlying mechanism through which *S. aureus* proteases disassemble a fully matured biofilm is complicated not only by the number of proteases involved but also by the myriad of protein targets. However, recent studies have shown that the production of proteases is positively regulated through the *S. aureus* quorum sensing system, *agr*. The *agr* system is activated upon detection of an autoinducing peptide (AIP) that is encoded and produced by the *agr* operon. The *agr* system induces the expression of both proteases and PSMs, which act as surfactants to disperse biofilms (Lister and Horswill, 2014). Thus, activation of the *agr* system can result in a shift from a biofilm state to a planktonic state of growth. This has been demonstrated through the addition of AIP to existing biofilms, which results in complete dispersal (Boles and Horswill, 2008), and through the use of fluorescent reporters, which demonstrated that cells detach from the biofilm after *agr* activation (Yarwood *et al.*, 2004).

## **1.6 Biofilm formation and quorum sensing in *S. aureus***

Qs often referred to as intercellular signaling play vital role in *S. aureus* virulence. In the past bacteria have been regarded as entities whose main role is to source for nutrient and proliferate (Fraune and Bosch, 2010). However, the recent findings of cell-to-cell communication often called quorum sensing has revealed that bacteria are capable of coordinated activity (Fuqua *et al.*, 2001).

### **1.6.1 The accessory gene regulator quorum sensing in *S. aureus***

The *agr* quorum-sensing system plays central role in the pathogenesis of *S. aureus* (Yarwood and Schlievert, 2003). *Agr* is a global regulator of the staphylococcal virulon also called accessory genes. These accessory genes encode cell wall proteins and secreted proteins of *S. aureus*. *Agr* controls the expression of majority of the extracellular protein genes present in *S. aureus*. The most important of these genes and their products are (a) superantigens (*sea*, *seb*, *sec*, *sed*, *eta*, *etb* and *tst* encoding enterotoxin A, enterotoxin B, enterotoxin C, enterotoxin D, exfoliatin A, exfoliatin B and toxic shock toxin-1) (b) cytotoxins (*hla*, *hlb*, *hld*, *hlg* and *lukS/F* encoding  $\alpha$ -hemolysin,  $\beta$ -hemolysin,  $\delta$ -hemolysin  $\gamma$ -Hemolysin and P-V leucocidin), (c)

enzymes (*SplA–F*, *ssp*, *aur*, *sspB*, *scp*, *geh*, *lip*, *fme*, *plc*, *nuc*, *hys*, *coa* and *sak* encoding serine protease-like, V8 protease, metalloprotease (aureolysin), cysteine protease, staphopain (protease II), glycerol ester (hydrolase), lipase (butyryl esterase), FAME (Fatty acid esterification), PI-phospholipase C, nuclease, hyaluronidase, coagulase and staphylokinase), (d) surface proteins (*spa*, *cna*, *fnbA*, *fnbB*, *clfA*, *clfB* encoding protein A, collagen binding protein, *fnbA* and *fnbB*, clumping factor A and clumping factor B) (e) capsular polysaccharides (*cap5* and *cap8* encoding polysaccharide capsular type 5 and polysaccharide capsular type 8) (Novick *et al.*, 2003).

*Agr* is a central transcriptional regulator that controls the expression of virulence-associated protein genes in *S. aureus* (Traber *et al.*, 2008). *Agr* suppresses the post-exponential-phase expression of cell surface binding proteins (responsible for the primary stages of colonization) and enhances the expression of secreted proteins (involved in the long-term survival of the organism at the site of infection). *Agr* has been linked to virulence in animal model associated infections and have been found to play a major role in human infection such as osteomyelitis, endocarditis and septic arthritis. Although the exact role of the *agr* locus differ with the type of infection model used (Yarwood *et al.*, 2004).

The production of virulence factors by *S. aureus* is controlled in response to cell density, availability of energy, superantigens and signals from the environment so that these factors are only secreted when needed. *In vitro*, the production of different extracellular proteins follows a specific order that is temporal in which surface proteins are produced before proteases or haemolysins and other degrading enzymes. Transcript profiling has shown that genes encoding adhesins decrease early in growth, whereas genes encoding proteins secreted by the bacteria increase during post exponential growth (Novick *et al.*, 2003). This expression pattern appears to correlate with the population cell density sensing *agr* which is generally activated in mid exponential phase thus increasing several secreted proteins and decreasing a number of surface proteins (Novick *et al.*, 2003). However, when energy or metabolites are not sufficient like in respiratory chain or citric acid cycle mutant's majority of the exoproteins are not synthesized allowing the bacteria to carry on its housekeeping roles. Also, some environmental signals affect the production of extracellular proteins, in some cases relating to the need to conserve resources under harmful conditions. Subinhibitory concentrations of ethanol and antibiotics that hinder the functions of ribosome have a general inhibitory effect on the synthesis of accessory gene proteins. The genetic variability of SAg gene is another response factor

controlling the production of virulence since these genes are known to cause toxinoses, and an organism expressing a toxin does not need other exoproteins (Novick *et al.*, 2003).

### 1.6.2 Regulatory factors identified in *S. aureus*

Apart from *agr*, other additional regulatory factors comprising several loci such as *sarA*, *rot*, *arlRS*, *svrA*, *sigB* and *saeRS* has been reported in *S. aureus* (Steinhuber *et al.*, 2003). These regulatory systems are two-component signal transduction systems that co-ordinately control the expression of *S. aureus* virulence factors that enable the organism to adapt to varied environments *in vitro* and *in vivo* (Liang *et al.*, 2005; Steinhuber *et al.*, 2003). These regulators play important role in the control of the expression of virulence factors such as hemolysins, protein A (*Spa*), fibronectin-binding proteins (*FnbpA* and *FnbpB* coded by *fnbA* and *fnbB*), capsular polysaccharide (CP, coded by the *cap* operon (Steinhuber *et al.*, 2003). These additional regulators allow the *S. aureus* to respond to environmental signals in addition to bacterial cell density, and sometimes counter *agr* activity (Yarwood and Schlievert, 2003). For example, the *S. aureus* accessory regulatory (*SarA*) protein influences expression of extracellular proteins and adhesins. This locus contains transcripts that are overlapping, *sarA*, *sarC*, and *sarB*. *SarA* binds to conserved regions termed *Sar* boxes within promoter regions of genes encoding cell surface proteins (*spa*, encoding protein A), genes encoding exoproteins (*hla*, encoding alpha-hemolysin) and *agr*. *SarA* binding to *agr* promoter elements augments both RNAII and RNAIII transcription and therefore contributes to virulence factor regulation indirectly. In several studies, *SarA* has been shown to control the expression of virulence genes *hla* and *spa* sometimes acting independently of *agr* showing that *SarA* regulates certain virulence factors on its own in an *agr*-independent manner (Dunman *et al.*, 2001). *ArlRS* comprises a two-component system that appears to counter *agr* autoinduction by repressing production of hemolysins and exoenzymes. Expression of *arlRS* was itself reduced in an *agr* mutant. An *arlS* mutant was enhanced for biofilm formation, despite the increased expression of *agr* and the presumed downregulation of surface-associated adhesion factors. *ArlRS* also appears to regulate autolytic activity. *SrrAB*, inhibit RNAIII expression and may itself be repressed by *agr*. The repressor of toxins (*Rot*) and the sigma factor B (*sigB*) affect the expression of many virulence associated genes. *Rot* counters *agr* activity by upregulating some of the genes that are downregulated by RNAIII, making it an antagonist of *agr* regulation and a mutation in *rot* was shown to partially restore the wild-type phenotype of an *agr* mutant. Sigma factor B, which responds to environmental stress also appears to at times counter *agr*

activity in that it increases the expression of some exoproteins early in growth (Yarwood and Schlievert, 2003).

### 1.6.3 The *agr* system in *S. aureus*

The *agr* operates a two-component signalling system. It is induced by a peptide, encoded within the locus that is the ligand for the histidine kinase component of the signalling module. Thus, *agr* is a sensor of population density or a quorum sensor (Wright *et al.*, 2005).

The *agr* system in *S. aureus* consist of an approx.3 kb locus containing divergent operons called RNAII and RNAIII transcribed from P2 and P3 which are non-overlapping promoters, (Manna and Cheung, 2001) (Figure 5). The P2 operon encodes proteins, *agrB*, *agrD*, *agrC* and *agrA* that generate the *agr*-sensing mechanism and encodes the RNAII transcript. *AgrB* is a transmembrane protein involved in (a) processing of the *agrD* product into an octapeptide; (b) processing and synthesis of the autoinducing peptide (AIP) that is the activating ligand for the signal receptor, *AgrC* whose role is to activate transcription of RNAIII (Geisinger *et al.*, 2006), (c) *AgrA* and *AgrC* form a two-component regulatory system in which the transmembrane component, *AgrC* (histidine kinase) binds the extracellular AIP activating autophosphorylation (dephosphorylation), followed by phosphorylation or dephosphorylation of the *AgrA* a response regulator which jointly with *SarA* increases the transcription of P2 and P3 (in the late-log phase of growth, when the concentration of the signal in the medium is high) leading to the secretion of RNAIII, which regulates transcription of the target genes through a few intercellular regulatory mediators including *saeRS* (Yarwood and Schlievert, 2003; Wright *et al.*, 2005).

Increased transcription of the P3 operon results in increased production of intracellular RNAIII. RNAIII encodes the toxin  $\delta$ -hemolysin (via *hld*) but, particularly, increases the transcription (and in certain instances, translation) of some secreted virulence factors, which include TSS toxin-1 and hemolysins. However, some toxins, such as enterotoxins A and K, produced in low levels and during exponential phase, are regulated by RNAIII. Other secreted toxins, for example enterotoxins B, C, and D, are only partly increased by RNAIII and can be produced in high concentrations independently of *agr* (Figure 5). RNAIII regulates the synthesis of rot a major pleiotropic transcription factor by blocking its translation. This interference of RNAIII with Rot translation is direct, involving RNAIII acting as a *trans* antisense pairing with complementary sequences in the 5' region of *rot*, and causing cleavage of the *rot* transcript (Geisinger *et al.*, 2006).

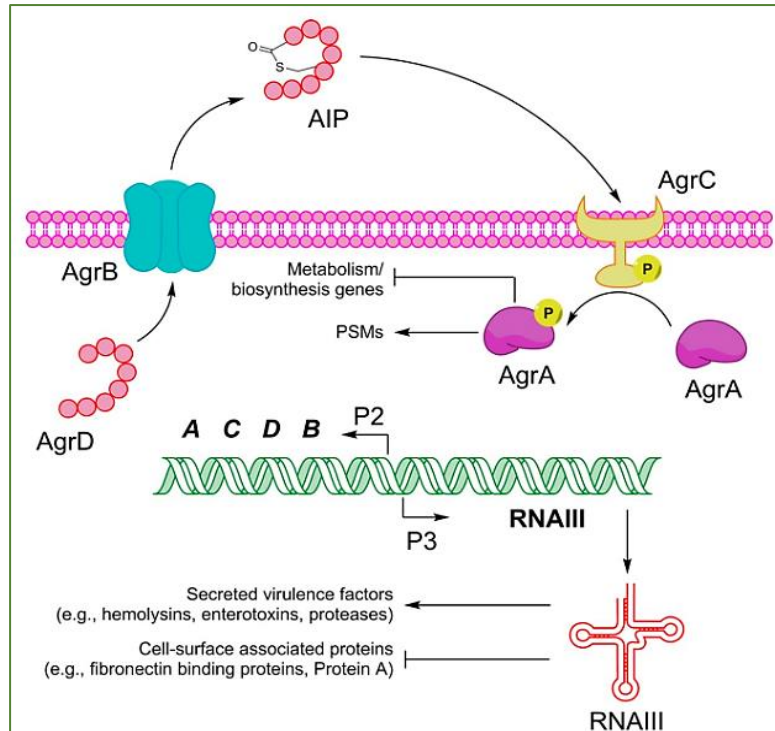


Figure 5. Schematic diagram of *S. aureus* accessory gene regulatory system (*agr*) (Salam and Quave, 2018).

## 1.7 Antibiotic resistance and resistance mechanisms in *S. aureus*

### 1.7.1 Antibiotics commonly used in the treatment of *S. aureus* infections and their mode of action

An antibiotic is a type of antimicrobial substance active against bacteria. Antibiotics are medications widely used in the treatment and prevention of bacterial infections (Liu and Breukink, 2016). The activity of antibiotics is to either kill or inhibit the growth of bacteria. There are ten main classes of antibiotics; they include penicillin, tetracyclines, cephalosporins, quinolones, lincomycin, macrolides, sulfonamides, glycopeptides, aminoglycosides and carbapenems. The antibiotics perform their functions in different ways exhibiting different mechanism of action. The most important antibiotic mechanisms include inhibition of cell wall synthesis, inhibition of protein synthesis and inhibition of DNA synthesis (del Giudice, Hubiche and Étienne 2012; Faron, Ledebor & Buchan, 2016).

To an extent, antibiotic activity and resistance appears to be influenced by differences in the bacterial structure. All bacterial cell walls contain a peptidoglycan layer also called murein and location of which varies between Gram-positive and Gram-negative bacteria (Liu and Breukink, 2016). Peptidoglycan layer acts as the bacterial cell wall's backbone, offering strength to the cell wall. In addition, the peptidoglycan layer helps maintain the rigidity of the

bacterial cell wall to prevent the cell from rupturing. Peptidoglycan layer is made up of amino acids that forms a mesh-like layer outside the plasma membrane of bacteria forming the cell wall. It is the sugar component of the peptidoglycan that contains alternating units of N-acetylmuramic acid and N-acetylglucosamine with the former having short peptide stems attached to it. Bacterial transpeptidases (detected as penicillin-binding proteins PBPs) are essential enzymes that catalyse this crosslinking step. Peptidoglycan production involves initial synthesis of precursors in the cytoplasm, transport of lipid-bound precursors across the cytoplasmic membrane, insertion of the glycan units into the cell wall, and lastly transpeptidation linking and maturation (Liu and Breukink, 2016).

#### **1.7.1.1 Inhibition of peptidoglycan synthesis**

Some antibiotics inhibit the synthesis of bacterial cell wall. These antibiotics include  $\beta$ -lactam compounds such as penicillins (e.g. ampicillin, penicillin G and methicillin), carbapenems and cephalosporins as well as  $\beta$ -lactamase inhibitors and monolactams (Kohanski, Dwyer & Collins, 2010). They are called beta-lactams because of the unusual 4-member ring that is common to all their members. Structurally, bacteria resemble primitive plants in that the cellular contents are surrounded by an inner peptidoglycan cell wall in addition to an inner plasma membrane. Specific antibacterial such as drugs in the  $\beta$ -lactams interfere with the synthesis of the peptidoglycan cell wall, weakening the peptidoglycan scaffold within the bacterial wall so that the structural integrity eventually fails (Kohanski *et al.*, 2010; Liu and Breukink, 2016). Penicillin irreversibly blocks bacterial cell wall synthesis by inhibiting the formation of peptidoglycan cross-links. Penicillin covalently binds to the enzyme transpeptidase that links the peptidoglycan molecules in bacteria, it inhibits the molecule so that it cannot react any further and cell wall cannot be further synthesized. The cell wall of the bacterium is weakened even further because the build-up of peptidoglycan precursors triggers bacterial cell wall hydrolysis and autolysins and destroys pre-existing peptidoglycan. Penicillin makes a great inhibitor because of its four membered beta lactam rings, which makes it especially reactive (Liu and Breukink, 2016). Penicillin acts as a suicide inhibitor by binding with the transpeptidase enzyme it inactivates itself.

#### **1.7.1.2 Creation of an alternate pathway**

A similar class of antibiotics that prevent a different step in cell wall synthesis are the vancomycin, teicoplanin and glycopeptides (Gardete and Tomasz, 2014). Vancomycin, a glycopeptide antibiotic with a significantly larger structure, also prevents cell wall construction

by interfering with transglycosylases. Vancomycin inhibits bacterial cell wall synthesis, which stops the bacteria growing and dividing properly. The cell walls are made of strings of sugars, crosslinked by short peptide chains. By binding to D -alanyl- D -alanine groups on the end of the peptide chains, it stops the crosslinks forming. This prevents the bacteria from building its strong peptidoglycan network (Gardete and Tomasz, 2014).

### **1.7.1.3 Inhibitors of protein synthesis**

Other antibiotic agents that display antibacterial effect by inhibiting synthesis of protein are the tetracyclines, macrolides, aminoglycosides and chloramphenicol which interfere with ribosome function (Trzcinski *et al.*, 2000). Protein synthesis is a complex, multi-step process involving many enzymes as well as conformational alignment. However, the majority of antibiotics that block bacterial protein synthesis interfere with the processes at the 30S subunit or 50S subunit of the 70S bacterial ribosome. The aminoacyl-tRNA synthetases that activate each amino acid required for peptide synthesis are not antibiotic targets. Instead, the primary steps in the process that are attacked are (1) the formation of the 30S initiation complex (made up of mRNA, the 30S ribosomal subunit, and formyl-methionyl-transfer RNA), (2) the formation of the 70S ribosome by the 30S initiation complex and the 50S ribosome, and (3) the elongation process of assembling amino acids into a polypeptide (Trzcinski *et al.*, 2000; del Giudice, Hubiche & Étienne 2012; Piątkowska *et al.*, 2012).

Tetracyclines, including doxycycline, prevent the binding of aminoacyl-tRNA by blocking the A (aminoacyl) site of the 30S ribosome (Trzcinski *et al.*, 2000). They are capable of inhibiting protein synthesis in both 70S and 80S (eukaryotic) ribosomes, but they preferentially bind to bacterial ribosomes due to structural differences in RNA subunits. Additionally, tetracyclines are effective against bacteria by exploiting the bacterial transport system and increasing the concentration of the antibiotic within the cell to be significantly higher than the environmental concentration (Trzcinski *et al.*, 2000; del Giudice *et al.*, 2012).

Aminoglycoside antibiotics have an affinity for the 30S ribosome subunit. Streptomycin, one of the most commonly used aminoglycosides, interferes with the creation of the 30S initiation complex. Kanamycin and tobramycin also bind to the 30S ribosome and block the formation of the larger 70S initiation complex (Rahimi, 2016).

Erythromycin, a macrolide, binds to the 23S rRNA component of the 50S ribosome and interferes with the assembly of 50S subunits. Erythromycin, roxithromycin, and clarithromycin

all prevent elongation at the transpeptidation step of synthesis by blocking the 50S polypeptide export tunnel. Elongation is prematurely terminated after a small peptide has been formed but cannot move past the macrolide roadblock (Piątkowska *et al.*, 2012).

#### **1.7.1.4 Inhibitors of topoisomerase synthesis**

Furthermore, antibiotics such as fluoroquinolones, quinolones, and sulphonamides are known to inhibit DNA and RNA synthesis (Correia *et al.*, 2017). Quinolones are a main group of antibiotics that interfere with DNA synthesis by inhibiting topoisomerase, most frequently topoisomerase II (DNA gyrase), an enzyme involved in DNA replication. DNA gyrase relaxes supercoiled DNA molecules and initiates transient breakages and re-joins phosphodiester bonds in super helical turns of closed-circular DNA. This allows the DNA strand to be replicated by DNA or RNA polymerases. The fluoroquinolones, second-generation quinolones that include levofloxacin, norfloxacin, and ciprofloxacin, are active against staphylococci (Correia *et al.*, 2017).

### **1.7.2 Development of antibiotic resistance in *S. aureus*.**

#### **1.7.2.1 Time line and brief history of antibiotic resistance in staphylococci**

In 1941, Penicillin was used to treat soldiers who suffered from staphylococcal infections during the Second World War (Quinn, 2013). After few years, resistance emerged and spread fast worldwide. Penicillin resistant *S. aureus* in hospitals increased in number between 1946 to 1948 from 6.5 % to 50% (Quinn, 2013). Since this number was still rising greatly in 1949, other natural antimicrobials agents were developed for medical care. These included macrolides, tetracyclines, chloramphenicol and macrolides. All these antimicrobials agents proved effective when they were first used to treat *S. aureus*. However, very quickly *S. aureus* developed resistance against these antimicrobials. Resistance of *S. aureus* was not to an antimicrobial agent only, but a combination of antimicrobials and multi-resistance *S. aureus* became a global problem in hospital settings in the year 1950 (Levy and Marshall, 2004; Marston *et al.*, 2016). After a period of 10 years, 1960s to be precise, other drugs such as cephalosporins and synthetic penicillinase stable  $\beta$ -lactams such as nafcillin, methicillin and oxacillin were introduced to help stabilize staphylococcal penicillinase (Chambers and DeLeo, 2009). Then in 1961, resistance to the newly discovered methicillin drug appeared and this spread fast all through the 1970s and reached 20 % of *S. aureus* at a major general hospital in Lagos, Nigeria, 10% of *S. aureus* in a general hospital setting in Birmingham, United Kingdom

and 15% of *S. aureus* from different infective sources in Denmark (Livermore *et al.*, 2000; Shittu *et al.*, 2011). In 1980s, gentamicin was introduced, and this led to a decrease of prevalence of MRSA though gentamicin resistant strain of *S. aureus* and MRSA began to emerge quickly during the same time (Yılmaz and Aslantaş, 2017). Then 1990s antimicrobials agents of the fluoroquinolone class were introduced. Later, MRSA clinical strains appeared resistant to ciprofloxacin (Didier *et al.*, 2011). This resistance was low because the spread of resistance was minimal compared to those of other antimicrobials. Till today, antimicrobial agents such as glycopeptides remain fairly active against MRSA. Similarly, and fusidic acid and Rifampicin are also considered as possible alternatives to treat *S. aureus* infections although fusidic acid resistance MRSA has been widely encountered in coagulase negative staphylococci of the *S. sciuri* species group (Dobie and Gray, 2004; Foster, 2017).

### **1.7.3. Resistant mechanisms exhibited by MRSA to selected clinically important drugs**

Various mechanisms by which *S. aureus* inactivates the activity of antimicrobials can be summarized into two main groups namely: (A) biochemical mechanisms and (B) genetic mechanisms.

#### **1.7.3.1 Biochemical mechanism of resistance**

##### **Acquisition of bla<sub>Z</sub> genes (Penicillin resistance)**

In the 20th century, penicillin was the first drug of choice used to treat *S. aureus* infections. But since the introduction of penicillin, *S. aureus* have been evolving and developing resistance to penicillin. Before this time, *S. aureus* infections such as skin rash and wounds were only treated with plants believed to possess healing properties but patients that develop bacteraemia infection due to *S. aureus* infections were more likely to die of their infection. The mode of action of penicillin is that it inhibits the penicillin binding protein (PBP) within the bacterial cell therefore preventing the PBP from diffusing across the peptidoglycan layer also known as murein resulting to a weakened cell wall. Inhibiting PBP simply means the bacteria dies because of osmosis (Deleo *et al.*, 2011; Deurenberg *et al.*, 2007). Then in 20<sup>th</sup> century, the discovery of penicillin and its curative action against infections was widely seen as the miracle cure for infections. However, soon after its implementation as a routine antibiotic across the world, penicillin resistant strains emerged in the hospital as well as in the community (Deurenberg *et al.*, 2007). Penicillin resistance is due to the acquisition of *bla<sub>Z</sub>* gene encoding  $\beta$ -lactam antibiotics. Generally, in staphylococci, beta lactam is an enzyme synthesized

extracellularly when they are exposed to lactam drugs for example Amoxicillin. The work of *blaZ* gene is that it hydrolyses the  $\beta$ -lactam thereby rendering the  $\beta$ -lactam very inactive. It is this inactivation that in-turn renders Penicillin based antibiotics such as Carbapenems and Cephalosporin in active in treatment of *S. aureus* infections (Alekhun and Levy, 2007).

### **Inactivation of beta lactam groups by penicillin binding proteins of *S. aureus***

*S. aureus* cell wall is surrounded by peptidoglycan which is 20-40 nm thick (Pinho *et al.*, 2001). The peptidoglycan is comprised of glycan chains which are short and are targeted by antibiotics such methicillin and penicillin in the beta-lactamase class (Pinho *et al.*, 2001). Cross linking takes place outside of the cytoplasmic membrane in a reaction catalysed by penicillin binding protein. Four different binding proteins are present in *S. aureus*; PBP1, PBP2a, PBP2b and PBP2c. All PBP have two main domains involved in transpeptidation and transglycosylation. The beta-lactam antibiotic, which look like the bond of the stem of peptide for cross linking, hinder the transpeptidation of the PBP domain which interfere with the cross-linking reaction causing the cell wall of the bacteria to become weak and cell ruptures due to osmosis (Fuda *et al.*, 2004; Villegas-Estrada *et al.*, 2008).

### ***S. aureus* resistance due to acquisition of plasmids**

Plasmids are extrachromosomal DNA molecules that can replicate independently of the chromosome and can integrate into the host cell (Chamber and Deleo 2009). Plasmids are acquired by community acquired MRSA (CA-MRSA) and are not necessary for cell survival. Plasmids acquired by CA-MRSA carry along with them high antibiotic resistance. For instance, Erythromycin drug resistance was accompanied by a 2kb plasmid. In previous research study, the  $\beta$ -lactamase resistance was found to have 41 kb plasmid which only codes for the  $\beta$ -lactamase resistance but also Mupirocin, Tetracycline, Cadmium resistance. Tetracycline and Trimethoprim resistance is due to the integration of a type-pT181 and acquisition of Tn4003-type plasmid (Lomovskaya and Watkins 2001; Chamber and Deleo 2009).

### **Acquisition of *mecA* gene and presence of phenol groups (Methicillin Resistance)**

The sudden evolution of antibiotic resistance by *S. aureus* to various antibiotics penicillinase resistance  $\beta$ -lactam prompted the implementation of the semi-synthetic penicillinase-resistant penicillin termed methicillin. Methicillin is quite different from Penicillin because of the presence of a phenol groups having a methoxy group in its structure. Methicillin works by inhibiting peptidoglycan synthesis in *S. aureus*. Inhibition is by the inhibition of PBP involved

in peptidoglycan synthesis. This mode of action appears quite like that Penicillin, except for the addition of methoxy group that also secretes an enzyme which decreases the affinity for  $\beta$ -lactamase (Fishovitz *et al.*, 2014; Llarrull *et al.*, 2009).

Shortly after the introduction of penicillin for medical use in the 1960's, resistant strains began to develop. Methicillin resistance in *S. aureus* occurs due to the expression of PBP2a which is 76KDa and methicillin-hydrolysing  $\beta$ -lactamase. PBP2a is a foreign PBP that is resistant to Methicillin and takes over the transpeptidation reaction. This PBP2a is coded for by a *mecA* gene which is a large stretch of foreign DNA with 40 to 60Kb). *S. aureus* acquired the *mecA* gene which is known to express PBP2 allegedly from *S. aureus*. Staphylococcal Cassette Chromosome (SCC) is a novel genetic element that carries *mecA* gene which facilitate resistance of  $\beta$ -lactamase and carrier of *mecA* gene across Staphylococcal species (Stryjewski and Corey, 2014).

### **Vancomycin resistance**

Vancomycin is a glycopeptide used to treat MRSA infections, and this led to vancomycin resistance. Vancomycin was first reported in 1988 among the enterococci, but suddenly in 2002, the first *S. aureus* isolate that was vancomycin resistance (VRSA) was reported. Vancomycin resistance in Staphylococcus species was found to develop as a result of the genetic exchange of some antimicrobial resistant genes between staphylococci and enterococci. The resistant genes were found on plasmids and transposons. VRSA was then characterized in 2002 and result revealed the presence of a composite plasmid that needed two main activities to occur. The first activity is the transfer of the plasmid of enterococci into a recipient strain of *S. aureus* and secondly a transposition that leads to composite plasmid which is composed of a staphylococcal plasmid and that of enterococci transposon (Chamber and Deleo 2009).

#### **1.7.3.2 Genetic mechanism of antibiotic resistance in *S. aureus***

The gene encoding virulence and antibiotic resistance are both located in *S. aureus* bacterial chromosome and plasmids. The genes are associated in clusters to form resistance or pathogenicity island which are transferred by integrons, phage or transposons called mobile genetic element (Kuroda *et al.*, 2001).

## ***S. aureus* genome**

*S. aureus* genome size varies from 2.5-3.1 Mb (Kuroda *et al.*, 2001). The genome contains approximately 2,500 open reading frames. Since the first two *S. aureus* genome sequences; N315 and Mu50, were analyzed and published in the year 2001, other genome sequences have also been studied. These include: MRSA252 and MSSA476, USA300-FPR3737, MW2, COL, USA300-HOU-MR, NCTC8325, ET3-1, JH-1 and JH-9, Newman and TW20 (Cocchiario *et al.*, 2006). The genome is comprised of genes which are most likely acquired by lateral gene transfer. *S. aureus* genome displays an overall conservation of sequence and structure, although this unique consistency is sometimes disrupted with tiny pockets of heterogeneity (Cocchiario *et al.*, 2006). The genome consists of two important parts (i) core genome that is conserved between the *S. aureus* lineages and (ii) the accessory genome (Lindsay, 2014). The core genome consists of genes that are used for daily events while the accessory genome contains the non-essential sequences mobile genetic elements. It is this difference and inclusions in the genome that accounts for both phenotypic and genotypic variations in *S. aureus* (Kuroda *et al.*, 2001; Lindsay, 2014).

### **(i) The core genome**

Approximately 80% of the *S. aureus* genes are contained in the core genome. These include cell surface genes, as well as genes encoding both regulatory and metabolic features. As a part of the core genome, the CV genes make up about 12% of the *S. aureus* genome, and often encode regulators of virulence genes or surface MSCRAMMs involved in human interactions during colonisation of the anterior nares, such as the surface protein (SpA) (Holden and Lindsay, 2008).

### **(ii) The accessory genome**

The remaining 20% of the *S. aureus* genome is the accessory genome, comprising of mobile genetic elements containing well over 50% of virulence factors in *S. aureus*. Mobile genetic elements (MGEs) include pathogenicity islands, chromosome cassettes, plasmids and transposons and bacteriophages. Many of these MGEs carry genes with both virulence and antibiotic resistance roles (Lindsay, 2014). MGEs are elements of dissemination of virulence and antibiotic resistance determinants. The MGEs are discussed below:

### **Staphylococcal cassette chromosome (SCC)**

The SCC is a DNA genetic element situated on the chromosome of MRSA. Five different members of the SCC family exist. They vary in length, structure and composition however each SCC member shares genomic insertion sites, inverted and direct repeat which allows the SCC to act as a carrier for the *mecA* gene (Lindsay, 2014). SCC types I-IV are associated with hospital acquired infections (HA-MRSA) for instance ST239-MRSA-III associated with hospital infections in East Coast of Australia in the 90's and ST250-MRSA -I which is the MRSA strain reported in Australia in the year 1960 (Plata, 2009).

### **Staphylococcal cassette chromosome (SCCmec)**

SCC is a major mobile genetic element that serves as the important vehicle responsible for gene exchange among *S. aureus* strains; SCCmec belong to the SCC family, the members of which serve as carriers of methicillin resistance (Plata *et al.*, 2009). SCCmec is a genomic island that is inserted at the 3' end of orf X and that is located near the replication origin of *S. aureus*. SCCmec is comprised of the *mec* gene complex, which codes both methicillin resistance and the *ccr* gene complex, which codes the recombinases responsible for its mobility and contains two site specific recombinase genes, *ccrA* and *ccrB* (Plata *et al.*, 2009). There are five different *mec* gene complexes which comprises of (*mecA*, *mecI*, and *mecR1*) and the insertion sequences comprising IS431 and IS1272.

- Class A IS431-*mecA*- *mecR1*-*mec I*,
- Class B IS431-*mecA*- $\Delta$ *mecR1*-IS1272,
- Class C1 IS431-*mecA*- $\Delta$ *mecR1*-IS431
- Class D IS431-*mecA*- $\Delta$ *mecR1*
- Class E *blaZ*-*mecA*- $\Delta$ *mecR1*-*mecI*

To date, eight SCCmec types (I-VIII) have been identified based on the allotype of recombinase gene (*ccr*) and the class of *mec* gene complex. These SCCmec types are distributed in different *S. aureus* strains. For example, SCCmec type I-III are harboured mostly by HA-MRSA strains (Diederer and Kluytmans, 2006; Turlej *et al.*, 2011). SCCmec types IV-VII of elements have been widely distributed among CA-MRSA strains. The type IV, V, VI and VII elements are

characterised by their small sizes and lack of resistance genes, other than *mecA* (Gill *et al.*, 2011). It is believed that SCCmec types IV harboured by the *S. aureus* community strains are acquired from the MRSA strains rather than an evolution of a hospital isolate that has found its way into the community (Gill *et al.*, 2011).

### **Pathogenicity islands**

*S. aureus* pathogenicity islands (SaPIs) are a family that generally carry few superantigen genes, encoding a range of TSST-1 and or enterotoxins. SaPIs are specifically integrated at certain chromosomal sites but can be mobilized following infection by certain staphylococcal bacteriophages or by induction of endogenous prophages (Novick, 2003). SaPIs is formed by integration of plasmids or by incorporation of bacteriophages carrying toxin genes (Penadés *et al.*, 2015).

### **Plasmids**

Plasmids are important genetic vehicle in *S. aureus* genome that carries antibiotic resistant genes. Several plasmids found in staphylococci, such as plasmid pUB110, belonging to a group of a small multicopy plasmids, is found incorporated in the type II SCCmec of some *S. aureus* strains. This plasmid encodes resistance to antimicrobials such as kanamycin, tobramycin, aminoglycosides and bleomycin. Resistance to tetracycline resistance is encoded by pT181 while penicillins and heavy metals, such as mercury, is encoded by pI258 (Shintani *et al.*, 2015).

### **Transposons (Tn)**

Transposons are small transferable pieces of DNA situated in *S. aureus* chromosome, which seem to be involved in modification or inactivation of certain cellular functions. Tn 554 is a site-specific transposon that encodes resistance to macrolide-lincosamide-streptogramin B antibiotics and spectinomycin. Tn 58001 carries a gene (*tet M*) which encodes tetracycline and aminocycline resistance (Hiramatsu *et al.*, 2004).

#### **1.7.4 MRSA 252 and antibiotic resistance**

Over many decades now, *S. aureus* has undergone genetic changes that have resulted in the emergence of antibiotic resistant strains that appears to be very successful at transmission and

causing human infections in the hospitals (Holden *et al.*, 2004). Due to the genetic changes, many genetic lineages have emerged and only a few of them have acquired SCCmec and this makes them become successful MRSA clones. Many of these hospital clones have developed multiple resistance to drugs, reduced susceptibility to vancomycin although very rare. MRSA 252 is an example of *S. aureus* strain found in the hospitals. MRSA 252 is an important clinical strain also known as EMRSA-16 clone (Holden *et al.*, 2004; Lim *et al.*, 2015). It is an antibiotic resistant strain with acquired SCCmec III and a major causative agent of human infections particularly wound infection in Europe, but recently, many of its isolates have been reported in countries like Nigeria and several other countries (Lim *et al.*, 2015). Based on genetic diversity, antibiotic resistance of MRSA 252 has been associated to horizontal acquisition of mobile DNA and genomic islands. Thus, most of the genes encoding vital metabolic functions in the enhance the survival and growth of MRSA 252 in the hospital settings, contributing immensely to the success of EMRSA-16 clone (Holden *et al.*, 2004; Lim *et al.*, 2015).

#### **1.7.5 Some identified factors for the emergence and spread of resistance in *S. aureus***

The emergence of resistance is a natural response of microbes to the presence of antimicrobial agents (Li and Webster, 2018). Factors responsible for the emergence and resistance of *S. aureus* includes (i) behavioural factors, (ii) inappropriate prescribing and dispensing of antibiotics (iii) patients and (iv) government.

Behavioural factors contribute to the increase in multidrug resistance by *S. aureus* species (Levy, 2002). These are the external factors and it includes the use of antibiotics in livestock's, misuse of antibiotics, inappropriate prescription and dispensing practices as well as improper hygienic practices. These involve the behavioural conduct of the doctors, patients, dispensers, agriculturists, government to prescription, usage and regulation of antibiotics. These factors are elucidated below.

Lack of access of prescribers to recent information about drug makes them prescribe drugs less rationally (Richardson, 2017; Li and Webster, 2018). Incentives and enticement from pharmaceutical companies makes the prescribers to prescribe drugs unnecessarily and inappropriately (Richardson, 2017). Moreover, it is a usual practice in many developing countries for antibiotics to be dispensed without appropriate prescription method. Worse of it is that in countries like Nigeria and her neighbouring countries, antibiotics are dispensed at any time over the counter with any prior prescription by a doctor. This form of practices had been

attributed to weak laws in the countries with resultant increase in multidrug resistant *S. aureus* species and high mortality and morbidity of *S. aureus* associated infections (Onanuga and Awhowho, 2012; Onanuga and Temedie, 2011).

Patients attitude has contributed immensely to the emergence of drug resistance through poor compliance to the usage of antibiotics (French, 2010; Ventola, 2015), especially if their symptoms are mild and could be resolved as soon as possible (Ventola, 2015). The attitudes of self-medication that is well practiced among patients has contributed to the emergence of multidrug *S. aureus* species to most of the first-generation drugs such as penicillin, streptomycin, ampicillin, cephalosporins (Rossolini, *et al.*, 2014).

Lastly, government contribute to emergence of resistance in *S. aureus* species because of weakness in legislation and enforcement allowing the circulation of substandard and counterfeit antimicrobial in the market. Poor regulation of advertisement and drug promotions increases sales and encourages use of antimicrobials unnecessarily. Lack of adequate training and certification of both prescribers and dispensers may be due to poor provision and regulation by government (Okeke, Lamikanra & Edelman, 1999; Shittu *et al.*, 2011; Tadesse *et al.*, 2017).

Currently, there are a few antibiotics available for treating *S. aureus* infections. However, increased resistance to many drugs has led to the severity of infections caused by the bacteria. In addition, weak immunity in human cells due to health problems such as diabetes, cancer and other immune-deficiency diseases and the unique ability of the bacteria to form biofilms as well as develop drug resistance have greatly increased the number of life threatening infections in human. As at today, bacterial infections still remain a major causative agent of human mortality. In this regard, plant oils (which are usually referred to as essential or vegetable oils) and their biologically active compounds are potential candidates as antibacterial agents. Several types of plant oils and their major active compounds from different medicinal plants have been reported by numerous authors to possess a wide range of inhibitory potentials for example antifungal, antibacterial, analgesic, antioxidant, antiviral and anti-inflammatory (Saxenaa, Joshib & Singhc, 2009; Orhan, Özçelik & Şener, 2011; Zakavi *et al.*, 2013; Bardaa *et al.*, 2016). The effect of antibacterial activity of plant oils may be to inhibit or destroy bacterial cells. Therefore, the potentials exhibited by plant oils have made them an interesting research area to search for alternatives to antibiotics that could help curb the menace of *S. aureus* infections.

## **1.8 Plant seed and nuts**

### **1.8.1 Nuts and seed types and their ethnobotanical uses**

#### **1.8.1.1 African walnut (*Tetracarpidium conophorum*- Mull. Arg)**

African walnut (*Tetracarpidium conophorum*- Mull. Arg) is a perennial creeping shrub (shown in Figure 6) that grows in temperate areas in Africa such as Cameroon, Gabon and Liberia including Nigeria (Ayoola, Onawumi, & Faboya, 2011). African walnuts are dry nuts which are encased in green pods. As African walnut matures, the outer covering dries and falls off leaving the segment tough black shell and the white seed (Figure 11). The white seed nut is the edible nut (Ekwe and Ihemeje, 2013). *T. conophorum* is often called by different names such as awusa (Yoruba), Ukpa in Igbo, kaso or ngak in Cameroon (Ayoola *et al.*, 2011). A bitter after taste is observed upon drinking water immediately after consumption of walnut and this has been attributed to the presence of alkaloids in the nut although phenols can confer such characteristic. African walnut tree is about 40m in length and are usually harvested between July to December (Ayoola *et al.*, 2011).

#### **1.8.1.2 Cashew nut (*Anacardium occidentale* L.)**

Cashew, (*Anacardium occidentale*), is an evergreen tropical shrub (Aliyu and Awopetu, 2007). Cashew is now propagated widely because of its nuts in areas of Africa particularly Nigeria, India, Tanzania, Vietnam, Madagascar, Asia and Philippines and Sri-Lanka (Azam-Ali and Judge, 2001). At maturity cashew fruit can appear as red or yellow (Akinhanmi, Atasié & Akintokun, 2008) (Figure 7). At the tip end of each cashew nut is a bean kidney shaped ovary called nuts with tough multiple layers of shell. Cashew nut tree is about 46ft tall (Aliyu and Awopetu, 2007).

#### **1.8.1.3 Fluted pumpkin (*Telfairia occidentalis*)**

Pumpkin (*T. occidentalis*) is a dioecious perennial crop cultivated in many nations of West Africa but is mainly cultivated in Nigeria (Aregheore, 2012). Common English names for the plant are fluted gourd, fluted pumpkin and Yoruba name is ugu (Aniekwe and Mbah, 2015). The plant is large ranging in size from 16 to 105 cm in length with an average diameter of 9cm. The seed count in the fluted gourd can be up to 196 per gourd, typically 3.4 to 4.9 cm in length for both pistillate and staminate varieties (Figure 8). Fluted pumpkin flowers grow in sets of

five showing a creamy-white and dark red petal unlike the light green colour of the young fruit and yellow colour when ripe (Odiaka, Akoroda & Odiaka, 2008).

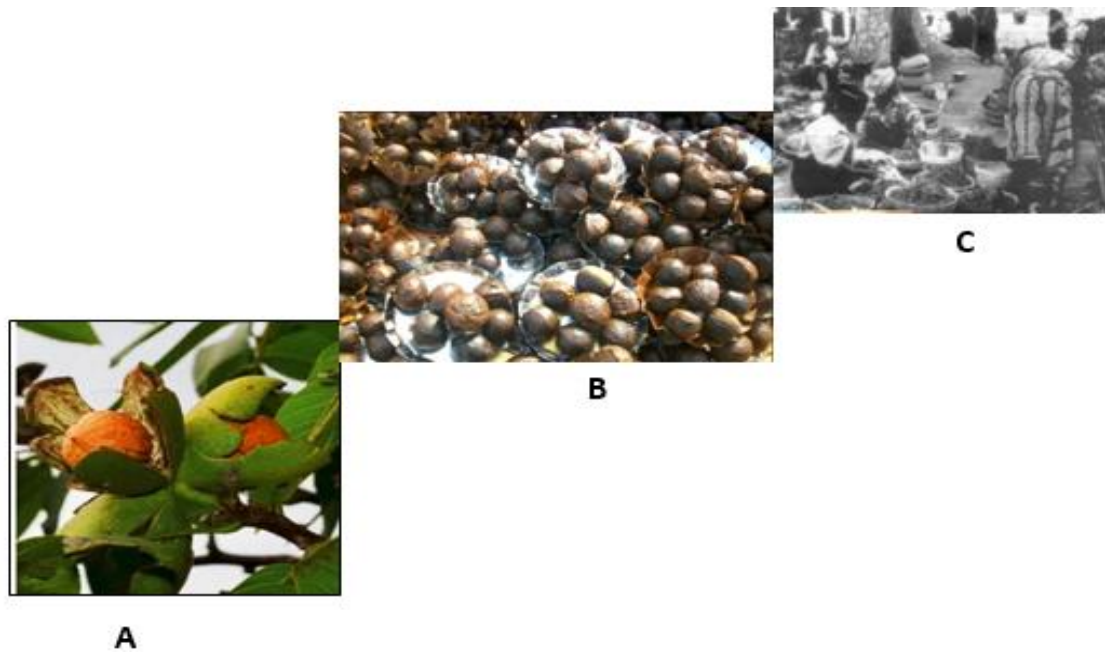


**Figure 6: African walnuts in Nigeria. (A) ripe-walnut still in its pod on the tree and (B) ripe walnuts in segmented black shells after removal from pod (C) display of walnut in open market in Lagos Nigeria.**

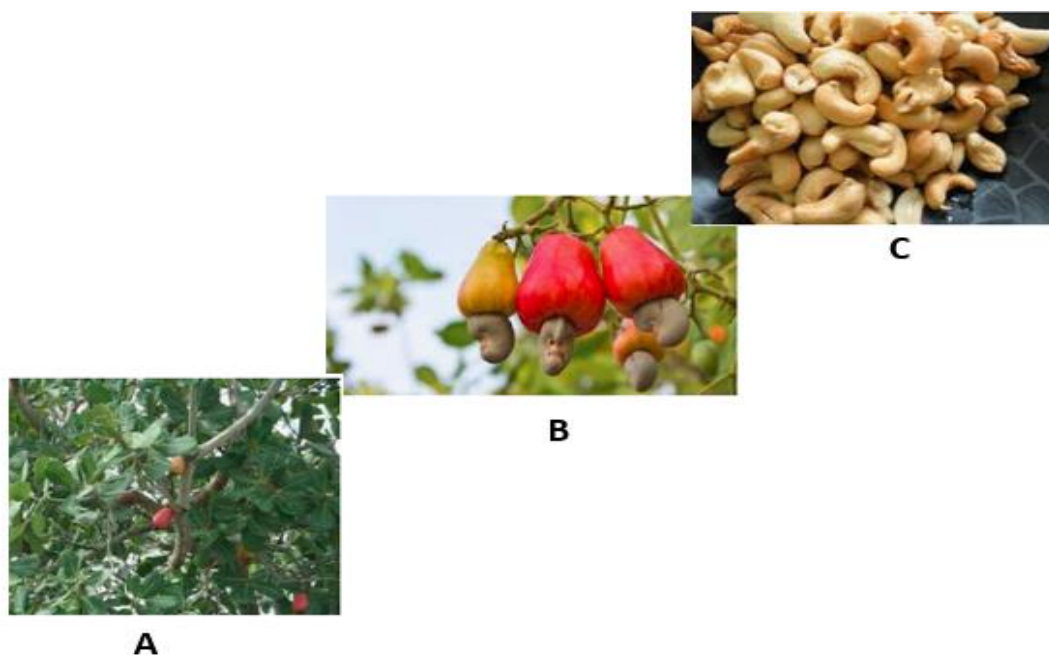


**Figure 7. Cashew nut in Nigeria. (A) Cashew tree showing nuts with different degree of ripening. (B) Ripe-cashew nut fruits and (C) processed sun-dried nuts.**

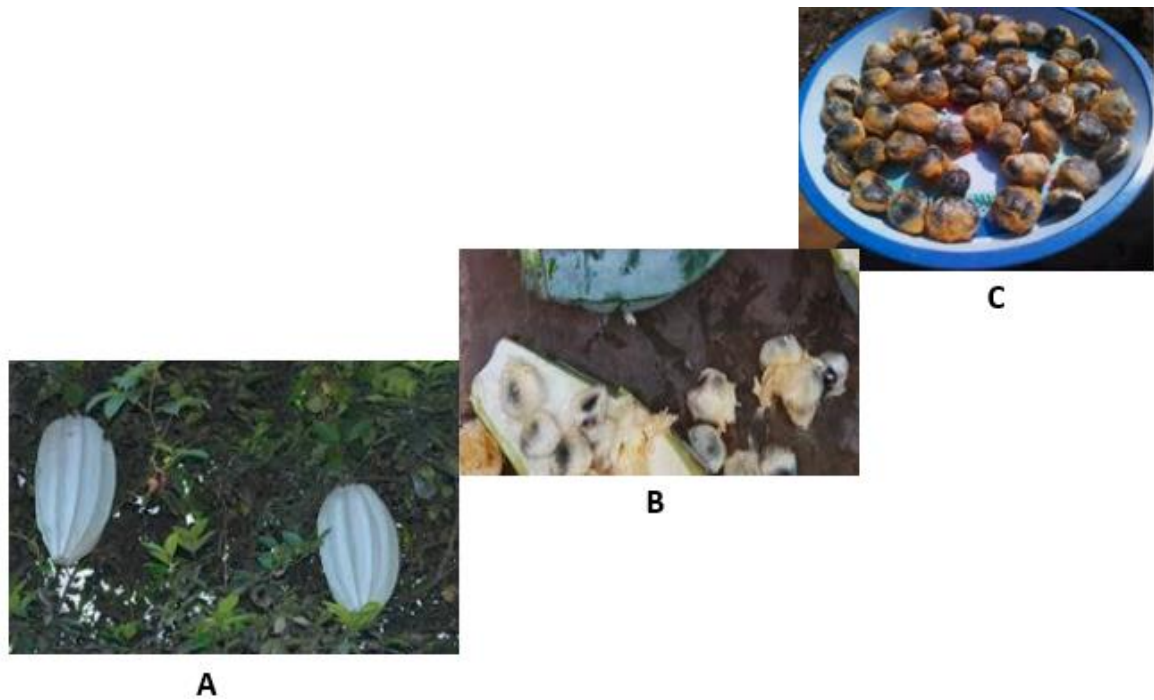


**Figure 8. Pumpkin seeds in Nigeria. (A) Ripe-fluted pumpkin on the tree (B) harvested and processing of pumpkin seed (C) sun-dried pumpkin seeds**

### **1.8.2 Ethno-botanical uses of nuts and seed**

African walnut is basically boiled and consumed as snacks. In the western and northern part of Nigeria, the nuts are either boiled or roasted and served as snacks to welcome visitors (Ekwe & IHEMEJE, 2013). In Cameroon, only adults are known consume walnuts until recent times. African walnut is also consumed raw for the of food as well as medicinal purposes (Akpuaka and Nwankwor, 2000), however, the leaves, bark and roots has been employed by herbal doctors in treatment of certain health issues (Ajaiyeoba and Fadare, 2006) (See Table 1). Cashew nuts are consumed as snacks. In different parts of Nigeria, cashew nuts are usually roasted and eaten (Olife, Jolaoso & Onwualu 2013). The leaves, bark and roots of cashew has also been used for treatment of health conditions (Alexander *et al.*, 2004). Fluted pumpkin seed is basically used in the southern part of Nigeria as food condiments. The seeds are also used in cookery. Different part of fluted pumpkin is used for medicinal purposes (Okpashi *et al.*,2013).

**Table 1. Ethnobotanical uses of African walnut, cashew and pumpkin seeds in Nigeria.**

Uses	Part of plant		
	African walnut	Cashew nut	Pumpkin seed
Treatment of chronic skin infections such as heat rash, eczema, boils Folliculitis.	Leaves, nuts and root	root and bark	Leaves and root
Treatment of fungal infections such as ringworm, nail infections	Nut, bark and leaves	Leaves, nuts and root	Seed and leaves
As pain relieve for abdominal pains and tooth ache when used as a tonic and beverage.	Root and bark	Leaves, root and bark	Leaves, root and bark
Treatment of diabetes, cramps and constipation	Nut, root and bark	Leaves and bark	Root and bark
Control of asthma, cough, diarrhoea	Root and bark	Root and bark	Root and bark
Cancer treatment and high blood pressure.	Nut, root and bark	root and bark	Leaves and root
Minor cuts and Wound infections	Nut, bark and leaves	Nut, bark and leaves	Seed, leaves and barks

Sources: Okpashi *et al.*, (2013); Dada, (2015); Oboh, Nwanna & Elusiyan (2010); Olife, Jolaoso & Onwualu, (2013); Akpuaka and Nwankwor, (2000); Ndie, Nnamani & Oselebe (2010); Ajaiyeoba and Fadare, (2006); Ekwe and IHEMEJE, (2013).

The scientific basis for the uses of walnut, cashew and pumpkin seed presented in Table 1 are yet to be fully researched and properly documented. It will be quite necessary to identify the key bioactive compounds.

## **1.9 Phytochemicals compound in nuts and antimicrobial activity of plant oils.**

### **1.9.1 Plant oils**

Edible oils obtained from plants are called vegetable oils. Edible oils are comprised of triglycerides (Rosillo-Calle *et al.*, 2009). Triglycerides are three molecules of fatty acids and ester of one molecule of glycerol. Fatty acids are main nutritional constituents present in edible seed and nut oils (Siyanbola *et al.*, 2013). Edible oils are usually classified as Oleic-Linoleic acid oils because they have a high amount of polyunsaturated linoleic acid and unsaturated fatty acids, such as the monounsaturated oleic acid. They are characterised by a higher ratio of polyunsaturated fatty acids to saturated fatty acids (Siyanbola *et al.*, 2013).

Edible oils also contain phytochemicals such as flavonoids, terpenoids and alkaloids. They are beneficial to human health. Most of the phytochemicals have been proven to have therapeutic activities such as antibacterial, antioxidant and antifungal roles (O'Brien *et al.*, 2005).

Edible oils can be extracted from plants seed and nuts by exerting pressure on the plant parts to squeeze out oil by mechanical process or by chemical method (O'Brien *et al.*, 2005). There are several types of vegetable oils derived from plant sources which include the most commonly consumed edible oils from cotton seed, sunflower, soybean, groundnut; and others such as castor, rapeseed, palm and coconut (Rosillo-Calle *et al.*, 2009). Edible oils also include the less known oils such as tiger nut, walnut, pumpkin and rice bran.

### 1.9.2 Bioactive phytochemicals compounds in nuts and their classifications

The term phytochemical compounds are synonymously used with bioactive compounds and are sometimes used interchangeably. In the study of Chen and Blumberg (2008) on phytochemical composition of nuts, they classified the bioactive components in nuts into 4 main classes namely Phenols and Phytosterols, Alkaloids, Carotenoids and Organosulfurs (see Figure 9). Phytochemical refers to chemicals derived from plants that is not regarded as important dietary nutrients but are believed to be beneficial to human health (Scalbert *et al.*, 2011).

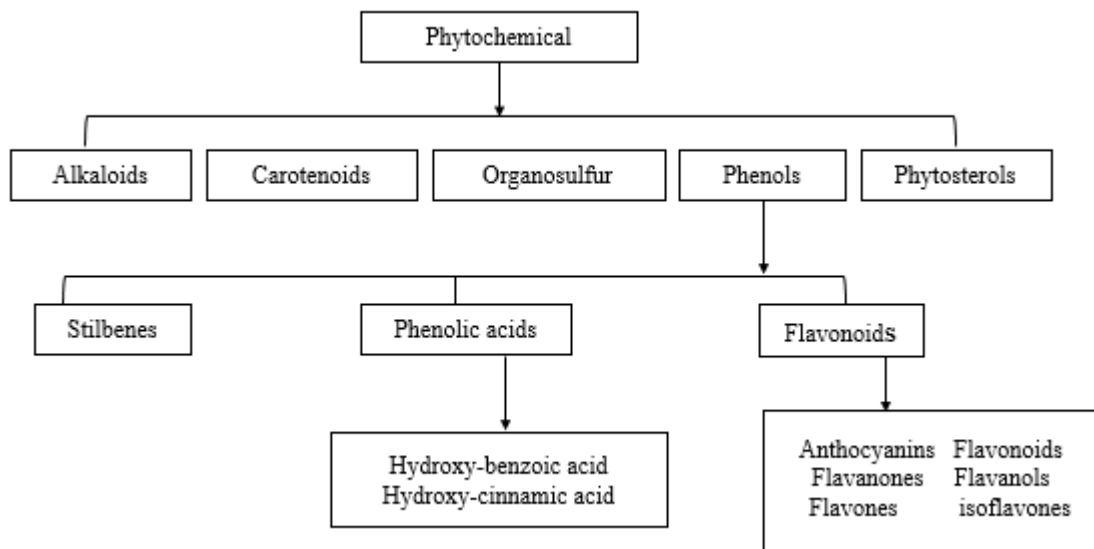
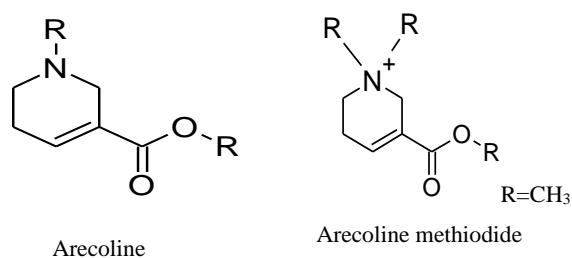


Figure 9. Classes of phytochemicals of nuts (Bolling *et al.*, 2011)

### 1.9.2.1 Alkaloids

Alkaloids are a class of naturally occurring organic compounds that mostly contain basic nitrogen atoms (Bolling *et al.*, 2011). Alkaloids belong to the category of secondary metabolites. The isolation of alkaloids dates back to nineteenth century (Jain *et al.*, 2017). The current use of modern methods and instrumentation has enabled the elucidation of alkaloid structures. Alkaloids are well-defined crystalline substances which react with acids to form salts. They may exist as N –oxides or in the free-state in plants (Jain *et al.*, 2017). Alkaloids contain carbon, hydrogen and nitrogen elements and oxygen. The functions of alkaloids in plants is still not unclear although study show that they may serve as defence of the plant against singlet oxygen which is responsible for damage to living tissues. The toxicity of alkaloids has also been suggestive that it acts as defence chemical against attacks by plant herbivores and microorganisms. In nuts, alkaloids occur in small amounts, usually < 0.08% (Scalbert *et al.*, 2011; Bolling *et al.*, 2011). Some of the alkaloids in nuts, found in Areca nut are arecolin, areacaine and guvacine, but only arecoline has antibacterial activity (Nwokota, 2015) (Figure 10).



#### Alkaloids found in nuts (Nwokota, 2015)

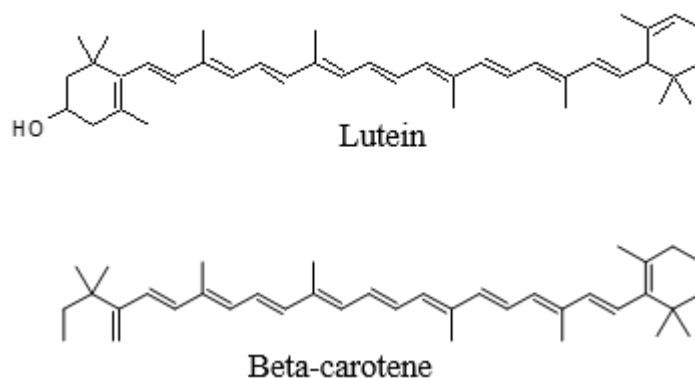


Figure 10. Alkaloids, phenol and carotenoids present in nuts (Chen and Blumberg, 2008)

### **1.9.2.2 Carotenoids**

Carotenoids are polyisoprenoids that naturally occurring in plants. Carotenoids are readily available in plant foods that are coloured (Alasalvar and Shahidi, 2009; Chen *et al.*, 2010). Nuts are not main sources of carotenoids (Halvorsen *et al.*, 2006). Carotenoids play two major roles in plants; firstly, they absorb light energy for photosynthesis, secondly and they protect chlorophyll from photo damage. There are well over 600 carotenoids that have been isolated from plants and characterised. In nuts, three major carotenoids are present in lower quantity;  $\beta$ -carotene, lutein, zeaxanthin and  $\beta$ -cryptoxanthin (Figure 10). Pistachos is an example of nut with low concentrations in  $\mu\text{g}/100\text{g}$   $\beta$ -carotene and lutein. Carotenoids are classified into two, xanthophylls and carotenes. Xanthophylls contain oxygen in their structure while carotenes are purely hydrocarbons and contain no oxygen in their structure (Chen *et al.*, 2010).

### **1.9.2.1 Phenolics**

Phenols are aromatic organic compounds which consists of one or more hydroxyl groups attached to an aromatic hydrocarbon group (Chen and Blumberg, 2008; Salcedo, de Mishima, & Nazareno, 2010). Phenol is a benzene derivative and is the simplest member of the phenolic group (Figure 10). its structure is a hydroxyl group (-OH) bonded to a phenyl ring and its formula is  $\text{C}_6\text{H}_5\text{OH}$  (Bullo *et al.*, 2011). Plant phenols are grouped into three classes; they include flavonoids, stilbenes and phenolic acids. The three classes all have a hydroxyl groups conjugated to an aromatic hydrocarbon. Phenolic compounds are ubiquitous in plant foods with total daily intakes estimated at 500-1000 mg (Chen & Blumberg, 2008). The total phenolic content among nuts varies widely based on varieties. For example, pistachios, pecans and walnuts are rich sources of phenolics (Chen and Blumberg, 2008).

### **1.9.2.2 Proanthocyanins**

Proanthocyanins, are polyphenol groups found in plant foods. They are flavanol oligomers and are composed primarily of epicatechin linked catechin. The size of proanthocyanins differs in plant foods and is ascertained by the level of polymerization. Polyphenol is found in walnut and other nuts (Coates & Howe, 2007).

### **1.9.2.3 Phytosterol and stilbenes**

Phytosterols are plant produced steroids which are lipophilic (Lagarda *et al.*, 2006). Sterols comprise of three six-carbon rings, one five-carbon ring conjugated to an aliphatic chain, and

a C3 hydroxyl group on the A ring. Phytosterols in nuts are mainly composed of  $\beta$ -sitosterol (Segura *et al.*, 2006). Stilbenes are chalcones because their arrangement comprise of phenyl groups. So far, resveratrol and piceid are types of stilbenes found in nuts (Fernández-Mar *et al.*, 2012).

### 1.9.3 Antibacterial activity of plant oils

Antibacterial activity of plant oils seed and nuts oils have been known to possess biological activity, particularly antifungal, antibacterial and antioxidant activities. Orhan *et al.*, (2011) found that oils of hazel nut and walnut had antibacterial effects against several bacterial strains such as *S. aureus*, *P. aeruginosa*, *Proteus mirabilis*, *Klebsiella pneumonia* and *E. coli*. *S. aureus*, and *E. coli*. Hammer *et al.*, (1999) analysed the antimicrobial activity of oils from 52 plant species on human pathogens such as *P. aeruginosa*, *Salmonella enteric subsp. enterica serotype typhimurium*, *Serratia marcescens* and *S. aureus*, *Acinetobacter baumannii*, *Aeromonas veronii* *C. albicans*, *E. coli* and *K. pneumonia* and stated that out of all the oils, only oregano, lemongrass, and bay inhibited all organisms while oils from pumpkin, sage and sweet almond, apricot kernel, evening primrose, macadamia, did not have any effect on the organisms. However, Oyewole and Abalaka, (2012) found that pumpkin oil can inhibit the growth of organisms like *Pseudomonas aeruginosa*, *Salmonella typhi* and *E coli* and *S. aureus*. Kubo *et al.*, (2006) investigated the antimicrobial activity of cashew nut shell liquid oil against methicillin resistant *S. aureus* (MRSA). He found that the oil exhibited inhibitory activity against the bacteria due to the presence of anacardic acid and other metabolites in the oil. Saxena *et al.*, (2009) found that walnut oil inhibited both sets of bacteria particularly, *Bacillus subtilis*, *B. licheniformis*, *S. aureus* and *K. pneumonia*. Similarly, Rhati *et al.*, (2014) found that walnut oil had antibacterial activity against *S. aureus*, *Proteus vulgaris*, *P. aeruginosa*, *K. pneumonia*, and *B. subtilis*. They reported that the activity could be due to the presence of alkaloids. Adeel *et al.*, (2014) showed that pumpkin oil had good antimicrobial action against *S. aureus* with very high zones of inhibition due to the presence of carotenoids. Based on the previous studies, walnut, cashew and pumpkin seeds were chosen for this study for further investigation of their antimicrobial potentials.

## 2.0 Hypothesis, aims and objectives of the research

**Hypothesis:** African walnut, cashew and pumpkin are nuts and seeds from Euphorbiaceae, Anacardiaceae and Cucurbitaceae from which oils are extracted and have antibacterial activity on staphylococcal species.

**Aims:** The main aim of this project, however, is to determine the biochemical characteristics and antimicrobial potential of seed and nut oils against *S. aureus*.

The objectives of this study are:

To grow biofilms of *S. aureus* ATCC 6538 and MRSA 252 in order to identify and study the expression of the virulence genes

To determine antibacterial activity of oils from African walnut, cashew and pumpkin oils and extracts.

To identify phytochemical constituents of African walnut, cashew and pumpkin oils and extracts.

To characterise the most effective oil and identify active components.

### Problem statement

After decades of antibiotic use, *S. aureus* have evolved in Nigeria and across the globe that have become resistant to most commonly used antibiotics (Akujobi *et al.*, 2013). These are the methicillin-resistant *Staphylococcus aureus* (MRSA). MRSA has increasingly become very important human pathogen in many countries in the world since its inception in 1961 and the first outbreak of infection in 1968 (Abdulgader *et al.*, 2015). Reports from the National Nosocomial Infections Surveillance System of the Centers for Disease Control and Prevention showed in August 2005 and October 2010 that MRSA on average accounts for 28-30% of *S. aureus* isolates causing nosocomial infection in hospitals and intensive care units (Akujobi *et al.*, 2013). There is evidence that hospital-acquired MRSA infection increases morbidity, risk of mortality, medical care costs and loss of productivity (Abdulgader *et al.*, 2015). Thus, a methicillin resistant and susceptible strain were used for this analysis to find active natural antimicrobials from plants that could be active against them to help curb the menace of multidrug resistant.

## **Research methodology**

Extraction of African walnut, cashew and pumpkin oils are followed by other analysis.

Different methodologies were used in this study including:

- 1. The extraction of oil from the nuts and seed of African walnut, cashew and pumpkin.**

Complex molecules contained in the oils were extracted using mechanical press and solvent extraction methods.

- 2. Antimicrobial assays**

The crude oils and solvent extracted oils as well as an active ingredient were tested in Methicillin resistant and susceptible *S. aureus* strains. Tests performed includes disc diffusion tests, minimum inhibition concentration (MIC), minimum biofilm inhibitory concentrations (MBIC), minimum biofilm eradication concentration (MBEC), scanning electron microscopy to observe biofilm growth, synergy test, fractional inhibitory concentration (FICI) to investigate their potential therapeutic activities.

- 3. Phytochemical analysis**

To identify active metabolites, standard methods were used to determine alkaloids, carotenoids, phenols etc of the oils and infra-red was performed.

- 4. Isolation of active compounds.**

Fractional distillation method was used to separate the cold pressed oil into fractions to obtain active component (s) that possessed biological activity.

- 5. Identification of active compound**

This was achieved by performing infra-red spectroscopic method, NMR; proton NMR and carbon NMR.

## Chapter 2. Materials and Methods

### 2.1 Materials

#### 2.1.1 Collection of plant materials and identification

Fresh African walnut (*Tetracarpidium conophorum*- Mull. Arg), cashew (*Anacardium occidentale* L.) and pumpkin seed (*Telfairia occidentalis*), of selected Nigerian plants that are used for the treatment of skin infections, burns and wounds were purchased in September through October 2016 from village farmers. For this study, an ethical approval from the University of Salford was obtained to stand in place for the Nagoya ethics that is yet to be implemented in Nigeria. Figure 11 and Table 2 shows the pictures and list of plant materials used in this study. The seeds and nuts were identified by a plant scientist in the Department of Biological Sciences, Olabisi Onabanjo University, Ogun State, Nigeria.

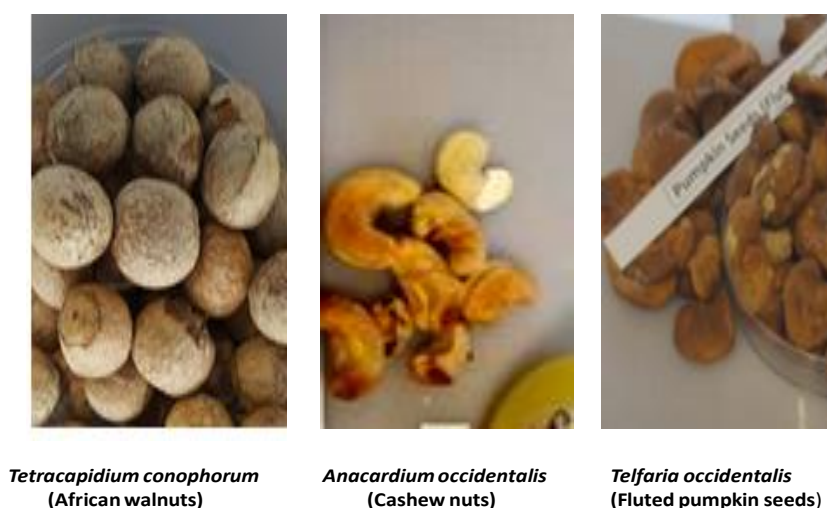


Figure 11. Plant seed and nuts used in this study

**Table 2. Plant materials used in this study**

Plant seed and nut used	Botanical name	Family	Traditional use	Place of collection	Month of collection
African walnut	<i>Tetracarpidium conophorum</i> -Mull Arg	Euphorbiaceae	Skin swellings and wound treatment, Reduction of growth of cancer cells	Ikotun central market, Alimosho	September
Cashew	<i>Anacardium occidentale</i> , L	Anacardiaceae	Eczema, syphilis related skin disorder and cough, eye, ear, wound healing	Ikotun central market, Alimosho	September
Pumpkin	<i>Telfaira occidentalis</i>	Cucurbitaceae commonly known as gourds	Skin and wound healing	Oja Oba Ado-Ekiti, Ekiti	October

### 2.1.2 Solvents, chemicals and media used in this study

#### Solvents

Solvents used for extraction and chemical studies were n-hexane (boiling point 61.2°C), chloroform (boiling point 61.2°C), petroleum ether (boiling point 42 - 62°C), obtained from Sigma Aldrich, Dorset, UK and Fisher Scientific, Loughborough, UK.

#### Chemical reagents

Extraction and phytochemical reagents including boron trifluoride (BF<sub>3</sub>-MeOH), ethyl alcohol, hydrochloric acid (HCl), potassium iodide, ferric chloride, wagner reagent, magnesium ribbon and lysostaphin were obtained from Sigma Aldrich, Dorset, UK, while saturated sodium chloride solution and anhydrous sodium sulphate reagent were obtained from Fisher Scientific, Loughborough, UK and Scientific Laboratory Supplies, UK. Scanning Electron Microscopy (SEM) materials including glutaraldehyde, sodium cacodylate buffer, sodium hydroxide, sodium phosphate dibasic, sodium phosphate monobasic and osmium tetroxide was purchased from Sigma Aldrich, Dorset, UK.

#### Media

Microbial culture media including Trypticase soy broth (TSB) and Trypticase soy agar (TSA) and Brain heart infusion (BHI) were purchased from Appleton Woods, Norton, UK. Mueller Hinton Broth (MHB) and Mueller Hinton Agar (MHA) was obtained from Sigma Aldrich,

Dorset, UK. Columbia blood agar base (CBAB) was obtained from ThermoScientific, Hampshire, UK.

### **Consumables**

Congo red, horse blood and glucose were purchased from ThermoScientific, Hampshire, UK. Materials for biofilm growth including Nunc 96-well plates with lids, polystyrene tissue culture plates and MBEC™ biofilm inoculator were obtained from Innovotech, Hertfordshire, UK. Glucose, parafilm, sterile loops and sterile petri-dishes 60 mm in size were obtained from Scientific Laboratory Supplies, UK. Mineral oil and safranin for staining biofilms was also obtained from Sigma Aldrich, Dorset, UK. Cotton buds, filter papers, universal tube (10 mL), pipettes (10 – 25 mL) and bacterial spreaders were obtained from Scientific Laboratory Supplies, UK.

#### **2.1.3 Bacterial strains used for antimicrobial susceptibility testing**

The bacterial strains used in this study were methicillin-susceptible (MSSA) laboratory strain *S. aureus* ATCC 6538, *Staphylococcus aureus* ATCC 12228 and methicillin-resistant (MRSA), a clinical wound isolate MRSA 252. Both ATCC 6538 and ATCC 12228 were obtained in the form of stock from the American Type Culture Collection (ATCC Manassas, VA, USA). MRSA 252 was collected from University of Salford, Manchester, UK. ATCC 6538 strain was selected because it is a standard strain for testing antimicrobial agents and drug discovery. In addition, it is known for its ability to form biofilms. ATCC 12228 was selected because it is a standard strain known to be a negative biofilm former. MRSA 252 was selected because it is among the pathogens often implicated with staphylococcal disease outbreaks in Europe and across the world and a biofilm former as well. All strains were preserved as stock in the freezer at  $-80^{\circ}\text{C}$ .

#### **2.1.4 Antibiotics discs**

A group of 12 antibiotics belonging to different mechanistic classes and potencies was initially explored for the disc diffusion test. These includes: vancomycin, chloramphenicol, gentamicin, erythromycin, penicillin G, streptomycin, rifampicin, oxacillin, linezolid and carbenicillin. (Table 3) shows the antibiotics concentrations. Antibiotic-impregnated discs (Thermo Fisher Scientific, UK) were stored in sealed cartridges along with desiccant at  $-20^{\circ}\text{C}$  in freezer. Only the working supply of discs was kept in the refrigerator at  $4^{\circ}\text{C}$  for one week. Before using the discs for assay, the discs are usually removed from refrigerator and left at room temperature

for 30 minutes. This was to ensure that the discs equilibrated at room temperature thus minimizing the amount of condensation that occurred when warm air comes in contact with cold discs.

**Table 3. Antibiotics used in the study**

Antibiotics were purchased from ThermoFisher Scientific, Uk. Their potency is given below

<b>Antibiotics</b>	<b>Antibiotics potency (µg)</b>
Vancomycin	10
Erythromycin	10
Chloramphenicol	10
Oxacillin	10
Streptomycin	10
Rifampicin	15
Gentamicin	10
Linezolid	10
Penicillin G	10
Carbenicillin	10
Trimethoprim	1.25
Ciprofloxacin	5
Cefoxitin	30
Oxacillin	5

## **2.2 Methods**

### **2.2.1 Extraction process of African walnut, cashew and pumpkin oils and their respective extracts**

#### **2.2.1.1 Preparation of plant materials for extraction**

After identification, the seeds and nuts were sorted, and damaged ones discarded. The seed and nuts were washed in cold water to remove dirt adhering to the surface. After washing, manual separation of the pulps from the seed and husk from the nuts was done. The seed and nuts were then sundried in shade for 14 days. The nuts and seeds were pulverised using MarlexExcella mixer/grinding machine (Amazon, UK), packed in air tight containers and kept in the refrigerator at 4°C for further processing.

### **2.2.1.2 Extraction of oils from African walnut, cashew and pumpkin using mechanical press method**

The method of choice for the extraction of the plant oils was screw press method. The advantage of using this method is to yield more oil and ensure that the vital components present in oil are preserved. The step wise method described by Jokic *et al.*, (2014) was used to extract oils from African walnut, cashew and pumpkin seeds. The extraction of oils from walnut, cashew and pumpkin were performed using a screw expeller (Model SPU 20, Senta, Serbia). African walnut, cashew and pumpkin oils were obtained by pressing 200 g of individual seed and nuts. The minimum and maximum nozzle size used was 7 and 12 mm, respectively. The frequency had a minimum of 10 Hz and a maximum of 20 Hz. The temperature of oil presses was between 70 and 100 °C. After pressing, the volume of each screw pressed oils was measured and after that the oil was centrifuged. The percentage yields of individual oil after three extractions were calculated by weight difference. Also, the average yield of each oil sample was obtained. In addition, the oil sample was recovered, and physical characteristics of the oil samples were observed. The extracted oils were stored in white bottles at 4 °C until analysed. After extraction, the physical properties of each extract were recorded, and the amount of extract obtained was measured using an analytical balance and result obtained was used to calculate the percentage yield of each oil sample.

### **2.2.1.3 Extraction of African walnut, cashew and pumpkin extracts using solvent extraction method**

To effectively extract the sample extracts needed for analysis, a standard procedure was developed this involved using the same amount of seeds/nuts and equal amount of solvents as well as the extraction time. By doing so, the final yield obtained from different solvents used were compared one to another. The extraction method was sequential extraction with solvents of increasing polarity. Petroleum ether, n-Hexane and chloroform were the solvents used for the extractions. Extractions of extract from African walnut, cashew and pumpkin were done separately at different times. Prior to extraction, the pulverized seed and nut samples were kept in an oven at 105 °C for 1 h to remove any moisture that may still be present. Thirty (30 g) of each dried sample seed was wrapped in a white muslin cloth and put into a porous thimble of the Soxhlet extractor, using 200 ml of different solvents such as chloroform, petroleum ether and n-hexane of HPLC grade with boiling range of 40-60 °C. The Soxhlet was coupled with condenser and flask already filled with the set up was heated heating mantle at 65 °C to allow

solvent boiling. In the process the solvent vapour travels up a distillation arm and flowed into the chamber housing the sample material. The extract seeps through the pores of the thimble and fills the siphon tube where it flows back down into the round bottom flask. The process was allowed to continue for 8 h until a clear solvent was obtained in the thimble chamber. At the end of the extraction, the resulting mixture of the extracts was filtered with a 10 mm Syringe-driven with a filter 0.45 micron to remove any impurities. The solvents were further removed completely with a rotary-evaporator (Model N-1, Eyela, Tokyo Rikakikal Co., Ltd., Japan). The extracts were stored in white bottles and tubes under nitrogen at 4 °C until analysed. After extraction, the physical properties of each extract were recorded, and the amount of extract obtained was measured using an analytical balance and result obtained was used to calculate the percentage yield of each oil sample.

#### **2.2.1.4 Oil and Extract Yield Determination (%)**

The method of Efeovbokhan *et al.*, (2015) was used to determine both the oil and extract yield of each sample. After evaporation of n-hexane, chloroform and petroleum ether solvents from the extracts, the weight of seeds, weight of each extract and the amount of solvent used for extraction were considered for the calculation of percentage yield of extracts which was recorded. To calculate the percentage yield of oil from African walnut, cashew and pumpkin the same was used. The weight of seeds, weight of oil obtained from African walnut, cashew and pumpkin were considered for the calculation. Percent yield of both the extracts and oils were calculated to know the amount of stock to prepare for further analysis. Percent yield was calculated to know the amount of stock to prepare for further analysis.

$$\text{Percentage yield of extracts} = \frac{\text{Weight of extracted extract (g)}}{\text{Weight of sample (g/nut)}} \times 100 \text{ (Equation 1)}$$

$$\text{Percentage yield of oil} = \frac{\text{Weight of extracted oil (g)}}{\text{Weight of sample (g/nut)}} \times 100 \text{ (Equation 2)}$$

#### **2.2.1.5 Preparation of standard concentrations of African walnut, cashew and pumpkin oils with their respective extracts**

The procedure described in Benson's Microbiological Applications Laboratory Manual (2001) was used to prepare the standard concentration of the oils and extracts. Two grams of the individual oil and extract was weighed and diluted with 2 mL of DMSO (0.05%). The dilution of the oils and extracts with DMSO led to the concentration of 1000 mg/mL individually.

Resultant stock samples were stored at 4°C in a clear glass volumetric flask. Working concentration was prepared by performing 2-fold dilution from stock.

### **2.3 Preliminary phytochemicals analysis of African walnut, cashew and pumpkin oils with their respective extracts**

Preliminary analysis of the various constituents of the oils and their respective extracts was performed to identify the possible phytochemical groups contained in each sample. In this study different qualitative phytochemical screens were performed on each oil sample and its extracts using various standard procedures (Mbatchou *et al.*, 2011) to identify their active constituents.

#### **2.3.1 Determination of Flavonoids**

Shinoda's Test

Briefly, 2 mL of each oil sample was put in three different 250 mL beakers and dissolved with 3 mL of ethyl alcohol each and reacted by few drops (10 drops) of diluted HCl followed by a magnesium ribbon. Formation of colours such as reddish, pink, or brown indicates the presence of flavonoids in the sample extract. This procedure was also used to determine flavonoids in each extract (Mbatchou *et al.*, 2011).

#### **2.3.2 Determination of alkaloids**

Wagner's Test

500 µL of each oil sample was put in three different tubes and acidified with 1 mL of 1.5% (v/v) HCl and dissolved with 500 µL of Wagner's reagent which is iodine prepared in potassium iodide solutions. Within 10 min a yellow or brown precipitate was observed. Appearance of yellow or brown precipitate indicates the presence of alkaloids. This procedure was used to determine alkaloids in each extract (Mbatchou *et al.*, 2011).

#### **2.3.3 Determination of saponins**

Foam test

To 2 mL of each oil sample and extract, 6 mL of deionised distilled water (ddH<sub>2</sub>O) was added and shaken vigorously; the presence of foams or bubbles indicated the presence of saponins.

### **2.3.4 Determination of tannins**

To 2 mL of each oil sample and extract, 500 µL of 10% of alcoholic ferric chloride was added; formation of brownish or blue-black colour indicates the presence of tannins.

### **2.3.5 Determination of phenol**

To 2 mL of each oil sample and extract, 2 mL of 5% aqueous ferric chloride were added and formation of blue colour within 3 minutes indicates the presence of phenols in both the oils and sample extracts.

### **2.3.6 Determination of terpenoids**

1 mL of each oil sample and extract of each solvent was placed into different 250 mL beakers and 500 µL of 100% chloroform was added followed by addition of 3-5 drops of concentrated sulphuric acid (100 %), formation of dark reddish-brown precipitate of each sample indicates the presence of terpenoids.

## **2.4 Identification and investigation of biofilm production in MRSA 252 and *S. aureus* ATCC 6538**

### **2.4.1 Identification of *S. aureus* isolates**

The strains were confirmed by several procedures which include:

- Morphological characteristics
- Biochemical test
- Antibiotic sensitivity test

#### **2.4.1.1 Morphological characteristics**

The characteristic colour and colony appearances (shapes) were determined using Habib *et al.*, (2015). To determine the colour and shapes based on Berge's method, one (1) to two (2) colonies of each bacterium was streaked onto TSA and CBAB plates respectively. After streaking, plates were then incubated at 37 °C for 24 h. After incubation colonial morphologies were determined.

#### **2.4.1.2 Biochemical tests**

Biochemical tests used to confirm the *S. aureus* strains include catalase test and coagulase test.

### **(i) Catalase test**

To test for catalase activity, the method of Darwish and Asfour, (2013) was modified. Modification was the use of 100 mL instead of 10-20 drops. 100 mL of hydrogen peroxide was put in white clear vials. Bacterial colonies 4-5 from both ATCC 6538 and MRSA 252 were picked up with inoculation loop and transferred onto hydrogen peroxide in glass vial, to test catalase activity. The production of gas bubbles constitutes positive reaction.

### **(ii) Coagulase test**

Tube coagulase test was used to test for coagulase. For detection of free coagulase 500  $\mu$ L of rabbit plasma was taken in a test tube. To this plasma 100  $\mu$ L of overnight broth culture of *S. aureus* strains was added. The tube was then rotated gently to mix the content together and then incubated at 37 °C, preferably in water bath for 2-4 h (Darwish and Asfour, 2013). Clotting of rabbit plasma by conversion of fibrinogen into fibrin by the Staphylococcal coagulase enzyme was considered as positive test. However, a weak coagulase positive strain will coagulate the plasma after overnight incubation.

### **(iii) Lysostaphin tests**

100 mL of over-night cultures of MRSA 252 and ATCC 6538 were mixed with 200 mL of PBS and 200 mL of reconstituted lysostaphin (1 mg/mL) and samples were incubated for 37°C for 2 h in an incubator. Samples were observed for turbidity and clean clear samples without turbidity were taken as positive. ATCC 12228 used as control was set up at the same time.

## **2.4.1.3 Antibiotic sensitivity test**

Two main antibiotic discs namely cefoxitin (30  $\mu$ g) and oxacillin (1  $\mu$ g) essential for the identification of methicillin susceptible and resistant MRSA 252 and ATCC 6538 were used.

## **2.4.2 Biofilm formation assays**

### **2.4.2.1 Phenotypic analysis**

#### **(i) Detection of slime production by congo red agar method**

Slime production was determined by cultivation of all *S. aureus* strains on congo red agar (CRA) plates as described by Darwish and Asfour, (2013). Briefly, CRA plates were prepared

using 3 g of TSA adding 0.1 g Congo red supplemented with 1 g (w/v) glucose in 100 mL of distilled water. The strains were inoculated in streaks and incubated at 37 °C under aerobic conditions for 24 h, followed by storage at room temperature for 48 h (Kaise and Nunes, 2012). Isolates were interpreted according to their colony phenotypes. Black colonies with dry consistency and rough surface edges were considered a positive indication of slime production, while black colonies with smooth, round and shiny surface and red colonies of dry consistency and rough edges were considered as intermediate slime producers. Red colonies with smooth, round, and shiny surface were indicative of negative slime production.

#### **(ii) Quantification of biofilm by microtiter plate (MTP) method**

MRSA 252, ATCC 12228 and *S. aureus* ATCC 6538 were grown overnight at 37 °C as pure cultures on TSA and CBAB plates. Groups of three single colonies morphologically similar were inoculated in 10 mL TSB. Suspensions were incubated for 18 h at 37°C (stationary phase >2.5) in a rotator shaker and then diluted at 1: 40 in a fresh sterile TSB with  $2-7 \times 10^7$ cfu/mL using 0.5 MacFarland standard tubes to compare the suspensions. This diluted suspension was used as the inoculum in the microtiter plate test. Microtiter plate test was performed according to Asthan *et al.*, (2013) and Darwish and Asfour, (2013). For each strain 1 mL aliquots of prepared suspension were inoculated into nine wells of the 24-well tissue culture plates (Corning Costa, UK) with the aid of a multichannel pipette. Each culture plate included a negative control, a negative biofilm former (ATCC 12228). The plates were incubated at 37°C for 12 h, 24 h and 48 h respectively and content of each well was removed by aspiration with 1 mL pipette tips and the wells were rinsed three times with 1 mL each of deionized water (total of 27 mL of deionized water was used to rinse each plate). The plates were dried in inverted position for 20 min. The attached bacteria were later fixed for 15 min at room temperature by adding 1 mL of methanol per well (9 mL in total/plate) for 20 min before the plates were emptied and left to dry overnight. Each well of the biofilm plates were then stained with 1 mL each of 0.1% safranin (9 mL in total/plate) for 15 min. Excess stain was rinsed off, and the plates were washed three times with distilled water, left to dry overnight and the next day plates were visually inspected for biofilm formation. After the visual inspection of plates, the safranin dye that was bound to the adherent cells was dissolved with 95% ethanol per well, and optical density was measured at 595 nm (OD<sub>595</sub>). The experiment was repeated three times. The optical density (OD<sub>595</sub>) of wells containing sterile. ATCC 12228 was used as the negative control. An OD<sub>595</sub> value of 0.5 was selected as the cut-off point to differentiate as

positive for biofilm formation. Biofilm formation for each strain was analyzed and categorized based on the absorbance value of the safranin-stained biofilms. Strains were considered as follows:

Strongly adherent ++++ (OD 595 > 3.0),

Highly adherent +++ (OD 595 > 2.0),

## **2.5 Screening of oils and extracts for antimicrobial activity against MRSA 252 and ATCC 6538**

### **2.5.1 Growth of *S. aureus* strains for analysis**

#### **2.5.1.1 Preparations of media for growth of bacterial strains**

Mueller Hinton Broth (MHB), Mueller Hinton agar (MHA), trypticase soy broth (TSB), trypticase soy agar (TSA) and Columbia blood agar base (CBAB) used as media for growth of bacterial cultures were sometimes made up in large volumes as follows: MHB, 23 g, MHA (38 g), TSB, 30 g, TSA (30 g) and CBAB (30 g) were made up in 1 Litre of deionised water and sterilised at 121°C for 15 minutes at 15 psi pressure.

#### **2.5.1.2 Growth of *S. aureus* strains on solid media**

ATCC 6538, ATCC 12228 and MRSA 252 were grown on solid media (TSA, MHA and CBAB), based on the method described by Vitko and Richardson, (2013). At times these three media were prepared same day. TSA was prepared by weighing out 3 g of TSA, into 100 mL of sterile deionised water (dH<sub>2</sub>O) to dissolve. Similarly, 2.3 g of MHA was weighed in 100 mL and 4.88 g of Columbia agar in 100 mL to dissolve. TSA, MHA and CBA media were then autoclaved at 121 °C for 60 min and poured into petri-plates to cool. After plates were cooled, sterile loops were used to streak out small amount of each bacterial strains from the frozen stock (-80°C) onto the TSA, MHA and CBA plates. This was done to make the strains visible as distinct colonies at the end of the streaks. Most importantly the bacterial colony appearances and morphology of the strains used in this study were carefully studied. The plates were then incubated for 24 h at 37°C in an incubator. After incubation, the cultured plates were sealed with parafilm and stored in the refrigerator at 4 °C for further use.

### **2.5.1.3 Preparation of overnight culture**

Overnight cultures were prepared using the method described by Vitko and Richardson, (2013). Using aseptic technique, single colonies of ATCC 6538, ATCC 12228 and MRSA from the streaked plates were transferred with sterile loops into 10 mL TSB broth or 10 mL MHB (depending on the analysis to be performed next day) and the bacterial cultures were then grown overnight for 16 – 18 h at 37 °C with shaking (200 rpm) in N-BIOTEK shaking incubator. The shaking was done to increase aeration. After incubation, bacterial growth was checked, which was characterized by a cloudy haze in the medium and the optical density was determined using a spectrophotometer. Following the overnight growth, the bacterial culture was in stationary phase an  $OD_{600} = > 2.5$ .

### **2.5.2 Maintenance of test organisms**

To be able to use the bacterial strains for a long period of time checks for no change in strain characteristics were performed. The bacterial strains were maintained for both short terms as well as for long term preservation.

#### **2.5.2.1 Short term maintenance**

For daily or weekly use of the bacterial strains short term maintenance method was followed. This was done to reduce the chance of the bacterial colony mutation when the culture is old. In this study, the strains were maintained for short time period (5 days) on agar plates. TSA and CBAB plates were used for this purpose. A single colony of each bacterium (ATCC 6538 and MRSA 252) was taken in a loop and was streaked on the agar plates by streak method to get more single colonies. The plates were incubated overnight at 37°C to get the colonies. Following day, the plates were sealed with parafilm and stored at 4°C refrigerator for the next use (Vitko, 2013). The parafilm helps to avoid any source of contamination in the plate while storing and it helps to maintain the moisture in the plate which prevents the bacterial colonies from drying. Using this method, the strains were stored in the refrigerator for a month. At times, the strains were sub-cultured on fifth day after culturing to maintain healthy bacterial colonies.

#### **2.5.2.2 Long term maintenance**

Long term bacterial maintenance is important because it helps to store the strain as stock sample (Vitko, 2013). The bacteria could be revived again for later use if the short term maintained bacterial strains are mutated (Vitko, 2013). For this study, long term maintenance of bacterial

strains was done in two ways: by keeping the bacterial strains supplied as stock in -80°C freezer or by preparing a glycerol stock in cryovials (as cryogenic stocks) containing 700 µL of overnight cultures in trypticase soy broth and 30% (v/v) glycerol (Vitko, 2013). Every 6 months, a loop full of each bacterial strain were thawed from the -80°C freezer, streaked on the agar plate and incubated overnight at 37°C to culture the bacterial strains. Next day, when the bacterial colonies were ready for use, four to five single colonies of the same morphology are picked up and inoculated in fresh TSB or MHB depending on the analysis to be conducted.

### **2.5.3 Antimicrobial susceptibility testing of seed and nut oils**

The antimicrobial activity of the extracted oils and respective extracts were tested by three main methods:

- Agar disc diffusion Method (Kirby Bauer)
- Minimum Inhibitory Concentration (MIC) and Minimum Biofilm Inhibitory Concentration (MBIC)
- Minimum Biofilm Eradication Concentration (MBEC)

#### **2.5.3.1 Agar diffusion method**

The agar diffusion assay is a method for quantifying the capacity of antimicrobial agents to inhibit bacterial growth (Boney *et al.*, 2008). It can be done in two ways, one is disk diffusion method, and another is well diffusion method. For this study the disk diffusion method was followed for the oils and the well diffusion was used for the extracts. Disc diffusion method for antimicrobial susceptibility testing was carried out based on recommendations given by the Clinical Laboratory Standards Institute, CLSI (CLSI, 2012; Jorgensen and Turnidge, 2015). The disk-diffusion method also called Kirby-Bauer sensitivity test was used to test the effectiveness of walnut oil, cashew oil, and pumpkin oil on *S. aureus* strains ATCC 6538 and MRSA 252. The effectiveness of these oils in combination with multiple commercial antibiotics was also determined using this method. This method was used as a preliminary check to select between efficient oils and antibiotics that could be used for further analysis and the synergism study. The disk diffusion method is performed using Mueller-Hinton Agar (MHA), which is the best medium for routine susceptibility tests because it has good reproducibility. Also, because MHA is low in trimethoprim, sulphonamide and tetracycline

inhibitors it gives satisfactory growth of most bacterial pathogens (Tendencia, 2004). This method was used to assess the antimicrobial activity of the oils only.

#### **(i) Preparation of impregnated disc**

10  $\mu$ L of oils (concentration 1000 mg/mL) from African walnut, cashew and pumpkin were used to impregnate sterilized 6 mm diameter blank discs (Oxoid, UK). For the screening of plant oils with commercial antibiotics, 10  $\mu$ L of a final concentration of each oil sample was used to impregnate the commercial standard antibiotics with known concentrations. Dimethyl sulfoxide 0.05 % (v/v) loaded discs (10  $\mu$ L) was used as a negative control. All impregnated discs were ensured to be fully dried in 40 °C incubator for 18 to 24 h prior to the application on Mueller Hinton Agar (MHA) plates. Standard antibiotic discs of all the discs impregnated with oils were used as positive controls and synergy test.

#### **(ii) Inoculum preparation for performing the disc diffusion test**

Inoculums for disc diffusion tests were prepared following the guidelines of the Clinical Laboratory Standards Institute, CLSI (CLSI, 2013) and National Committee for Clinical Laboratory Standards NCCLS (2012). Briefly, using aseptic techniques, bacteria strains (ATCC 6538 and MRSA 252) were cultured in 10 mL of Mueller Hinton Broth (MHB) overnight or to stationary phase ( $OD_{600} > 2.5$ ). From the overnight culture, using streak plate method, a loop full of both strains were streaked across the MHA plate and incubated at 37 °C for 24 hours. From the incubated MHA culture plates, inoculums were prepared by making a direct broth suspension of four to five *S. aureus* strains ATCC 6538 and MRSA 252 well isolated colonies of the same morphological type from an 18 to 24-hour culture into a freshly prepared 10 mL of Mueller Hinton Broth (MHB), and incubated in a shaking incubator (Camlab, UK) at 37 °C, 200 rpm for 18 h with 200 rpm to stationary phase ( $OD_{600} > 2.5$ ). The bacterial suspensions were adjusted to achieve a turbidity equivalent to a 0.5 McFarland,  $1.0 \times 10^8$  to  $1.5 \times 10^8$  colony forming units per millilitre CFU/mL. This was done by diluting the overnight cultures 1:100 by transferring 0.1 mL of the bacterial suspension to 9.9 mL of sterile TSB before growing back in the shaking incubator for approximately 2-3 hours (mid-log phase) to obtain 0.08 to 0.10  $OD_{625}$  corresponding to  $1.5 \times 10^8$  CFU/mL. The correct density of the turbidity standard was verified using a spectrophotometer with a 1-cm light path and matched cuvette (Star Labs, UK) to determine the absorbance at 625 nm. Blank of MHB alone was used to calibrate the spectrophotometer before measuring the samples. To ensure conformity of the

suspension's turbidity with McFarland standard, both the suspension and the prepared McFarland standard were also compared visually. Furthermore, the inoculum suspension was used within 30 min of standardisation, which is a very important factor to avoid any change of the size of inoculum or loss of their viability. The viable cell density was confirmed by serially diluting and plating on TSA.

### **(iii) Inoculation of test plates with standardized bacteria**

100  $\mu\text{L}$  of standardised bacterial inoculum were spread over the plate's surfaces containing Mueller-Hinton agar using a sterile cotton swab to get a uniform microbial growth on both control and test plates. For uniformity of bacterial growth, a sterile cotton swab was dipped into the standardised bacterial inoculum suspension, and then it was streaked over the entire dried surface of 40 mm MHA plates twice. The agar plate was swirled about  $60^\circ\text{C}$  each time to ensure that the inoculum was evenly distributed on the entire agar surface. To get rid of excess moisture from the inoculated plates their lids were left partly open for about 5-10 min in an oven but not less than 15 min.

### **(iv) Application of impregnated discs to inoculated agar plates**

Using sterile forceps, the discs which had been impregnated with 10  $\mu\text{L}$  of plant oil samples (African walnut oil, cashew nut oil and pumpkin oil) alone, with commercial antibiotics with known concentration were applied on the inoculated MHA once it has completely dried. Commercial antibiotics with known concentration impregnated with 10  $\mu\text{L}$  of plant oil samples were also placed on the MHA plates. The disks were pressed gently to ensure uniform contact with agar surface so that the oils can penetrate the agar. Furthermore, each one of the test plates was comprised of no more than four treated discs which were placed about equidistance to each other to avoid the overlapping of inhibition zone. The four treated discs includes: 1 disc moistened with 10  $\mu\text{L}$  of 0.05% (v/v) DMSO was placed on the inoculated agar plate as a negative control, 1 disc moisten with 10  $\mu\text{L}$  of oil sample (1000 mg/mL) only, 1 antibiotic disc of known concentration of antibiotics and another moistened with 10  $\mu\text{L}$  oil sample. A wide range of antibiotic was used (Table 5). All agar petri-dishes were sealed with sterile laboratory parafilm to avoid evaporation of the test oil samples. The plates were left for 30 min at room temperature to allow the diffusion of oil, and then they were inverted and incubated at  $37^\circ\text{C}$  for 24 h. Control plates were prepared using DMSO and mineral oil. After the incubation period, the zones of inhibition around the treated discs were measured in millimeter (mm) with

a ruler and interpreted using the CLSI zone diameter interpretative standards. Zones were classified as resistant or susceptible based on the diameter of the zones. Studies were performed in triplicate to ensure reproducibility, and mean value was calculated. The means were analyzed by two-way analysis of variance (ANOVA).

### **2.5.3.2 Minimum inhibitory concentration (MIC) of African walnut, cashew and pumpkin oils with their respective extracts**

To effectively identify the concentration range for biofilm experiments, initially the minimum inhibitory concentration (MIC) of African walnut oil, cashew oil and pumpkin oil and their respective extracts were determined by the micro broth dilution assay using 96 well microtiter plates described by Mahboubi *et al.*, (2011) and Sallleh *et al.*, (2016). The inoculum of MRSA 252 and ATCC 6538 were prepared from 18 h overnight cultures and suspensions were standardized to 0.5 McFarland standard turbidity. The standardised oils were prepared in a concentration range of 0.98 – 500 mg/mL. In setting the 96 well microtiter plate, wells A-F were reserved in each plate for negative control. 100  $\mu$ L of sterile TSB was added to the wells from rows B to H. After this, 100  $\mu$ L of the stock solution of each oil sample (from 1000 mg/mL) were added to the wells at rows A and B. Then both the mixture of samples and sterile broth 100  $\mu$ L at row B was transferred to each well to obtain a two-fold serial dilution of the stock oil samples (concentration of 500, 250, 125, 62.5, 31.25, 15.6, 7.8, 3.9, 1.95 and 0.98 mg/mL. After serially diluting the oil samples, 100  $\mu$ L of each standardized inoculum ( $10^8$  CFU/mL) was added to each well. The final volume in each well was 200  $\mu$ L. Streptomycin sulphate for bacteria 20  $\mu$ g/mL was used as positive control to monitor the results. The plates were then incubated at 37 °C for 24 h. Thereafter, the optical density (OD) values of the samples in each well/plate were measured at 600 nm ( $OD_{600}$ ) wavelength. MIC was defined as the lowest walnut, cashew and pumpkin oil concentration resulting in no visible growth compared to the control bacterial suspension (growth control that is untreated control). Wells (G-H) with sterile TSB served as negative control.

### **2.5.3.3 Determination of MICs of antibiotics**

Different concentrations of streptomycin, chloramphenicol and vancomycin, was prepared by diluting their powders in sterile distilled water. Rifampicin and trimethoprim were prepared by diluting the powders in dimethyl sulfoxide (DMSO) to completely dissolve since they do not dissolve in water. MICs of antibiotics namely vancomycin, chloramphenicol, rifampicin,

streptomycin and trimethoprim, gentamicin, for *S. aureus* strains in biofilm were determined using the broth micro-dilution method as recommended by the CLSI, (2013) and described by Xing *et al.*, (2012). For this analysis, under a septic condition, biofilms were developed by growing cultures of *S. aureus* in MHB prepared overnight at 37°C for 18 h without shaking. Overnight cultures were diluted 10-fold (1:10) in fresh MHB giving OD<sub>600</sub> = 0.4 resulting in 5.0×10<sup>5</sup> cfu/mL. Following standardization 100 µL of the bacterial cultures were distributed into each well of the 96 well microtiter plate and incubated at 37°C for 24 h for biofilm formation. After 24 h incubation, the 96 well microtiter plate containing *S. aureus* biofilms were washed three times with 4 mL of sterile PBS to remove any free floating bacteria and a serial two-fold dilution of each antibiotic sample prepared in water or DMSO resulting in concentrations ranging from 50 µg/mL to 0.195 µg/mL for vancomycin and streptomycin, 125 to 0.49 µg/mL for trimethoprim and rifampicin, 250 to 0.98 µg/mL for gentamicin and lastly 100 to 0.41 µg/mL was added to each well in the 96-well plate (100 µL per well) and incubated at 37 °C for 24 h. Each of the antibiotics was separately tested. Rows G-H in the plate served as negative control wells for media only and antibiotic alone, while column 12 served as positive controls containing biofilm and saline. After incubation, growth on the plates were assessed by measuring the optical density at 600 nm by using a FLUOstar Omega plate reader (LABTECH, UK).

#### **2.5.3.4 Minimum biofilm inhibitory concentration (MBIC) of African walnut, cashew and pumpkin oils with their respective extracts**

Plant oils and extracts which showed clear inhibition zone and is within the breakpoint established in the CLSI, (2012) guidelines for antibacterial susceptibility testing were further tested to determine their MBIC values by broth micro-dilution. MRSA 252 and ATCC 6538 biofilms were first performed by placing 100 µL of the standardized inoculums 10<sup>8</sup> CFU/mL into rows B-H of the 96-well polystyrene tissue culture plates covered with lid and incubated for 24 h at 37 °C. After 24 h of incubation, the bottom of each well of the 96 well microtiter plate was visually inspected for biofilm formation (adherent cells). When biofilm formation was confirmed, the free-floating cells (planktonic cells) in each well was carefully removed and each plate was rinsed with 200 µL of 1X sterile PBS to remove all free-floating cells from the wells. After washing, 100 µL of the freshly diluted TSB containing two-fold serial dilutions of each oil sample prepared to achieve concentration ranging from 0.98 -500 mg/mL was placed into each well. This dilution was to achieve a recommended final cell count of about 5

$\times 10^5$  CFU/mL after incubation for 24 h at 37 °C. After the incubation time, supernatant from all wells was discarded and biofilms that adhered to the bottom of the wells were incubated with 200  $\mu$ L of 0.1 mol/L of HCl (per well) for 90 min at room temperature. After this, HCl was replaced by 0.1 % safranin and the plates incubated for 35 min at room temperature (Figure 12). Nonbounded safranin was removed by rinsing the wells three times (3X) with distilled water, and thereafter each well of the plates were incubated with 125  $\mu$ L of 0.2 mol NaOH at 37°C for 1 h. After incubation, 100  $\mu$ L from the stained dissolved biofilm in each well was pipetted to a sterile new flat-bottom 96-well microtiter polystyrene plate and its intensity was measured at a wavelength of 600 nm using a plate reader.

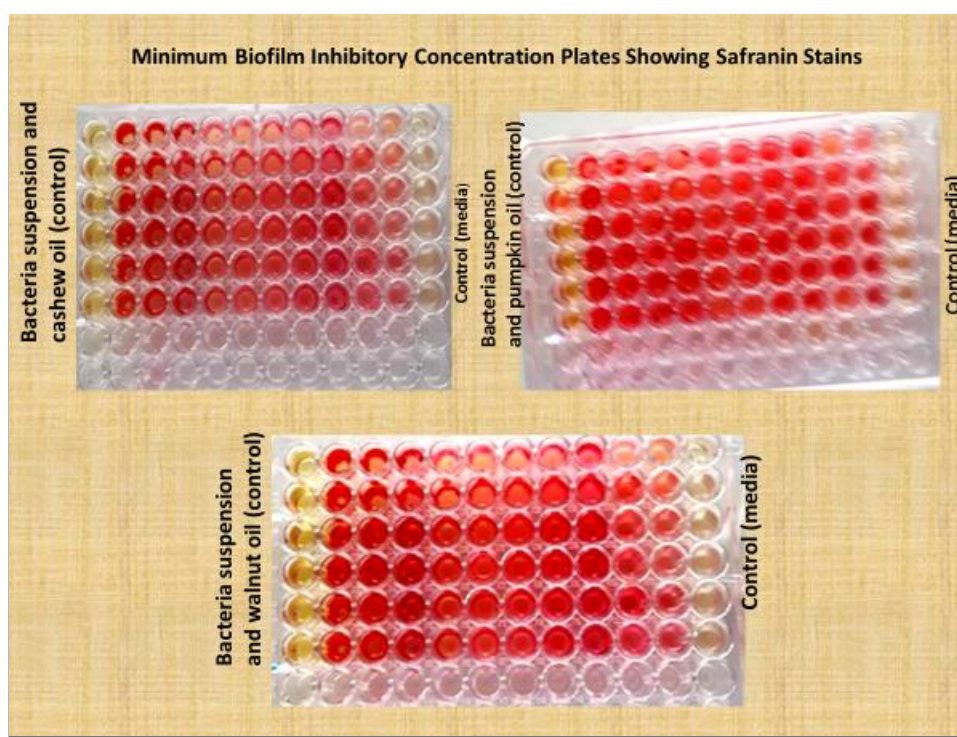


**Figure 12.** Example of separately prepared plates with oils for biofilm inhibitory concentration determined by broth microdilution method and safranin staining.

#### **2.5.3.5 Determination of minimum biofilm eradication concentration of African walnut, cashew and pumpkin oils on preformed biofilms**

Protocol outlined in the MBEC procedural manual for high throughput antimicrobial susceptibility testing of biofilms was followed strictly for this analysis. Broth microdilution procedure was employed to investigate the antimicrobial efficacy particularly the inhibitory effect of walnut oil, cashew oil and pumpkin oil against MRSA 252 and ATCC 6538 preformed

biofilms. In addition, other similar procedures for determining MBEC described by Nair *et al.*, (2016) and Deborah Corca-huber, (2012) was used. In this study MBEC was defined as the minimum concentration of oils that prevents a re-grow of MRSA 252 and ATCC 6538 biofilms or can eradicate their biofilms.

#### **(i) Growing subculture for MBEC assay**

In this assay, two subcultures of *S. aureus* strains were first prepared. A first subculture of *S. aureus* strains was streaked out on TSA plate and incubated statistically at 37 °C for 24 h. After 24 h, the first subculture was checked for purity that is no contaminant. The second subcultures were streaked out from the first culture and incubated at 37 °C for 24 h again.

#### **(ii) Inoculation and biofilm formation**

To successfully grow biofilm for MBEC assay, the MBEC™ Biofilm Inoculator with 96 well Base was used. Overnight inoculums were diluted to give a final organism density of  $1.5 \times 10^8$  CFU/mL in TSB which was poured into a reagent reservoir. Using a multichannel pipette, 150 µL of the inoculum was added to each well of the 96 well microtiter base packaged with the MBEC™ Biofilm Inoculator. The biofilm inoculator with peg lids was placed onto the 96 well microtitre base. While dispensing the inoculum into the wells, it was ensured that the orientation of the plate matches the orientation of the lid (i.e. peg A1 was inserted into well A1 of the microtiter plate, this was to ensure that the device was fitted correctly. The volume of 150 µL inoculum was used in this step to ensure that the biofilm covers a surface area of the peg that is immersed, entirely, by the volume of plant oils used in the challenge plate set up described below. The microtiter plate was placed in the incubator at 37°C for 48 h without shaking at 110 rpm.

#### **(iii) Biofilm growth check**

The peg lids were checked for biofilm growth by preparing a rinse plate for the individual oil. This was done by filling each well of a new sterile 96-well Nunc plate (Innovotech USA) with 200 µL of sterile distilled water (dH<sub>2</sub>O) to rinse the dispersed cells from the biofilms that have formed on the pegs of the MBEC™ device. Rinsing was done by immersing by the peg lid into the rinse plate for approximately 10 seconds. Following the rinse step and prior to the use of the antimicrobial challenge plate, the biofilm growth check (BGC) pegs (about 2 pegs) were broken off with sterilized (flamed) pliers and placed into 200 µL of TSB recovery media in

row A of a new sterile 96-well microtiter plate. The recovery plate was then transferred to the sonicator and sonicated on high amplitude for 30 minutes to dislodge the biofilm. Following sonication, 180  $\mu\text{L}$  of TSB was placed into each well of rows B-H, directly below the BGC pegs in row A of the recovery plate. A serial dilution ( $10^0$ - $10^7$ ) was prepared by transferring 20  $\mu\text{L}$  from each well in row A to each well in row B and so on down each of the 8 rows, mixing well and discarding tips between each transfer. 20  $\mu\text{L}$  from each well was removed and plated on TSA plates. Plates were incubated for  $37^\circ\text{C}$  for 48 h and colonies counted to determine the biofilm density on the pegs (Biofilm Growth Check).

#### **(iv) Preparation of the antimicrobial challenge plate**

Using a sterile nunc brand 96 well microtiter plate, the following steps described how the challenged plate was aseptically prepared. The challenge plate was prepared fresh on the day of the challenge for the three oil samples. 200  $\mu\text{L}$  of TSB was added to each well in columns 11 and 12 of the challenge plate. These wells served as the sterility controls, growth controls and biofilm growth checks. 100  $\mu\text{L}$  of TSB for the oil sample was added to each well in columns 1-10, rows B-H. 100  $\mu\text{L}$  of the standardised oil sample was added to each well in columns 1 to 10, row A of the microtiter plate and added to each well in columns 1-10, of rows B and C. Using a multichannel micropipette, the contents of columns were carefully and properly mixed in 1 to 10, row C by pipeting up and down. After mixing, 100  $\mu\text{L}$  was transferred from the wells in row C to the corresponding wells in row D. The contents of columns 1-10, row D was mixed and 100  $\mu\text{L}$  was transferred from each well to the corresponding wells in row E. The serial dilution and transfer process were repeated down the length of the microtiter plate until reaching row H. This dilution was performed for only the challenge columns (columns 1 to 10). After this, a multichannel pipette, was used to remove 100  $\mu\text{L}$  from each well in columns 1-10, row H and discarded. Then 100  $\mu\text{L}$  of TSB was added to each well in columns 1-10, rows C-H so that at the end each well of the challenge plate contains 200  $\mu\text{L}$ . Aseptically, the freshly prepared challenge plate was covered with lid and allowed to stand at room temperature for 30 min to equilibrate prior to use. Oxacillin was used as positive control in this analysis.

#### **(V) Antimicrobial challenge and recovery of the biofilm**

Following the rinse step and after breaking off the BGC pegs, the MBEC™ lid was transferred with biofilm growth to the prepared challenge plate described above and incubated for  $37^\circ\text{C}$  for 24 h. A new recovery plate was prepared by placing 200  $\mu\text{L}$  of TSB in each well (including growth and sterility control wells) of a new, sterile 96-well microtiter plate. The MBEC™ lid

from the challenge plate was transferred to the recovery plate and left to stand for 30 min to equilibrate. After the equilibration time, the recovery plate was transferred to the sonicator and sonicated on high speed for 30 min to dislodge the biofilms. After this the recovery plate is incubated at 37°C for 6, 12, 24 and 48 respectively. After each growth time conditions, the MBEC values, were determined by visually checking for turbidity in the wells of the recovery plate and plating out 100 µL of suspension per well on TSA. The mean of the viable counts of different concentrations of each oil sample per well for each bacterium was compared and analysed using one-way analysis of variance (ANOVA) with Bonferroni posttests. Result is reported in log reduction.

## **2.6 Molecular study of MRSA 252 and *S. aureus* ATCC 6538 virulence genes**

### **2.6.1 Scanning electron microscopy**

#### **2.6.1.1 Preparation of MRSA 252 and *S. aureus* ATCC 6538 biofilms for scanning electron microscopy (SEM)**

Before determining the appropriate timepoints for RNA extraction, changes in the morphological surfaces of each strain was initially observed using SEM along the different growth time point. Biofilms of MRSA 252 and ATCC 6538 cells for SEM analysis were grown on 24-well polystyrene tissue culture plates using the methods described by Asthan *et al.*, (2013) and Stepanovic *et al.*, (2007). Briefly, standardized inoculums of MRSA 252 and ATCC 6538 cells were prepared from overnight culture. This was done by diluting overnight culture 1:10 in fresh TSB supplemented with glucose (to enhance biofilm formation) and 5 ml aliquots were placed into each well (6 wells) of the polystyrene plate covered with lid. Plate for each strain was incubated in static position at 37 °C for 6 h, 12 h, 24 h and 48 h. After incubation at each time point, the plates were carefully washed two times with 4 ml deionized water to remove all planktonic cells. After washing, adhered cells were fixed with 4 % glutaraldehyde for 4 h. At each growth time point, the bottom of each well of polystyrene plate was cut to lens shape suitable for scanning electron microscopy. After cutting, the pieces were rinsed three times with 0.1 M sodium cacodylate buffer, and then fixed with osmium tetroxide for 1 h at 4 °C and samples dehydrated with 90 % ethanol. The samples were then mounted on pin tubs. All experiments were performed in duplicates at different scans.

## **2.6.2 RNA isolation from and MRSA 252 and *S. aureus* ATCC 6538**

### **2.6.2.1 Preparation of *S. aureus* biofilm cells for RNA isolation process**

The method described by Qiu *et al.*, (2011) and Atshan *et al.*, (2013) was used for this analysis. MRSA 252 and ATCC 6538 biofilm cells ( $5 \times 10^5$  CFU/mL) was separately grown on 24-well polystyrene tissue culture plates for 24 h at 37 °C after which they were treated with using the MBIC values of 31.25 and 15.6 mg/mL of African walnut oil, 125 and 62.5 mg/mL of pumpkin oils for 12, 24 and 48 h. Thereafter, each well of the plates were washed twice with 200 ml of sterile distilled water (dH<sub>2</sub>O). Biofilm was also grown for 6 h but it was used as control sample. After washing, the adhering bacterial cells in each well were disrupted and re-suspended in 1 mL of cold sterile distilled water by rapidly scraping them from the plate surface until no visible adherent layer was left. This was achieved using sterile micropipette tips and the bacterial suspensions were immediately incubated with 2 mL of RNA Protect (Qiagen) to stabilize the RNA before the bacterial cells were lysed. The bacterial suspensions were immediately vortexed for 5 s and incubated for 5 min at room temperature. The bacterial suspension was pelleted by centrifugation at 10000 xg for 10 min and the supernatant was discarded and residual supernatants were removed by gently dabbing the inverted tube onto a tissue paper and the cell pellets were obtained.

### **2.6.2.2 RNA isolation**

To the cell pellets (0.56 g from 12 h pellet, 0.98 g from 24 h and 1.2 g from 48 h pellet) and obtained after centrifugation, 200 µL TE buffer (30 mM Tris-Cl, 1 mM EDTA, pH 8.0) containing lysostaphin (12.5 µg/mL of 1mg/mL) and 200µl Qiagen proteinase K was prepared and then added to the pellets which was mixed by vertexing for 10 s thereafter, the suspension was incubated on a heat block for 30 min. During incubation, suspension was vortexed for 10 s at least every 5 – 10 min. After incubation, 700 µL RNeasy lysis buffer; RLT (with 10 µL β-mercapthoethanol per mL) was added and vortexed vigorously and centrifuged for 2 min at 12000 xg. Then, the supernatant was transferred into a new Eppendorf tube and 70 % ethanol (500 µL) was added and it was mixed immediately by pipetting up and down five times. The half of the mixture (700 µL) was then transferred to a RNeasy spin column and centrifuged for 15 s at 12000 xg. The flow through was discarded after centrifugation and reinserted in the collection tube. This step was repeated thrice to collect all bacterial lysate. Bacterial lysate was washed by 350 µL buffer RW1 and centrifuged for 15 s at 12000 xg and the flow through discarded. DNase 1 was prepared according to the manufacture's instruction. 10 µL DNase 1

was added to 70  $\mu\text{L}$  Buffer RDD, and added directly onto the centre of the RNeasy spin column membrane before incubation at room temperature for 15 min. Genomic DNA (gDNA) was removed from the mini spin column by buffer RW1 (350  $\mu\text{L}$ ) by centrifuging for 15 s at 12000  $\times g$ . The flow through was discarded and the mini spin columns placed in new tubes. RPE buffer (500  $\mu\text{L}$ ) was added two times to the same RNeasy spin column in two separate steps and centrifuged at 12000  $\times g$  for 15 s and 2 min, respectively, prior to discarding the flow through from the collection tube. RNA was eluted into a new 1.5 mL collection tube by adding 30  $\mu\text{l}$  of RNase-free water directly to the spin column and centrifuging at 12000  $\times g$  for 1 min. This step was repeated twice to elute all RNA.

### **2.6.2.3 Determination of RNA concentration**

After isolation, the RNA was kept on ice while proceeding to determine the RNA concentration of the samples using Nanodrop 2000 spectrophotometer (ThermoScientific, UK). Nanodrop was used to assess the yield and purity of RNA samples. RNA samples with an absorbance ratio 260/280 between 1.9–2.2 and 260/230 greater than 2.0 were used for further analysis.

## **2.6.3 Reverse transcription polymerase chain reaction (RT-PCR)**

### **2.6.3.1 cDNA synthesis**

The RNA extracted from both the treated and untreated biofilm cells were reverse transcribed into complementary DNA (cDNA) using a RevertAid first strand cDNA synthesis kit which consisted of three different steps which are described below. In the first step, random hexamer primer (1  $\mu\text{L}$ ), nuclease free water (1  $\mu\text{L}$ ), was added to 10  $\mu\text{L}$  RNA (10  $\text{ng}/\mu\text{L}$ ) giving a total volume of 12 and incubated at 65  $^{\circ}\text{C}$  for 5 min. After which the mixture was immediately placed on ice to chill. In the second step, reverse transcription master mix was prepared using the kit components supplemented with 12  $\mu\text{L}$  of the already prepared template RNA giving a total volume of 20  $\mu\text{L}$  (Table 4). In the third step, reverse transcription was performed in a thermal cycle. The thermal cycle settings were; primer annealing at 25  $^{\circ}\text{C}$  for 5 min (step 1), then reverse transcription at 42  $^{\circ}\text{C}$  for 60 min (step 2), and finally inactivation/termination of the enzyme at 70  $^{\circ}\text{C}$  for 5 min to stop the reaction (step 3). The final cDNA products were stored at -20  $^{\circ}\text{C}$  until further use.

**Table 4. Reverse transcription master mix components and volume used for the second step reaction of cDNA synthesis**

Component	Volume ( $\mu\text{L}$ )	
	Positive Sample	Negative Sample
Reverse transcription master mix		
5x reaction buffer	4	4
Ribolock RNase inhibitor	1	1
10 Mm dNTP mix	2	2
Revert Aid M-MuLV RT	1	1
Template RNA	11 (varied)	0
Random Hexamer	1	12
Final volume	20	20

### 2.6.3.2 Reverse transcription PCR (RT-PCR)

Complementary DNA sequences of the target genes used in this study were amplified through RT-PCR Table 5. The thermocycling time for the amplification of each adhesion and biofilm genes primer set (*icaA*, *icaB*, *icaC*, *icaD*, *fnbA*, *fnbB*, *fib*, *clfA*, *clfB*, *cna*, *ebps* and *eno*), antibiotic and food poisoning genes (*mecA*, *blaZ*, *emrA*, *seA*, *seB*) and selected reference genes (16S rRNA, *tpiA*, *rrsC*, *gmk*, *glyA*, *proC*, *rho*, *pyK*, *gyrA* and *gapdh*), is shown in tables 6-7 below.

**Table 5. The RT-PCR reaction mixture for all the target genes analysed in *S. aureus* ATCC6538**

Component	Volume ( $\mu\text{L}$ )
My Taq Red 2x mix	25
Forward Primer	1
Reverse Primer	1
Template cDNA	2
Nuclease free water	21
Total volume	50

**Table 6. The thermocycling temperatures and times used for RT-PCR amplification of each primer sets of adhesion and biofilm genes**

PCR phases	Temperature (°C)	Time (s)
Initial denaturation	95	60
Denaturation	95	15
Annealing	60	20
Elongation	72	10
Final hold		4°C

**Table 7. The thermocycling temperatures and times used for RT-PCR amplification of each primer sets of antibiotics and enterotoxins gene**

PCR phases	Temperature (°C)	Time (s)
Initial denaturation	95	1800
Denaturation	95	5
Annealing	55	30
Elongation	72	20
Final hold		4°C

## 2.6.4 Quantitative real time PCR (qRT-PCR)

### 2.6.4.1 Selection of optimal reference genes for normalization in quantitative RT-PCR of MRSA 252 and *S. aureus* ATCC 6538 biofilms

Ten reference genes were tested based on their common usage as endogenous control genes in previous studies. The genes were *tpiA*, *rrsC*, *proC*, *rho*, *rpoD*, *gyrA*, *glyA*, *gmk*, *pyk* and *16S rRNA*. Although 9 genes were eventually tested. The primers were obtained from previous publications and were confirmed whether they are present in *S. aureus* strains tested. The methods of Eleaume, (2000) and Crawford *et al.*, (2014) was used for the determination of the gene expression levels of the reference genes in MRSA 252 and ATCC 6538. The expression levels of nine selected reference genes in *S. aureus* biofilms at 12 h, 24 h and 48 h were calculated using cycle threshold values (Ct values) obtained after qRT-PCR analysis. Two reference gene normalization algorithms described in different software programs: geNorm (version 3.5) and NormFinder (version 0.953) was used to assess the expressional stability of the nine selected candidate reference genes.

### 2.6.4.2 Quantitative PCR analysis of target genes

Quantitative real time PCR was carried out to quantify the expression of the target genes on cDNA from MRSA 252 and *S. aureus* ATCC 6538 using the SensiFast SYBR Lo-ROX Kit. Multiple reference genes (16 S rRNA, *gmk* and *gyrA*) identified to be suitable for the analysis were used for normalization. Amplification plots and melting curves were used to confirm the PCR primers. After extracting RNA from each growth time point, the RNA concentration of each extract was normalized, and cDNA was obtained. Five microlitres (5 µL) of cDNA from the reverse transcription reaction (20 µL) was added to 45 µL of nuclease free water to obtain a final volume of 50 µL and the standard curve was obtained by a 10-fold serial dilution which was made as follows: 100%, 10%, 1%, 0.1% and 0% cDNA. The qPCR reaction was set up as described in Table 8 and analysed using the MJ Opticon Monitor Version 3.1 software.

**Table 8: The qPCR reaction temperature for the reference and target genes**

PCR phase	Temperature (°C)	Time (s)
Denaturation	95	300
Denaturation	95	20
Annealing	60	20
Extension	72	20

1 cycle  
40 cycles

### 2.6.4.3 Analysis qPCR results of the reference genes using the softwares

(i) Using the geNorm (version 3.5) The Ct values were first transformed/converted into relative quantification data using the delta-ct method. To achieve this data, the delta-ct formula was used:

$$Q = E^{-\Delta ct}$$

$$Q = E^{-(\text{min ct} - \text{sample ct})}$$

Q = Sample quantity relative to sample with highest expression  
 E = amplification efficiency (2 = 100%)  
 Min = lowest Ct value = Ct of sample with highest expression

Thus:

- a. The sample with the highest expression (lowest ct value) was set to 1
- b. The min Ct (lowest Ct value) was subtracted from the sample Ct. The result obtained was calculated in excel using the power function. And finally, the converted quantities; raw Cq values were directly analyzed by geNORM.

The geNorm software calculates the expression stability value (M) which are used to evaluate each individual reference gene candidate or each combination of reference genes, called a normalization factor (NF). Graph showing the M values of each reference gene (produced by the geNorm software) was used to identify the best stable individual reference genes. The most stable expressed genes yielded the lowest M value. GeNorm helps to identify a suite of reference gene and ends up by suggesting a pair of genes that shows high correlation and should be suitable for normalization of qPCR studies in *S. aureus*.

## (ii) Analysis using the NormFinder software

The NormFinder software computes a different type of stability value based on the intragroup and intergroup variation of the expression data. The software instructions from each package were followed when inputting the RT-qPCR data, fetching the output, and interpreting the analysis results.

### 2.6.4.4 Primer sequences used in this study

**Table 9: Primer sequences used in this study**

Primer pairs of selected adhesion and biofilm formation genes.					
Genes	Nucleotide sequence of primers (5' – 3')	Accession number	Annealing temp (°C)	Amplicon size	References
<i>icaA</i> (intercellular adhesion gene)	GAGGTAAAGCCAACGCACTC CCTGTAACCGCACCAAGTTT	AF086783	60	151	Atshan <i>et al.</i> , (2013)
<i>icaB</i> (intercellular adhesion gene)	ATACCGGCGACTGGGTTTAT TTGCAAATCGTGGGTATGTGT	AF086783	60	141	Atshan <i>et al.</i> , (2013)
<i>icaC</i> (intercellular adhesion gene)	CTTGGGTATTTGCACGCATT GCAATATCATGCCGACACCT	AF086783	60	209	Atshan <i>et al.</i> , (2013)
<i>icaD</i> (intercellular adhesion gene)	ACCCAACGCTAAAATCATCG GCGAAAATGCCCATAGTTTC	AF086783	60	198	Atshan <i>et al.</i> , (2013)
<i>fnbA</i> (fibronectin binding protein A)	AAATTGGGAGCAGCATCAGT GCAGCTGAATTCCCATTTTC	X95848.1	60	121	Atshan <i>et al.</i> , (2013)
<i>fnbB</i> (fibronectin binding protein B)	ACGCTCAAGGCGACGGCAAAG ACTTTCTGCATGACCTTCTGCACCT	X62992.1	60	197	Atshan <i>et al.</i> , (2013)
<i>fib</i> (fibrinogen binding protein)	CGTAACAGCAGATGCGAGCG TGCATCAGTTTTTCGCTGCTGGTTT	X72014.1	60	239	Atshan <i>et al.</i> , (2013)
<i>clfA</i> (clumping factor A)	ACCCAGGTTTCAGATTCTGGCAGCG TCGCTGAGTCGGAATCGCTTGCT	Z18852.1	60	245	Atshan <i>et al.</i> , (2013)

<b><i>clfB</i> (clumping factor B)</b>	AACTCCAGGGCCGCCGGTTG CCTGAGTCGCTGTCTGAGCCTGAG	A1224764.1	60	159	Atshan <i>et al.</i> , (2013)
<b><i>cna</i> (collagen binding protein)</b>	AATAGAGGGCCACGACCGT GTGCCTTCCCAAACCTTTTGAGCA	M81736.1	60	156	Atshan <i>et al.</i> , (2013)
<b><i>ebps</i> (elastin binding protein)</b>	GCACCGTGTTGCCTTCGAACT GGTGCAGCTGGTGCAATGGGTGT	U48826.2	60	191	Atshan <i>et al.</i> , (2013)
<b><i>eno</i> (laminin binding protein)</b>	TGCCGTAGGTGACGAAGGTGGTT TGCCGTAGGTGACGAAGGTGGTT	AF065394.1	60	195	Atshan <i>et al.</i> , (2013)
<b>Primer pairs of selected reference genes</b>					
<b><i>glyA</i> (Serine/glycine hydroxymethyl transferase A)</b>	CTACAAACTCACAGCCAC GTATCGGAAGCGGTTAT	NC_10788	55	98	Crawford <i>et al.</i> , (2014)
<b><i>gmk</i> (Guanylate kinase)</b>	CCATCTGGAGTAGGTAAAGG CTACGCCATCAACTTCAC	NC_10788	55	120	Crawford <i>et al.</i> , (2014)
<b><i>gyrA</i> (DNA gyrase subunit A)</b>	GTGTTATCGTTGCTCGTG CGGTGTCATACCTTGTC	NC_10788	55	97	Eleaume (2004)
<b><i>proC</i> (Pyrroline 5 – carboxylate reductase)</b>	GGCAGGTATTCCGATTGA CCAGTAACAGAGTGTCCAAC	NC_10788	55	104	Eleaume (2004)
<b><i>pyk</i> (pyruvate kinase)</b>	GCATCTGTACTCTTACGTCC GGTGACTCCAAGTGAAGA	NC_10788	55	89	Eleaume (2004)
<b><i>rho</i> (transcription terminal factor rho)</b>	GGAAGATACGACGTTTCAGAC GAAGCGGGTGGAAGTTTA	NC_10788	55	144	Eleaume (2004)
<b><i>rpoD</i> (RNA polymerase sigma factor)</b>	CACGAGTGATTGCTTGTC GATACGTAGGTCGTGGTATG	NC_10788	55	146	Crawford <i>et al.</i> , (2014)
<b><i>rrsC</i> (16S ribosomal rRNA subunit)</b>	CATGCTGATCTACGATTACT CCATAAAGTTGTTCTCAGTT	NC_10788	55	82	Crawford <i>et al.</i> , (2014)
<b><i>tpiA</i> (Triosephosphate isomerase B)</b>	GGTGAAACAGACGAAGAG TTACCAGTCCGATTGCC	NC_10788	55	145	Crawford <i>et al.</i> , (2014)
<b><i>16S rRNA</i></b>	GGGACCCGCACAAGCGGTGG GGGTTGCGCTCGTTGCGGCA	NC_10788	55	191	Eleaume (2004)

Primer pairs of antibiotic genes					
Genes	Nucleotide sequence of primers (5' – 3')	Accession number	Annealing temp (°C)	Amplicon size	References
<i>mecA</i> (Methicillin resistant gene)	TCCAGATTACACAACCTCACCAGG CCTTCATATCTTGTAACG		55	162	Steggar <i>et al.</i> , (2012)
<i>blaZ</i> (penicillin resistant gene)	TCCAGATTACAACCTCACCAGG CCTTCATATCTTGTAACG		55	173	Steggar <i>et al.</i> , (2012)
RNAIII (transcripts of agr locus)	GAATTTGTTCACTGTGTCGATAATCCAT TT GAAGGAGTGATTTCAATGGCACAAGAT AT	AP0031352	55	97	Eleaume (2004)
RNAII (transcript of agr locus)	TATGAATAAATGCGCTGATGATATACC ACG TTTTAAAGTTGATAGACCTAAACCACG ACC	AP0031352	55	101	Eleaume (2004)
<i>seA</i> (staphylococcal enterotoxin)	TGTTTCGGGTATTTGAAGATGG CGTTTCATAAGGCGAGTTGTT		55	154	Qui (2011)

#### 2.6.4.5 Data analysis using the standard curve method

The experiment of 22 selected genes at 12 h, 24 h and 48 h was calculated relative to the calibrator sample at 6 h and internal control 16 S rRNA, *gmk* and *gyrA*. The 6 h time point was chosen as calibrator since at this point of growth the strain did not form or showed any cell associated biofilm/fibrous material, in contrast to the 12 h, 24 h, and 48 h biofilm formation which was clearly seen on 24-well polystyrene plate. For each experimental sample, amplification plot, standard curves and melting curves were generated from 72°C to 90°C, reading every 1°C, hold at 30 s and data was subjected to analysis using the Livak method commonly known as the delta delta CT ( $\Delta\Delta CT$ ) or double delta CT and gene expression fold changes were calculated using  $2^{-(ddct)-method}$ .

#### 2.6.4.6 Agarose gel electrophoresis

The RNA samples after each extraction as well as RT-PCR samples from *S. aureus* biofilms at 6 h, 12 h, 24 h and 48 h were assessed by using 1 % agarose gel electrophoresis. The agarose gel was prepared by mixing 1 g of agarose with 100 mL of 0.5x TBE (Tris-borate EDTA) in a 250 mL Duran bottle then heating the mixture in a microwave oven. After the agarose had cooled to 55°C, 4  $\mu$ L of gel red was added and the content was swirled round severally to ensure proper mixing and poured into a gel tray to solidify/set for 35 min. The gel was subjected to

electrophoresis at 100 V for 120 min. The band sizes were imaged and recorded by UV-trans illumination and Gene Snap software.

## **2.7 Screening of oils of African walnut, cashew and pumpkin oils for synergy, biofilm kill time and determining the efficacy of oils in the treatment of staphylococcal infections using *Galleria mellonella* as an *in-vivo*-model**

### **2.7.1 Synergy test**

#### **2.7.1.1 Checker board assay**

Checkerboard method was used to further evaluate the synergic effect of walnut, cashew and pumpkin oil with conventional antibiotic drugs as observed in the disc diffusion test.

#### **2.7.1.2 Preparation of the microtiter plates for the checker board assay for antibiotics**

Overnight culture of *S. aureus* inoculum was diluted fresh with sterile MHB (1:100) to obtain a final concentration of  $1 \times 10^6$  cfu/ml. 100  $\mu$ L of this suspension was first distributed into each well of the micro-dilution plates and incubated for 24 h at 37 °C. After 24 h of pre-formed biofilm, the cell suspensions were gently aspirated and fresh 100  $\mu$ L of MHB was distributed into each well of the micro-dilution plates. Each of the antibiotic drugs tested (100  $\mu$ L working solutions) were serially diluted in MHB along the first column, while the second drug (plant oils) solution were serially diluted along the first row. Dilutions were started from the last well with a higher concentration towards the first well for each of the drugs tested. These concentrations were then diluted along the ordinate (vertical axis) and abscissa (horizontal axis) to obtain varying concentrations of the combined drugs. Antibiotics that had their MICs previously determined were used for the assay. The different concentrations used for checkerboard assay was same as those used individually. The entire resulting checkerboard contained each double serial dilution/combination of the two antimicrobial agents (plant oils and antibiotics), with wells that contain the highest concentration of each antibiotic at opposite corners. Controls containing antibiotics alone, plant oil alone, growth control (bacteria suspension alone), sterility control inocula in TSB alone were all included in the experiment as described in previous sections. The microtiter plates were incubated at 37°C for 24 h, and the MIC of the combination of both antimicrobial compounds was determined by visual inspection and read using the plate reader.

### 2.7.1.3 Fractional inhibition concentration

Calculation of the fractional inhibitory concentration (FIC) and FICI index (FICI) were determined as described by Mahboubi *et al.*, (2014) using the following equation.

$$\text{FIC of walnut oil} = \frac{\text{MIC (Walnut oil in combination with antibiotic)}}{\text{MIC (Walnut oil alone)}} \quad \text{Equation 3}$$

$$\text{FIC of pumpkin oil} = \frac{\text{MIC (pumpkin oil in combination with antibiotic)}}{\text{MIC (pumpkin oil alone)}} \quad \text{Equation 4}$$

All the antibiotics were calculated using the same equation. The ( $\Sigma$ FIC) index determines the interaction between the plant oils and antibiotics where the interaction is interpreted according to a range of values; values less than 0.5 as synergistic, values greater than 0.5-1 as additives.

### 2.7.2 Biofilm time-kill assay

The rate of kill of *S. aureus* within biofilms upon treatment with African walnut, cashew and pumpkin oil was evaluated. MRSA 252 and *S. aureus* ATCC 6538 biofilms pre-formed over 48 h were treated using in 24-well plate with 100  $\mu$ L of 62.5 mg/mL and 31.25 mg/mL of African walnut oil and 100  $\mu$ L of pumpkin oil at 250 mg/mL and 125 mg/mL dilution and 100  $\mu$ L of cashew oil at 500 mg/mL dilution previously made with TSB (MBEC concentrations were used). The biofilms were treated for 12, 24 and 48 h. The same procedure described in previous sections was used but the concentration of oils differs.

### 2.7.3 Preliminary assessment of the pathogenicity of MRSA 252 and ATCC 6538 and efficacy of African walnut oil in treating staphylococcal infections

#### 2.7.3.1 Collection of *Galleria mellonella*

Two hundred *G. mellonella* were purchased from Pet Home, Salford, UK. For the experiment, larvae in the fifth instar of their life cycle were used. The weights of the larvae varied, but on average their weights were between 100 and 290 mg. Very low weight and skin decolorization larvae with any obvious abnormalities were rejected. The larvae were used within a period of 6 days of purchase and no food or water was given to them. This was to starve them before infecting them. The larvae boxes containing approximately 45 larvae each after sorting were stored in 15 °C before use in the laboratory as previously reported by (Tsai, Loh & Proft 2016).

### 2.7.3.2 Bacterial strain and preparation for larval infection

Bacterial strains used in this experiment are MRSA 252 and ATCC 6538 strains. The method used to prepare bacterial strains for infection was a modification of the method described by Loh *et al.*, (2013). Briefly, single colonies of MRSA 252 and ATCC 6538 were both inoculated into TSB in 10 mL conical sterile tubes and cultured at 200 rpm in a shaking incubator (Camlab, UK) overnight at 37°C for 18 h. Next day the overnight culture in TSB with an optical density of >2.5 at 600 nm ( $OD_{600} = >2.5$ ) was obtained. 1 mL of the cultures obtained for MRSA 252 and ATCC 6538 strains were separately transferred into 2 mL Eppendorf tubes and centrifuged at 5000  $\times g$  for 10 min and re-suspended in PBS (1 mL) for washing and repeated centrifugation. Washing of the bacterial suspensions were done twice after which the washed cultures were re-suspended in 1 mL PBS again. Bacterial cultures were thereafter serially diluted with PBS saline to obtain dilutions of bacterial suspensions to final concentrations ranging from  $10^0$  to  $10^{-4}$  dilutions. These dilutions were prepared aseptically by transferring 100  $\mu\text{L}$  of the washed bacterial cells into a sterile 1.5 mL Eppendorf which contained 900  $\mu\text{L}$  sterile PBS, the suspension was mixed by gently shaking and pipetting the samples up and down two times. Another 100  $\mu\text{L}$  of this dilution was removed and transferred to a new tube containing 900  $\mu\text{L}$  sterile PBS. This process was again repeated the fourth time to produce 8 log dilutions. But 3 dilutions ( $10^0$ ,  $10^{-1}$ ,  $10^{-2}$  and  $10^{-3}$ ) were used for this experiment. The infecting dose was confirmed for each experiment by serial dilution and viable count of bacteria using the spread plate method. To test for infecting dose of MRSA 252 and ATCC 6538, twenty (20) *G. mellonella* larvae were set up as follows for the experiment;

**Group A** consisted of 20 non-infected larvae which served as negative control for the experiment

**Group B** consisted of 20 larvae inoculated with PBS and 20 mg of ampicillin to serve as positive control.

**Group C** consisted of 20 larvae for each dilution with 10  $\mu\text{L}$  MRSA 252/ATCC 6538 bacterial suspension aliquots injected into them through the last left proleg. Each strain was injected separately.

### 2.7.3.3 *G. mellonella* injection procedure

A 10  $\mu\text{L}$  Hamilton syringe (Fisher scientific, UK) 701N, with 10  $\mu\text{L}$  volume, 26 s, needle size was used to inject 10  $\mu\text{L}$  of PBS and ampicillin into them. Ampicillin was co-injected into them

to prevent infection by bacteria that are naturally present on the surface of the larvae (Tsai *et al.*, 2016). Although the area to inject was cleaned with ethanol 70 % swab (Ramarao *et al.*, 2012). In addition, 10  $\mu$ L of bacterial suspension of MRSA 252 and ATCC 6538 were also injected into the larvae. Similarly, the different bacterial dilutions prepared  $10^0$ ,  $10^{-1}$ ,  $10^{-2}$  and  $10^{-3}$  were also injected into the larvae groups. Both groups A, B and C were studied parallel in the infection investigation.

#### **2.7.3.4 Pathogenicity and monitoring of *G. mellonella* with MRSA 252 and ATCC 6538**

After injection, the different groups of larvae were incubated in petri-plates at 37°C in an incubator and survival was monitored every day (5 days). Daily, post infection check was carried out on *G. mellonella* larvae for the following features: melanisation, survival, cocoon formation. The number of dead versus survival larvae was recorded for each strain and group tested. An infective dose of bacteria was defined as one capable of causing an innate immune response, leading to the formation of melanin plaques around bacteria recognizable by the entire darkening of the cuticle. These plaques appear dark through the cuticle (Tsai *et al.*, 2016). The groups of larvae were incubated at 37 °C for 5 days, as bacterial virulence changes with temperature and this experiment was designed to mimic the development of infection in humans. In addition, *G. mellonella* were considered dead when they showed no movement in response to slightest touch with forceps and the development of melanin (black coloration). Each experiment was repeated at least three times, and representative experiments are presented here.

#### **2.7.3.5 Assessing the efficacy of African walnut oil in the treatment of staphylococcal infections using *G. mellonella***

To determine the efficacy of African walnut oil in treating infected *G. mellonella*, different formulated larvae groups were injected with lethal doses of MRSA 252 and ATCC 6538 ( $10^6$  CFU/mL) and then treated with 10  $\mu$ L of 31.25 and 15.6 mg/mL of walnut oil and vancomycin. The groups of larvae were incubated at 37 °C for 5 days and *G. mellonella* were considered dead when they showed no movement in response to slightest touch with forceps and the development of melanin (black coloration). Each experiment was repeated at least three times, and representative experiments are presented here.

## **2.8 Identification of the most active oil**

Identification of the active compounds were conducted according to bioassay guided isolation protocol. Briefly the active oil (walnut oil) obtained from screw press was first trans-esterified and separated by vacuum fractional distillation, followed by bioassay test to determine which fraction were most likely to have the active substances. The different fractions were finally analysed by spectrometry technique to possibly identify their molecular structures.

### **2.8.1 Analytical methods for identification of fatty acids in African walnut oil**

African walnut oil was extracted as described in section 3 of this thesis. In a bid to further confirm the activity of the screw pressed walnut oil and identify the fatty acids present in it, the oil was first trans-esterified into fatty acid methyl ester. After transesterification, the antimicrobial activity of the methyl ester product was tested for antimicrobial activity on MRSA 252 and *S. aureus* ATCC 6538. Further analytical investigations including GC-MS, infra-red, NMR and UV visible was conducted to identify the fatty acids in the oil that may be responsible for its activity. Except otherwise mentioned all analytical analysis was conducted on walnut oil alone.

#### **2.8.1.1 Fatty acid methyl ester (FAME) analysis**

African walnut oil was trans-esterified into (FAME) and the fatty acids were analysed as fatty acid methyl esters. Transesterification (Boron trifluoride methanolysis-BF<sub>3</sub>-MeOH) of walnut oil was done in accordance with the guidelines of International Olive Oil Council (IOOC, 2006). Briefly screw pressed walnut oil (1 g) sample was placed in a vial with screw cover and 2 mL of 0.5 mol/L NaOH-methanol solution was added. The mixture was heated at 100°C for 7 min and allowed to cool. After cooling, 3 mL of 14% BF<sub>3</sub>-MeOH reagent was added and the vial was sealed and heated for another 5 min at 100°C. After cooling, 3 mL of hexane and 7 mL of saturated NaCl solution were added and shaking vigorously. The resulting hexane layer (3 mL) sample was dried with anhydrous sodium sulphate and was left in a rack at room temperature (25°C) to settle. The upper hexane layer that was clear containing methyl esters was decanted into amber Agilent vials and stored at -20°C for GC analysis and other antimicrobial analysis.

### **2.8.1.2 FAME standard mix preparation**

A standard known as Supelco 37 component FAME mix (Supelco, Merck, Bellefonte, UK) containing methyl esters of fatty acids ranging from C8 – C24 including monounsaturated and polyunsaturated fatty acids was used for the experiment as reference to aid in the identification of fatty acids. Stock of mixed supelco standard was prepared by weighing 100 mg into a 100 mL volumetric flask and made up to volume with hexane (HPLC grade) therefore making a 1 mg/mL stock.

### **2.8.1.3 Gas liquid chromatography/mass spectrometry (GC-MS) analysis**

A trans-esterified sample of African walnut oil was sent to GlycoAnalytics Services, San Diego, United States) for accurate analysis. African walnut methyl ester sample was pre-analysed by injecting 1 $\mu$ L and profiling of fatty acids were done using an Agilent 6890N Gas Chromatography device (Agilent Technologies, Wokingham, United States). Profiling and quantification of fatty acids were achieved using Restek-5MS (30 m x 30 mm x 0.25  $\mu$ m) column. Column temperature was programmed at 80°C for 3 min, and then raised to 220°C at 4°C min<sup>-1</sup> and then held for 3 min. The carrier gas was helium with a column flow rate of 1.12 cm<sup>3</sup> and the Mass detector transfer line temp: 280°C. The fatty acids were identified and quantified by comparing sample peak retention times with those of known mixed supelco 37 standards of known composition and mass fragmentation pattern of standard mixture of FAME (Supelco, UK). Also, peaks were identified by comparing the mass spectra with the mass spectral data base in NIST Library 2008.

## **2.8.2 Fractionation of the active African walnut oil**

### **2.8.2.1 Vacuum fractional distillation**

African walnut oil previously extracted using cold press method was further purified by fractional distillation. Fractional distillation is a process of separating a mixture of compounds into different fractions (Silvestre *et al.*, 2016). Briefly, the method described by Torres *et al.*, (2012) and Silvestre *et al.*, (2016) was used for the analysis. Walnut oil was fractionated using vacuum distillation. Vacuum was used because the boiling of the expected fatty acid compounds is far above 230 °C (230-361 °C). A volume of 250 ml of walnut oil was introduced in a round bottom flask that has three different outputs for different purposes; output B had a capillary tube to control and stabilize the ebullition occurring in the round bottom flask; the

output temperature controller 1 (output TC1) was used to introduce a temperature sensor to monitor the oil temperature during the distillation process in order to prevent high temperatures, and lastly the third output (output B) was used to connect the packed column. Fractional distillation was done by heating the walnut oil sample and fractions evaporate and then condense in its own compartment. The size of the fractionating column was 1.5 m in height and it was packed with titanium alloy. This alloy material was selected to prevent corrosion. Temperatures in the condensers were controlled by a thermostatic bath TECNAL, Model TE 2000) and the maintenance of the pressure of the system made by vacuum pump (TECNAL, Model TE 058).

### 2.8.3 Molecular structure identification

#### 2.8.3.1 Attenuated total reflectance fourier transform infrared spectroscopy (ATR-FTIR)

Infrared spectrum of the oils and fractions were measured using ATR-FTIR (Fourier transform infrared) spectrometer (Nicolet iS10, ThermoScientific, UK). The spectrophotometer is equipped with a detector of deuterated triglycine sulphate and connected to the software of an OMNIC operating system. Drops of oil samples were covered on the surface in contact with attenuated total reflectance (ATR) on a multibounce plate of zinc crystal at room temperature 25°C (Figure 13). FTIR spectra were collected in the frequency range of 4000 – 600  $\text{cm}^{-1}$ . At each point of measurement, the plate was carefully cleaned twice with acetone and dried with soft tissue before filling it with next sample. The spectra were recorded as transmittance values at each data point.



Figure 13: ATR-FTIR spectrophotometer

### 2.8.3.2 Ultraviolet visible spectroscopy analysis (Uv-visible)

The molecular absorption UV-visible spectra of the oils and extracts were determined by measuring the absorbance at 200-900 wavelength. Prior to measurement all samples were dissolved 1:100 in their corresponding solvents. Background noise was removed by blanking with corresponding solvents (chloroform, petroleum ether and n-hexane). A computer control spectrophotometer (Cary 300, Varian, UK) was used with a glass quart cuvette of a 1 cm optical path (Figure 14). Spectrophotometers are set to have linear absorbances from 0 to 1. The software package was used for data acquisition and processing.



Figure 14: UV-visible spectrophotometer

### 2.8.3.3 Nuclear magnetic resonance (NMR) spectrometry

NMR experiments were performed using Bruker AV400 NMR spectrometer (400 MHz) situated in the NMR laboratory of Salford Analytical Services centre. Samples of each fraction were dissolved in deuterated dimethyl sulfoxide-d<sub>6</sub> (DMSO-d<sub>6</sub>) and placed in 5 mm NMR tubes (Norell, United States). A drop of tetramethylsilane (TMS) was added to the sample solutions to serve as reference for the proton nuclear magnetic resonance <sup>1</sup>H, <sup>13</sup>Carbon attached proton test (APT) and carbon NMR (<sup>13</sup>C NMR) spectra δ (0) ppm. The NMR experiments were further analysed using Topspin software under automation controlled by iconmr.

## **2.8.4 Antimicrobial activity of fractions**

### **2.8.4.1 Disc diffusion assay of fractions**

Standardisation of bacterial cultures were performed as described in section 2.5.5.1 of this thesis. Briefly, freshly cultured test organisms were adjusted to a 0.5 Mc Farland standard turbidity, and then the bacteria strains were inoculated on Mueller Hinton (MHA) agar plates, respectively. The solution (15  $\mu\text{L}$ ) of each pure fraction (100 %) was embedded onto 6 mm sterile paper discs. The impregnated discs were placed onto inoculated agar plates and incubated at 37 °C for 24-48 h. At the end of the incubation time, the diameter of the zone sides of the paper discs were recorded in millimeters. All tests were performed under sterile conditions in triplicate. DMSO (15  $\mu\text{L}$ ) was used as negative control.

## **Chapter 3. Extraction of Plant Seed and Nut Oils and their Respective Extracts**

### **3.1 Introduction**

In recent years, many plant oils and their various constituents have been extensively studied for their antimicrobial properties against bacterial pathogens (Bansod and Rai, 2008). Oils from plants have been reported useful for the cure of various human health problems (Bansod and Rai, 2008). Oils have been used to treat skin infections, wounds and other health conditions. Their antimicrobial, antibacterial and antifungal properties make them active against bacterial pathogens. Nigeria has a wide variety of plant seed and nuts cultivated in different climatic regions of the country. Many compounds existing naturally in these crops have been reported useful for therapeutic purposes since ancient times (Tulp and Bohlin, 2004). Therefore, for this study African walnut, cashew and pumpkin were chosen based on their reported potentials in ancient times for treatment of bacterial infections

Seed and nuts oil extraction was carried out by screw press method, in order to preserve vital constituents contained in walnut, cashew and pumpkin. Having found that these plants contain an abundant quantity of secondary metabolites, which encompass physicochemical properties and to maximise the oil quality, the method of extraction helped to reduce the loss of active components. Plant extract was also extracted using soxhlet extraction method described by Jokić *et al.*, (2014).

This study used a screw press method and solvent extraction method that relies mainly on the capability of the solvents used to breakopen the cell wall of the seed and nuts, diffuse into the cells, solubilize the metabolites and lastly diffuse into the extractants. This procedure does not require the use of any other treatments to the seed and nut that may possibly affect the secondary metabolites that was extracted.

Ionescu *et al.*, (2017) investigated that oils can be obtained from seed or nuts through solvent extraction or mechanical methods and that pressing of oils involves the application of pressure using screw press or hydraulic press to force out oil. Thus, Ionescu and his co-authors thought that mechanical pressing is however, preferable because it yields good quality oil and it costs less to extract oils.

Puspita, (2015) determined that oil extraction is usually performed by a polar organic solvent such as ethanol and methanol targeting to extract a few compounds, this can be linked to the

ability of the solvents to increase cell wall permeability, facilitating the most efficient extraction of large amounts of polar and medium to low polarity compounds. Also, the use of less polar solvents such as hexane and chloroform are useful for the extraction of non-polar substances for example terpenoids and lipids.

This chapter is focussed on the extraction of plant oils and their extracts, physical characteristics of the oils and extract and preliminary assessment of both the oils and extracts.

## 3.2 Results

### 3.2.1 Extraction of African walnut, cashew and pumpkin oils

#### 3.2.1.1 Preparation of seed and nuts for extraction

The nuts and seed of African walnut, cashew and pumpkin were obtained from the healthy seeds and nuts which were sorted, oven dried and milled into powder. The milled seeds and nuts were then grounded into fine powder. The powders were packaged in airtight containers to maintain optimal conditions before extraction.

#### 3.2.1.2 Extraction and yield of African walnut, cashew and pumpkin oils

Oil was extracted from African walnut, cashew nut and pumpkin seeds using the screw press method. This involved pressing each respective seed and nut sample using an oil expelling machine. The recovery of oils after each extraction was recorded and a total average of the recovery of three extractions was used to calculate the percentage yield of oils sample (Table 10). A graphical representation of the percentage oil yields is presented in Figures 15. Furthermore, the physical appearances of the pressed oils are as shown below (Figure 17).

**Table 10. Yield of oils obtained from screw press after each extraction**

List of oils	Fresh weight of seeds (g)	Yield of oils (in gram)			Average yield of oils (g)	Percentage yield (%) calculated on average
		1 <sup>st</sup> extraction	2 <sup>nd</sup> extraction	3 <sup>rd</sup> extraction		
Pumpkin	200	25.00	25.67	24.50	25.06	12.53
Cashew	200	50.00	52.00	51.99	51.33	25.67
African walnut	200	18.00	17.90	18.02	17.97	8.99

A graphical illustration of the percentage oil yields is presented in Figures 15.

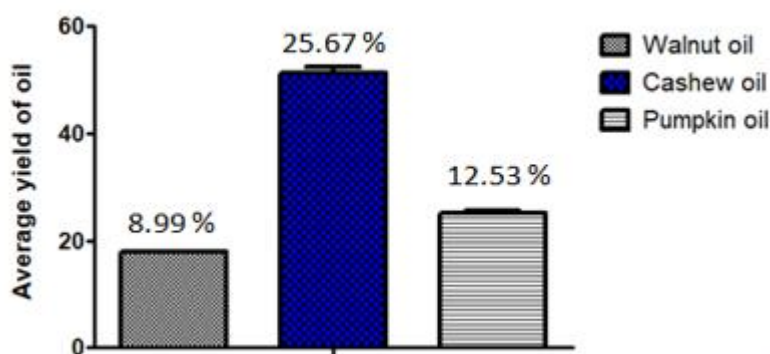


**Figure 15. A graphical representation of the average percentage yield of African walnut, cashew and pumpkin oils.**

Figure 15 shows the calculated percentage yield of extracted oils from African walnut, cashew and pumpkin. Each value on the graph depicts the mean yield of African walnut, cashew and pumpkin oils calculated after three independent extractions using the oil expeller. Percentage values above the bars represent the % yield of each oil sample. Bar values are represented as mean  $\pm$  SD. Using the screw press method, the percentage oil yield of African walnut, cashew and pumpkin was 8.99, 25.67 and 12.53 %. Cashew oil had the highest yield (25.67), followed closely by pumpkin oil (12.53 %) and lastly walnut oil (8.99 %).

### **3.2.1.3 Extraction and percentage yield of African walnut, cashew and pumpkin extracts**

In this study African walnut, cashew and pumpkin seed extracts were extracted with n-hexane, petroleum ether and chloroform using the soxhlet's extractor for 8 hours. The extracts were quantified after evaporating the solvents in a rotatory vacuum for 2 hours. The average yield of each extract was then determined as dry weight and percentage yield of each extract was calculated (Table 11, 12 and 13). Also graphical representation of the yield of African walnut, cashew and pumpkin extracts is shown below (Figure 16).

**Table 11. Average yields and percentage yield of extracts of African walnut (*Tetracapidium conophorum*).**

Serial No	Fresh weight of seeds (g)	Solvent Volume (mL)	Name of solvent	Average yield/recovery of extract after evaporation, dry weight (grams)	% Yield of extract
1	30	200	n-hexane	5.42	18.06
2	30	200	Petroleum ether	3.75	12.5
3	30	200	chloroform	3.59	11.97

**Table 12. Average yields and percentage yield of cashew (*Anacardium occidentale*)**

Serial No	Fresh weight of seeds (g)	Solvent Volume (mL)	Name of solvent	Average yield /recovery of extract after evaporation, dry weight (grams)	% Yield of extract
1	30	200	n-hexane	12.0	40.25
2	30	200	Petroleum ether	6.41	21.37
3	30	200	chloroform	5.01	16.70

**Table 13. Average yields and percentage yield of fluted pumpkin (*Telfaira occidentalis*)**

Serial No	Fresh weight of seeds (g)	Solvent Volume (mL)	Name of solvent	Average yield /recovery of extract after evaporation, dry weight (grams)	% Yield of extract
1	30	200	n-hexane	9.03	30.01
2	30	200	Petroleum ether	7.76	25.86
3	30	200	chloroform	5.96	19.86

According to Table 11-13, average dry weight and % yield of each plant extracts differs based on the type of solvent used for the extraction. African walnut (*Tetracapidium conophorum*) extracts obtained from n-hexane, petroleum ether and chloroform gave different dry weights of extracts and % yield. Based on Table 11, African walnut n-hexane extract dry weight was 5.42 gram with 18.02 % yield. Petroleum extract of walnut dry weight was 3.75 g with a % yield of 12.5 %. Chloroform extract of walnut dry weight was 3.59 g with a % yield of 11.97 %. From this result n-hexane extract of walnut gave the highest dry weight and % yield of extract followed closely by petroleum ether extract of walnut with a dry weight of 3.75 g and 12.5 % yield. Chloroform extract gave the least dry weight of 3.59 g and 11.97 % yield of extract.

Furthermore, Table 12 shows cashew (*Anacardium occidentale*) extracts. The case of cashew oil was not too different from African walnut and pumpkin. The n-hexane, petroleum ether and chloroform also gave varied dry weights of cashew extracts and % yield. Hexane extract of cashew dry weight was 12.0 g giving 40.25 % yield. Petroleum ether extract of cashew dry weight was 6.41 g giving a % yield of 21.35 % and lastly chloroform extract of cashew dry weight was 5.01 g giving a % yield of 16.70 %. Of all the results obtained in Table 11-13 n-hexane extract of African walnut, cashew and pumpkin gave better dry weights and % yield. Also, the result shows that the nuts of African walnut, cashew and seed of pumpkin dissolved better in n-hexane than petroleum and chloroform. In addition, petroleum ether even seems

good for the African walnut, cashew seed and pumpkin nut extraction. This is probably because n-hexane and petroleum ether extract are non-polar solvents capable of dissolving non-polar vegetable oils.

Based on Table 13 pumpkin seed (*Telfaira occidentalis*) extracts obtained from n-hexane, petroleum ether and chloroform also gave different dry weights of extracts and % yield. Pumpkin n-hexane extract dry weight was 9.03 g giving 30.01 % yield. Petroleum ether extract dry weight was 7.76 g with a % yield of 25.86 %. Chloroform extract of pumpkin dry weight was 5.96 g with a % yield of 19.56 %. From this result, the n-hexane extract of pumpkin gave the highest dry weight and % yield of extract. The second highest dry weight and percentage of yield was obtained from petroleum ether extract which gave a dry weight of 7.76 g and % yield of 25.86 %. Lastly chloroform extract of pumpkin gave the least dry weight of extract 5.96 g and 19.86 % yield.

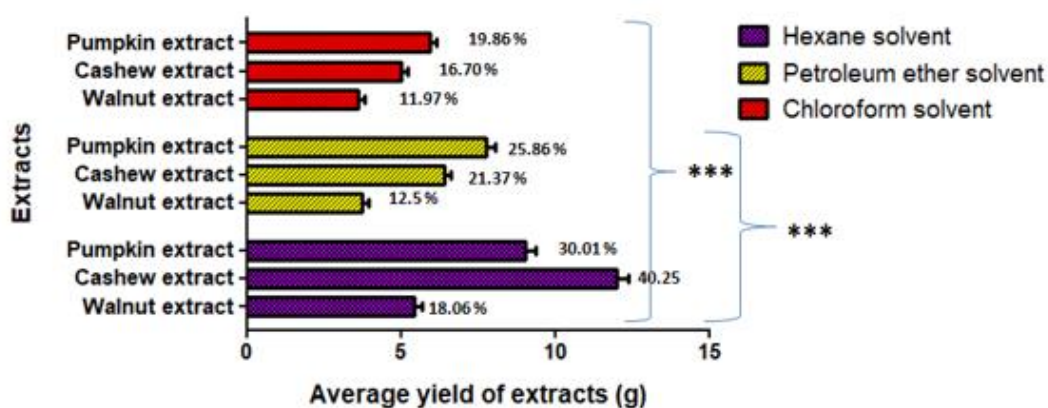


Figure 16. Graphical representation of the percentage yield of African walnut, cashew and pumpkin extracts

Figure 16 shows the average yield after consecutive extractions, and percentage yield of African walnut, cashew and pumpkin extracts compared to the initial weight of starting materials, the solvent types (petroleum ether, chloroform and n-hexane) used for the extraction. Each value on the graph represents the mean yield of each extracts obtained at three independent experiments  $\pm$  SD (n=3); two-way ANOVA using Bonferroni post-tests was used to test for significance difference between the extracts. Asterisks represent significant differences  $***p < 0.001$  between the three solvents used and between hexane and chloroform extracts. The average yield of each extract (dry weight) was determined after extraction, drying off the solvents and filtered. The average yield of extract in this study is the means of three independent extractions.

### 3.2.2 Physical characteristics of oils and extracts of African walnut, cashew and pumpkin

Both the screw pressed oils and extracts were assessed physically before using them for further analysis. After obtaining the wet extracts of African walnut, cashew and pumpkin seed from n-hexane, petroleum ether and chloroform, the wet extracts were dried separately in a rotator vacuum to get rid of the solvents and this became the dry weight samples. The dry extracts were then filtered and their physical characteristics in terms of colour and texture were recorded (Figure 18). For the screw pressed oils drying was not necessary so after extraction the physical characteristics were assessed immediately (Figure 17). Physical appearance of each oil and extracts was observed and results presented tables below.

**Table 14. Physical appearances of screw pressed oils**

Alphabetical order	Name of oil samples	Oil samples description
A	African walnut	Light brown
B	Pumpkin	Thick and brownish
C	Cashew	Light and yellowish

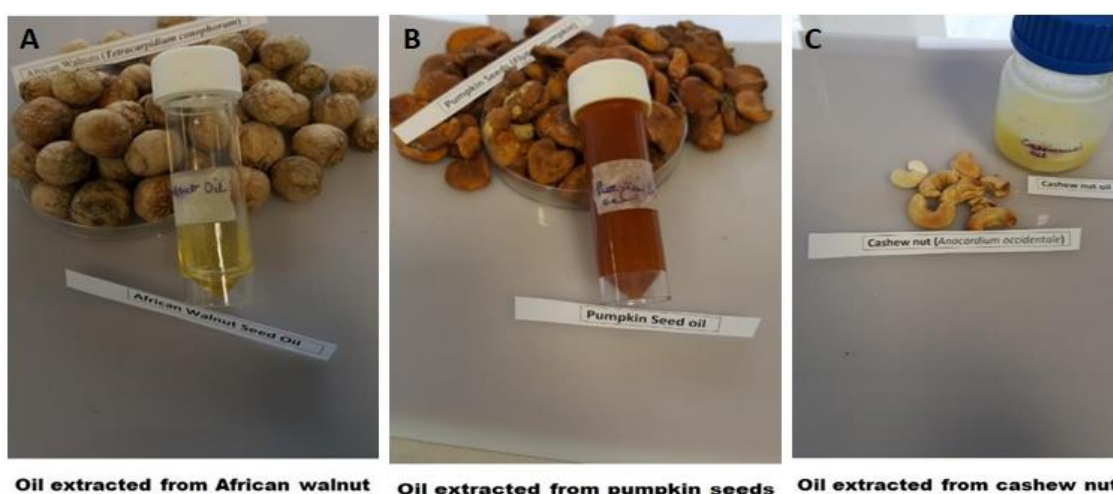


**Figure 17. Physical appearances of each oil sample as observed after extraction.**

The screw pressed oil extraction was started with the healthy nuts and seed of African walnut (*Tetracapidium conophorum*), cashew (*Anacardium occidentale*) and pumpkin (*Telfaira occidentalis*). The extraction resulted in light slightly brown oil, light and yellow oil of cashew and thick golden-brown oil of pumpkin.

Physical appearance of African walnut, cashew and pumpkin extracts are presented in Table 15 to 17 and Figure 18 below.

**Table 15. Physical appearances of solvent extracted African walnut (*Tetracarpidium conophorum*).**

Alphabetical order	Name of extract and solvent used	Extract description
A	African walnut	
	Hexane	Light and golden brown in color
	Chloroform	Light and golden brown in color
	Petroleum ether	Light and slightly brown in color

**Table 16. Physical appearances of solvent extracted cashew (*Anacardium occidentale*)**

Alphabetical order	Name of extract and solvent used	Extract description
B	Cashew	
	Hexane	Light and yellow in color
	Chloroform	Light and yellow in color
	Petroleum ether	Light and yellow in color

**Table 17. Physical appearances of solvent extracted pumpkin (*Telfaira occidentalis*)**

Alphabetical order	Name of extract and solvent used	Extract description
C	African walnut	
	Hexane	Thick and brown in color
	Chloroform	Thick and brown in color
	Petroleum ether	Thick and golden brown in color

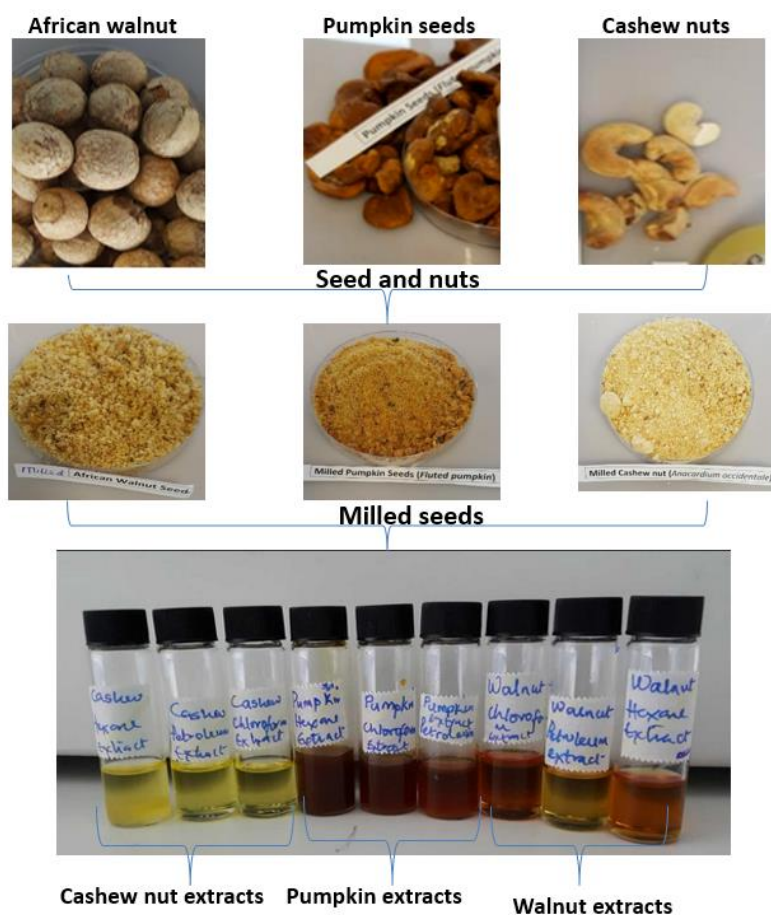


**Figure 18. Physical appearances of extracts of walnut, cashew and pumpkin**

Figure 18 shows the appearances and characteristic colours of African walnut, cashew and pumpkin extracts after extraction with n-hexane, petroleum ether and chloroform. Solvent extraction of African walnut with n-hexane, chloroform and petroleum ether yielded a light and golden-brown extracts. Solvent extraction of cashew with hexane, chloroform and petroleum ether yielded light yellow extracts. Solvent extraction of pumpkin with hexane, chloroform and petroleum ether yielded thick brown and golden-brown extracts.

### **3.2.3 Phytochemical screening of oils of African walnut, cashew and pumpkin with their respective extracts**

Initial screening of the oils and crude extracts constituents was performed to ascertain the phytochemical groups contained in each preparation. The results revealed the presence of saponin, terpenoid alkaloid, flavonoid, phenol and tannin in the screw pressed oils of African walnut and pumpkin. Alkaloids and terpenoids were not detected in chloroform and petroleum ether extracts of walnut and pumpkin. Saponin was not detected in screw pressed oil of cashew as well in its n-hexane and petroleum ether extract. Flavonoid was not detected in the cashew

chloroform and petroleum ether extract. From the results, oils of walnut, cashew and pumpkin had most of the vital photochemical present in them. Phytochemical results are presented in Tables 18-20.

**Table 18. Preliminary qualitative photochemical results of African walnut (*Tetracarpidium conophorum*)**

Phytochemical tests	African walnut and extracts			
	Hexane	Chloroform	Petroleum ether	Screw/Cold pressed oil
Flavonoids	+	+	+	+
Alkaloids	+	-	-	+
Saponins	+	+	+	+
Tannins	+	+	+	+
Terpenoids	-	-	-	+
Phenol	+	-	-	+

**Table 19. Preliminary qualitative photochemical results of cashew (*Anacardium occidentale*)**

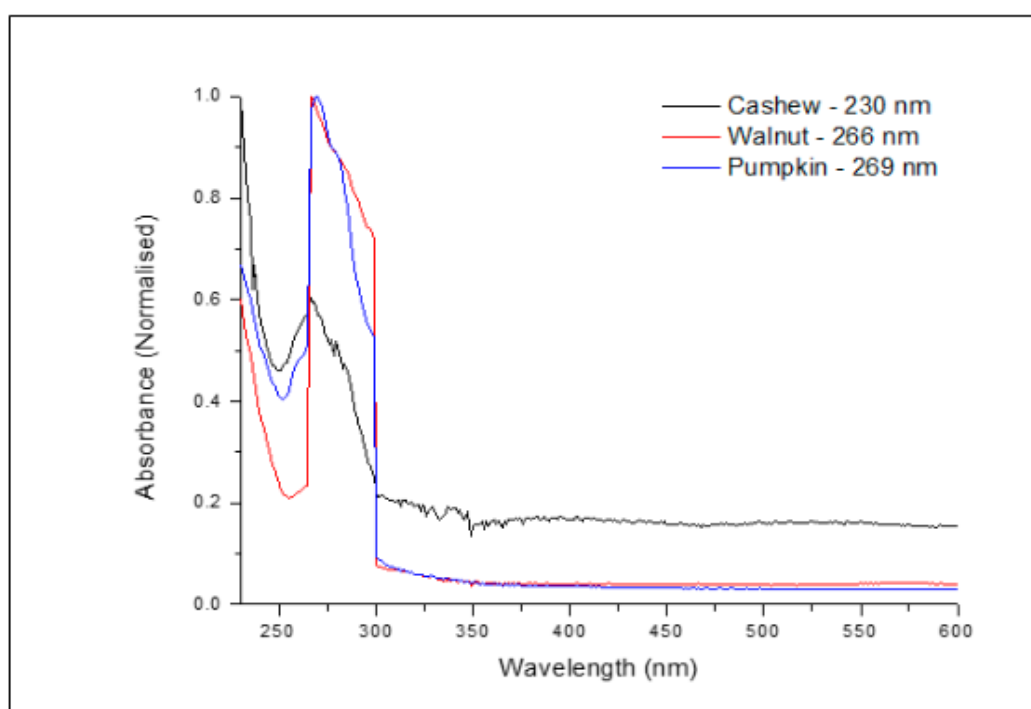
Phytochemical tests	Cashew and extracts			
	Hexane	Chloroform	Petroleum ether	Screw/Cold pressed oil
Flavonoids	+	+	-	+
Alkaloids	+	-	-	+
Saponins	-	-	+	-
Tannins	+	+	+	+
Terpenoids	+	+	+	-

**Table 20. Preliminary qualitative phytochemicals result of pumpkin (*Telfaira occidentale*)**

Phytochemical tests	Pumpkin oil and extracts			
	Hexane	Chloroform	Petroleum ether	Screw/Cold pressed oil
Flavonoids	+	+	+	+
Alkaloids	+	+	-	+
Saponins	+	+	+	+
Tannins	-	+	+	+
Terpenoids	+	-	-	+

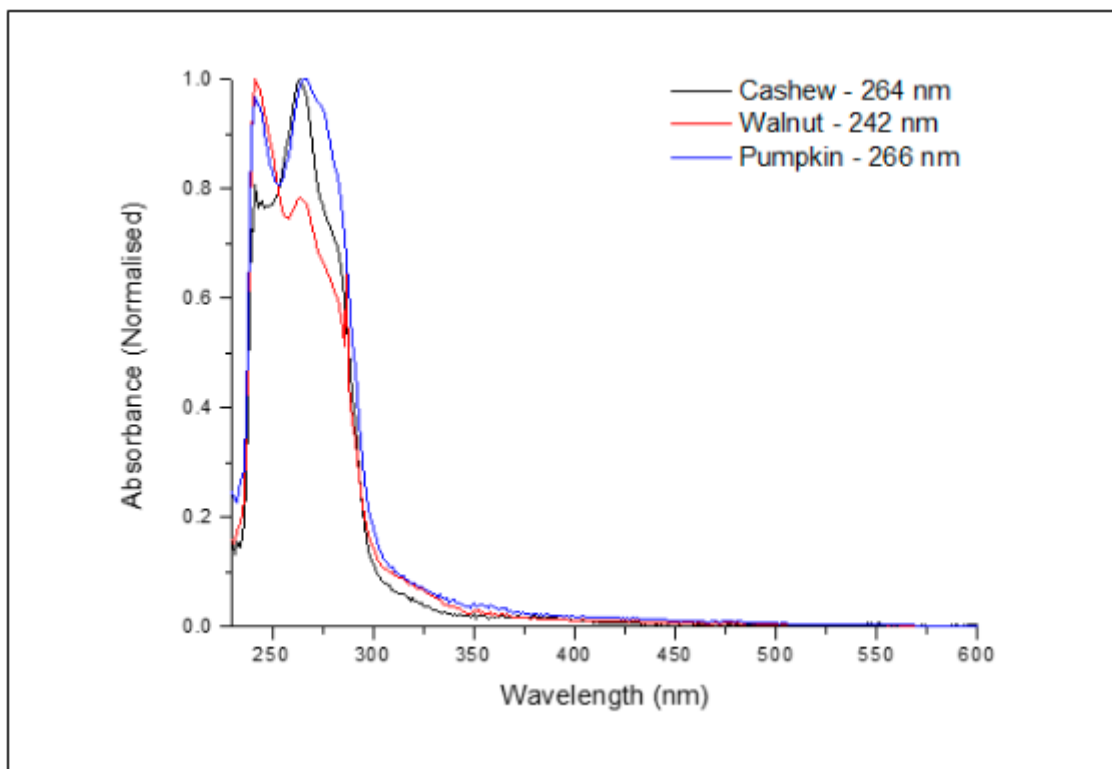
### 3.2.4 Ultraviolet absorption of plant oils and extracts

The ultraviolet absorption spectra of African walnut, cashew and pumpkin oils and extracts were measured from a solution consisting of a 1:100 dilution of the oils and crude extracts extracted with n-hexane, chloroform and petroleum ether. The UV-visible spectrophotometer used for the analysis was Cary 300 (Varian, UK). During measurements, background readings were first removed by measuring the spectra against the corresponding solvents (chloroform, petroleum ether and n-hexane). Glass quart cuvette of a 1 cm optical path was used to measure the absorbance. Due to nature of the colour of both the oils and extracts, the wavelength range for measurement was taken from 200 to 900 nm to cover all the pigment spectral range occurring in extracts (Puspita, 2015).



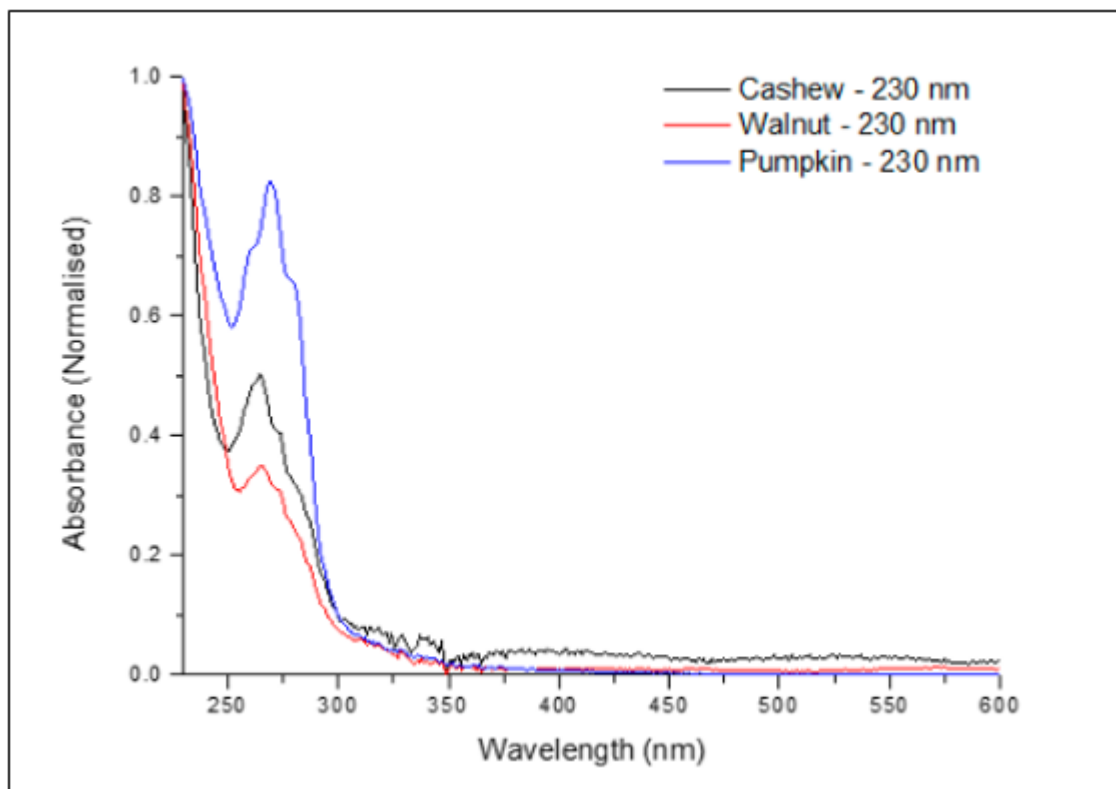
**Figure 19. Ultra-violet absorption spectrum of African walnut, cashew and pumpkin oils.**

Figure 19 shows the visible spectrum of screw pressed oils of African walnut, cashew and pumpkin. In the ultra violet region strong absorption peaks between 200 nm and 300 nm were observed for the oils. Oils of African walnut, cashew and pumpkin has the maximum absorption at a value of  $\lambda=266$  nm,  $\lambda=230$  nm and  $\lambda=269$  nm. Based on the data on the graphs, the three oils have absorption values less than 1.



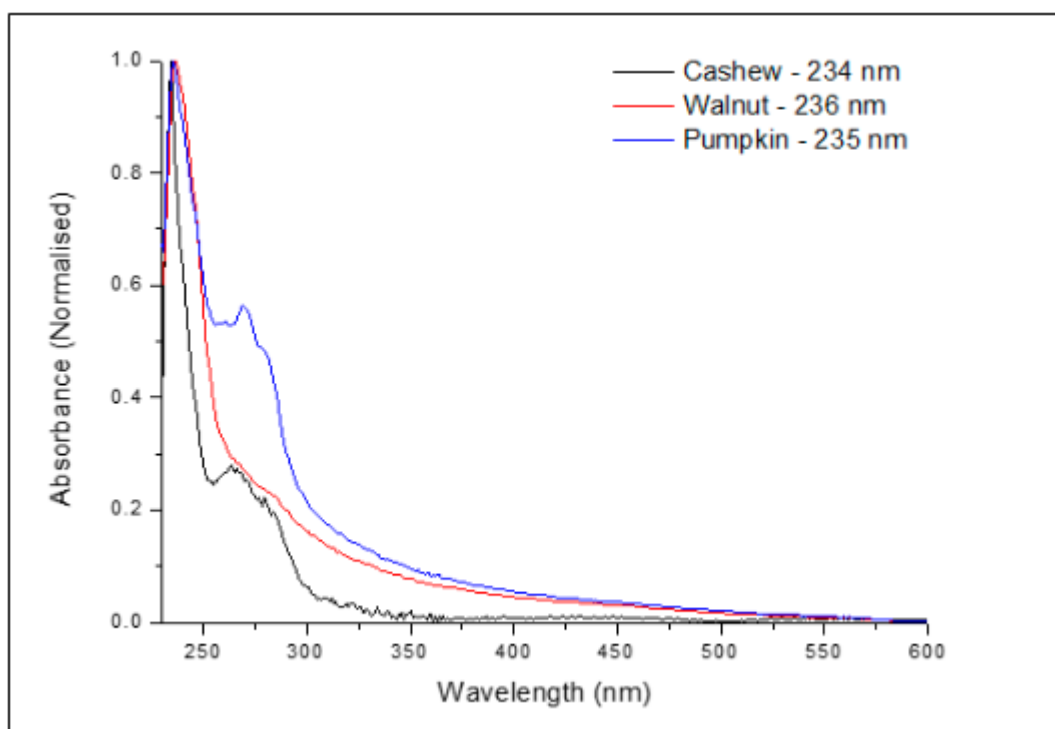
**Figure 20. Ultra-violet absorption spectrum of African walnut, cashew and pumpkin chloroform extracts.**

Figure 20 shows the visible spectrum of chloroform extracts of African walnut, cashew and pumpkin. In the ultra violet region strong absorption peaks between 200 nm and 300 nm were observed for the chloroform extracts. Chloroform extracts of African walnut has the maximum absorption at a value of  $\lambda=242$  nm. Cashew has maximum absorption at a value of  $\lambda=264$  nm while pumpkin extract has  $\lambda=266$  nm. It can be seen from the graphs that the three extracts showed absorption values less than 1. Although African walnut and pumpkin extracts showed more peaks than cashew extract.



**Figure 21. Ultra-violet absorption spectrum of African walnut, cashew and pumpkin petroleum ether extracts.**

Figure 21 shows the visible spectrum of petroleum ether extracts of African walnut, cashew and pumpkin. In the ultra violet region strong absorption peaks between 200 nm and 300 nm were observed for the petroleum ether extracts. Petroleum ether extracts of African walnut has the maximum absorption at a value of  $\lambda=230$  nm. Cashew has maximum absorption at a value of  $\lambda=230$  nm while pumpkin extract has  $\lambda=230$  nm. it can be seen from the graphs that the three extracts showed absorption values less than 1.



**Figure 22. Ultra-violet absorption spectrum of African walnut, cashew and pumpkin hexane extracts.**

Figure 22 shows the visible spectrum of hexane extracts of African walnut, cashew and pumpkin. In the ultra violet region strong absorption peaks between 200 nm and 300 nm were observed for the hexane extracts. Hexane extracts of African walnut has maximum absorption at a value of  $\lambda=236$  nm. Cashew has maximum absorption at a value of  $\lambda=234$  nm while pumpkin extract has  $\lambda=235$  nm. It can be seen from the graphs that the three extracts showed absorption values less than 1.

### 3.2.5 FTIR spectra analysis

ATR-FTIR of the oils were measured by the instrument Nicolet iS10 (ThermoScientific, UK). Infrared (IR) spectra were identified and analysed by OMNIC spectra software in a controlled computer. FTIR spectrophotometer was used to identify the functional groups of the active components present in oils from African walnut, cashew and pumpkin based on the peak values in the region of IR radiation. The IR spectra were accounted in % transmittance and the wave number region for analysis was  $4000-600\text{ cm}^{-1}$  (mid-infrared range). The results of FTIR analysis confirmed the presence of alkanes, alkenes, alkynes, aliphatics, aldehydes and esters in the oils which may be responsible for the antimicrobial activity of the oils (Figure 23-25).

### 3.2.5.1 FTIR spectra of African walnut oil

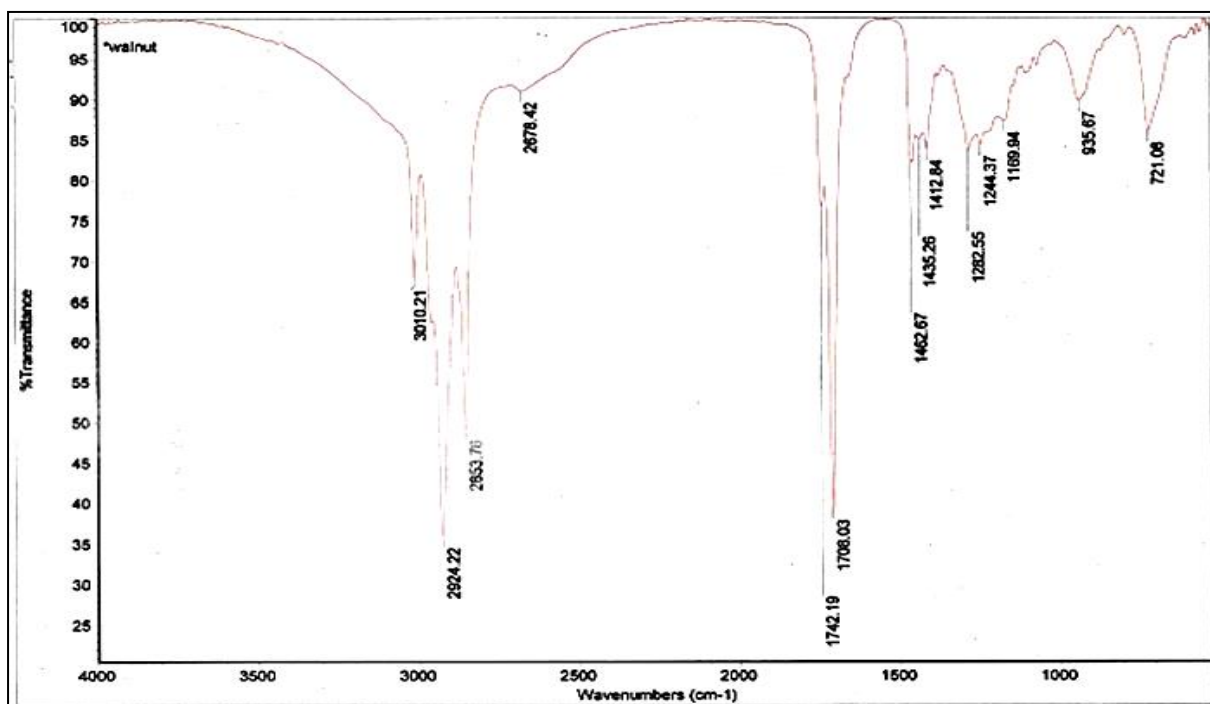


Figure 23. FTIR spectrum of African walnut oil.

Table 21. Infrared absorption of African walnut oil

Frequency (cm <sup>-1</sup> )	Peak assignment
3010	= C-H (cis) stretch Fatty acid back bone
2924	C-H methyl stretch asymmetrical
2853	C-H methyl stretch symmetrical Aliphatic group of triglycerides
2678	-CH <sub>2</sub> asymmetrical stretch
1742	-C=O stretch
1706	-C=O stretch
1462	C-H methylene scissoring
1435	C-H methylene scissoring
1412	C-H methylene scissoring
1282	-C-O stretch
1244	-C-O ester weak bending
1169	-C-O stretch; -CH <sub>2</sub> weak bending
936	C-H bending conjugated
721	cis-CH=CH bending conjugated

The IR frequencies in this study was assigned according to Tay *et al.*, (2002) and Liang *et al.*, (2012). Results presented in table 21 shows the position of absorption bands with the appropriate vibration in spectral range from 4000 to 600 cm<sup>-1</sup> for walnut oil.

### 3.2.5.2 FTIR of cashew oil

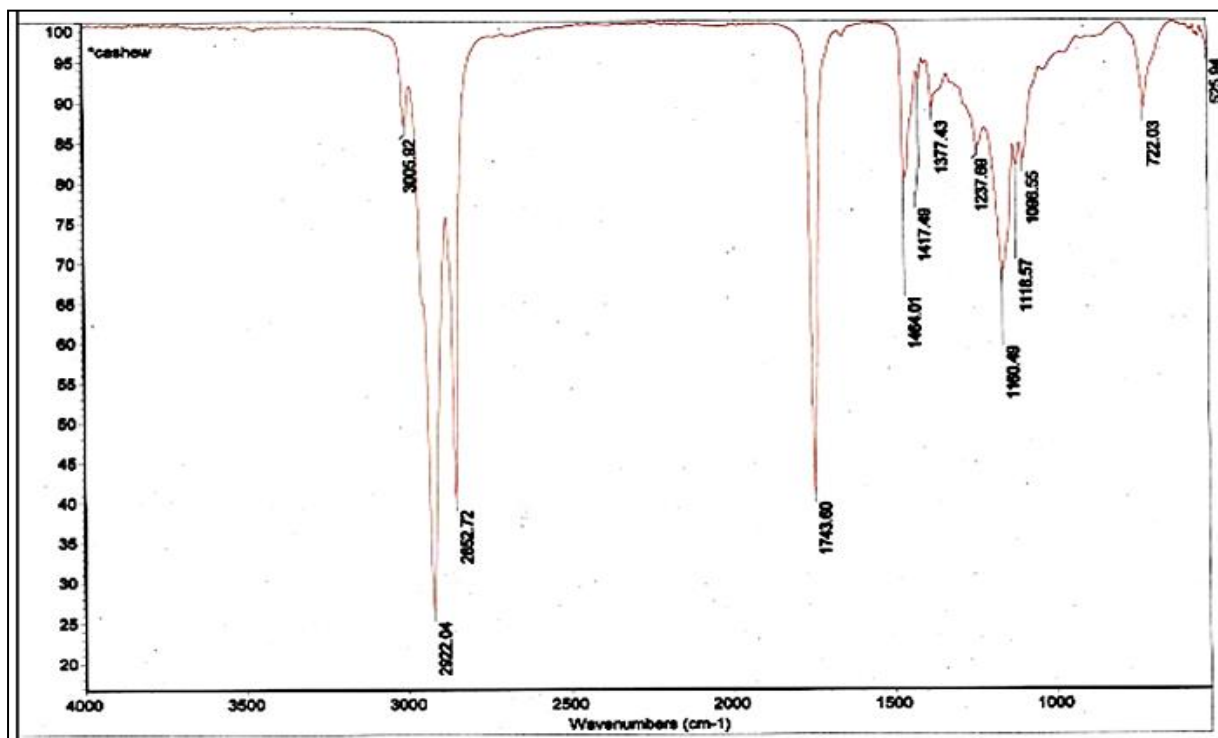


Figure 24. FTIR spectrum of cashew oil.

Table 22. Infrared absorption of cashew oil

Frequency (cm <sup>-1</sup> )	Peak assignment
3006	Trans C-H stretch Fatty acid back bone
2822	-CH <sub>2</sub> symmetrical stretch, aliphatics group triglycerides
2052	-CH <sub>2</sub> asymmetrical stretch
1743	-C=O in ester stretch
1484	-CH <sub>2</sub> bending
1417	cis = C-H bending
1377	-C-H or -CH <sub>3</sub> bending
1237	C-O or -CH <sub>2</sub> stretch
1160	C-O stretch or CH <sub>2</sub> bending
1116	Trans RCH=CHR
1096	-HC=CH trans bending
1000	-HC=CH trans bending
825	=CH <sub>2</sub> wagging
722	cis-CH=CH bending conjugated

The IR frequencies in this study was assigned according to Tay *et al.*, (2002) and Liang *et al.*, (2012). Results presented in table 22 shows the position of absorption bands with the appropriate vibration in spectral range from 4000 to 600 cm<sup>-1</sup> for cashew oil.

### 3.2.5.3 FTIR of pumpkin oil

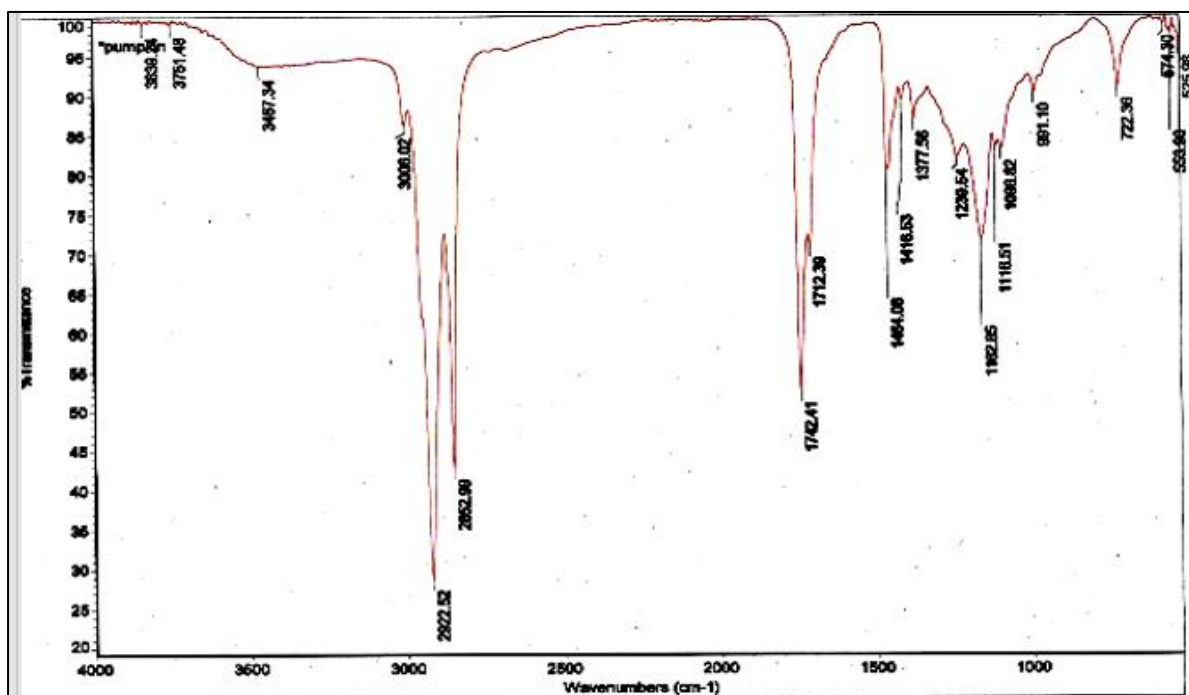


Figure 25. FTIR spectrum of pumpkin oil.

Table 103. Infrared absorption of pumpkin oil

Frequency (cm <sup>-1</sup> )	Peak assignment
3638	Trans C-H stretch Fatty acid back bone
3751	Trans C-H stretch Fatty acid back bone
3467	Trans C-H stretch Fatty acid back bone
3006	Trans C-H stretch Fatty acid back bone
2922	--C—H, CH <sub>2</sub> symmetrical stretch
2852	-C-H, -CH <sub>2</sub> asymmetrical stretch. Aliphatic group of triglycerides
1742	-C=O ester stretch
1712	-C=O in acid
1464	cis = C-H bending
1416	-C-H, -CH <sub>3</sub> bending
1377	-C-H, -CH <sub>3</sub> bending
1239	-C-O stretch or - CH <sub>2</sub> bending
1162	-C-O stretch or - CH <sub>2</sub> bending
1116	-C-O stretch or - CH <sub>2</sub> bending
1006	- C-O stretch
991	-HC=CH trans bending out of plane
722	cis-CH=CH bending conjugated

The IR frequencies in this study was assigned according to Tay *et al.*, (2002) and Liang *et al.*, (2012). Results presented in table 23 shows the position of absorption bands with the appropriate vibration in spectral range from 4000 to 600 cm<sup>-1</sup> for pumpkin oil.

### 3.3 Discussion

In this study, screw press method and solvent extraction was used to extract oils and extracts from African walnut, cashew and pumpkin to determine the efficient method in terms of antibacterial activity and yield of material. Results obtained in this experiment suggests that screw pressed oil has better antimicrobial activity than solvent extracted samples. Although, solvent extraction of three different solvents with different polarities gave higher yield of extracts. In the screw pressed oil samples, cashew oil produced the highest percentage yield of oil 25.67 %, followed by pumpkin oil 12.5% and lastly by walnut oil 8.99 %. The solvent extracts; chloroform, petroleum ether and n-hexane extract of walnut had percentage yield of 11.97%, 12.5 % and 18.06%, cashew had 16.70 %, 21.37 % and 40.25 %, pumpkin had 19.86 %, 25.86 % and 30.01 % respectively. N-hexane gave the highest yield of extracts. Physical observations of the screw pressed oil samples, African walnut, pumpkin and cashew oils were brown to yellow. Similarly, physical observation of the extracts, n-hexane, chloroform and petroleum ether were golden brown to yellow in colour. This result correlates with the findings of a research study performed by Odewole and colleagues (2015), who performed soxhlet extraction using various organic solvents to obtain pumpkin extracts. The authors reported that the yield was high when polar and non-polar solvents such as methanol, n-hexane and petroleum ether were used. Of the three solvents used by the authors, n-hexane produced the highest yield followed by petroleum ether and methanol. The result obtained was also like that of Okpashi and his colleagues (2013) who conducted soxhlet extraction using n-hexane and petroleum ether. The authors reported that the two solvents yielded high percentage of pumpkin extracts. However, n-hexane gave the highest yield. The increase in yield was thought to vary due to the different boiling points of the solvents used.

Phytochemical study of the oils and extracts shows the presence of saponin, alkaloid, flavonoid, tannin, and terpenoids in the extracts of cashew and pumpkin with n-hexane having the highest combinations of phytochemicals. The n-hexane extract of walnut shows the presence of various phenols, flavonoids, alkaloids, saponins and tannins, which seem to be different to that of cashew and pumpkin. Phytochemical-analysis presented in this thesis appears similar to the literatures. Iyewoka and co-workers (2016) reported that, from GC-MS analysis, walnut oil showed a positive result for alkaloids, terpenes, phenols, flavonoids and tannins. Also, the n-hexane extracts of walnut obtained from soxhlet extraction reported by Nyong *et al.*, (2009), gave positive result for alkaloids, tannins flavonoids, saponins. Mbatchou and Kosoona (2011) reported that from soxhlet extraction of cashew with n-hexane, alkaloids, flavonoids, steroids,

terpenoids were present and tannins was absent. Similarly, the result obtained corroborates the finding of Dorathy and Karpagam (2017). They authors conducted a preliminary phytochemical screening of cashew, using soxhlet extraction method with chloroform, petroleum ether and many other extracts. The authors found that the extracts showed the presence of alkaloids, saponin, phenol, tannin but absent for flavonoids.

Characterization of the oil samples and crude extracts was performed by using the uv-vis spectroscopy. All oil samples and extracts exhibited main bands within the range of wavelength 200-300 nm region in which the UV absorption for majority of the organic compounds such as flavonoids, tannin and phenols fall (Harborne, 1998; Tay *et al.*, 2002; Maduabuchi and Onyebuchi 2016).

Furthermore, FTIR spectroscopy analysis was used to screen the oils constituents, as it is a sensitive technique in identifying the functional groups present in samples (Rohman and Man, 2010). FTIR is used in phytochemical studies as a fingerprinting instrument for comparing the purified natural compound with a known standard (Christy *et al.*, 2004; Puspita, 2015; Altemini *et al.*, 2017). Therefore, the mass spectra presented in this study represents a fingerprint for the molecules. This fingerprint can be used to identify the compound to determine the purity of the natural compounds or the presence of contaminants resulting from the complex extraction and purification procedures. The absorbance of the FTIR light by the organic compound present in the oil samples corresponded to the energy required to cause the stretching or bending of the molecular bonds within each molecule. Different types of bonds require specific amounts of energy to initiate such molecular vibrations and accordingly, absorbed different frequencies of the FTIR radiation. Consequently, the absorption peaks plotted in each of the spectra reflects the types of chemical bonds present in the molecules. The FTIR spectra obtained for African walnut, cashew and pumpkin oils exhibited well defined spectral regions varied in the range of 4000–600  $\text{cm}^{-1}$ . The FTIR spectrum of African walnut oil shows, alkanes, alkene, esters and aldehyde compounds were present in the spectral range of 3010-2678  $\text{cm}^{-1}$  and 1462-1412  $\text{cm}^{-1}$ , 936-721  $\text{cm}^{-1}$ , 1282-1169  $\text{cm}^{-1}$  and 1742-1706  $\text{cm}^{-1}$ . Cashew oil also had alkanes, alkenes, esters and aldehydes in the range of 3006-2052  $\text{cm}^{-1}$  and 1484-1377  $\text{cm}^{-1}$ , 1096-722  $\text{cm}^{-1}$ , 1160-1237  $\text{cm}^{-1}$  and 1743  $\text{cm}^{-1}$ . Pumpkin also had alkanes in the range of 3638-2852  $\text{cm}^{-1}$  and 1377-1464  $\text{cm}^{-1}$ , esters 1006-1239  $\text{cm}^{-1}$ , aldehyde 1742-1712  $\text{cm}^{-1}$  and alkenes 991-525  $\text{cm}^{-1}$ . While comparing FTIR spectra of the oils, cashew oil spectra appear to have similar fingerprints with similar functional groups with those of pumpkin oil with minor shifts. Similar peaks with

frequency ( $\text{cm}^{-1}$ ) was observed at regions of  $1116 \text{ cm}^{-1}$ ,  $1377 \text{ cm}^{-1}$  and  $3006 \text{ cm}^{-1}$  in both cashew and pumpkin oils and  $1742 \text{ cm}^{-1}$  was observed in both African walnut and pumpkin oil. These similar peak regions denote the C – O stretching, C – H bending and C = O stretch of ester, alkane and aldehyde which indicate the roles of the oils in lysis of bacterial cell wall as the exhibit antimicrobial activity through formation of a complex with the bacterial cell wall. According to Nazzaro *et al.*, (2013), alkanes and aldehyde group has good antibacterial activity on bacteria.

In conclusion, the extraction of African walnut, cashew and pumpkin using both the screw method and solvent extraction with various solvents with different ranges and polarity gave varying yield of oils and extracts. African walnut and cashew had the highest yield of oils while the n-hexane extracts yielded more extract. The oils and extracts gave positive results for various phytochemicals such as tannin, saponins, phenols, alkaloids and flavonoids as the UV-visible spectrums. The IR spectra also suggested the occurrence of numerous functional groups related to oils and extracts. Overall, the data presented in this study provides confirmatory evidence of the rich mixture of constituents within the African walnut, cashew and pumpkin plant oils that could potentially play vital role in the biological and therapeutic uses as observed in these plants.

## **Chapter 4. Establishing the Methodology for the Identification and Biofilm formation of Methicillin Resistant (MRSA 252) and Susceptible *S. aureus* (ATCC 6538)**

### **4.1 Introduction**

Staphylococci pathogenic strains are the main cause of acute and severe infections due to their capability to form biofilms (Asthan *et al.*, 2012; Gowrishankar *et al.*, 2016). Although biofilm forming characteristics have been demonstrated by the pathogenic strains of the genus *Staphylococcus*, particularly, *S. aureus* and *S. epidermidis*, it is not well investigated in methicillin resistant staphylococcus aureus (MRSA) which have evolved from numerous clonal lineages of MRSA through acquisition of Staphylococcal cassette chromosome mec (SCCmec), known as mobile genetic element (DeLeo *et al.*, 2011; Gowrishankar *et al.*, 2016). The biofilm forming ability of MRSA has led to difficulty in treating Staphylococcal infections including its enhanced tendency to spread and cause deleterious human diseases across the globe. The initial monolayer of the bacteria that get stuck to a polymeric surface changes within few days to a common biofilm that includes bacteria and a slimy polymeric substance called extracellular slime material (Stoodley *et al.*, 2002). The spread of the bacteria and EPS production results in an increased drug resistance because antibiotics are prevented from reaching the bacteria that are protected by biofilm (Asthan *et al.*, 2012). Numerous studies have reported that the production of biofilm is caused by attachment at late phases of bacterial development (Stepanovic *et al.*, 2007; Archer *et al.*, 2011; Asthan *et al.*, 2012; Gowrishankar *et al.*, 2016). In this process, the bacterial attaches to each other by polysaccharide intercellular adhesion called PIA, which is produced by *icaADBC* operon (Archer *et al.*, 2011).

This chapter is focused on establishing the methodology of the identification of *S. aureus* strains, biofilm forming ability of MRSA 252 and *S. aureus* ATCC 6538. Finally, a discussion is presented to provide an overview of the biofilm formation of the strains.

## 4.2 Results

### 4.2.1 Confirmation of the strains

The strains used for this study were confirmed.

#### 4.2.1.1 Colony morphology of the strains on different agar media

MRSA 252 and *S. aureus* ATCC 6538 were grown on solid media so as to confirm them through their characteristic morphological appearances. MRSA 252 and *S. aureus* 6538 were confirmed before using them for analysis. TSA a general-purpose media was used to grow ATCC 6538. TSA was used to allow enough nutrients for the strain to grow. Columbia blood base agar, a selective media was used to grow MRSA 252 to specifically identify the strain. *S. aureus* ATCC 6538 and MRSA 252 were grown on TSA and Columbia agar to study their colony appearances and morphologies by visual observations. Visual observation of both strains was carefully conducted on the plates after streaking out a loop full of the frozen stock and overnight culture of each respective strain on TSA and Columbia agar and incubating the plates at 37°C for 24 h (Figure 26). Colony appearances and morphologies of each strain as observed visually are shown in Table 24.

**Table 24. Colony and morphological characteristics of MRSA 252 and *S. aureus* ATCC 6538 after 24 hours of culturing on different growth media**

Colony appearances and morphologies	ATCC 6538	MRSA 252
	Growth on TSA	Growth on Columbia blood base agar
Shape	Circular	Circular
Elevation	convex	convex
Size	moderate	moderate
Texture	rough	rough
Appearance	shiny	shiny
Pigmentation	golden yellow	Golden cream colonies

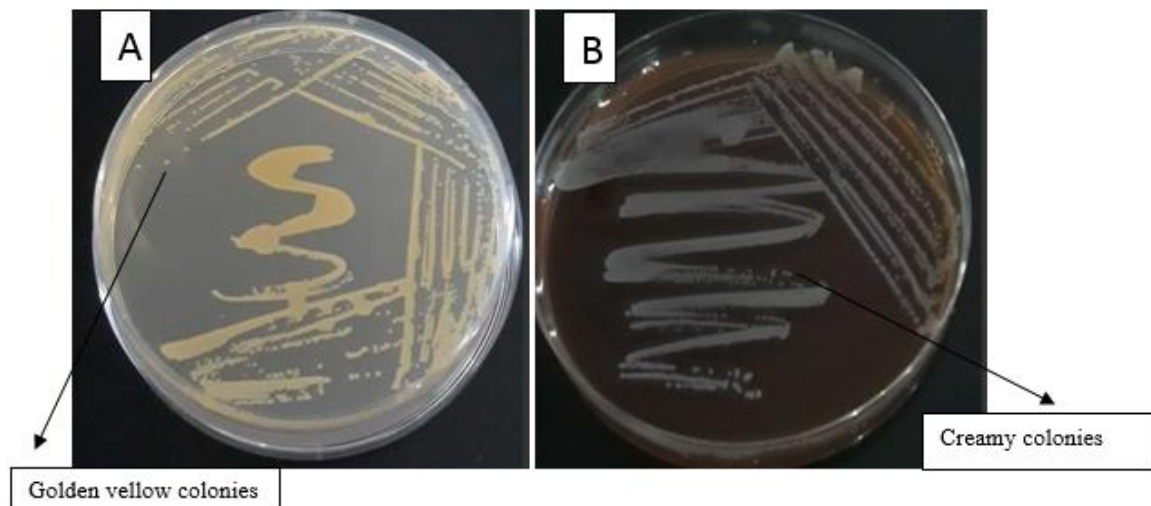
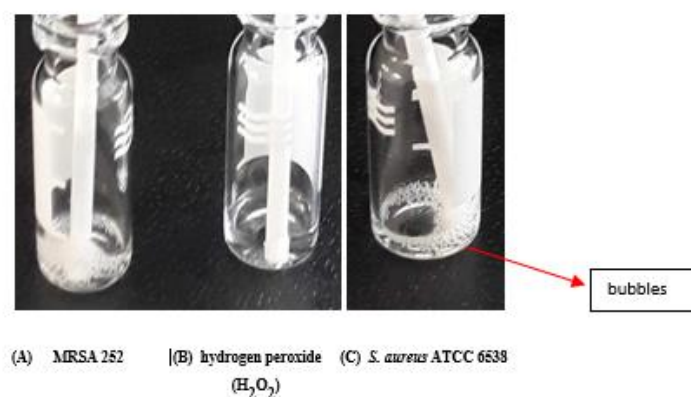


**Figure 26. Appearance of ATCC6538 and MRSA 252 on TSA and Columbia blood base agar**

Figure 26 shows Plate A: ATCC 6538 on TSA agar plate, plate B: MRSA 252 on Columbia blood base agar plate. Streaks showing growth of ATCC 6538 and MRSA 252 on TSA and Columbia agar. (A) Golden yellow colonies observed for ATCC 6538 on TSA (B) creamy colonies observed for MRSA 252 on Columbia blood base agar (B). Their growth on both plates was used to confirm the strains before using them for further analysis.

#### 4.2.1.2 Biochemical tests of *S. aureus* strains

Both MRSA 252 and *S. aureus* ATCC 6538 tested positive for catalase and lysostaphin tests which is a 2-5 h test. Both strains were also positive for coagulase test. These three methods were used for the rapid detection of the staphylococcus strains.



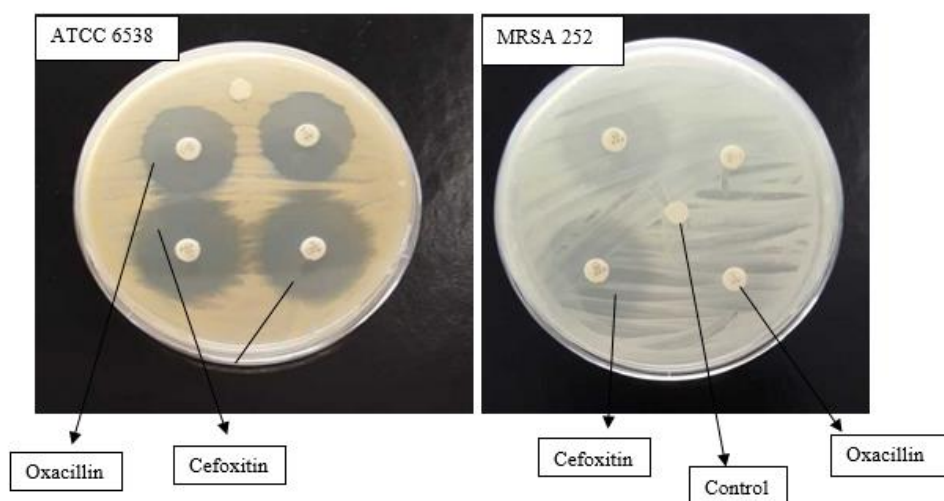
**Figure 27. Catalase test results of MRSA 252 and *S. aureus* ATCC 6538**

Figure 27 shows the formation of bubbles because of the breakdown of H<sub>2</sub>O<sub>2</sub> into oxygen and water. (A) Bubble formation from a loop full of 4-8 colonies of MRSA 252. (B) Negative

control: hydrogen peroxide solution alone (C) Bubble formation in *S. aureus* ATCC 6538 after placing 4-8 colonies into 20 mL of H<sub>2</sub>O.

#### 4.2.2 Antibiotic sensitivity test

Based on the CLSI method, MRSA 252 and ATCC 6538 were both screened for susceptibility and resistance using oxacillin 1 µg and cefoxitin 30 µg. Screening was performed using the disc diffusion method and the resulting clear zones were measured in diameter (mm).



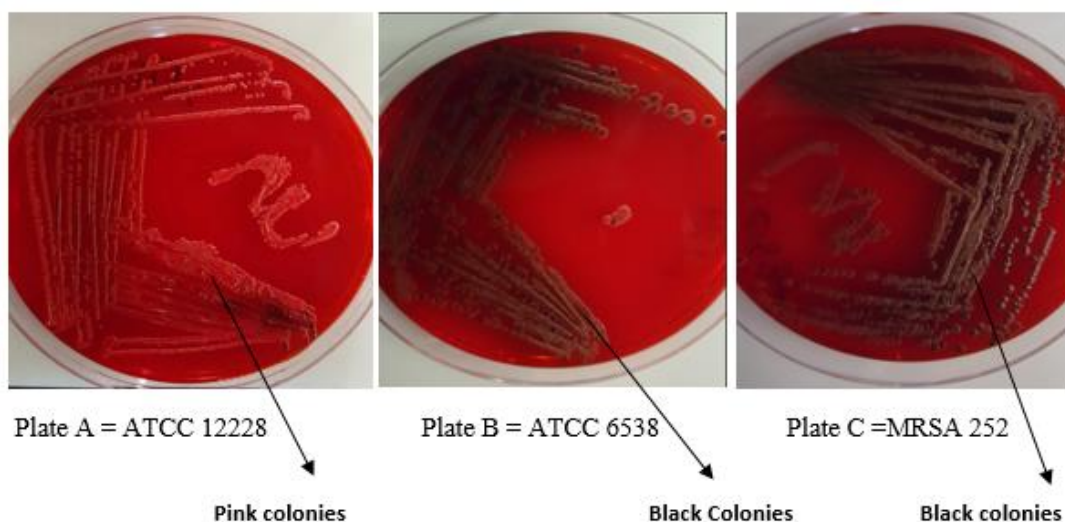
**Figure 28. Antibiotic confirmatory test of ATCC 6538 and MRSA 252**

Cefoxitin drug had a clear zone of 21 mm while oxacillin gave 19 mm. Similarly, MRSA 252 had a zone of 21 mm without a clear zone and no zones was obtained for oxacillin. Result therefore indicates that MRSA 252 is resistant to cefoxitin and oxacillin confirming that it is a methicillin resistant strain. Whereas ATCC 6538 is sensitive to both cefoxitin and oxacillin.

#### 4.2.3 Biofilm formation assay

##### 4.2.3.1 Phenotypic detection of MRSA 252 and *S. aureus* ATCC 6538 slime production on Congo red agar

The qualitative slime production was assessed on the basis of the color of *S. aureus* colonies developed on Congo red agar. Congo red agar was used to detect the ability of MRSA 252 and ATCC 6538 to form biofilm (slime) before using them for further analysis. To carry out this assay, Congo red agar was supplemented with glucose to help support the growth of the strains. Biofilm formation ability of the strains on CRA were characterized by the formation of black colonies.



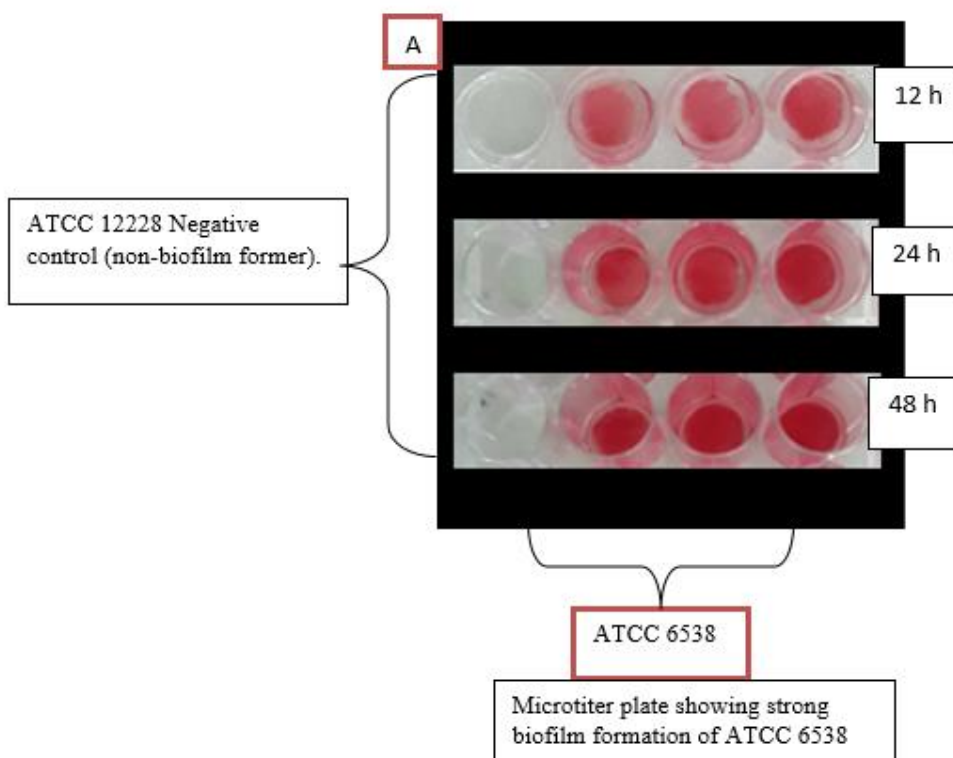
**Figure 29. Biofilm (slime) productions by ATCC 12228, ATCC 6538 and MRSA 252 on CRA plates**

Figure 29 show Plate A: Red colonies, non-biofilm former (negative biofilm producer); Plate B: black colonies of ATCC 6538, positive biofilm former; Plate C: black colonies of MRSA 252 positive biofilm former. Result shows that MRSA 252 and ATCC 6538 are positive biofilm formers producing black colonies on Congo red agar while ATCC 12228 was considered a negative biofilm producer. Based on the colony colors produced by each strain on Congo red, they were classified into very black, black and pink biofilm former showing various degrees of biofilm production.

#### **4.2.4 Quantification of biofilm formation by microtiter plate (MTP) method**

##### **4.2.3.2 Visual inspection of biofilm formation on 24-well tissue culture plates**

The biofilm forming ability of MRSA 252, ATCC 6538 and ATCC 12228 were visually examined for biofilm formation (adhered cells) on the 24 well polystyrene microtiter plates using the microtiter plate method (MTP). MRSA 252 and ATCC 6538 were grown separately in 24-well tissue culture plates containing TSA supplemented with 1% glucose. Figure 30 and 31 shows biofilm formation of ATCC 6538 and MRSA 252 on the polystyrene microtiter plates.



**Figure 30. Biofilm formation of ATCC 6538 on 24-well tissue culture microtiter plate.**

Figure 30 shows biofilm formation of ATCC 6538 on 24 –well polystyrene microtiter plate with surfaces stained with safranin. Visual observations of the microtiter plates revealed that there was evidence of biofilm formation for ATCC 6538 at 12 h, 24 h and 48 h. Biofilm formation was seen to be strong at 24 h and stronger at 48 h. At 48 hours the biofilm looked thicker on the 24-well plate. However, no biofilm formation was observed on the plates for ATCC 12228 which served as a negative control. At 12 h, microtiter plates had small biofilms formed compared to 24 and 48 hours. The results were reproduced at least three times and were confirmed in subsequent experiments. This result suggests that ATCC 6538 is a strong adherent biofilm former and capable of forming strong biofilms from 24 hours. Based on the result ATCC 6538 is moderately strong biofilm former.

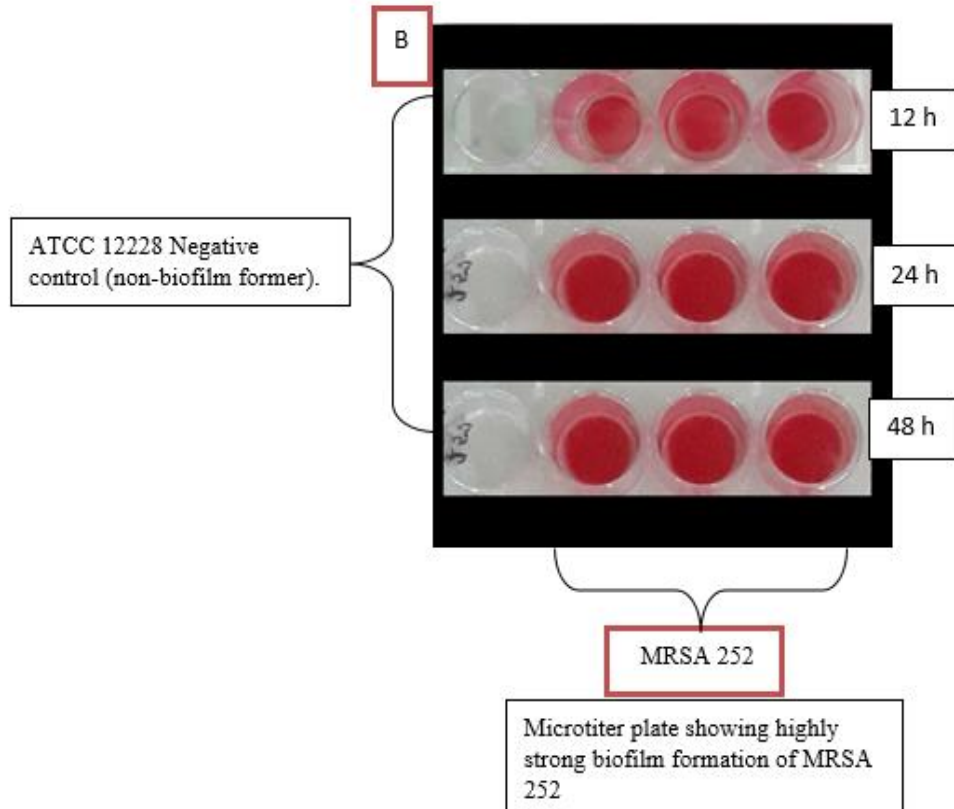


**Figure 31. Biofilm formation of MRSA 252 on 24-well tissue culture microtiter plate.**

Figure 31 shows biofilm formation of MRSA 252 on 24 –well polystyrene microtiter plate with surfaces stained with safranin. Visual observations of the microtiter plates showed that there was evidence of biofilm formation for MRSA 252 at 12 h, 24 h and 48 h, Biofilm formation was strong at 12 h and highly strong at 24 h and 48 h. Biofilm at 12 hours appears fairly strong, stronger and highly adherent at 24 and 48 hours. Compared to ATCC 6538, MRSA 252 seems to form stronger biofilms. However, no biofilm formation was observed on the plates for ATCC 12228 which served as a negative control. The results were reproduced at least three times with three technical replicates and were confirmed in subsequent experiments. Based on the result, MRSA 252 is a strongly adherent biofilm former.

#### **4.2.3.3 Quantification of *S. aureus* biofilms**

*Invitro* biofilm formation was spectrophotometrically quantified by performing polystyrene microtiter plate (MTP) assay as described above. After the visual inspection of ATCC 12228, ATCC 6538 and MRSA 252 microtiter plates for biofilm formations at 12, 24 and 48 hours, the safranin dye that was bound to the adherent cells was dissolved with 95% ethanol per well, and absorbance was measured at 595 nm (OD 595 nm). The optical density reading of wells containing ATCC 12228 was used as the negative control and an optical density value of 0.5

was selected as the cut-off point to differentiate as positive for biofilm formation and each strain was categorized based on the optical density value of the safranin-stained biofilms.

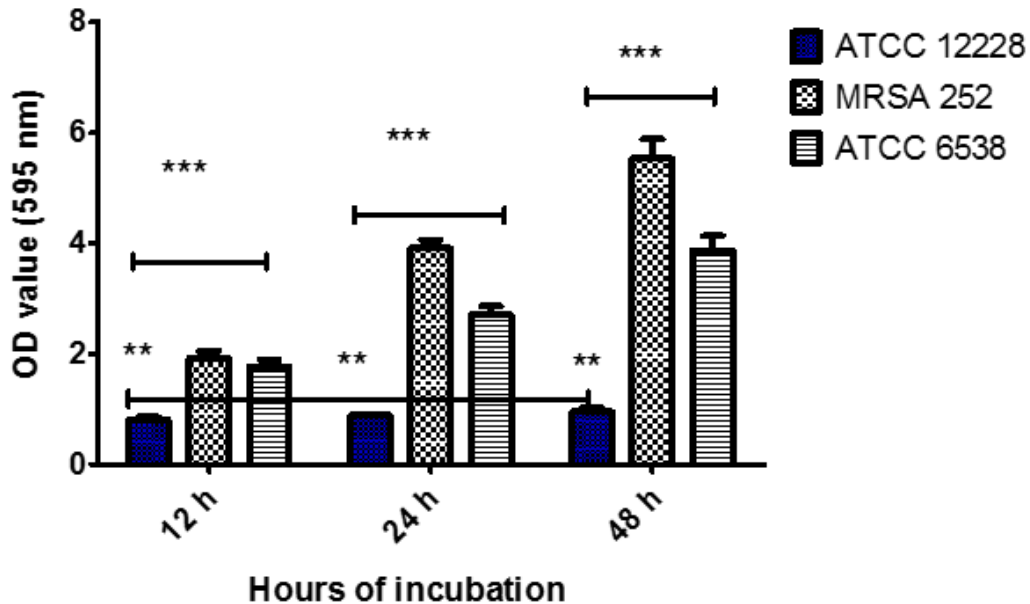


Figure 32. Quantification of ATCC 12228, ATCC 6538 and MRSA 252 biofilms formed on polystyrene microtiter plate after 12 h, 24 h and 48 hours at OD 595 nm.

Figure 32 shows that MRSA 252, ATCC 6538 produced biofilms that were adherent at varied levels: *S. aureus* strains were tested at three growth time point 12, 24 and 48 hours. Bar graphs represent the mean of biofilm formations  $\pm$  SD on 24-well tissue culture plates. The mean values refer to the mean OD values  $\pm$  standard deviation of three to four independent experiments with three technical replicates per condition. The OD<sub>595</sub> of the adherent cells bound to safranin stained wells were measured at OD<sub>595</sub>. In addition, biofilm formation of *S. aureus* strains seems to progressively increase with time of incubation because at 12 hours, optical densities of MRSA 252 and ATCC 6538 were low as 1.96 and 1.8. At 24 hours, OD of both MRSA 252 and ATCC 6538 were 3.91 and 2.71. Surprisingly at 48 hours an increased OD of 5.5 and 3.87 was measured. Therefore, based on the results ATCC 6538 was highly adherent with OD 595 values nm of >3.0. The MRSA 252 was strongly adherent with an OD<sub>595</sub> nm value of >4.0. While ATCC 12228 strain was negatively adherent (OD 595 < 0.5) which is less than the cut off selected to differentiate the positive biofilm formers. Bar graphs represent the mean of biofilm formations  $\pm$  SD on 24-well tissue culture plates. Data were analyzed by two-way ANOVA using Bonferroni post-tests. Significant interactions (\*\*\*) $p$ <0.001; (\*\*) $p$ <0.01) were observed. Two-way ANOVA revealed significant differences

between growth and time points of biofilm formation. Significant effects for growth ( $F(213.97) = ***p < 0.001$ ) and time ( $F(94.05) = ***p < 0.001$ ) indicates that these two factors acted individual.

### 4.3 Discussion

In this study, conventional methods were used for identification of MRSA 252 and *S. aureus* ATCC 6538 which are methicillin resistant and susceptible *S. aureus* strains. Initial identification of *S. aureus* strains was performed using different biochemical methods. The bacterial strains ATCC 6538 and MRSA 252 isolates colonial and morphological appearances were examined on TSA and CBAB. These agar media (TSA and CBAB) are general purpose media that allows robust growth and promotes distinct colony morphology, good pigmentation and well-defined haemolytic reactions (Vitko and Richardson, 2013). In this study trypticase soy agar and Columbia blood base agar supported the growth of ATCC 6538 and MRSA 252 producing circular shapes, convex elevations, moderate sizes, shiny appearances with golden yellow and creamy pigmentations on TSA and CBAB plates. Carotenoid pigment called staphyloxanthin is responsible for the characteristics golden yellow colour observed in ATCC 6538. Catalase is a protein enzyme that breaks down hydrogen peroxide secreted by phagocytes. Catalase does not appear to be of necessary for the normal growth of *S. aureus* strains but it serves as a defense mechanism against destruction by phagocytic cells (Dezfulian *et al.*, 2010). Lysostaphin is a metalloenzyme consisting of zinc which is capable of exhibiting a lytic action against *S. aureus* (Dezfulian *et al.*, 2010). From this study biochemical tests results showed that *S. aureus* ATCC 6538 and MRSA 252 were both catalase and lysostaphin positive.

*S. aureus* has the ability to produce biofilm (Vasudevan 2003; Caizza and O'Toole, 2003; López, Vlamakis & Kolter 2010), which assist bacteria to adhere to biotic or abiotic surfaces (Goyal *et al.*, 2014) and is capable to adhere and produce biofilm consequently causing infections and morbidity (López, Vlamakis & Kolter 2010; Ribet and Cossart, 2015). The ability of *S. aureus* to form biofilm is the vital reason for eradication of infections and recurring infection of skin (Montgomery *et al.*, 2015), blood (Corey, 2009), heart valves (in human (Pollit *et al.*, 2018)). Biofilm formation facilitates adhesion of *S. aureus* to the surfaces of skin, blood vessels and tissues. It also facilitates persistence of bacteria in the human tissue by protecting the bacterial cells against the various mechanisms of the host defense (Ribet and Cossart, 2015). In this study, phenotypic expression of biofilm formation in *S. aureus* was investigated by modified Congo red agar assay and microtiter tissue culture plate method. These two methods were chosen to detect slime production and to quantify the adherence level since biofilm formation is to be further studied. Figure 29 shows a variable biofilm formation of

MRSA 252 and *S. aureus* ATCC 6538 tested. Based on the results *S. aureus* 6538 and MRSA 252 was considered biofilm producers by Congo red agar method, in which MRSA 252 produced very black colonies compared to ATCC 6538 that produced black colonies. Similar findings have been reported in previous studies. A study on biofilm formation conducted by Yousefi *et al.*, (2016), reported varying degrees of black colonies ranging from very black to black colonies in MSSA strains and MRSA clinical isolates. In another work carried out by Gowrishankar and co-workers (2016), they found MRSA strains to be slime producers, producing varying degrees of black colonies. Growing *S. aureus* strains on Congo red agar plates were also in agreement with Hammadi *et al.*, (2014) and findings of Arslan and Ozkardes, (2007). The authors recorded that Congo red agar was important in detection of *S. aureus* slime formation from human. The *S. aureus* strains they tested produced black colonies with smooth round and shiny surfaces. Black colonies produced by ATCC 6538 and MRSA 252 in this study were black colonies with smooth shiny surfaces. While the pink colonies produced by ATCC 12228 was considered negative biofilm former. This result appears to be in contrast with the report of Cucarella and his colleagues who considered black or pink rough colonies as positive result after their biofilm formation study (Cucarella *et al.*, 2009). However, the result correlates with those of Yousefi *et al.*, (2016) and Atshan *et al.*, (2012).

Safranin-staining is predominantly used to detect the presence of extracellular substances and is used to measure quantify the amount of biofilm formed by *S. aureus* (Stepanovic *et al.*, 2000). Biofilm formation of MRSA 252 and *S. aureus* ATCC 6538 was evaluated first by visual observation of the 24 well polystyrene microtiter plates at 12, 24 and 48 h and secondly by safranin staining technique. Visual observation showed that MRSA 252 and ATCCC 6538 were biofilm formers, forming biofilm in different capacities. Both strains form fairly strong biofilms at 12 h while much stronger and highly adherent biofilms were formed at 24 and 48 h. It is worthy to note that at 12 h, ATCC 6538 biofilms were not much compared to that MRSA 252. For the safranin technique (Figure 30 and 31) the optical density was measured and was observed that OD readings of MRSA 252 and *S. aureus* ATCC 6538 were low at 12 h (OD<sub>595</sub> = 1.96 and 1.8), at 24 h (OD<sub>595</sub> = 3.91 and 2.71) and surprisingly at 48 h (OD<sub>595</sub> = 5.5 and 3.87) an increased biofilm formation was observed. These values were far higher than the cut-off value of OD<sub>595</sub><0.5 set for positive biofilm formers indicating that MRSA 252 was a strong and highly adherent biofilm former while ATCC 6538 was a moderately strong adherent biofilm former. According to Stepanovic *et al.*, (2000) the ability of biofilm formation can be classified into 4 main categories: non-adherent, weakly, moderately and strongly adherent

based on the OD<sub>595</sub>. However, following Stepanovic *et al.*, (2000) classification method, MRSA 252 and ATCC 6538 tested in this study were classified as strongly and moderately adherent. In this study, the tested MRSA 252 and ATCC 6538 were both cultured in TSB with 1 % glucose for enhancement of biofilm formation which is composed of polysaccharides called Poly-N acetylglucosamine or Polysaccharide intercellular adhesion (PIA). Furthermore, safranin resolubilized with 95 % ethanol resulted in high OD because it resolubilized the dye bound to the cells attached to the well of the 24 well microtiter plate.

## **Chapter 5. Screening of Plant Seed and Nut Oils and their Respective Extracts for Antimicrobial Activity against MRSA 252 and *S. aureus* ATCC 6538**

### **5.1 Introduction**

*S. aureus* has a remarkable ability to adapt to the human environment and huge capacity to quickly develop resistance to numerous antibiotics (Bastista *et al.*, 2017). *S. aureus* is a gram positive bacterium that resides permanently on the surface of human skin and in the nose of healthy individuals across the globe causing a range of human infections ranging from mild infections such as superficial or epidermal skin lesions, to very chronic infections including inflammation of the inner lining of the heart (endocarditis), bone infections (osteomyelitis), inflammation of the alveoli (pneumonia), inflammation of the lining of the brain and spinal cord (meningitis), blood infections (septicaemia), presence of viable bacteria in the blood (bacteraemia) and inflammation by exotoxins (toxic shock syndrome) (Qiu *et al.*, 2011; Kim *et al.*, 2015). In addition, *S. aureus* is known to form biofilms, and the bacteria residing in biofilm have been reported to be very resistant to antibiotics (Nair *et al.*, 2016). A biofilm is composed of microbial cells living together within an EPS composed of extracellular DNA (eDNA), polysaccharides intercellular adhesion (PIA), proteins, and amyloid fibrils (Garret 2008). In nature, *S. aureus* has been found to form biofilm on both biotic (living) and abiotic (non-living) surfaces, including indwelling hospital devices for example bone and joint prostheses, heart valves, implanted catheters), human tissues, food and food processing facilities (Chamdit and Siripermpool, 2011). Because of their complexity, biofilms confer microorganisms enclosed in the extracellular matrix very high levels of antibiotic resistance (Chamdit and Siripermpool, 2011). Previous research studies have showed that microbes enclosed in biofilm become less susceptible to antibiotics thereby hindering the effectiveness of antimicrobial drugs, leading to both persistent and severe infections which are of global concerns (Chamdit and Siripermpool, 2011; Atshan *et al.*, 2013; Chamdit and Siripermpool, 2011; Dakheel *et al.*, 2016; Belbase *et al.*, 2017; Reffuveille *et al.*, 2017).

Some decades ago, *S. aureus* strains resistant to a range of betalactam antibiotics such as oxacillin, cefotaxime and methicillin emerged not long after the introduction of penicillin. These strains cannot be treated with most conventional betalactams, thus making glycopeptides (vancomycin otherwise known as teicoplanin) and cyclic lipopeptides (daptomycin) the only

drug of choice for staphylococcal infections. But surprisingly, MRSA also emerged as major causes of hospital acquired, and community acquired infections and as resistant strains of vancomycin and daptomycin thus making infections increasingly very difficult to treat (Nair *et al.*, 2016). The emergence of MRSA worsened the problem of staphylococcal infections as the newly introduced drugs; vancomycin, daptomycin and linezolid which was the last resort drug after all other drug options failed to produce adequate response to treatment of staphylococcal infections (Nair *et al.*, 2016). In 1997 vancomycin resistant *S. aureus* strains was first isolated. Shortly after this year VRSA isolates were also identified in USA and across the globe (Chen and Huang, 2014). Similarly, vancomycin - intermediate *S. aureus* (VISA) with MIC of 8 µg/ml was reported in France, Germany, United State, United Kingdom and Japan. This pattern of developing resistance to antibiotics by *S. aureus* has also been identified in much newer antibiotics developed between year 2000 and 2010. Linezolid the new oxazolidinone antimicrobial which was introduced in 2000 led to the first linezolid - resistant methicillin resistant strain recovered from a patient after treatment with linezolid for peritonitis associated with dialysis (Tsiodras *et al.*, 2001). Furthermore, daptomycin a semi synthetic lipopeptide antibiotic was introduced in 2003 and within 2 years daptomycin resulted in the first daptomycin – resistant MRSA strain reported in patient suffering from high grade MRSA bacteremia (Mangili *et al.*, 2005). In view of all this resistance issues, MRSA is a global problem and particularly worrisome is the significant increase of MRSA with reduced susceptibility to the newly identified drugs in the class of glycopeptides and cyclic lipopeptide.

Plant oils have been used for different purposes including alternative medicine, pharmaceutical therapies, and natural therapies for decades (Kayode and Kayode 2011). Cashew, (*Anacardium occidentale*) is a genus in the family Anacardiaceae and it is found in tropical regions such as Brazil. Cashew nut oil has been known for years for its therapeutic purpose. Cashew oil from leaves, barks, flower and fresh shoots has been reported to possess several biological activities which includes antimicrobial, antioxidant, and antitumor. In a study conducted by Hassan *et al.*, (2016), cashew nut oil showed activity against gram positive strains such as *Acinetobacter anitratus*, methicillin resistant *S. aureus* (MRSA), *Proteus vulgaris*, *Pseudomonas aeruginosa*, *S. aureus*, *S. epidermidis*, *Serratia marcescens* and fungal species including *Candida albicans* and *Candida tropicalis*. The potency of the oil was evaluated using standard Kirby Bauer disc diffusion and minimum inhibition concentration (MIC) which showed clear zones and MIC values ranging from 6250 – 12500 µg/mL and 6250 – 50000 µg/mL for all the bacterial strains and *Candida tropicalis* while *C. albicans* had the lowest MIC value of 3125 µg/mL. In another

research study, da Silva *et al.*, (2016) evaluated the antimicrobial activity of oil from cashew flower against *Streptococcus mutans*, *Lactobacillus acidophilus*, *S. aureus*, *MRSA*, *Enterococcus faecalis*, *Streptococcus pyogenes*, *Pseudomonas aeruginosa*, *Proteus mirabilis*, *Escherichia coli*, *Klebsiella pneumoniae*, *Helicobacter pylori*, *Salmonella cholerae suis*, *Candida albicans* and *Candida tropicalis* using agar diffusion. With this method, they found that cashew flower oil was able to inhibit the growth of both the bacterial and fungal species. Similarly, Parasa *et al.*, (2011) investigated the ability of 70% of three organic solvent extract of cashew oil (acetone extract, methanol extract and chloroform extract) to inhibit about 15 clinical isolates of *MRSA* from different hospitals in South India. They used the well-diffusion method and found that with 70% acetone extract 19-25 mm clear zones of inhibition were produced by cashew oil against the clinical isolates.

Fluted pumpkin (*Telfaira occidentalis*) is a tropical vine grown in many West African countries, but is mainly cultivated in Nigeria, Benin and Cameroon as a leaf vegetable which is used in herbal medicine (Oyewole and Abalaka, 2012; Dada, 2017). Fluted pumpkin is a genus in the family of Cucurbitaceae. The leafy vegetable has been known for decades to possess both antimicrobial and antiviral properties (Dada, 2017). Many researchers have reported the medicinal activities of fluted pumpkin. Nwakanma *et al.*, (2014) investigated the effect of *Telfaira occidentalis* leaf oil against two commonly known pathogenic strains - *S. aureus* and *E. coli*. In the study, the disc diffusion method and dilution techniques were used. The oil from the leaf of *Telfaira occidentalis* was found to produce 1.00 mm diameter clear zones of inhibition against *S. aureus* and a 2.00 mm diameter zone against *E. coli*. Also, the dilution test showed that 8 µg/ml of the oil was able to inhibit the growth of *S. aureus*. In another study, Oyewole and Abalaka (2012) investigated the activity of leaf extract of fluted pumpkin on *Salmonella typhi*, *E. coli* and *Streptococcus faecalis* using both the disc diffusion method and MIC method. In the study, they found that the leaf extract showed high antibacterial activity against *S. faecalis* ( $6 \pm 1.10$  mm at 5.0 mg), *E. coli* ( $20 \pm 0.58$  mm at 500 mg/mL) and *S. typhi* ( $11 \pm 0.70$  mm at 50mg/mL). The MIC was 0.5 mg/mL, 5.0 mg/mL and 500 mg/mL for *E. coli*, *S. typhi* and *S. faecalis*.

African walnut (*Tetracapidium conophorum*) is a genus in the family Euphorbiaceae. *Tetracapidium conophorum* is cultivated in Cameroon and Nigeria (Ayoola *et al.*, 2011). It is commonly called African walnut. African walnut oil has been known for decades as healing oil. Walnut oil is widely used in medicine for the treatment of fungal infections, skin infections,

respiratory diseases and ulcers. African walnut oil has been reported to possess antimicrobial, antioxidant, antimicrobial, antiviral and immunosuppressive activities. Only few publications have reported the antimicrobial activity of walnut oil isolated from the leaves and roots of this walnut specie (Ajaiyeoba and Fadare, 2006; Ogbolu, 2012). Walnut oil has been shown to be very effective against bacterial species. In one study, the disc Kirby Bauer diffusion method was used to determine the activity of *T. conorphorum* on both gram positive and gram-negative strains including *Bacillus subtilis*, *Bacillus licheniformis*, *S. aureus* and *Klebsiella pneumonia* and it was suggested that clear zones of inhibition seen on cultured plates signify the antimicrobial activity of walnut oil (Saxenaa *et al.*, 2009). Also, Rhati *et al.*, (2014) reported that walnut oil has antibacterial activity against *S. aureus*, *Proteus vulgaris*, *Pseudomonas aeruginosa*, *Bacillus subtilis* and *E. coli*. They reported that the activity of walnut oil was due mainly to the presence of alkaloids a phytochemical that is present in significant amount. Similarly, Orhan *et al.*, (2009) has demonstrated walnut oil and hazel nut oil had antibacterial effects against *S. aureus*, *E. faecalis* and *E. coli*, *Proteus mirabilis*, *K. pneumonia* with MIC of 8 µg mL, 4 µg mL, 16 µg mL and 32 µg mL respectively.

Most research studies are based on the antimicrobial activities of extracts obtained from leaves, flowers, roots, and shoots of walnut, cashew and fluted pumpkin and as such only very little information is available on the nut and seed oils and its effect on *S. aureus* biofilm formation. Based on the findings of previous studies, firstly, the Kirby Bauer disc diffusion assay was performed to check for the activity of walnut oil, pumpkin oil and cashew oil against *S. aureus*. This served as a preliminary screening for subsequent experiments. Secondly, exploration whether the oil samples that were active in the disc diffusion assay are also effective in inhibiting or eradicating *S. aureus* biofilm was performed. To do this, the Minimum Inhibition Concentration (MIC), Minimum Biofilm Inhibition Concentration (MBIC) and Minimum Biofilm Eradication Concentration (MBEC) methods were used to determine the concentration needed to inhibit or eradicate *S. aureus* biofilm. All these tests determined if the plant oil samples tested could be good antimicrobial agents.

## 5.2. Results

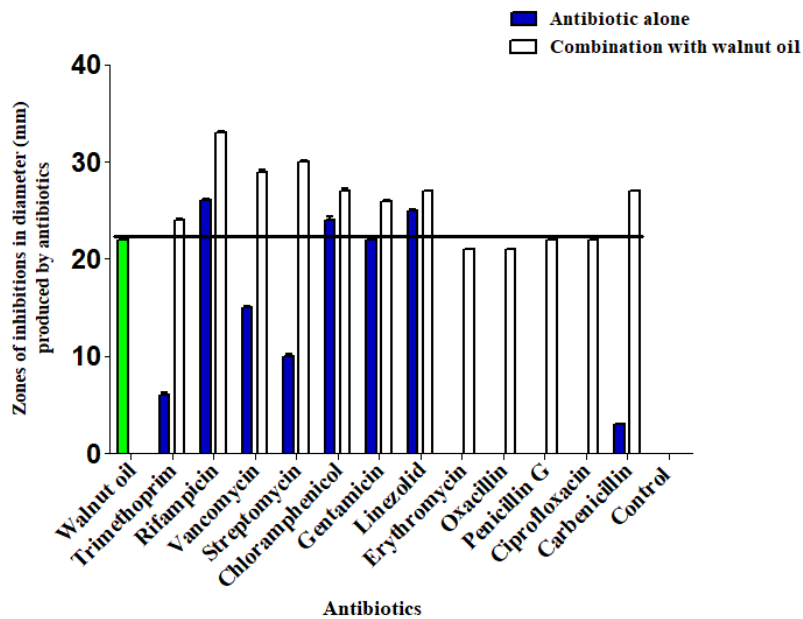
### 5.2.1 Antibiotic sensitivity testing of seed and nut oils against MRSA 252 and *S. aureus* ATCC 6538

Preliminary evaluation of the antibacterial activity of African walnut, cashew and pumpkin oils against MRSA 252 and ATCC 6538 and some selected antibiotics was evaluated before using the oils for further analysis. In determining the antibacterial activities of walnut, cashew and pumpkin oils, the Kirby-Bauer disk diffusion assay was first conducted. In this assay, resultant zones of inhibitions produced by oils alone, antibiotic disks and combination disks were measured in millimetre (mm) with a ruler and interpreted using the CLSI zone diameter interpretative standards. Studies were performed in triplicate to ensure reproducibility, and mean value was calculated.

#### 5.2.1.1 African walnut oil effect on MRSA 252

African walnut (*Tetracarpidium conophorum*) oil showed significant antibacterial activity against the tested MRSA 252 (Figure 33 and 34). The results of the antibacterial activity of African walnut oil against the tested MRSA 252 showed that MRSA 252 was susceptible to a range of antibiotics belonging to the class of nucleic acid inhibitors and cell wall synthesis inhibitors, intermediary metabolism inhibitors and protein synthesis inhibitors. Antibacterial susceptibility testing with African walnut oil alone produced larger zones of inhibitions indicating that it is highly capable of killing MRSA 252. For test with antibiotics alone, MRSA 252 was seen to be susceptible to antibiotics such as streptomycin, vancomycin, linezolid and gentamicin, rifampicin, and chloramphenicol. The bacterium was susceptible because it produced clear zones of inhibitions. However, MRSA 252 was observed to be very resistant to drugs such as trimethoprim, penicillin G, ciprofloxacin, oxacillin, and erythromycin. This was because no zones were produced by the antibiotics. However, because trimethoprim and carbenicillin produced clear zones that are not up to 12 mm diameter, MRSA 252 was still classified as been resistant to the drugs. The antibiotics produced varied effects in combination with walnut oil. Combination of walnut oil with chloramphenicol, rifampicin, gentamicin and linezolid antibiotics showed an indifference effect against MRSA 252. The diameter of zone (mm) of the resultant combination did not show difference between the African walnut oil alone and antibiotic disk alone. The combination of trimethoprim, vancomycin, carbenicillin and streptomycin led to a synergistic effect on MRSA 252. In this case the diameter of the zones obtained resulted in a combination effect of both the antibiotic disc alone and African walnut oil. In the synergistic effect, the applied antibiotics and essential oil work together to

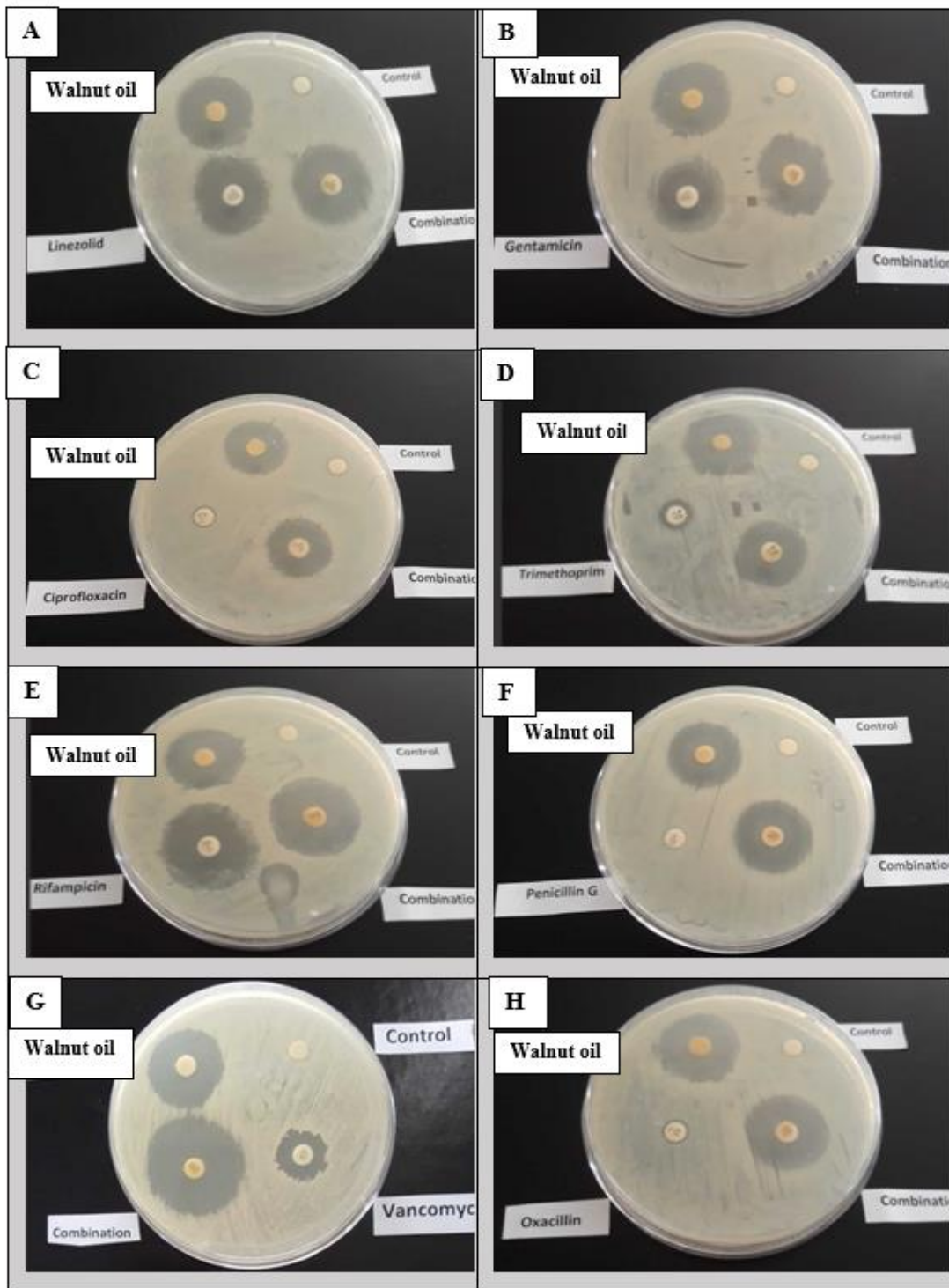
produce an effect more potent than if each antibiotic or oil were applied singly. This explains the synergistic effect of carbenicillin which appears to be enhanced by activity of African walnut oil even though it did not produce much inhibitory effect alone. While combination of African walnut oil with erythromycin, oxacillin, penicillin G and ciprofloxacin led to a potentiating effect where no zone was recorded for the antibiotics alone. For the control (DMSO) no growth was observed in all the plates.



**Figure 33. Resistant pattern of MRSA 252 to commercial antibiotics and synergy effect of African walnut oil with antibiotics**

Data on the graph is the diameter of clear zones of inhibition (mm). Bars represent the means standard deviation (SD) of three repeated experiments (n=3). Statistical analysis was performed using the two-way ANOVA with Bonferroni posttests and significant differences in the data were established at  $P < 0.05$  ( $P < 0.0001$ ). The green bar and blue bars represent the mean diameter zone of African walnut oil alone and antibiotic alone while the white bars represent the diameter of zones of combination effect of antibiotic with African walnut oil on MRSA 252. The line represents a threshold that limits the zones of inhibition of walnut oil against MRSA 252.

**Antibacterial activities (zones of inhibition) of African walnut oil and its synergistic effect with selected antibiotics on MRSA 252**



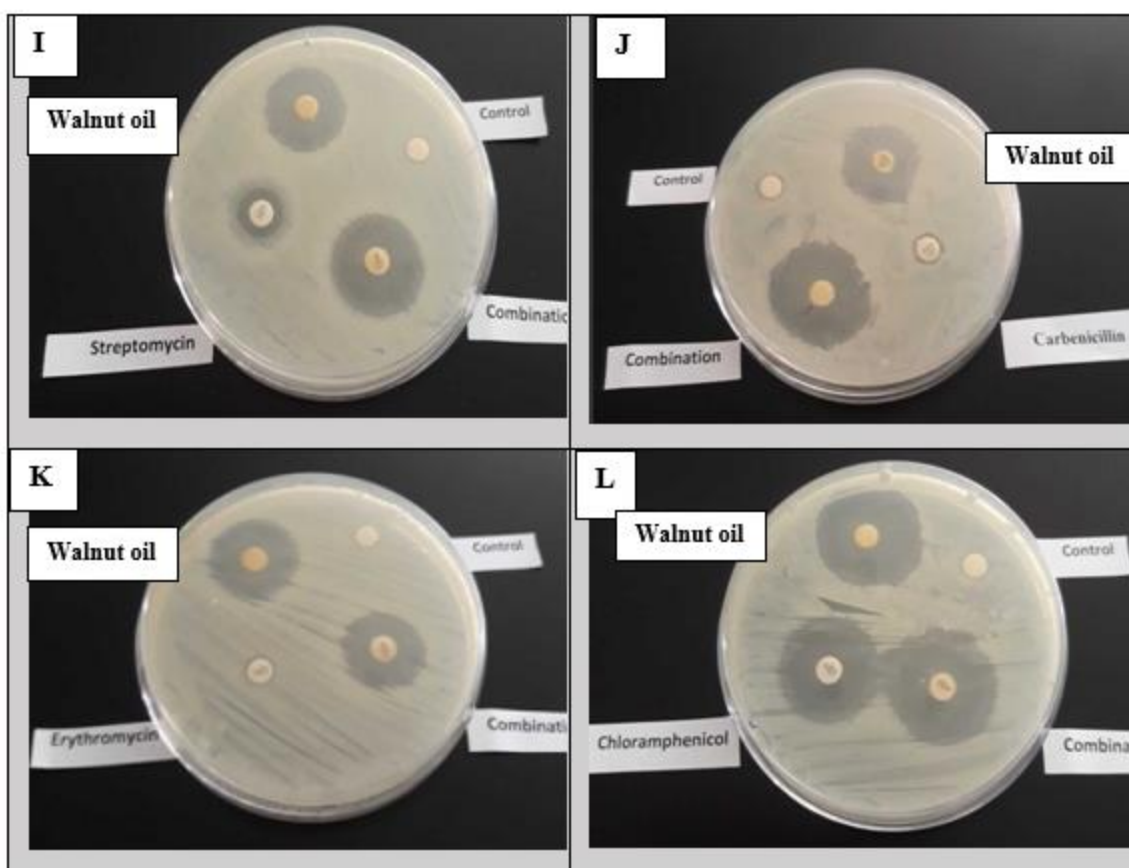


**Figure 34. Disk diffusion assay identifies African walnut oil and some selected commercial antibiotics with antimicrobial activity.**

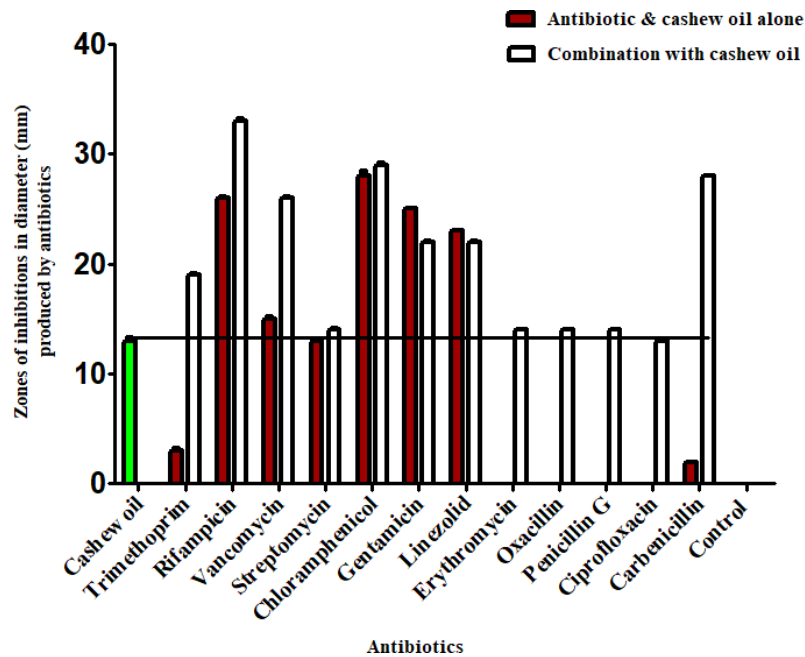
Figure 34 shows the representative plates for disk diffusion assay. Disk diffusion assay was conducted by impregnating 6 mm disks separately with African walnut oil, antibiotics and combination of antibiotics with standard concentrations of antibiotics and allowed to dry in the oven for 30 minutes before placing them individually on plates and incubated for 24 hours. Control disc in all the plates contains 10  $\mu$ L of DMSO. (A). Antibacterial activity of African walnut oil, linezolid 10  $\mu$ g and combination of 10  $\mu$ L African walnut oil + linezolid 10  $\mu$ g. (B). Antibacterial activity of walnut oil, gentamicin 10  $\mu$ g and combination of 10  $\mu$ L walnut oil + gentamicin 10  $\mu$ g. (C). Antibacterial activity of African walnut oil, ciprofloxacin 5  $\mu$ g and combination of 10  $\mu$ L walnut oil + ciprofloxacin 5  $\mu$ g. (D). Antibacterial activity of walnut oil, trimethoprim 1.25  $\mu$ g and combination of 10  $\mu$ L African walnut oil + trimethoprim 1.25  $\mu$ g. (E). Antibacterial activity of walnut oil, rifampicin 15  $\mu$ g and combination of 10  $\mu$ L walnut oil + rifampicin 15  $\mu$ g. (F). Antibacterial activity of African walnut oil, penicillin G 15  $\mu$ g and combination of 10  $\mu$ L walnut oil + penicillin G 15  $\mu$ g. (G). Antibacterial activity of African

walnut oil, vancomycin 30 µg and combination of 10 µL walnut oil + streptomycin 30 µg. (H). Antibacterial activity of walnut oil, oxacillin 30 µg and combination of 10 µL African walnut oil + oxacillin 30 µg. (I). Antibacterial activity of African walnut oil, streptomycin 10 µg and combination of 10 µL walnut oil + streptomycin 10 µg. (J). Antibacterial activity of walnut oil, carbenicillin 10 µg and combination of 10 µL African walnut oil + carbenicillin 10 µg. (K). Antibacterial activity of walnut oil, erythromycin 15 µg and combination of 10 µL walnut oil + erythromycin 15 µg. (L). Antibacterial activity of African walnut oil, chloramphenicol 10 µg and combination of 10 µL walnut oil + chloramphenicol 10 µg.

#### **5.2.1.2 Cashew oil effect on MRSA 252**

Cashew (*Anacardium occidentale*) oil showed low inhibitory activity against the tested MRSA 252 (Figure 35 and 36). The result of antibacterial susceptibility testing represented in Figure 33 below showed that MRSA 252 was susceptible to a range of antibiotics belonging to different classes of drugs. Antibacterial susceptibility testing with cashew oil alone showed that cashew oil produced smaller zones of inhibitions compared to walnut oil indicating that it has low activity against MRSA 252. For tests with antibiotics alone, MRSA 252 was seen to be susceptible to a range of antibiotics such as streptomycin, linezolid and rifampicin, vancomycin, gentamicin and chloramphenicol. The antibiotics were susceptible because they produced clear zones of inhibitions. However, MRSA 252 was observed to be very resistant to drugs such as trimethoprim, penicillin G, ciprofloxacin, oxacillin, carbenicillin and erythromycin which were similar to walnut oil. This was because no clear zones were produced by the antibiotics. For combination test, the antibiotics produced varied effects when combined with cashew oil. Combination of cashew oil with trimethoprim, chloramphenicol, rifampicin, vancomycin and carbenicillin gave a synergistic effect with cashew oil which shows that the diameter of the zone obtained for combination was equal to that of walnut oil and the individual antibiotics. Chloramphenicol and rifampicin exhibited a key-hole synergy against MRSA 252. An indifferent effect was observed when cashew oil was combined with linezolid, gentamicin, and streptomycin, in this case the diameter of the zones obtained was just the same as that of antibiotic alone or slightly greater. Although the combination zone obtained for gentamicin was smaller. Since no zone was produced by ciprofloxacin, erythromycin, oxacillin and penicillin G, combination of cashew oil with the antibiotics led to a potentiating effect where no zone was recorded for the antibiotics alone but clear zones were obtained for combination

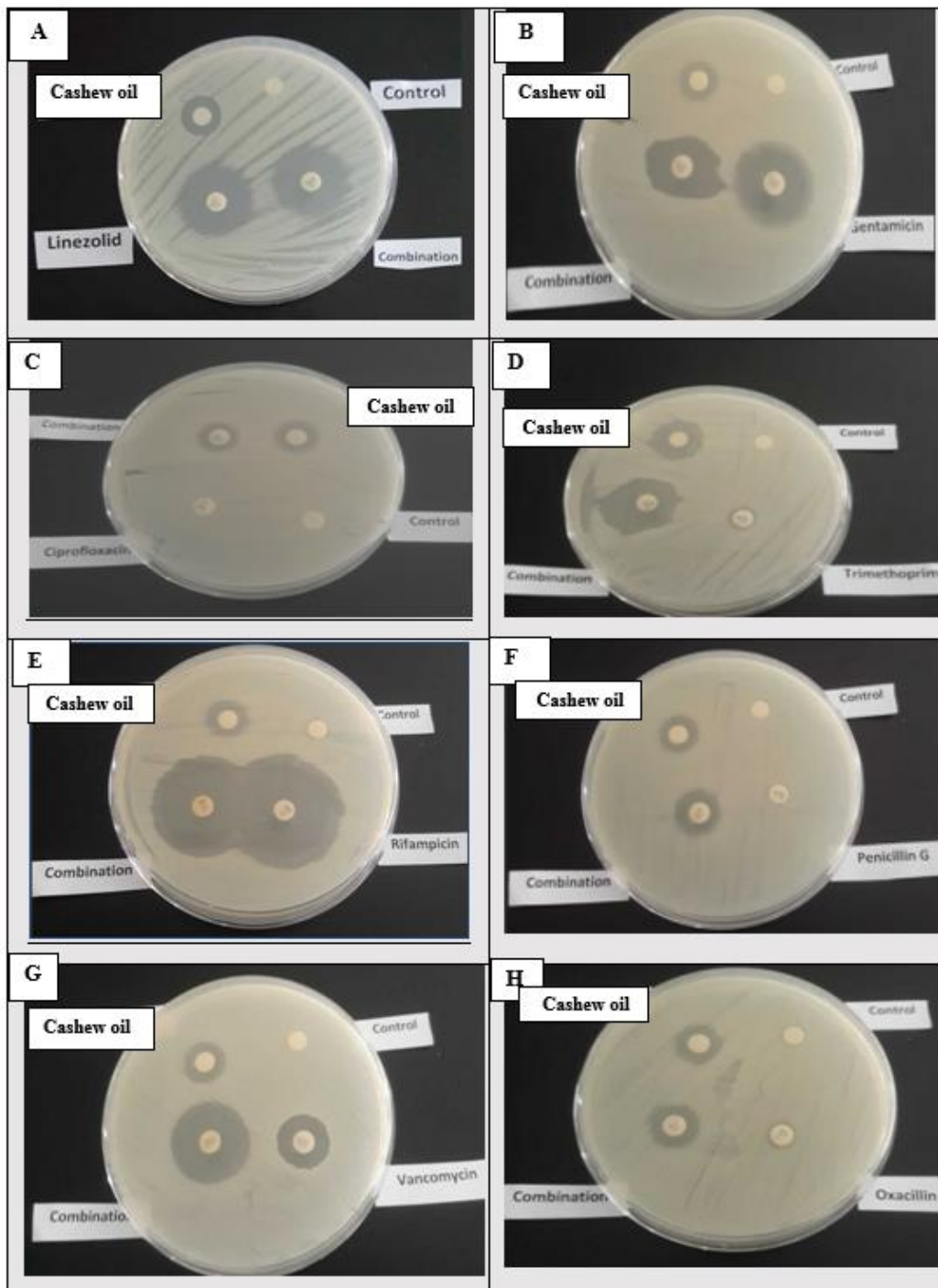
which was almost equal to cashew oil zone alone. For the control (DMSO) no growth was observed in all the plates.

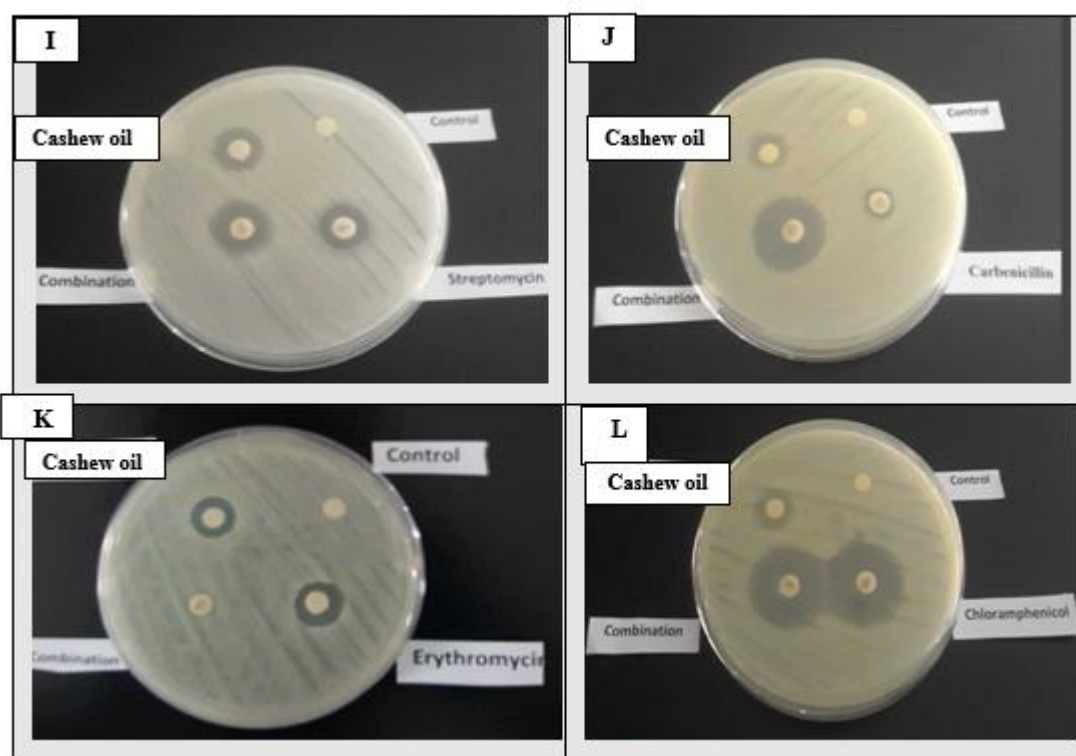


**Figure 35. Resistant pattern of MRSA 252 to commercial antibiotics and synergy effect of cashew oil with antibiotics.**

Data on the graph is the diameter of clear zones of inhibition (mm). Bars represent the means standard deviation (SD) of three repeated experiments (n=3). Significant differences in the data were established at  $P < 0.05$  ( $P < 0.0001$ ) using two-way ANOVA with Bonferroni post-tests. The green and brown bars represent the mean diameter zone of cashew oil alone and antibiotic alone while the white bars represent the diameter of zones of combination effect of antibiotic with cashew oil on MRSA 252. The line represents a threshold that limits the zones of inhibition of cashew oil against MRSA 252.

**Antibacterial activities (zones of inhibition) of cashew oil and its synergistic effect with selected antibiotics on MRSA 252**





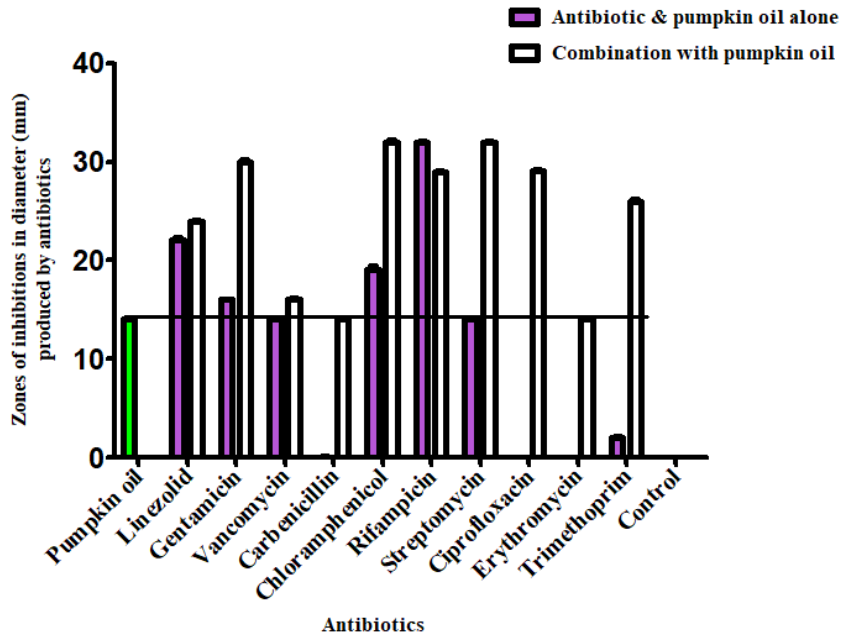
**Figure 36. Disk diffusion assay identifies cashew oil and some selected commercial antibiotics with antimicrobial activity.**

Figure 36 shows the representative plates for disk diffusion assay showing the antibacterial activity of cashew oil against MRSA 252. Control disc in all the plates contained 10  $\mu$ L of DMSO. (A). Antibacterial activity of cashew oil, linezolid 10  $\mu$ g and combination of 10  $\mu$ L cashew oil + linezolid 10  $\mu$ g. (B). Antibacterial activity of cashew oil, gentamicin 10  $\mu$ g and combination of 10  $\mu$ L cashew oil + gentamicin 10  $\mu$ g. (C). Antibacterial activity of cashew oil, ciprofloxacin 5  $\mu$ g and combination of 10  $\mu$ L cashew oil + ciprofloxacin 5  $\mu$ g. (D). Antibacterial activity of cashew oil, trimethoprim 1.25  $\mu$ g and combination of 10  $\mu$ L cashew oil + trimethoprim 1.25  $\mu$ g. (E). Antibacterial activity of cashew oil, rifampicin 15  $\mu$ g and combination of 10  $\mu$ L cashew oil + rifampicin 15  $\mu$ g. (F). Antibacterial activity of cashew oil, penicillin G (15  $\mu$ g) and combination of 10  $\mu$ L cashew oil + penicillin G (15  $\mu$ g). (G). Antibacterial activity of cashew oil, vancomycin 30  $\mu$ g and combination of 10  $\mu$ L cashew oil + vancomycin 30  $\mu$ g. (H). Antibacterial activity of cashew oil, oxacillin 30  $\mu$ g and combination of 10  $\mu$ L cashew oil + oxacillin 30  $\mu$ g. (I). Antibacterial activity of cashew oil, streptomycin 10  $\mu$ g and combination of 10  $\mu$ L cashew oil + streptomycin 10  $\mu$ g. (J). Antibacterial activity of cashew oil, carbenicillin 10  $\mu$ g and combination of 10  $\mu$ L cashew oil + carbenicillin 10  $\mu$ g. (K). Antibacterial activity of cashew oil, erythromycin 15  $\mu$ g and combination of 10  $\mu$ L cashew oil

+ erythromycin 15 µg. (L). Antibacterial activity of cashew oil, chloramphenicol 10 µg and combination of 10 µL cashew oil + chloramphenicol 10 µg. Studies were performed in triplicate to ensure reproducibility, and mean value was calculated.

### **5.2.1.3 Fluted pumpkin oil effect on MRSA 252**

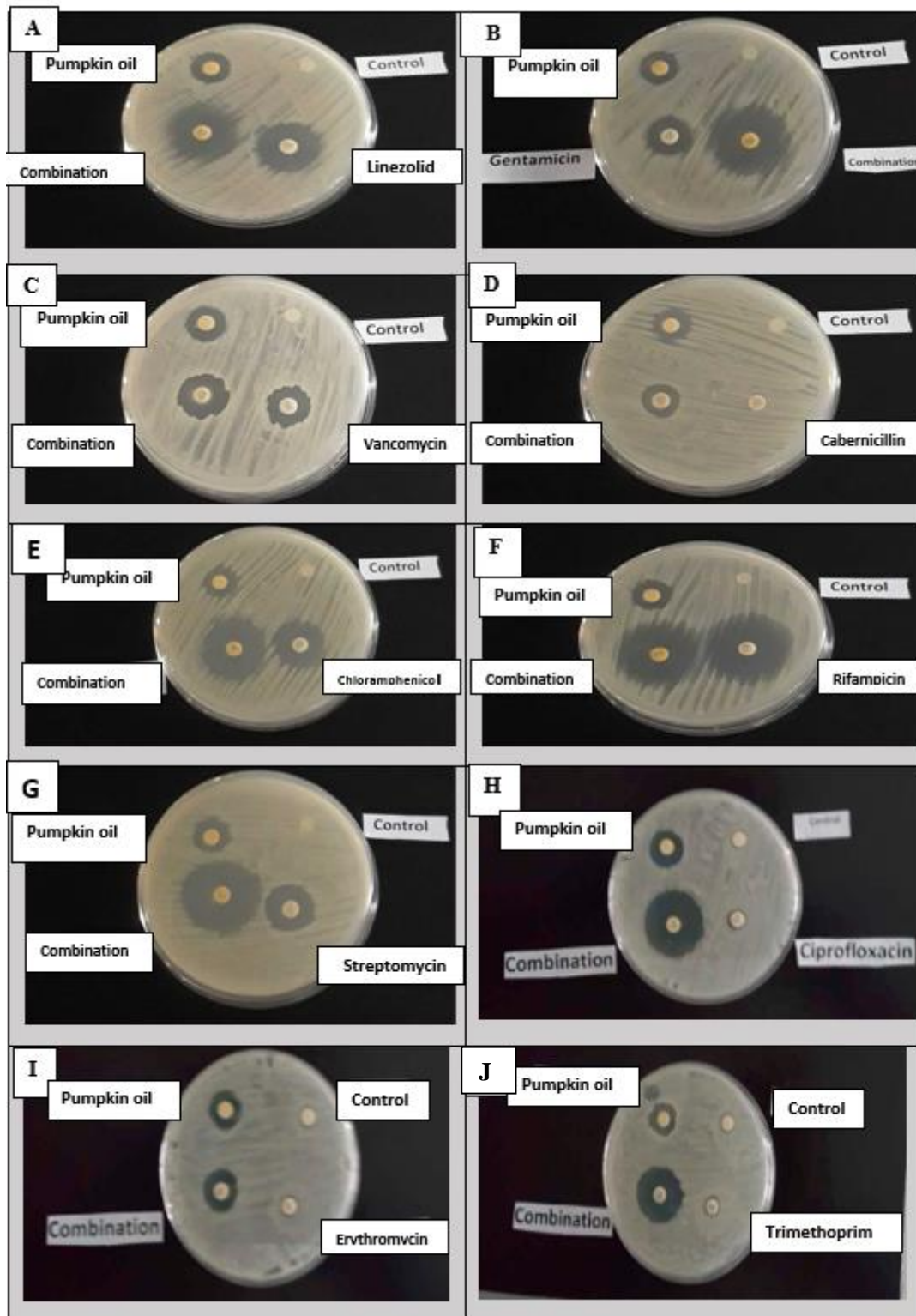
Fluted pumpkin (*Telfaria occidentalis*) oil showed significant inhibitory activity against MRSA 252 (Figure 37 and 38). The result of antibacterial susceptibility testing presented below showed that MRSA 252 was susceptible to a range of antibiotics belonging to different classes of drugs. Antibacterial susceptibility testing with pumpkin oil alone showed that the oil produced moderately bigger and clear zones of inhibitions compared to cashew oil indicating that it has high activity against MRSA 252. According to the results, MRSA 252 appears to be susceptible to a range of antibiotics such as streptomycin, rifampicin, vancomycin, gentamicin and resistant to ciprofloxacin, erythromycin, trimethoprim and carbenicillin. Clear zones with different diameter (mm) were obtained for streptomycin, rifampicin, vancomycin, gentamicin while no zones were obtained for ciprofloxacin, and carbenicillin. Combination of pumpkin oil with gentamicin, streptomycin, trimethoprim, chloramphenicol led to a synergistic effect against MRSA 252. Whereas combination of pumpkin oil with linezolid and vancomycin led to indifference effect against MRSA 252. A potentiation effect was obtained when pumpkin oil was combined with antibiotics such as ciprofloxacin, erythromycin and carbenicillin. For the control (DMSO) no growth was observed in all the plates.



**Figure 37. Resistant pattern of MRSA 252 to commercial antibiotics and synergy effect of fluted pumpkin oil with antibiotics.**

Data on the graph is the diameter of clear zones of inhibition (mm). Bars represent the means standard deviation (SD) of three repeated experiments (n=3). Significant differences in the data were established at  $P < 0.05$  ( $P < 0.001$ ) using two-ANOVA with Bonferroni posttests. The green and purple bars represent the mean diameter zone of fluted pumpkin oil alone and antibiotic alone while the white bars represent the diameter of zones of combination effect of antibiotic alone with pumpkin oil on MRSA 252. The line represents a threshold that limits the zones of inhibition of pumpkin oil against MRSA 252.

**Antibacterial activities (zones of inhibition) of fluted pumpkin oil and its synergistic effect with selected antibiotics on MRSA 252**



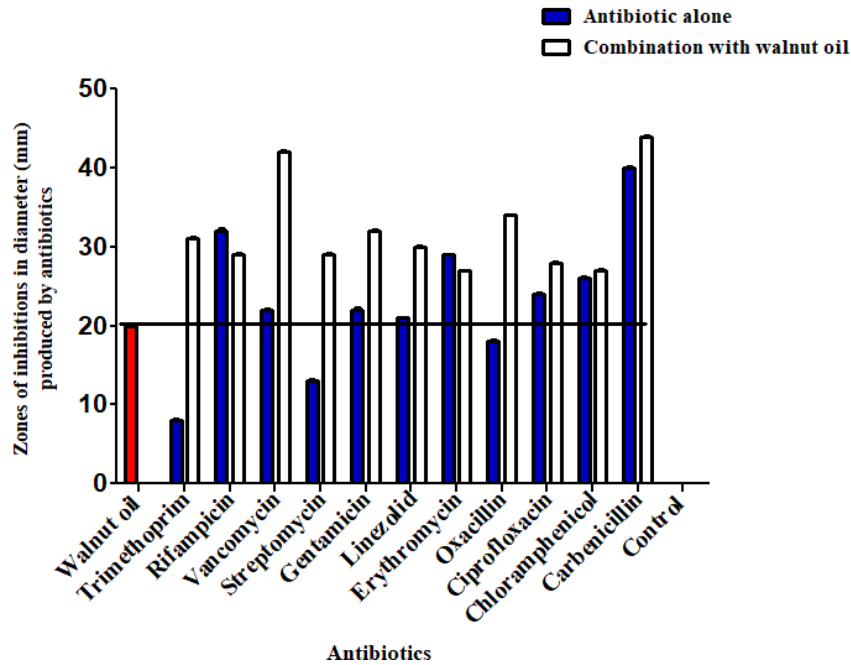
**Figure 38. Disk diffusion assay identifies fluted pumpkin oil and selected commercial antibiotics with antimicrobial activity.**

Figure 38 shows the representative plates for disk diffusion assay. The representative plates for disk diffusion assay showing the antibacterial activity of pumpkin oil against MRSA 252. Control disc in all the plates contained 10  $\mu$ L of DMSO. (A). Antibacterial activity of pumpkin oil, linezolid 10  $\mu$ g and combination of 10  $\mu$ L pumpkin oil + linezolid 10  $\mu$ g. (B). Antibacterial activity of pumpkin oil, gentamicin 10  $\mu$ g and combination of 10  $\mu$ L pumpkin oil + gentamicin 10  $\mu$ g. (C). Antibacterial activity of pumpkin oil, vancomycin 30  $\mu$ g and combination of 10  $\mu$ L pumpkin oil + vancomycin 30  $\mu$ g. (D). Antibacterial activity of pumpkin oil, carbenicillin 10  $\mu$ g and combination of 10  $\mu$ L pumpkin oil + carbenicillin 10  $\mu$ g. (E). Antibacterial activity of pumpkin oil, chloramphenicol 10  $\mu$ g and combination of 10  $\mu$ L pumpkin oil + chloramphenicol 10  $\mu$ g. (F). Antibacterial activity of pumpkin oil, rifampicin 15  $\mu$ g and combination of 10  $\mu$ L pumpkin oil + rifampicin 15  $\mu$ g. (G). Antibacterial activity of pumpkin oil, streptomycin 10  $\mu$ g and combination of 10  $\mu$ L pumpkin oil + streptomycin 10  $\mu$ g. (H). Antibacterial activity of cashew oil, ciprofloxacin 5  $\mu$ g and combination of 10  $\mu$ L cashew oil + ciprofloxacin 5  $\mu$ g. (I) Antibacterial activity of cashew oil, erythromycin 15  $\mu$ g and combination of 10  $\mu$ L cashew oil + erythromycin 15  $\mu$ g. (J). Antibacterial activity of cashew oil, trimethoprim 1.25  $\mu$ g and combination of 10  $\mu$ L cashew oil + trimethoprim 1.25  $\mu$ g. Studies were performed in triplicate to ensure reproducibility, and mean values were calculated.

#### **5.2.1.4 African walnut oil effect on *S. aureus* ATCC 6538**

African walnut (*Tetracarpidium conophorum*) oil showed significant inhibitory activity against ATCC 6538 (Figure 39 and 40). The results obtained from the disc diffusion test showed that ATCC 6538 was susceptible to most of the antibiotics tested. Antibacterial susceptibility testing with African walnut oil alone produced larger zones of inhibitions indicating that walnut oil has the capability to kill ATCC 6538. For test with antibiotics alone, ATCC 6538 was susceptible to trimethoprim, erythromycin, oxacillin, ciprofloxacin, streptomycin, vancomycin, linezolid, rifampicin and chloramphenicol. This result confirms the susceptibility character of ATCC 6538. For combination test, the antibiotics produced varied effects in combination with walnut oil. Combination of walnut oil with ciprofloxacin, erythromycin, rifampicin, gentamicin chloramphenicol and linezolid showed an antagonistic effect against ATCC 6538 because the combination zones were smaller than zones of African walnut oil and antibiotics alone. Combination of African walnut oil with ciprofloxacin, gentamicin, trimethoprim, vancomycin, oxacillin and streptomycin led to a synergistic effect against ATCC 6538. Gentamicin exhibited a strong synergistic effect with African walnut oil against ATCC

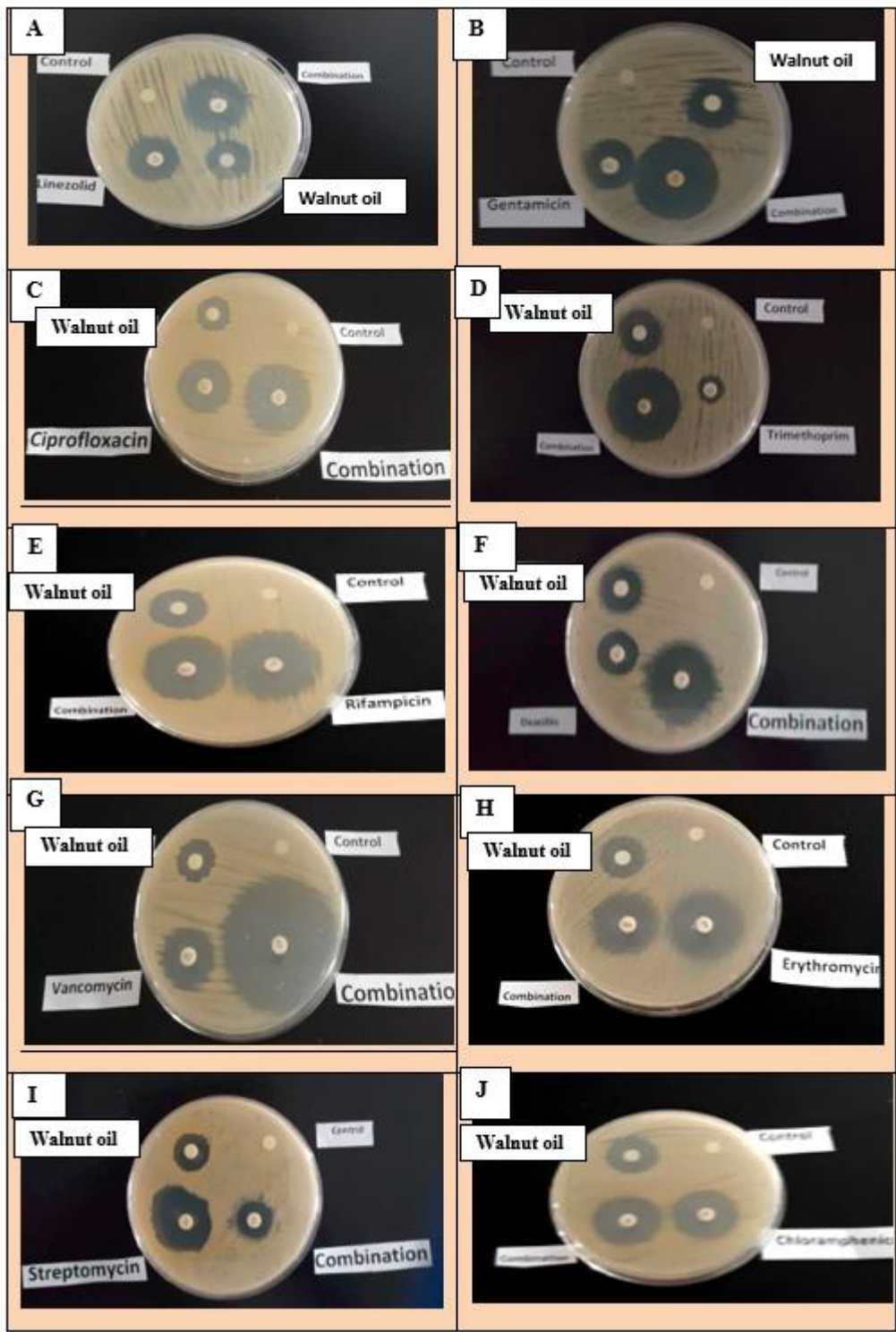
6538 indicated by the key hole formation. Carbenicillin exhibited a key-hole synergy against ATCC 6538. For the control no growth was observed in all the plates.

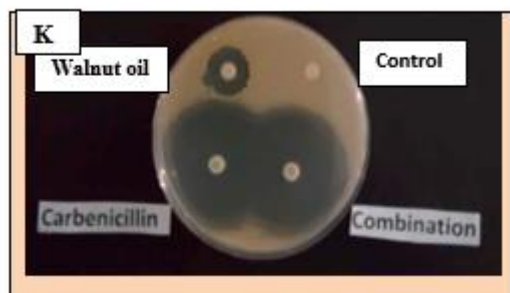


**Figure 39. Resistant pattern of ATCC 6538 to commercial antibiotics and synergy effect of African walnut oil with antibiotics**

Data on the graph is the diameter of clear zones of inhibition (mm). Bars represent the means standard deviation (SD) of three repeated experiments (n=3). Significant differences in the data were established at  $P < 0.05$  ( $P < 0.0001$ ) using two-way ANOVA with Bonferroni posttests. The red and blue bars represent the mean diameter zone of walnut oil alone and antibiotics alone while the white bars represent the zones of combination effect of antibiotics alone with African walnut oil on ATCC 6538. The line represents a threshold that limits the zones of inhibition of walnut oil against ATCC 6538.

**Antibacterial activities (zones of inhibition) of African walnut oil and its synergistic effect with selected antibiotics on *S. aureus* ATCC 6538**





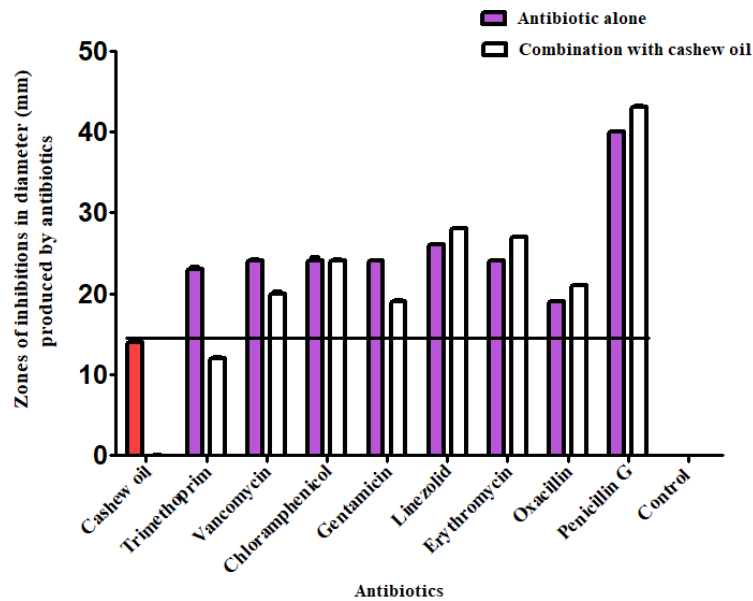
**Figure 40. Disk diffusion assay identifies walnut oil and selected commercial antibiotics with antimicrobial activity.**

Figure 40 shows the representative plates for disk diffusion assay of walnut oil against ATCC 6538. Control disc in all the plates contained 10  $\mu$ L of DMSO. (A). Antibacterial activity of walnut oil, linezolid 10  $\mu$ g and combination of 10  $\mu$ L walnut oil + linezolid 10  $\mu$ g. (B). Antibacterial activity of walnut oil, gentamicin 10  $\mu$ g and combination of 10  $\mu$ L walnut oil + gentamicin 10  $\mu$ g. (C). Antibacterial activity of walnut oil, ciprofloxacin 5  $\mu$ g and combination of 10  $\mu$ L walnut oil + ciprofloxacin 5  $\mu$ g. (D). Antibacterial activity of walnut oil, trimethoprim 1.25  $\mu$ g and combination of 10  $\mu$ L walnut oil + trimethoprim 1.25  $\mu$ g. (E). Antibacterial activity of walnut oil, rifampicin 15  $\mu$ g and combination of 10  $\mu$ L walnut oil + rifampicin 15  $\mu$ g. (F). Antibacterial activity of walnut oil, oxacillin 30  $\mu$ g and combination of 10  $\mu$ L walnut oil + oxacillin 30  $\mu$ g. (G). Antibacterial activity of walnut oil, vancomycin 30  $\mu$ g and combination of 10  $\mu$ L walnut oil + vancomycin 30  $\mu$ g. (H). Antibacterial activity of walnut oil, erythromycin 15  $\mu$ g and combination of 10  $\mu$ L walnut oil + erythromycin 15  $\mu$ g. (I). Antibacterial activity of walnut oil, erythromycin 15  $\mu$ g and combination of 10  $\mu$ L walnut oil + erythromycin 15  $\mu$ g. (J). Antibacterial activity of walnut oil, streptomycin 10  $\mu$ g and combination of 10  $\mu$ L walnut oil + streptomycin 10  $\mu$ g. (K) Antibacterial activity of pumpkin oil, carbenicillin 10  $\mu$ g and combination of 10  $\mu$ L pumpkin oil + carbenicillin 10  $\mu$ g. (L). Antibacterial activity of pumpkin oil, chloramphenicol 10  $\mu$ g and combination of 10  $\mu$ L pumpkin oil + chloramphenicol 10  $\mu$ g. Studies were performed in triplicate to ensure reproducibility, and mean values were calculated.

#### **5.2.1.5 Cashew oil effect on *S. aureus* ATCC 6538**

Cashew (*Anacardium occidentale*) oil showed low inhibitory activity against ATCC 6538 (Figure 41 and 42). The result of antibacterial susceptibility testing presented below shows that ATCC 6538 was susceptible to most of the antibiotics such as trimethoprim, erythromycin, gentamicin, streptomycin, vancomycin, linezolid, penicillin G and chloramphenicol. Cashew

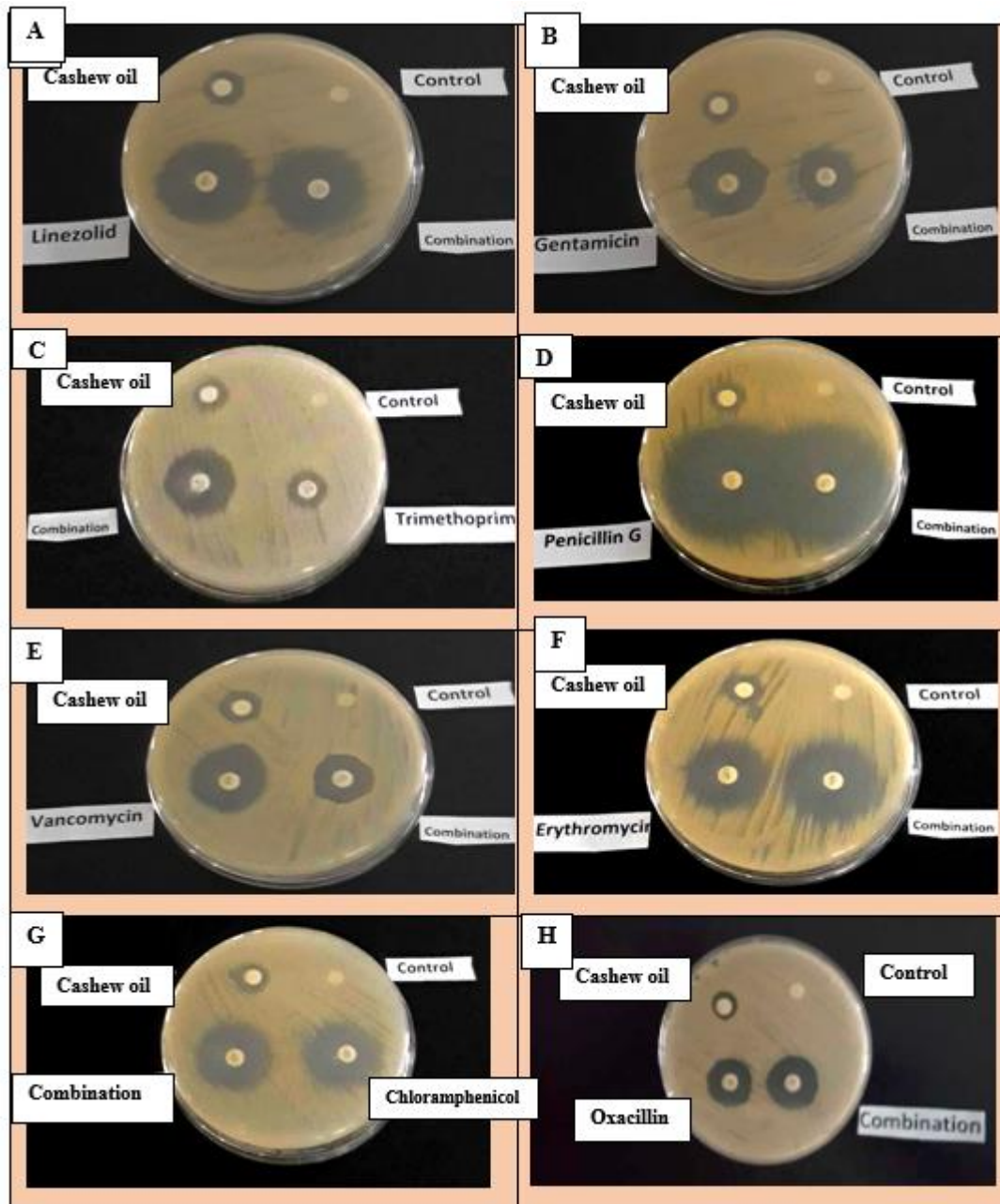
oil alone produced smaller zones (13 mm) indicating that it has low activity against ATCC 6538. For combination test, the antibiotics produced varied effects in combination with cashew oil. Combination of cashew oil with trimethoprim and penicillin G produced synergistic effect. Combination of cashew oil with gentamicin produced an antagonistic effect whereas combination with vancomycin, erythromycin and chloramphenicol produced an indifference effect.



**Figure 41. Resistant pattern of ATCC 6538 to commercial antibiotics and synergy effect of cashew oil with antibiotics**

Data on the graph is the diameter of clear zones of inhibition (mm). Bars represent the means standard deviation (SD) of three repeated experiments (n=3). Significant differences in the data were established at  $P < 0.05$  ( $P < 0.001$ ) using two-way ANOVA with Bonferroni posttests. The red and purple bars represent the mean diameter zone of cashew oil alone and antibiotics alone while the white bars represent the zones of combination effect of antibiotics alone with cashew oil. The line represents a threshold that limits the zones of inhibition of cashew oil against ATCC 6538.

**Antibacterial activities (zones of inhibition) of cashew oil and its synergistic effect with selected antibiotics on *S. aureus* ATCC 6538**



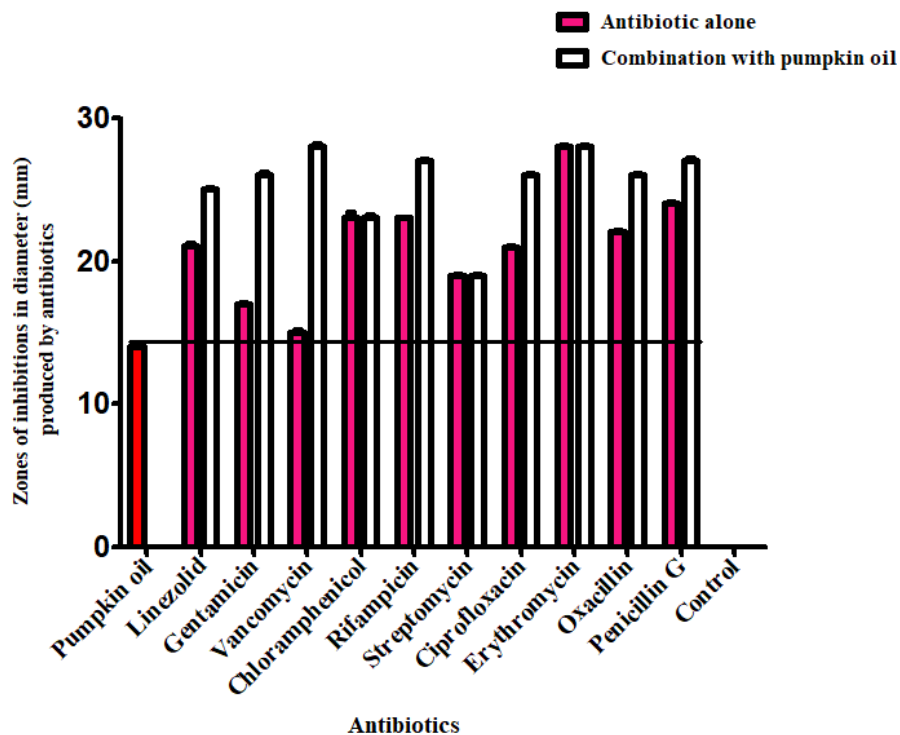
**Figure 42. Disk diffusion assay identifies cashew oil and selected commercial antibiotics with antimicrobial activity.**

Figure 42 shows the representative plates for disk diffusion assay of cashew oil against ATCC 6538. Control disc in all the plates contained 10  $\mu$ L of DMSO. A. Antibacterial activity of cashew oil, linezolid 10  $\mu$ g and combination of 10  $\mu$ L cashew oil + linezolid 10  $\mu$ g. B. Antibacterial activity of cashew oil, gentamicin 10  $\mu$ g and combination of 10  $\mu$ L walnut oil + gentamicin 10  $\mu$ g. C. Antibacterial activity of cashew oil, trimethoprim 1.25  $\mu$ g and

combination of 10  $\mu$ L cashew oil + trimethoprim 1.25  $\mu$ g. D. Antibacterial activity of cashew oil, penicillin G (15  $\mu$ g) and combination of 10  $\mu$ L cashew oil + penicillin G (15  $\mu$ g). E. Antibacterial activity of cashew oil, vancomycin 30  $\mu$ g and combination of 10  $\mu$ L cashew oil + vancomycin 30  $\mu$ g. F. Antibacterial activity of cashew oil, erythromycin 15  $\mu$ g and combination of 10  $\mu$ L cashew oil + erythromycin 15  $\mu$ g. I. Antibacterial activity of cashew oil, erythromycin 15  $\mu$ g and combination of 10  $\mu$ L cashew oil + erythromycin 15  $\mu$ g. G. Antibacterial activity of cashew oil, chloramphenicol 10  $\mu$ g and combination of 10  $\mu$ L cashew oil + chloramphenicol 10  $\mu$ g. Resultant zones of inhibitions produced by cashew oil alone, antibiotic disks and combination disks were measured in millimetre (mm) with a ruler and interpreted using the CLSI zone diameter interpretative standards. Studies were performed in triplicate to ensure reproducibility, and mean values were calculated.

#### **5.2.1.6 Fluted pumpkin oil effect on *S. aureus* ATCC 6538**

Fluted pumpkin (*Telfaria occidentalis*) oil showed significant inhibitory activity against ATCC 6538 (Figure 43 and 44). The disc diffusion test showed that ATCC 6538 was susceptible to most of the antibiotics tested. Antibacterial susceptibility testing with pumpkin oil alone produced moderately large zones of inhibitions indicating that pumpkin oil has the capability to kill ATCC 6538. For test with antibiotics alone, ATCC 6538 was susceptible to erythromycin, oxacillin, ciprofloxacin, streptomycin, vancomycin, linezolid, rifampicin, penicillin G and chloramphenicol. This result confirms the susceptibility character of ATCC 6538. For combination test, the antibiotics produced varied effects in combination with pumpkin oil. Combination of pumpkin oil with vancomycin, rifampicin and erythromycin led to a synergistic effect against ATCC 6538. Synergy between rifampicin and erythromycin was indicated by key-hole formation which was different from vancomycin synergy. An antagonistic effect was observed when pumpkin oil was combined with penicillin G. Combination of pumpkin oil with chloramphenicol and streptomycin resulted in an indifference effect against ATCC 6538. Because the combination results for ciprofloxacin and oxacillin were high and didn't result into synergy; their activities were categorized as indifference effects against ATCC 6538. For the control no growth was observed in all the plates.



**Figure 43. Resistant pattern of ATCC 6538 to commercial antibiotics and synergy effect of fluted pumpkin oil with antibiotics**

Data on the graph is the diameter of clear zones of inhibition (mm). Bars represent the means standard deviation (SD) of three repeated experiments (n=3). Significant differences in the data were established at  $P < 0.05$  ( $P < 0.0001$ ) using two-way ANOVA. The red and pink bars represent the mean diameter zone of pumpkin oil alone and antibiotics alone while the white bars represent the zones of combination effect of antibiotics alone with pumpkin oil on ATCC 6538. The line represents a threshold that limits the zones of inhibition of pumpkin oil against ATCC 6538.

**Antibacterial activities (zones of inhibition) of fluted pumpkin oil and its synergistic effect with selected antibiotics on *S. aureus* ATCC 6538**

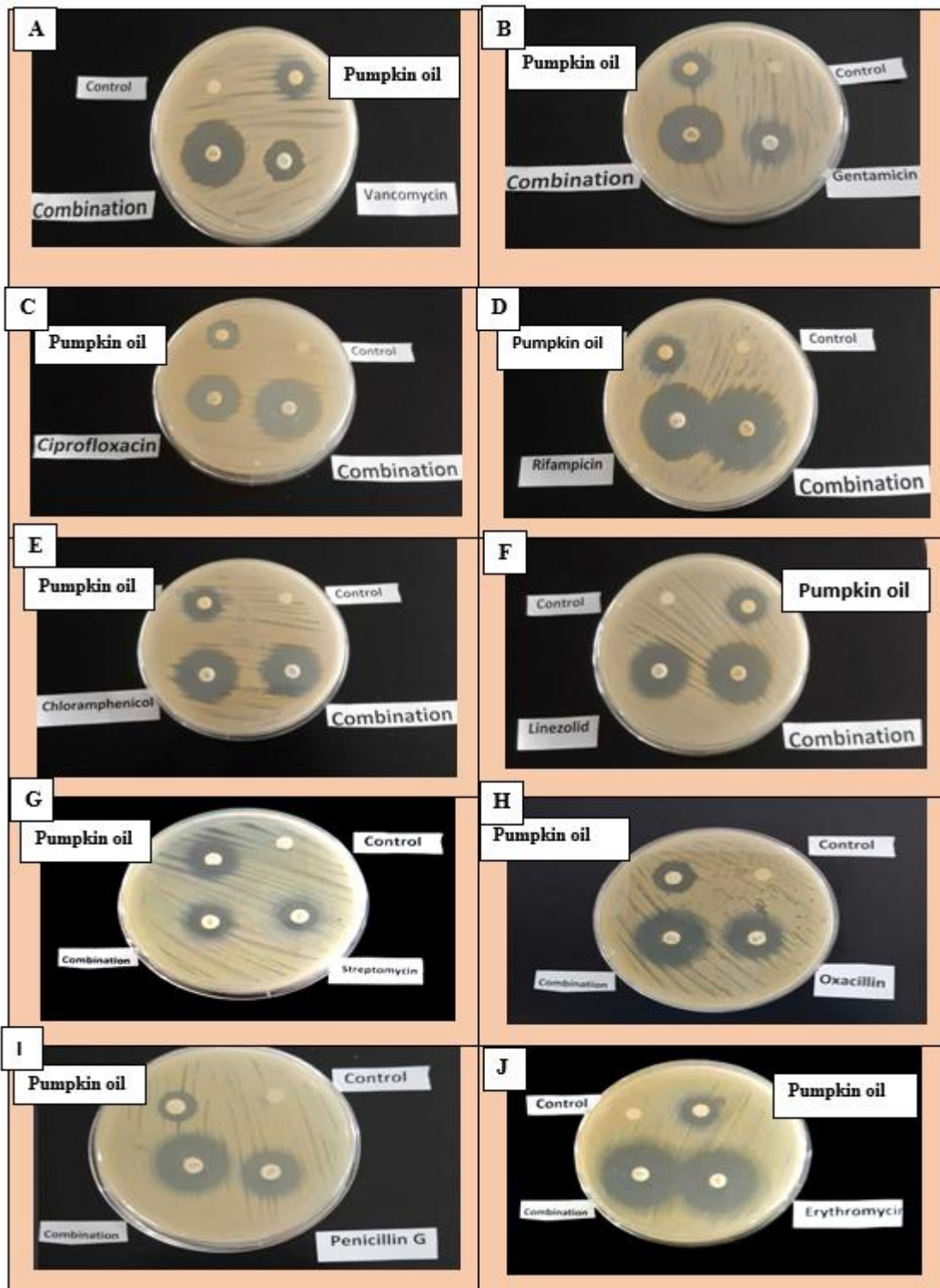


**Figure 44.** Disk diffusion assay identifies fluted pumpkin oil and selected commercial antibiotics with antimicrobial activity.

Figure 44 shows the representative plates for disk diffusion assay of pumpkin oil against ATCC 6538. Control disc in all the plates contained 10  $\mu$ L of DMSO. (A). Antibacterial activity of pumpkin oil, vancomycin 30  $\mu$ g and combination of 10  $\mu$ L pumpkin oil + vancomycin 30  $\mu$ g. (B). Antibacterial activity of pumpkin oil, gentamicin 10  $\mu$ g and combination of 10  $\mu$ L pumpkin oil + gentamicin 10  $\mu$ g. (C). Antibacterial activity of pumpkin oil, ciprofloxacin 5  $\mu$ g and combination of 10  $\mu$ L cashew oil + ciprofloxacin 5  $\mu$ g. (D). Antibacterial activity of cashew oil, rifampicin 15  $\mu$ g and combination of 10  $\mu$ L cashew oil + rifampicin 15  $\mu$ g. (E). Antibacterial activity of pumpkin oil, chloramphenicol 10  $\mu$ g and combination of 10  $\mu$ L pumpkin oil + chloramphenicol 10  $\mu$ g. (F). Antibacterial activity of pumpkin oil, linezolid 10  $\mu$ g and combination of 10  $\mu$ L pumpkin oil + linezolid 10  $\mu$ g. (G). Antibacterial activity of pumpkin oil, streptomycin 10  $\mu$ g and combination of 10  $\mu$ L pumpkin oil + streptomycin 10  $\mu$ g. (H). Antibacterial activity of pumpkin oil, oxacillin 30  $\mu$ g and combination of 10  $\mu$ L pumpkin oil + oxacillin 30  $\mu$ g. (I). Antibacterial activity of pumpkin oil, erythromycin 15  $\mu$ g and combination of 10  $\mu$ L pumpkin oil + erythromycin 15  $\mu$ g. (J). Antibacterial activity of pumpkin oil, penicillin G (15  $\mu$ g) and combination of 10  $\mu$ L pumpkin oil + penicillin G (15  $\mu$ g). Studies were performed in triplicate to ensure reproducibility, and mean values were calculated.

## **5.2.2 Oil control plates and well diffusion results of African walnut, cashew and fluted pumpkin extracts**

Control plates of ATCC 6538 and MRSA 252 cultured with DMSO and mineral oil did not show any zone of inhibitions as compared to the clear zones obtained previously for African walnut, cashew and pumpkin oils and extracts.

### **5.2.2.1 Oil control**

The oil control plates show no zones of inhibition were produced by MRSA 252 and ATCC 6538 when cultured with DMSO and mineral oil (Figure 45).

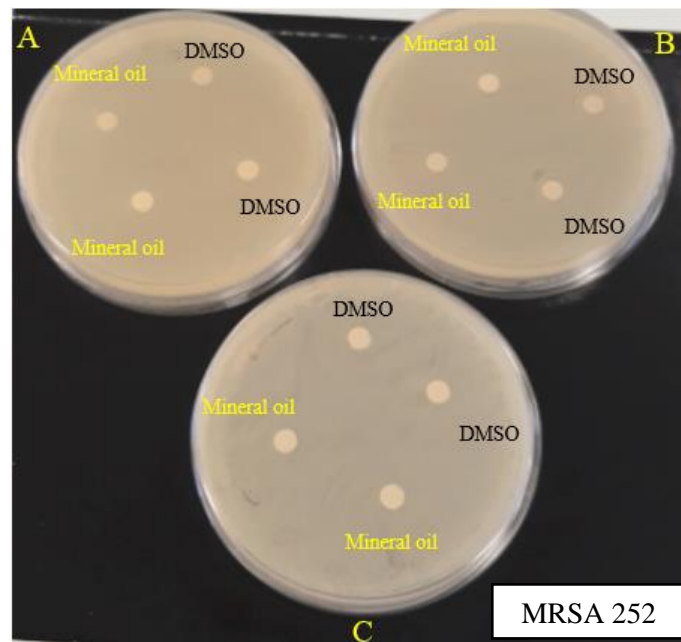
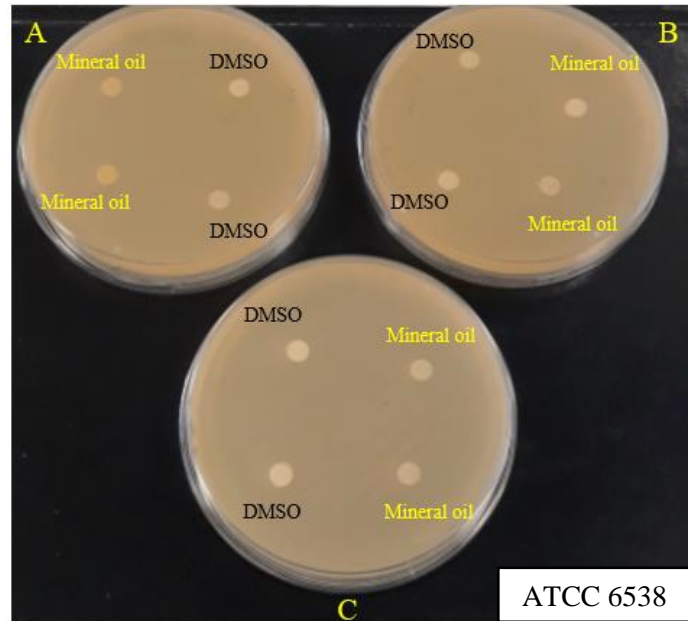


**Figure 45. Control plates of ATCC 6538 and MRSA 252 showing no zone of inhibitions with DMSO and mineral oil.**

#### **5.2.2.2 Effect of African walnut extracts on MRSA 252 and *S. aureus* ATCC 6538**

A well diffusion assay was used to test the antibacterial activity of extracts of African walnut, cashew and pumpkin. The extracts were obtained from three solvents-hexane, chloroform and petroleum ether. This assay was used as a preliminary test to ascertain the activity of each extract. The result is presented in Figure 46.

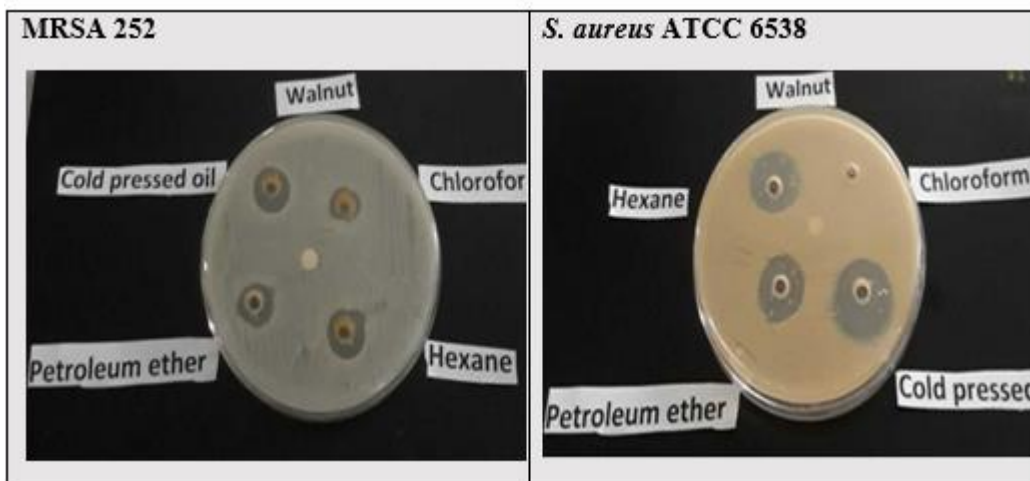


**Figure 46. Representative plates for well diffusion of African walnut extracts against MRSA 252 and ATCC 6538.**

Figure 46 shows that the pressed oil, hexane and petroleum extract of African walnut had significant activity against MRSA 252 and ATCC 6538. The diameter of the zones of ATCC 6538 were higher than those of MRSA 252, For MRSA 252 the zones were clear with 14 mm (petroleum ether), 16 mm (hexane), 10 mm (chloroform) and 17 mm (pressed oil). For ATCC 6538, the zones were also clear with large zones 18 mm (petroleum ether), 20 mm (hexane) and 25 mm (pressed oil). No zone was observed for chloroform. However, the result indicated that the hexane and the pressed oil had more activity against the two strains. In this assay 20 uL of each extract was used. In addition, control discs contained 20 uL of DMSO alone. 20 uL was used to allow a proper diffusion of the extracts into the agar plate.

### 5.2.2.3 Effect of fluted pumpkin extracts on MRSA 252 and *S. aureus* ATCC 6538

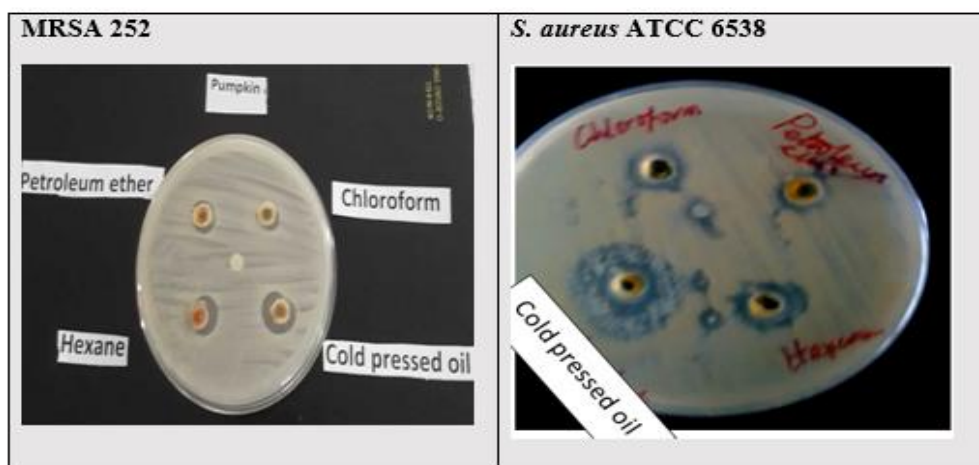


**Figure 47. Representative plates for well diffusion of fluted pumpkin extracts against MRSA 252 and ATCC 6538**

Figure 47 shows that the pressed oil, hexane and petroleum extract of African walnut had significant activity against both MRSA 252 and ATCC 6538. The diameter of the zones of ATCC 6538 were higher than those of MRSA 252, For MRSA 252 the zones were clear with 12 mm (petroleum ether), 14 mm (hexane), 9 mm (chloroform) and 17 mm (pressed oil). For ATCC 6538, the zones were also clear with large zones >10mm (7 mm petroleum ether and chloroform 9 mm), 12 mm (hexane) and 24 mm (pressed oil). However, the result indicates that the hexane and the pressed oil had more activity against the two strains. In this assay 20 uL of each extract was used. In addition, control discs contained 20 uL of DMSO alone.

### **5.2.3 Minimum inhibitory concentration and minimum biofilm inhibitory concentration of oils against MRSA 252 and *S. aureus* ATCC 6538 planktonic and biofilms**

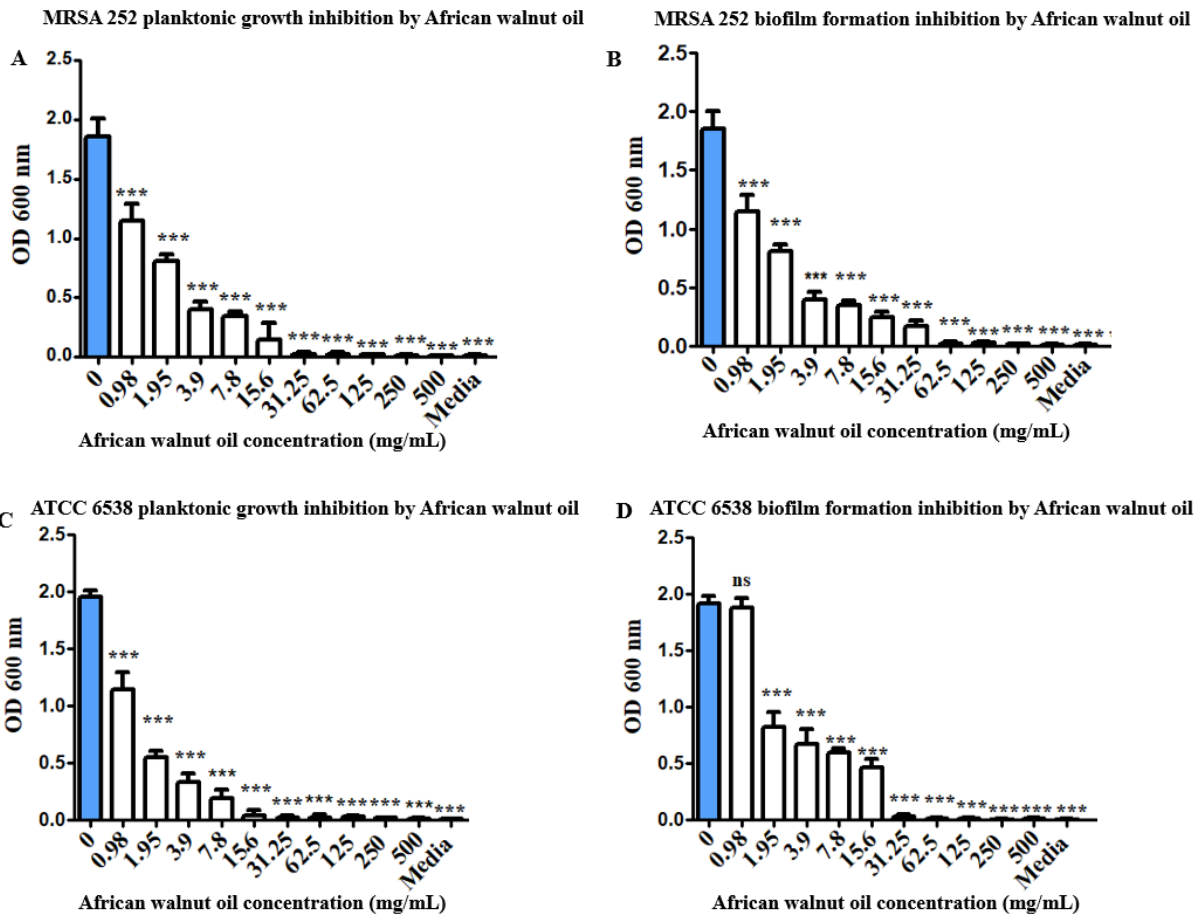
The antibacterial activity testing of MRSA 252 and ATCC 6538 was determined to ascertain whether the staphylococci strains were susceptible to African walnut oil, cashew oil and pumpkin oil along with their respective extracts. For the antibacterial susceptibility testing the assays Minimum Inhibition Concentration (MIC), Minimum Bactericidal Concentration, Minimum Biofilm Inhibitory Concentration (MBIC) and Minimum Bactericidal Eradication Concentration (MBEC) were performed to determine whether African walnut, cashew and pumpkin oils with their extracts that were active in the disc diffusion assay are effective in inhibiting planktonic growth and biofilm formation of MRSA 252 and *S. aureus* ATCC 6538. To effectively determine the antibacterial activity of African walnut, cashew and pumpkin oil and identify their concentration range for the following biofilm experiments, initially the MICs of walnut oil, cashew oil and pumpkin oil was determined following the CLSI Standard Broth Micro-dilution procedure. The activities of each oil sample on MRSA 252 and ATCC 6538 planktonic growth were investigated by determination of MICs of MRSA 252 and ATCC 6538 growth in TSB medium. *S. aureus* ATCC 6538 and MRSA 252 were cultured separately in the presence of different concentrations of walnut oil, cashew oil and pumpkin oil for 24 hours at 37°C to determine their MICs. In the context of this study, MIC was defined as the lowest oil concentration at which no visible turbidity was seen after 24 h hours of culture. All MIC and experiments were carried out in triplicate with three independent repetitions. MIC was defined as the lowest oil concentration with no growth after 24 h culture.

MBICs was defined as the lowest concentration of oil required to inhibit the growth of MRSA 252 and *S. aureus* ATCC 6538 biofilms or, in other words, it was considered as the lowest concentration of oil that prevents visible growth medium used to collect biofilms. For

determining the MBECs of the individual oils, the MBEC<sup>TM</sup>-HTP plate method was used to monitor the reduction in MRSA 252 and *S. aureus* ATCC 6538 counts of 48 h preformed biofilms in a recovery medium after challenging the strains with African walnut, cashew and pumpkin oils in a concentration range of 0.98 to 500 mg/mL and each oil sample has its MBEC value within this range. MBECs was defined as the lowest concentration of oil required to eradicate the biofilms of MRSA 252 and *S. aureus* ATCC 6538 or, in other words, it was considered as the lowest concentration of oil that prevents visible growth in the recovery medium used to collect biofilms.

#### **5.2.3.1 MICs and MBICs of African walnut oil against MRSA 252 and ATCC 6538 planktonic and biofilm growth**

African walnut oil significantly (Dunnett's test =  $P < 0.05$ ) inhibited the planktonic growth of MRSA 252 and *S. aureus* ATCC 6538 after 24 h of incubation (Figure 48 A & C). Figure 48 A & C showed that MRSA 252 and *S. aureus* ATCC 6538 were both susceptible to walnut oil at different concentrations tested. MICs of African walnut oil against planktonic cells of MRSA 252 was 15.6 mg/mL and ATCC 6538 was 7.8 mg/mL (Figure 48 A & C). Based on the results obtained African walnut oil revealed remarkable antibacterial effect against MRSA 252 and *S. aureus* ATCC 6538. MBIC values of MRSA 252 and ATCC 6538 biofilm cells were 31.25 and 15.6 mg/mL. MBIC results in Figure 48 B & D showed that walnut oil exhibited high antibacterial activity against MRSA 252 and *S. aureus* ATCC 6538 biofilms. From the data on the graph, walnut oil proved to be dose dependently successful in its ability to significantly ( $P < 0.05$ ) (Dunnett's test) inhibit biofilm formation of *S. aureus* ATCC 6538 and MRSA 252 in the 96-well plate after incubation for 24 hours at 37°C. Although the MBIC values are higher than the MIC values, they are considered low showing that African walnut oil can inhibit the growth of MRSA 252 and *S. aureus* ATCC 6538 biofilms at minimally low concentrations.



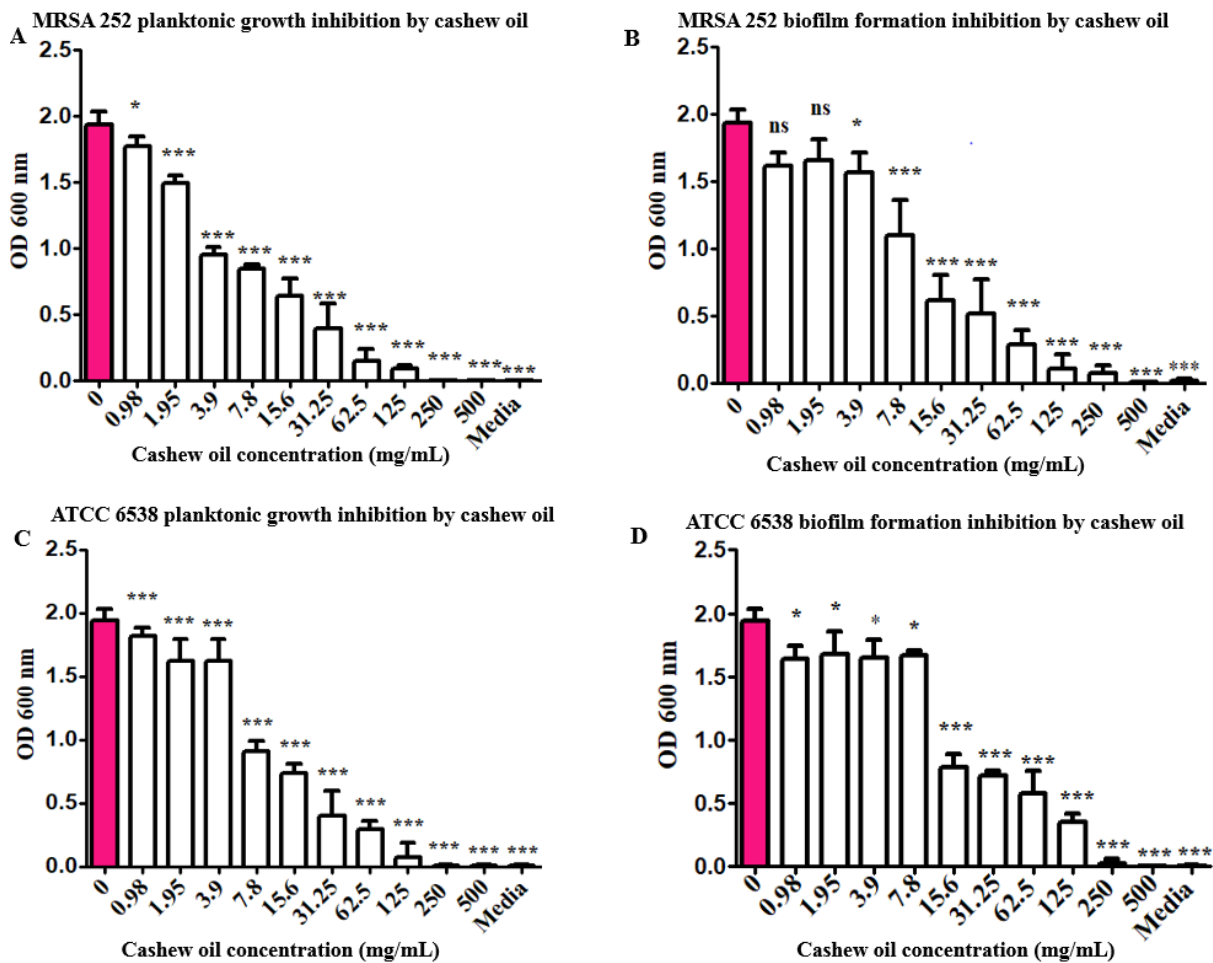
**Figure 48. Minimum inhibitory concentration and minimum biofilm inhibitory concentration of African walnut oil tested against MRSA 252 and *S. aureus* ATCC 6538 planktonic cells and preformed biofilms after 24 hours of incubation at 37°C in 96-well tissue culture polystyrene plate.**

Figure 48 shows (a) MRSA 252 planktonic growth inhibition by African walnut oil (b) MRSA 252 biofilm formation inhibition by African walnut oil (c) ATCC 6538 planktonic growth inhibition by African walnut oil and (d) ATCC 6538 biofilm formation inhibition by African walnut oil. Data on the graphs represent the mean OD values (Mean  $\pm$  SD) of three independent experiments (n=3) and the error bars indicate standard deviations of the means. For MIC, the OD of the planktonic growth cultures of MRSA and ATCC 6538 are shown, and MBIC, the absorbance of safranin stained cells attached to the surface of the 96-well plates after washing are showed for MRSA and ATCC 6538. Statistical analysis of the mean OD600 nm was performed using one-way ANOVA with Dunnett's comparison test. Asterisks (\*\*\*) above the columns indicates significant difference of each mean with walnut oil with the corresponding growth control group ( $p < 0.0001$ ). No significant (ns) difference at  $P > 0.05$ . Two controls were used: Media only without oil was used as negative blank and bacterial suspension used as positive growth control.

### **5.2.3.2 MICs and MBICs of cashew oil against MRSA 252 and ATCC 6538 planktonic and biofilm growth**

MICs of 125 mg/mL was obtained for MRSA 252 and ATCC 6538 planktonic growth cells (Figure 49 A & C). Cashew oil inhibited the growth planktonic cells of MRSA 252 and *S. aureus* ATCC 6538 significantly (Dunnett's test =  $P < 0.05$ ). Cashew oil showed very moderate inhibitory effect on *S. aureus* strains. Compared to walnut oil, cashew oil required higher concentrations to be an effective antimicrobial agent. MRSA 252 and *S. aureus* ATCC 6538 showed low susceptibility to cashew oil exhibiting the highest MICs of 125 mg/mL for both MRSA 252 and ATCC 6538 planktonic growth. (Figure 49 A & C).

In addition, MBIC results of cashew oil effect on MRSA 252 and *S. aureus* ATCC 6538 is shown in Figure 49 B & D. Cashew oil had an MBIC value of 250 mg/mL for MRSA 252 and 250 mg/mL for *S. aureus* ATCC 6538 indicating that a higher concentration is needed to inhibit biofilm formation in both strains. These values are higher than their MIC values. However, a weak antibacterial activity was observed and as such cashew oil was regarded as an antibacterial agent that is less active at inhibiting biofilm formation of MRSA 252 and *S. aureus* ATCC 6538.



**Figure 49. Minimum inhibitory concentration and minimum biofilm inhibitory concentration of cashew oil tested on MRSA 252 and *S. aureus* ATCC 6538 planktonic cells and preformed biofilms formed after 24 hours of incubation at 37°C in 96-well tissue culture polystyrene plates.**

Figure 49 shows (a) MRSA 252 planktonic growth inhibition by cashew oil (b) MRSA 252 biofilm formation inhibition by cashew oil (c) ATCC 6538 planktonic growth inhibition by cashew oil and (d) ATCC 6538 biofilm formation inhibition by cashew oil. Data on the graphs represent the mean OD values (Mean  $\pm$  SD) of three independent experiments (n=3) and the error bars indicate standard deviations of the means. For MIC, the OD of the planktonic growth cultures of MRSA 252 and ATCC 6538 are shown, and MBIC, the absorbance of safranin stained cells attached to the surface of the 96-well plates after washing are showed for MRSA 252 and ATCC 6538. Statistical analysis of the mean OD600 nm was performed using one-way ANOVA with Dunnett's test. Asterisks (\*\*\*) above the columns indicates significant difference of each column with walnut oil with the corresponding growth control group ( $p < 0.0001$ ). No significant (ns) difference at  $P > 0.05$ . Two controls were used: Media only without oil was used as negative blank and bacterial suspension used as positive growth control.

### 5.2.3.3 MICs and MBICs of fluted pumpkin oil against MRSA 252 and ATCC 6538 planktonic and biofilm growth

MIC of fluted pumpkin oil is presented in (Figure 50 A & C). Pumpkin oil inhibited the growth of planktonic cells of MRSA 252 and *S. aureus* ATCC 6538 significantly (Dunnett's test) and the inhibitory effect was observed to be concentration dependent. After 24 h of incubation with pumpkin oil, MRSA 252 and *S. aureus* ATCC 6538 showed high susceptibility to pumpkin oil exhibiting low MICs of 31.25 mg/mL and 62.5 mg/mL respectively.

MBIC results for fluted pumpkin oil activity against MRSA 252 and *S. aureus* ATCC 6538 is presented in Figure 50 B & D. The MBIC value varied between the strains and result indicates that pumpkin oil has high inhibitory activity against MRSA 252 and *S. aureus* ATCC 6538 biofilm formation. Pumpkin MBIC values for MRSA 252 and ATCC 6538 was 125 and 62.5 mg/mL. Pumpkin oil was considered an effective antibacterial agent.

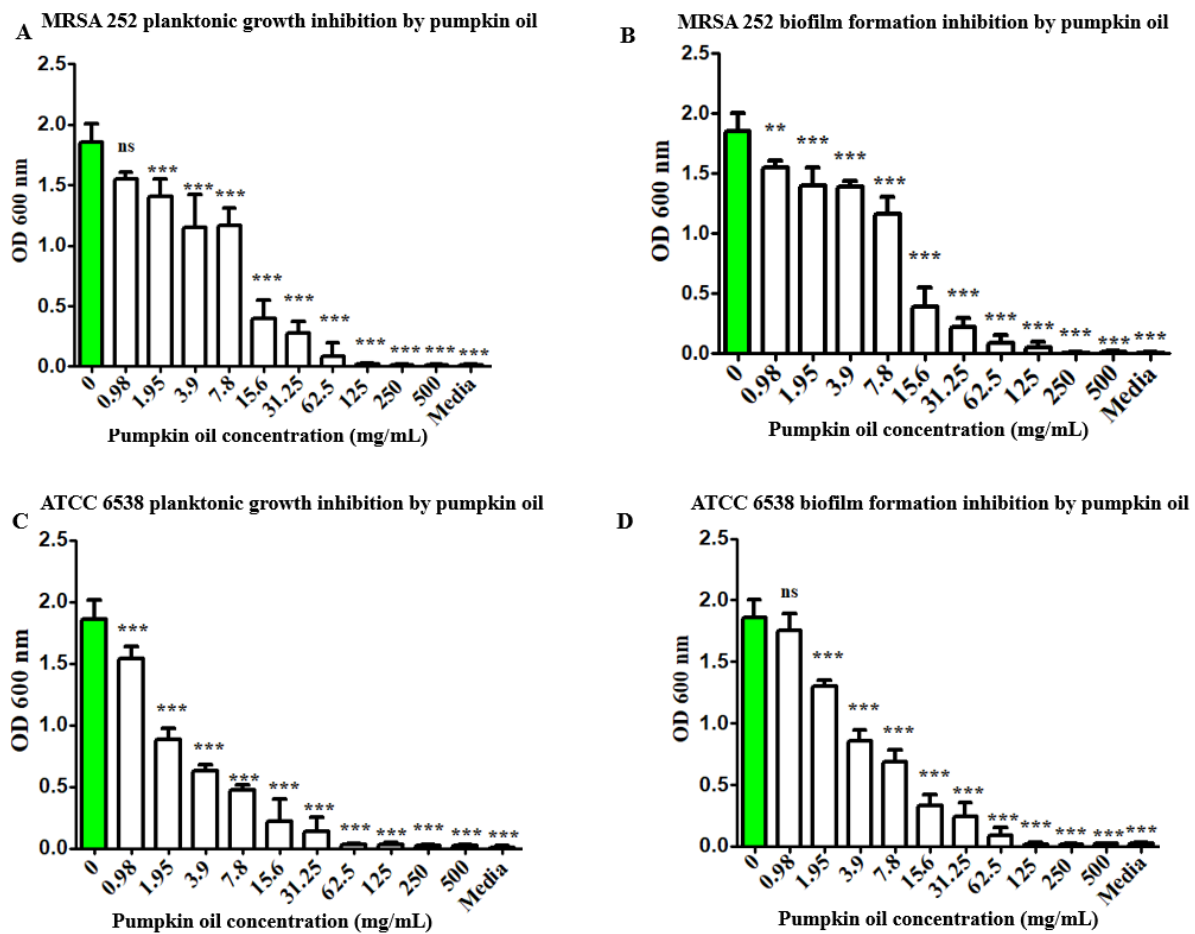


Figure 50. Minimum inhibitory concentration and minimum biofilm inhibitory concentration fluted pumpkin oil tested on MRSA 252 and *S. aureus* ATCC 6538 planktonic cells and preformed biofilms formed after 24 hours of incubation at 37°C in 96-well tissue culture plates.

Figure 50 shows (a) MRSA 252 planktonic growth inhibition by fluted pumpkin oil (b) MRSA 252 biofilm formation inhibition by pumpkin oil (c) ATCC 6538 planktonic growth inhibition by pumpkin oil and (d) ATCC 6538 biofilm formation inhibition by pumpkin oil. Data on the graphs represent the mean OD values (Mean  $\pm$  SD) of three independent experiments (n=3) and the error bars indicate standard deviations of the means. For MIC, the OD of the planktonic growth cultures of MRSA and ATCC 6538 are shown, and MBIC, the absorbance of safranin stained cells attached to the surface of the 96-well plates after washing are showed for MRSA and ATCC 6538. Statistical analysis of the mean OD600 nm was performed using one-way ANOVA with Dunnett's test. Asterisks (\*\*\*) above the columns indicates significant difference of each column with walnut oil with the corresponding growth control group ( $p < 0.0001$ ). No significant (ns) difference at  $P > 0.05$ . Two controls were used: Media only without oil was used as negative blank and bacterial suspension used as positive growth control.

In summary, a comparison of the results of inhibitory activity of walnut oil (Figure 48 A - D), pumpkin oil (Figure 49 A - D) and cashew oil (Figure 50 A - D) on MRSA 252 and ATCC 6538 planktonic and biofilm growth shows that low concentrations of walnut oil and pumpkin oil are required to inhibit the growth MRSA 252 and ATCC 6538 cells and the oils are considered effective antimicrobial agent on MRSA 252 and ATCC 6538 strains. In addition, cashew oil exhibited weak activity against MRSA 252 and ATCC 6538. However, of the three oils tested, walnut oil had the highest activity. Cashew oil was referred to as a weak antibacterial agent.

#### **5.2.4 MICs and MBICs of African walnut, cashew and fluted pumpkin extracts against MRSA 252 and *S. aureus* ATCC 6538 planktonic and biofilms**

African walnut, cashew and pumpkin extracts obtained from hexane, petroleum ether was tested. Chloroform extracts were not tested because the zone of inhibition obtained was smaller than 12 mm diameter as specified in CLSI guidelines. All the hexane and petroleum extracts of walnut, cashew and pumpkin were able to significantly (Dunnett's test =  $P < 0.05$ ) inhibit growth of planktonic cells of the two tested bacterial strains. The MIC and MBIC values varied among the various extracts tested. The effects of the different extracts on cell growth in 96-well microtiter plates was also dose dependent.

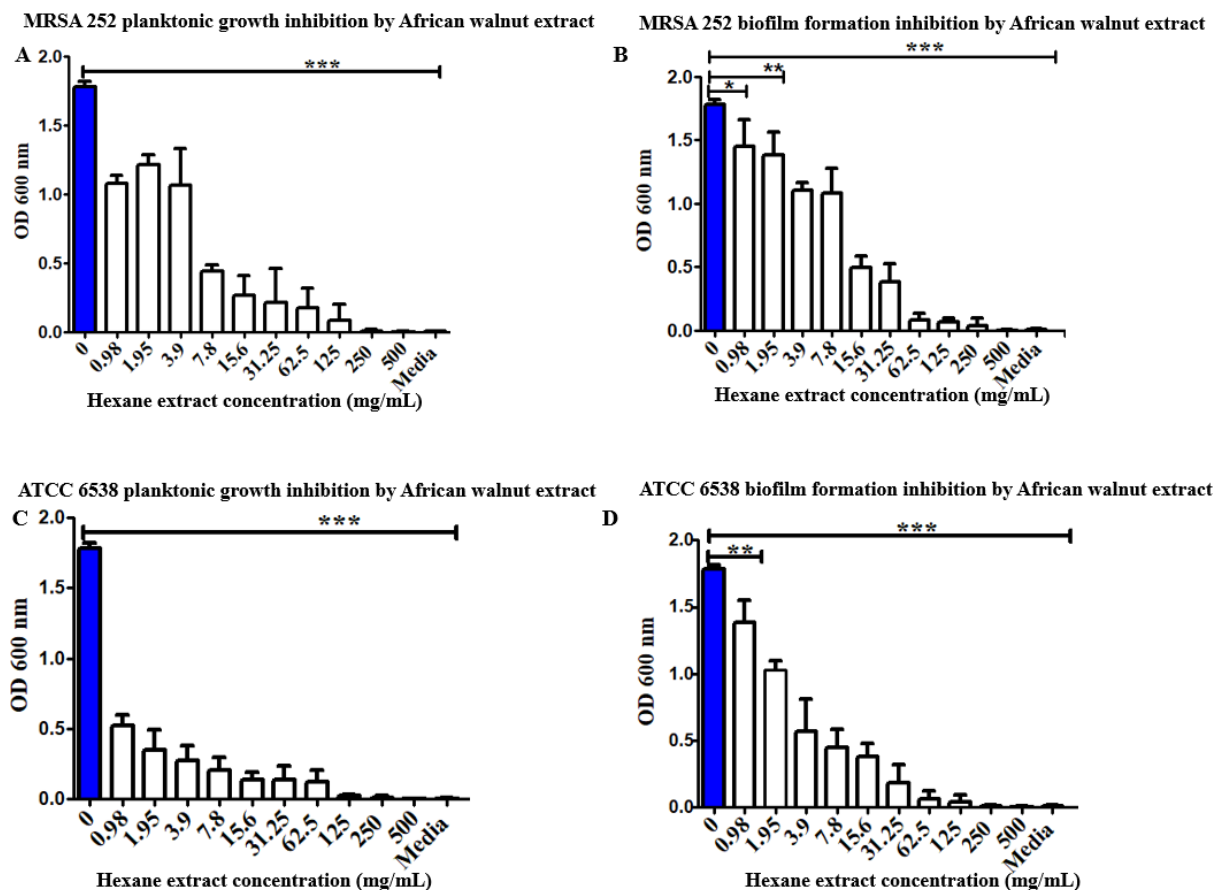
All the active and weak extracts of walnut, pumpkin and cashew were further used to determine the MBIC of the various extracts against MRSA 252 and *S. aureus* ATCC 6538. Some of the

MBIC values were relatively higher than the MIC values of both MRSA 252 and *S. aureus* ATCC 6538. Biofilm formation of MRSA 252 and *S. aureus* ATCC 6538 were observed to be significantly inhibited slightly by the active hexane extracts of walnut and pumpkin oil.

#### **5.2.4.1 MICs and MBICs of hexane extract of African walnut against MRSA 252 and ATCC 6538 planktonic and biofilm growth**

The lowest concentration considered as the MIC values of hexane extract that completely inhibited the growth of both MRSA 252 and *S. aureus* ATCC 6538 planktonic cells was 125 and 62.5 mg/mL since no turbidity was observed at these concentrations in the 96-well microtiter plates (Figure 51 A & C). This result showed that both strains were susceptible to African walnut hexane extract at high (125 mg/mL) and low (62.5 mg/mL) concentrations. The hexane extract exhibited concentration dependent concentrations. OD<sub>600</sub> readings of the TSB culture medium for each strain decreased with increased extract concentration. This result suggests that hexane extract of African walnut possess high antibacterial activity on ATCC 6538.

The hexane extract of African walnut oil significantly ( $P>0.05$ ) inhibited biofilm formation of MRSA 252 and *S. aureus* ATCC 6538 in microtiter plates at a concentration of 250 and 125 mg/mL. The inhibitory activity of walnut hexane extract on MRSA 252 and ATCC 6538 was good compared to MBICs of other extracts indicating that hexane extract of walnut possesses strong antibacterial activity. The hexane extract appeared to be active on ATCC 6538 than MRSA 252 (Figure 51).



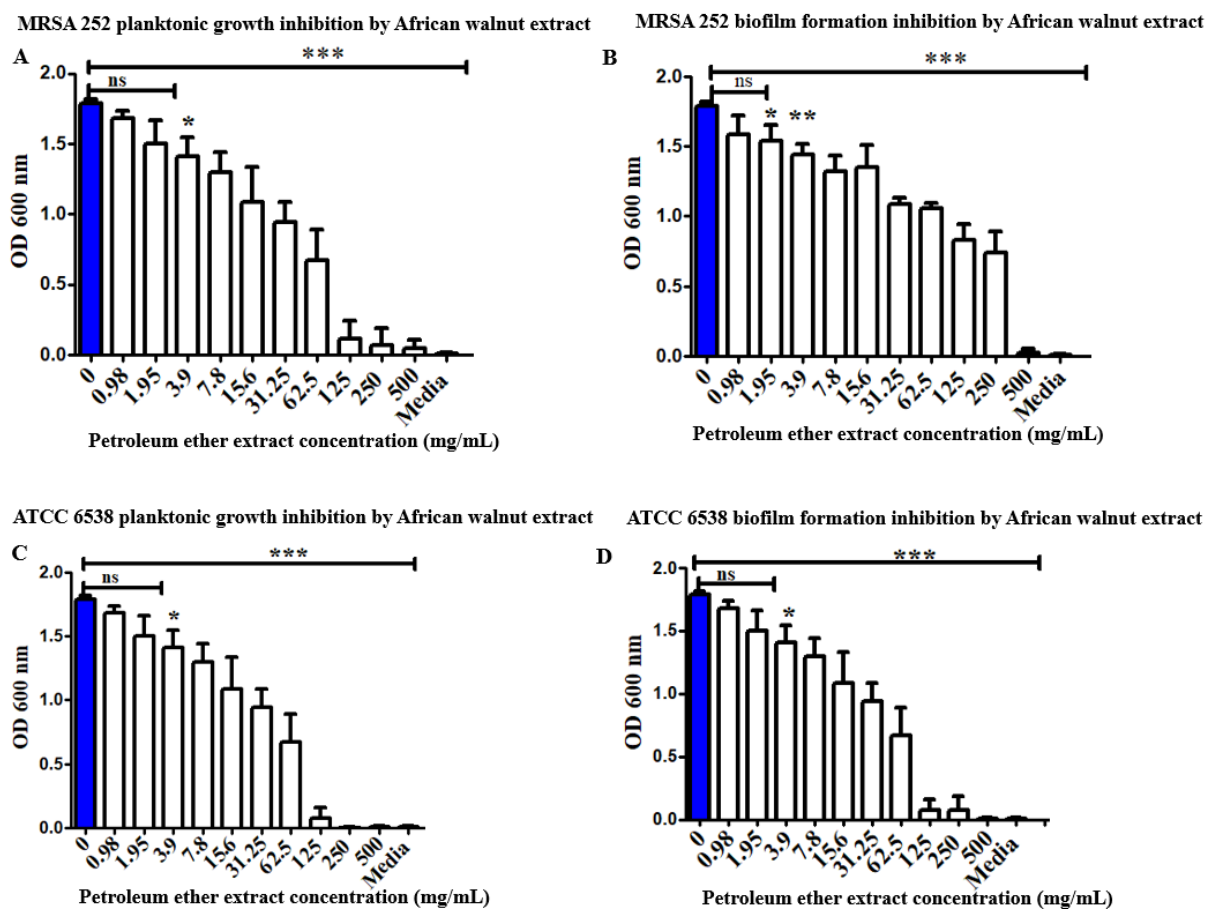
**Figure 51. Minimum inhibitory concentration and minimum biofilm inhibitory concentration of hexane extract African walnut tested on *S. aureus* ATCC 6538 and MRSA 252 planktonic cells and biofilms formed after 24 hours of incubation at 37°C in 96-well tissue culture polystyrene plates**

Figure 51 shows (a) MRSA 252 planktonic growth inhibition by African walnut hexane extract (b) MRSA 252 biofilm formation inhibition by African walnut hexane extract (c) ATCC 6538 planktonic growth inhibition by African walnut hexane extract and (d) ATCC 6538 biofilm formation inhibition by African walnut hexane extract. Data on the graphs represent the mean OD values (Mean  $\pm$  SD) of three independent experiments (n=3) and the error bars indicate standard deviations of the means. For MIC, the OD of the planktonic growth cultures of MRSA 252 and ATCC 6538 are shown, and MBIC, the absorbance of safranin stained cells attached to the surface of the 96-well plates after washing are showed for MRSA and ATCC 6538. Statistical analysis of the mean OD600 nm was performed using one-way ANOVA with Dunnett's test. Asterisks (\*\*\*) above the columns indicates significant difference of each column with walnut oil with the corresponding growth control group ( $p < 0.0001$ ). No significant (ns) difference at  $P > 0.05$ . Two controls were used: Media only without oil was used as negative blank and bacterial suspension with walnut extract was used as positive growth control to monitor the growth of MRSA 252 and *S. aureus* ATCC 6538.

### 5.2.4.2 MICs and MBICs of petroleum ether extract of African walnut against MRSA 252 and ATCC 6538 planktonic and biofilm growth

Petroleum ether extract of African walnut inhibited the planktonic growth of both MRSA 252 and *S. aureus* ATCC 6538 at higher concentrations of 500 mg/mL and 125 mg/mL (Figure 52 A & C). However, ATCC 6538 was more susceptible to petroleum ether extract at this concentration tested (Figure 52 C). Whereas, MRSA 252, inhibition at 500 mg/mL concentration is high and does not show that the strain was susceptible to petroleum ether extract. Compared to hexane extract, petroleum ether extract requires higher concentrations of 500 mg/mL to successfully inhibit the growth of MRSA 252 planktonic cells. Based on the results, petroleum ether extract exhibited weak activity against ATCC 6538 and a much weaker effect on MRSA 252.

On the other hand, petroleum ether extract of African walnut inhibited biofilm formation in MRSA 252 and *S. aureus* ATCC 6538 at very high concentrations of 500 and 250 mg/mL. On the basis of these results, hexane extract of walnut appeared more effective than the petroleum ether extracts. The petroleum ether extract was therefore considered a weak antibacterial agent.



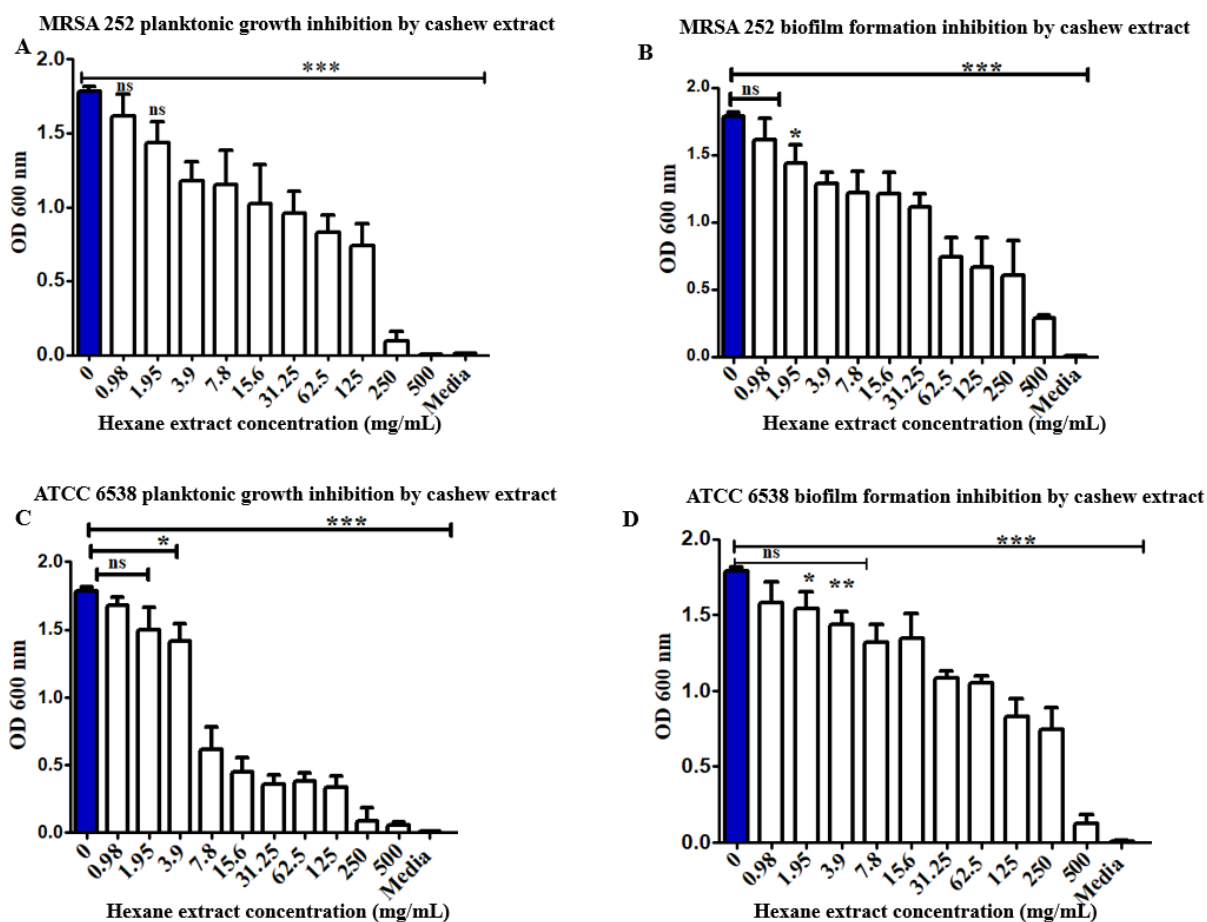
**Figure 52. Minimum inhibitory concentration and minimum biofilm inhibitory concentration of African walnut petroleum ether extract tested on *S. aureus* ATCC 6538 and MRSA 252 planktonic cells and biofilms formed after 24 hours of incubation at 37°C in 96-well tissue culture polystyrene plate**

Figure 52 shows (a) MRSA 252 planktonic growth inhibition by African walnut petroleum ether extract (b) MRSA 252 biofilm formation inhibition by African walnut petroleum ether extract (c) ATCC 6538 planktonic growth inhibition by African walnut petroleum ether extract and (d) ATCC 6538 biofilm formation inhibition by African walnut petroleum ether extract. Data on the graphs represent the mean OD values (Mean  $\pm$  SD) of three independent experiments (n=3) and the error bars indicate standard deviations of the means. For MIC, the OD of the planktonic growth cultures of MRSA 252 and ATCC 6538 are shown, and MBIC, the absorbance of safranin stained cells attached to the surface of the 96-well plates after washing are showed for MRSA and ATCC 6538. Statistical analysis of the mean OD600 nm was performed using one-way ANOVA with Dunnett's test. Asterisks (\*\*\*) above the columns indicates significant difference of each column with walnut oil with the corresponding growth control group ( $p < 0.0001$ ). No significant (ns) difference at  $P > 0.05$ . Two controls were used: Media only without oil was used as negative blank and bacterial suspension with African walnut extract was used as positive growth control to monitor the growth of MRSA 252 and *S. aureus* ATCC 6538.

**5.2.4.3 MICs and MBICs of hexane extract of cashew against MRSA 252 and ATCC 6538 planktonic and biofilm growth**

The MIC values of the tested cashew extracts against MRSA 252 and *S. aureus* ATCC 6538 are shown in Figure 53 A & C. The hexane extract of cashew exhibited considerably high MIC values of 250 and 500mg/mL against MRSA 252 and *S. aureus* ATCC 6538 planktonic cells. Result showed that cashew extract possesses much weaker antibacterial activity and will require 250 and 500 mg/mL to completely inhibit planktonic growth of MRSA 252 and ATCC 6538.

Biofilm formation of MRSA 252 and *S. aureus* ATCC 6538 were inhibited at 500 mg/mL concentrations. The MBIC values for the hexane extract of cashew against MRSA 252 and *S. aureus* ATCC 6538 were considerably higher indicating that a higher concentration is required to inhibit biofilm formation by MRSA 252 and *S. aureus* ATCC 6538.



**Figure 53. Minimum inhibitory concentration and minimum biofilm inhibitory concentration of cashew hexane extract tested on *S. aureus* ATCC 6538 and MRSA 252 planktonic cells and biofilms formed after 24 hours of incubation at 37°C in 96-well tissue culture polystyrene plate**

Figure 53 shows (a) MRSA 252 planktonic growth inhibition by hexane extract (b) MRSA 252 biofilm formation inhibition by hexane (c) ATCC 6538 planktonic growth inhibition by hexane and (d) ATCC 6538 biofilm formation inhibition by hexane. Data on the graphs represent the mean OD values (Mean  $\pm$  SD) of three independent experiments (n=3) and the error bars indicate standard deviations of the means. For MIC, the OD of the planktonic growth cultures of MRSA 252 and ATCC 6538 are shown, and MBIC, the absorbance of safranin stained cells attached to the surface of the 96-well plates after washing are showed for MRSA and ATCC 6538. Statistical analysis of the mean OD600 nm was performed using one-way ANOVA with Dunnett's test. Asterisks (\*\*\*) above the columns indicates significant difference of each column with walnut oil with the corresponding growth control group ( $p < 0.0001$ ). No significant (ns) difference at  $P > 0.05$ . Two controls were used: Media only without oil was used as negative blank and bacterial suspension with cashew extract was used as positive growth control to monitor the growth of MRSA 252 and *S. aureus* ATCC 6538.

#### **5.2.4.4 MICs and MBICs of petroleum ether extract of cashew against MRSA 252 and ATCC 6538 planktonic and biofilm growth**

In the case of petroleum ether extract, the MIC value of the tested extract against MRSA 252 and *S. aureus* ATCC 6538 are shown in Figure 54 A & C. Petroleum ether extract of cashew failed to inhibit the growth of MRSA 252 and ATCC 6538 planktonic cells even at the highest concentration of 500 mg/ml of cashew extract tested. This therefore indicates that more than 500 mg/mL of the extract is required to significantly inhibit the growth of both MRSA 252 and ATCC 6538 respectively.

Similarly, the antibacterial activity of petroleum ether extract from cashew nut could not inhibit biofilm formation in MRSA 252 and *S. aureus* ATCC 6538 even at a higher concentration. A higher concentration of the extract >500 mg/ml is needed to inhibit biofilm formation of MRSA 252 and ATCC 6538 in biofilms. The result indicates that cashew extracts possessed weak antibacterial activity (Figure 54 B & D).

Based on the results, both the hexane and petroleum extracts of cashew appeared very weak to inhibit the growth of MRSA 252 and *S. aureus* ATCC 6538 planktonic cells. Compared to other extracts, cashew extract seems to be the weakest antibacterial extract.

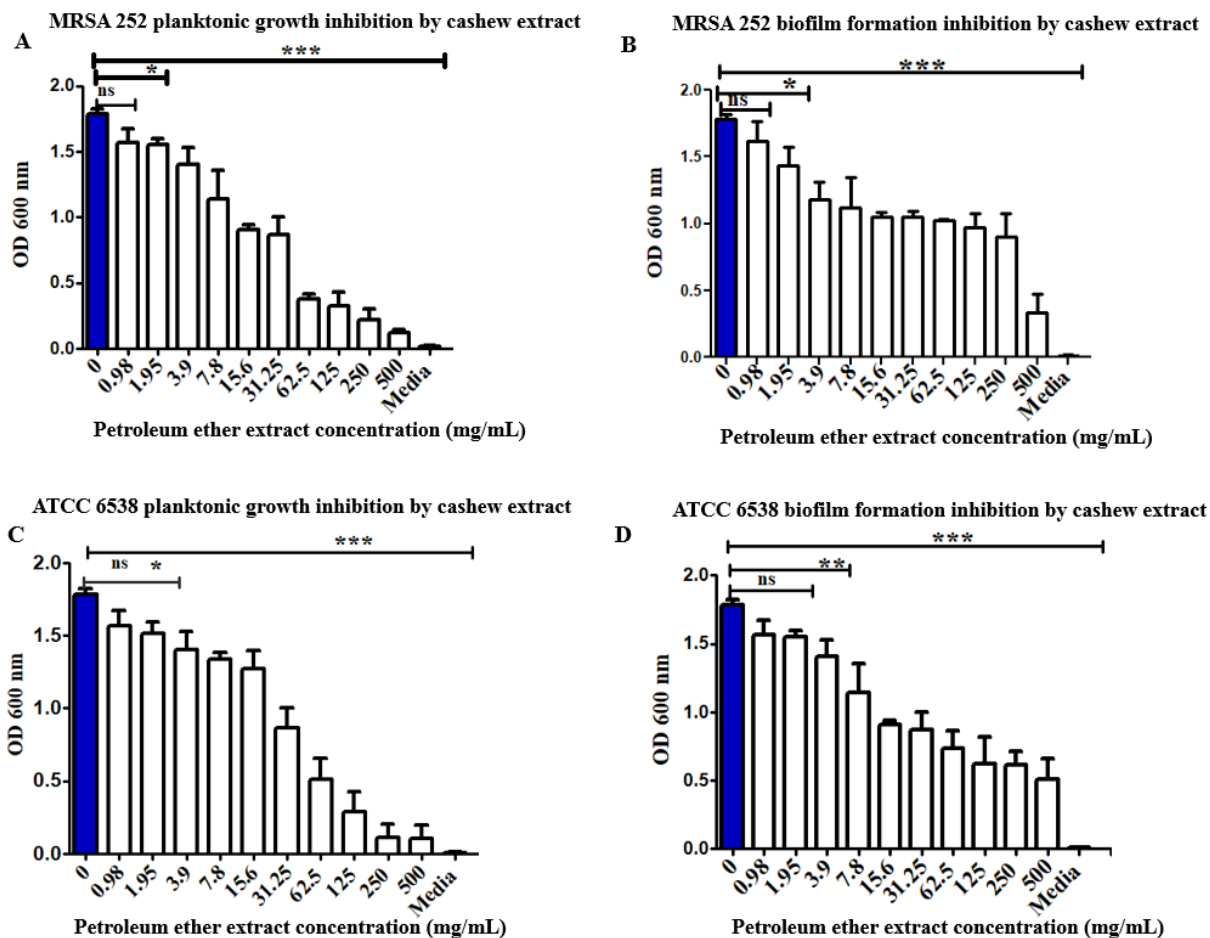


**Figure 54. Minimum inhibitory concentration and minimum biofilm inhibitory concentration of cashew petroleum ether extract tested on *S. aureus* ATCC 6538 and MRSA 252 planktonic cells and biofilms formed after 24 hours of incubation at 37°C in 96-well microtiter polystyrene plate**

Figure 54 shows (a) MRSA 252 planktonic growth inhibition by cashew petroleum ether extract (b) MRSA 252 biofilm formation inhibition by cashew petroleum ether extract (c) ATCC 6538 planktonic growth inhibition by cashew petroleum ether extract and (d) ATCC 6538 biofilm formation inhibition by cashew petroleum ether extract. Data on the graphs represent the mean OD values (Mean ± SD) of three independent experiments (n=3) and the error bars indicate standard deviations of the means. For MIC, the OD of the planktonic growth cultures of MRSA 252 and ATCC 6538 are shown, and MBIC, the absorbance of safranin stained cells attached to the surface of the 96-well plates after washing are showed for MRSA and ATCC 6538. Statistical analysis of the mean OD600 nm was performed using one-way ANOVA with Dunnett’s test. Asterisks (\*\*\*) above the columns indicates significant difference of each column with walnut oil with the corresponding growth control group (p < 0.0001). No significant (ns) difference at P>0.05. Two controls were used: Media only without

oil was used as negative blank and bacterial suspension with cashew extract was used as positive growth control to monitor the growth of MRSA 252 and *S. aureus* ATCC 6538.

#### **5.2.4.5 MICs and MBICs of hexane extract of fluted pumpkin against MRSA 252 and ATCC 6538 planktonic and biofilm growth**

The MIC values of the tested fluted pumpkin seed extracts against MRSA 252 and *S. aureus* ATCC 6538 are shown in Figure 55 A & C. Hexane extract of pumpkin inhibited planktonic growth of MRSA 252 and *S. aureus* ATCC 6538 at a concentration of 250 and 62.5 mg/mL. From the result, ATCC 6538 planktonic appears to very susceptible to hexane extract than MRSA 252 planktonic cells. MRSA 252 planktonic cell was weakly susceptible. The result obtained showed that hexane extract had high antibacterial activity on the growth of ATCC 6538 planktonic cells alone.

The MBIC value of fluted pumpkin hexane on MRSA 252 and *S. aureus* ATCC 6538 was 500 and 125 mg/mL. MRSA 252 and ATCC 6538 were inhibited at higher concentrations of pumpkin extract suggesting that a higher concentration of the hexane extract is needed to inhibit biofilm formation of both strains (Figure 55 B & D).

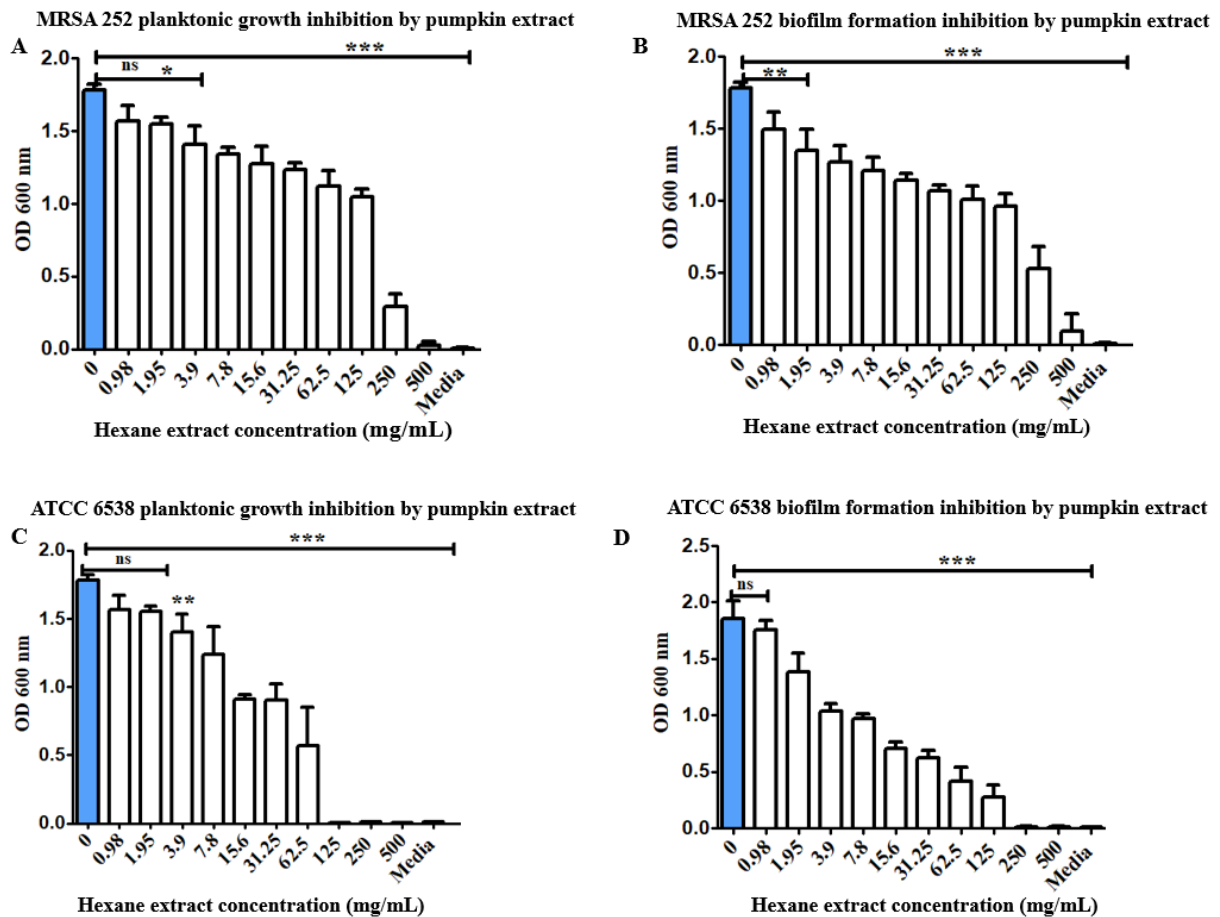


**Figure 55. Minimum inhibitory concentration and minimum biofilm inhibitory concentration of pumpkin hexane extract tested on *S. aureus* ATCC 6538 and MRSA 252 planktonic cells and biofilms formed after 24 hours of incubation at 37°C in 96-well tissue culture polystyrene plate**

Figure 55 shows (a) MRSA 252 planktonic growth inhibition by pumpkin hexane extract (b) MRSA 252 biofilm formation inhibition by pumpkin hexane extract (c) ATCC 6538 planktonic growth inhibition by pumpkin hexane extract and (d) ATCC 6538 biofilm formation inhibition by pumpkin hexane extract. Data on the graphs represent the mean OD values (Mean  $\pm$  SD) of three independent experiments (n=3) and the error bars indicate standard deviations of the means. For MIC, the OD of the planktonic growth cultures of MRSA 252 and ATCC 6538 are shown, and MBIC, the absorbance of safranin stained cells attached to the surface of the 96-well plates after washing are showed for MRSA and ATCC 6538. Statistical analysis of the mean OD600 nm was performed using one-way ANOVA with Dunnett's test. Asterisks (\*\*\*) above the columns indicates significant difference of each column with walnut oil with the corresponding growth control group ( $p < 0.0001$ ). No significant (ns) difference at  $P > 0.05$ . Two controls were used: Media only without oil was used as negative blank and bacterial

suspension with pumpkin extract was used as positive growth control to monitor the growth of MRSA 252 and *S. aureus* ATCC 6538.

#### **5.2.4.6 MICs and MBICs of petroleum ether extract of fluted pumpkin against MRSA 252 and ATCC 6538 planktonic and biofilm growth**

For petroleum ether extract, MIC value of the tested extract against MRSA 252 and *S. aureus* ATCC 6538 are shown in Figure 56 A & C. MIC value for MRSA 252 and *S. aureus* ATCC 6538 was 250 and 500 mg/mL. This result indicates that the extract possesses weak antibacterial activity against the staphylococcus strains. The MBIC of petroleum ether extract was 500 mg/mL for both MRSA 252 and ATCC 6538. However, the hexane extract still appears more effective than the petroleum ether 56 B & D.

A critical examination of the activity of hexane extract and petroleum ether extracts of pumpkin seed showed that only the hexane extract of walnut oil possessed higher antibacterial activity against ATCC 6538 and MRSA 252 and was considered the strongest antibacterial agent.

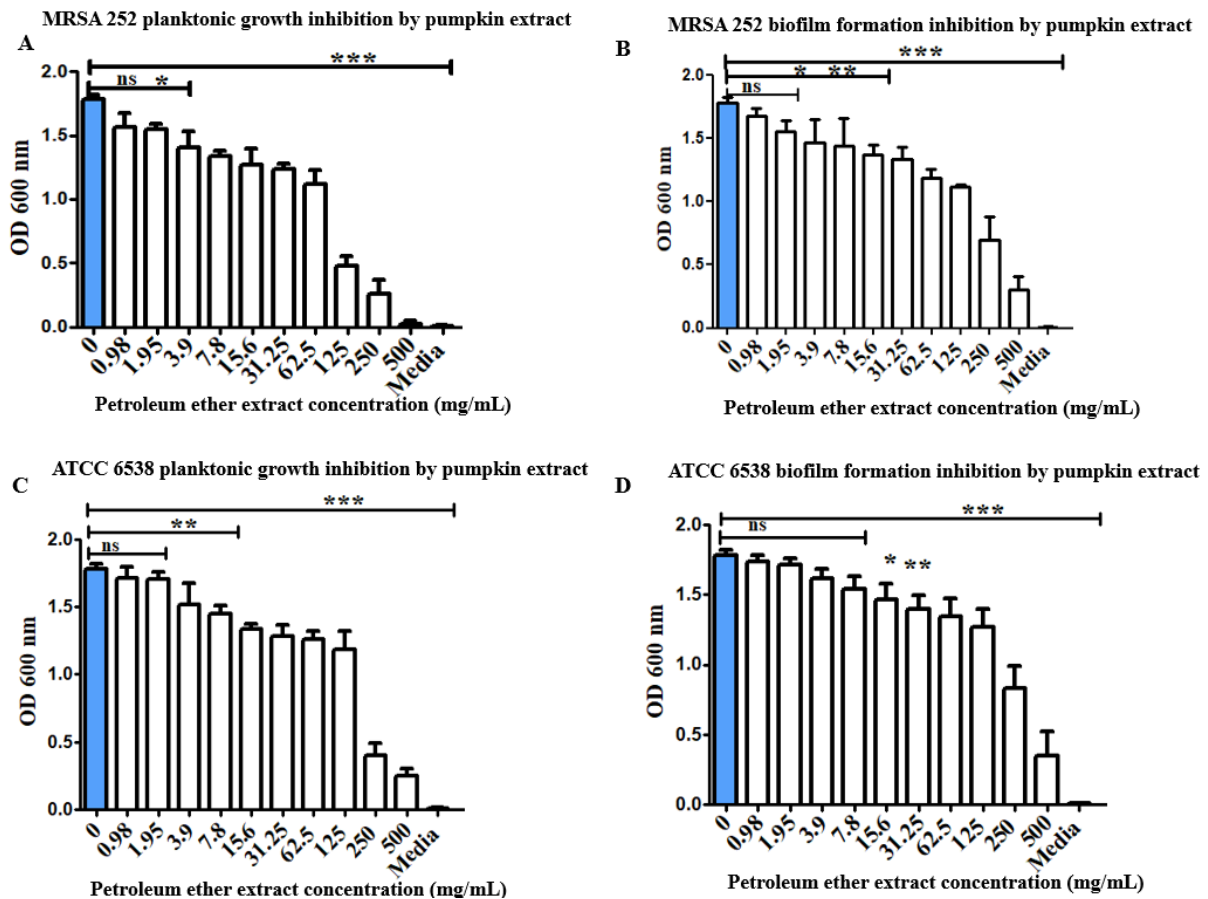


Figure 56. Minimum inhibitory concentration and minimum biofilm inhibitory concentration of pumpkin petroleum ether tested on *S. aureus* ATCC 6538 and MRSA 252 planktonic cells and biofilms formed after 24 hours of incubation at 37°C in 96-well tissue culture polystyrene plate

Figure 56 shows (a) MRSA 252 planktonic growth inhibition by pumpkin ether extract (b) MRSA 252 biofilm formation inhibition by pumpkin petroleum ether extract (c) ATCC 6538 planktonic growth inhibition by pumpkin petroleum ether extract and (d) ATCC 6538 biofilm formation inhibition by pumpkin petroleum ether extract. Data on the graphs represent the mean OD values (Mean  $\pm$  SD) of three independent experiments (n=3) and the error bars indicate standard deviations of the means. For MIC, the OD of the planktonic growth cultures of MRSA 252 and ATCC 6538 are shown, and MBIC, the absorbance of safranin stained cells attached to the surface of the 96-well plates after washing are showed for MRSA and ATCC 6538. Statistical analysis of the mean OD600 nm was performed using one-way ANOVA with Dunnett's test. Asterisks (\*\*\*) above the columns indicates significant difference of each column with walnut oil with the corresponding growth control group ( $p < 0.0001$ ). No significant (ns) difference at  $P > 0.05$ . Two controls were used: Media only without oil was used as negative blank and bacterial suspension with pumpkin extract was used as positive growth control to monitor the growth of MRSA 252 and *S. aureus* ATCC 6538.

### **5.2.5 Minimum biofilm eradication concentration of African walnut, cashew fluted pumpkin oils against MRSA 252 and *S. aureus* ATCC 6538 biofilms**

Biofilm eradication activities of the oils were determined using the minimum biofilm eradication concentration high throughput (MBEC<sup>TM</sup>-HTP) procedure which is in two main stages. (i) Determination of biofilm growth on MBEC<sup>TM</sup>-HTP pegs and (ii) recovery of biofilm cells after a challenge with antibacterial agents at different concentrations. The results are presented below. To effectively quantify the eradication effect of the different oil sample, the minimum biofilm eradication concentration (MBEC) assay was used to determine the total number of viable cells in the treated versus non-treated MRSA 252 and *S. aureus* ATCC 6538 biofilms. In doing this assay, firstly biofilm growth check of MBEC<sup>TM</sup>-HTP pegs cultured differently with aliquots of 100  $\mu$ L ( $10^8$  CFU/mL) of MRSA 252 and *S. aureus* ATCC 6538 incubated for 48 h at 37 °C was first performed. The 48 h biofilms formed by each bacterium on the MBEC peg was regarded as their respective preformed biofilms. Viable bacteria count of the MBEC<sup>TM</sup>-HTP pegs was also regarded as the mean cell density of each bacterium. Biofilm growth check of the MBEC<sup>TM</sup>-HTP pegs was necessary to have an idea of the total biofilm viable count of each bacteria per well. Secondly, each individual well having pegs with biofilms was then challenged with different concentrations of African walnut, cashew and pumpkin oils in the range of 0.98 - 500 mg/mL and recovered with fresh 100  $\mu$ L of TSB broth placed in wells of new 96-well microtiter plate. After challenging each well with oil concentrations in the range of 0.98 - 500 mg/mL, recovery of MRSA 252 and ATCC 6538 biofilm cells were determined by total viable count using the spread plate method for direct spot counting. The reduction in total viable count after treatment is reported in log<sub>10</sub> CFU/mL.

#### **(i) Biofilm growth check on MBEC pegs**

Biofilms of MRSA 252 and *S. aureus* ATCC 6538 were grown to an overall mean density of  $8.37 \pm 0.49$  and  $8.33 \pm 0.30$  log<sub>10</sub> cfu peg<sup>-1</sup> (respectively) in tryptic soy broth medium enriched with glucose (Figure 57 and 58). This growth was for 48 h of incubation at 37°C. Mean and standard deviation calculations for cell densities were based on pooled data from three to four growth experiments performed with control. The mean viable cell counts and standard deviation (SD) for *S. aureus* ATCC 6538 and MRSA 252 on the pegs of A1-H1 row of the MBEC<sup>TM</sup>-HTP assay are presented in (Figure 57 and 58). The cell density of biofilms grown on the different rows of pegs in the MBEC<sup>TM</sup>-HTP assay were not statistically significant ( $p =$

0.1914 for MRSA 252;  $p = 0.7332$  for ATCC 6538. Both strains also formed statistically equivalent biofilms across the different rows of pegs (A-H) in the microtiter plates.

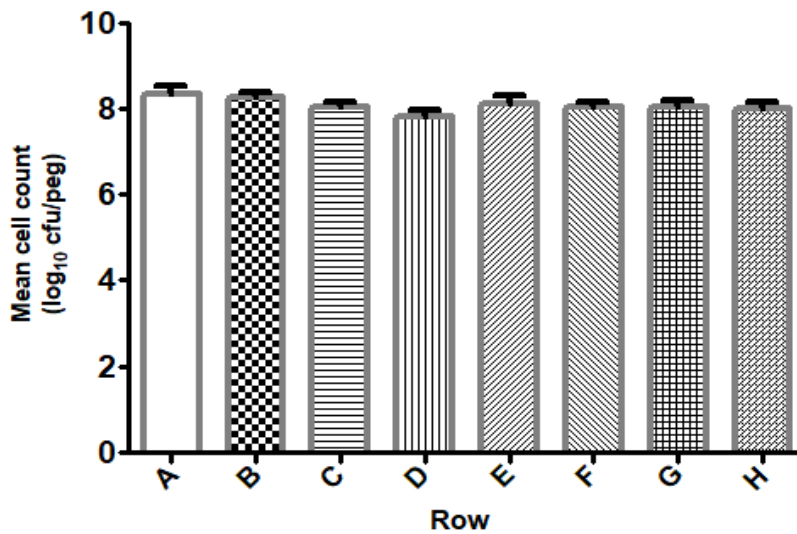


Figure 57. Preformed biofilms of ATCC 6538 on MBEC pegs.

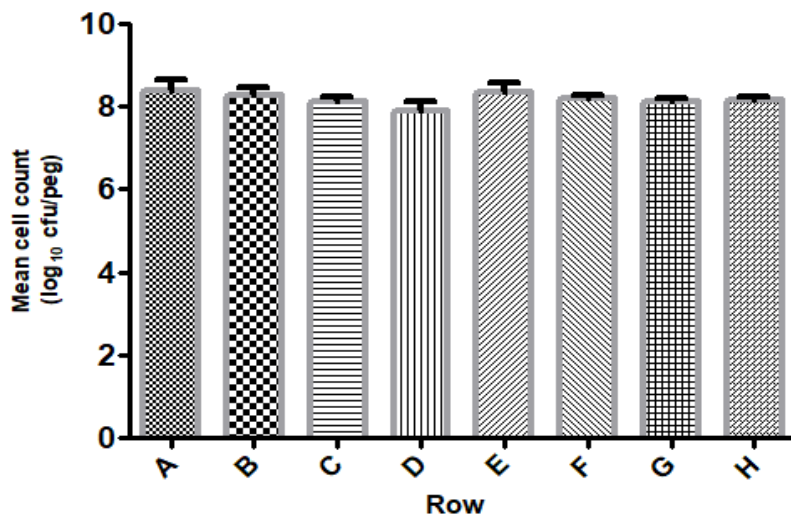


Figure 58. Preformed biofilms of MRSA 252 on MBEC pegs.

Figure 57 and 58 shows mean cell density of ATCC 6538 and MRSA 252 biofilms on the pegs in different rows of the MBEC assay after 48 hours of incubation. Each value is expressed as the mean and standard deviation of 3 to 4 trials. There is no significant difference between cell density of biofilms in the different rows ( $p = 0.6709$  using one-way ANOVA, the Bonferonni's multiple comparison test to compare all means). Mean cell density of ATCC 6538 on the pegs in different rows of the MBEC assay. Each value is expressed as the mean and standard

deviation of 3 to 4 trials. There is no significant difference between cell density of biofilms in the different rows ( $p =$  and 0.7332 using one-way ANOVA). Based on the p-values obtained, the biofilm cell density of MRSA 252 and ATCC 6538 were significant different.

**(ii) Eradication activity of African walnut oil against MRSA 252 and ATCC 6538.**

In order to effectively determine whether African walnut oil, cashew oil and pumpkin oil could also act as bactericidal agents in biofilms using the MBEC™-HTP plate, the colony forming unit (CFU) reduction was monitored in MRSA 252 and *S. aureus* ATCC 6538 48 h preformed biofilms with initial count of 8.37 log<sub>10</sub> CFU/mL and 8.33 log<sub>10</sub> CFU/mL per peg of bacteria treated with different concentrations of African walnut, cashew and pumpkin oil respectively for 48 h. MBEC was used to evaluate the ability of African walnut, cashew and pumpkin oils to disrupt/eradicate preformed biofilm of MRSA 252 and *S. aureus* ATCC 6538. The bacterial count of biofilm cells of MRSA 252 and ATCC 6538 at 6, 12, 24 and 48 h in recovery media after challenging the cells on the pegs with different concentrations of African walnut, cashew and pumpkin oils (0.98 -500 mg/mL) was calculated and the results are expressed as Log<sub>10</sub> cfu/mL (log reduction) of the treated versus non-treated bacterial sample. The results are reported as log reductions to know whether the oils are effective in reducing the pathogens tested. The greater the log reduction value, the more effective the oil is at killing the bacterial strains. Results are presented in table 25.

**Table 25. MRSA 252 and *S. aureus* ATCC 6538 counts in 12 h, 24 h and 48 h-biofilms, in growth recovery media expressed as log<sub>10</sub> cfu/mL, after exposure to different concentrations of African walnut oil.**

African Walnut oil conc. mg/mL	Viable cell count reduction in 6 h, 12, 24 and 48 h biofilms of MRSA 252 and ATCC 6538 after exposure to African walnut oil. Results are expressed as log <sub>10</sub> cfu/mL							
	MRSA 252				<i>S. aureus</i> ATCC 6538			
	6 h	12 h	24 h	48 h	6 h	12 h	24 h	48 h
<b>Growth control</b>	8.37 ± 0.49	8.44 ± 0.42	8.60 ± 0.53	8.64 ± 0.60	8.33 ± 0.30	8.43 ± 0.64	8.46 ± 0.59	8.53 ± 0.48
0.98	8.29 ± 0.56	6.59 ± 0.71	5.34 ± 0.41	3.34 ± 0.41	8.43 ± 0.43	8.16 ± 0.54	5.34 ± 0.41	3.78 ± 0.86
1.95	7.60 ± 0.78	5.99 ± 1.09	4.66 ± 1.16	2.99 ± 0.58	7.88 ± 0.70	7.82 ± 0.78	4.66 ± 1.29	3.33 ± 0.88
3.9	7.21 ± 0.81	6.02 ± 1.44	4.02 ± 0.72	1.85 ± 0.52	7.28 ± 0.96	6.68 ± 0.58	3.85 ± 0.51	2.52 ± 0.51
7.8	6.95 ± 0.33	5.43 ± 1.21	3.43 ± 1.21	1.69 ± 0.56	7.72 ± 0.80	5.94 ± 0.65	4.36 ± 0.59	2.03 ± 0.97

15.6	4.88 ± 1.00	3.63 ± 0.59	3.13 ± 0.71	1.54 ± 0.14	4.88 ± 0.94	4.35 ± 0.87	3.21 ± 0.66	1.52 ± 0.94
31.5	3.66 ± 1.52	3.16 ± 0.92	2.25 ± 0.16	0.27 ± 0.08	4.32 ± 0.57	2.83 ± 0.60	1.37 ± 0.89	1.01 ± 0.58
62.5	3.21 ± 0.97	2.21 ± 0.58	1.89 ± 0.42	0.29 ± 0.13	3.21 ± 0.59	2.21 ± 0.58	No counts	No counts
125	2.48 ± 0.95	1.77 ± 0.89	No counts	No counts	2.55 ± 0.49	1.76 ± 0.56	No counts	No counts
250	2.07 ± 0.48	1.41 ± 0.48	No counts	No counts	1.51 ± 0.58	1.41 ± 0.55	No counts	No counts
500	1.70 ± 0.43	1.24 ± 0.51	No counts	No counts	1.50 ± 0.46	1.24 ± 0.65	No count	No counts
20 mg/mL Oxacillin	0.91 ± 0.16	0.91 ± 0.16	0.91 ± 0.16	0.91 ± 0.16	0.91 ± 0.16	0.91 ± 0.16	0.91 ± 0.16	0.91 ± 0.16

Table 25. Shows the viable count of recovery cells in the recovery medium after 6 h, 12 h, 24 h and 48 h incubation periods. Results at different growth time points shows log reduction of viable counts of MRSA 252 and ATCC 6538 biofilms after treatment with African walnut oil.

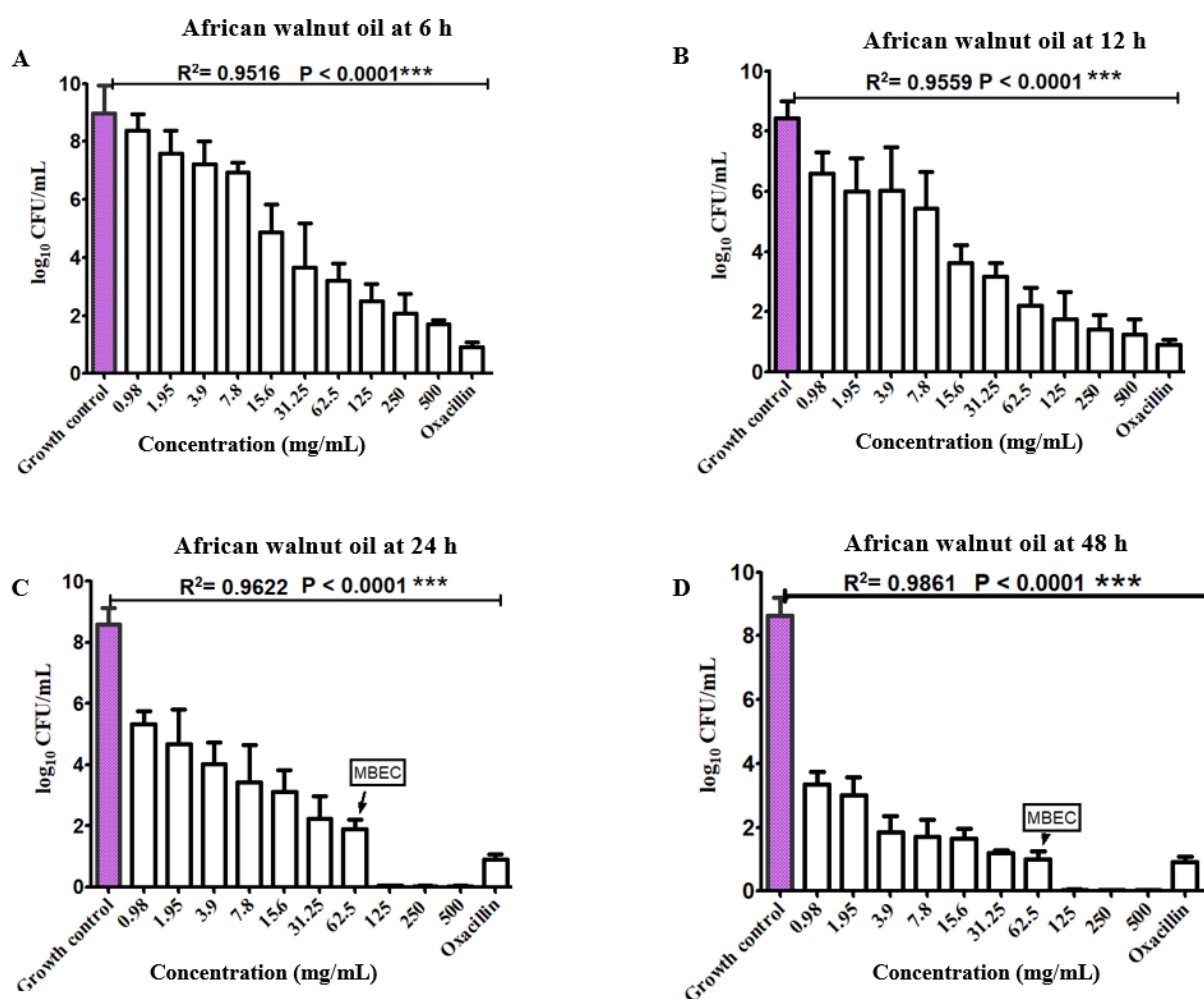


Figure 59. Reduction of MRSA 252 preformed biofilm on pegs following exposure to increasing concentrations of African walnut oil at 0.98-500 mg/mL after 6, 12, 24 and 48 h of incubation at 37°C.

Figure 59 shows the bactericidal effect of African walnut oil on MRSA 252 preformed biofilms. In addition, data on the graph shows the log of the mean CFU/peg after 6, 12, 24 and 48 h incubation of the TSB recovery medium at 37°C. The control in this experiment CFU/peg obtained for the untreated peg after the total 48 h incubation period and biofilm growth check with 8.37 log<sub>10</sub> CFU/mL per/peg served as the reference (growth control) for treatment efficacy. Data were obtained from three independent experiments (n=3). Significant differences in comparison to the untreated controls (growth control) and the negative control oxacillin 20 mg/mL were performed. Statistical analysis was performed using one-way ANOVA: \*\*\*, P<0.0001 with Bonferroni's post-tests. Both the positive and negative controls were included in the experiment to monitor the recovery of the bacterial isolate in biofilm.

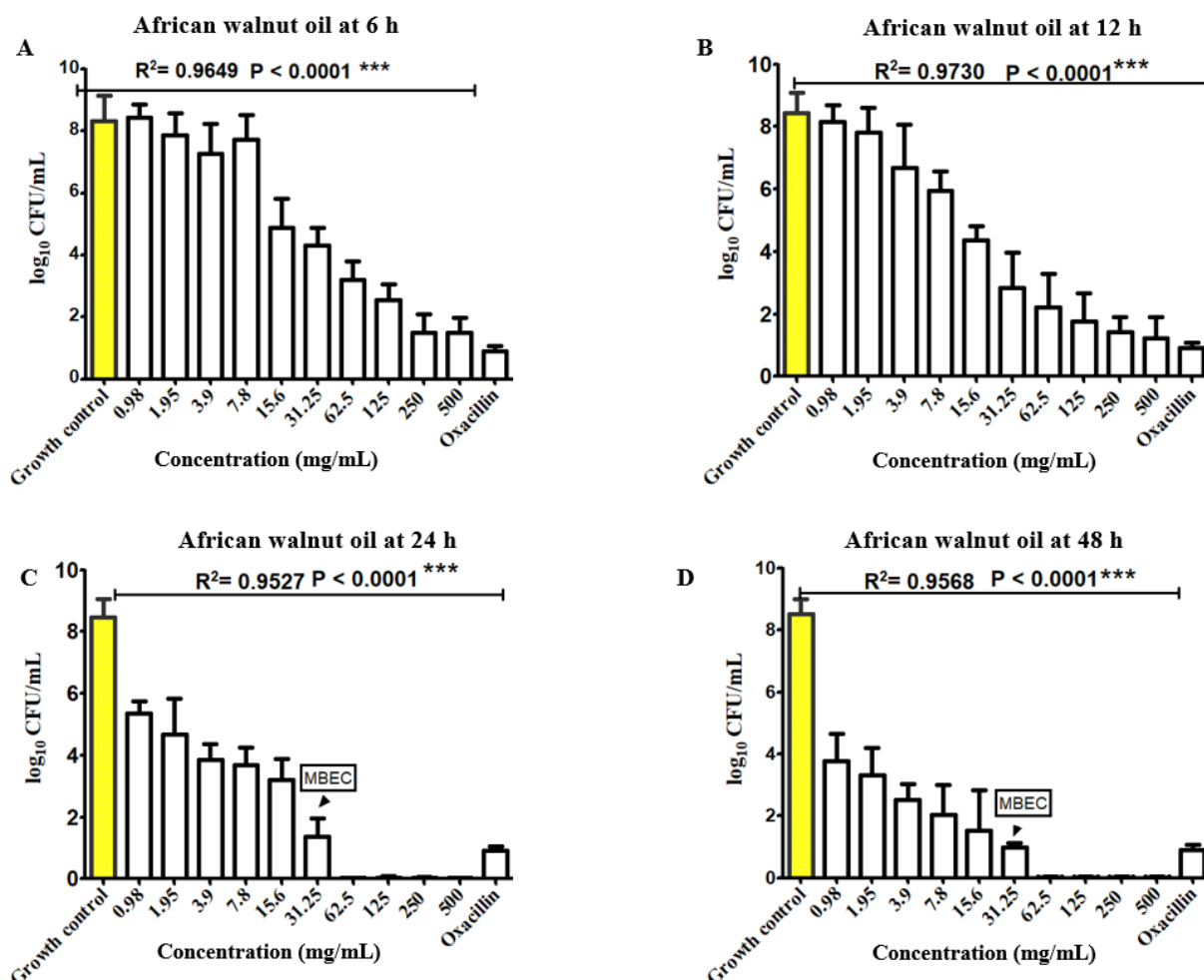


Figure 60. Reduction of *S. aureus* ATCC 6538 preformed biofilm on pegs following exposure to increasing concentrations of African walnut oil at 0.98-500 mg/mL after 6, 12, 24 and 48 h of incubation at 37°C.

Figure 60 shows the bactericidal effect of African walnut oil on *S. aureus* ATCC 6538 preformed biofilms. In addition, data on the graph shows the log of the mean CFU/peg after 6, 12, 24 and 48 h incubation of the TSB recovery medium at 37°C. The control in this experiment CFU/peg obtained for the untreated peg after the total 48 h incubation period and biofilm growth check with 8.33 log<sub>10</sub> CFU/mL per/peg served as the reference (growth control) for treatment efficacy. Data were obtained from three independent experiments (n=3). Significant differences in comparison to the untreated controls (growth control) and the negative control oxacillin 20 mg/mL were performed. Statistical analysis was performed using one-way ANOVA: \*\*\*, P<0.0001 with Bonferroni's post-tests. Both the positive and negative controls were included in the experiment to monitor the recovery of the bacterial isolate in biofilm.

From the MBEC result of MRSA 252 and ATCC 6538, the challenge of MRSA 252 and *S. aureus* ATCC 6538 with African walnut oil resulted in significant decrease of viable biofilm cells in recovery medium at 6 h, 12 h, 24 h and 48 h (Figure 59 - 60). Bacterial counts in both MRSA 252 and ATCC 6538 biofilms started to decrease drastically in viable count after exposure to 15.6 mg/mL of African walnut oil for 6 h. (Figure 59 – 60). However, despite the decrease at this concentration, at 24 and 48 h a better reduction in viable count was observed at 62.5 mg/mL and 31.25 mg/mL concentration of MRSA 252 and ATCC 6538 biofilm. MBEC was considered the lowest oil concentration able to prevent a recovery of microbial growth. Using this definition, it could be seen that the MBEC of African walnut oil was 62.5 mg/mL and 31.25 mg/mL concentration active against MRSA 252 causing approximately 5 log reductions and ATCC 6538 causing >7 log reduction after 24 and 48h. Therefore, African walnut oil was considered highly effective because it was able to eradicate staphylococcal strains progressively starting from 6, 12, 24 and 48 hours at low concentration as seen on the graph.

### **(iii) Eradication activity of Cashew oil against MRSA 252 and ATCC 6538**

Cashew oil was considered weakly effective because it was weak in eradicating MRSA 252 and ATCC 6538 biofilm cells progressively from 6, 12, 24 and 48 hours at the different concentrations tested. Cashew oil exhibited similar eradication activity against MRSA 252 and ATCC 6538 at 500 mg/mL concentration for MRSA 252 and ATCC 6538 respectively. Bacterial counts of MRSA 252 and ATCC 6538 biofilm cells started to decrease significantly (p < 0.0001) immediately after exposure to 31.25 mg/mL of walnut oil for 6 h. The data on the

graphs and table 26 shows a time and concentration-dependent decrease of bacterial counts recorded as log reduction. (MBEC).

**Table 26. MRSA 252 and *S. aureus* ATCC 6538 counts in 12 h, 24 h and 48 h-biofilms, in growth recovery media expressed as log<sub>10</sub> cfu/mL, after exposure to different concentrations of cashew oil.**

Cashew oil conc. mg/mL	Viable cell count reduction in 6 h, 12, 24 and 48 h biofilms of MRSA 252 and ATCC 6538 after exposure to cashew oil. Results expressed as log <sub>10</sub> cfu/mL.							
	MRSA 252				<i>S. aureus</i> ATCC 6538			
	6 h	12 h	24 h	48 h	6 h	12 h	24 h	48 h
<b>Growth control</b>	8.37 ± 0.49	8.64 ± 0.40	8.64 ± 0.56	8.66 ± 0.56	8.33 ± 0.30	8.33 ± 1.07	8.34 ± 0.62	8.39 ± 0.87
0.98	8.15 ± 0.69	7.16 ± 0.54	6.42 ± 0.93	4.18 ± 0.80	7.52 ± 0.91	7.16 ± 0.54	6.15 ± 0.51	4.99 ± 0.69
1.95	7.69 ± 0.68	6.59 ± 1.10	5.17 ± 0.19	3.26 ± 1.18	7.39 ± 0.93	6.60 ± 1.09	5.67 ± 0.47	4.81 ± 1.29
3.9	7.39 ± 0.78	5.68 ± 1.26	4.81 ± 0.47	3.68 ± 0.87	6.69 ± 1.32	5.68 ± 1.26	4.48 ± 0.55	3.81 ± 0.62
7.8	7.08 ± 0.47	5.37 ± 1.14	5.17 ± 0.97	3.00 ± 0.58	6.16 ± 1.26	5.37 ± 1.14	4.43 ± 0.52	3.10 ± 1.1
15.6	6.28 ± 0.61	4.97 ± 0.96	4.37 ± 0.61	2.61 ± 1.00	6.03 ± 0.73	4.97 ± 0.96	4.44 ± 0.67	2.66 ± 0.90
31.5	5.09 ± 0.18	3.93 ± 1.00	3.00 ± 0.87	1.36 ± 1.26	4.88 ± 1.00	3.93 ± 1.00	2.89 ± 0.17	2.44 ± 0.68
62.5	4.91 ± 0.97	3.54 ± 1.16	2.38 ± 0.78	2.65 ± 0.74	4.79 ± 1.0	3.54 ± 1.16	2.54 ± 0.65	1.27 ± 0.68
125	3.27 ± 0.57	2.13 ± 0.51	1.58 ± 0.59	1.12 ± 0.89	4.42 ± 0.75	3.13 ± 0.51	2.15 ± 0.63	1.15 ± 0.68
250	2.34 ± 0.51	1.40 ± 0.36	1.37 ± 0.39	1.31 ± 1.06	4.37 ± 0.71	1.57 ± 1.08	1.06 ± 0.52	1.15 ± 0.68
500	1.70 ± 0.16	1.41 ± 0.56	1.03 ± 0.13	No colonies	1.42 ± 0.47	1.17 ± 0.46	No colonies	No colonies
20 mg/mL Oxacillin	0.91 ± 0.16	0.91 ± 0.16	0.91 ± 0.16	0.91 ± 0.16	0.91 ± 0.16	0.91 ± 0.16	0.91 ± 0.16	0.91 ± 0.16

Table 26 shows the viable count of recovery cells in the recovery medium after 6 h, 12 h, 24 h and 48 h incubation periods. Results at different growth time points shows log reduction of viable counts of MRSA 252 and ATCC 6538 biofilms after treatment with cashew oil.

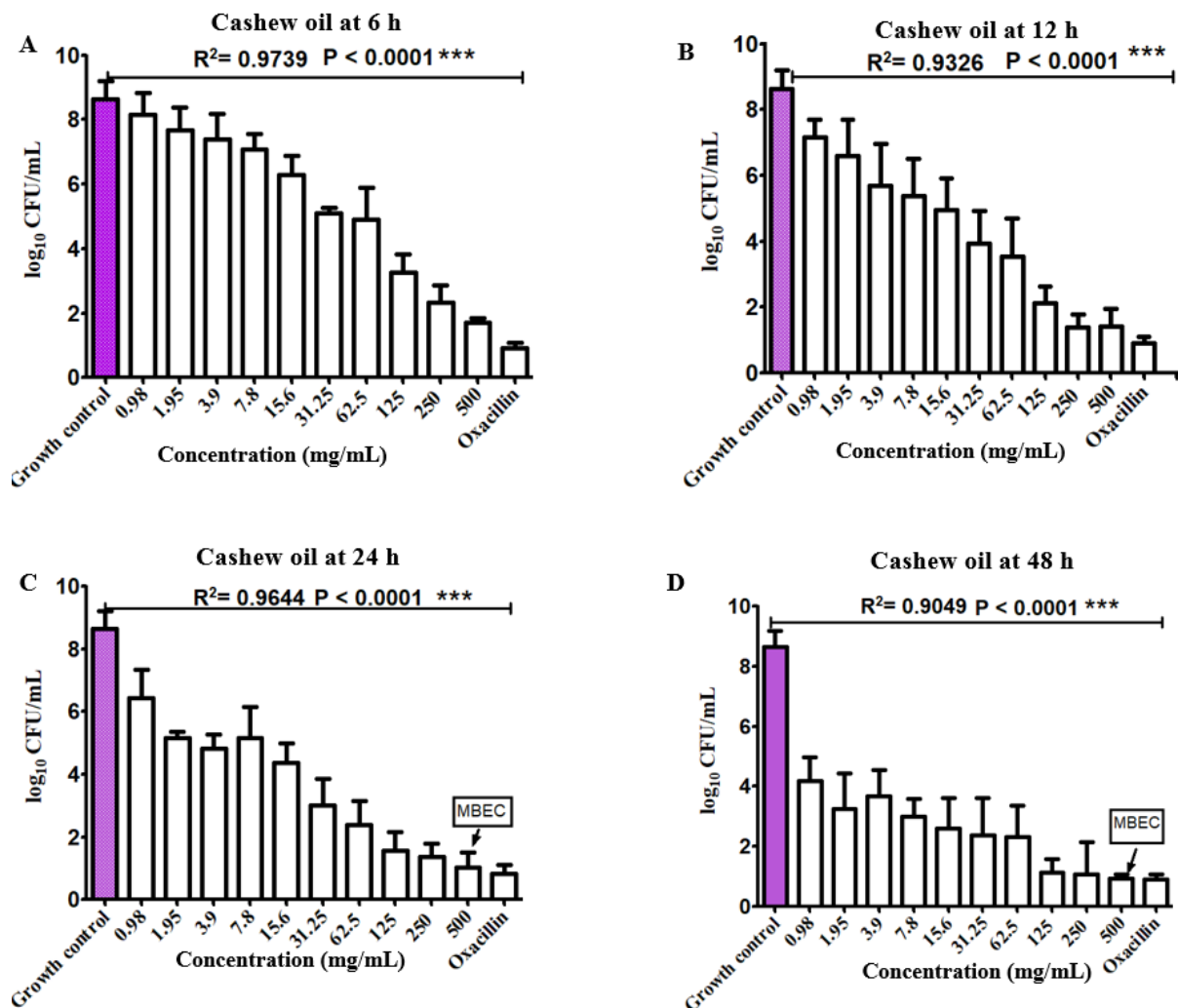
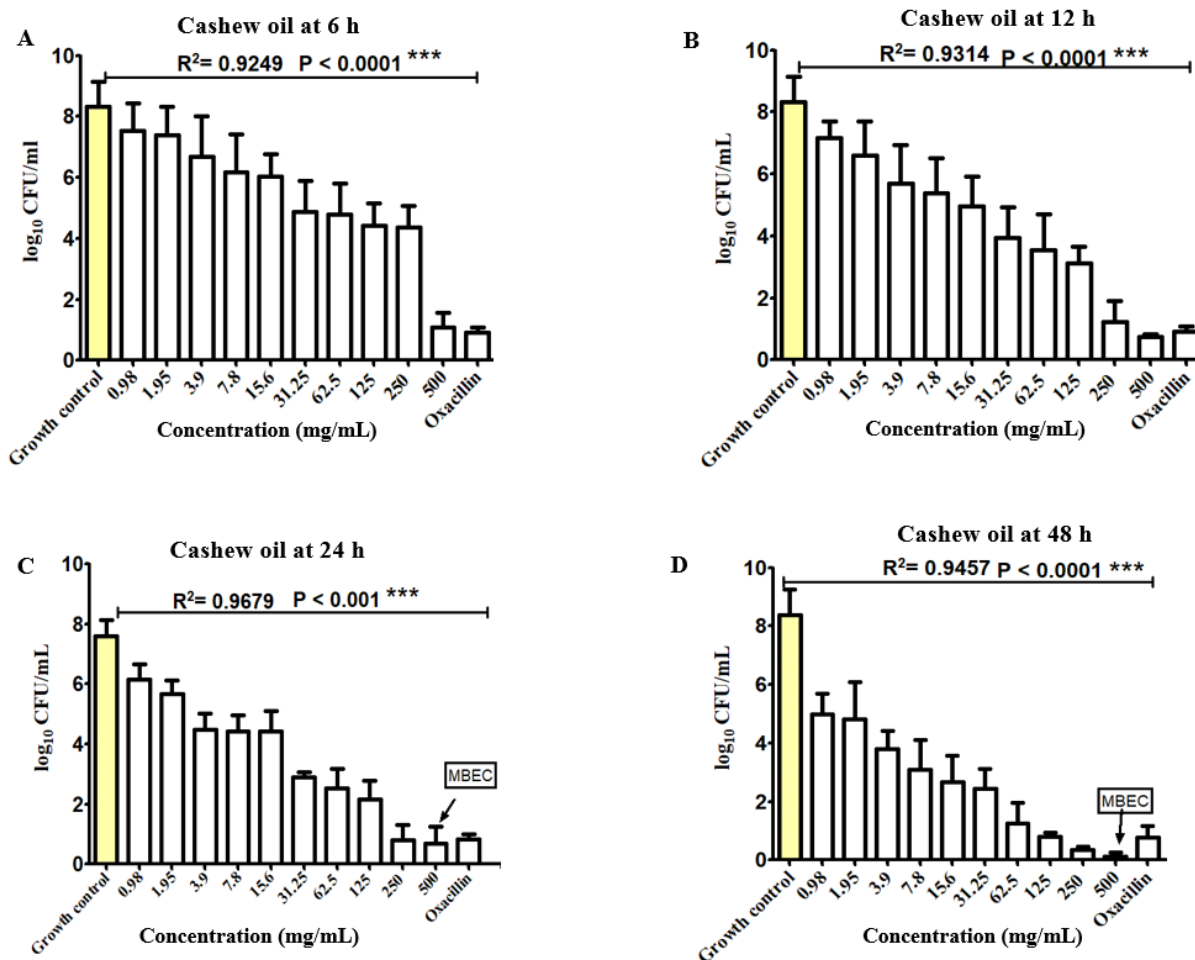


Figure 61. Reduction of MRSA 252 preformed biofilm on pegs following exposure to increasing concentrations of cashew oil at 0.98-500 mg/mL after 6, 12, 24 and 48 h of incubation at 37°C.

Figure 61 shows the bactericidal effect of cashew oil on MRSA 252 preformed biofilms. In addition, data on the graph shows the log of the mean CFU/peg after 6, 12, 24 and 48 h incubation of the TSB recovery medium at 37°C. The control in this experiment CFU/peg obtained for the untreated peg after the total 48 h incubation period and biofilm growth check with 8.37 log<sub>10</sub> CFU/mL per/peg served as the reference (growth control) for treatment efficacy. Data were obtained from three independent experiments (n=3). Significant differences in comparison to the untreated controls (growth control) and the negative control oxacillin 20 mg/mL were performed. Statistical analysis was performed using one-way ANOVA: \*\*\*, P<0.0001 with Bonferroni's post-tests. Both the positive and negative controls were included in the experiment to monitor the recovery of the bacterial isolate in biofilm.



**Figure 62. Reduction of *S. aureus* ATCC 6538 preformed biofilm on pegs following exposure to increasing concentrations of cashew oil at 0.98-500 mg/mL after 6, 12, 24 and 48 h of incubation at 37°C.**

Figure 62 shows the bactericidal effect of cashew oil on ATCC 6538 preformed biofilms. In addition, data in the graph shows the log of the mean CFU/peg after 6, 12, 24 and 48 h incubation of the TSB recovery medium at 37°C. The control in this experiment CFU/peg obtained for the untreated peg after the total 48 h incubation period and biofilm growth check with 8.33 log<sub>10</sub>CFU/mL per/peg served as the reference (growth control) for treatment efficacy. Data were obtained from three independent experiments (n=3). Significant differences in comparison to the untreated controls (growth control) and the negative control oxacillin 20 mg/mL were performed. Statistical analysis was performed using one-way ANOVA: \*\*\*, P<0.0001 with Bonferroni's post-tests. Both the positive and negative controls were included in the experiment to monitor the recovery of the bacterial isolate in biofilm.

From the MBEC result of MRSA 252 and ATCC 6538, the challenge of MRSA 252 and *S. aureus* ATCC 6538 with cashew oil resulted in minimal significant decrease of viable biofilm cells in recovery medium at 6 h, 12 h, 24 h and 48 h (Figure 61-62). However, bacterial counts

in MRSA 252 and ATCC 6538 biofilms started to decrease drastically in viable count after exposure to 31.25 mg/mL of cashew oil after 6 h. Despite the decrease at this concentration, better reduction in viable count was observed at 24 and 48 h with 500 mg/mL concentration. These concentrations led to MRSA 252 and ATCC 6538 causing approximately >7 log reduction after 6, 12, 24 and 48 h. Therefore, cashew oil was considered weakly effective because its MBEC concentration was high and will require much concentration of cashew oil to eradicate the strains. In addition, based on the data on the graph, MBEC activity of cashew oil was seen to be concentration dependent and time dependent.

### (iii) Eradication activity of fluted pumpkin oil on MRSA 252 and ATCC 6538

Fluted pumpkin oil was considered slightly effective because it could effectively eradicate MRSA 252 and ATCC 6538 biofilms progressively from 6, 12, 24 and 48 h at the different concentrations tested. The MBEC of pumpkin oil was 250 mg/mL and 125 mg/mL for MRSA 252 and ATCC 6538 respectively. Bacterial counts in MRSA 252 and ATCC 6538 biofilms started to decrease significantly ( $p < 0.0001$ ) immediately after exposure to 125 mg/mL of pumpkin oil after 6 h. (Figure 63 and 64). The data on the graphs below also showed a time and concentration-dependent decrease of bacterial counts recorded as log reduction (MBEC). The challenge of MRSA 252 with pumpkin oil resulted in significant reduction of viable bacterial cells in recovery medium after 6 h, 12 h, 24 h and 48 h.

**Table 27. MRSA 252 and *S. aureus* ATCC 6538 counts in 12 h, 24 h and 48 h-biofilms, in growth recovery media expressed as log<sub>10</sub> CFU/mL, after exposure to different concentrations of fluted pumpkin oil.**

Fluted pumpkin oil conc. mg/mL	Viable cell count reduction in 6 h, 12, 24 and 48 h biofilms of MRSA 252 and ATCC 6538 after exposure to pumpkin oil. Results expressed as log <sub>10</sub> CFU/mL							
	MRSA 252				<i>S. aureus</i> ATCC 6538			
	6 h	12 h	24 h	48 h	6 h	12 h	24 h	48 h
<b>Growth control</b>	8.37 ± 0.49	8.37 ± 0.49	8.60 ± 0.53	8.64 ± 0.55	8.33 ± 0.30	8.34 ± 0.65	8.46 ± 0.62	8.53 ± 0.48
0.98	7.15 ± 1.23	7.03 ± 0.23	5.92 ± 0.89	3.57 ± 1.02	7.65 ± 0.10	6.75 ± 0.38	5.25 ± 0.45	3.57 ± 1.00
1.95	6.99 ± 0.34	6.99 ± 0.34	5.23 ± 1.02	3.33 ± 0.56	7.26 ± 1.30	5.98 ± 0.62	4.92 ± 0.32	2.66 ± 0.52
3.9	7.32 ± 0.78	5.69 ± 0.98	5.05 ± 0.43	3.21 ± 0.41	7.10 ± 1.49	5.36 ± 0.98	4.72 ± 0.56	2.21 ± 0.56
7.8	7.27 ± 1.09	5.4 ± 1.38	3.71 ± 0.28	3.21 ± 0.41	7.31 ± 1.99	4.67 ± 0.25	3.04 ± 0.31	2.54 ± 0.48

15.6	6.30 ± 0.49	4.91 ± 0.31	3.31 ± 0.30	2.68 ± 0.59	6.57 ± 0.97	4.91 ± 0.32	2.64 ± 0.57	2.00 ± 0.48
31.5	6.47 ± 0.83	3.84 ± 1.03	2.36 ± 0.62	2.05 ± 0.17	6.32 ± 0.57	3.84 ± 1.03	1.16 ± 0.25	1.05 ± 0.17
62.5	5.92 ± 1.03	3.92 ± 0.49	1.92 ± 0.58	2.21 ± 0.40	5.97 ± 1.00	3.92 ± 1.07	1.12 ± 0.32	1.04 ± 0.34
125	5.58 ± 1.51	2.23 ± 1.04	1.50 ± 0.58	1.19 ± 0.34	2.58 ± 0.30	1.58 ± 0.43	1.00 ± 0.21	No colonies
250	4.21 ± 0.68	1.88 ± 0.78	1.48 ± 0.56	1.01 ± 0.38	2.34 ± 0.50	1.50 ± 0.45	No colonies	No colonies
500	2.69 ± 1.40	1.83 ± 0.78	1.39 ± 0.41	0.78 ± 0.67	1.72 ± 0.30	1.35 ± 0.34	No colonies	No colonies
Oxacillin Negative control	0.91 ± 0.16	0.91 ± 0.16	0.91 ± 0.16	0.91 ± 0.16	0.91 ± 0.16	0.91 ± 0.16	0.91 ± 0.16	0.91 ± 0.16

Table 27 shows the viable count of recovery cells in the recovery medium after 6 h, 12 h, 24 h and 48 h incubation periods. Results at different growth time points shows log reduction of viable counts of MRSA 252 and ATCC 6538 biofilms after treatment with pumpkin oil.

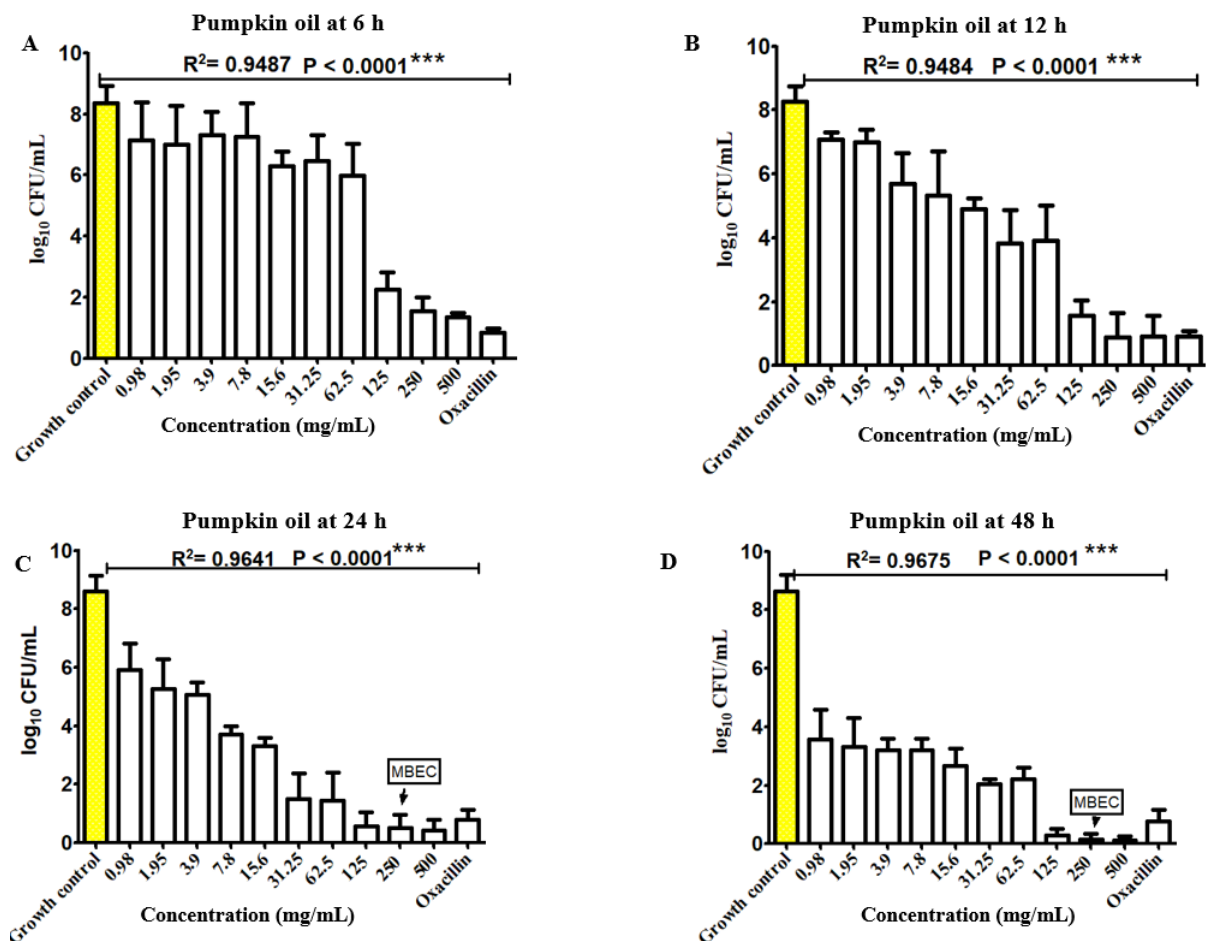
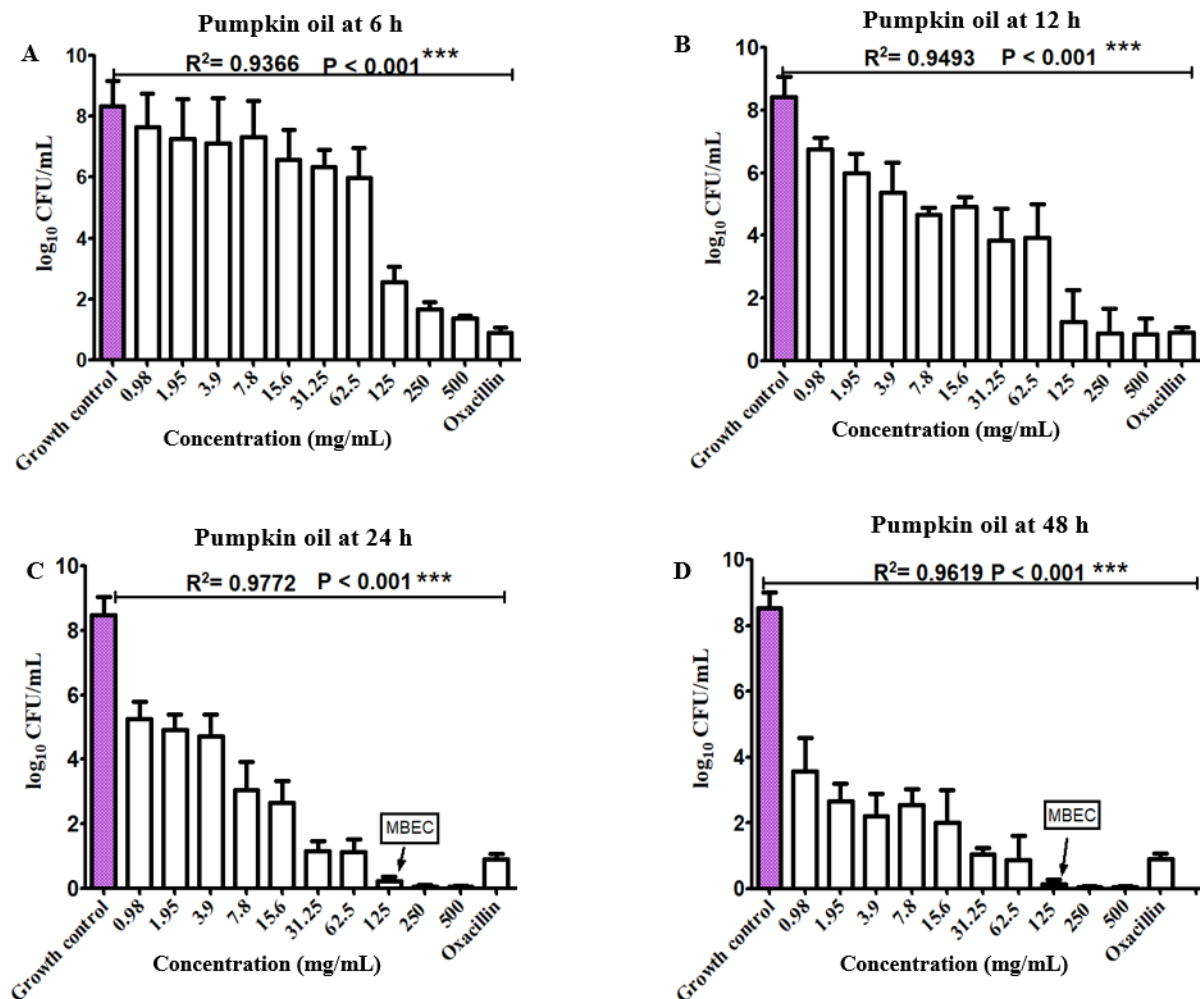


Figure 63. Reduction of MRSA 252 preformed biofilm on pegs following exposure to increasing concentrations of fluted pumpkin oil at 0.98-500 mg/mL after 6, 12, 24 and 48 h of incubation at 37°C.

Figure 63 shows the bactericidal effect of fluted pumpkin oil on MRSA 252 preformed biofilms. In addition, data on the graph shows the log of the mean CFU/peg after 6, 12, 24 and 48 h incubation of the TSB recovery medium at 37°C. The control in this experiment CFU/peg obtained for the untreated peg after the total 48 h incubation period and biofilm growth check with 8.37 log<sub>10</sub> CFU/mL per/peg served as the reference (growth control) for treatment efficacy. Data were obtained from three independent experiments (n=3). Significant differences in comparison to the untreated controls (0 mg/mL-growth control) and the negative control oxacillin 20 mg/mL were performed. Statistical analysis was performed using one-way ANOVA: \*\*\*, P<0.0001 with Bonferroni's post-tests. Both the positive and negative controls were included in the experiment to monitor the recovery of the bacterial isolate in biofilm.



**Figure 64. Reduction of ATCC 6538 preformed biofilm on pegs following exposure to increasing concentrations of fluted pumpkin oil at 0.98-500 mg/mL after 6, 12, 24 and 48 h of incubation at 37°C.**

Figure 64 shows the bactericidal effect of fluted pumpkin oil on ATCC 6538 preformed biofilms. In addition, data on the graph shows the log of the mean CFU/peg after 6, 12, 24 and

48 h incubation of the TSB recovery medium at 37°C. The control in this experiment CFU/peg obtained for the untreated peg after the total 48 h incubation period and biofilm growth check with 8.33 log<sub>10</sub> CFU/mL per/peg served as the reference (growth control) for treatment efficacy. Data were obtained from three independent experiments (n=3). Significant differences in comparison to the untreated controls (growth control) and the negative control oxacillin 20 mg/mL were performed. Statistical analysis was performed using one-way ANOVA: \*\*\*, P<0.0001 with Bonferroni's post-tests. Both the positive and negative controls were included in the experiment to monitor the recovery of the bacterial isolate in biofilm.

In summary, the MBEC results of MRSA 252 and ATCC 6538 showed that the challenge of MRSA 252 and *S. aureus* ATCC 6538 with fluted pumpkin oil resulted in significant decrease of viable biofilm cells in recovery medium at 6 h, 12 h, 24 h and 48 h (Figure 63 - 64). Bacterial counts in both MRSA 252 and ATCC 6538 biofilms started to decrease drastically in viable count after exposure to 15.6 mg/mL pumpkin oil for 6 h. However, despite the reduction at this concentration, at 24 and 48 h a better reduction in viable count was observed although a higher concentration at 250 mg/mL and 125 mg/ml for MRSA 252 and ATCC 6538 respectively. MBEC was considered the lowest oil concentration able to prevent a recovery of microbial growth after antimicrobial exposure. Using this definition, it could be seen that pumpkin oil was active at 125 mg/mL and 250 mg/mL concentration against ATCC 6538 and MRSA 252 causing approximately 5 log reduction and >7 log reduction after 24 and 48h. Therefore, fluted pumpkin oil was considered effective at 125 mg/mL against ATCC 6538 and less active at 250 mg/mL because much of the oil is required to cause a viable reduction of the strains in biofilm.

### 5.3 Discussion

In this study, different oils of African walnut, cashew and pumpkin showed significant antibacterial activity against methicillin resistant and susceptible *S. aureus* as assessed by the diameter of zone of inhibition of the oils. In addition, a few of the respective extracts of walnut, cashew and pumpkin also showed significant antibacterial activity. Although the low values recorded for some plant oils and extract may be attributed to fact that the oils and extracts in crude forms contain very little quantity of bioactive components. At the same time, many workers have reported their findings on bioactivity of crude extracts of plants with such range of diameter of zones obtained (El-Bashiti *et al.*, 2017). Although leaves, flowers, roots and shoot extracts of African walnut (*Tetracarpidium conophorum*), fluted pumpkin *Telfairia occidentalis*) and cashew (*Anacardium occidentale*) has been widely studies for their antimicrobial activity but the antimicrobial potential of the oils of these plants has not been extensively explored. The oils of African walnut in general showed a high inhibitory activity against MRSA 252 and ATCC 6538 in a zone of clearance (disc diffusion assay) indicating that they are bactericidal towards MRSA 252 and ATCC 6538. In this study, disc diffusion data presented in this study showed that African walnut, cashew and pumpkin oils exhibited antibacterial activity against MRSA 252 and *S. aureus* ATCC 6538 with African walnut oil at a concentration of 1000 mg/mL (10  $\mu$ L/disc) exhibiting stronger activity compared to cashew and pumpkin oils. Using the Kirby baurer (Disc diffusion) test the oils of African walnut, cashew and pumpkin used in this study produced activity against MRSA 252 and ATCC 6538 with different diameter of zones. All the tested bacteria were sensitive to the three oils. From the results African walnut oil, had larger zone ( $23.04 \pm 0.21$  mm), pumpkin oil had large zone ( $15.33 \pm 0.21$  mm) and cashew had moderately sized zones ( $13.01 \pm 0.21$  mm) against MRSA 252. Similarly, African walnut oil had large zones ( $19.00 \pm 0.22$ ), pumpkin had large zones ( $17.04 \pm 0.22$  mm) and cashew had relatively sized zones ( $13.50 \pm 0.22$  mm) against ATCC 6538. Results obtained in this study are similar with the findings of Rathi *et al.*, (2014) who tested antimicrobial activity of black walnut oil. The dried chopped nut was extracted using the cold press method. The oil was tested using the agar well diffusion method against both the gram negative (*Klebsiella pneumonia*, *Pseudomonas aeruginosa*, *Escherichia coli*, *Proteus vulgaris*), gram positive (*Bacillus subtilis*, *S. aureus*) for its antimicrobial activity. The authors found that walnut oil showed antimicrobial activity against all the pathogens tested. *S. aureus* (31 mm), *Bacillus subtilis* 11 mm, *Klebsiella pneumonia* (24 mm), *Pseudomonas aeruginosa* (22 mm) and *Proteus vulgaris* (12 mm). But the result indicated that black walnut oil produced

larger zone against *S. aureus* compared to other strain. Therefore, the result showed that black walnut oil had the potential to cure bacterial infections caused by the pathogenic strains. In addition, results obtained for pumpkin oil was similar to those of Adeel *et al.*, (2014) who reported that pumpkin seed oil exhibited strong antibacterial activity against *S. aureus*. The activity of pumpkin seed oil showed an average diameter of 17.03 mm. Similarly, pumpkin oil result was in line with those of Chonoko and Rufai, (2011) who found that pumpkin oil exhibited strong antibacterial activity against *S. aureus* (15.2 mm). In summary, the three oils tested had antibacterial effect against MRSA 252 and ATCC 6538 with significant difference in contrast to control. However walnut, pumpkin and cashew oil showed significant ( $P < 0.0001$ ) antimicrobial activity against MRSA 252 and ATCC 6538 compared to cashew oil. All diameter of zones measured in this study were based on CLSI, (2013) guidelines.

Furthermore, the findings in this study indicated that African walnut, cashew and pumpkin extracts exhibited antibacterial activities against *S. aureus* at the concentration of 1000 mg/mL (20  $\mu$ L/well). The antibacterial activity of extracts of African walnut, cashew and pumpkin obtained from solvent extraction with hexane, petroleum ether and chloroform were evaluated against MRSA 252 and ATCC 6538 using agar disc diffusion and agar well diffusion test. MRSA 252 and ATCC 6538 tested were sensitive to hexane and petroleum ether extracts only. Hexane extract of African walnut had 16 mm and 20 mm clear zones of diameter against MRSA 252 and ATCC 6538. Petroleum ether extract had 14 mm and 18 mm diameters of zones while chloroform did not produce zones against ATCC 6538 and less than 10 mm against MRSA 252. In addition, extracts of pumpkin showed activity against MRSA 252 producing clear zones of 12 mm, 14 mm and 9 mm for petroleum ether, hexane and chloroform extracts. Whereas against ATCC 6538, petroleum ether, hexane and chloroform extracts produced 7 mm, 12 mm and 9 mm were produced. Results obtained in this study were in accordance with those obtained in previous studies. For example, Ukpai Grace *et al.*, (2016) tested antimicrobial activity of nuts of *Tetracarpidium conophorum* on *S. aureus*, *Streptococcus pyogenes*, *Escherichia coli*, *Pseudomonas aeruginosa*, *Klebsiella pneumoniae*, *Candida albicans*, and *Aspergillus Spp.* Aqueous, ethanol and hexane extract of *T. conophorum* nut was used. For ethanol and hexane 20 g of the material was macerated into 200 mL of each solvent and extraction was done in air tight container to prevent evaporation of solvent. Hexane and ethanol extracts were dried in a warm air oven at 50°C for the solvents to evaporate. The result showed that the inhibition zone of diameter of the hexane and ethanol extracts of *T. conophorum* plant on gram positive *S. aureus* ranged from 10-14 mm, the zone of *S. pyogenes* was 12-17 while the zones of diameter

of the gram-negative bacterial species were in range of 12-18 mm and However, the hexane and ethanol extract of *T. conophorum* was found to produce better inhibitory activity against *S. pyyogenes* than *S. aureus*. In another study carried out Allaie *et al.*, (2018) examined the antibacterial activity of nut extracts of *Juglans regia* against some clinical isolates (*E. coli*, *S. aureus*, *S. saprophyticus*, *K. pneumonia*, *Proteus mirabilis*, and *P. aeruginosa* responsible for urinary tract infection. The result showed that among the three nut extracts tested against the isolates causing UTIs, hexane extract was moderately active on gram positive (*S. aureus* (9 mm) and *S. saprophyticus* (7 mm) strains compared to the ethyl acetate, and methanolic extracts that were highly effective.

In the present study, the possible effects of conventional antibiotics and combination effect of plant oils with antibiotics were evaluated. In the disc diffusion assay, antibiotics alone and combination with African walnut, cashew and pumpkin oils exhibited antibacterial activity against MRSA 252 and ATCC 6538 but at different concentrations. In this combinational study, MRSA 252 and ATCC 6538 exhibited different patterns of resistance and susceptibility. This combination might prove the benefit of using a combination with the lower dose of antibiotic alone (Aminnezhad *et al.*, 2013). In this study lower antibiotic doses were used for the combinational study to allow effective combination of the drugs and oils. MRSA 252 was observed to be susceptible to drugs like streptomycin, vancomycin, linezolid, gentamicin, rifampicin chloramphenicol but resistant to trimethoprim, penicillin G, ciprofloxacin, oxacillin, carbenicillin and erythromycin. However, combination of African walnut oil with antibiotics such as trimethoprim, vancomycin, carbenicillin and streptomycin led to synergy. Combination of cashew oil with trimethoprim, chloramphenicol, rifampicin, vancomycin and carbenicillin led to synergy. Combination of pumpkin oil with gentamicin, streptomycin, trimethoprim, chloramphenicol led to a synergistic effect against MRSA 252. Based on the results, MRSA 252 appears to have better synergy with drugs in the class of aminoglycosides, glycopeptide, sulphonamides and chloramphenicol. Against ATCC 6538, combination of African walnut oil with streptomycin, carbenicillin, vancomycin, oxacillin, gentamicin, ciprofloxacin and trimethoprim resulted in synergy. Combination of cashew oil with trimethoprim and penicillin G led to synergy while combination of pumpkin oil with vancomycin, rifampicin and erythromycin led to synergy aminoglycosides, glycopeptide, sulphonamides. In general, African walnut oil and pumpkin oil resulted in better synergistic effects with antibiotics against MRSA 252 and ATCC 6538.

Plants edible oils have already been known to exhibit strong antimicrobial properties (Tabassum and Vidyasagar, 2014). However, the effect of edible oils on the formation of biofilms has not been thoroughly investigated. The effect of African walnut, cashew and pumpkin oils from nuts and seed on the formation of bacterial biofilm has never been reported before. The ability of *S. aureus* to form biofilm is a major virulence factor and contributes to the success of disease development (Batista *et al.*, 2017). Previous studies on other plant oils have showed that bacteria in the biofilm mode of growth are much more resistant to antibacterial agents than their planktonic counterparts (Nostro *et al.*, 2007; Nuryastuti *et al.*, 2009; Chamdit and Siripermpool 2012; Kavanaugh *et al.*, 2012; Al-Shuneigat *et al.*, 2014). The greater resistance of *S. aureus* in the mature biofilm EPS, when compared to that of its cells in planktonic cell culture can be linked to the bacterial biofilms ability to reduce the entry and dissemination of antimicrobials in its interior. Once a bacterium is enveloped in matrix (biofilm), the cells are protected from antimicrobials, environment and the immune response of the host. In this study, results obtained have demonstrated that walnut oil and pumpkin oil has an excellent antibacterial potential against MRSA 252 and ATCC 6538 planktonic and biofilm cells. At higher concentration, African walnut, cashew and pumpkin oils exerted an antibacterial activity. Against MRSA 252 and ATCC 6538 the MIC of walnut oil were 15.6 and 7.8 mg/mL. Cashew oil had an MIC of 125 and 125 mg/mL. Pumpkin had an MIC value of 62.6 and 31.25 mg/mL. MBICs values for both strains were 31.25 mg/mL and 15.6 mg/mL (walnut oil), 125 and 62.5 mg/mL (pumpkin oil), 250 mg/mL for both MRSA 252 and ATCC 6538 (Cashew oil). Based on the result, African walnut and pumpkin oil showed strong inhibitory activity on the growth of MRSA 252 and ATCC 6538 planktonic and biofilm cells. However, cashew oil exhibited weak inhibitory activity against MRSA 252 and ATCC 6538.

MIC of hexane and petroleum ether extracts of African walnut, cashew and pumpkin against MRSA 252 and ATCC 6538 planktonic and biofilm cells were determined using the broth micro-dilution technique. MIC of hexane extract of the African walnut oil against MRSA 252 and ATCC 6538 was 125 and 62.5 mg/mL while MIC of petroleum ether extract against MRSA 252 and ATCC 6538 was 500 and 125 mg/mL. MICs of hexane extract of cashew against MRSA 252 and ATCC 6538 was 250 and 500 mg/mL (hexane extract) and MICs of petroleum ether extracts was 500 mg/mL for both strains. For pumpkin oil, MICs of hexane extract against MRSA 252 and ATCC 6538 was 250 and 62.5 mg/mL and MICs of petroleum ether extracts was 250 and 500 mg/mL for both strains. MBIC of hexane and petroleum ether extracts of African walnut against MRSA 252 and ATCC 6538 was 250 and 125 mg/mL, and 250 and 500

mg/mL. MBIC of hexane and petroleum ether extracts of cashew against MRSA 252 and ATCC 6538 was 500 mg/mL for the two strains, MBIC of hexane and petroleum ether extracts of pumpkin against MRSA 252 and ATCC 6538 was 500 and 125 mg/mL, and lastly 500 mg/mL for the two strains.

Treatment with antibacterial drugs may kill free-floating cells but fail to eradicate bacteria embedded within biofilm, which can then act as a source responsible for human recurrent infection (Tabassum and Vidyasagar, 2014). After treatment with standard antibiotic, a few of drug resistant bacteria may still exist that repopulates the biofilm. Subsequent retreatment of the biofilms that repopulated resulted in reduced bacterial counts indicating that the repopulated biofilm is very resistant to antibiotics. In this study, the ability of oils of walnut, cashew and pumpkin to eradicate biofilms formed by MRSA 252 and ATCC 6538 at different time point was investigated. This was done to firstly ascertain whether the oils can eradicate the established biofilms of the strains, secondly, to determine the appropriate concentration and time that the oils will be able to eradicate the biofilms of the strains. To effectively perform the experiments, mature biofilms of MRSA 252 and ATCC 6538 in a 96-well Nunc plate grown for 48 h with an initial count of 8.37 and 8.33 log<sub>10</sub> CFU/mL per peg/well of bacteria were treated with walnut, cashew and pumpkin oils at ten concentrations. African walnut, cashew and pumpkin oil were found to significantly reduce viabilities of biofilm cells. Whereas, the cell viability of MRSA 252 and ATCC 6538 growth control was observed to increase to 8.64 log<sub>10</sub> CFU/mL per peg/well and 8.53 log<sub>10</sub> CFU/mL per peg/well. Pumpkin oil was also able to reduce cell viabilities of MRSA 252 and ATCC 6538 biofilms from an initial count from 8.37 and 8.33 log<sub>10</sub> CFU/mL per peg/well. The use of African walnut, cashew and pumpkin oils for the susceptibility tests in this study showed which oils are more efficient against MRSA 252 and ATCC 6538 preformed biofilms after 48 h. African walnut oil was significantly efficient against *S. aureus* MRSA 252 and ATCC 6538 embedded in biofilms as it was observed to eradicate MRSA 252 and ATCC 6538 biofilms at low concentrations of 31.25 and 62.5 mg/mL after 12 h but with more better eradication after 24 and 48 h giving low or no counts of viable cells in recovery media. Cashew oil could not completely eradicate the biofilms of MRSA 252 and ATCC 6538 but significantly decreased its cells re-occurring growth rate after 24 h of incubation in different concentrations but better at 500 mg/mL concentration. After African walnut oil, pumpkin oil showed better activity against ATCC 6538 at 125 mg/mL concentration compared to MRSA 252 at 250 mg/mL.

Results by Unachukwu, Nwakanma & Ekuma, (2018), is in line with the results of our study. They carried out an antibacterial evaluation of *T. occidentalis* leaf extract against *S. aureus* and two *E. coli* clinical strains using both the disc diffusion and dilution methods. The leaf extract produced no inhibitory activity on *E. coli* isolates but inhibited the growth of *S. aureus*. In another study, Apagu and coworkers (2017), studied the antibacterial activity of the leaf extracts of *T. occidentalis* on *S. typhi*, *E. coli*, *P. auriginosa*, *S. aureus* and *S. feacalis*, using disc diffusion method with standard antibiotic drugs as positive control for comparison. *T. occidentalis* extract produced higher antibacterial activity against *S. aureus*. Similarly, Ayepola and Ishola, (2009) investigated the antibacterial activity of the leaves and stem bark of cashew (*A. occidentale*) on gram-positive and gram-negative organisms including *K. pneumoniae*, *S. aureus*, *B. subtilis*, *S. typhi*, *C. albicans* and *E. coli* using disc diffusion with ampicillin as a standard control. The mean diameter of the zones of inhibition exhibited by the extracts was between 13 mm and 22 mm. *S. aureus* and *B. subtilis* showed the highest zones of inhibition (13 and 22 mm) to the leaf extracts. Agedah, Bawo & Nyananyo, (2010) investigated the antimicrobial capabilities of plant extract derived from the leaves of the cashew plant, *A. occidentale* on two common human pathogens of clinical importance, *E. coli* and *S. aureus* using disc diffusion method and ampicillin as a standard antibiotic. The two clinical strains were sensitive to the extracts, but *S. aureus* was more sensitive with a larger zone of inhibition (13 mm).

## Chapter 6. Molecular study of MRSA 252 and *S. aureus* ATCC 6538 Virulence Genes

### 6.1 Introduction

*S. aureus* is a prominent gram-positive pathogen capable of causing infections associated with indwelling medical devices. The ability of this pathogen to form biofilm on surfaces of either biotic or abiotic surfaces is perhaps the major factor contributing to *S. aureus* acquired infections. Biofilm formation involves the attachment of the bacteria to solid materials which results in the subsequent assemblage of microbial communities embedded in polymeric substances (Atshan *et al.*, 2013). Therefore, infections caused by this notorious pathogen are becoming chronic in wound infections and on hospital devices including orthopaedic and prosthetic implants such as wires, pins, prosthetic joints, screws, nails, external fixators, plates, and mini-large fragment implants. However, other devices that are prone to *S. aureus* biofilm infection include the indwelling hospital devices such as urinary, intravenous and endotracheal catheters and heart valves (Archer *et al.*, 2011). In the on-set of *S. aureus* infections, adhesion is a vital step in the formation of biofilm communities which is enhanced by the production of a variety of protein and non-protein adhesins that mediate attachment to a great multitude of human factors which include extracellular matrix and plasma protein, intercellular adhesion or human host cells which is vital for biofilm formation and accumulation (Heilmann, 2011).

Protein adhesins are classified either in the MSCRAMMs family which are the covalently anchored proteins or in the family of proteins that are non-covalently anchored to the cell wall but by other means such as ionic and hydrophobic means. Examples of such proteins include the SERAM proteins (secretable expanded repertoire adhesive molecule) family, or membrane spanning proteins. Non-protein adhesins is composed of the polysaccharide intercellular adhesin (PIA), teichoic acids and lipoteichoic acid (Heilmann, 2011). During implant infection, the implant becomes coated with host extracellular matrix (ECM) proteins including fibrinogen (*fib*), fibrinectin A and B (*fnbA* and *fnbB*), collagen (*cna*), laminin (*eno*), clumping factors A and B (*clfA* and *clfB*), elastin (*ebps*), providing a suitable surface for MSCRAMMs to bind. MSCRAMMs can bind to one or more host molecules and thus escape immune system and then develop infections. MSCRAMMs are proteinaceous adhesins on *S. aureus* surface that mediate the adhesion of the bacterium to ECM. These MSCRAMMs are attached covalently to the cell wall of *S. aureus* by sortase enzymes (Abdolmajid *et al.*, 2015) and sec pathway.

Furthermore, MSCRAMMs play vital role in staphylococcal biofilm formation, in addition to the *ica* locus that produces the PIA. The development of *S. aureus* biofilm is mostly facilitated by the production of polysaccharide intercellular adhesion (PIA). The production of this PIA matrix results in complex cell clustering with several distinct layers. In *S. aureus* PIA is a polysaccharide composed of poly- $\beta$  (1-6)-*N*-acetylglucosamine (PNAG), with partially deacetylated residues, positively charged, whose synthesis is mediated by the *icaADBC* operon. It serves as a protective outer covering around the cells, protecting them against human immune defences and drug treatment (Atshan *et al.*, 2013; Mirzaee *et al.*, 2014). The intercellular adhesion (*ica*) operon is composed of the *icaADBC* genes that encodes protein and are responsible for the production of PIA and capsular polysaccharide adhesion in majority of staphylococcal strains. The gene *icaA* is encoding the N-acetylglucosamyltransferase. This enzyme is not always active and stable *in vitro*, but of both *icaA* and *icaD* helps to increase N-acetylglucosamyltransferase activity and production of slime (Arciola *et al.*, 2006; Mirzaee *et al.*, 2014). Gene *icaB* encodes an extracellular protein with an unknown function and is responsible for the deacylation of fully developed PIA. *IcaC* encodes a transmembrane protein which is believed to be involved in the secretion and elongation of polysaccharides. Therefore, experiments conducted in this chapter identified virulence genes in *S. aureus* ATCC 6538 and MRSA 252 associated with biofilm formation, adhesion to biotic surfaces, antibiotic resistance, quorum sensing and food poisoning. Also, experiments were geared towards determining the expression levels of the virulence genes that were found to be present in the strains, then their expression levels before and after treatment with walnut and fluted pumpkin oils in strains were determined.

## 6.2 Results

### 6.2.1 Preparation of MRSA 252 and ATCC 6538 for SEM

*S. aureus* bacteria undergo gradual morphological changes at different growth phases during biofilm formation therefore it was necessary to initially determine the growth phases at different time points exhibited by MRSA 252 and ATCC 6538 biofilms (using SEM) at which they produce morphological structures before performing, RNA extraction and RT-PCR analysis. To effectively determine this, MRSA 252 and ATCC 6538 biofilm growth curves were performed. This was performed by growing their standardized suspension ( $1.5 \times 10^{-6}$  cells) on 6-well polystyrene tissue culture plates and their growth was monitored over a period of 48 h by measuring their absorbance at optical density of 600 nm using the spectrophotometer. Result is presented in Figure 65. Based on the growth curve results, biofilms formed at 6, 12, 24 and 48 h corresponding to lag, log and stationary phases of growth were examined for morphological changes, using Scanning electron microscopy (SEM). Result is presented in Figure 65-69.

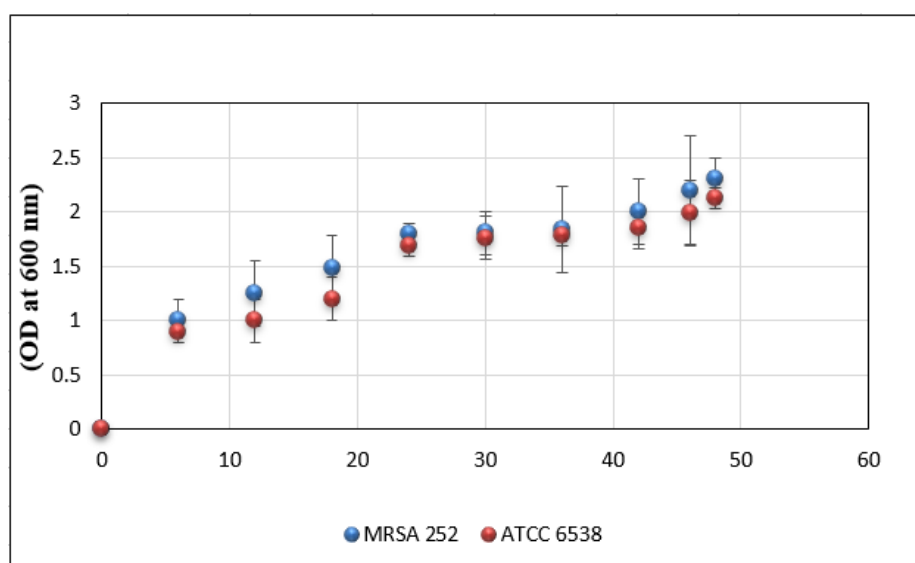


**Figure 65. Growth curve of MRSA 252 and ATCC 6538 grown in trypticase soy broth enriched with 1 % glucose at 37 °C for 48 h.**

Values on the graph are means of three repeated OD readings and error bars indicate standard deviations of the means. As shown in Figure 65, the OD is plotted versus time and the growth of MRSA 252 seem to be slightly faster than ATCC 6538 entering exponential phase at 6 h. In this graph, bacterial biofilm formation MRSA 252 and ATCC 6538 on 96-well plates was monitored at 0, 6, 12, 18, 24, 30, 36, 42, 46 and 48 h using quantitative culturing. As shown

in Figure 65, three distinct patterns of biofilm formation were observed for each strain (lag, exponential and stationary phase): biofilm formation by *S. aureus* MRSA 252 and ATCC 6538 progressed at an early (lag) phase characterized by a rapid biofilm formation in 6-8 h without thick fibrous biofilm materials, followed by a slow intermediate phase observed up to 18 h. After the 18 h growth time point, *S. aureus* biofilm growth reached stationary phase. Growth pattern of biofilm formation by ATCC 6538 was slightly different from that of MRSA 252 at 6 h to 24 h. In addition, biofilm formation by MRSA 252 and ATCC 6538 gradually increased in growth up to 24 and 48 h. Biofilms grown to 12 h, 24 and 48 h were used in subsequent experiments. These observations are similar with that reported by Szczotka-Flynn *et al.*, (2009) and Atshan *et al.*, (2013). Szczotka-Flynn *et al.*, (2009) observed that *S. aureus* strains formed biofilms on lenses exhibiting three main phases of growth which includes lag, exponential and stationary phases. Atshan *et al.*, (2013) showed that the growth of *S. aureus* clones in tryptic soy broth was faster with clones entering an exponential phase early at 6 h and reaching a plateau phase of growth at 22 h.

## 6.2.2 Scanning electron microscopy (SEM)

### 6.2.2.1 SEM of MRSA 252

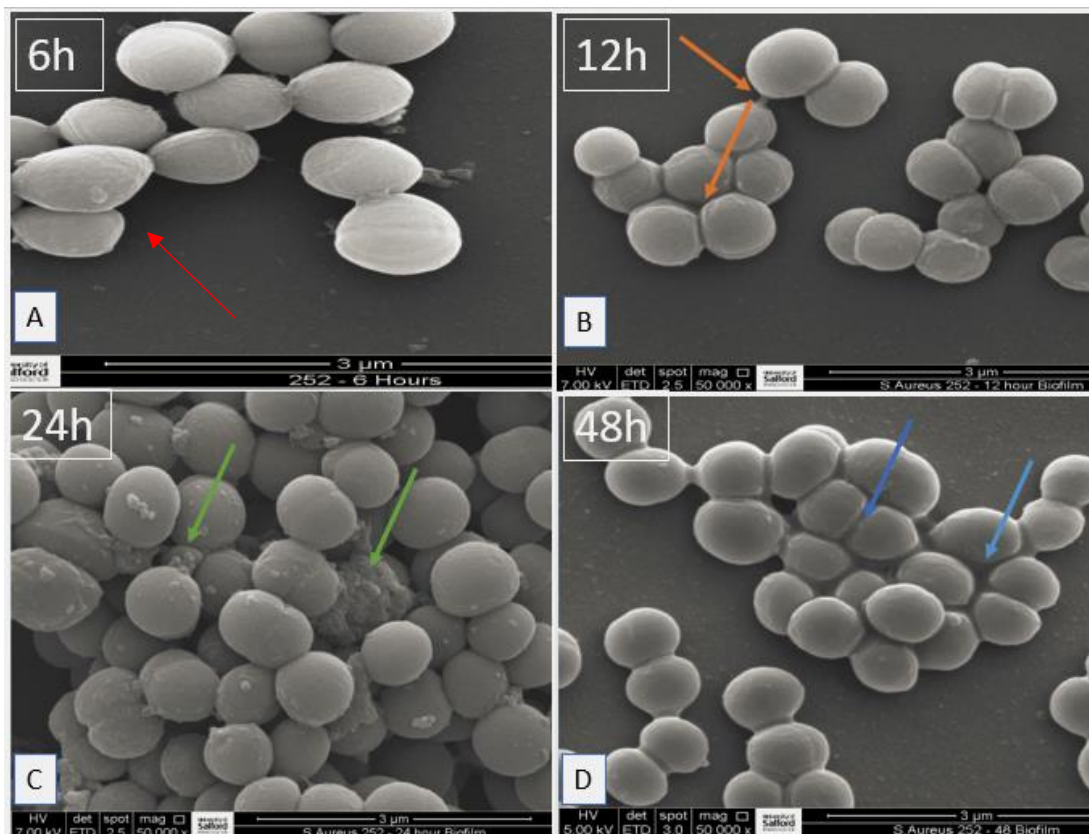


**Figure 66.** SEM images (A-D) of MRSA 252 grown in trypticase soy broth enriched with glucose for 6, 12, 24 and 48 h respectively, then imaged with FEI Quanta FEG 250 FESEM. Images of MRSA 252 shows clusters of biofilms at 6 h, mesh-like biofilm at 12 h, thick fibrous biofilm at 24 h and dense mesh-like structures with arrow heads at 48 h as depicted with red, orange, green and blue coloured arrows.

On the biofilm micrographs, HV and det (Everhart-Thornley Detector) represents the accelerating emission volatage, which is 7 kv and 5 kv. Spot on the micrographs means the resolution of the images and magnification at 50,000 x is the enlargement of the image. (A) Clusters of biofilms at 6 h (B) Biofilm at 12 h with meshwork like structures sticking the cells together (C) Biofilm with thick fibrous material observed at 24 h. (D) Biofilm with increased meshwork like structures which became denser with arrow head. The orange arrow used in labelling B shows the meshwork and arrow head of MRSA 252 biofilm formed at 12, green arrows in C shows fibrous materials formed at 24 h and blue arrows indicates dense layers of meshwork holding the cells together.

#### 6.2.2.2 SEM of *S. aureus* ATCC 6538

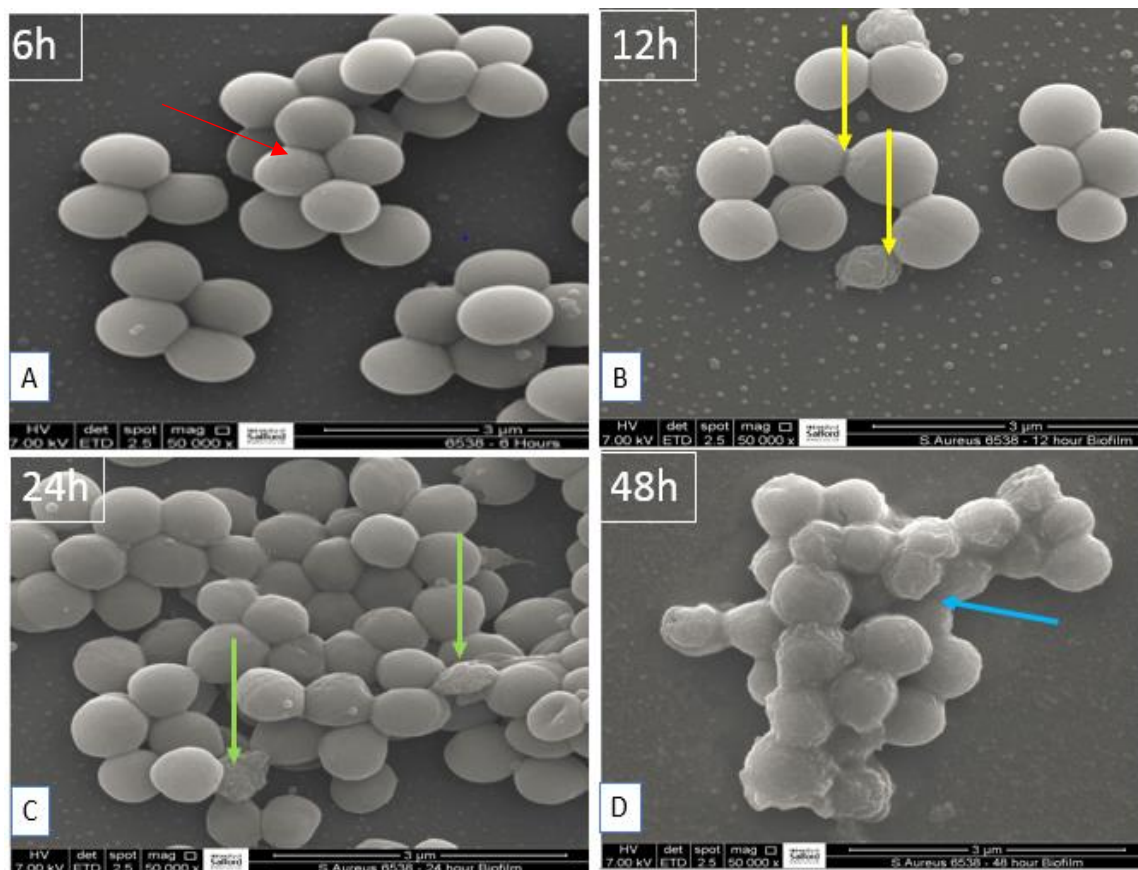


**Figure 67.** SEM images (A-D) of ATCC 6538 grown in trypticase soy broth enriched with glucose for 6, 12, 24 and 48 h respectively, then imaged with FEI Quanta FEG 250 FESEM. Images of ATCC 6538 shows clusters of biofilms at 6 h, mesh-like biofilm at 12 h, thick fibrous biofilm at 24 h and dense mesh-like structures with arrow heads at 48 h as depicted with red, yellow, green and blue coloured arrows.

On the biofilm micrographs, HV and det (Everhart-Thornley Detector) represents the accelerating emission voltage, which is 7 kv and 5 kv. Spot on the micrographs means the resolution of the images and magnification at 50,000 x is the enlargement of the image. (A) Clusters of biofilms at 6 h (B) Biofilm at 12 h with meshwork like structures sticking the cells together (C) Biofilm with thick fibrous material observed at 24 h. (D) Biofilm with increased meshwork like structures which became denser with arrow head. The yellow arrow used in labelling B shows the little meshwork like structures and arrow head of ATCC 6538 biofilm formed at 12, green arrows in C shows little fibrous materials formed at 24 h and blue arrows indicates dense layers of meshwork holding the cells together.

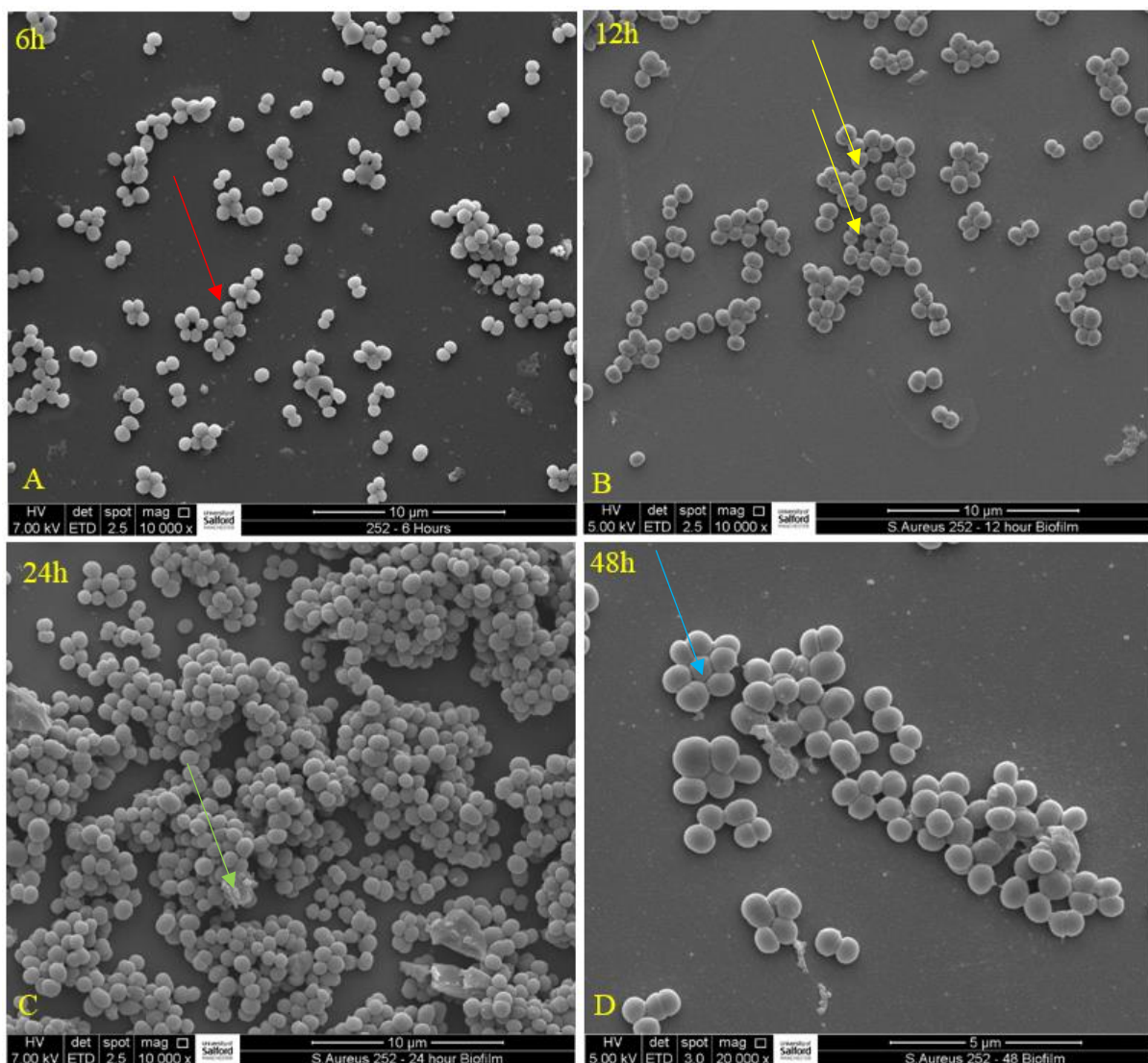


**Figure 68.** SEM images (A-D) of MRSA 252 grown in trypticase soy broth enriched with glucose for 6, 12, 24 and 48 h respectively, then imaged with FEI Quanta FEG 250 FESEM. Images of MRSA 252 shows clusters of biofilms at 6 h, mesh-like biofilm at 12 h, thick fibrous biofilm at 24 h and dense mesh-like structures with arrow heads at 48 h as depicted with red, yellow, green and blue coloured arrows. Magnification of images is at 10,000 x and 20,000 x.

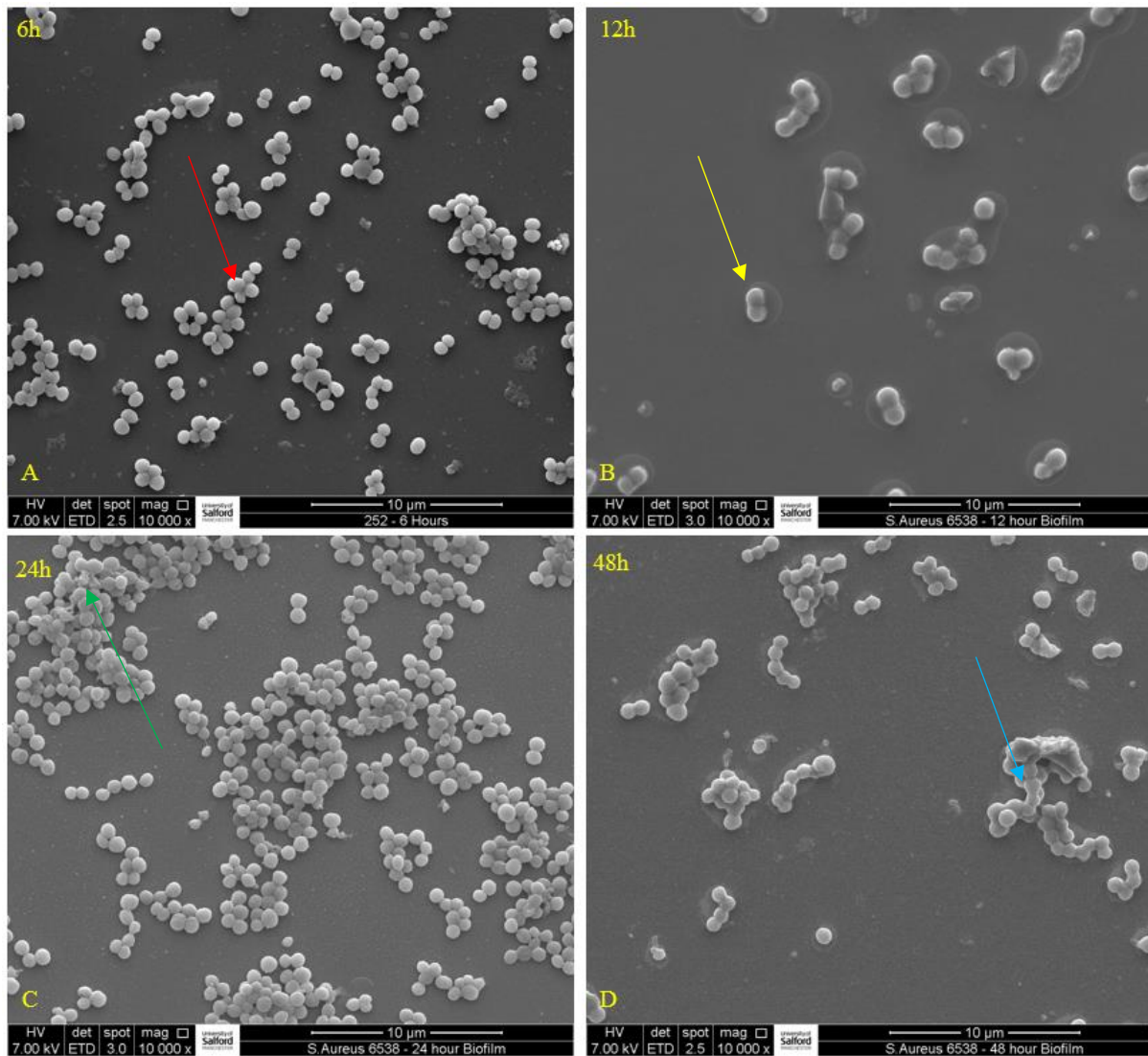


**Figure 69.** SEM images (A-D) of ATCC 6538 grown in trypticase soy broth enriched with glucose for 6, 12, 24 and 48 h respectively, then imaged with FEI Quanta FEG 250 FESEM. Images of ATCC 6538 shows clusters of biofilms at 6 h, mesh-like biofilm at 12 h, thick fibrous biofilm at 24 h and dense mesh-like structures with arrow heads at 48 h as depicted with red, yellow, green and blue coloured arrows. Magnification of images is at 10,000 x.

In summary, as observed in Figure 66 to 69, morphological observations of MRSA 252 and ATCC 6538 biofilm cultures at 12, 24 and 48 h showed that both strains started to exhibit little surface mesh like structures at 12 h with arrow heads which became denser with fibrous materials at 24. However, no fibrous materials and arrow heads was observed at 6 h. This observation correlates with other reports. Szczotka-Flynn *et al.*, (2009) observed that *S. aureus* strains formed biofilms on lotrafilcon A as dense mesh networks of bacterial cells arranged in clusters with visible extracellular matrix. Similarly, Asthan *et al.*, (2013) reported that *S. aureus* clones grew in tryptic soy broth at different stages of growth, forming thick and dense meshwork like structures particularly at 24 and 48 h. Asthan and his coworkers were of the

opinion that the *S. aureus* clones exhibited different morphological structures (Asthan *et al.*, 2013). Based on the observation in this study MRSA 252 biofilms appears to exhibit pronounced and steady surface structural changes at 12 h, 24 h and 48 h compared to ATCC 6538. As such, 12, 24 and 48 h time points were further studied with 6 h growth time point which was used as time control.

### 6.2.3 RNA extraction and gel electrophoresis of the RNA extracted from MRSA 252 and *S. aureus* ATCC 6538 biofilms.

RNA extracted from ATCC 6538 and MRSA 252 were of good purity. The quality and quantity of RNA extracted from 6, 12, 24 and 48 h biofilms at different growth time points was found to be intact before and after walnut, cashew and fluted pumpkin oil treatments.

#### 6.2.3.1 Gel electrophoresis of RNA extracted from MRSA 252 and *S. aureus* ATCC 6538 biofilms at 6, 12, 24 and 48 h.

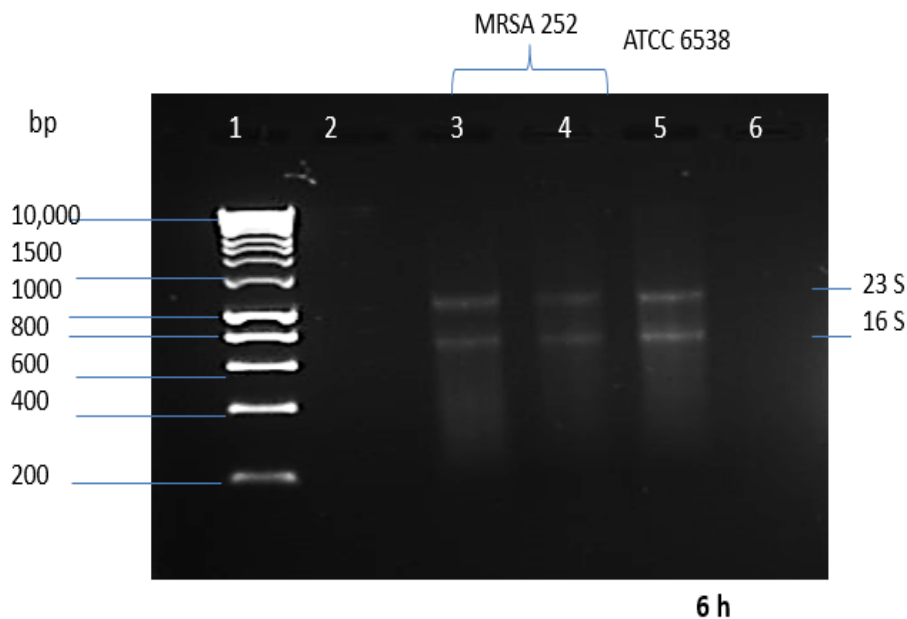


**Figure 70. Agarose gel electrophoresis of RNA extracted from MRSA 252 and *S. aureus* ATCC 6538 biofilms at 6 h.**

Lane 1; H is 1Kb base ladder marker. H, Hyperladder 1 Kb size marker Lanes 3 and 4 (7  $\mu$ L each) of RNA extracted from *S. aureus* ATCC 6538 biofilm and Lanes 7, 8 and 9 (7 and 8  $\mu$ L each) of RNA extracted from MRSA 252 biofilm at 6 h respectively.

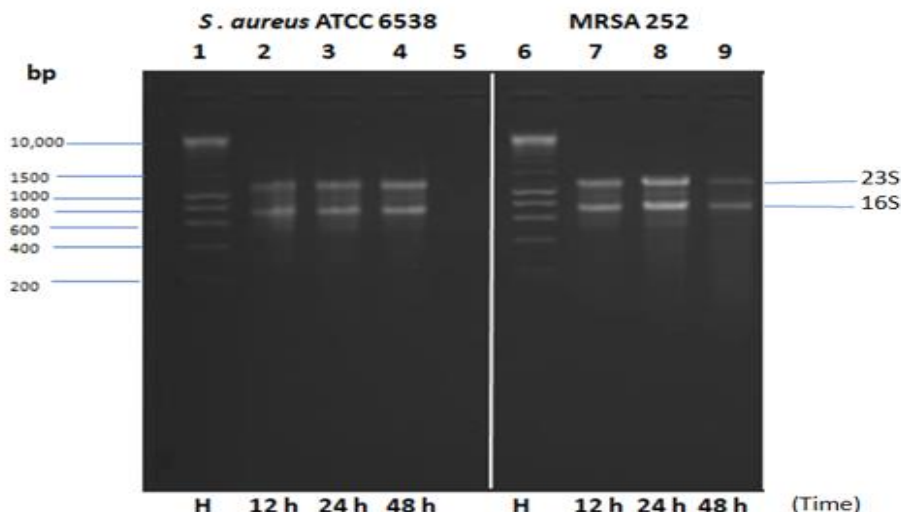


**Figure 71.** Agarose gel electrophoresis of RNA extracted from MRSA 252 and *S. aureus* ATCC 6538 biofilms at 12 h, 24 h and 48 h.

Lane 1; H is 1Kb base ladder marker. H, Hyperladder 1 Kb size marker. Lanes; 2, 3 and 4 (7  $\mu$ L each) of RNA extracted from *S. aureus* ATCC 6538 biofilm and Lanes 7, 8 and 9 (8  $\mu$ L each) of RNA extracted from MRSA 252 biofilm at 12 h, 24 h and 48 h respectively.

The gels show that the RNA extraction was successful indicated by the presence of intact ribosomal RNA bands from MRSA 252 and *S. aureus* ATCC 6538 biofilms.

### 6.2.3.2 Agarose gel electrophoresis of RNA extracted from MRSA 252 biofilms after treatment with fluted pumpkin, African walnut and cashew oils.

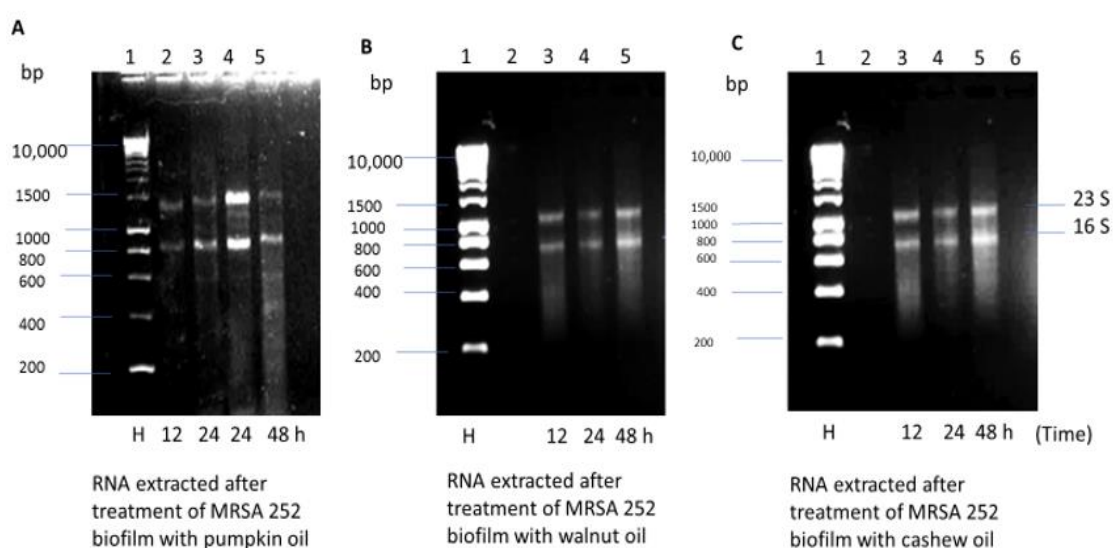


**Figure 72.** Agarose gel electrophoresis of RNA extracted from MRSA 252 biofilms after 12 h, 24 h and 48 h treatment with fluted pumpkin, African walnut and cashew oils.

Lane 1 of A, B and C; H, Hyperladder 1kb size marker. (A) Lanes; 2 (12 h), 3 (24 h) and 5 (48 h) (7  $\mu$ L each) of RNA extracted from MRSA 252 biofilm treated with pumpkin oil. Lane 4; (24 h) is 8  $\mu$ L of RNA extracted from MRSA 252 treated with pumpkin oil. (B) Lanes 3 (12 h), 4 (24 h) and 5 (48 h) (7  $\mu$ L each) of RNA extracted from MRSA 252 biofilm treated with walnut oil. Lastly, Lanes 3 (12 h); 5 (24 h) and 6 (48 h) (7  $\mu$ L each) of RNA extracted from MRSA 252 biofilm treated with cashew oil.

Figure 72 show that the RNA extraction after treatment of MRSA 252 with oils was successful confirming the presence of intact ribosomal RNA bands (23S & 16S) 1200 and 800 bp for total RNA extracted from MRSA 252 biofilm after treatment with fluted pumpkin, African walnut, cashew oils at 12 h, 24 h and 48 h. This indicates that the RNA is still likely intact in the three samples.

### 6.2.3.3 Agarose gel electrophoresis of RNA extracted from *S. aureus* ATCC 6538 after treatment with African walnut, cashew and fluted pumpkin oils

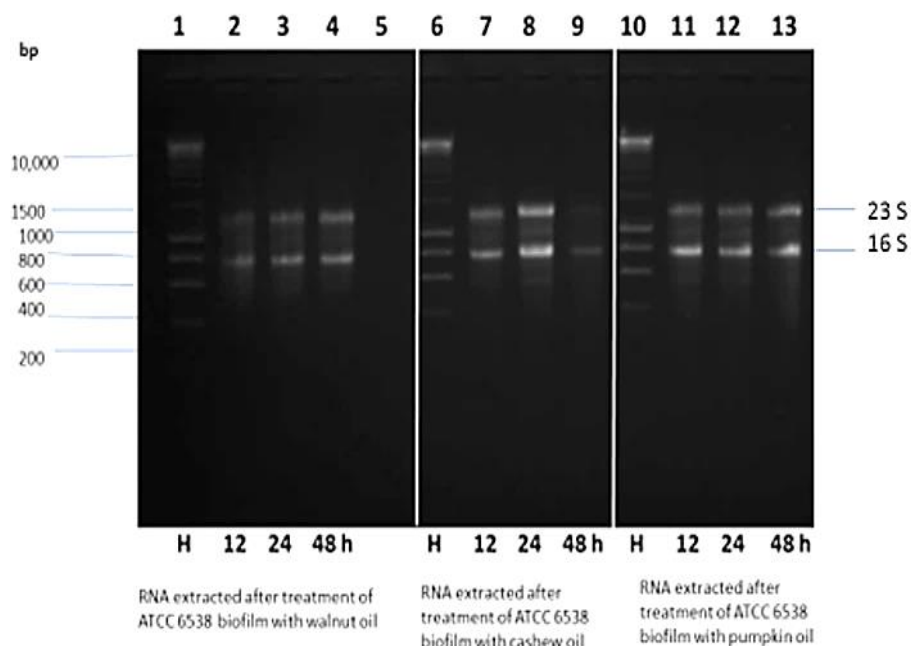


**Figure 73. Agarose gel electrophoresis of rna extracted from *S. aureus* atcc 6538 biofilms after 12 h, 24 h and 48 h treatment with African walnut, cashew and fluted pumpkin oils.**

Lanes 1, 6 and 10; H, Hyperladder 1kb size marker. Lanes; 2 (12 h), 3 (24 h) and 4 (48 h) (7  $\mu$ L each) of RNA extracted from ATCC 6538 biofilm treated with African walnut oil. Lane 7; (12 h), 8 (24 h), and 9 (48 h) (7  $\mu$ L each) of RNA extracted from ATCC 6538 biofilm treated with cashew oil. Lanes; 11 (12 h), 12 (24 h) and 13 (48 h) (7  $\mu$ L each) of RNA extracted from ATCC 6538 biofilm treated with fluted pumpkin oil.

Figure 73 show that RNA extraction after treatment with oils was successful confirming the presence of intact ribosomal RNA bands (23S & 16S) 1200 and 800 bp for total RNA extracted

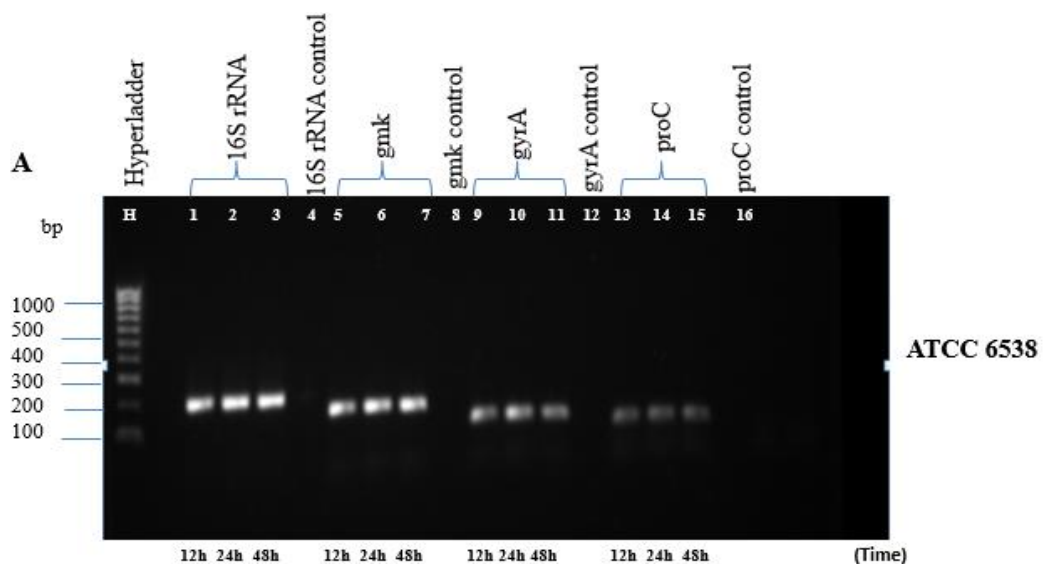
from ATCC 6538 biofilm after treatment with fluted pumpkin, African walnut, cashew oils at 12 h, 24 h and 48 h. This indicates that the RNA is still likely intact in the three samples.

## 6.2.4 Reverse transcription PCR products from RNA extracted from ATCC 6538 and MRSA 252 biofilms.

### 6.2.4.1 RT-PCR products of selected reference genes

The cDNA synthesis generated enough products and all the primers used in this study showed single bands. Reverse transcription polymerase chain reaction (RT-PCR) was carried out on cDNA obtained from ATCC 6538 and MRSA 252 using specific primers of the reference and target genes to confirm that the PCR products yielded a single band of correct size. The RT-PCR products of selected reference genes namely; 16S rRNA, *gmk*, *gyrA*, *proC*, *tpiA*, *glyA*, *pyK*, *gapdh*, *rho* and *rpoD* were identified and genes that were successfully amplified were considered present in strains tested and were further assessed for suitability in gene expression analysis.

**Amplified PCR products for 16S rRNA, *gmk*, *gyrA* and *proC* of MRSA 252 and *S aureus* ATCC 6538 biofilms at 12 h, 24 h and 48 h.**



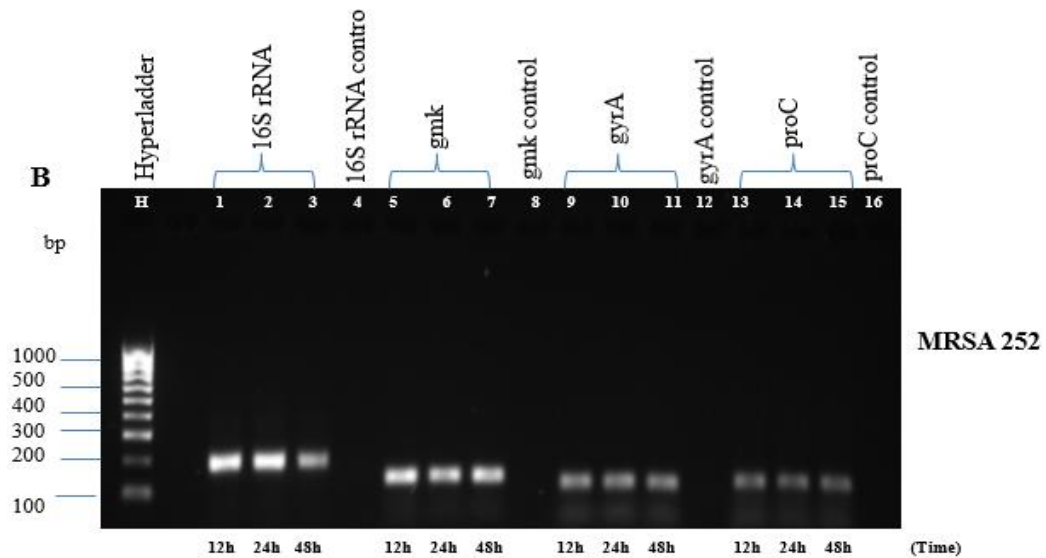


**Figure 74.** Agarose gels showing the RT-PCR products of the 16S rRNA, *gmk*, *gyrA* and *proC* genes of (A) *S. aureus* ATCC 6538 and (B) MRSA 252 biofilms at 12, 24 and 48 h.

(A) Lane H represents Hyperladder 100 (100bp). Lane 1-3, 16S rRNA; lane 5-7, *gmk*; lane 9-11, *gyrA*; lane 13-15, *proC*. Control lanes are Lane 4, 16S rRNA; lane 8, *gmk*; lane 12, *gyrA* and lane 16, *proC*. Control lanes are negative primer control lanes for the PCR products. (B) Lane H represents Hyperladder 100 (100bp). Lane 1-3, 16S rRNA; lane 5-7, *gmk*; lane 9-11, *gyrA*; lane 13-15, *proC*. Control lanes are Lane 4, 16S rRNA; lane 8, *gmk*; lane 12, *gyrA* and lane 16, *proC*. Control lanes are negative primer control lanes for the PCR products.

Figure 74 shows the amplification of 16S rRNA, *gmk*, *gyrA* and *proC* genes were identified using gel electrophoresis. However, the gel of ATCC 6538 revealed the presence of *proC*, 16S rRNA, *gmk* and *gyrA* genes. For MRSA 252, 16S rRNA, *gmk*, *gyrA* and *proC* were present. Furthermore, the amplification of 16S rRNA, *gmk* and *gyrA* of both MRSA 252 and ATCC 6538 resulted in amplification of single products of 16S rRNA, *gmk*, *gyrA* with clear bands at the expected 199, 120 and 97 bp regions. While *proC* was visible at 104 bp region in MRSA 252.

**Amplified PCR products for *tpiA*, *glyA*, *pyk* and *gapdh* of *S. aureus* ATCC 6538 and MRSA 252 biofilms at 12 h, 24 h and 48 h.**

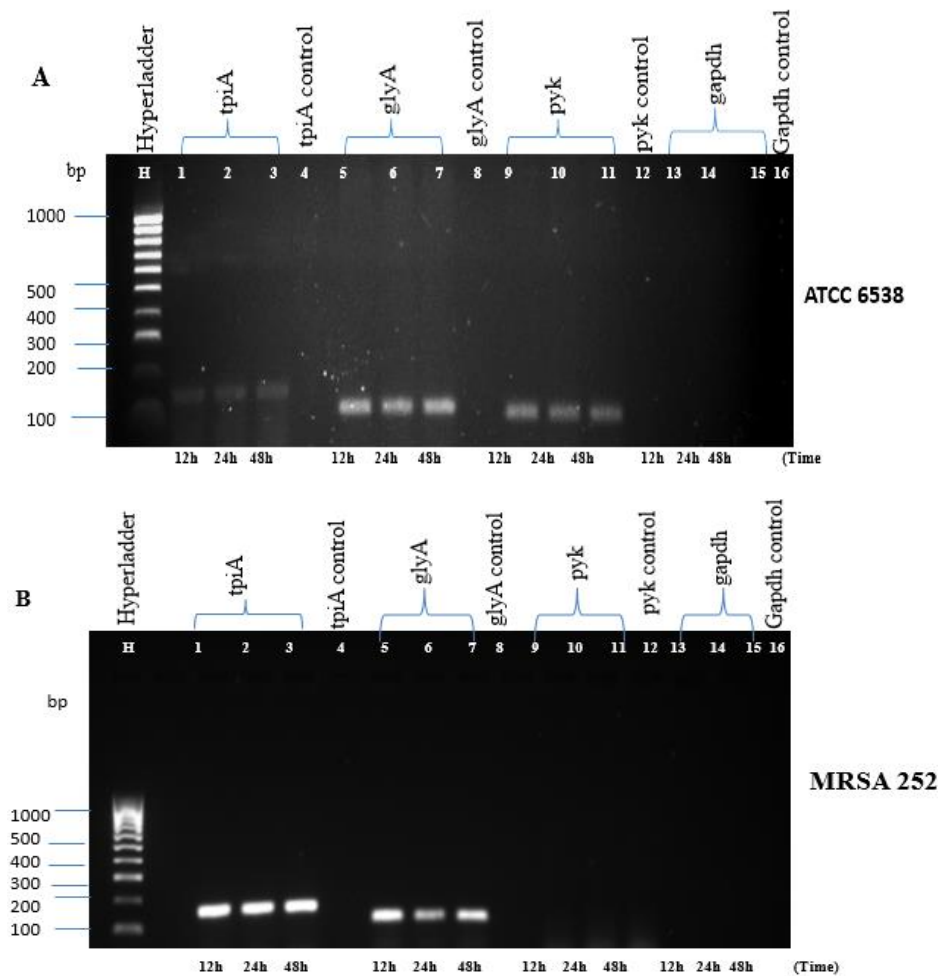


**Figure 75. Agarose gels showing the RT-PCR products of the *tpiA*, *glyA*, *pyk* and *gapdh* genes of (A) *S. aureus* ATCC 6538 and (B) MRSA 252 biofilms.**

(A) Lane H represents Hyperladder 100 (100bp). Lane 1-3, *tpiA*; lane 5-7, *glyA*; lane 9-11, *pyk*; lane 13-15, *gapdh*. Control lanes are Lane 4, *tpiA*; lane 8, *glyA*; lane 12, *pyk* and lane 16, *gapdh*. Control lanes are negative primer control lanes for the PCR products. (B) Lane H represents Hyperladder 100 (100bp). Lanes 1-3, *tpiA*; lane 5-7, *glyA*; lane 9-11, *pyk*; lane 13-15, *gapdh*. Control lanes are Lane 4, *tpiA*; lane 8, *glyA*; lane 12, *pyk* and lane 16, *gapdh*. Control lanes are negative primer control lanes for the PCR products.

Figure 75 shows the reference genes; *tpiA*, *glyA*, *pyk* and *gapdh* were identified using gel electrophoresis. ATCC 6538 was positive for *tpiA*, *glyA* and *pyk* except *gapdh*. Whereas MRSA 252 was positive for *tpiA* and *glyA* only and absent of *pyk* and *gapdh* genes. In addition, the amplification of *tpiA*, *glyA* and *pyk* genes in ATCC 6538 resulted in amplification of single products of 145, 98 and 89 bp. Similarly, MRSA 252 was positive for *tpiA* and *glyA* giving clear bands at 145 and 98 bp regions. No bands can be seen in the primer control lanes.

**Amplified PCR products for *rho* and *rpod* of *S. aureus* ATCC 6538 and MRSA 252 biofilms at 12 h, 24 h and 48 h.**

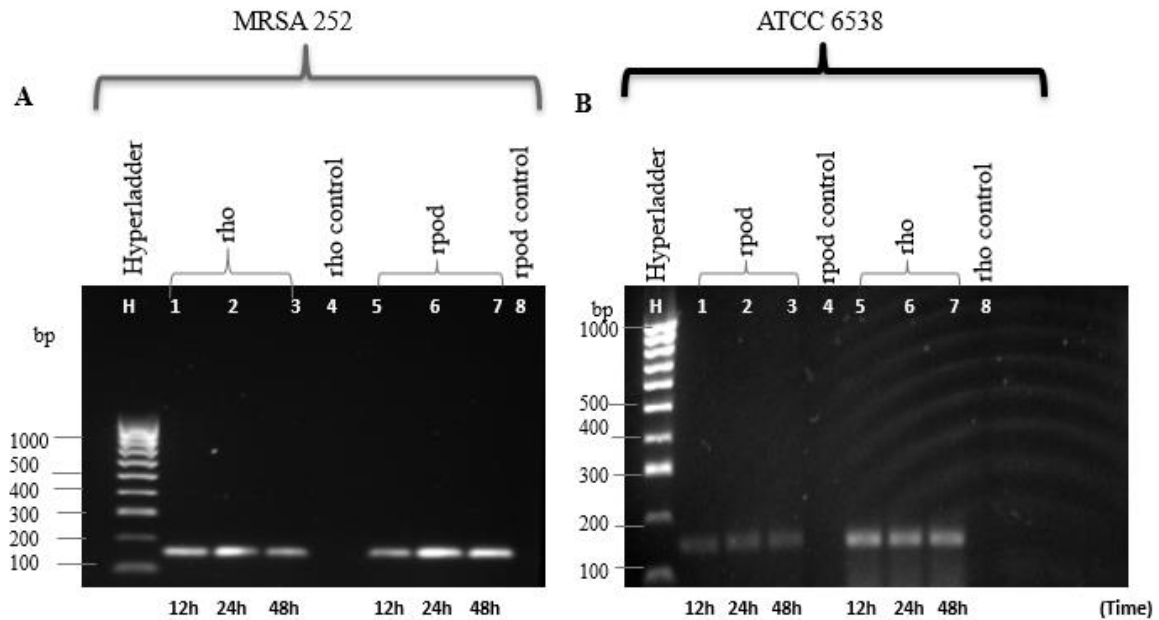


**Figure 76. Agarose gels showing the RT-PCR products of the *rho* and *rpod* genes of (a) *S. aureus* ATCC 6538 and (b) MRSA 252 biofilms.**

(A) Lane H represents Hyperladder 100 (100bp). Lane 1-3, *rho* and lane 5-7, *rpod*. Control lanes are Lane 4, *rho* and lane 8, *rpod*. (B) Lane H represents Hyperladder 100 (100 bp). Lanes 1-3, *rpod* and lanes 5-7, *rho*. Control lanes are Lane 4, *rpod* and lane 8 *rho*. Control lanes are negative primer control lanes for the PCR products.

Figure 76 shows that primer pairs of *rho* and *rpod* resulted in amplification of genes *rho* and *rpod* in both MRSA 232 and ATCC 6538. These agarose gels revealed single products of *rho* and *rpod* with clear bands at 144 and 146 regions. No additional bands were observed.

**Amplified PCR products for *rrsC* of *S aureus* ATCC 6538 and MRSA 252 biofilms at 12 h, 24 h and 48 h.**

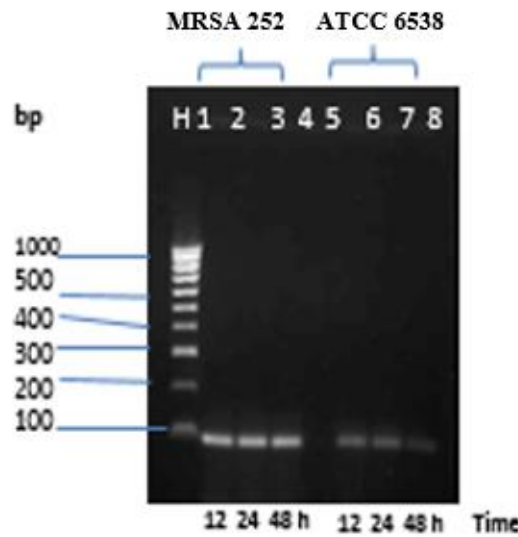


**Figure 77. Agarose gel electrophoresis of RT-PCR products of *rrsC* gene for *S. aureus* ATCC 6538 and MRSA 252 biofilms.**

Lanes 1-3, *rrsC* of MRSA 252 and lane 5-7, *rrsC* of ATCC 6538. H represents Hyperladder 100 (100bp). Control lanes are Lane 4 and lane 8. Control lanes are negative primer control lanes for the PCR products.

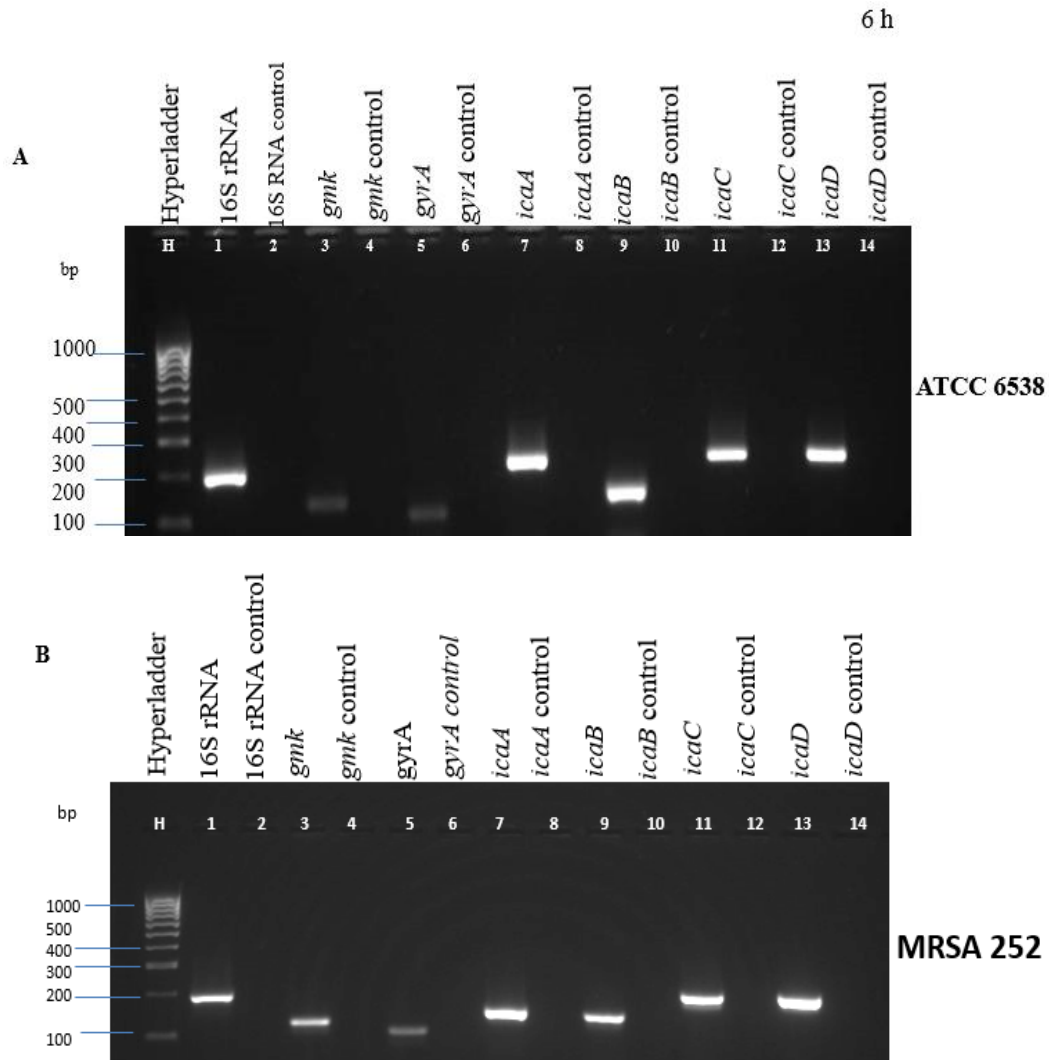
Figure 77 shows that the primer resulted in the amplification of single products of *rrsC*. This indicates that ATCC 6538 and MRSA 252 are positive for *rrsC* giving visible bands at 82 bp regions. No additional bands were observed.

**6.2.4.2 RT-PCR products of adhesion and biofilm genes in ATCC 6538 and MRSA 252 at different growth time points.**

RT-PCR was used to identify the adhesion (*icaA*, *icaB*, *icaC* and *icaD*) and biofilm genes (*fnbA*, *fnbB*, *fib*, *clfA*, *clfB*, *cna*, *ebps* and *eno*) present in *S. aureus* ATCC 6538 and MRSA 252 cultured cells and biofilms at 6 h, 12 h, 24 h and 48 h growth time points.

(i) Amplified PCR products at 6 h growth time point

Amplified PCR products for 16S rRNA, *gmk*, *gyrA*, *icaA*, *icaB*, *icaC* and *icaD* of *S aureus* ATCC 6538 and MRSA 252 cultured cells at 6 h.



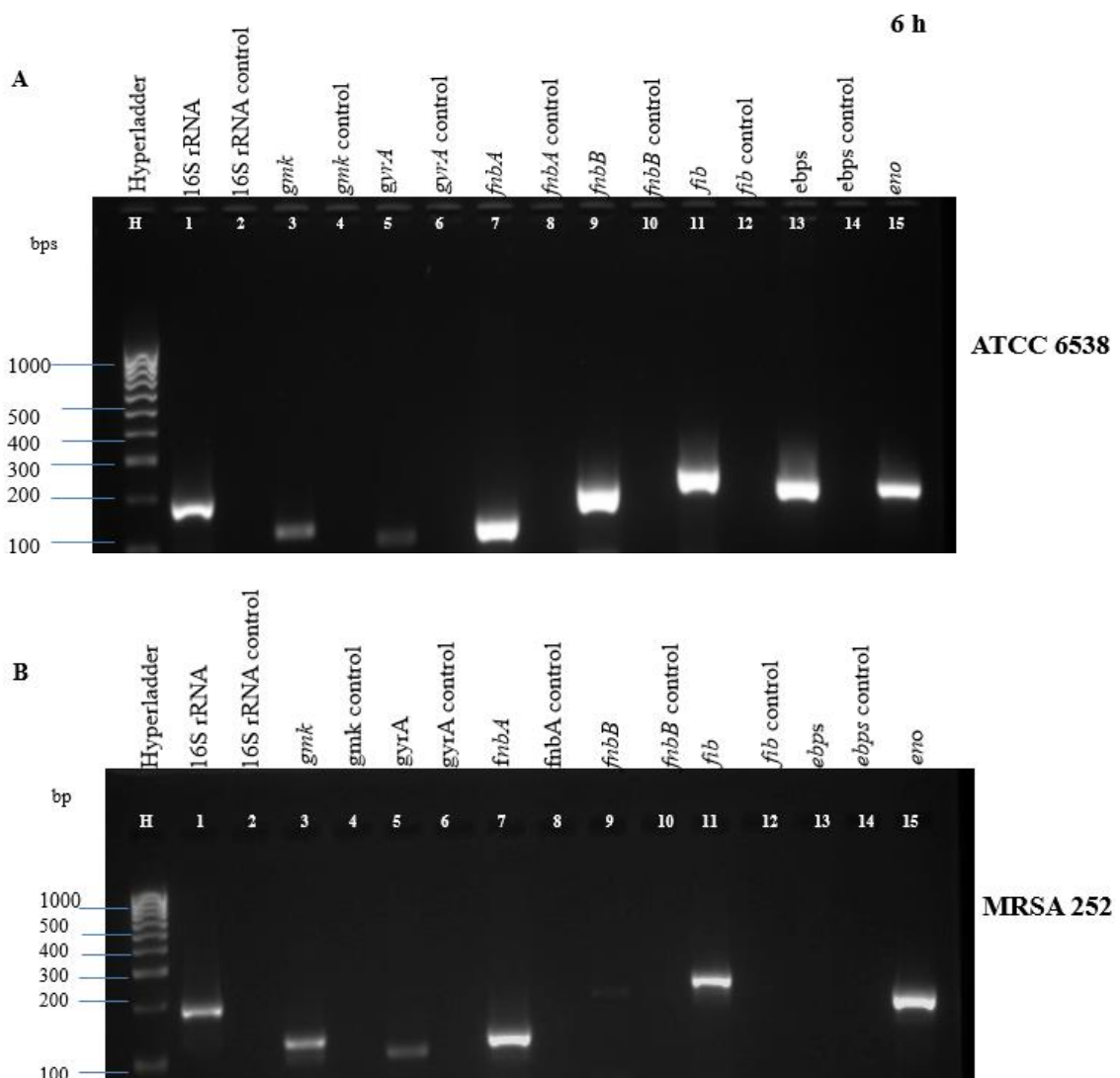
Agarose gel electrophoresis of RT-PCR amplification products of 16S rRNA, *gmk*, *gyrA*, *icaA*, *icaB*, *icaC* and *icaD* genes for (A) *S. aureus* ATCC 6538 and (B) MRSA 252 cultured for 6 h.

(A) Lane 1, 16S rRNA; lane 3, *gmk*; lane 5, *gyrA*; lane 7, *icaA*; lane 9, *icaB*; lane 11, *icaC*; lane 13, *icaD*. H represents Hyperladder 100 (100bp). Control lanes are Lane 2, 16S rRNA; lane 4, *gmk*; lane 6, *gyrA*; lane 8, *icaA*; lane 10, *icaB*; lane 12, *icaC*; lane 14, *icaD*. Control lanes are negative primer control lanes for the PCR products.

(B) (A) Lane 1, 16S rRNA; lane 3, *gmk*; lane 5, *gyrA*; lane 7, *icaA*; lane 9, *icaB*; lane 11, *icaC*; lane 13, *icaD*. H represents Hyperladder 100 (100bp). Control lanes are Lane 2, 16S rRNA; lane 4, *gmk*; lane 6, *gyrA*; lane 8, *icaA*; lane 10, *icaB*; lane 12, *icaC*; lane 14, *icaD*. Control lanes are negative primer control lanes for the PCR products.

The gels show that all the intercellular adhesion target genes are expressed in MRSA 252 and *S. aureus* ATCC 6538 at 6 h. 16S rRNA, *gmk*, *gyrA*, *icaA*, *icaB*, *icaC* and *icaD* bands seems to be intense. In addition, Clear bands were observed at the expected 191 bp, 121 bp, 98 bp, 151 bp, 140 bp, 209 bp and 211 bp regions. No bands can be seen in the primer control lanes showing that amplification was not due to contamination of materials.

**Amplified PCR products for 16S rRNA, *gmk*, *gyrA*, *fnbA*, *fnbB*, *fib*, *ebps* and *eno* of *S. aureus* ATCC 6538 and MRSA 252 cultured cells at 6 h.**



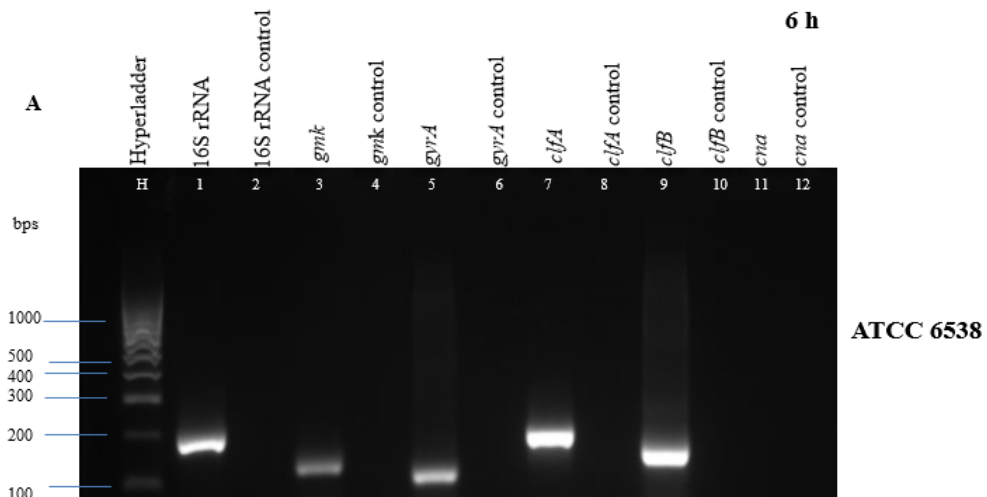
**Agarose gel electrophoresis of RT-PCR amplification products of 16S rRNA, *gmk*, *gyrA*, *fnbA*, *fnbB*, *fib*, *ebps* and *eno* for (A) ATCC 6538 and (B) MRSA 252 cells cultured for 6 h.**

(A) Lane 1, 16S rRNA; lane 3, *gmk*; lane 5, *gyrA*; lane 7, *fnbA*; lane 9, *fnbB*; lane 11, *fib*; lane 13, *ebps*; lane 15, *eno*. H represents Hyperladder 100 (100bp). Control lanes are Lane 2, 16S rRNA; lane 4, *gmk*; lane 6, *gyrA*; lane

8, *fnbA*; lane 10, *fnbB*; lane 12, *fib*; lane 14, *ebps*. Control lanes are negative primer control lanes for the PCR products. (B) Lane 1, 16S rRNA; lane 3, *gmk*; lane 5, *gyrA*; lane 7, *fnbA*; lane 9, *fnbB*; lane 11, *fib*; lane 13, *ebps*; lane 15, *eno*. H represents Hyperladder 100 (100bp). Control lanes are Lane 2, 16S rRNA; lane 4, *gmk*; lane 6, *gyrA*; lane 8, *fnbA*; lane 10, *fnbB*; lane 12, *fib*; lane 14, *ebps*. Control lanes are negative primer control lanes for the PCR products.

The gels show the amplification of 16S rRNA, *gmk*, *gyrA*, *fnbA*, *fnbB*, *fib*, *ebps* and *eno* in MRSA 252 and *S. aureus* ATCC 6538. Clear bands of the target genes were observed at the expected 191 bp, 121 bp, 98 bp, 121 bp, 197 bp, 239 bp, 191 bp and 195 bp regions. Gene *ebps* was present in ATCC 6538 but was conspicuously absent in MRSA 252. Also, no additional band sizes were observed. No bands can be seen in the primer control lanes because no cdna template was used.

**Amplified PCR products for 16S rRNA, *gmk*, *gyrA*, *clfA*, *clfB* and *cna* of *S aureus* ATCC 6538 and MRSA 252 cultured cells at 6 h.**



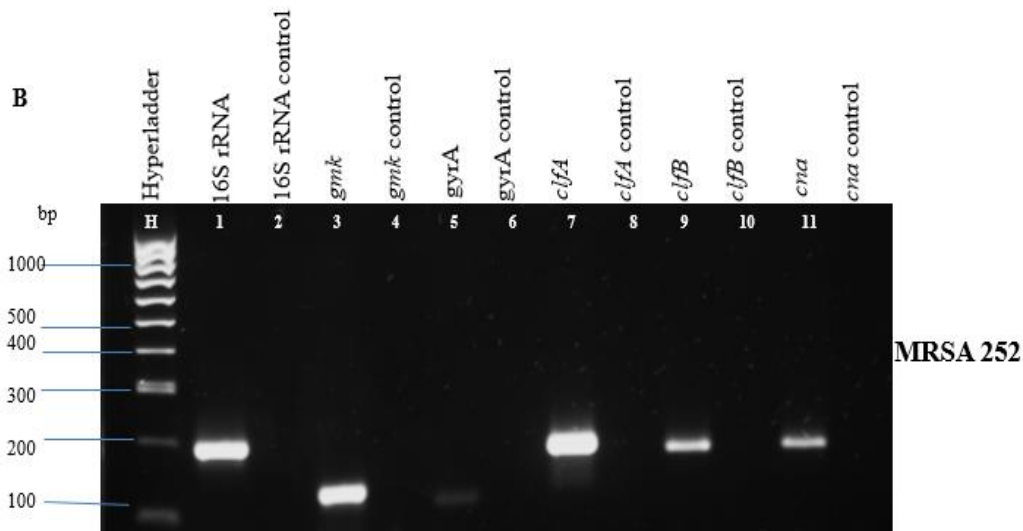


**Figure 78. Agarose gel electrophoresis of RT-PCR amplification products of 16S rRNA, *gmk*, *gyrA*, *clfA*, *clfB* and *cna* of (a) MRSA 252 and (b) ATCC 6538 cells cultured at 6 h.**

(A) Lane 1, 16S rRNA; lane 3, *gmk*; lane 5, *gyrA*; lane 7, *clfA*; lane 9, *clfB*; lane 11, *cna* H represents Hyperladder 100 (100bp). Control lanes are Lane 2, 16S rRNA; lane 4, *gmk*; lane 6, *gyrA*; lane 8, *clfA*; lane 10, *clfB*; lane 12, *cna*. Control lanes are negative primer control lanes for the PCR products. (B) Lane 1, 16S rRNA; lane 3, *gmk*; lane 5, *gyrA*; lane 7, *clfA*; lane 9, *clfB*; lane 11, *cna*. H represents Hyperladder 100 (100bp). Control lanes are Lane 2, 16S rRNA; lane 4, *gmk*; lane 6, *gyrA*; lane 8, *clfA*; lane 10, *clfB*; lane 12, *cna*. Control lanes are negative primer control lanes for the PCR products because no cDNA template was used.

Figure 78 shows that MRSA 252 and *S. aureus* ATCC 6538 is positive for 16S rRNA, *gmk*, *gyrA*, *clfA*, and *clfB* giving visible clear bands at the expected 191 bp, 121 bp, 98 bp, 245 bp and 159 bp regions. ATCC 6538 is *cna* negative while MRSA 252 is *cna* positive giving band in the 156 bp region. The reason for *cna* not showing any visible band is unknown, the PCR was repeated several times with varied PCR conditions.

**Amplified PCR products for 16S rRNA, *gmk*, *gyrA*, *RNAII*, *RNAIII*, *Sea* and *Seb* of *S. aureus* ATCC 6538 and MRSA 252 cells cultured at 6 h.**

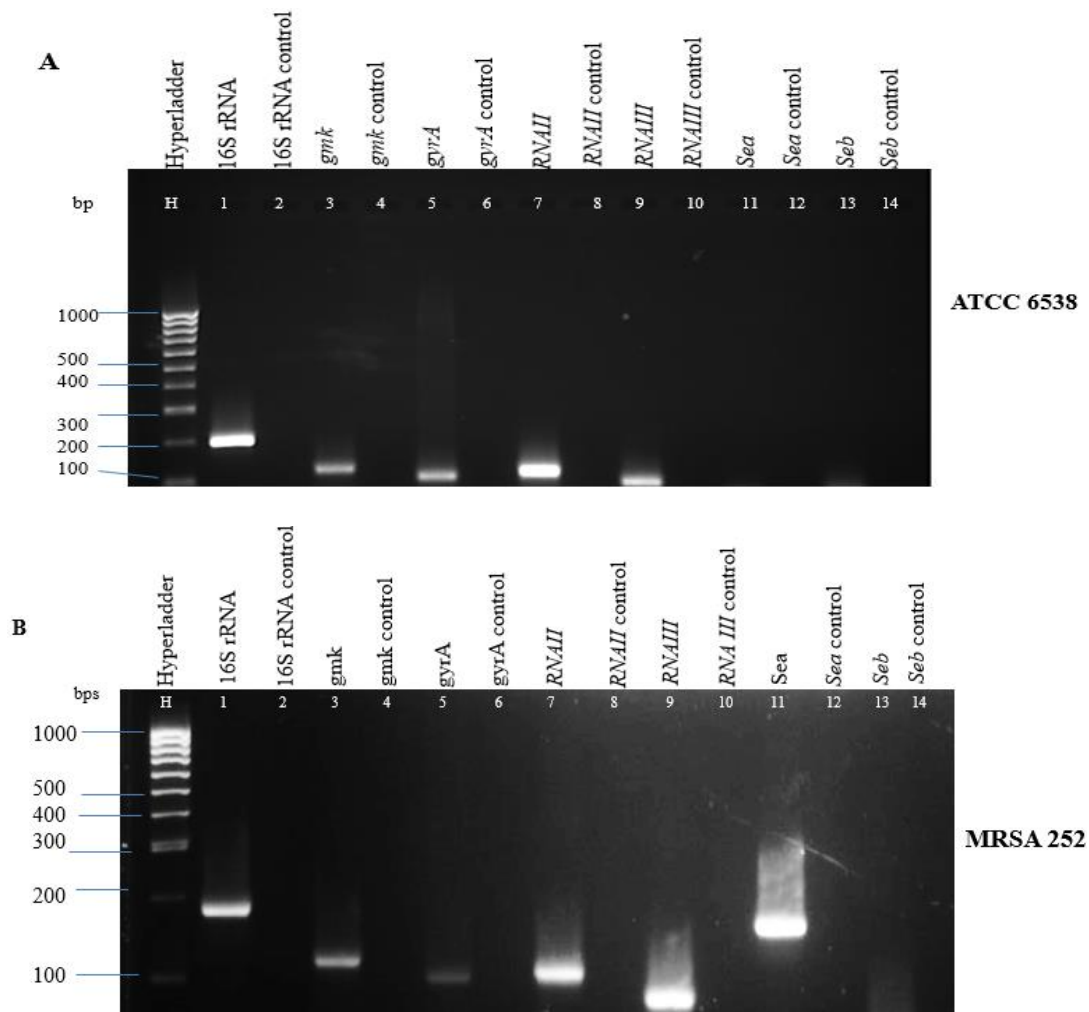


**Figure 79. Agarose gel electrophoresis of RT-PCR amplification products of 16S RNA, *gmk*, *gyrA*, *RNAII*, *RNAIII*, *sea*, and *seb* genes for (a) *S. aureus* ATCC 6538 and (b) MRSA 252 cells.**

(A) Lane 1, 16S rRNA; lane 3, *gmk*; lane 5, *gyrA*; lane 7, *RNAII*; lane 9, *RNAIII*; lane 11, *sea* and lane 13, *seb*. H represents Hyperladder 100 (100bp). Control lanes are Lane 2, 16S rRNA; lane 4, *gmk*; lane 6, *gyrA*; lane 8, *RNAII*; lane 10, *RNAIII*; lane 12, *sea* and lane 14, *seb*). (B) Lane 1, 16S rRNA; lane 3, *gmk*; lane 5, *gyrA*; lane 7, *RNAII*; lane 9, *RNAIII*; lane 11, *sea* and lane 13, *seb*. H represents Hyperladder 100 (100bp). Control lanes are Lane 2, 16S rRNA; lane 4, *gmk*; lane 6, *gyrA*; lane 8, *RNAII*; lane 10, *RNAIII*; lane 12, *sea* and lane 14, *seb*. Control lanes in gels A and B are negative primer control lanes for the PCR products because no cDNA template was used.

Figure 79 shows that MRSA 252 and *S. aureus* ATCC 6538 biofilms are positive for 16S rRNA, *gmk*, *gyrA*, *RNA II*, and *RNA III* genes at 6 h. However, at this same time point only MRSA 252 was positive for *sea*. Gene *sea* was not seen in ATCC 6538. All the bands of the genes appeared indicating that their amplification was successful and resulted in single clear

visible bands observed at the expected 191 bp, 121 bp, 98 bp, 73 bp, 53bp and 154 bp regions. No bands can be seen in the primer control lanes.

**Amplified PCR products for 16S rRNA, *gmk*, *gyrA*, *mecA*, *emrA*, and *blaZ* of *S aureus* ATCC 6538 and MRSA 252 cells cultured at 6 h.**

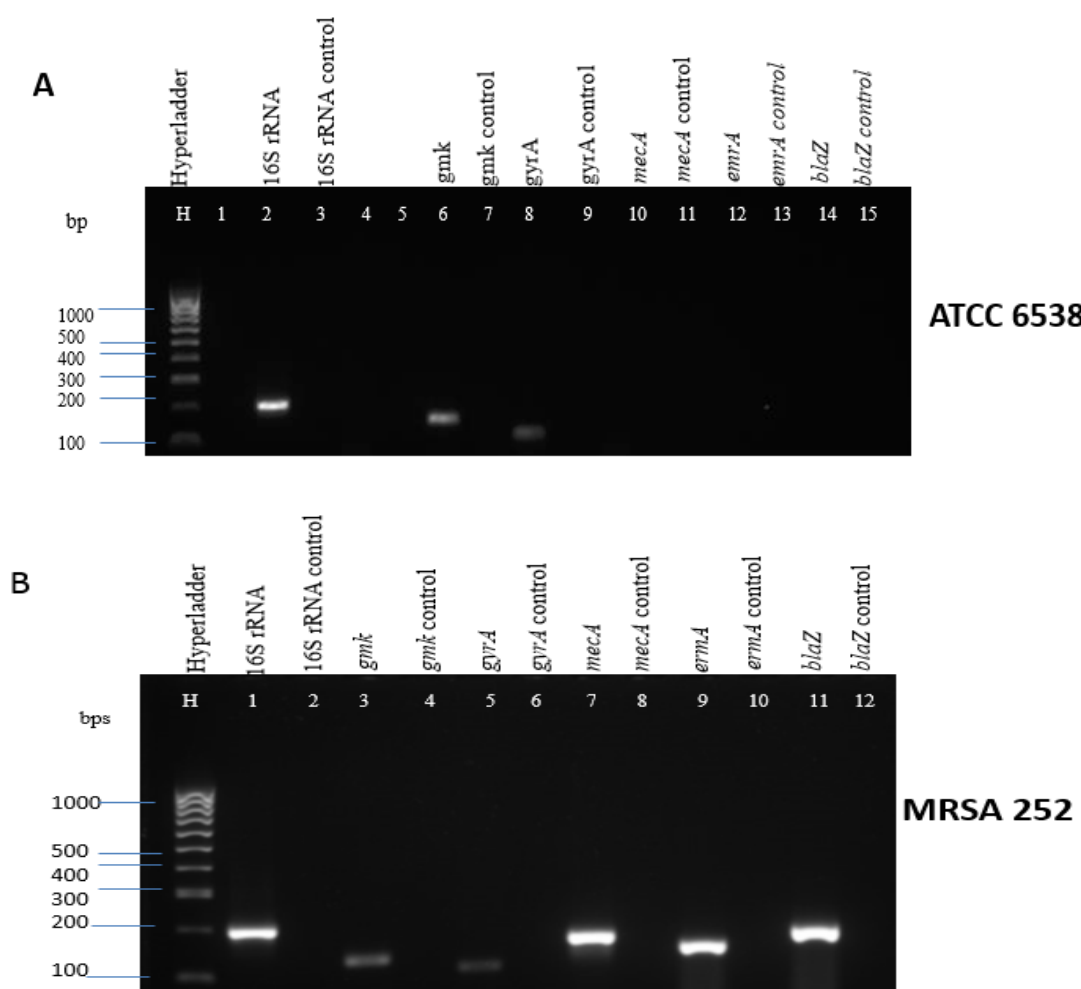


**Figure 80. Agarose gel electrophoresis of RT-PCR amplification products of 16S rRNA, *gmk*, *gyrA*, *mecA*, *emrA* and *blaZ* genes for (a) *S. aureus* ATCC 6538 and (b) MRSA 252 cultured cells.**

(A) Lanes 1, 16S rRNA; lanes 3, *gmk*; lanes 5 *gyrA*; lane 7, *mecA*, lane 9, *emrA* and lanes 14, *blaZ*. H represented Hyperladder 100 (100bp). Control lanes are Lane 2, 16S rRNA; lane 4, *gmk*; lane 6, *gyrA*; lane 8, *mecA*; lane 10, *emrA* and lane 12, *blaZ*. Control lanes are negative primer control lanes for the PCR products. (B) Lanes 1, 16S rRNA; lanes 3, *gmk*; lanes 5, *gyrA*; lanes 7 *mecA*, lanes 9, *emrA* and *blaZ*. H represented Hyperladder 100 (100bp). Control lanes are Lane 2, 16S rRNA; lane 4, *gmk*; lane 6, *gyrA*; lane 8, *mecA*, lanes 10, *emrA* and Lanes 11, *blaZ*. Control lanes are negative primer control lanes for the PCR products.

Figure 80 shows that MRSA 252 and *S. aureus* ATCC 6538 biofilms are positive for 16S rRNA, *gmk*, *gyrA*, *mecA*, *emrA* and *blaZ* genes at 6 h. However, *mecA* and *blaZ* were not seen

in ATCC 6538. MRSA 252 contained *mecA* and *blaZ* genes probably because it is a methicillin resistant strain. Most of the bands of the genes in both gels appeared indicating that their amplification resulted in single clear visible bands observed at the expected 191 bp, 121 bp, 98 bp, 139 bp and 173 bp regions. No bands can be seen in the primer control lanes.

**Amplified PCR products for 16S rRNA, *gmk*, *gyrA* and *agrA* genes of *S aureus* ATCC 6538 and MRSA 252 cells cultured at 6 h.**

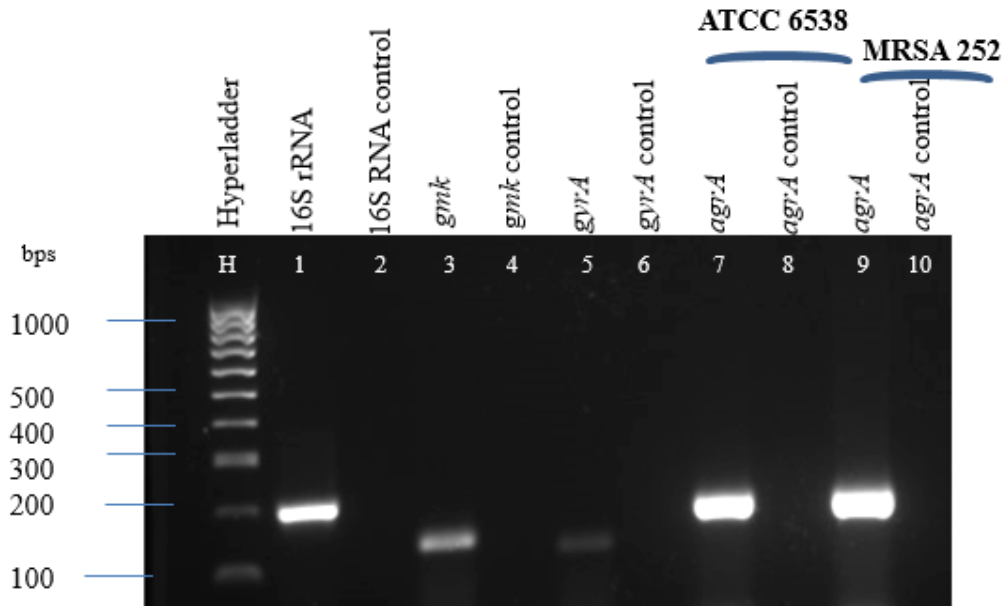


**Figure 81. Agarose gel electrophoresis of RT-PCR amplification products of *agrA* gene for *S. aureus* ATCC 6538 and MRSA 252 biofilms.**

Lanes 7, *agrA* for ATCC 6538; lanes 9, *agrA* for MRSA 252. H represented Hyperladder 100 (100bp). Control lanes are Lane 8 and 10. Control lanes are negative primer control lanes for the PCR products.

Figure 81 shows that MRSA 252 and *S. aureus* ATCC 6538 cells are positive for *agrA* gene at 6 h. All the *agrA* bands appeared indicating that the amplification resulted in single clear visible bands observed at the expected 111 bp regions. No bands can be seen in the primer control lanes.

(ii) Amplified PCR products at 12 h, 24 h and 48 h growth time point.

Amplified PCR products for 16S rRNA, *gmk*, *gyrA*, *icaA* and *icaB* of *S aureus* ATCC 6538 and MRSA 252 biofilms at 12 h, 24 h and 48 h.

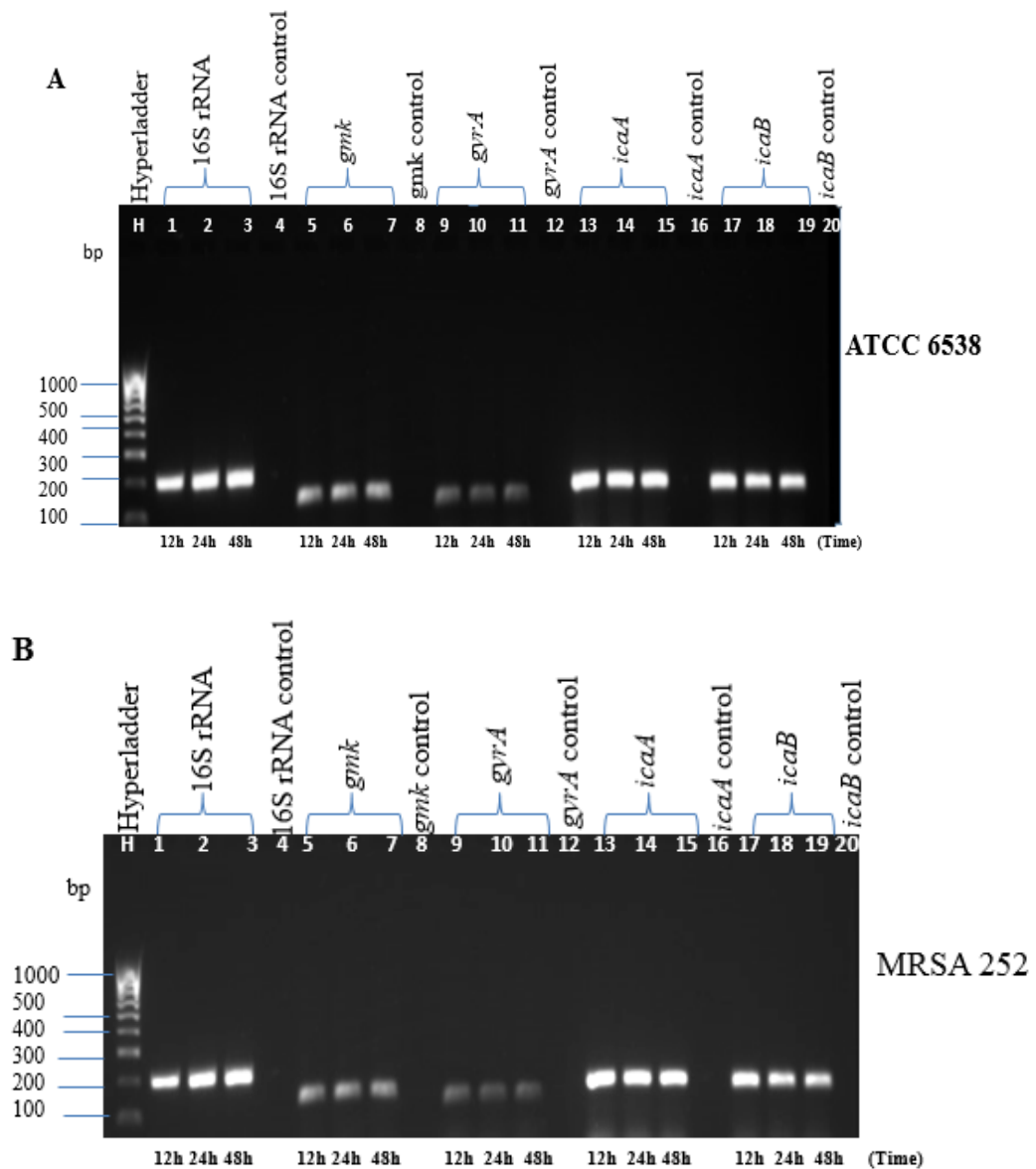
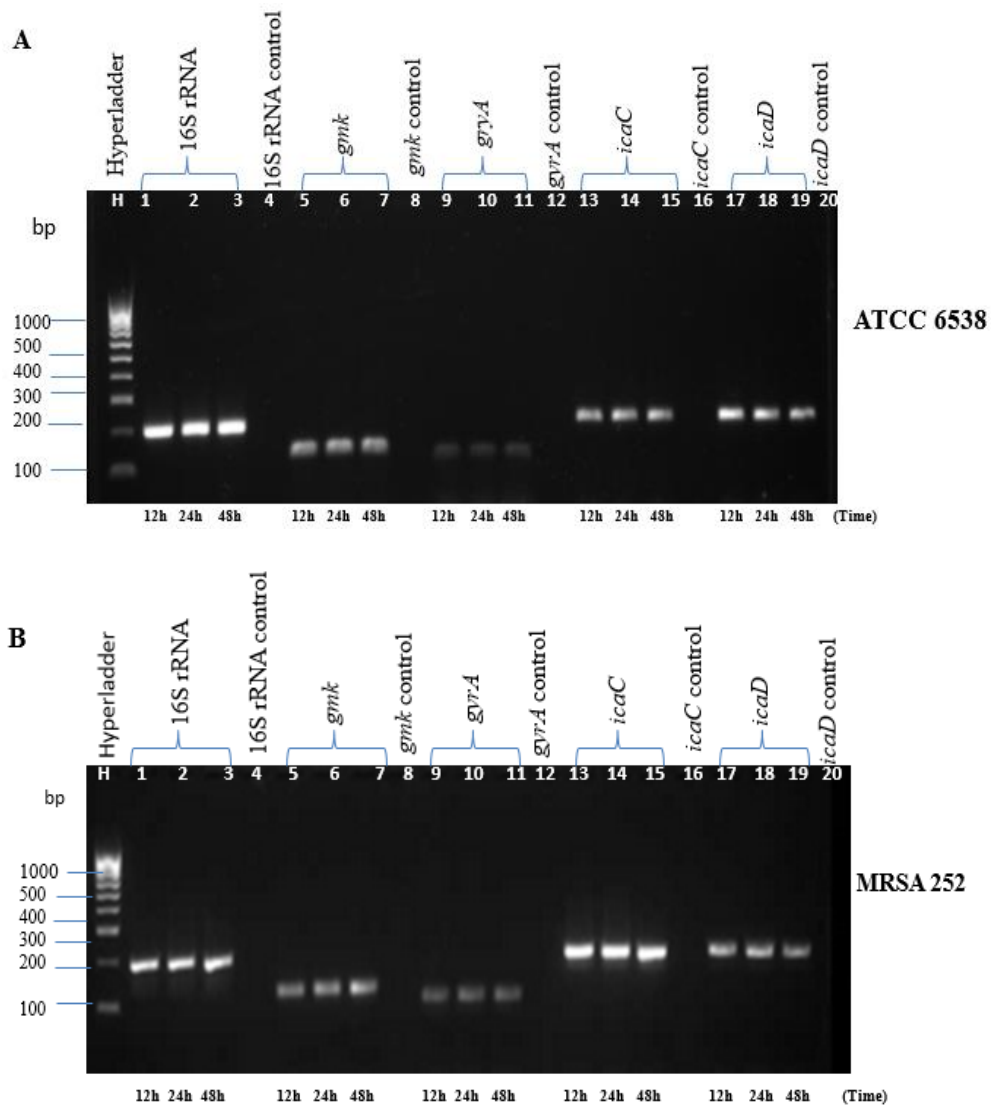


Figure 82. Agarose gel electrophoresis of RT-PCR amplification products of 16S rRNA, *gmk*, *gyrA*, *icaA* and *icaB* genes for (a) *S. aureus* ATCC 6538 and (b) MRSA 252 biofilms.

(A) Lanes 1-3, 16S rRNA; lanes 5-7, *gmk*; lanes 9-11, *gyrA*; lanes 13-15, *icaA* and lanes 17-19, *icaB*. H represented Hyperladder 100 (100bp). Control lanes are Lane 4, 16S rRNA; lane 8, *gmk*; lane 12, *gyrA*; lane 16, *icaA* and lanes 20, *icaB*. Control lanes are negative primer control lanes for the PCR products. (B) Lanes 1-3, 16S rRNA; lanes 5-7, *gmk*; lanes 9-11, *gyrA*; lanes 13-15, *icaA* and lanes 17-19, *icaB*. H represented Hyperladder 100 (100bp). Control lanes are Lane 4, 16S rRNA; lane 8, *gmk*; lane 12, *gyrA*; lane 16, *icaA* and lanes 20, *icaB*. Control lanes are negative primer control lanes for the PCR products.

Figure 82 shows that the control genes and target genes are expressed in MRSA 252 and *S. aureus* ATCC 6538 biofilms at 12, 24 and 48 h. This shows that the control genes; 16S rRNA, *gmk*, *gyrA* as well as the target genes; *icaA* and *icaB* are present in MRSA 252 and ATCC 6538 at 12 h, 24 h and 48 h. Genes *gmk* and *gyrA* appeared faint but despite the faint bands, amplification resulted in single clear visible bands observed at the expected 121 and 98 bp. Also, 16S rRNA, *icaA* and *icaB* gave single clear visible bands at 12, 24 and 48 h with the bands observed at the expected 191 bp, 151 bp and 141 bp regions. No bands can be seen in the primer control lanes.

**Amplified PCR products for 16S rRNA, *gmk*, *gyrA*, *icaC* and *icaD* of *S. aureus* ATCC 6538 and MRSA 252 biofilms at 12 h, 24 h and 48 h.**

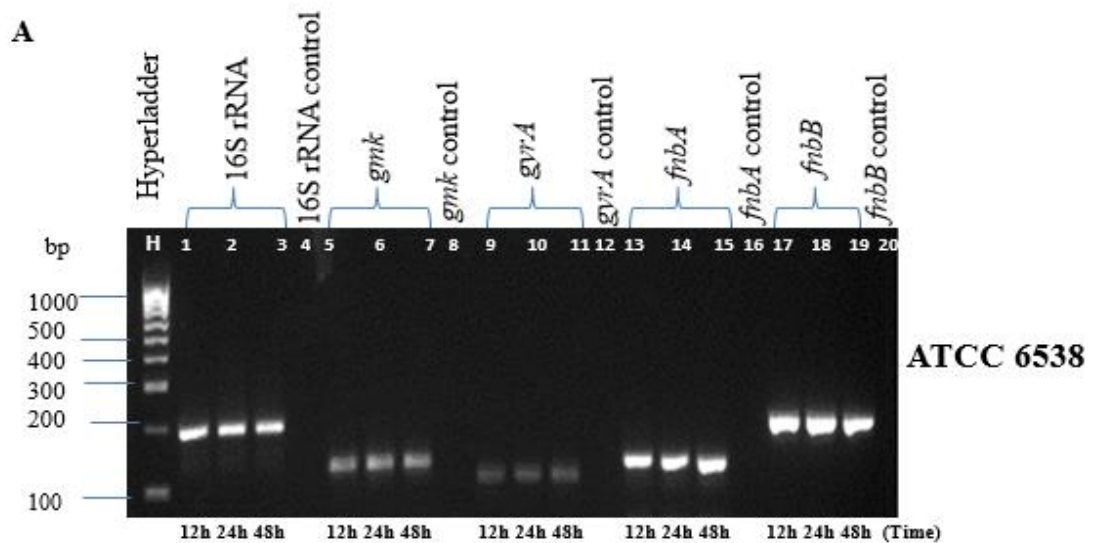


**Figure 83. Agarose gel electrophoresis of RT-PCR amplification products of 16S RNA, *gmk*, *gyrA*, *icaC* and *icaD* genes for (a) *S. aureus* ATCC 6538 and (b) MRSA 252 biofilms.**

(A) Lanes 1-3, 16S rRNA; lanes 5-7, *gmk*; lanes 9-11, *gyrA*; lanes 13-15, *icaC* and lanes 17-19, *icaD*. H represented Hyperladder 100 (100bp). Control lanes are Lane 4, 16S rRNA; lane 8, *gmk*; lane 12, *gyrA*; lane 16, *icaC* and lanes 20, *icaD*. Control lanes are negative primer control lanes for the PCR products. (B) Lanes 1-3, 16S rRNA; lanes 5-7, *gmk*; lanes 9-11, *gyrA*; lanes 13-15, *icaC* and lanes 17-19, *icaD*. H represented Hyperladder 100 (100bp). Control lanes are Lane 4, 16S rRNA; lane 8, *gmk*; lane 12, *gyrA*; lane 16, *icaC* and lanes 20, *icaD*. Control lanes are negative primer control lanes for the PCR products.

Figure 83 shows that MRSA 252 and *S. aureus* ATCC 6538 biofilms are positive for 16S rRNA, *gmk*, *gyrA*, *icaC* and *icaD* genes at 12, 24 and 48 h. All the bands of the genes appeared prominent indicating that their amplification was successful and resulted in single clear visible bands observed at the expected 191 bp, 121 bp, 98 bp, 209 bp and 211 bp regions. No bands can be seen in the primer control lanes.

**Amplified PCR products for 16S rRNA, *gmk*, *gyrA*, *fnbA* and *fnbB* of *S aureus* ATCC 6538 and MRSA 252 biofilms at 12 h, 24 h and 48 h.**



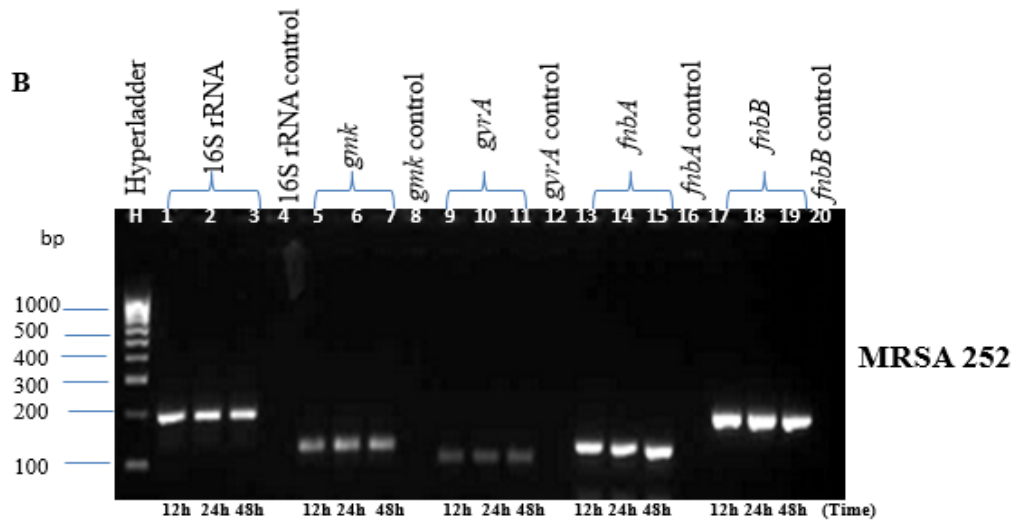


**Figure 84. Agarose gel electrophoresis of RT-PCR amplification products of 16S RNA, *gmk*, *gyrA*, *fnbA* and *fnbB* genes for (a) *S. aureus* ATCC 6538 and (b) MRSA 252 biofilms**

(A) Lanes 1-3, 16S rRNA; lanes 5-7, *gmk*; lanes 9-11, *gyrA*; lanes 13-15, *fnbA* and lanes 17-19, *fnbB*. H represented Hyperladder 100 (100bp). Control lanes are Lane 4, 16S rRNA; lane 8, *gmk*; lane 12, *gyrA*; lane 16, *fnbA* and lanes 20, *fnbB*. Control lanes are negative primer control lanes for the PCR products. (B) Lanes 1-3, 16S rRNA; lanes 5-7, *gmk*; lanes 9-11, *gyrA*; lanes 13-15, *fnbA* and lanes 17-19, *fnbB*. H represented Hyperladder 100 (100bp). Control lanes are Lane 4, 16S rRNA; lane 8, *gmk*; lane 12, *gyrA*; lane 16, *fnbA* and lanes 20, *fnbB*. Control lanes are negative primer control lanes for the PCR products.

Figure 84 shows that MRSA 252 and *S. aureus* ATCC 6538 biofilms are positive for 16S rRNA, *gmk*, *gyrA*, *fnbA* and *fnbB* genes at 12, 24 and 48 h. All the bands of the genes appeared indicating that their amplification was successful and resulted in single clear visible bands observed at the expected 191 bp, 121 bp, 98 bp, 121 bp and 197 bp regions. No bands can be seen in the primer control lanes.

**Amplified PCR products for 16S rRNA, *gmk*, *gyrA*, *fib* and *cna* of *S aureus* ATCC 6538 and MRSA 252 biofilms at 12 h, 24 h and 48 h.**

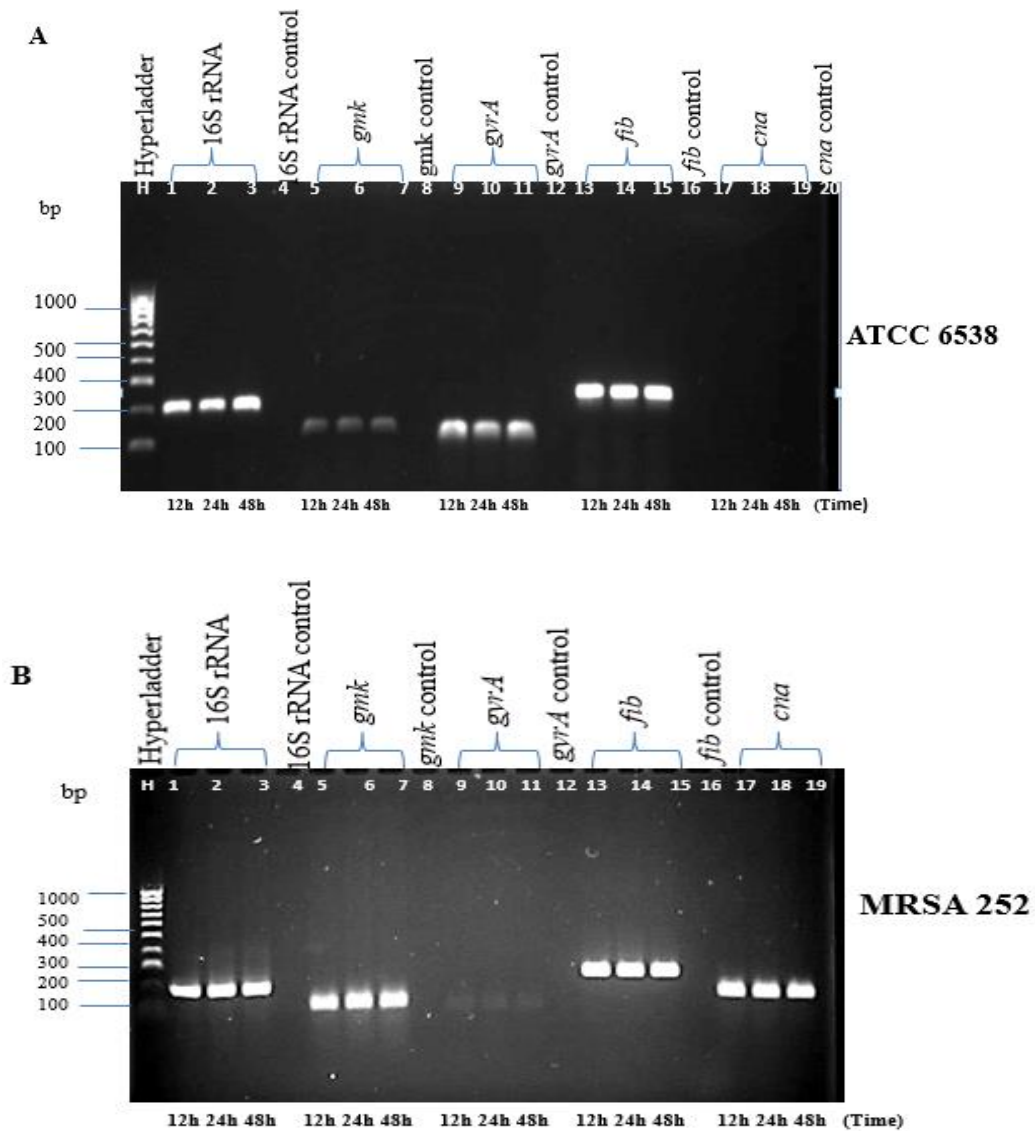
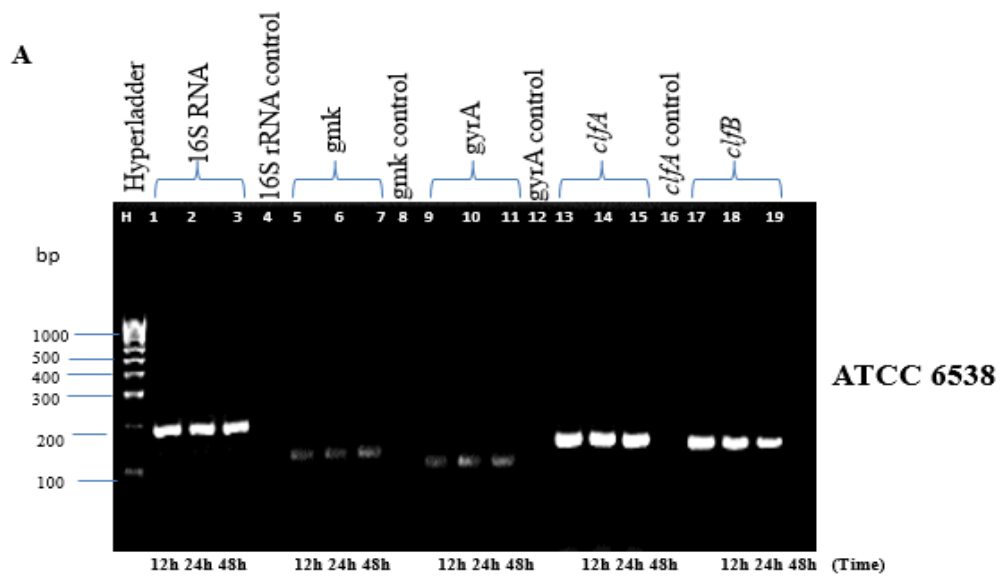


**Figure 85. Agarose gel electrophoresis of RT-PCR amplification products of 16S rRNA, *gmk*, *gyrA*, *fib* and *cna* genes for (a) *S. aureus* ATCC 6538 and (b) MRSA 252 biofilms.**

(A) Lanes 1-3, 16S rRNA; lanes 5-7, *gmk*; lanes 9-11, *gyrA*; lanes 13-15, *fib* and lanes 17-19, *cna*. H represented Hyperladder 100 (100bp). Control lanes are Lane 4, 16S rRNA; lane 8, *gmk*; lane 12, *gyrA*; lane 16, *fib* and lanes 20, *cna*. Control lanes are negative primer control lanes for the PCR products. (B) Lanes 1-3, 16S rRNA; lanes 5-7, *gmk*; lanes 9-11, *gyrA*; lanes 13-15, *fib* and lanes 17-19, *cna*. H represented Hyperladder 100 (100bp). Control lanes are Lane 4, 16S rRNA; lane 8, *gmk*; lane 12, *gyrA*; lane 16, *fib* and lanes 20, *cna*. Control lanes are negative primer control lanes for the PCR products.

Figure 85 shows that MRSA 252 and *S. aureus* ATCC 6538 biofilms are positive for 16S rRNA, *gmk*, *gyrA*, *fib* and *cna* genes at 12, 24 and 48 h. All the bands of the genes appeared prominent indicating that their amplification was successful and resulted in single clear visible bands observed at the expected 191 bp, 121 bp, 98 bp, 239 bp and 156 bp regions. Despite the faintness of *gyrA* band in MRSA 252 it was seen at the 98 bp region as expected. Gene *cna* was not observed in ATCC 6538 but was present in MRSA 252. No bands can be seen in the primer control lanes.

**Amplified PCR products for 16S rRNA, *gmk*, *gyrA*, *clfA* and *clfB* of *S aureus* ATCC 6538 and MRSA 252 biofilms at 12 h, 24 h and 48 h.**



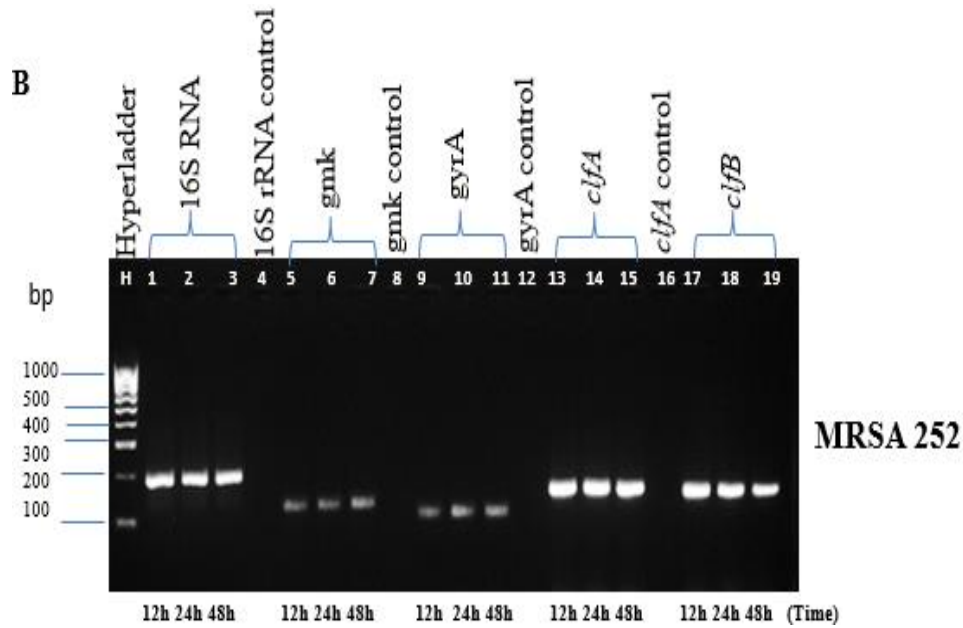


**Figure 86. Agarose gel electrophoresis of RT-PCR amplification products of 16S RNA, *gmk*, *gyrA*, *clfA* and *clfB* genes for (a) *S. aureus* ATCC 6538 and (b) MRSA 252 biofilms**

(A) Lanes 1-3, 16S rRNA; lanes 5-7, *gmk*; lanes 9-11, *gyrA*; lanes 13-15, *clfA* and lanes 17-19, *clfB*. H represented Hyperladder 100 (100bp). Control lanes are Lane 4, 16S rRNA; lane 8, *gmk*; lane 12, *gyrA* and lane 16, *clfA*. Control lanes are negative primer control lanes for the PCR products. (B) Lanes 1-3, 16S rRNA; lanes 5-7, *gmk*; lanes 9-11, *gyrA*; lanes 13-15, *fib* and lanes 17-19, *cna*. H represented Hyperladder 100 (100bp). Control lanes are Lane 4, 16S rRNA; lane 8, *gmk*; lane 12, *gyrA* and lane 16, *clfA*. Control lanes are negative primer control lanes for the PCR products.

Figure 86 shows that MRSA 252 and *S. aureus* ATCC 6538 biofilms are positive for 16S rRNA, *gmk*, *gyrA*, *clfA* and *clfB* genes at 12, 24 and 48 h. All the bands of the genes appeared prominent indicating that their amplification resulted in single clear visible bands observed at the expected 191 bp, 121 bp, 98 bp, 165 bp and 159 bp regions. No bands can be seen in the primer control lanes.

**Amplified PCR products for 16S rRNA, *gmk*, *gyrA*, *ebps* and *eno* of *S aureus* ATCC 6538 and MRSA 252 biofilms at 12 h, 24 h and 48 h.**

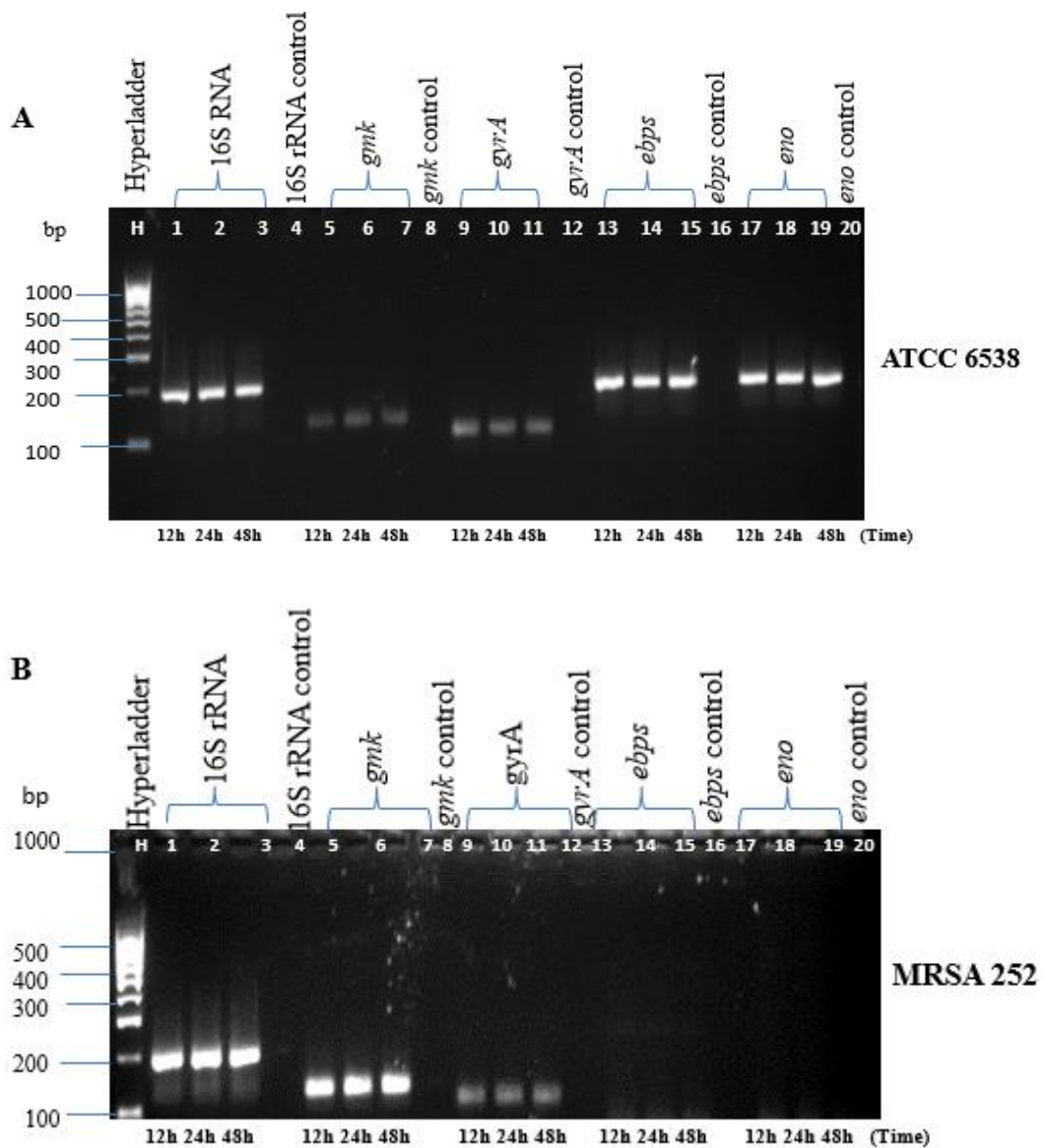


**Figure 87. Agarose gel electrophoresis of RT-PCR amplification products of 16S rRNA, *gmk*, *gyrA*, *ebps* and *eno* genes for (a) *S. aureus* ATCC 6538 and (b) MRSA 252 biofilms.**

(A) Lanes 1-3, 16S rRNA; lanes 5-7, *gmk*; lanes 9-11, *gyrA*; lanes 13-15, *ebps* and lanes 17-19, *eno*. H represented Hyperladder 100 (100bp). Control lanes are Lane 4, 16S rRNA; lane 8, *gmk*; lane 12, *gyrA*; lane 16, *ebps* and lanes 20, *eno*. Control lanes are negative primer control lanes for the PCR products. (B) Lanes 1-3, 16S rRNA; lanes 5-7, *gmk*; lanes 9-11, *gyrA*; lanes 13-15, *ebps* and lanes 17-19, *eno*. H represented Hyperladder 100 (100bp). Control lanes are Lane 4, 16S rRNA; lane 8, *gmk*; lane 12, *gyrA*; lane 16, *ebps* and lanes 20, *eno*. Control lanes are negative primer control lanes for the PCR products.

Figure 87 shows that MRSA 252 and *S. aureus* ATCC 6538 biofilms are positive for 16S rRNA, *gmk*, *gyrA*, *ebps* and *eno* genes at 12, 24 and 48 h. However, *ebps* was not seen in MRSA 252. Most of the bands of the genes appeared indicating that their amplification resulted in single clear visible bands observed at the expected 191 bp, 121 bp, 98 bp, 191 bp and 195 bp regions. No bands can be seen in the primer control lanes.

### 6.2.5 RT-PCR products of selected antibiotic and staphylococcal food poisoning genes.

Amplified PCR products for 16S rRNA, *gmk*, *gyrA*, *mecA* and *blaZ* genes of *S aureus* ATCC 6538 and MRSA 252 biofilms at 12 h, 24 h and 48 h.

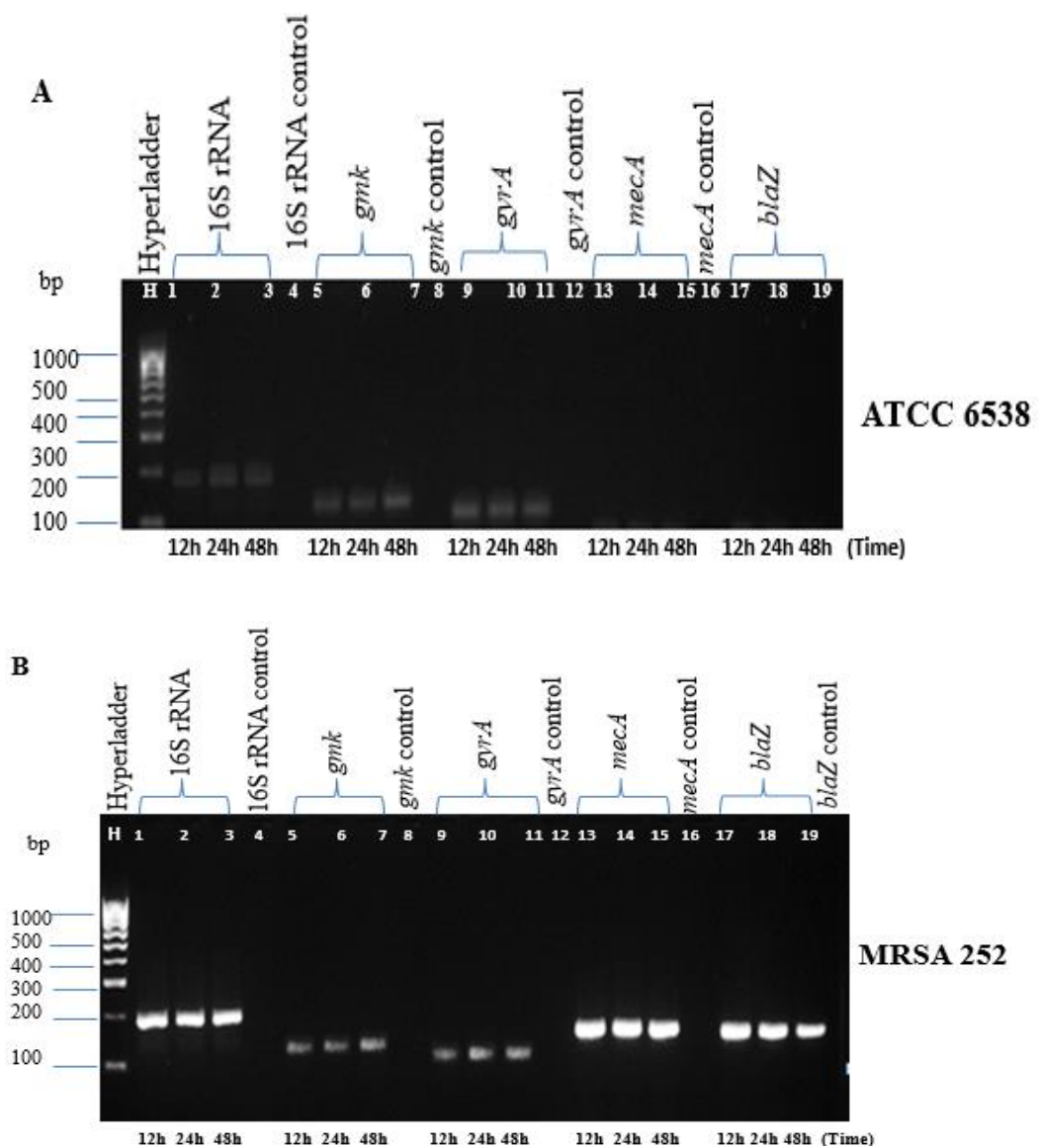
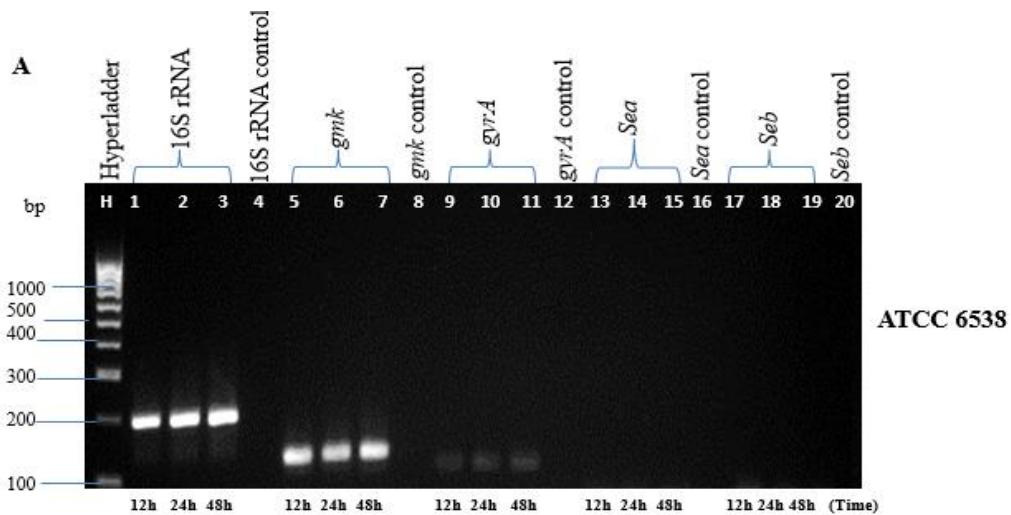


Figure 88. Agarose gel electrophoresis of RT-PCR amplification products of 16S rRNA, *gmk*, *gyrA*, *mecA* and *blaZ* genes for (a) *S. aureus* ATCC 6538 and (b) MRSA 252 biofilms.

(A) Lanes 1-3, 16S rRNA; lanes 5-7, *gmk*; lanes 9-11, *gyrA*; lanes 13-15, *mecA* and lanes 17-19, *blaZ*. H represented Hyperladder 100 (100bp). Control lanes are Lane 4, 16S rRNA; lane 8, *gmk*; lane 12, *gyrA*; lane 16, *mecA* and lanes 20, *blaZ*. Control lanes are negative primer control lanes for the PCR products. (B) Lanes 1-3, 16S rRNA; lanes 5-7, *gmk*; lanes 9-11, *gyrA*; lanes 13-15, *mecA* and lanes 17-19, *blaZ*. H represented Hyperladder 100 (100bp). Control lanes are Lane 4, 16S rRNA; lane 8, *gmk*; lane 12, *gyrA*; lane 16, *mecA* and lanes 20, *blaZ*. Control lanes are negative primer control lanes for the PCR products.

Figure 88 shows that MRSA 252 and *S. aureus* ATCC 6538 biofilms are positive for 16S rRNA, *gmk*, *gyrA*, *mecA* and *blaZ* genes at 12, 24 and 48 h. However, *mecA* and *blaZ* were not seen in ATCC 6538. MRSA 252 contained the *mecA* and *blaZ* probably because it is a methicillin resistant strain. Most of the bands of the genes appeared indicating that their amplification resulted in single clear visible bands observed at the expected 191 bp, 121 bp, 98 bp, 162 bp and 173 bp regions. No bands can be seen in the primer control lanes.

**Amplified PCR products for 16S rRNA, *gmk*, *gyrA*, *sea* and *seb* genes of *S aureus* ATCC 6538 and MRSA 252 biofilms at 12 h, 24 h and 48 h.**



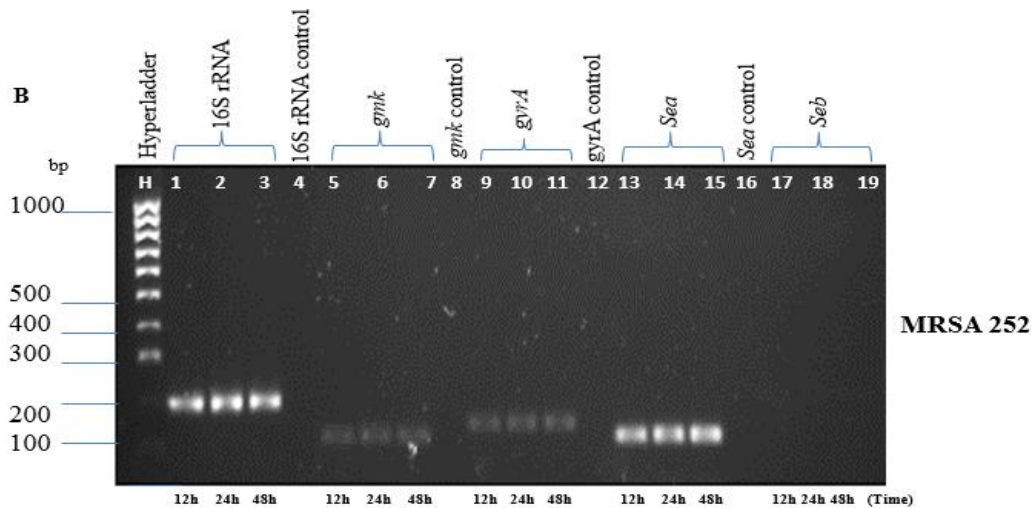


**Figure 89. Agarose gel electrophoresis of RT-PCR amplification products of 16S rRNA, *gmk*, *gyrA*, *sea* and *seb* genes for (A) *S. aureus* ATCC 6538 and (B) MRSA 252 biofilms.**

(A) Lanes 1-3, 16S rRNA; lanes 5-7, *gmk*; lanes 9-11, *gyrA*; lanes 13-15, *sea* and lanes 17-19, *seb*. H represented Hyperladder 100 (100bp). Control lanes are Lane 4, 16S rRNA; lane 8, *gmk*; lane 12, *gyrA*; lane 16, *sea* and lanes 20, *seb*. Control lanes are negative primer control lanes for the PCR products. (B) Lanes 1-3, 16S rRNA; lanes 5-7, *gmk*; lanes 9-11, *gyrA*; lanes 13-15, *sea* and lanes 17-19, *seb*. H represented Hyperladder 100 (100bp). Control lanes are Lane 4, 16S rRNA; lane 8, *gmk*; lane 12, *gyrA* and lane 16, *sea*. Control lanes are negative primer control lanes for the PCR products.

Figure 89 shows that MRSA 252 biofilm was positive for 16S rRNA, *gmk*, *gyrA* and *sea* genes and no *seb* gene at 12, 24 and 48 h. However, *sea* and *seb* genes were absent in ATCC 6538. MRSA 252 contained the *sea* gene probably because it is associated with staphylococcal food poisoning. The bands of the genes that are present in MRSA 252 indicates that their amplification resulted in single clear visible bands observed at the expected 191 bp, 121 bp, 98 bp and 154 bp regions. No bands can be seen in the primer control lanes.

## 6.2.6 RT-PCR products of selected quorum sensing genes

Amplified PCR products for 16S rRNA, *gmk*, *gyrA*, *RNA II*, *RNA III* and *agrA* genes of *S aureus* ATCC 6538 and MRSA 252 biofilms at 12 h, 24 h and 48 h.

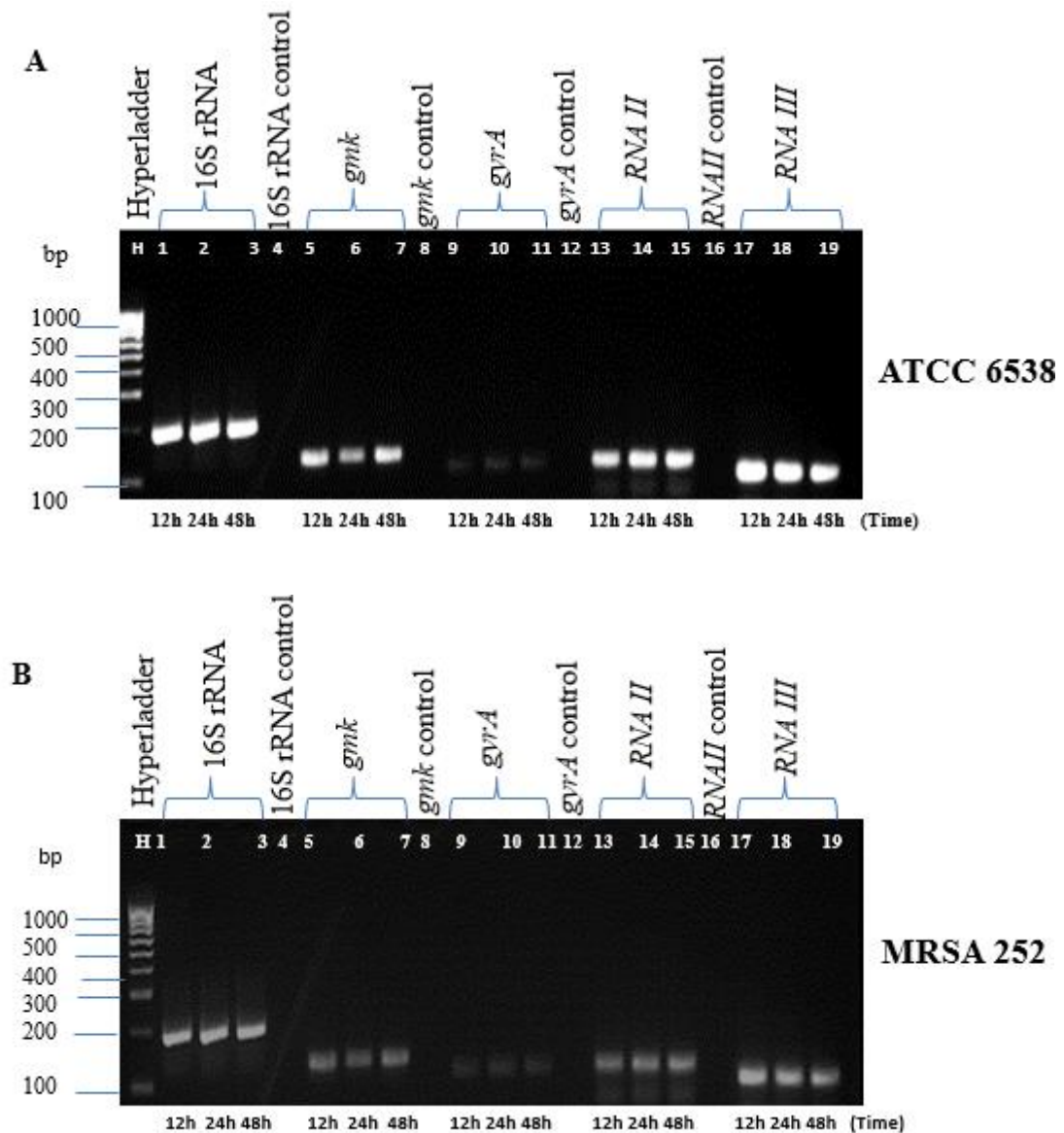


**Figure 90.** Agarose gel electrophoresis of RT-PCR amplification products of 16S rRNA, *gmk*, *gyrA*, *RNAII* and *RNAIII* genes for (a) *S. aureus* ATCC 6538 and (b) MRSA 252 biofilms.

(A) Lanes 1-3, 16S rRNA; lanes 5-7, *gmk*; lanes 9-11, *gyrA*; lanes 13-15, *RNA II* and lanes 17-19, *RNA III*. H represented Hyperladder 100 (100bp). Control lanes are Lane 4, 16S rRNA; lane 8, *gmk*; lane 12, *gyrA*; lane 16, *RNA II*. Control lanes are negative primer control lanes for the PCR products. (B) Lanes 1-3, 16S rRNA; lanes 5-7, *gmk*; lanes 9-11, *gyrA*; lanes 13-15, *RNA II* and lanes 17-19, *RNA III*. H represented Hyperladder 100 (100bp). Control lanes are Lane 4, 16S rRNA; lane 8, *gmk*; lane 12, *gyrA*; lane 16, *RNA II*. Control lanes are negative primer control lanes for the PCR products.

Figure 90 shows that MRSA 252 and *S. aureus* ATCC 6538 biofilms are positive for 16S rRNA, *gmk*, *gyrA*, *RNA II* and *RNA III* genes at 12, 24 and 48 h. All the bands of the genes appeared indicating that their amplification was successful and resulted in single clear visible bands observed at the expected 191 bp, 121 bp, 98 bp, 101 bp and 97 bp regions. No bands can be seen in the primer control lanes.

**Amplified PCR products for 16S rRNA, *gmk*, *gyrA* and *agrA* genes of *S aureus* ATCC 6538 and MRSA 252 biofilms at 12 h, 24 h and 48 h**

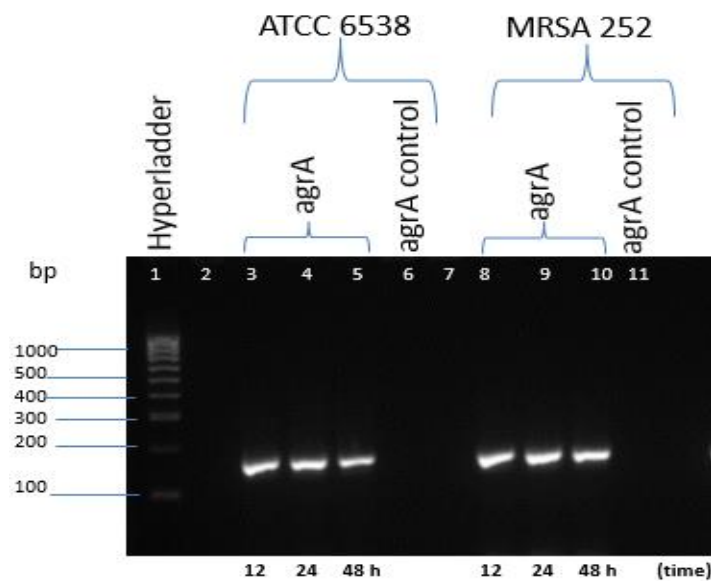


**Figure 91. Agarose gel electrophoresis of RT-CR amplification products of *agrA* gene for *S. aureus* ATCC 6538 and MRSA 252 biofilms.**

(A) Lanes 3-5, *agrA* for ATCC 6538; lanes 8-10, *agrA* for MRSA 252. H represented Hyperladder 100 (100bp). Control lanes are Lane 6 and 11. Control lanes are negative primer control lanes for the PCR products.

Figure 91 shows that MRSA 252 and *S. aureus* ATCC 6538 biofilms are positive for *agrA* gene at 12, 24 and 48 h. All the *agrA* bands appeared indicating that the amplification resulted in single clear visible bands observed at the expected 111 bp regions. No bands can be seen in the primer control lanes.

### **6.2.7 Analysis of the quantitative real time PCR (qRT-PCR) results of selected reference genes**

Quantitative real time PCR is a fluorescent based technique used to measure the level of expression of target genes with the aid of fluorescent dye such as SYBR Green (Bioline, UK). By plotting fluorescence against the cycle number, an amplification plot that represents the accumulation of product over the duration of the PCR reaction was generated.

Appropriate normalization was performed to sort out experimental errors that may arise from extraction of RNA and generation of cDNA. The use of multiple stable reference genes is generally accepted as the method of choice for RT-qPCR data normalization (Turabelidze *et al.*, 2010; Crawford *et al.*, 2016). Thus, multiple reference genes (16S rRNA, *gmk* and *gyrA*) was used in this study for accurate normalization of the target genes, as it is assumed that their expression levels are constant in the bacterial cells. Each run of qPCR has a standard curve that was generated through serial dilution of cDNA.

#### **6.2.7.1 Amplification efficiency and determination of PCR efficiency of reference genes**

The quantification cycle (Ct) for each gene expression reaction was plotted against the log of cDNA concentration, and the slopes of the curves were used to calculate the PCR efficiency values for the reference genes, which ranged from 95 to 105 for ATCC 6538 and 88 to 100 for MRSA 252 with regression coefficients and target genes which ranged from 95 to 102 for ATCC 6538 and 95 to 103 for MRSA 252 with regression coefficients (Table 28). For melting points of the qPCR products all primers amplified well. Melting curve analysis showed a single peak for both the reference genes studied. For RT-PCR analysis of the target genes, only the genes found to be positive and present in both MRSA 252 and ATCC 6538 were assessed for expression levels in the strains. This was to allow a relative comparison of the expression levels of each gene in MRSA and MSSA strain.

**Table 28. Reference and target genes efficiency determination, amplicon melting points and  $r^2$  values for the curves.**

	ATCC 6538	MRSA252	ATCC 6538	MRSA252	ATCC 6538	MRSA252
<b>Reference genes</b>	r <sup>2</sup> on the amplification curve		PCR amplification efficiency (%)		Melting temperature (°C)	
tpiA	0.964	0.991	102	100	80	80
rrSC	0.997	0.891	101	100	80	80
proC	0.913	0.796	95	88	80	80
rho	0.981	0.698	103	90	79	79
rpod	0.991	0.987	103	95	80	80
gyrA	0.991	0.975	97.6	97.6	80	80
glyA	0.976	0.876	95.9	99	80	80
gmk	0.987	0.997	96	100	75-80	75-80
16S rRNA	0.995	0.666	105	100	85	85
	ATCC 6538	MRSA252	ATCC 6538	MRSA252	ATCC 6538	MRSA252
<b>Target genes</b>	r <sup>2</sup> on the amplification curve		PCR amplification efficiency (%)		Melting temperature (°C)	
icaA	0.908	0.78	100	100	80	80
icaB	0.942	0.803	104	100	80	80
icaC	0.995	0.994	95	102	80	80
icaD	0.717	0.942	100	99	80	80
fnbA	0.976	0.771	101	97	80	80
fnbB	0.948	0.843	100	98	80	80
fib	0.678	0.78	100	99	80	80
clfA	0.699	0.664	102	101	80	80
clfB	0.994	0.993	100	100	80	80
agrA	0.913	0.991	99	103	80	80
eno	0.993	0.976	100	95	80	80
mecA	-	0.866	-	95	85	85

### 6.2.7.2 Assessment of stability and validation of reference genes

Relative expression levels (Ct values) of the reference genes investigated in ATCC 6538 and MRSA 252 biofilms were entered into the geNorm Microsoft Excel (Microsoft Canada, Mississauga, ON) application which calculated stability values (M values) for each gene listed above. GeNorm excel was also used to calculate normalization factors using combinations of the most stably expressed genes and calculated the pairwise variation between these factors to identify the optimum number of reference genes to use. The three genes with the lowest individual M values were used in combination (*16S rRNA*, *gmk*, *gyrA*) for subsequent expression analysis. M-value results are present in Figure 92 and 93.

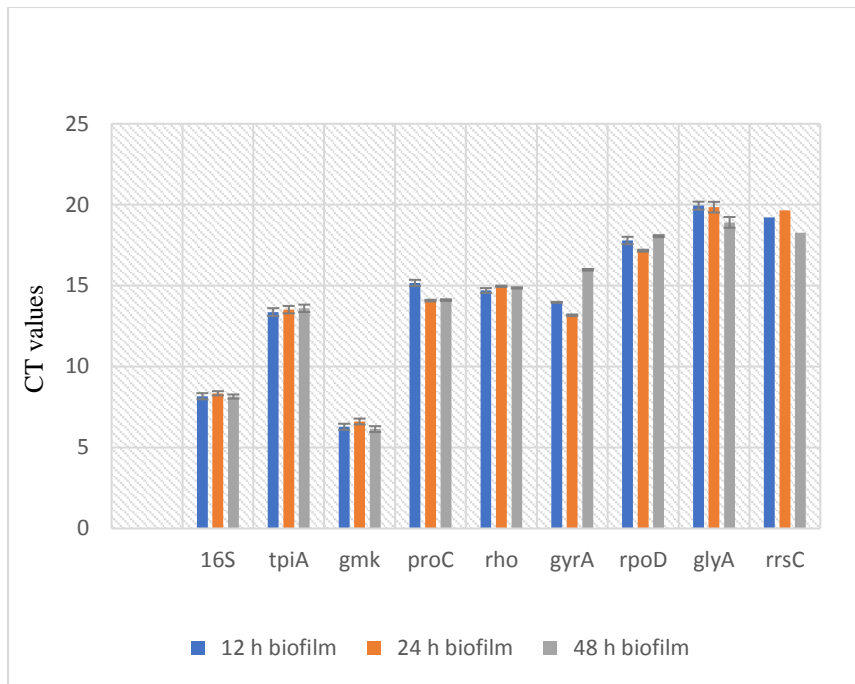


**Figure 92. Mean Ct values obtained from RT-qPCR expression levels of nine reference genes in ATCC 6538. Values are means of triplicate readings. Error bars are standard deviation of means of ct values.**

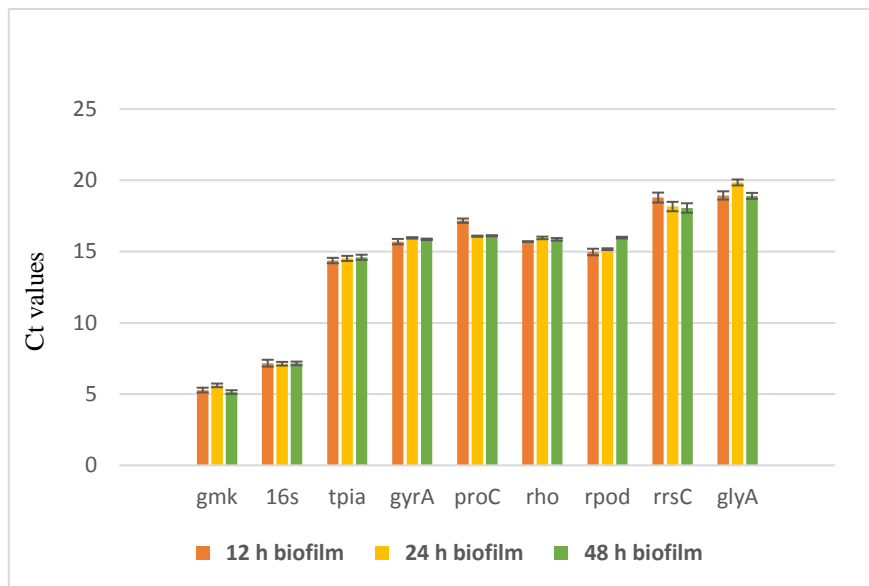


**Figure 93. Mean Ct values obtained from RT-qPCR expression levels of nine reference genes in MRSA 252. Values are means of triplicate readings. Error bars are standard deviation of means of ct values**

Figure 92 and 93 shows the histogram representing the mean Ct values of nine housekeeping/reference genes determined in three different time points: 12 h, 24 h and 48 h biofilm formation. For each condition, Ct was measured from three independent cDNA (12 h, 24 h and 48 h cDNA); the means are represented in the histogram. The genes showed a wide range of expression levels. However, for ATCC 6538, 16S rRNA presented the highest

expression with low mean Ct value ( $8.22 \pm \text{SD } 0.11$ ), *gmk* ( $6.43 \pm \text{SD } 0.24$ ), *tpiA* ( $13.49 \pm \text{SD } 0.12$ ), *rho* ( $14.84 \pm \text{SD } 0.13$ ) *proC* ( $14.45 \pm \text{SD } 0.24$ ) and *gyrA* ( $18.34 \pm \text{SD } 0.40$ ). Figure 8.6 B, shows MRSA 252, 16S rRNA presented the highest expression with low mean Ct value ( $7.15 \pm \text{SD } 0.16$ ), *gmk* ( $5.34 \pm \text{SD } 0.15$ ), *tpiA* ( $14.49 \pm \text{SD } 0.18$ ), *rho* ( $15.84 \pm \text{SD } 0.16$ ) *proC* ( $16.45 \pm \text{SD } 0.19$ ) and *gyrA* ( $15.84 \pm \text{SD } 0.40$ ). Low Ct value indicates higher gene expression.

In Figure 94 and 95 below, the expression stability (*M*) assessment of the nine reference genes as obtained using the geNorm applet was done by first transforming the mean Ct values into quantities for relative comparison. The transformed relative quantities were entered into the Microsoft Excel visual basic application geNorm, which calculated stability values (M values) for nine references based on the mean Ct values. The genes with the lowest M values have the most stable expression. The reference genes all achieved high expression stability criterion, with  $M < 0.788$ , which is well below the default limit of 1.5 recommended by geNorm to identify reference genes with stable expression.

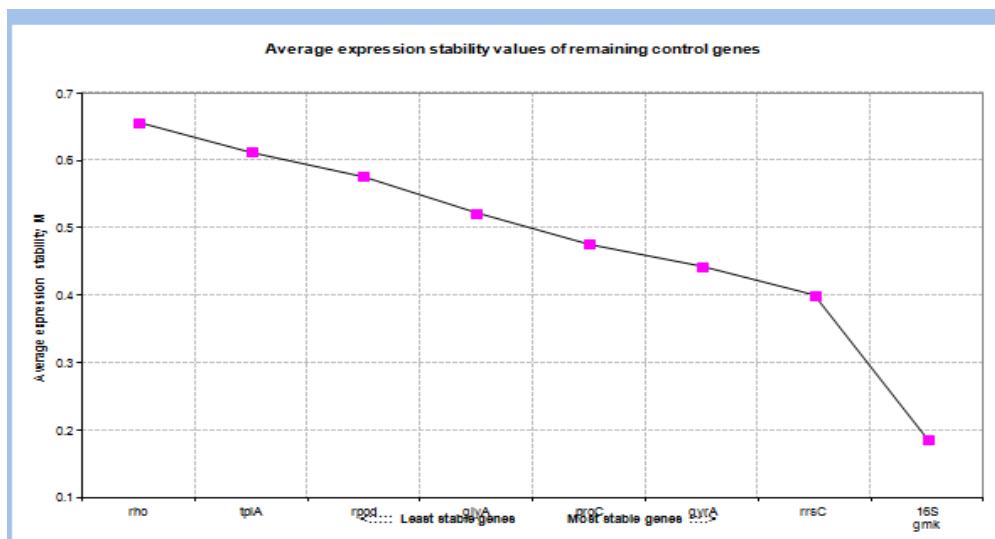
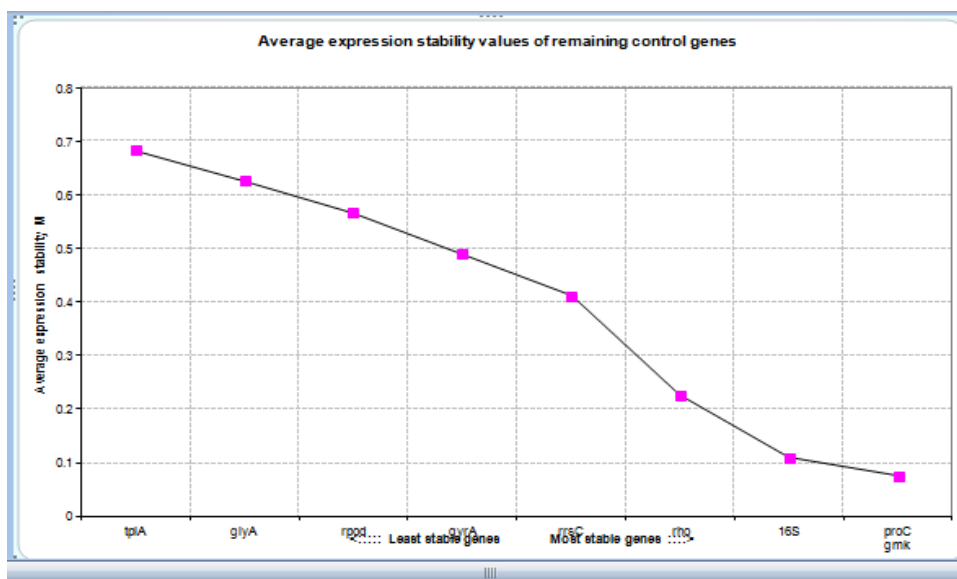


Figure 94. Stability value ranking of the reference genes in ATCC 6538, as determined by geNorm



**Figure 95.** The stability value ranking of the reference genes in MRSA 252, as determined by geNorm.

Figure 94 and 95 shows that M represents the mean pairwise variation between an individual reference gene and all other tested reference genes. The most stable reference genes are those that are still included, i.e., those that exhibit the lowest M values. Shown is the stability ranking of the reference genes in all samples. Genes are ranked from left to right in order of increasing expression stability (decreasing M value). The summary of the stability value of each gene generated by geNorm software is given in Table 29-30.

**Table 29.** Stability (M) value calculated using the GeNorm software

Reference genes	geNORM (M values) M < 1.5 values	Reference genes	geNORM (M values) M < 1.5 values
<b>ATCC 6538</b>		<b>MRSA 252</b>	
rho	0.788	tpiA	0.692
tpiA	0.656	glyA	0.621
rpoD	0.588	rpoD	0.583
glyA	0.531	gyrA	0.521
proC	0.485	rrsC	0.432
gyrA	0.412	rho	0.222
rrsC	0.421	16 s	0.120
gmk	0.189	gmk	0.09
16 s	0.189	proC	0.09

In this analysis, all the reference genes presented M values less than the geNorm threshold of 1.5, which is considered as stable. However, the two genes with the lowest individual M values and one with minimally low M value were used in combination for subsequent expression analysis. The stability was again assessed using the normFinder software for a better

confirmation. Using the NormFinder program the nine reference genes were further assessed for their expression stability (M).

**Table 30. Stability (M) values calculated using the NormFinder software**

Gene name	Stability value		Predicted stability with combinations	geNORM (M values) M < 1.5 values
	ATCC6538	MRSA 252		
<b>16S</b>	<b>0.058</b>	<b>0.048</b>	M value of ATCC 6538	
tpiA	0.305	0.256	Stability value of 16S with stability value of gmk	0.031
rrsC	0.199	0.221		
proC	0.135	0.176		
rho	0.198	0.178	M value of MRSA 252	
rpod	0.334	0.231	Stability value of proC with stability value of gmk	0.093
gyrA	0.080	0.095		
glyA	0.305	0.062		
<b>gmk</b>	<b>0.008</b>	<b>0.009</b>		

The result obtained from both the geNorm and NormFinder programs for the stability test of the nine reference genes tested indicates that 16S and gmk are the two most stable genes. These results seem to correlate each other. However, normFinder suggests that gmk is the most stable gene. Other stable genes identified by geNorm include proC, rrsC and gyrA. Thus, 16S, gmk and gyrA were chosen for this study.

### **6.2.7.3 Analysis of the quantitative real time PCR (qRT-PCR) results of selected target genes**

RT-PCR expression results of selected target genes in MRSA 252 and ATCC 6538 biofilms at different growth time points before and after treatment with African walnut, cashew and pumpkin oils are presented below.

Expression results of *icaA* gene in MRSA 252 and *S. aureus* ATCC 6538 biofilms before and after treatment with African walnut and fluted pumpkin oils.

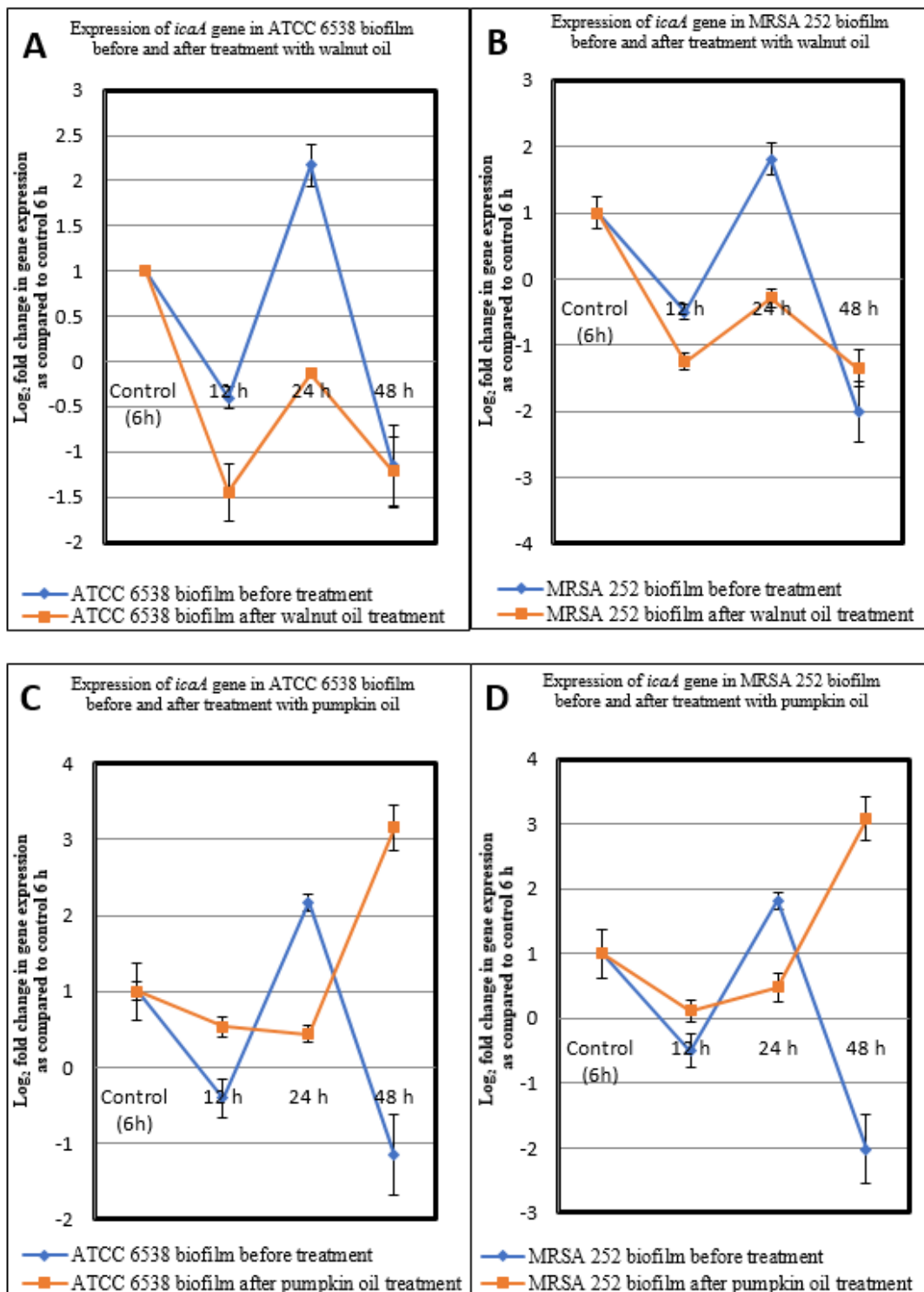


Figure 96. The expression of *icaA* gene in biofilms of MRSA 252 and *S. aureus* ATCC 6538 before and after treatment with African walnut and fluted pumpkin oils.

MRSA 252 and ATCC 6538 were cultured with African walnut oil (31.25 and 15.6 mg/mL) and pumpkin oil (125 and 62.5 mg/mL) for 12, 24 and 48 h. Expression of *icaA* in MRSA 252 and ATCC 6538 was monitored by quantitative real time PCR (qRT-PCR) and data presented on the graph is log base 2-fold change. Expression of *icaA* was normalized to untreated control sample (calibrator) at 6 h and three reference genes (16S rRNA, *gmk* and *gyrA*). (A) expression of *icaA* in ATCC 6538 biofilm before and after treatment with African walnut oil (B) expression of *icaA* in MRSA 252 biofilm before and after treatment with African walnut oil (C) expression of *icaA* in ATCC 6538 biofilm before and after treatment with pumpkin oil (D) expression of *icaA* in MRSA 252 biofilm before and after treatment with pumpkin oil. The data on the graphs are values of three biological replicates with three technical replicates performed independently for each oil treatment. Error bars (n=3) represents standard deviation of log transformed values of fold change and were analysed using t-test.

Based on the data on the graph, no oil controls of MRSA 252 and ATCC 6538 exhibited varying degrees of expression at 12 h, 24 and 48 h. Generally, at 12 h, *icaA* was down-regulated, at 24 h, it was up-regulated and at 48 h it was down-regulated. However, after treatment of ATCC 6538 biofilm with pumpkin oil *icaA* gene was down-regulated at 12 and 24 h with fold change 0.536 and 0.433 ( $P = 0.01$ ) (t-test) and up regulated at 48 h (3.16) ( $P = 0.02$ ). In MRSA 252 biofilm, *icaA* gene was down-regulated at 12 h (0.111), 24 h (0.475) and up-regulated at 48 h (3.08) ( $P = 0.01$ ). On the other hand, African walnut oil significantly down-regulated *icaA* in ATCC 6538 and MRSA 252 biofilms giving fold changes of -1.446 ( $P = 0.04$ ), -0.133 ( $P = 0.02$ ), -1.211 and -1.248 ( $P = 0.016$ ), -0.29, -1.36 ( $P = 0.01$ ) at 12, 24 and 48 h. Result shows that at 24 h when the gene was up-regulated, both oils were able to down-regulate the gene. But an up-regulation was observed at 48 h in both strains after pumpkin oil treatment. The expression pattern of *icaA* gene in both MRSA 252 and ATCC 6538 was completely different from the control sample.

Expression results of *icaB* gene in MRSA 252 and *S. aureus* ATCC 6538 biofilms before and after treatment with African walnut and fluted pumpkin oils.

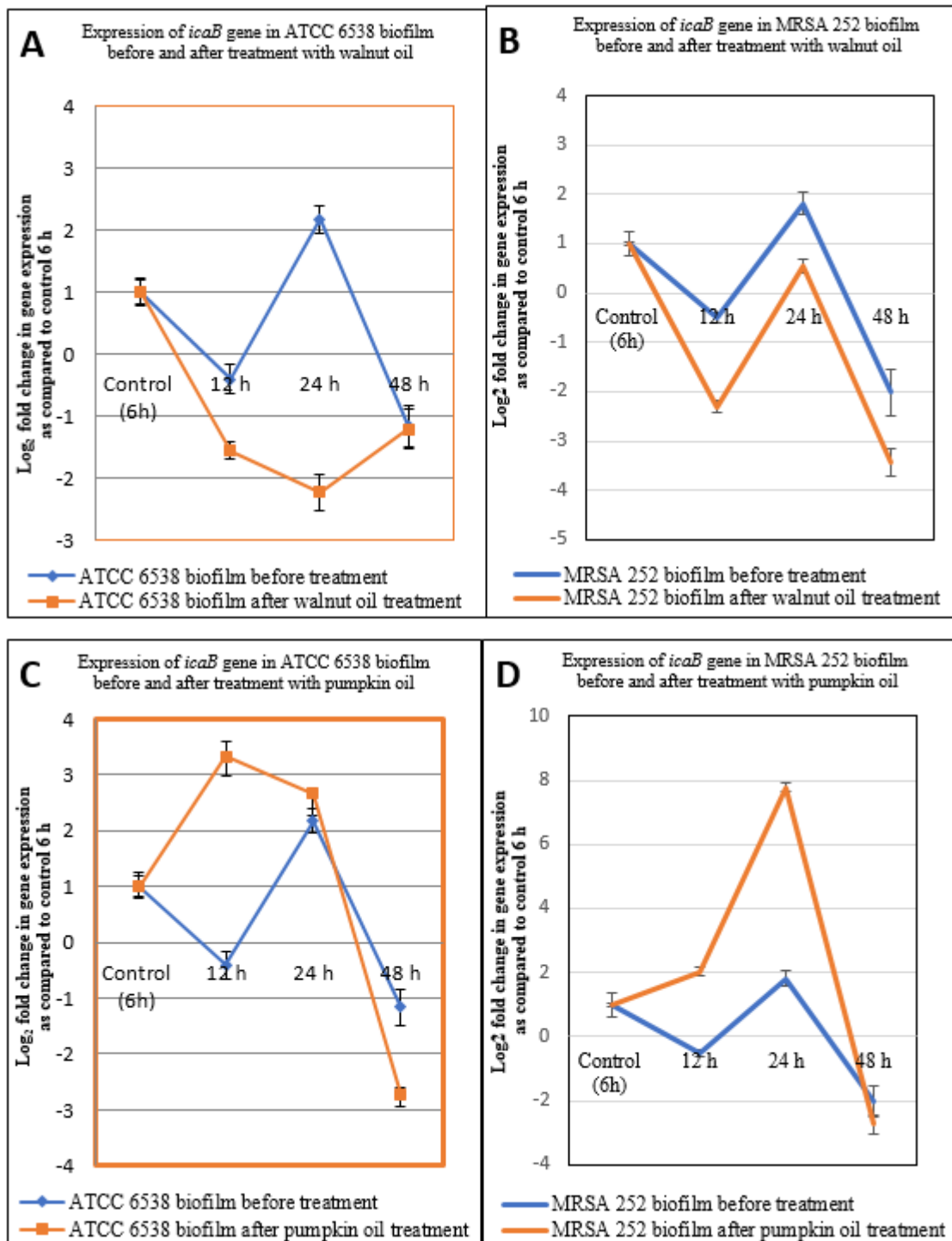
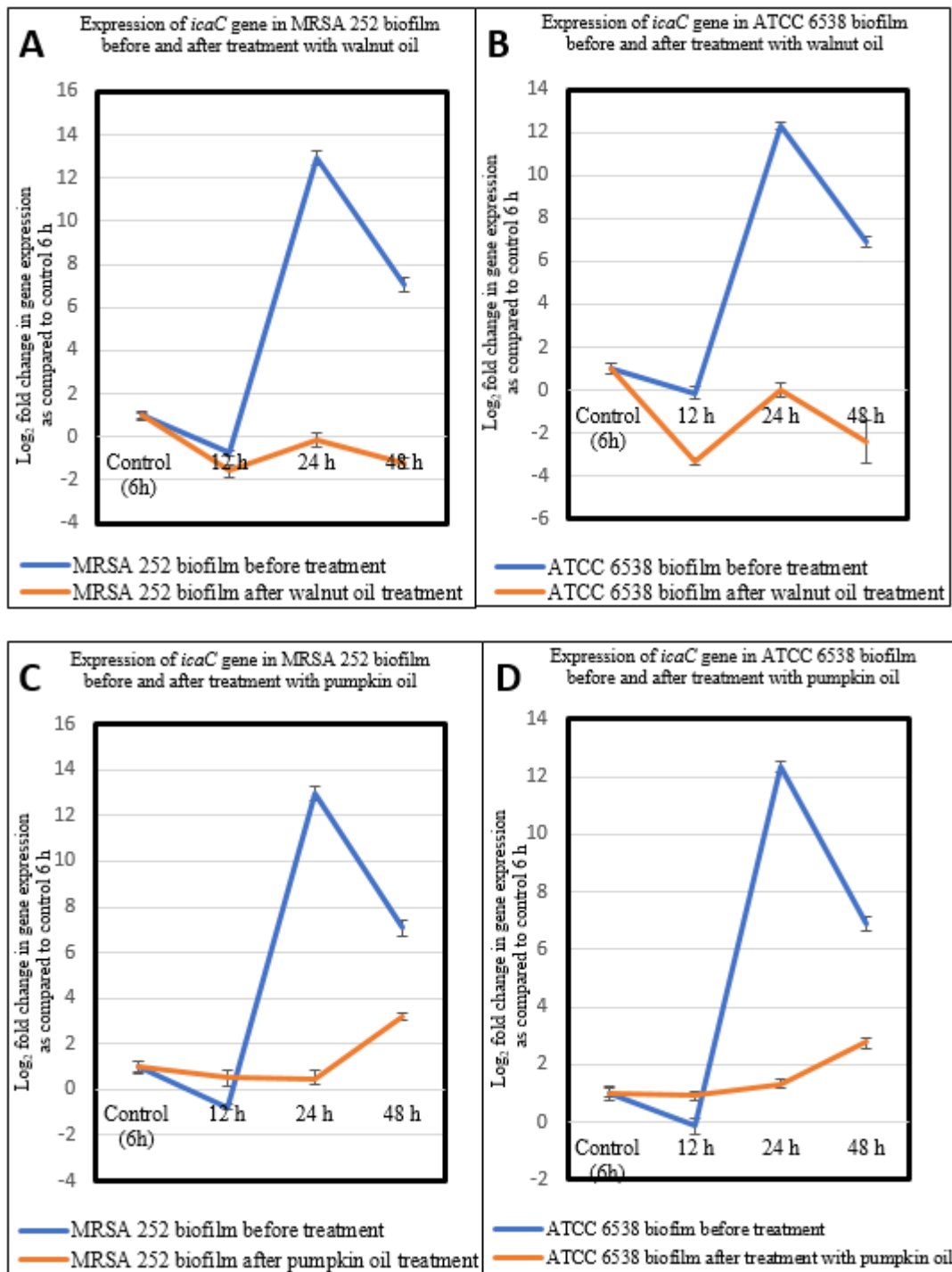


Figure 97. The expression of *icaB* gene in biofilms of MRSA 252 and *S. aureus* ATCC 6538 before and after treatment with African walnut and fluted pumpkin oils.

MRSA 252 and ATCC 6538 were cultured with African walnut oil (31.25 and 15.6 mg/mL) and pumpkin oil (125 and 62.5 mg/mL) for 12, 24 and 48 h. Expression of *icaB* in MRSA 252 and ATCC 6538 was monitored by qRT-PCR and data presented on the graph is log base 2-fold change. Expression of *icaB* was normalized to untreated control sample (calibrator) at 6 h and three reference genes (16S rRNA, *gmk* and *gyrA*). (A) expression of *icaB* in ATCC 6538 biofilm before and after treatment with African walnut oil (B) expression of *icaB* in MRSA 252 biofilm before and after treatment with African walnut oil (C) expression of *icaB* in ATCC 6538 biofilm before and after treatment with pumpkin oil (D) expression of *icaB* in MRSA 252 biofilm before and after treatment with pumpkin oil. The data on the graphs are values of three biological replicates with three technical replicates performed independently for each oil treatment. Error bars (n=3) represents standard deviation of log transformed values of fold change and were analysed using t-test.

Quantitative RT-PCR results shows that *icaB* was down-regulated in MRSA 252 and ATCC 6538 biofilms after treatment with oils. Based on the data on the graph, no oil controls of MRSA 252 and ATCC 6538 exhibited varying degrees of expression at 12 h, 24 and 48 h. Generally, at 12 h, *icaB* was down-regulated, at 24 h, it was up-regulated and at 48 h it was down-regulated. After treatment of ATCC 6538 biofilm with pumpkin oil surprisingly, *icaB* gene was up-regulated at 12 h (3.32), 24 h (2.664) ( $P = 0.02$ ) and down-regulated at 48 h (-2.737) ( $P = 0.01$ ). In MRSA 252 biofilm, *icaB* gene was also up-regulated at 12 h (2.032), 24 h (7.786) and down-regulated at 48 h (-2.737) ( $P = 0.03$ ). On the other hand, African walnut oil significantly down-regulated *icaB* in ATCC 6538 and MRSA 252 biofilms giving fold changes of -1.569 ( $P = 0.01$ ), -2.237, -1.211 ( $P = 0.03$ ) and -2.301, -0.536 and -3.442 ( $P = 0.02$ ) at 12, 24 and 48 h. But at 12 h, *icaB* gene was up-regulated in ATCC 6538. Treatment of ATCC 6538 biofilms with pumpkin oil seem to provoke an up-regulation of *icaB* gene at 12 and 24 h instead of a down-regulation. The expression pattern of *icaB* gene in both MRSA 252 and ATCC 6538 was completely different from the control sample.

**Expression results of *icaC* gene in MRSA 252 and *S. aureus* ATCC 6538 biofilms before and after treatment with African walnut and fluted pumpkin oils.**



**Figure 98.** The expression of *icaC* gene in biofilms of MRSA 252 and *S. aureus* ATCC 6538 before and after treatment with African walnut and fluted pumpkin oils.

MRSA 252 and ATCC 6538 were cultured with African walnut oil (31.25 and 15.6 mg/mL) and pumpkin oil (125 and 62.5 mg/mL) for 12, 24 and 48 h. Expression of *icaC* in MRSA 252 and ATCC 6538 was monitored by qRT-PCR and data presented on the graph is log base 2-fold change. Expression of *icaC* was normalized to untreated control sample (calibrator) at 6 h and three reference genes (16S rRNA, *gmk* and *gyrA*). (A) expression of *icaC* in MRSA 252 biofilm before and after treatment with African walnut oil (B) expression of *icaC* in ATCC 6538 biofilm before and after treatment with African walnut oil (C) expression of *icaC* in MRSA 252 biofilm before and after treatment with pumpkin oil (D) expression of *icaC* in ATCC 6538 biofilm before and after treatment with pumpkin oil. The data on the graphs are values of three biological replicates with three technical replicates performed independently for each oil treatment. Error bars (n=3) represents standard deviation of log transformed values of fold change and were analysed using t-test.

Figure 98 shows that *icaC* was down-regulated in MRSA 252 and ATCC 6538 biofilms after treatment with oils. Based on the data on the graph, no oil controls of MRSA 252 and ATCC 6538 exhibited varying degrees of expression at 12 h, 24 and 48 h. Generally, at 12 h, *icaC* was down-regulated, at 24 h, it was up-regulated and at 48 h it remained up-regulated which was quite different to the pattern of growth regulation exhibited by *icaABD*. However, it was observed that the treatment of MRSA 252 and ATCC 6538 biofilms at 12, 24 and 48 h with pumpkin oil led to a significant down-regulation of *icaC* in the strains giving fold changes of 0.536, 0.43, 3.16 ( $P = 0.01$  and  $P = 0.03$  for 24 and 48 h) and 0.941, 1.321 and 2.815 ( $P = 0.03$ ). Furthermore, treatment of MRSA 252 biofilm with walnut oil significantly resulted in down-regulation of *icaC* gene with fold changes of -1.569 ( $P = 0.03$ ), -0.133, and -1.211 ( $P = 0.018$ ) at 12, 24 and 48 h. This pattern was different in ATCC 6538 which gave fold change values of -3.293 ( $P = 0.23$ ), 0.02 and -2.380 with ( $P = 0.04$  for 12, and 48 h). Again, the expression pattern of *icaC* gene observed after African walnut and pumpkin oil treatments of both MRSA 252 and ATCC 6538 biofilms were completely different from the control sample.

Expression results of *icaD* gene in MRSA 252 and *S. aureus* ATCC 6538 biofilms before and after treatment with African walnut and fluted pumpkin oils.

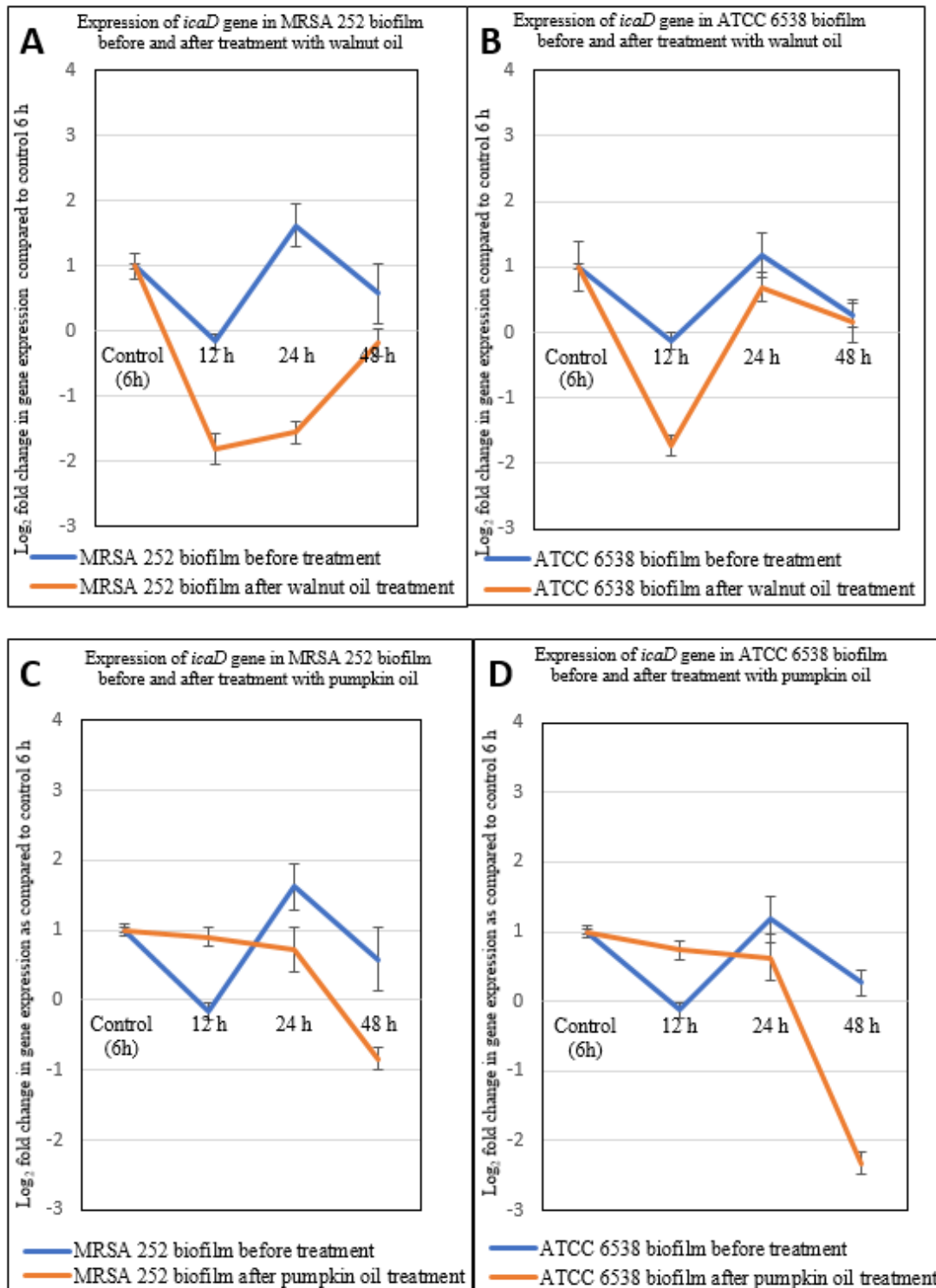


Figure 99. The expression of *icaD* gene in biofilms of MRSA 252 and *S. aureus* ATCC 6538 before and after treatment with African walnut and fluted pumpkin oils

MRSA 252 and ATCC 6538 were cultured with African walnut oil (31.25 and 15.6 mg/mL) and pumpkin oil (125 and 62.5 mg/mL) for 12, 24 and 48 h. Expression of *icaD* in MRSA 252 and ATCC 6538 was monitored by qRT-PCR and data presented on the graph is log base 2-fold change. Expression of *icaD* was normalized to untreated control sample (calibrator) at 6 h and three reference genes (16S rRNA, *gmk* and *gyrA*). (A) expression of *icaD* in MRSA 252 biofilm before and after treatment with African walnut oil (B) expression of *icaD* in ATCC 6538 biofilm before and after treatment with African walnut oil (C) expression of *icaD* in MRSA 252 biofilm before and after treatment with pumpkin oil (D) expression of *icaD* in ATCC 6538 biofilm before and after treatment with pumpkin oil. The data on the graphs are values of three biological replicates with three technical replicates performed independently for each oil treatment. Error bars (n=3) represents standard deviation of log transformed values of fold change and were analysed using t-test.

Figure 99 shows that *icaD* was down-regulated in MRSA 252 and ATCC 6538 biofilms after treatment with oils. According to the data on the graph, no oil controls of MRSA 252 and ATCC 6538 exhibited varying degrees of expression at 12 h, 24 and 48 h. Generally, at 12 h, *icaD* was down-regulated, at 24 h, it was up-regulated and at 48 h it was down-regulated. It was observed that the treatment of MRSA 252 and ATCC 6538 biofilms with pumpkin oil resulted to down-regulation of *icaD* in the strains giving fold changes of 0.903, 0.722, -0.8365 (P = 0.026) and 0.731, 0.623 (P = 0.04) and -2.321 (P = 0.01). Although, *icaD* gene was generally down-regulated, it appeared more down-regulated in ATCC 6538 with fold change value of -2.321. Expression of *icaD* gene after walnut oil treatment in MRSA 252 and ATCC 6538 was also down-regulated giving fold change values of -1.800, -1.556 (P = 0.13), -0.168 and -1.727, 0.688 and 0.163 (P = 0.02). Treatment of MRSA 252 and ATCC 6538 biofilms with oils did not cause any up-regulation of *icaD* gene. The expression pattern of *icaD* gene observed after treating MRSA 252 and ATCC 6538 biofilms with African walnut and pumpkin oils were completely different from the control sample.

Expression results of *fnbA* gene in MRSA 252 and *S. aureus* ATCC 6538 biofilms before and after treatment with African walnut and fluted pumpkin oils.

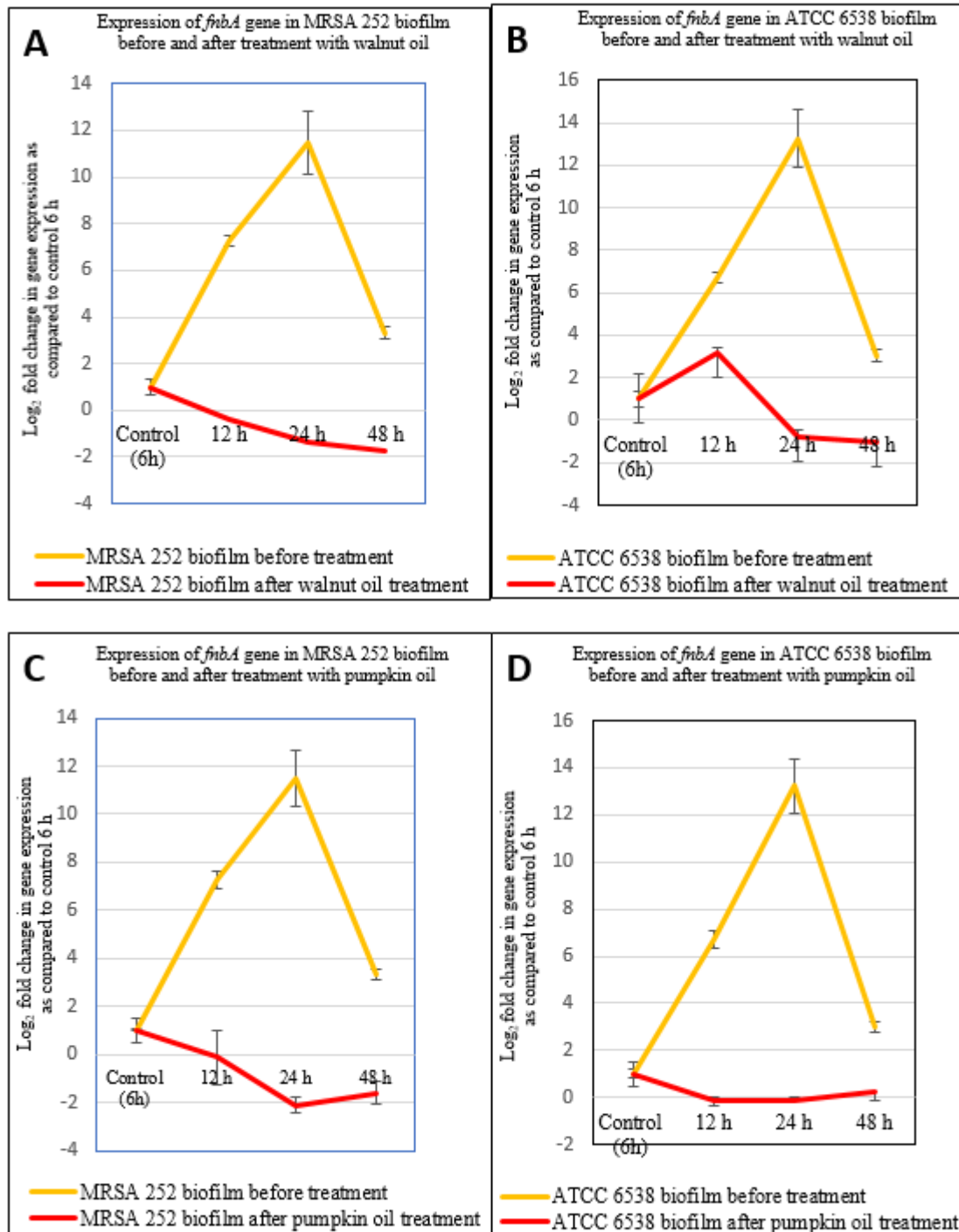
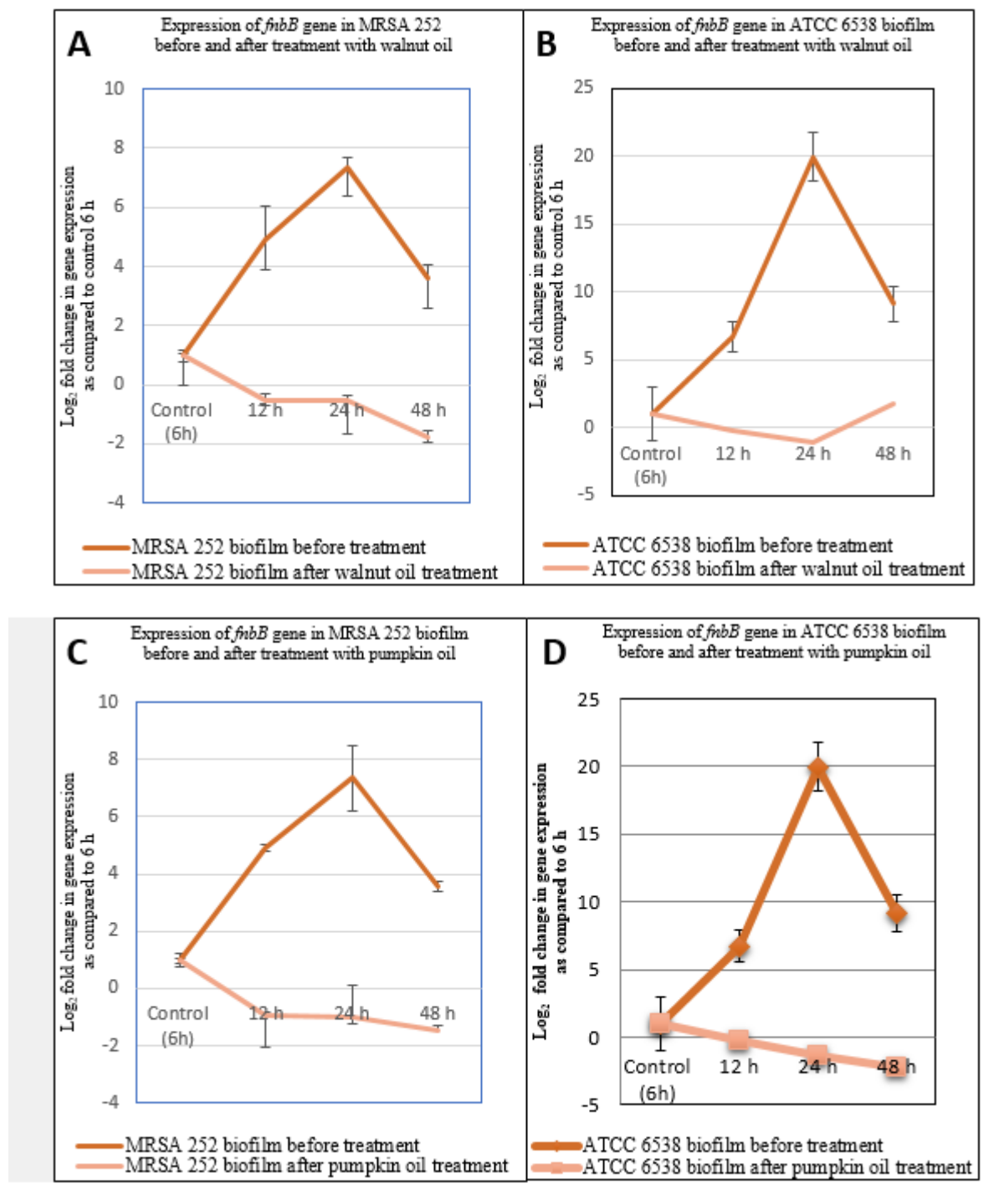


Figure 100. The expression of *fnbA* gene in biofilms of MRSA 252 and *S. aureus* ATCC 6538 before and after treatment with African walnut and fluted pumpkin oils.

MRSA 252 and ATCC 6538 were cultured with African walnut oil (31.25 and 15.6 mg/mL) and pumpkin oil (125 and 62.5 mg/mL) for 12, 24 and 48 h. Expression of *fnbA* in MRSA 252 and ATCC 6538 was monitored by qRT-PCR and data presented on the graph is log base 2-fold change. Expression of *fnbA* was normalized to untreated control sample (calibrator) at 6 h and three reference genes (16S rRNA, *gmk* and *gyrA*). (A) expression of *fnbA* in MRSA 252 biofilm before and after treatment with African walnut oil (B) expression of *fnbA* in ATCC 6538 biofilm before and after treatment with African walnut oil (C) expression of *fnbA* in MRSA 252 biofilm before and after treatment with pumpkin oil (D) expression of *fnbA* in ATCC 6538 biofilm before and after treatment with pumpkin oil. The data on the graphs are values of three biological replicates with three technical replicates performed independently for each oil treatment. Error bars (n=3) represents standard deviation of log transformed values of fold change and were analysed using t-test.

Figure 100 shows that *fnbA* was down-regulated in MRSA 252 and ATCC 6538 biofilms after treatment with oils. Based on the data on the graph, no oil controls of MRSA 252 and ATCC 6538 exhibited varying degrees of expression at 12 h, 24 and 48 h. Based on the results, the pattern of expression of *fnbA* in MRSA 252 and ATCC 6538 appears very different compared to that of *icaABDC* genes. In the expression pattern observed before treatment of biofilms, *fnbA* gene in no oil control at 12, 24 and 48 h were up-regulated. Thus, it was further observed that after the treatment of MRSA 252 and ATCC 6538 biofilms with pumpkin oil, *fnbA* was down-regulated in the strains giving fold changes of -0.120 (P = 0.01), -2.120, -1.599 (P = 0.02) and -0.120, -0.152 and 0.251 (P = 0.22). Similarly, African walnut oil treatment of MRSA 252 and ATCC 6538 biofilms, down-regulated *fnbA* gene giving fold change values of -0.355 (P = 0.01), -1.358, -1.776 (P = 0.03) and 3.167 (P = 0.10), -0.761 and -1.023 (P = 0.04). African walnut oil appears to cause an up-regulation of *fnbA* gene at 12 h. The expression pattern of *fnbA* gene observed after oil treatments of both MRSA 252 and ATCC 6538 biofilm was completely different from the control sample.

**Expression results of *fnbB* gene in MRSA 252 and *S. aureus* ATCC 6538 biofilms before and after treatment with African walnut and fluted pumpkin oils.**



**Figure 101.** The expression of *fnbB* gene in biofilms of MRSA 252 and *S. aureus* ATCC 6538 before and after treatment with African walnut and fluted pumpkin oils.

MRSA 252 and ATCC 6538 were cultured with African walnut oil (31.25 and 15.6 mg/mL) and pumpkin oil (125 and 62.5 mg/mL) for 12, 24 and 48 h. Expression of *fnbB* in MRSA 252 and ATCC 6538 was monitored by qRT-PCR and data presented on the graph is log base 2-

fold change. Expression of *fnbB* was normalized to untreated control sample (calibrator) at 6 h and three reference genes (16S rRNA, *gmk* and *gyrA*). (A) expression of *fnbB* in MRSA 252 biofilm before and after treatment with African walnut oil (B) expression of *fnbB* in ATCC 6538 biofilm before and after treatment with African walnut oil (C) expression of *fnbB* in MRSA 252 biofilm before and after treatment with pumpkin oil (D) expression of *fnbB* in ATCC 6538 biofilm before and after treatment with pumpkin oil. The data on the graphs are values of three biological replicates with three technical replicates performed independently for each oil treatment. Error bars (n=3) represents standard deviation of log transformed values of fold change and were analysed using t-test.

Figure 101 shows that *fnbB* was down-regulated in MRSA 252 and ATCC 6538 biofilms after treatment with oils. According to the data on the graph, no oil controls of MRSA 252 and ATCC 6538 exhibited varying degrees of expression at 12 h, 24 and 48 h. The pattern of expression of *fnbA* in MRSA 252 and ATCC 6538 seem similar to that of *fnbB* gene with up-regulation at 12, 24 and 48 h growth time points. However, treatment of biofilms of MRSA 252 and ATCC 6538 with pumpkin oil resulted in the repression of *fnbB* at 12, 24 and 48 h giving fold change values of -0.943 (P = 0.03), -1.029, -1.490 (P = 0.05) and -0.286 (P = 0.02), -1.358 (P = 0.04) and -2.251 (P = 0.03). Whereas, the treatment of MRSA 252 and ATCC 6538 biofilms with walnut oil led to down-regulation of -0.556, -0.533 (P = 0.05) -1.776 (P = 0.15) and -0.136 (P = 0.001), -1.029 (P = 0.03). and 1.775 (P = 0.13). The expression pattern of *fnbB* gene observed after walnut and pumpkin oil treatments of both MRSA 252 and ATCC 6538 was completely different from the control sample.

**Expression results of *fib* gene in MRSA 252 and *S. aureus* ATCC 6538 biofilms before and after treatment with African walnut and fluted pumpkin oils.**

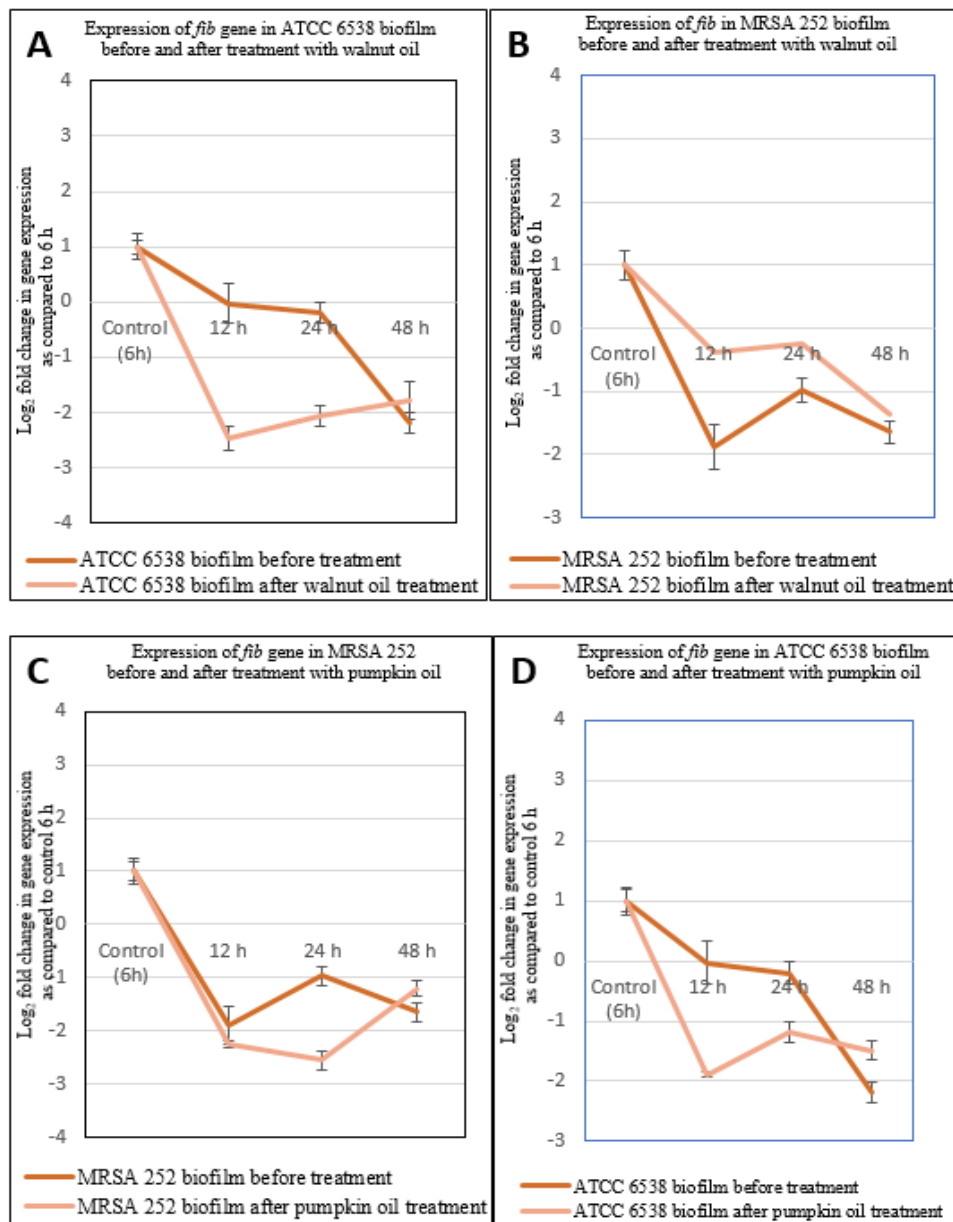


**Figure 102. The expression of *fib* gene in biofilms of MRSA 252 and *S. aureus* ATCC 6538 before and after treatment with African walnut and pumpkin oils**

MRSA 252 and ATCC 6538 were cultured with 31.25 and 15.6 mg/mL (African walnut oil) and pumpkin oil (125 and 62.5 mg/mL) of African walnut and pumpkin oils for 12, 24 and 48 h. Expression of *fib* in MRSA 252 and ATCC 6538 was monitored by qRT-PCR and data presented on the graph is log base 2-fold change. Expression of *fib* was normalized to untreated control sample (calibrator) at 6 h and three reference genes (16S rRNA, *gmk* and *gyrA*). (A) expression of *fib* in ATCC 6538 biofilm before and after treatment with walnut oil (B)

expression of *fib* in MRSA 252 biofilm before and after treatment with walnut oil (C) expression of *fib* in MRSA 252 biofilm before and after treatment with pumpkin oil (D) expression of *fib* in ATCC 6538 biofilm before and after treatment with pumpkin oil. The data on the graphs are values of three biological replicates with three technical replicates performed independently for each oil treatment. Error bars (n=3) represents standard deviation of log transformed values of fold change and were analysed using t-test.

Figure 102 shows that *fib* was down-regulated in MRSA 252 and ATCC 6538 biofilms after treatment with oils. According to the data on the graph, no oil controls of MRSA 252 and ATCC 6538 exhibited varying degrees of expression at 12 h, 24 and 48 h. The pattern of expression of *fib* in MRSA 252 and ATCC 6538 appears different to that of *fnbA* and *fnbB* gene. In its normal expression before treatment, *fib* was down-regulated at 12 h, 24 h and 48 h. Gene with up-regulation at 12, 24 and 48 h growth time points. However, treatment of biofilms of MRSA 252 and ATCC 6538 with pumpkin oil resulted in the further down-regulation of *fib* giving fold change values of -1.89, (P = 0.21) -1.12, -1.49 (P = 0.05) and -2.25, -2.56- (P = 0.14) and -1.21 (P = 0.04). African walnut oil, down-regulated *fib* giving fold changes of -2.47, -2.06 (P = 0.12) and -1.78 in MRSA 252 and -0.377, -0.246 (P = 0.02) and -1.356 (P = 0.04) in ATCC 6538. The expression pattern of *fib* gene observed after walnut and pumpkin oil treatments of both MRSA 252 and ATCC 6538 was completely different from the control sample.

**Expression results of *clfA* genes in MRSA 252 and *S. aureus* ATCC 6538 biofilms before and after treatment with African walnut and fluted pumpkin oils.**

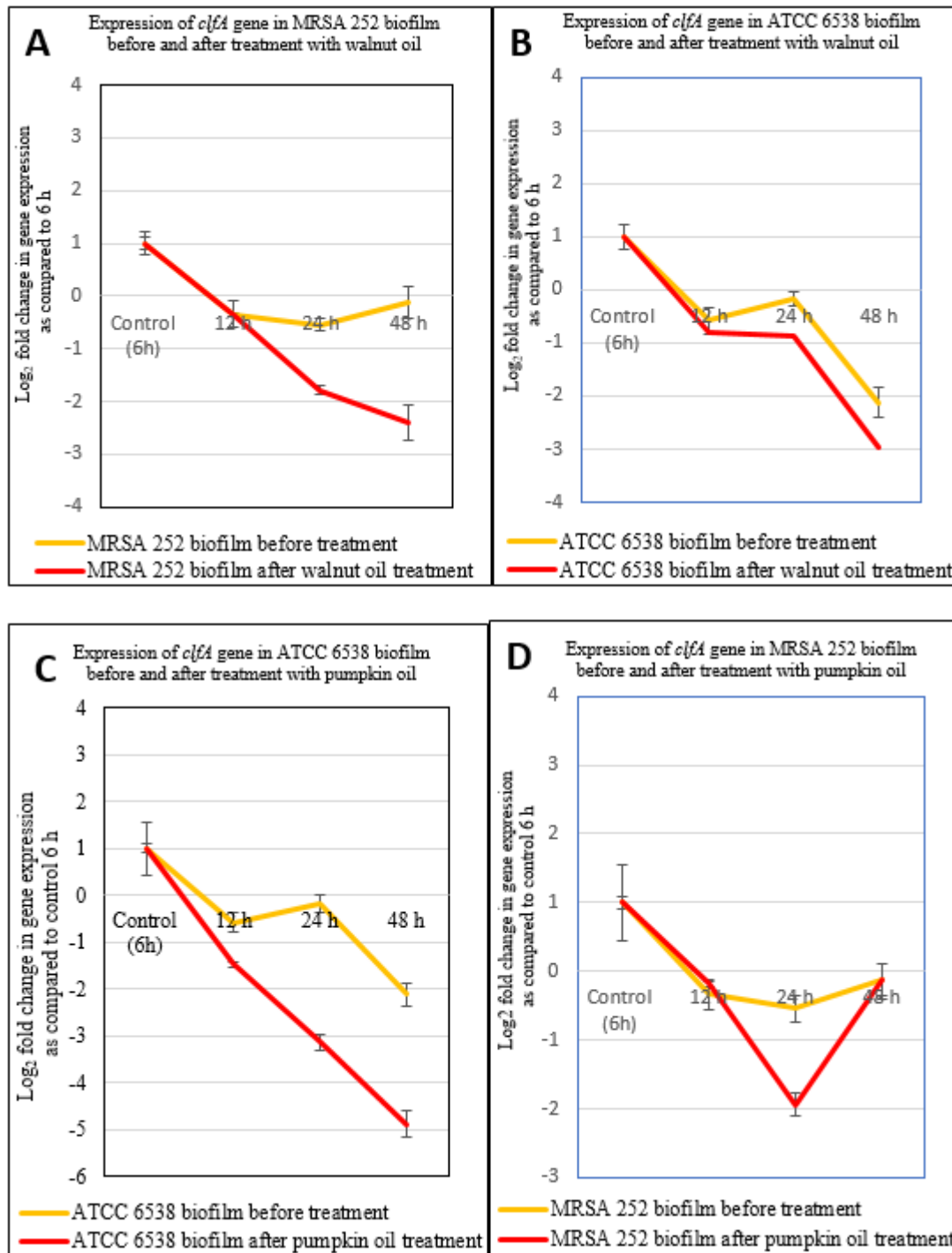


**Figure 103.** The expression of *clfA* gene in biofilms of MRSA 252 and *S. aureus* ATCC 6538 before and after treatment with African walnut and fluted pumpkin oils.

MRSA 252 and ATCC 6538 were cultured with African walnut oil (31.25 and 15.6 mg/mL) and pumpkin oil (125 and 62.5 mg/mL) for 12, 24 and 48 h. Expression of *clfA* in MRSA 252 and ATCC 6538 was monitored by qRT-PCR and data presented on the graph is log base 2-

fold change. Expression of *clfA* was normalized to untreated control sample (calibrator) at 6 h and three reference genes (16S rRNA, *gmk* and *gyrA*). (A) expression of *clfA* in MRSA 252 biofilm before and after treatment with African walnut oil (B) expression of *clfA* in ATCC 6538 biofilm before and after treatment with African walnut oil (C) expression of *clfA* in ATCC 6538 biofilm before and after treatment with pumpkin oil (D) expression of *clfA* in MRSA 252 biofilm before and after treatment with pumpkin oil. The data on the graphs are values of three biological replicates with three technical replicates performed independently for each oil treatment. Error bars (n=3) represents standard deviation of log transformed values of fold change and were analysed using t-test.

Figure 103 shows that *clfA* was down-regulated in MRSA 252 and ATCC 6538 biofilms after treatment with oils. According to the data on the graph, no oil controls of MRSA 252 and ATCC 6538 exhibited varying degrees of expression at 12 h, 24 and 48 h. The pattern of expression of *clfA* gene observed in MRSA 252 and ATCC 6538 is a down-regulation of the gene at 12, 24, 48 h. Therefore, treatment of MRSA 252 and ATCC 6538 biofilms with African walnut and pumpkin oil only further down-regulated the gene. Gene *clfA* was down-regulated after walnut oil treatment with fold changes of -0.358 (P = 0.02), -1.79, -2.38 (P = 0.038), and -0.811, -0.863 (P = 0.03) and -2.96 (P = 0.14) in MRSA 252 and ATCC 6538. Whereas pumpkin oil down-regulated the gene giving fold change values of -0.184, -1.943, -0.13 (P = 0.04) and -1.47, -3.13 (P = 0.23) and -4.89 (P = 0.05) in MRSA 252 and ATCC 6538 respectively.

**Expression results of *clfB* genes in MRSA 252 and *S. aureus* ATCC 6538 biofilms before and after treatment with African walnut and fluted pumpkin oils.**

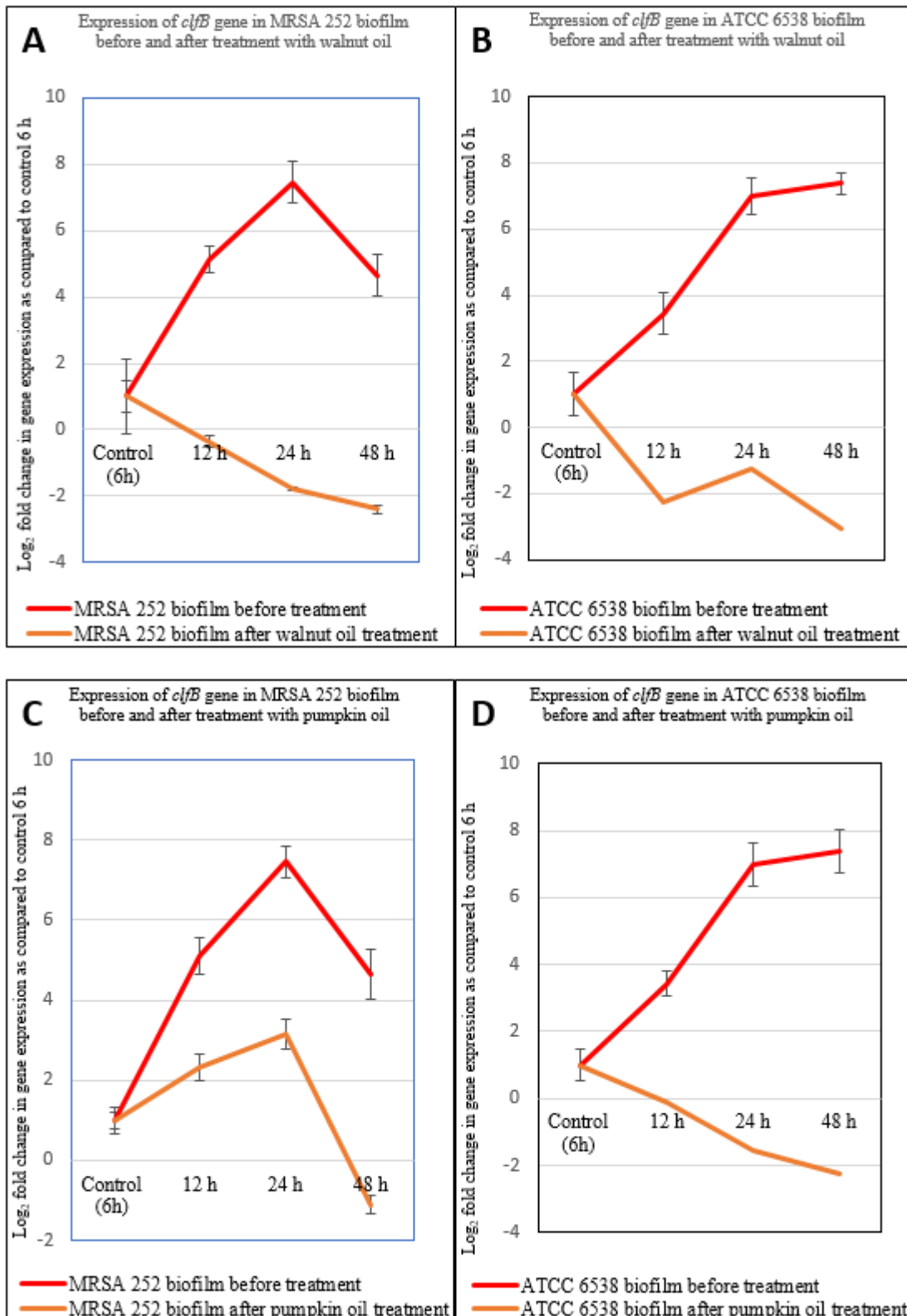


**Figure 104.** The expression of *clfB* gene in biofilms of MRSA 252 and *S. aureus* ATCC 6538 before and after treatment with African walnut and fluted pumpkin oils.

MRSA 252 and ATCC 6538 were cultured with African walnut oil (31.25 and 15.6 mg/mL) and pumpkin oil (125 and 62.5 mg/mL) for 12, 24 and 48 h. Expression of *clfB* in MRSA 252 and ATCC 6538 was monitored by qRT-PCR and data presented on the graph is log base 2-fold change. Expression of *clfB* was normalized to untreated control sample (calibrator) at 6 h and three reference genes (16S rRNA, *gmk* and *gyrA*). (A) expression of *clfB* in MRSA 252 biofilm before and after treatment with African walnut oil (B) expression of *clfB* in ATCC 6538 biofilm before and after treatment with African walnut oil (C) expression of *clfB* in MRSA 252 biofilm before and after treatment with pumpkin oil (D) expression of *clfB* in ATCC 6538 biofilm before and after treatment with pumpkin oil. The data on the graphs are values of three biological replicates with three technical replicates performed independently for each oil treatment. Error bars (n=3) represents standard deviation of log transformed values of fold change and were analysed using t-test.

Figure 104 shows that *clfB* was down-regulated in MRSA 252 and ATCC 6538 biofilms after treatment with oils. According to the data on the graph, no oil controls of MRSA 252 and ATCC 6538 exhibited varying degrees of expression at 12 h, 24 and 48 h. The pattern of expression of *clfB* gene observed in MRSA 252 and ATCC 6538 is that the gene is up-regulated all through the different time points. However, treatment of MRSA 252 and ATCC 6538 biofilms with African walnut and pumpkin oil down-regulated the gene at 12, 24 and 48 h. Gene *clfB* was down-regulated with fold changes of -0.354 (P = 0.01), -1.79, -2.40 (P = 0.21) in MRSA 252 and -2.252 (P = 0.04), -1.25 (P = 0.02), -3.06 (P = 0.14) in ATCC 6538. Whereas pumpkin oil up-regulated the gene giving 2.316 (P = 0.26), 3.151 (P = 0.33), -1.10 (P = 0.03) fold changes in MRSA 252 and down-regulation in ATCC 6538 with -0.12 (P = 0.01), -1.538 (P = 0.03) and -2.252 (P = 0.05) fold changes respectively.

**Expression results of *agrA* genes in MRSA 252 and *S. aureus* ATCC 6538 biofilms before and after treatment with African walnut and fluted pumpkin oils.**

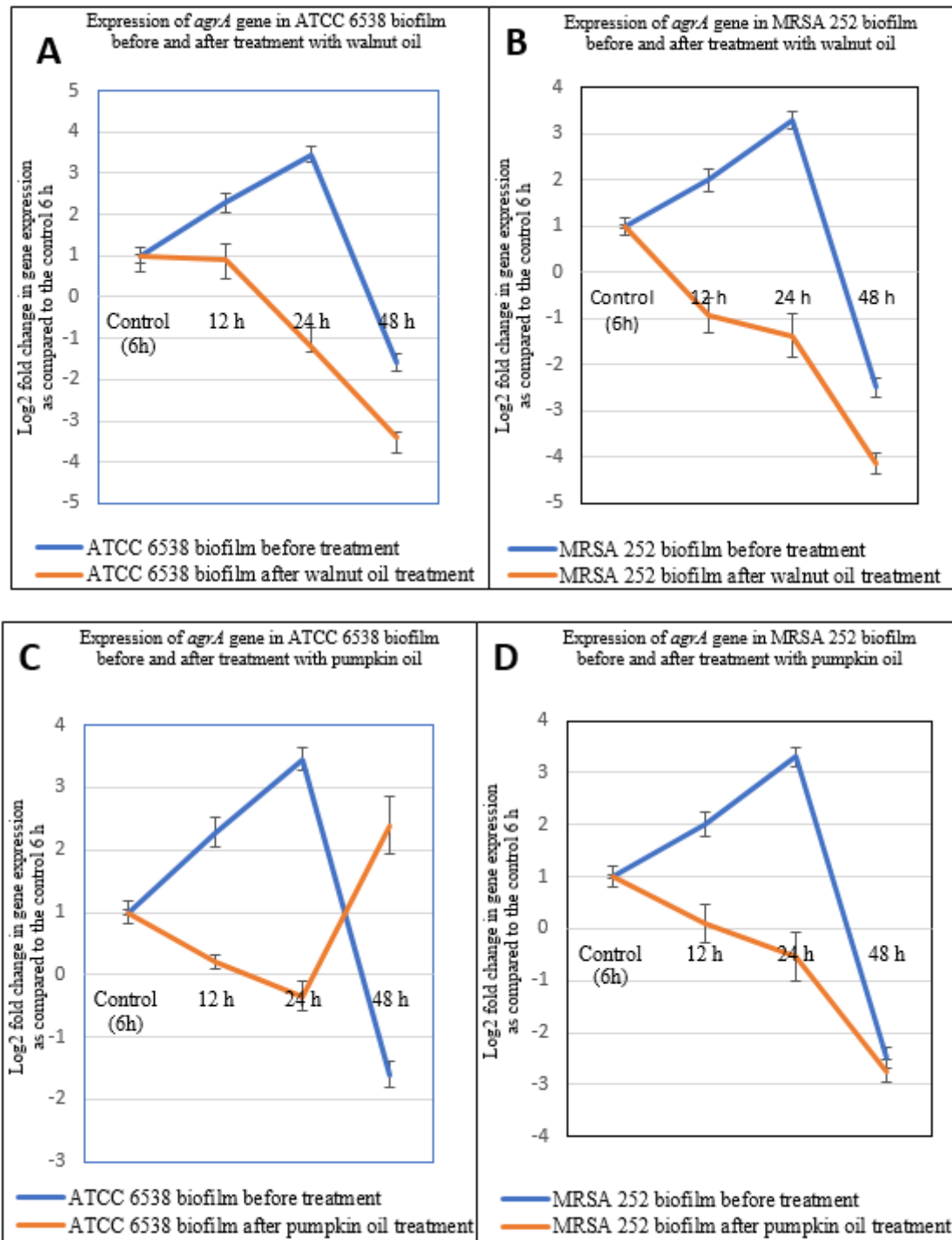


**Figure 105.** The expression of *agrA* gene in biofilms of MRSA 252 and *S. aureus* ATCC 6538 before and after treatment with African walnut and fluted pumpkin oils.

MRSA 252 and ATCC 6538 were cultured with African walnut oil (31.25 and 15.6 mg/mL) and pumpkin oil (125 and 62.5 mg/mL) for 12, 24 and 48 h. Expression of *agrA* in MRSA 252 and ATCC 6538 was monitored by qRT-PCR and data presented on the graph is log base 2-fold change. Expression of *agrA* was normalized to untreated control sample (calibrator) at 6 h and three reference genes (16S rRNA, *gmk* and *gyrA*). (A) expression of *agrA* in ATCC 6538 biofilm before and after treatment with African walnut oil (B) expression of *agrA* in MRSA 252 biofilm before and after treatment with African walnut oil (C) expression of *agrA* in MRSA 252 biofilm before and after treatment with pumpkin oil (D) expression of *agrA* in ATCC 6538 biofilm before and after treatment with pumpkin oil. The data on the graphs are values of three biological replicates with three technical replicates performed independently for each oil treatment. Error bars (n=3) represents standard deviation of log transformed values of fold change and were analysed using t-test.

Figure 105 shows that *agrA* was down-regulated in MRSA 252 and ATCC 6538 biofilms after treatment with oils. According to the data on the graph, no oil controls of MRSA 252 and ATCC 6538 exhibited varying degrees of expression at 12 h, 24 and 48 h. The pattern of expression of *agrA* gene observed in MRSA 252 and ATCC 6538 is that the gene is up-regulated at 12 and 24 h time points. However, treatment of MRSA 252 and ATCC 6538 biofilms with walnut oil down-regulated the gene at 12, 24 and 48 h. Walnut oil down-regulated *agrA* gene giving fold changes of -0.934 (P = 0.02), -1.385 (P = 0.25), -4.152 (P = 0.14) and 0.89 (P = 0.01), -1.184, (P = 0.02) -3.418 (P = 0.17) in MRSA 252 and ATCC 6538. Whereas in MRSA 252 pumpkin oil down-regulated the gene at 12 h and 24 h with 0.1, -0.535- (P = 0.03) and -2.377 (P = 0.30) -fold changes. On the other hand, pumpkin oil also down-regulated *agrA* gene in ATCC 6538 but an up-regulation was observed at 48 h (2.396).

**Expression results of *eno* genes in MRSA 252 and *S. aureus* ATCC 6538 biofilms before and after treatment with African walnut and fluted pumpkin oils.**

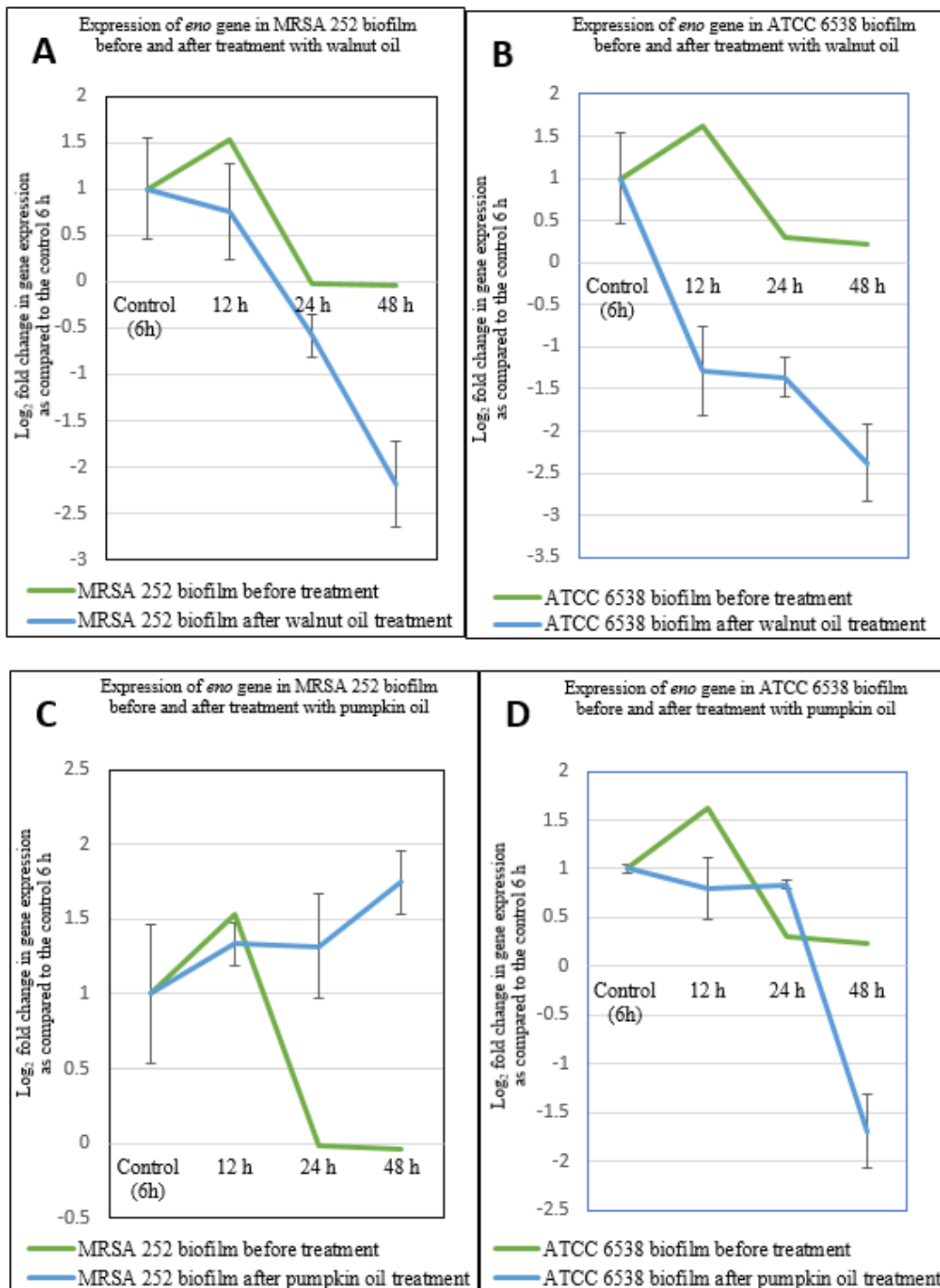


**Figure 106.** The expression of *eno* gene in biofilms of MRSA 252 and *S. aureus* ATCC 6538 before and after treatment with African walnut and fluted pumpkin oils.

MRSA 252 and ATCC 6538 were cultured with African walnut oil (31.25 and 15.6 mg/mL) and pumpkin oil (125 and 62.5 mg/mL) for 12, 24 and 48 h. Expression of *eno* in MRSA 252 and ATCC 6538 was monitored by qRT-PCR and data presented on the graph is log base 2-fold change. Expression of *eno* was normalized to untreated control sample (calibrator) at 6 h and three reference genes (16S rRNA, *gmk* and *gyrA*). (A) expression of *eno* in MRSA 252 biofilm before and after treatment with African walnut oil (B) expression of *eno* in ATCC 6538 biofilm before and after treatment with African walnut oil (C) expression of *eno* in MRSA 252 biofilm before and after treatment with pumpkin oil (D) expression of *eno* in ATCC 6538 biofilm before and after treatment with pumpkin oil. The data on the graphs are values of three biological replicates with three technical replicates performed independently for each oil treatment. Error bars (n=3) represents standard deviation of log transformed values of fold change and were analysed using t-test.

Figure 106 shows that *eno* was down-regulated in MRSA 252 and ATCC 6538 biofilms after treatment with oils. According to the data on the graph, no oil controls of MRSA 252 and ATCC 6538 exhibited varying degrees of expression at 12 h, 24 and 48 h. The pattern of expression of *eno* gene observed in MRSA 252 and ATCC 6538 is that the gene is up-regulated only at 12 h only. However, treatment of MRSA 252 and ATCC 6538 biofilms with African walnut oil and pumpkin oil only further down-regulated the gene at 12, 24 and 48 h. Although pumpkin oil up-regulated the gene in MRSA 252 at 48 h. Based on the results, African walnut oil down-regulated *eno* gene giving fold changes of 0.749, -0.578 (P = 0.03), -2.184 (P = 0.13) and -1.286 (P = 0.05), -1.359 (P = 0.03), -2.381(P = 0.24) in MRSA 252 and ATCC 6538. Whereas in ATCC 6538 and MRSA 252 pumpkin oil down-regulated the gene but at 48 h a -2.377-fold changes showing an up-regulation was observed in MRSA 252.

**Expression results of *mecA* and *blaZ* genes in MRSA 252 biofilms before and after treatment with African walnut and fluted pumpkin oils.**

The expression levels of antibiotic resistance genes (*mecA* and *blaZ* genes) were assessed in MRSA 252 biofilm because it was only positive in this strain.

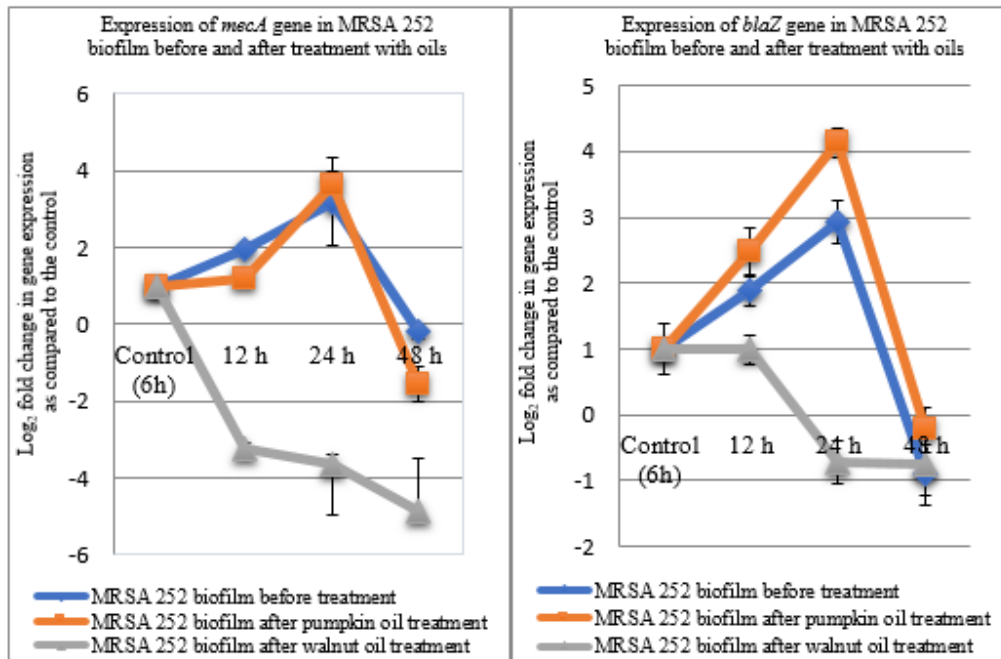


**Figure 107. The expression of *mecA* and *blaZ* gene in biofilms of MRSA 252 before and after treatment with African walnut and fluted pumpkin oils.**

MRSA 252 were cultured with African walnut oil (31.25 mg/mL) and pumpkin oil (125) for 12, 24 and 48 h. Expression of *mecA* and *blaZ* in MRSA 252 was monitored by qRT-PCR and data presented on the graph is log base 2-fold change. Expression of *mecA* and *blaZ* was normalized to untreated control sample (calibrator) at 6 h and three reference genes (16S rRNA, *gmk* and *gyrA*). (A) expression of *mecA* in MRSA 252 biofilm before and after treatment with African walnut and pumpkin oil oils at different growth time points. (B) expression of *blaZ* in MRSA 252 biofilm before and after treatment with African walnut and pumpkin oils. The data on the graphs are values of three biological replicates with three technical replicates performed independently for each oil treatment. Error bars (n=3) represents standard deviation of log transformed values of fold change and were analysed using t-test.

Figure 107 shows that *mecA* and *blaZ* genes were down-regulated in MRSA 252 biofilms after treatment with African walnut oil. On the other hand, an up-regulation was observed after pumpkin oil treatment. According to the data on the graph, no oil controls of MRSA 252

exhibited varying degrees of expression at 12 h, 24 and 48 h. The pattern of expression of *mecA* and *blaZ* genes observed in MRSA 252 is that the genes are up-regulated only at 12, 24 and 48 h. However, treatment of MRSA 252 biofilms with walnut oil succeeded in down-regulating the *mecA* gene giving fold changes of -3.23, -3.623 (P = 0.16) and -4.852 (P = 0.02) and *blaZ* gene giving fold changes of 0.993, -0.713 and -0.761 (P = 0.02).

## 6.4 Discussion

To establish the molecular process of biofilm formation in staphylococcal strains; MRSA 252 and ATCC 6538, this study attempted to ascertain the levels of expression of genes involved in biofilm production which includes *fnbA*, *fnbB*, *clfA*, *clfB*, *fib*, *eno*, *ebps* and intercellular adhesion genes A, B, C and D (*icaADBC*) genes. In addition, the expression levels of antibiotic resistance genes (*blaZ*, *mecA*) as well as regulatory gene (*agrA*) were ascertained. In this study, scanning electron microscopy (SEM) was used to show the growth phases of MRSA 252 and *S. aureus* ATCC 6538 biofilms on 24-well microtiter polystyrene tissue plates model for 6 h, 12 h, 24 h, 48 h. This model shows that the biofilm growth at the different growth time points studied was satisfactory and allows gradual changes (such as slime production, formation of arrow heads and division) in the complexity of the biofilms be observed (Figure 63 and 64).

In addition, RNA extraction from the biofilms of MRSA 252 and *S. aureus* ATCC 6538 grown on 24-well polystyrene plates for 12 h, 24 h, 48 h and the amplification of RT-PCR products, visualized on agarose gels electrophoresis allows the confirmation of the presence of 21 genes found to be strongly associated with their pathogenicity. Each of these genes have been identified in literature to play significant roles in adhesion, biofilm formation, antibiotic resistance, food poisoning genes and biofilm regulatory genes (Asthan *et al.*, 2013). Although some of the confirmed genes were only present in MRSA 252 strain probably because of its link in antibiotic resistance. The genes include intercellular adhesion genes *icaADBC*, biofilm related genes such as fibrinogen (*fib*), fibrinectin A and B (*fnbA* and *fnbB*), collagen (*cna*), laminin (*eno*), clumping factors A and B (*clfA* and *clfB*), elastin (*ebps*), staphylococcal food poisoning genes including enterotoxin genes (*Sea*), antibiotic resistant genes (*mecA* *ermA*, *blaZ*), and quorum sensing transcripts of the *agrA* system (*agrA*, *RNAII* and *RNAIII*). Staphylococcal food poisoning genes are just associated with food poisoning only. However, ATCC 6538 contained all of the *ica* genes, biofilm related genes except *cna*, *agrA* transcripts, no enterotoxin genes (*Sea*) and antibiotic resistant genes (*mecA* *ermA*, *blaZ*). MRSA 252 has all of the genes except *ebps*.

In gene expression analysis, a few authors have emphasized the need to perform qRT-PCR using suitable reference genes. Crawford and his co-workers who worked on choosing suitable reference genes in *Staphylococcus pseudintermedius* reported that multiple reference genes particularly three genes with M values below 1 is necessary for obtain accurate results (Crawford *et al.*, 2014). Similarly, Shito *et al.*, (2014) identified suitable reference genes that

could be used to normalise *S. aureus* in acidic and stress adaptation models. In another study, Thesis and his friends used qRT-PCR to identify suitable internal controls that could be used for gene expression studies in MRSA strains since they are of the opinion that housekeeping genes are easily affected by growth in the presence of antimicrobial compounds. In this study multiple reference genes whose stability was firstly determined by the geNORM and normFinder softwares were used to study gene expression in MRSA 252 and *S. aureus* ATCC 6538 strains. The most stable genes; 16S rRNA, *gmk* and *gyrA* were selected as stable based on their gene stability measure M values (Figure 95 and 96). The multiple reference genes were used in order to measure the gene expression levels of each target gene correctly. However, because 16S rRNA is known to produce multiple gene copies that might cause overflow of the signal systems in qPCR, other genes such as *gmk* and *gyrA* which are single copy housekeeping genes were included in the analysis.

Gene expression analysis was performed on selected virulence genes found to be present in MRSA 252 and ATCC 6538. In staphylococcal biofilms, production of *icaADBC* and extracellular slime play significant role in staphylococcal biofilm formation (Lister and Horswill 2014; Nourbakhsh and Namvar 2016; Saba *et al.*, 2018). One of the main objectives of this study is to determine whether the biofilm genes coding for *icaADBC*, biofilm related genes, antibiotic resistant genes as well as regulatory genes are expressed at different levels along the growth time points of biofilm formation and whether the expressions of these genes could be down-regulated with natural antimicrobials such as oils of walnut and pumpkin. A previous study conducted by Resch and his co-workers on biofilm and planktonic cells, showed that intercellular adhesion gene expression is essential for formation of biofilm in staphylococci between 6 and 8 h of growth which they found to be the beginning of biofilm development. However, the result obtained in this study are contradictory, where the *icaADBC* expression levels were found to be down-regulated at 6 and 12 h in MRSA 252 and ATCC 6538. However, in a similar study by Asthan *et al.*, (2013), *icaADBC* genes were found to be down-regulated between 6-12 h, up-regulated at 24 h and down-regulated at 48 h in MRSA clones. Results obtained in this study seem to correlate with that of Asthan *et al.*, (2013), where *icaABCD* were down-regulated at 6 and 12 h, up-regulated at 24 h and down-regulated again at 48 h. Of all the *icaADBC* genes tested *icaC* expression levels have been found to increase in MRSA 252 and ATCC 6538 biofilms at the exponential and post exponential phase. Similarly, it has been shown by Vandecasteele *et al.*, (2003) and Asthan *et al.*, (2013) that *icaC* was the only gene that is highly expressed at 24 and 48 h in *icaA* gene family. Its increase at 48 h was linked to

factors such as environmental factors, growth media and the nature of the strain which play significant roles in the regulation of biofilm gene expression (Vandecasteele *et al.*, 2003; Beloin *et al.*, 2006).

A confirmation of a series of microbial surface components known to facilitate adhesion of staphylococci to host factors were also performed. These surface components are known as MSCRAMMs and they can bind to one or more host ECM factors including fibrinogen (*fib*), fibrinectin A and B (*fnbA* and *fnbB*), collagen (*cna*), laminin (*eno*), elastin binding protein (*ebps*), clumping factors A and B (*clfA* and *clfB*). Many of these MSCRAMMs showed high level of expression at 12 h and the level of expression of the genes remained up-regulated during the entire biofilm growth time points. *ClfB* expression level was high at 12 h, followed by *fnbA*, B and *ebps* which showed increased fold change at 24 h and 48 h in MRSA 252 and ATCC 6538. In a previous report, Ytheir *et al.*, (2012), reported that the expression level of *clfA* in Newman strain was up-regulated after 24 h growth time point. Surprisingly, genes *fnbA* and *fnbB* encoding fibronectin binding protein A and B was highly expressed in early and in mature growth phases of biofilm cells observed at 12 h, 24 h and 48 h. Therefore, in this present study, six out of the eight MSCRAMMs were up-regulated all through the different growth time points tested. Gene *clfA* and *fib* were not up-regulated at all. The results presented in our study are contradictory to the results obtained by Kot, Sytykiewicz & Sprawka, (2018) who showed that among the biofilm genes, *fib* gene was significantly enhanced after 12 h. In this study, *fib* gene was down-regulated at the different growth time points before treatment with oils. In this study, as in the case of genes encoding MSCRAMMs, the *icaADBC* genes are up-regulated at 24 h signifying the beginning and peak of biofilm formation. This indicates that products of these genes are associated with the initial colonization phase during biofilm formation by *S. aureus*, rather than maturation and its persistence (Asthan *et al.*, 2013). At the later colonization stage (stationary phase), when the cells are already attached to the surface and biofilm formation begins and growing of cells is retarded due to nutrient depletion, increase of expression levels of these *icaADBC* genes is probably no more necessary. Our results were in concordance with the results obtained by Beenken *et al.* (2004), who did not observe an increase in *icaD* expression at exponential stage but at postexponential stages of biofilm formation (24 h). Overall, the gene expression levels of the *icaADBC* genes was observed to fluctuate over time in MRSA 252 and ATCC 6538 tested with variations in expression levels.

It has been reported that antimicrobial drugs that exhibit little or no effect on bacterial growth can affect the expression of *S. aureus* virulence factors when used at subinhibitory concentrations. The antibiotics may induce regulation of the virulence genes or result in aggravation or attenuation of the infection (Qiu *et al.*, 2012). Similarly, after confirming the presence of *icaABDC* genes, biofilm related genes and a few antibiotic resistant genes in MRSA 252 and ATCC 6538 biofilms, the test whether walnut and pumpkin oils found to be active in MICs and MBICs would mediate the inhibition of the virulence genes was determined. Using qRT-PCR, walnut oil was found to significantly decrease the expression of *icaABDC* genes as well as other biofilm associated and mostly especially the *agrA* gene that coordinately regulate most of the virulence genes studied. After the treatment of MRSA 252 and ATCC 6538 biofilms with varying concentrations of walnut oil and pumpkin oil, all the *icaABCD* genes and MSCRAMMs were found to be down-regulated although there was some up-regulation of some genes.

## **Chapter 7. Screening African Walnut, Cashew and Pumpkin Oils for Synergy, Kill Kinetics and Establishing the Efficacy of African Walnut Oil in the Treatment of Staphylococcal Infections using *Galleria mellonella* as an *in-vivo* model**

### **7.1 Introduction**

*S. aureus* is an important hospital and community acquired pathogen (Wang and Ruan, 2017). *S. aureus* has been established to be responsible for infections acquired in the hospital causing diseases in 3% of all patient admissions in UK and 10% in Nigeria and other countries like Ethiopia and Burkina Faso (David and Daum, 2010; Thwaites, 2010; Ige *et al.*, 2011; Mbim *et al.*, 2016). Not only does this pathogen cause numerous infections, but *S. aureus* in many hospitals across the world are becoming increasingly resistant to numerous antibiotics (Fair and Tor, 2014, Mbim *et al.*, 2016). The rise in staphylococcal infections involving resistant and multidrug resistant bacteria and of resistance to antibiotics has limited the therapeutic options of treating staphylococcal infections (Magiorakos *et al.*, 2012, Blair *et al.*, 2015). Increased resistance presents a major challenge to public health since it reduces the effectiveness of antimicrobial drugs as well as increases mortality (Smith and Coast, 2002, Ventola, 2015).

The burden of infectious diseases is high in developed and underdeveloped countries as is the emergence of multidrug pathogens that arise due to poor infection control in hospitals and health-care facilities (Okeke *et al.*, 2007; Ventola, 2015), absence of new antibiotics being discovered (Newell *et al.*, 2010), availability and lastly misuse of antibiotics (Elder *et al.*, 2016). Methicillin resistant *S. aureus* (MRSA) and enterococci resistant to vancomycin are important resistant organisms among the Gram-positive bacteria associated with nosocomial infections in human (Rice, 2006, Hughes *et al.*, 2018). Many hospitals in the developed and under-developed countries including parts of Europe, Japan, and the US, 40-60% of all hospital *S. aureus* are now MRSA (Levy and Marshall, 2004). Worse of it is that a higher percentage 70-80% of all hospital *S. aureus* in Nigeria and the neighbouring countries like Cameroon and Chad are also now resistant to methicillin (Boswihi and Udo, 2018; Tadesse *et al.*, 2018). The emergence of resistance in *Klebsiella pneumoniae*, *Pseudomonas aeruginosa*, *Escherichia coli*, *Acinetobacter* which are Gram negative bacteria are also making the treatment of hospital infections difficult to treat (Nordmann *et al.*, 2009). Recently it has been reported that majority of the drugs that have previously been used in the past in the treatment of infections have

suddenly become less effective against the deleterious pathogens (Ventola, 2015, Kok, *et al.*, 2015). Hence, there is an urgent need to find natural antimicrobials that could serve as alternative therapy for the treatment of multidrug resistant pathogens (Savoia, 2012, Upadhyay *et al.*, 2014, Cheesman *et al.*, 2017).

Based on history, plants have been reported useful in folk medicine across the world. In earlier days people use local herbs to treat staphylococcal infections because they found them as remedies. In those days people first used plants as food and if allows proper digestion, the plants are then linked with some curative properties. Till today many vegetable oils including those from walnut, pumpkin, cashew have been used in folk medicine throughout the world and the medicinal potentials of these oils have been investigated (Petrovska, 2012, Pan *et al.*, 2014, Yuan *et al.*, 2016). African walnut, cashew and pumpkin oils have been reported to possess antifungal, antibacterial, antiviral, anti-inflammatory and analgesic properties (Olajide *et al.*, 2004; Souza *et al.*, 2017; Ajileye *et al.*, 2015) and have also found application in food, cosmetic and pharmaceutical products. The oils have been used for relieving cold symptoms such as cough, cold, sore throat and other staphylococcal infections. In addition, the oils are sometimes used as an antiseptic, treatment of skin infections such as heat rash, and respiratory disorders (Hayes *et al.*, 2016). Oils from African walnut, cashew and pumpkin could be obtained from the leaves, roots barks, shoots, nuts, seeds and suppose to possess powerful antimicrobial properties (Akinhanmi *et al.*, 2008; Bou *et al.*, 2016). However, none of walnut and cashew oils obtained from nuts have received adequate attention about their activity against drug resistant and susceptible bacteria although the chemical composition of the oils has been extensively studied (Crews *et al.*, 2005; Dogan and Akgul, 2005; Uzunova *et al.*, 2015; Poggetti *et al.*, 2018;). On the other hand, synergies of walnut, cashew and pumpkin oils in combination with antibiotics have not been examined.

Recently, the use of models in the study of human pathogens has gain momentum over the 5 years. Very few simple animal models exist which reflect either the biofilm nature of growth of pathogens or the treatment of infection influenced by biofilm development in vivo. Using *G. mellonella* model to study interaction between the host and microbe provides many advantages for example low cost rearing, convenience ethical status (Bokhari *et al.*, 2017). Of recent, *G. mellonella*, the greater wax moth, emerged as a reliable host model to study the pathogenesis of many multidrug resistant pathogen (Bokhari *et al.*, 2017).

Surprisingly, the wax worm has the ability to survive under optimum temperature at 37°C just as most human pathogens do and which is vital for synthesis of virulence factors. To date, a correlation between the capability of a human pathogen to kill wax worm has been established (Desbois and Coote, 2011). Here, experiments conducted in this chapter aimed to evaluate the bactericidal activity of oils from African walnut, cashew and fluted pumpkin on MRSA 252 and ATCC 6538 biofilms. This was evaluated using biofilm time kill assay or growth curves to really ascertain the time and concentration of each oil sample that is sufficient to kill the strains. Investigate the possible synergistic action of the oils with drugs belonging to different categories that have been popularly useful in the treatment of staphylococcal infections but because of the insurgent of antibiotic resistance has now developed reduced potency/activity and lastly study the efficacy of the active oil in treating staphylococcal infections using *G. mellonella* model.

## 7.2 Result

### 7.2.1 Biofilm time-kill assay

The time kill kinetics of African walnut, cashew and pumpkin oil was performed to determine their rate of bactericidal action on MRSA 252 and ATCC 6538 biofilms after been found out to have bactericidal effects when the MBEC experiment was performed. This investigation was performed against MRSA 252 and *S. aureus* ATCC 6538 biofilms grown to stationary phase (48 hours). Results of the time kill curves of MRSA 252 and ATCC 6538 biofilms are presented below.

#### **Biofilm time kill assay of MRSA 252 and ATCC 6538 after treatment with African walnut oil**

The time exposure viability curve for the addition of 100  $\mu$ L of African walnut oil at 62.5 mg/mL and 31.25 mg/mL dilution made with TSB to preformed MRSA 252 and ATCC 6538 formed within 48 h with a viable count of ( $2.32 \times 10^8 = \log 8.37$ ) and ( $2.12 \times 10^8 = \log 8.33$ ) is presented in Figure 108 and 109. Approximately 5 log cycle reductions of MRSA 252 biofilm cells were detected and the time kill curve obtained showed that the bacterial count decreased rapidly 5 log reductions in 2 h, 6 logs in 4 and 6 h. Then over 8 h bacterial count decreased gradually. The viability of MRSA 252 isolate was abolished within 8 h. Therefore, the time at which 90% of the bacterial biofilm killed by African walnut oil for this experiment was approximately in the period between 6 and 8 h. Therefore, from the result African walnut oil at MBEC concentration 62.5 mg/mL was bactericidal against MRSA 252 biofilms as it rapidly achieved approximately 5 log (99.999 %) reductions in 2 h, 6 logs in 4 and 6 h. However, killing of MRSA 252 and ATCC 6538 at 8 h and 2 h indicates that very little time is required by walnut oil to kill MRSA 252 and ATCC 6538. Therefore African walnut oil is regarded as highly effective antibacterial oil. Similarly, for ATCC 6538 biofilm 6 log cycle reductions of ATCC 6538 biofilm cells was detected and the time kill curve obtained showed that the bacterial count decreased rapidly at 2 h. Then over 4 h bacterial count decreased gradually. The viability of MRSA 252 biofilm was abolished early within 6 h (Figure 108). However, killing of ATCC 6538 biofilms at 2 h indicates that very little time is required by walnut oil to kill ATCC 6538. Result shows that African walnut oil at MBEC value of 31.25 mg/mL was highly bactericidal against ATCC 6538 biofilms as it rapidly achieved approximately 6 log reductions in 2 h (Figure 109).

**Table 31. Biofilm time-killing of African walnut oil against MRSA 252 and *S. aureus* ATCC 6538**

Microorganism MRSA 252									
Time (h)	0	2	4	6	8	10	12	22	24
Count (CFU/mL)	2.32 x 10 <sup>8</sup>	3.20 x 10 <sup>3</sup>	2.15 x 10 <sup>3</sup>	2.06 x 10 <sup>3</sup>	0	0	0	0	0
log <sub>10</sub> CFU/mL	8.37	3.72	3.15	2.08	0	0	0	0	0
Microorganism <i>S. aureus</i> ATCC 6538									
Time (h)	0	2	4	6	8	10	12	22	24
Count (CFU/mL)	2.12 x 10 <sup>8</sup>	2.23 x 10 <sup>8</sup>	0	0	0	0	0	0	0
log <sub>10</sub> CFU/mL	8.33	3.83	0	0	0	0	0	0	0

In the above table, the values represent the mean±SD (n=3), SD: standard deviation, CFU: colony forming unit.

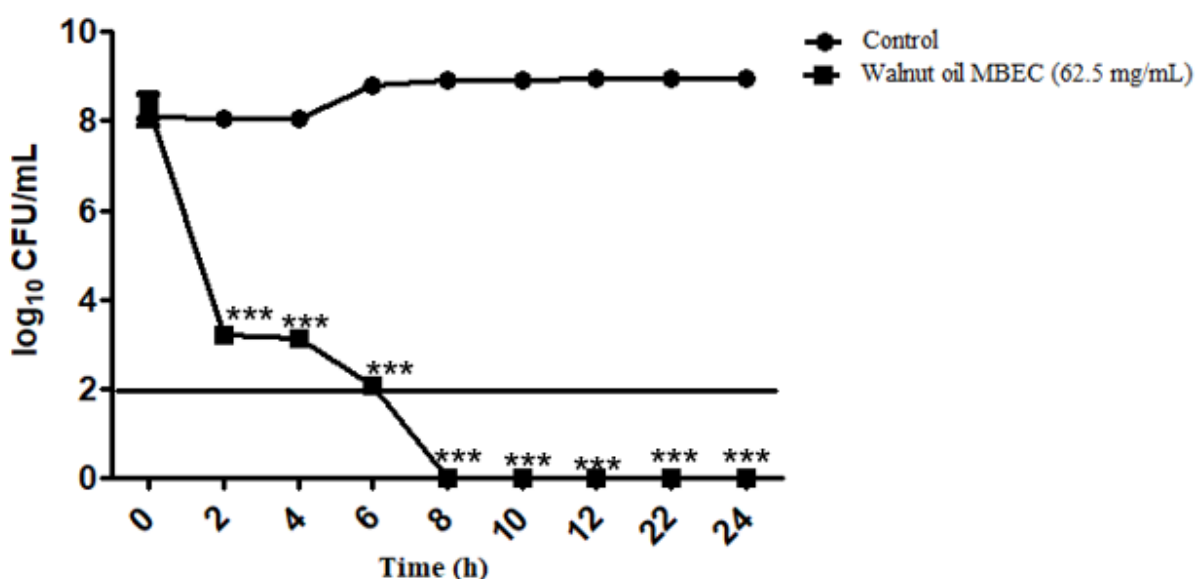


**Figure 108. Time exposure viability curve (log<sub>10</sub>CFU/mL over 24 h) for mature MRSA 252 biofilm incubated with African walnut oil at MBEC (62.5 mg/mL) for 24 h at 37°C**

Data on the graph represent the log of the mean colony forming units of three independent experiments (n=3). Values are the mean±SD (n=3), CFU: colony forming unit, time (X-axis): time intervals needed for killing MRSA 252. Log (CFU/mL) (Y-axis) shows viability of MRSA 252 at different times. The line drawn across the graph indicates that bacterial count was from 10<sup>2</sup>. Statistical analysis was performed with Bonferroni's post-test (Two-way Anova), asterisk on the graph signifies a significant difference between the mean CFU/mL compared with control \*\*\*P<0.0001 (P<0.05).

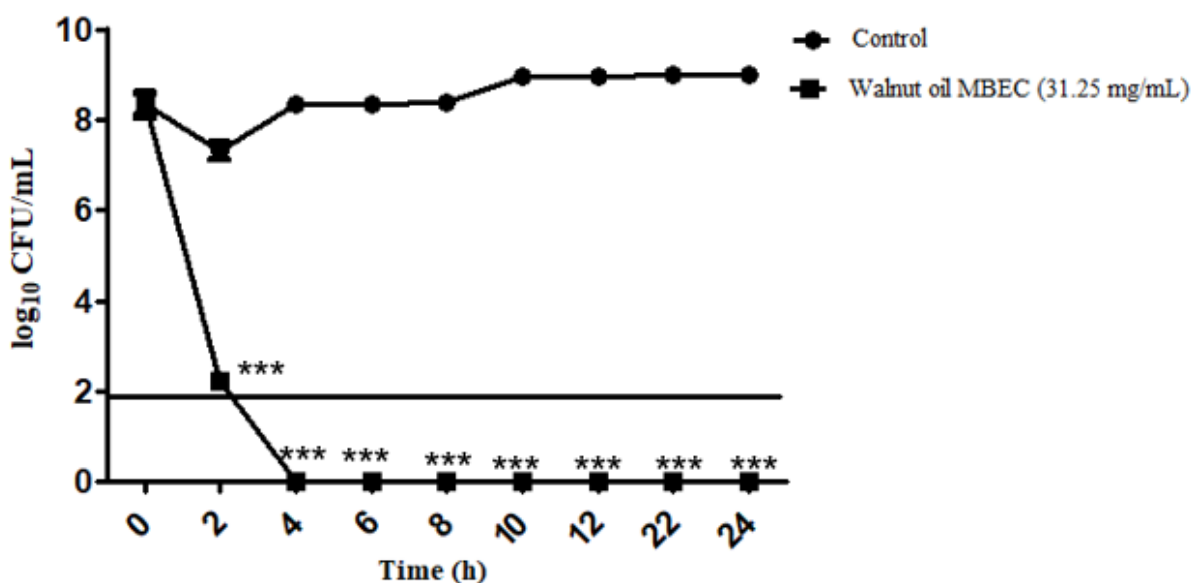


**Figure 109. Time exposure viability curve (log<sub>10</sub>CFU/mL over 24 h) for preformed ATCC 6538 biofilm incubated with African walnut oil at MBEC (31.25 mg/mL) for 24 h at 37°C.**

Data on the graph represent the log of the mean colony forming units of three independent experiments (n=3). Values are the mean±SD (n=3), CFU: colony forming unit, time (X-axis): time intervals needed for killing ATCC 6538. Log (CFU/mL) (Y-axis) shows viability of ATCC 6538 at different times. Asterisk on the graph signifies a significant difference between the mean CFU/mL compared with control \*\*\*P<0.001 (P<0.05).

### **Biofilm time killing assay of cashew oil against MRSA 252 and ATCC 6538**

The time exposure viability curve for the addition of 100 µL of cashew oil at 500 mg/mL dilution previously made with TSB to preformed MRSA 252 and ATCC 6538 formed within 48 h with a viable count of (2.32 X 10<sup>8</sup> = log 8.37) and (2.12 X 10<sup>8</sup> = log 8.33) is presented in Figure 110 and 111. For MRSA 252 biofilm 4 log cycle reductions (99.99 %) of MRSA 252 biofilm cells was detected and the time kill curve obtained showed that the bacterial count decreased rapidly at 4 h. Then over 4 h bacterial count decreased gradually. The viability of MRSA 252 biofilm was abolished within 24 h. However, killing of MRSA 252 biofilms at 22 h indicates that much longer time is required by cashew oil to kill MRSA252. Result shows that cashew oil at MBEC value of 500 mg/mL was not bactericidal against MRSA 252 biofilms despite that it rapidly achieved approximately 4 log reductions in 4 h. Similarly, approximately 4 log cycle reductions (99.99 %) of ATCC 6538 biofilm cells were detected and the time kill curve obtained showed that the bacterial count decreased rapidly at 4 log reductions in 2 h. Then over 4 h bacterial count decreased gradually. The viability of ATCC 6538 isolate was abolished within 22 h. Therefore, the time at which 99.99% of the bacterial biofilm were killed by cashew oil for this experiment was approximately in the period between 24 and 22 h.

Therefore, from the result cashew oil at MBEC concentration 500 mg/mL was not bactericidal against ATCC 6538 biofilms this is because despite that it rapidly achieved approximately 4 log reductions in 2 h, killing still progressed to 22-24 h in both strains. However, killing of MRSA 252 and ATCC 6538 at 24 and 22 h indicates that much longer time is required by cashew oil to kill MRSA 252 and ATCC 6538. Therefore, cashew oil is regarded as weak antibacterial oil.

**Table 32. Biofilm time-killing of cashew oil against MRSA 252 and *S. aureus* ATCC 6538**

Microorganism: MRSA 252									
Time (h)	0	2	4	6	8	10	12	22	24
Count (CFU/mL)	2.32 x 10 <sup>8</sup>	1.80 x 10 <sup>6</sup>	1.68 x 10 <sup>4</sup>	1.81 x 10 <sup>5</sup>	1.34 x 10 <sup>5</sup>	1.00 x 10 <sup>2</sup>	1.34 x 10 <sup>2</sup>	1.0 x 10 <sup>4</sup>	0
log <sub>10</sub> CFU/mL	8.37	6.25	4.23	5.26	5.13	5.00	4.13	4.00	0
Microorganism: <i>S. aureus</i> ATCC 6538									
Time (h)	0	2	4	6	8	10	12	22	24
Count (CFU/mL)	2.12 x 10 <sup>8</sup>	2.12 x 10 <sup>4</sup>	1.50 x 10 <sup>4</sup>	2.80 x 10 <sup>3</sup>	1.50 x 10 <sup>3</sup>	2.00 x 10 <sup>2</sup>	1.40 x 10 <sup>2</sup>	0	0
log <sub>10</sub> CFU/mL	8.33	4.33	4.18	3.45	3.17	2.30	2.15	0	0

In the above table, the Values represented are the mean ± SD (n=3), SD: standard deviation, CFU: colony forming unit.

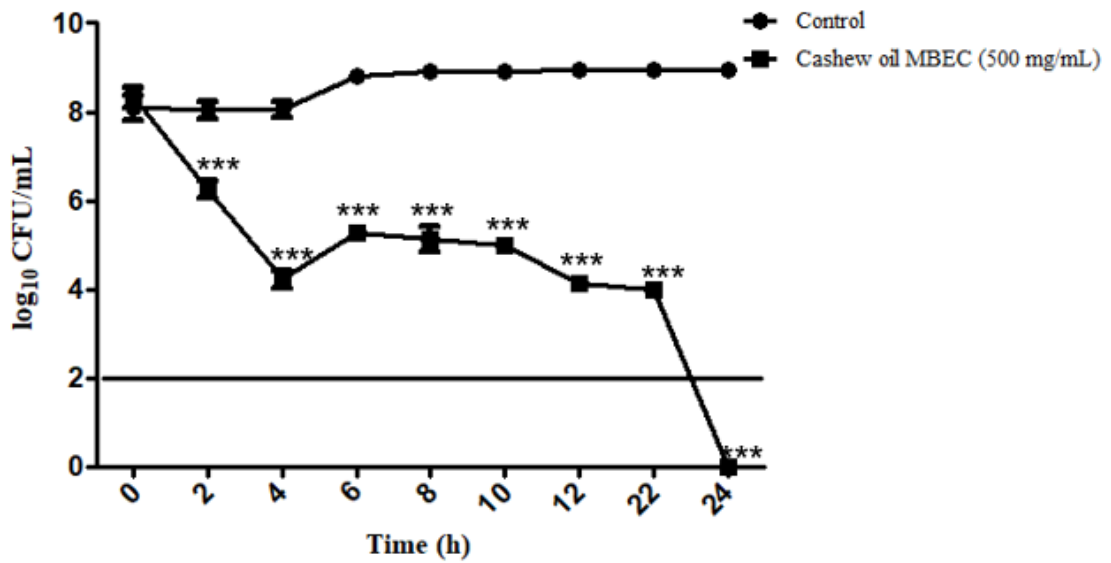


Figure 110. Time exposure viability curves (log<sub>10</sub>CFU/mL over 24 h) for preformed MRSA 252 biofilm incubated with cashew oil at MBEC (500 mg/mL) at 37°C.

Data on the graph represent the log of the mean colony forming units of three independent experiments (n=3). Values are the mean±SD (n=3), CFU: colony forming unit, time (X-axis): time intervals needed for killing MRSA 252. Log (CFU/mL) (Y-axis) shows viability of MRSA 252 at different times. Asterisk on the graph signifies a significant difference between the mean CFU/mL compared with control \*\*\*P<0.0001 (P<0.05).

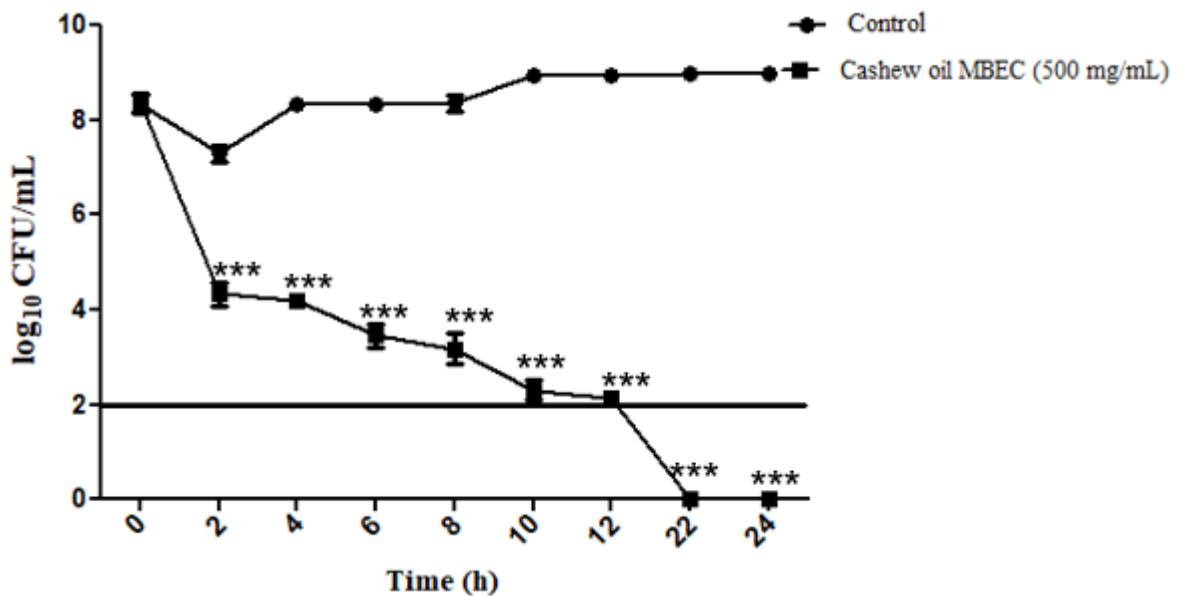


Figure 111. Time exposure viability curves (log<sub>10</sub>CFU/mL over 24 h) for preformed ATCC 6538 biofilm incubated with cashew oil at MBEC (500 mg/mL) at 37°C

Data on the graph represent the log of the mean colony forming units of three independent experiments (n=3). Values are the mean±SD (n=3), CFU: colony forming unit, time (X-axis): time intervals needed for killing ATCC 6538. Log (CFU/mL) (Y-axis) shows viability of ATCC 6538 at different times. Asterisk on the graph signifies a significant difference between the mean CFU/mL compared with control \*\*\*P<0.0001 (P<0.05).

### **Biofilm time kill assay of MRSA 252 and ATCC 6538 after treatment with pumpkin oil**

The time exposure viability curve for the addition of 100 µL of pumpkin oil at 250 mg/mL and 125 mg/mL dilution previously made with TSB to preformed MRSA 252 and ATCC 6538 formed within 48 h with a viable count of ( $2.32 \times 10^8 = \log 8.37$ ) and ( $2.12 \times 10^8 = \log 8.33$ ) is presented in Figure 112 and 113. Approximately 4 log cycle reductions of MRSA 252 biofilm cells at 2 h was detected and the time kill curve obtained showed that the viable count of bacteria decreased rapidly from 4 h then over 12 h bacterial count decreased gradually to over 24 h. The viability of MRSA 252 isolate was abolished within 12 and 24 h. Therefore, the time at which 99.99% of the bacterial biofilm is killed by pumpkin oil in this experiment is between 12 and 24 h. Therefore, from the result pumpkin oil at MBEC concentration of 250 mg/ml was only minimally bactericidal against MRSA 252 biofilms as killing of MRSA 252 seem to require more time. Similarly, for ATCC 6538 biofilm approximately 5 log reductions (99.999) was detected and the time kill curve obtained showed that the bacterial count decreased rapidly at 2 h. Then over 6 h bacterial count decreased gradually. The viability of ATCC 6538 biofilm was abolished within 10 h. However, killing of ATCC 6538 biofilms at 10 h indicates that not much time is required by pumpkin oil to kill ATCC 6538. Result shows that pumpkin oil at MBEC value of 125 mg/mL was bactericidal against ATCC 6538 biofilms as it rapidly achieved approximately 5 log reductions in 2 h.

**Table 33. Biofilm time-killing of pumpkin oil against MRSA 252 and *S. aureus* ATCC 6538**

ATCC 6538									
Time (h)	0	2	4	6	8	10	12	22	24
Count (CFU/mL)	$2.12 \times 10^8$	$1.8 \times 10^3$	$1.7 \times 10^3$	$1.7 \times 10^2$	$2.10 \times 10^2$	0	0	0	0
log <sub>10</sub> CFU/mL	8.33	3.25	3.23	3.23	2.30	0	0	0	0

MRSA 252									
Time (h)	0	2	4	6	8	10	12	22	24
Count (CFU/mL)	$2.32 \times 10^8$	$2.2 \times 10^4$	$1.5 \times 10^3$	$2.80 \times 10^2$	$1.5 \times 10^1$	$1.1 \times 10^1$	0	0	0
log <sub>10</sub> CFU/mL	8.37	4.34	3.18	2.45	1.17	1.04	0	0	0

In the above table, the values represented are the mean  $\pm$  SD (n=3), SD: standard deviation, CFU: colony forming unit.

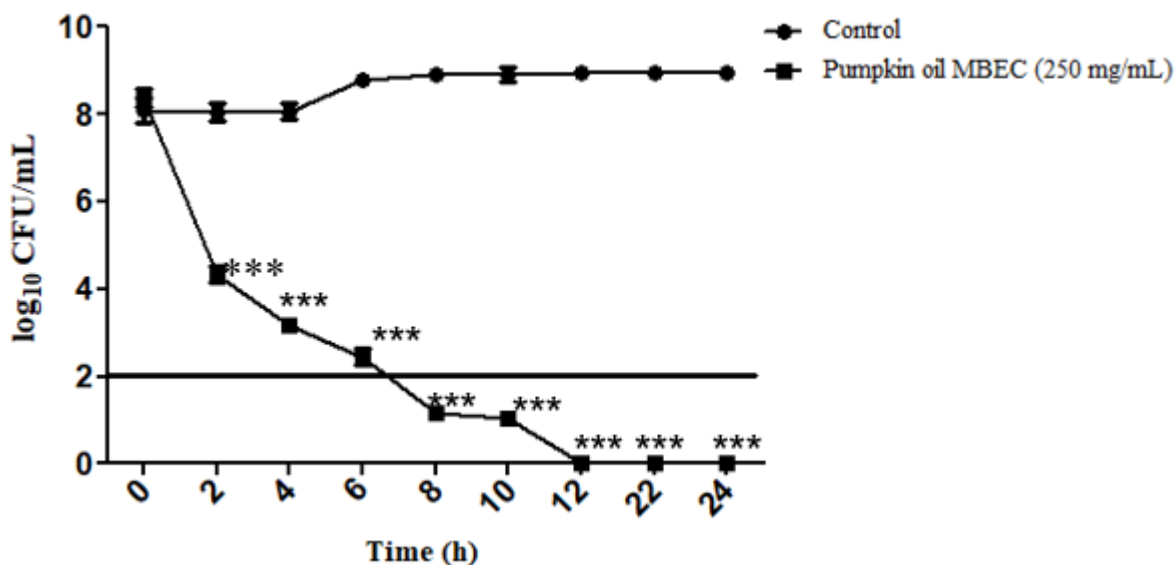


**Figure 112. Time exposure viability curve (log<sub>10</sub>CFU/mL over 24 h) for preformed MRSA 252 biofilm incubated with pumpkin oil at MBEC (250 mg/mL) for 24 h at 37°C**

Data on the graph represent the log of the mean colony forming units of three independent experiments (n=3). Values are the log of mean $\pm$ SD (n=3) CFU/mL, CFU: colony forming unit, time (X-axis): time intervals needed for killing MRSA 252. Log (CFU/mL) (Y-axis) shows viability of MRSA 252 at different times. Asterisk on the graph signifies a significant difference between the mean CFU/mL compared with control \*\*\*P<0.0001 (P<0.05).

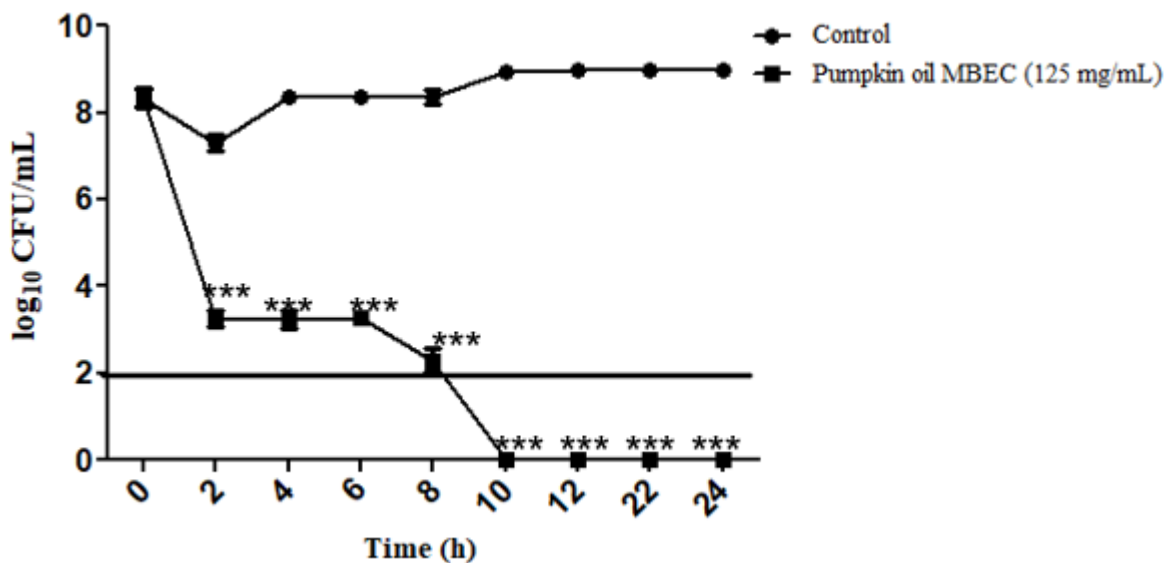


**Figure 113. Time kill exposure viability curve (log<sub>10</sub>CFU/mL over 24 h) for preformed ATCC 6538 biofilm incubated with pumpkin oil at MBEC (125 mg/mL) for 24 h at 37°C**

Data on the graph represent the log of the mean colony forming units of three independent experiments (n=3). Values are the log of mean±SD (n=3) CFU/mL, CFU: colony forming unit, time (X-axis): time intervals needed for killing ATCC 6538. Log (CFU/mL) (Y-axis) shows viability of ATCC 6538 at different times. Asterisk on the graph signifies a significant difference between the mean CFU/mL compared with control \*\*\*P<0.0001 (P<0.05).

## 7.2.2 Synergy activity of plant oils with antibiotics.

### 7.2.2.1 Checkerboard assay

A series of 4 trials of the individual MIC determination assays for antibiotics were performed in triplicates and consistent results were obtained. The MIC was determined as the smallest antimicrobial concentration that inhibited bacterial growth as indicated by the darkest purple colour. For example, where there was ambiguity in the colour determination, the well with the darker purple coloured was chosen as the MIC. The purple colour was chosen because they indicate complete inhibition of the bacteria while the light purple colour indicates partial inhibition. However, the MICs of individual antibiotic as observed in the plate below indicates antibacterial inhibition was complete. Figure 114 shows a representative plate of antibiotic MIC.

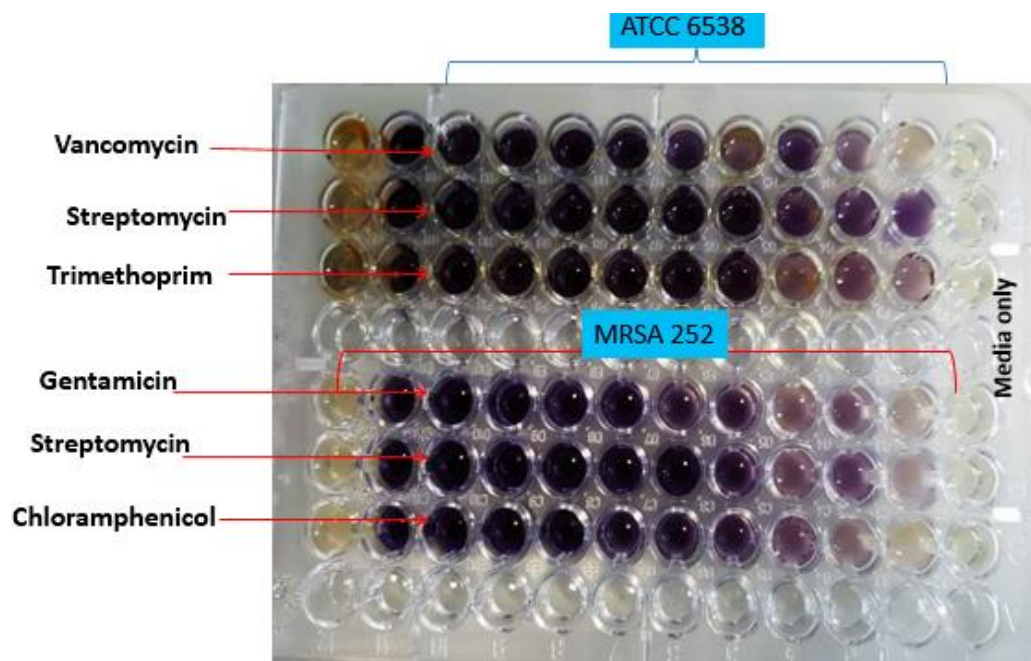


**Figure 114. Representative trial microtiter plate for the individual MIC determination trials.**

In testing for the efficacy of oils with antibiotics, cashew oil was not used because of its weak activity. The efficacy of African walnut and pumpkin oil combined with antibiotics were determined by checkerboard assay, and the results are presented below. In most of the antibiotics tested, the MIC value of African walnut oil and pumpkin oil combined with many antibacterial agents decreased predominantly, suggesting that both oils exhibited synergistic activity. This is the first report concerning the synergistic effects of walnut and pumpkin oil in combination with antibiotics against methicillin susceptible and resistant strains. In the checkerboard assay, several dilutions below the MIC to above the MICs were tested for each oil sample and antibiotic tested against MRSA 252 and ATCC 6538. Antibiotic combinations and oils tested includes;

- Vancomycin, streptomycin with walnut oil against MRSA 252
- Vancomycin, trimethoprim and streptomycin with African walnut oil against *S. aureus* ATCC 6538.
- Gentamicin, chloramphenicol with pumpkin oil against MRSA 252
- Vancomycin and rifampicin with pumpkin oil against *S. aureus* ATCC 6538.

Antibiotics used in testing for drug interactions are those found promising in the disc diffusion test. Interpretation of FICI index was carried out for each combination treatments with African walnut and pumpkin oils tested on MRSA 252 and ATCC 6538 (tables 34-37). FICI index

values were calculated considering all combinations of the oils and antibiotics. In this analysis, synergistic activity of African walnut oil with vancomycin was 0.37 (FICI 0.50) and streptomycin (FICI 0.75) when tested against MRSA 252. However, combination of African walnut oil with vancomycin was 0.50 (FICI 0.50), trimethoprim (FICI 0.19) and streptomycin (FICI 0.56) when tested on *S. aureus* ATCC 6538. The “best combination” of African walnut oil and vancomycin, and trimethoprim are the ones giving the lowest FIC Index value (FIC Index  $\leq 0.5$ ) against MRSA 252 and ATCC 6538, an indifference interaction (FIC Index  $>0.5$ ) was observed in the combination of African walnut oil with streptomycin for the two strains.

**Table 34. Fractional inhibitory concentration (FIC) indices of African walnut oil combined with antibiotics.**

	MRSA 252								
Antimicrobials	1	2	3	4	5	6	7	8	9
Vancomycin ( $\mu\text{g/mL}$ )	50	25	12.5	6.25	3.125	1.56	0.78	0.39	0.195
Streptomycin ( $\mu\text{g/mL}$ )	50	25	12.5	6.25	3.125	1.56	0.78	0.39	0.195
Walnut oil (mg/mL)	250	125	62.5	31.25	15.6	7.8	3.9	1.95	0.98
	<i>S. aureus</i> ATCC 6538								
Vancomycin ( $\mu\text{g/mL}$ )	50	25	12.5	6.25	3.125	1.56	0.78	0.39	0.195
Trimethoprim ( $\mu\text{g/mL}$ )	125	62.5	31.25	15.6	7.8	3.9	1.95	0.98	0.49
Streptomycin ( $\mu\text{g/mL}$ )	50	25	12.5	6.25	3.125	1.56	0.78	0.39	0.195
Walnut oil (mg/mL)	250	125	62.5	31.25	15.6	7.8	3.9	1.95	0.98

**Key:**

- The MIC concentrations of each antibiotic is highlighted in yellow
- The MIC concentrations of each antibiotic and oil combination is highlighted in pink
- The MIC concentrations of each oil in combination with drug is highlighted in green
- The MIC concentrations of African walnut oil alone is highlighted in brown.

**Table 35. FIC and FIC index results from the combination of African walnut oil and antibiotics on MRSA 252 and ATCC 6538**

MRSA 252							
Antibiotics/Anti bacterial agent	Antibiotics combinations	FIC of oil and drug		FICI			Interpretation
		FIC of drug	FIC of walnut oil	FICI calculation			
Vancomycin	African walnut oil + Vancomycin	0.78/3.125	1.95/15.6	0.249	0.125	0.37	Synergy
Streptomycin	African walnut oil + Streptomycin	1.56/6.25	7.8/15.6	0.25	0.5	0.75	Indifference
<i>S. aureus</i> ATCC 6538							
Antibiotics/Anti bacterial agent	Antibiotics combinations	FIC of oil + drug		FICI			Interpretation
		FIC drug	FIC oil	FICI calculation			
Vancomycin	African walnut oil + vancomycin	0.78/3.125	1.95/7.8	0.249	0.25	0.50	Synergy
Trimethoprim	African walnut oil + trimethoprim	0.98/15.6	0.98/7.8	0.06	0.13	0.19	Synergy
Streptomycin	African walnut oil + streptomycin	0.39/6.25	3.9/7.8	0.06	0.5	0.56	Synergy

**Table 36. Fractional inhibitory concentration (FIC) and (FICI) indices (FICI) of pumpkin oil combined with antibiotics on MRSA 252 and ATCC 6538**

Antimicrobials	MRSA 252								
	1	2	3	4	5	6	7	8	9
Gentamicin (µg/mL)	250	125	62.5	31.25	15.6	7.8	3.9	1.95	0.98
Chloramphenicol (µg/mL)	100	50	25	12.5	6.25	3.125	1.625	0.813	0.406
Pumpkin oil (mg/mL)	500	250	125	62.5	31.25	15.6	7.8	3.9	1.9
<i>S. aureus</i> ATCC 6538									
Vancomycin (µg/mL)	50	25	12.5	6.25	3.125	1.56	0.78	0.39	0.195
Rifampicin (µg/mL)	125	62.5	31.25	15.6	7.8	3.9	1.95	0.98	0.49
Pumpkin oil (mg/mL)	500	250	125	62.5	31.25	15.6	7.8	3.9	1.9

**Key:**

- The MIC concentrations of each antibiotic is highlighted in yellow
- The MIC concentrations of each antibiotic and oil combination is highlighted in pink
- The MIC concentrations of each oil in combination with drug is highlighted in green
- The MIC concentrations of pumpkin oil alone is highlighted in brown.

**Table 37. FIC and FICI data results from the combination of pumpkin oil with antibiotics**

MRSA 252							
Antibiotics/Antibacterial agent	Antibiotics combinations	FIC of oil + drug		FICI			Interpretation
		FIC of drug	FIC of oil	FICI calculation			
Gentamicin	Pumpkin oil + Gentamicin	7.8/62.5 =0.125	3.9/ 62.5 =0.26	0.125	0.26	0.19	Synergy
Chloramphenicol	Pumpkin oil + Chloramphenicol	1.62/6.25 =0.2	31.25/62.5 = 0.5	0.2	0.5	0.76	Indifference

ATCC 6538							
Antibiotics/Antibacterial agent	Antibiotics combinations	FIC of oil + drug		FICI			Interpretation
		FIC of drug	FIC of oil	FICI calculation			
Vancomycin	Pumpkin oil + vancomycin	1.56/3.125	3.9/31.25	0.50	0.125	0.625	indifference
Rifampicin	Pumpkin oil + trimethoprim	7.8/15.6	1.95/31.25	0.5	0.06	0.56	Indifference

### 7.2.3 Assessing the efficacy of African walnut oil in the treatment of staphylococcal infections using *G. mellonella* as an *in vivo* model.

#### 7.2.3.1 Establishing pathogenicity of MRSA 252 and ATCC 6538 against *G. mellonella*.

To effectively study the pathogenicity of staphylococcal strains; MRSA 252 and ATCC 6538, three main groups A, B and C was constituted as explained below. However, group C was further expanded to contain dilution series infected with infective doses of the strains. Except otherwise mentioned, each infective dose stated in group C was constituted for each strain.

**Group A** consisted of 20 non-infected larvae which served as negative control for the experiment

**Group B** consisted of 20 larvae inoculated with PBS and 20 mg of ampicillin to serve as positive control.

**Group C** consisted of 20 larvae for each dilution ( $10^0$ ,  $10^{-1}$ ,  $10^{-2}$  and  $10^{-3}$ ) of MRSA 252 and *S. aureus* ATCC 6538.

Numerous studies have shown that melanisation and development of black thick *plaques* on the body surface of *G. mellonella* after infection is an important marker indicating that the immune response of the worm has been affected (Loh *et al.*, 2013; Tsai *et al.*, 2016; Yang *et al.*, 2017). In this present study, melanisation was found to develop gradually on the body surfaces of the infected *G. mellonella* larvae after infecting them with MRSA 252 and ATCC 6538. This was found to increase gradually, and more deaths were recorded. Figure 115 show melanisation in *G. mellonella* larvae.

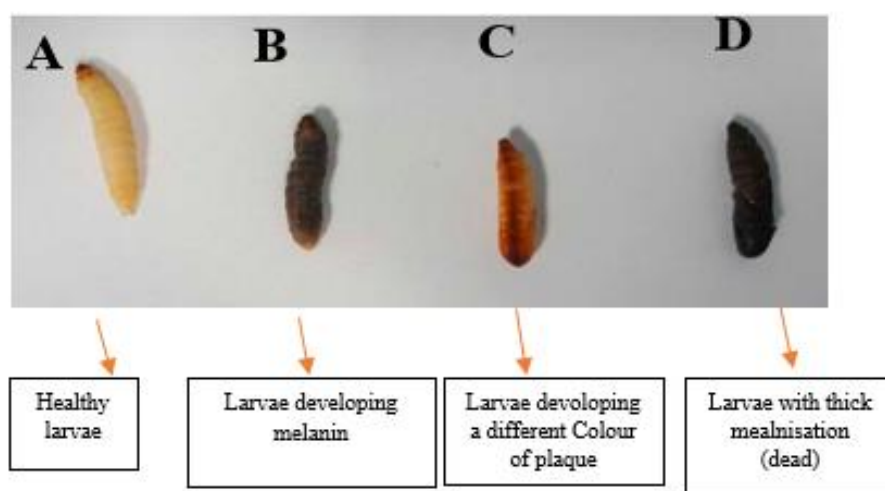


**Figure 115. Observed changes in *G. mellonella* before, after infection and with combinational treatment.**

*G. mellonella* infection model a) A healthy caterpillar prior to injection with infective doses of MRSA 252 and ATCC 6538 biofilm cells. (b) Infected larvae developed melanin and move sluggishly. (c) Larvae develop a different colour after treatment with walnut oil, with this colour larvae were not sluggish and dead. (d) Subsequent death of the caterpillar with a high level of melanisation and hardening.

To determine the infective dose of each bacterial strain to be used the total viable count was determined. In order to enumerate viable bacterial colonies, an assumption was made that each bacterial colony that grew on an agar plate when cultured arose from one living (viable) cell, therefore it was possible to determine the total viable bacterial count defined as colony forming units (CFU) per ml of the original culture. The general acceptance range for counting colony forming units on agar plates is 30 to 300 colonies (Loh *et al.*, (2013). In this present study, dilution  $10^{-5}$  of both strains fell within the acceptance range of 186 and 172 colony forming

units grown on the agar plate. The CFU/mL of the original culture was calculated using the following formula: CFU/mL = number of colonies per ml plated/Total dilution factor.

A log dilution of  $10^{-5}$  showed 186 colonies, however only 100  $\mu$ L of the dilution was plated, therefore the number of colonies was divided by 0.1 ml before being divided by the total dilution factor.

$$\text{Therefore; CFU/mL} = (186/0.1\text{mL})/10^{-5} = 1860 \times 10^{-5} = 1.86 \times 10^{-8} \text{ CFU/mL}$$

The above calculation was used to determine the CFU/mL; however, the larvae were only injected with 10  $\mu$ L of each culture, a dilution of  $10^{-2}$ . Therefore, it was possible to determine that 10  $\mu$ L of the original culture contained  $1.86 \times 10^{-6}$  CFU for MRSA 252 and  $1.72 \times 10^{-6}$  CFU for ATCC 6538. From this the dilutions injected into the larvae were obtained (Table 38).

**Table 38. CFU/Larvae per 10  $\mu$ L injections of infecting doses of MRSA 252 and ATCC 6538 calculated from the original CFU counts.**

Dilution	CFU/Larva Amount injected in 10 $\mu$ L	
	MRSA 252	ATCC 6538
$10^0$	$1.86 \times 10^{-6}$	$1.72 \times 10^{-6}$
$10^{-1}$	$1.86 \times 10^{-5}$	$1.72 \times 10^{-5}$
$10^{-2}$	$1.86 \times 10^{-4}$	$1.72 \times 10^{-4}$
$10^{-3}$	$1.86 \times 10^{-3}$	$1.72 \times 10^{-3}$

Different groups of *G. mellonella* larvae were infected with  $10^0$  ( $1.86 \times 10^{-6}$ ),  $10^{-1}$  ( $1.86 \times 10^{-5}$ ),  $10^{-2}$  ( $1.86 \times 10^{-4}$ ), and  $10^{-3}$  ( $1.86 \times 10^{-3}$ ), dilutions of MRSA 252 and  $10^0$  ( $1.72 \times 10^{-6}$ ),  $10^{-1}$  ( $1.72 \times 10^{-5}$ ),  $10^{-2}$  ( $1.72 \times 10^{-4}$ ), and  $10^{-3}$  ( $1.72 \times 10^{-3}$ ) dilutions of ATCC 6538 at the stationary phase of growth. Bacterial infecting doses of MRSA 252 and ATCC 6538 strains represent a virulent and susceptible strain doses. The survival of the larvae was monitored over a period of 5 days following injection of the bacterial suspensions (infective doses). MRSA 252 strain caused time-dependent larval death that was determined by touch-induced lack of larval movement and in most cases, larval death was accompanied by quick melanisation of the larvae. Compared to ATCC 6538, MRSA 252 induced higher larval mortality at the different bacterial inoculum infection dose particularly with the  $10^0$  dilution used after 1 day indicating an increased virulence exhibited by this strain in this model. *G. mellonella* larvae infected with MRSA 252 were observed to develop high level of melanisation and hardening. In the control PBS-injected larvae, no mortality was observed in the control PBS-injected larvae. In addition,

no melanisation was even observed. ATCC 6538 was observed to exhibit an avirulent behaviour because only 10 deaths were recorded within the 5 days. These results obtained in this experiment show that, *G. mellonella* larvae succumb to *S. aureus* infection and appear to show strain differences and pathogenicity. Results for *G. mellonella* death and survival recorded within 5 days is presented in Figure 116

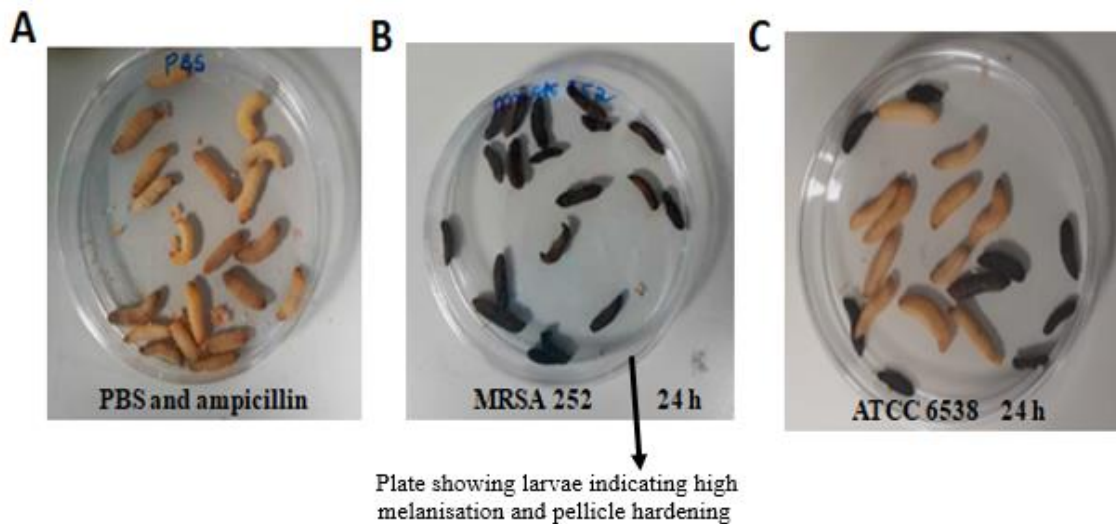


**Figure 116.** One day (24 h) post inoculation of *G. mellonella* larvae infected with 10  $\mu$ L of 100 infecting doses of MRSA 252 and ATCC 6538 biofilm cultures (stationary phase cultures).

*G. mellonella* used for each group test were injected with 10  $\mu$ L of  $10^0$  infecting dose aliquots of MRSA 252 and ATCC 6538, injected into them through the last left proleg. (A) One day (1 day) post inoculation of *G. mellonella* infected with 10  $\mu$ L of PBS and ampicillin (B) *G. mellonella* infected with 10  $\mu$ L MRSA 252 and (C) *G. mellonella* larvae infected 10  $\mu$ L ATCC 6538.

Below, both the dead and survivors were continually monitored for other lower infective doses of the strains that were also used. Pathogenicity test result of *S. aureus* ATCC 6538 against *G. mellonella* larvae on day 5 shows that a greater number of larvae survived after been infected with  $10^{-3}$  (80 %) biofilm cells compared with the groups infected with  $10^0$  (45 %),  $10^{-5}$  (45 %) and  $10^{-4}$  (55 %). In contrast, MRSA 252 biofilm cells exhibited virulence at all levels with the  $10^{-6}$  cells (0 % survivor) been the most effective. Survivors were also recorded at  $10^{-5}$  (19.0 %),  $10^{-4}$  (30 %) with  $10^{-3}$  (35 %) being the least effective culture. Figure 117 and 118 below shows day 5 survivors of *G. mellonella* larvae after been infected with 10  $\mu$ L biofilm cells of MRSA 252 at the different infecting doses.

Day 5 samples of *G. mellonella* larvae after injection with infecting doses of MRSA 252

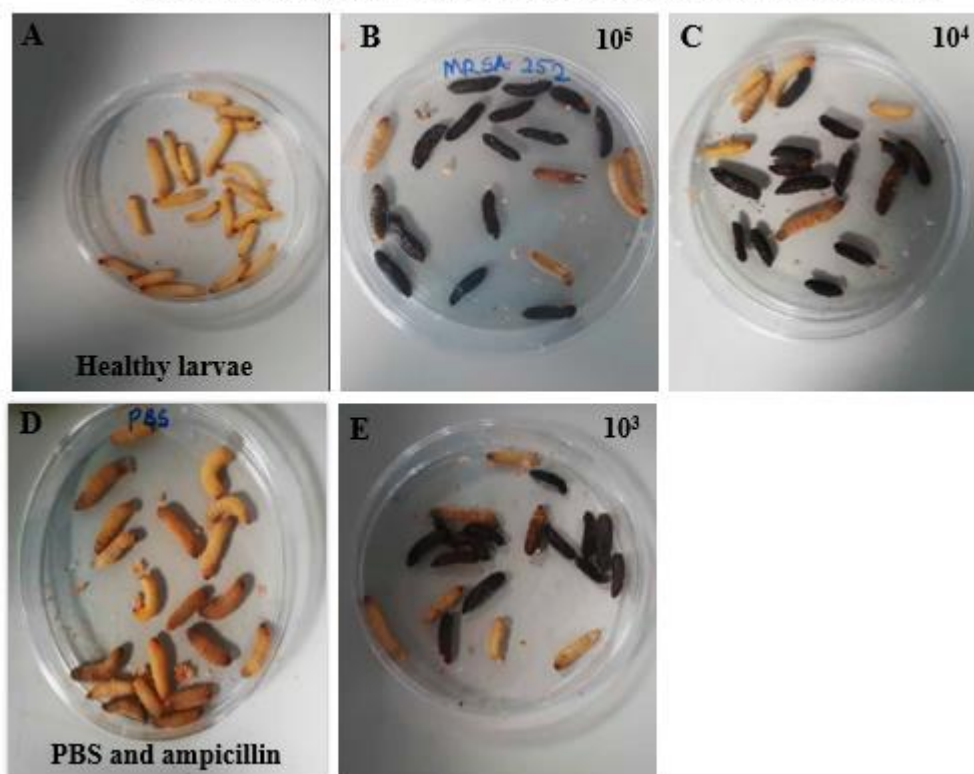


**Figure 117. Representative photographs of petri-plates containing *G. mellonella* infected with MRSA 252 biofilm cultures.**

(A) Healthy larvae of *G. mellonella* larvae. (B) *G. mellonella* infected with MRSA 252 ( $1.86 \times 10^5$  CFU/larvae). (C) *G. mellonella* infected with MRSA 252 ( $1.86 \times 10^4$  CFU/larvae). (D) *G. mellonella* larvae injected with PBS and ampicillin (10  $\mu$ L). (E) *G. mellonella* injected with MRSA 252 ( $1.86 \times 10^3$  CFU/larvae). Photographs were obtained 5 days after the infection of each strain. 20 *G. mellonella* were used for each group tested.

Figure 117 show that *G. mellonella* gradually developed melanin which appear intense as observed in the picture. With time, the larvae appeared sluggish to any slightest touch with forcep. The results obtained show that *G. mellonella* was susceptible to MRSA 252. Within 5 days each group recorded few deaths. Death was recorded as dose dependent. Dose  $10^6$  was the most effective. This tested was repeated three times for thorough observation. Figure 118 show the percentage of dead and survivors from MRSA 252 infecting doses in each group tested within 5 days.

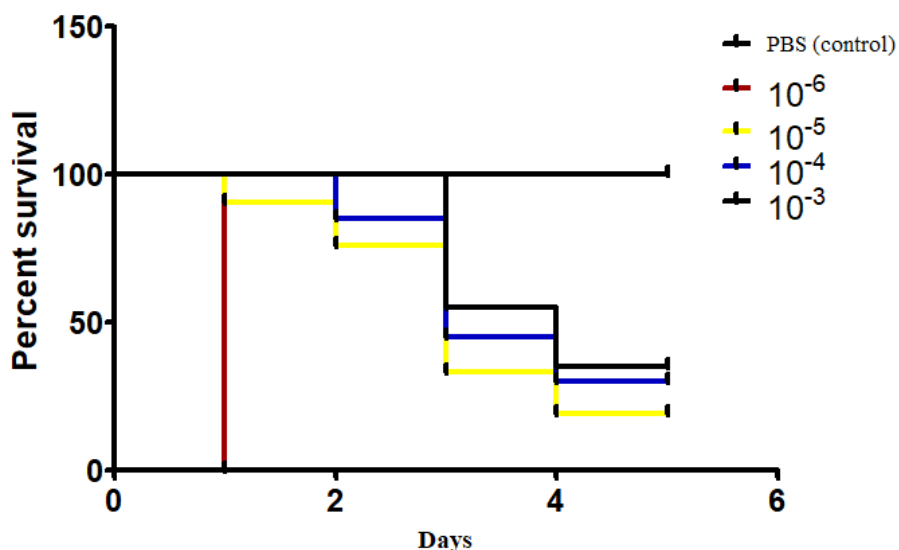


**Figure 118. The survival of *G. mellonella* larvae infected with MRSA 252.**

*G. mellonella* larvae (n=20 per group) were infected with varying concentration of MRSA 252 or PBS by injection of 10 ul of each infective dose obtained from stationary phase biofilm cultures via the proleg while restrained between the thumbs. Kaplan-Meier survival curves were drawn for inoculums of  $10^0$  ( $1.86 \times 10^{-6}$ ),  $10^{-1}$  ( $1.86 \times 10^{-5}$ ),  $10^{-2}$  ( $1.86 \times 10^{-4}$ ), and  $10^{-3}$  ( $1.86 \times 10^{-5}$ ) dilutions. Statistical analysis show \*p < 0.05 (0.0001) was obtained using the Log Rank Mantel-Cox test indicating significant difference between survivals per day.

**Table 39. Survivors and dead recorded between day 1 to 5 after infecting *G. mellonella* with MRSA 252 infecting doses.**

Days	PBS (control)	$10^{-6}$	$10^{-5}$	$10^{-4}$	$10^{-3}$
0	100.000	100.000	100.000	100.000	100.000
1		90.000	90.47619		
2		60.000	76.19048	85.000	
3		15.000	33.33333	45.000	70.000
4		0.000	19.04762	30.000	35.000
5	100.000	0.000	19.04762	30.000	35.000

Based on the result presented in Figure 117 and Table 39, a greater survival by larval group that has been infected with  $10^{-3}$  CFU/larva (35%) was observed compared with the groups that had been infected with  $10^{-4}$  (30%),  $10^{-5}$  (19%) and  $10^{-6}$  CFU/Larva (0%).

Figure 119 and 120 below shows day 5 survivors of *G. mellonella* larvae after infected with 10  $\mu$ L biofilm cells of *S. aureus* ATCC 6538 at the different infecting doses.

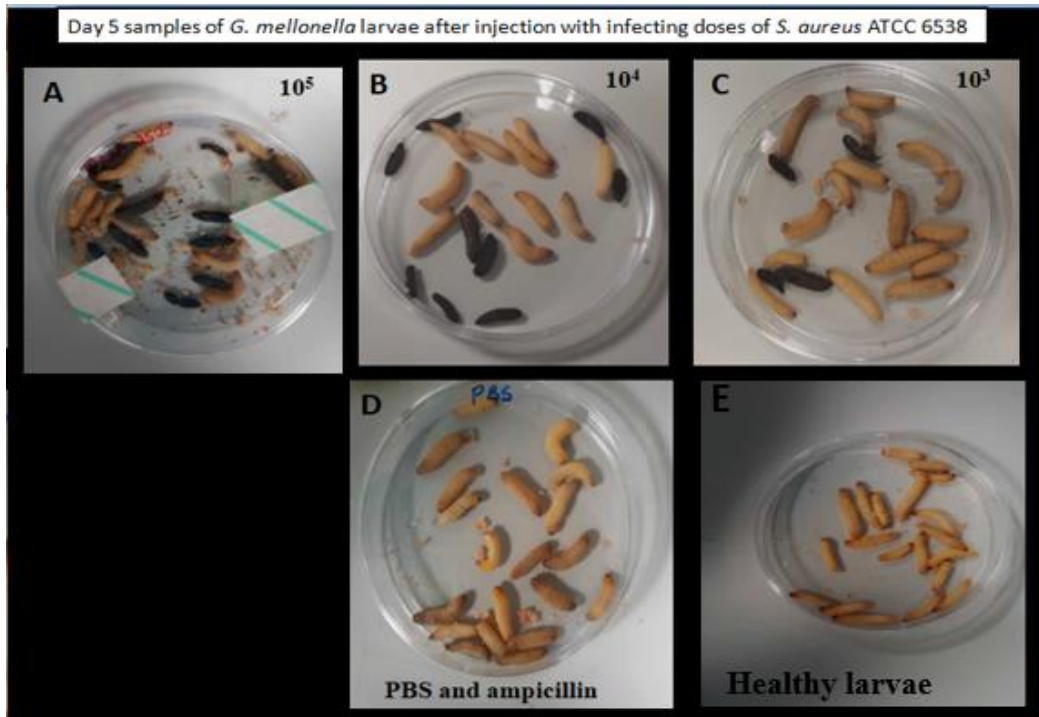


**Figure 119. Representative photographs of petri-plates containing *G. mellonella* infected with *S. aureus* ATCC 6538**

(A) *G. mellonella* infected with ATCC 6538 ( $1.72 \times 10^5$  CFU/larvae) (B) *G. mellonella* infected with *S. aureus* ATCC 6538 ( $1.72 \times 10^4$  CFU/larvae) (C) *G. mellonella* injected with *S. aureus* ATCC 6538 ( $1.72 \times 10^3$  CFU/larvae). (D) *G. mellonella* larvae injected with PBS and ampicillin (10  $\mu$ L) and (E) Healthy larvae of *G. mellonella*. Photographs were obtained 5 days after the infection of each strain. 20 *G. mellonella* were used for each group tested.

Figure 119 shows that *G. mellonella* gradually developed melanin which was not too intense as observed in the picture. Although with time, the larvae appeared sluggish to any touch with forcep. The results obtained show that *G. mellonella* was susceptible to ATCC 6538 even though it is a methicillin susceptible strain. Within 5 days each group recorded few deaths. Death was recorded as dose dependent. However, dose  $10^6$  was the effective dose. This tested was repeated three times for thorough observation. Figure 120 below shows the percentage of dead and survivors from ATCC 6538 infecting doses in each group tested within 5 days.

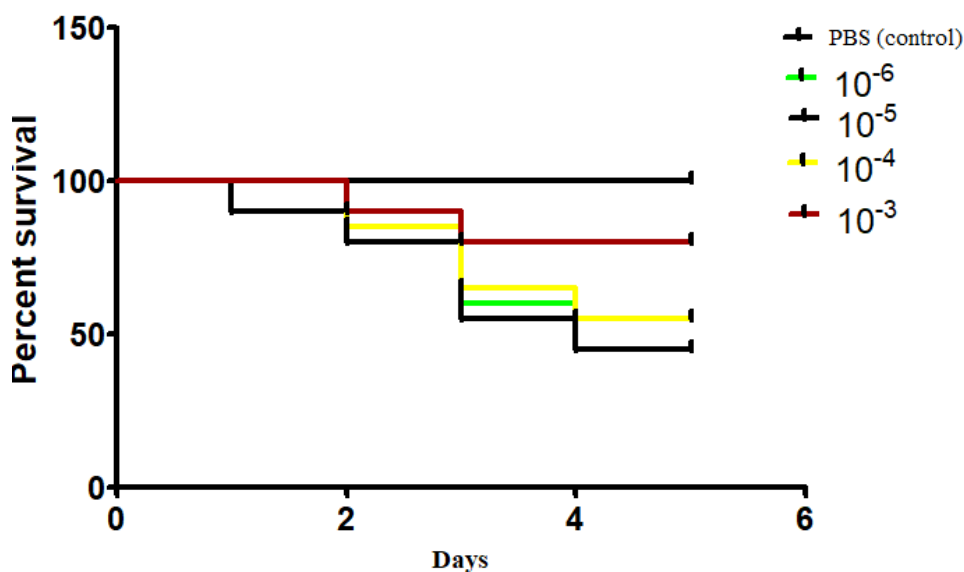


**Figure 120. The survival of *G. mellonella* larvae infected with ATCC 6538**

*G. mellonella* larvae (n=20 per group) were infected with varying concentration of ATCC 6538 or PBS by injection of 10  $\mu$ L of each infective dose obtained from stationary phase biofilm cultures via the proleg while restrained between the thumbs. Kaplan-Meier survival curve were drawn at an inoculum of  $10^0$  ( $1.72 \times 10^{-6}$ ),  $10^{-1}$  ( $1.72 \times 10^{-5}$ ),  $10^{-2}$  ( $1.72 \times 10^{-4}$ ), and  $10^{-3}$  ( $1.72 \times 10^{-3}$ ) dilutions at the end of 5 days. However, daily deaths and survivors were recorded individually. Statistical value \*p < 0.05 (0.0001) was obtained using the Log Rank Mantel-Cox test indicating significant difference between survivals per day.

**Table 40. Survivors and dead recorded between day 1 to 5 after infecting *G. mellonella* with ATCC 6538 infecting doses.**

Days	PBS (control)	$10^{-6}$	$10^{-5}$	$10^{-4}$	$10^{-3}$
0	100.000	100.00	100.00	100.00	100.00
1.		90.000	90.000		
2.		80.000	80.000	85.000	90.000
3.		60.000	55.000	65.000	80.000
4.		45.000	45.000	55.000	
5.	100.000	45.000	45.000	55.000	80.000

Based on the result presented in Figure 119 and Table 40, a greater survival by larval group that has been infected with  $10^{-3}$  CFU/larva (80%) was observed compared with the groups that had been infected with  $10^{-4}$  (55%),  $10^{-5}$  (45%) and  $10^{-6}$  CFU/Larva (45%). A higher percentage survival was obtained for ATCC 6538 compared to MRSA 252. PBS control larvae group had 100 % survivors.

### 7.2.3.2 Combination therapy with African walnut oil

The efficacy of African walnut oil against MRSA 252 infections, groups of 15-20 larvae were challenged with  $10^6$  lethal doses of MRSA 252 then treated against melanisation with single dose of African walnut oil. Vancomycin was included in this experiment to serve as antibiotic commonly used in the treatment of staphylococcal infection and control. Two different concentrations (15.6 mg/mL, 31.25 mg/mL and 62.5mg/mL) of African walnut oils (found to have inhibitory activity) was prepared in DMSO but two dilutions, 15.6 mg/mL and 31.25 mg/mL was used for the experiment.

Day 5 samples of *G. mellonella* larvae after injection with infecting dose ( $10^6$  CFU/Larva) of MRSA 252 and ATCC 6538 and treated with antibiotic and African walnut oil.

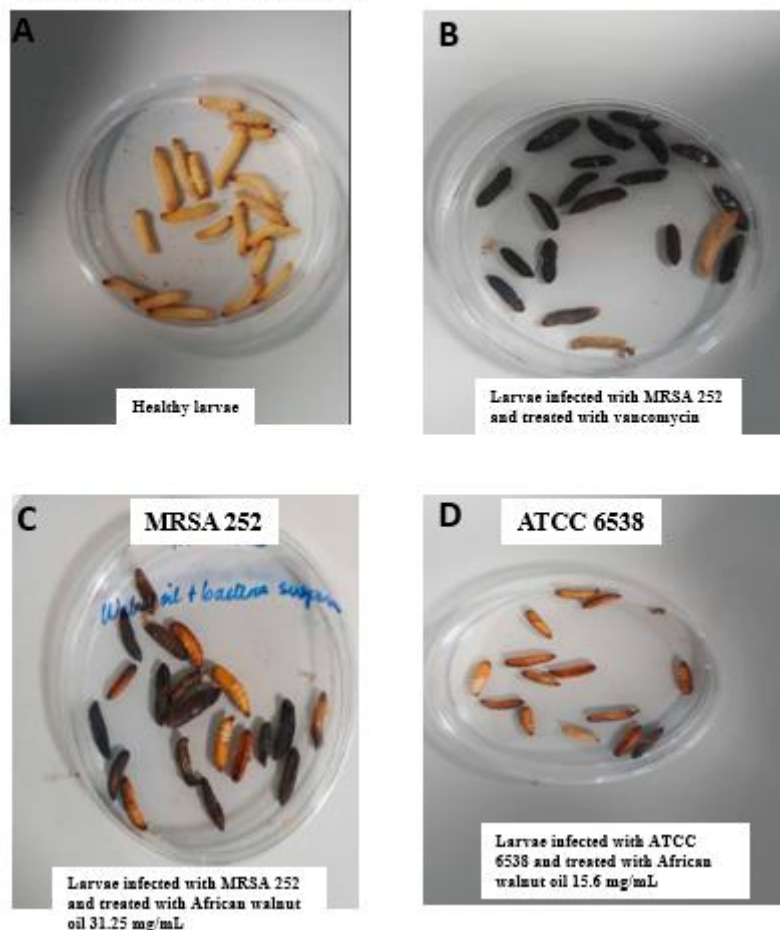


**Figure 121. Visual observation of *G. mellonella* before and after treatment with antibiotic and African walnut oil for 5 days**

(A) Healthy *G. mellonella* larvae. (B) *G. mellonella* larvae infected with MRSA 252 and treated with vancomycin (100  $\mu$ g/mL). (C) *G. mellonella* larvae infected with MRSA 252 and treated with African walnut oil (31.25 mg/mL by injecting this amount into the larvae). (D) *G. mellonella* larvae infected with ATCC 6538 and treated with

African walnut oil (15.6 mg/mL by injecting this amount into the larvae). Infecting dose of MRSA and ATCC 6538 found effective  $10^0$  ( $1.86 \times 10^{-6}$ ) CFU/mL and  $10^0$  ( $1.72 \times 10^{-6}$ ) was used.

Figure 121 shows the efficacy of African walnut oil in the treatment of staphylococcal infections using *G. mellonella* as an *in vivo* model. This efficacy was assessed in the post inoculated *G. mellonella* larvae by checking for melanin development and sluggishness. Larvae group infected with 10  $\mu$ L of infecting dose of MRSA 252 and treated with 10  $\mu$ L of 100  $\mu$ g/mL of vancomycin were observed to have started dying on the second day after treatment and death was within day 2 to 4. Larvae group infected with 10  $\mu$ L of infecting dose of MRSA 252 and treated with walnut oil 31.25 mg/mL were observed to survive gradually but death was recorded with day 2 to 4. Although 7 survivors were still observed on day 5. Larvae group infected with 10  $\mu$ L of infecting dose of ATCC 6538 were observed to survive until day 5 even after treatment with 15.6 mg/mL of walnut oil. However, the development of brownish pellicles was observed in both the MRSA 252 and ATCC 6538 treated with walnut oil which was quite different to the blackish melanin observed in vancomycin and 24 h infected MRSA 252 and ATCC 6538. Also observed is that sluggishness characterized as death symptom was not also observed. This shows a promising indicator of survival in *G. mellonella* larvae even after infection with staphylococcal infections. This test was repeated three times for thorough observation. Figure 122 shows the percentage of dead and survivors from MRSA 252 and ATCC 6538 infected groups and treated with antibiotic and African walnut oil. The test in each group was within 5 days.

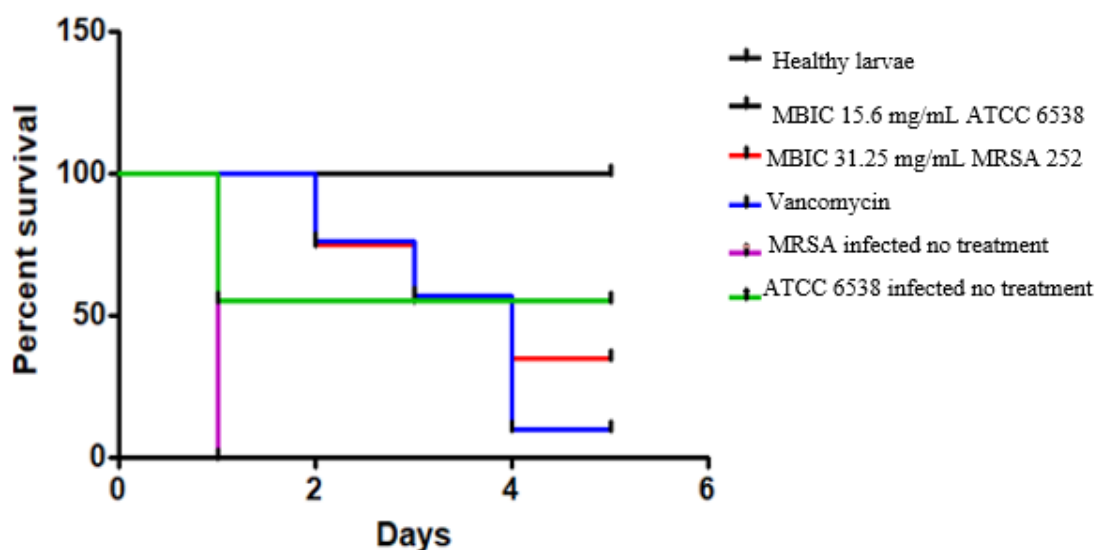


Figure 122. Percentage survival from *G. mellonella* (n=15-20 per group) groups infected MRSA 252 and ATCC 6538 and treated with antibiotic and African walnut oil.

Kaplan-Meier survival curve were drawn at an inoculum of  $10^0$  ( $1.86 \times 10^{-6}$ ) MRSA 252 and  $10^0$  ( $1.72 \times 10^{-6}$ ) ATCC 6538 dilutions at the end of 5 days. However, daily deaths and survivors were recorded individually. Statistical value  $*p < 0.05$  (0.0001) was obtained using the Log Rank Mantel-Cox test indicating significant difference between survivals per day.

**Table 41. Survivors and dead recorded between day 1 to 5 after infecting *G. mellonella* with ATCC 6538 and MRSA 252 infecting dose ( $10^{-6}$  CFU/Larva) and treatment with antibiotic and African walnut oil.**

Days	Healthy	MBIC 15.6 mg/mL ATCC 6538	MBIC 31.26 mg/mL MRSA 252	Vancomycin	MRSA infected no treatment	ATCC 6538 infected no treatment
	Survivors recorded			Dead recorded		
0	100.000	100.000	100.000	100.000	100.000	100.000
1						90.000
2			75.000	85.000		80.000
3			55.000			60.000
4			35.000			45.000
5	100.000	100.000	35.000		100.000	45.000

Based on the result presented in Figure 122 and table 41 a greater survival by larval group that was infected with  $10^{-6}$  CFU/larva was recorded after injection with vancomycin, 15.6 mg/mL and 31.25 mg/mL of African walnut oil. After injection of 15.6 mg/mL African walnut oil into *G. mellonella* infected with ATCC 6538, 100% survivors were recorded although brownish pellicles were observed. After injection of 31.25 mg/mL walnut oil into *G. mellonella* infected with MRSA 252, 35% survivors were recorded although similar brownish pellicles alongside melanin were observed. Whereas *G. mellonella* injected with  $10^{-6}$  CFU/larva of MRSA 252 and ATCC 6538 alone recorded dead of 100% and 45%.

### 7.3 Discussion

To consider oils of African walnut and pumpkin as natural antimicrobials with potential for the development of a new chemotherapy drug for the treatment of staphylococcal infections, it is important to consider its antimicrobial action on cells enclosed in biofilms (Batista *et al.*, 2017). For that purpose, biofilm time kill assay was performed which determines the time of action of a compound antimicrobial activity. The used strains are *S. aureus* ATCC 6538 and MRSA 252 the sensitive and resistant strains that had their growth in mature biofilm eradicated by the oils particularly African walnut and pumpkin oil at the tested concentration (MBEC = 62.5 and 31.25mg/mL for walnut oil) and (MBEC = 125 and 250 mg/mL for pumpkin oil). Biofilm kinetic time assay for walnut oil and pumpkin oil has provided a platform to visually observe antibacterial action of minimum bactericidal concentrations of walnut and pumpkin oils against MRSA 252 and ATCC 6538 biofilm growth. Visually in the sense that bacterial colonies from exposed cultures of MRSA 252 and ATCC 6538 were counted at growth time points after plating on TSA plates and log CFU/mL was calculated. From the results, ATCC 6538 strain with reduced/low biofilm production, 31.25 mg/mL achieved bactericidal activity at 2 h after exposure. In contrast, MRSA 252 observed to be a strong biofilm former, 62.5 mg/mL African walnut oil achieved bactericidal activity at 6 h. indicating that despite the high biofilm produced by MRSA 252, bactericidal activity was achieved early. Although not as early as the 2 h observed for ATCC 6538. An initial 6-log reduction at 2 and 4 h for MRSA 252 and a rapid 2-log reduction at 2 h for ATCC 6538 after which the bacterial count dropped to zero. The mean CFU/mL assessed after 48 h from the preformed biofilms were significantly different between the low-and high-biofilm-producing strains (2.12 and 2.32 CFU/mL, respectively;  $P < 0.001$ ). Cashew oil appeared to be low in bactericidal activity against MRSA 252 and ATCC 6538 because already, its MBEC value was high and exhibited low activity on the strains. Against MRSA 252 bactericidal killing was achieved at 24 h while killing of ATCC 6538 was at 22 h then viable count dropped to zero. Bactericidal killing of pumpkin oil was achieved at 10 h and 8 h for MRSA 252 and ATCC 6538 with an initial log reduction 4-5 log reduction in the strain. Overall, results obtained for the bactericidal activity the oils on the strains shows that the varying biofilm forming ability of the strains manifested in the bactericidal activity of the individual oil tested. However, African walnut oil achieved bactericidal activity promptly on both the susceptible and resistant staphylococcal strains.

The concept of synergism is applied to treat infections caused by harmful pathogens to tackle the complex multiple-drug resistance problems (Yap *et al.*, 2014). A review by Rayner and Munckhof, (2005) compiled antibiotics belonging to different categories with failure rates due to increased resistance. It is for this reason; synergism of African walnut oil and pumpkin were examined for their synergistic activity with antibiotics with a view finding alternative therapies to staphylococcal infections. Vancomycin and trimethoprim were the drug of choice for MRSA infections for several decades, increased treatment failure rates coinciding with the spread of vancomycin *S. aureus* (VISA) have cast doubt on the reliable use of vancomycin and other drugs. The synergistic effect of vancomycin and trimethoprim was investigated, and FIC index interpretations have demonstrated that the African walnut and pumpkin oils appear to work synergistically with glycopeptide and sulphonamide drugs such as vancomycin and trimethoprim. This was evidently depicted in the FIC index interpretation which affirmed the synergistic action of African walnut oil with MRSA 252 and ATCC 6538 with FICI indexes of 0.37 and 0.5 (FICI<0.5). Similar activity was observed for trimethoprim with FICI (0.19) for ATCC 6538.

Adequate infection models that have similar genetic and immune responses to human disease are the key to analysing the molecular basis of bacterial pathogenesis (Tsai *et al.*, 2016). Recently, the larva of the greater wax moth *G. mellonella* has been reported as an easy-to-use model organism for several pathogenic bacteria (Pollitt *et al.*, 2018; Yang *et al.*, 2017). Because of these similarities, the response against MRSA 252 and ATCC 6538 infection by various means, such as the bacterial concentration capable of killing *G. mellonella*, infection, morphology and melanization in response to infection was investigated. One main limitation of *G. mellonella* larvae is their ability to survive at either 30°C - 37°C. the mammalian body temperature. In this study larval death caused by MRSA 252 and ATCC 6538 was not dependent on the post-infection incubation temperature, as evidenced by the killing rate at 37 °C. The strains used herein are all capable of causing disease, as they were obtained from human lesions and wounds with clinical signs of skin infections. In this study, for the first time the use of *G. mellonella* larva as an alternative host for studying MRSA 252 and ATCC 6538 virulence is investigated. One of the aspects of the present work was to investigate the pathogenicity of MRSA 252 and ATCC 6538 against *G. mellonella*. To establish *S. aureus* infection, standardized stationary phase biofilm cultures of MRSA 252 and ATCC 6538 in two concentrations were used to challenge *G. mellonella* for 5 days. Groups of *G. mellonella* infected with 10 uL of 10<sup>-6</sup> MRSA 252 strain all died within 24 h while lesser death

was recorded in  $10^{-5} - 10^{-4}$ . Therefore, indicating that 100 % of MRSA 252 inoculum induced death in the larvae. However, ATCC 6538 infected with the same CFU/mL  $10^{-6}$  could not induce high death. This difference is probably due to a threshold over which processes leading to larval death are induced via the overwhelming activation of the innate immune system (Grounta *et al.*, 2016).

Surprisingly inspection of the morphology and survival rate of *G. mellonella* group infected with single doses of MRSA 252 and vancomycin (100 µg/mL) showed that the larvae started to developed melanin characterized as death on the second day of infestation and all through within the 5 days study period. Group of *G. mellonella* infected with MRSA 252 and African walnut oil 31.25 mg/mL had some members of the group developing brownish pellicle on the second day which was different from the blackish melanized pellicle observed in group infected with MRSA 252 and vancomycin and the infected non-treated group. While some in the group developed melanin. The members with brownish pellicle were seen to survive three days after this development with only few dead. The group infected with MSSA 15.6 mg/mL had greater survival with no dead recorded after 5 days. But from the third day of infestation, brownish pellicles were observed. Considering the results, overall greater survival of *G. mellonella* was recorded after the infection treatment of MRSA 252 and *S. aureus* ATCC 6538 using African walnut oil.

## Chapter 8. Identification of Active type of Components in African Walnut Oil

### 8.1 Introduction

African walnut (*Tetracarpidium conophorum*- Mull. Arg) is a perennial climbing shrub which grows mainly in Africa, particularly in the Western regions of Africa (Uzunova *et al.*, 2015). It is mainly found in Nigeria and other neighbouring countries such as Equatorial Guinea and Cameroon, Gambia, Sierra Leone and Gabon (Ojeda-Amador *et al.*, 2018). Nuts of African walnuts grow in pods which contains 2 to 5 nuts. The nut is composed of two cotyledons which are encased in a hard-shell-like case. Usually, after maturity, the nuts are harvested between month of June and September. In Nigeria, the nuts are consumed as snacks. Also, the flour is used as a soup thickener especially by the Yoruba tribe (Bada *et al.*, 2010). In ethnobotanical medicine, the nut is extensively used in decoctions for treatment of several ailments such as dysentery, constipation, abdominal cramps and general fever, as well as in management of chronic diseases such as diabetes, malaria, male sterility dysfunctions, cancer and high blood pressure (Bada *et al.*, 2010; Rahimi *et al.*, 2011; Kris-Etherton, 2014; Zibaenezhad *et al.*, 2016). African walnut leaves are scrubbed between the hands to get exudates for first hand treatments of wounds and as home remedies for skin infections such as rash, eczema (Ajaiyeoba and Fadare, 2006; Lin, Zhong & Santiago 2017; Dawid-Pać, 2013). African Walnut oil is known for its curative potential, general body nourishment and hence ability to boost the immune system of the humans (Ajaiyeoba and Fadare, 2006).

African walnuts contain kernels that have high amount of glyceride oil (Uzunova *et al.*, 2015). It varies widely (53-76%), depending on the cultivation place, variety, place of growing and irrigation process of walnut trees. Regarding the fatty acid composition of African walnut unsaturated fatty acids are predominant particularly – linolenic, oleic and linoleic acid. The different ratio of these acids determines the nutritional content of African walnut oil. In addition, monounsaturated fatty acids also have a beneficial effect on human health (Crews *et al.*, 2005; Ojeda-Amador *et al.*, 2018). The present study is a preliminary investigation of the active compounds in walnut oil that may be responsible for its antibacterial activity.

## 8.2 Results

### 8.2.1 Identification of fatty acid methyl esters (FAMES) of Supelco 37 standards mix using GC-MS spectrometry

#### 8.2.1.1 Fatty acid profile of Supelco 37 standard FAME mix

GC-MS was used to separate and identify the compounds in FAME mix (C8 - C24) standard. In the FAME mix, 33 out of 37 compounds were identified and their retention times are presented. Table 42 presents the list of the FAME compounds identified. Identification of FAME standards were necessary to allow effective comparison of their retention times with those of African walnut oil.

**Table 42. Elution order and retention times of compounds observed in standard FAME mix (C8 - C24) from GC-MS analysis.**

S/N	FAME C8-C24 mix components	Retention time (min)
1	Caprylic acid (C8:0)	5.193
2	Capric acid (C10:0)	8.135
3	Undecylic acid (C11:0)	11.247
4	Lauric acid (C12:0)	14.163
5	Tridecanoic acid (C13:0)	17.309
6	Myristoleic acid (C14:1)	20.151
7	Myristic acid (C14:0)	20.561
8	Pentadecanoic acid (C15:1, cis 10)	23.404
9	Pentadecanoic acid (C15:0)	23.800
10	Palmitic acid (C16:0)	26.309
11	Palmitoleic acid (C16:1)	26.989
12	Heptadecanoic acid (C17:1, cis 10)	29.420
13	Heptadecanoic acid (C17:0)	30.073
14	$\alpha$ -linolenic acid (C18:3,	32.387
15	Linoleic acid (C18:2)	32.087
16	Oleic acid (C18:1, cis 9)	32.275
17	<u>Linolelaidic</u> acid (C18:2)	32.350
18	Elaidic acid (C18:1, trans 9)	32.470
19	Stearic acid (C18:0)	33.054
20	Arachidonic acid (C20:4 n6),	36.776
21	Arachidonate acid (C20:4),	36.964
22	Ticosatrienoic acid (C20:3, cis 11)	37.286
23	Eicosadienoic acid (C20:2, cis11)	37.821
24	Eicosenoic acid (C20:1, cis 11)	37.599
25	Eicosenoic acid (C20:2, trans 11)	37.807
26	Arachidic acid (C20:0)	38.688
27	Heneicosylic acid (C21:0)	41.346

28	Docosahexaenoic acid (C22:6)	41.943
29	Erucic Acid (C22:1)	43.246
30	Behenic Acid (C22:0)	43.907
31	Tricosylic acid (C23:0)	46.464
32	Nervonic acid (C24:1)	48.720
33	Lignoceric acid (C24:0)	49.583

The table above shows the profile of fatty acids methyl esters. Arrangement of the compounds was from Frau and Frau, (2010).

### 8.2.1.2 Chromatograms of FAME mix (C8 - C24) standard

**Standard FAME mix-expanded (5-30 min)**

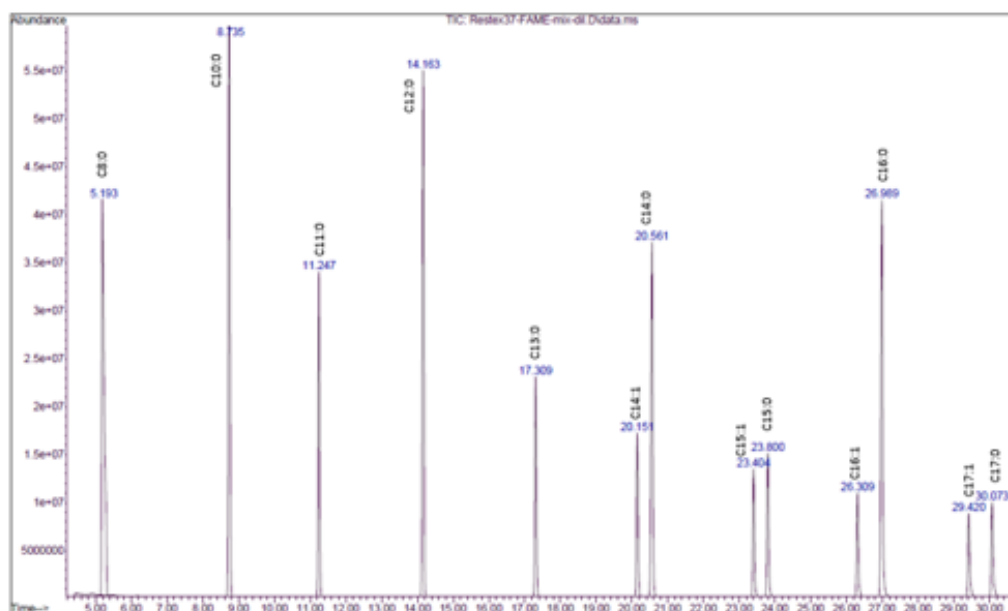


**Figure 123. GC-MS chromatogram showing peaks of fatty acid methyl esters (C8:C17) and their retention times identified in Supelco standard FAME mix.**

### Standard FAME mix-expanded (31-39 min)

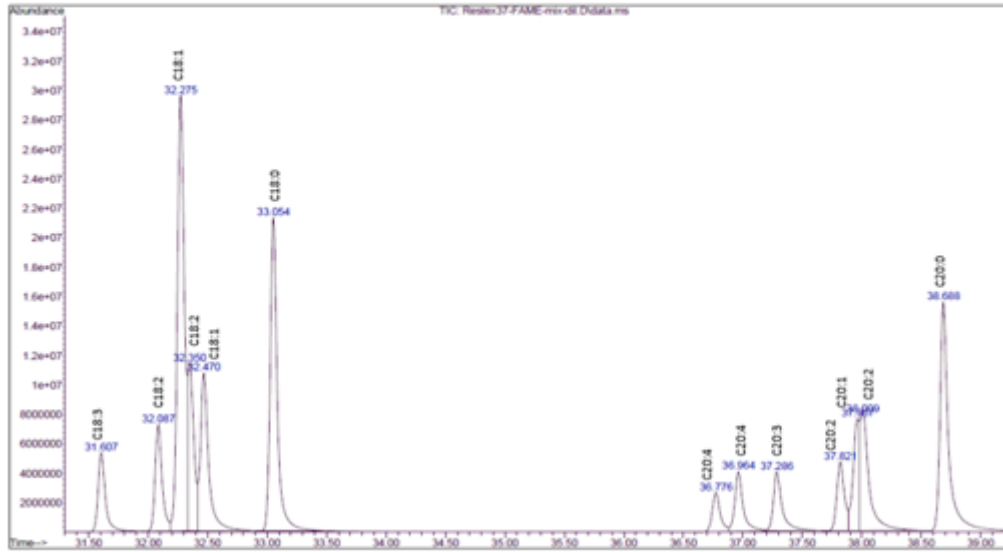


Figure 124. GC-MS chromatogram showing peaks of fatty acid methyl esters (C18:C20) and their retention times identified in Supelco standard FAME mix.

### Standard FAME mix-expanded (41-50 min)

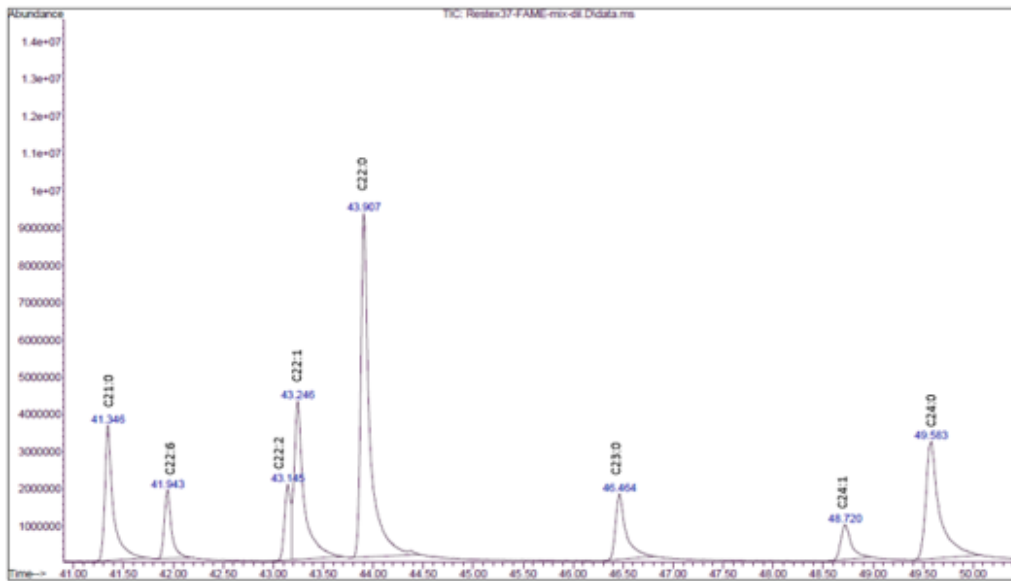


Figure 125. GC-MS chromatogram showing peaks of fatty acid methyl esters (C21:C24) and their retention times identified in Supelco standard FAME mix.

### 8.2.2 Fatty acid profile of African walnut oil (GC-MS results of walnut oil FAME)

The fatty acid profile of African walnut oil was determined as corresponding methyl esters, using gas chromatography. Chromatogram of fatty acid methyl esters identified in African walnut oil is presented in Figure 127. The chromatogram clearly shows that there are 5 (five) major peaks with retention times ranging from 18.68 to 32.39 min. Although 4 (four) other minor peaks were also observed. The peak with the greatest abundance is shown by the highest peak with retention time of 32.39 min having relative percentage of 80.59%. Further analysis by mass spectrometry indicates that this peak is methyl linolenate, characterized by a molecular ion at  $m/z = 292$ , which is in very good agreement with the molecular weight of methyl linolenate. Mass spectra of other peaks showed good evidence that the final product of transesterification is purely a mixture of fatty acid methyl esters. Furthermore, the distribution of fatty acids based on percentage area (Figures 126), shows that the five main fatty acids methyl esters identified included saturated, monounsaturated and polyunsaturated fatty acids. The saturated fatty acids identified include palmitic acid and stearic acid. Only one monounsaturated fatty acid eicosenoic acid was identified. Also, the polyunsaturated fatty acids were dominantly linoleic and linolenic acid otherwise called  $\alpha$  linolenic acid (alpha linolenic acid). Besides the fatty acids reported other minor fatty acids observed include caprylic acid (C8:0 this means the compound has 8 carbon atoms and zero bonds), myristic acid (C14:0), palmitoleic acid (C16:1), heptadecanoic acid (C17:1, cis 11), heptadecanoic acid (C17:0) and arachidic acid. List of fatty acid methyl esters identified in African walnut oil is presented in Table 43. In addition, a pie chart showing their distribution is shown in Figure 151. The GC-MS spectrum of the individual peak is presented in Figure 152.

**Table 43. Fatty acid methyl ester profile of African walnut oil**

Peak No	Fatty acid methyl ester	Area %	Molecular weight (g/mol)	Retention times
1	Palmitic acid (C16:0)	1.53	270	26.98
2	Linoleic acid (C18:2)	13.05	294	32.16
3	Linolenic acid (C18:3)	80.59	292	32.39
4	Stearic acid (C18:0)	4.41	298	33.07
5	Eicosenoic acid (C20:0)	0.42	325	18.68

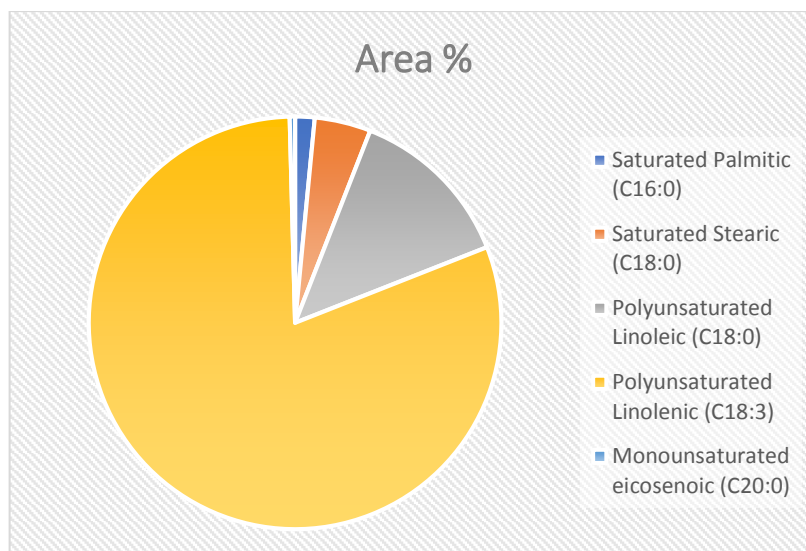


**Figure 126. Fatty acids methyl esters identified in African walnut oil and proportion through GC-MS results.**

Result shows a higher percentage of polyunsaturated fatty acid linolenic acid with 80.59%.

### 8.2.2.1 Chromatograms and spectra results of FAME of African walnut oil

Figure 127 below shows the GC-MS spectrum of fatty acid methyl esters identified in African walnut oil.

**African walnut oil FAME (the peaks labelled was confirmed from the mass fragmentation spectra).**

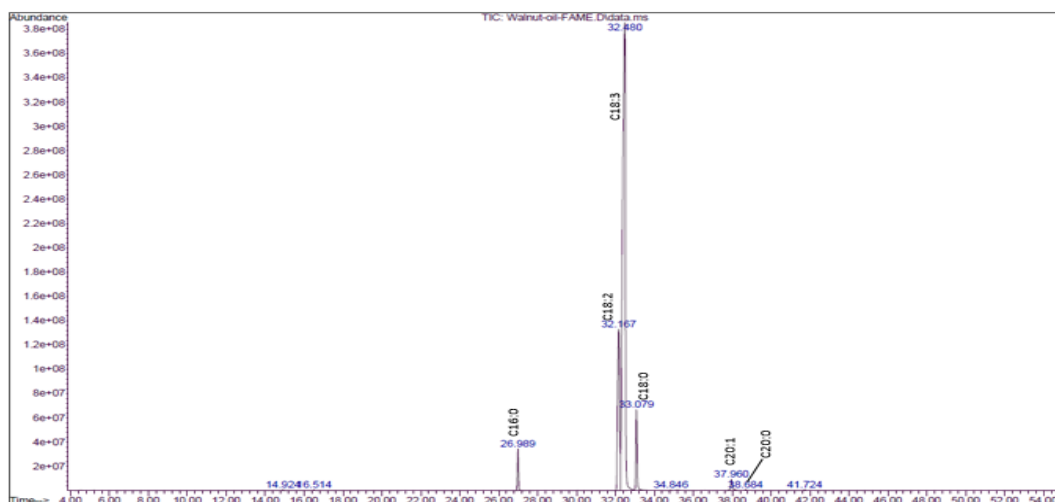


**Figure 127. GC-MS chromatogram of major fatty acid methyl esters identified in African walnut oil with their retention times.**

Figure 127 shows the presence of five (5) major fatty acids between C16:0 and C20:1 which includes palmitic, linoleic, linolenic, stearic and eicosenoic acid as listed in Table 43. In the chromatogram, the peak with the greatest abundance is shown by the highest peak with retention time of 32.39 min and is Linolenic (C18:3). On the spectra's, the mass of the fragment

divided by the charge is called the mass to charge ratio (M/Z). The x-axis represents the M/Z ratios. The y-axis represents the signal intensity (abundance) for each of the fragments detected during the scan.

### Mass fragmentation of peak 32.39 min, (C18:3)

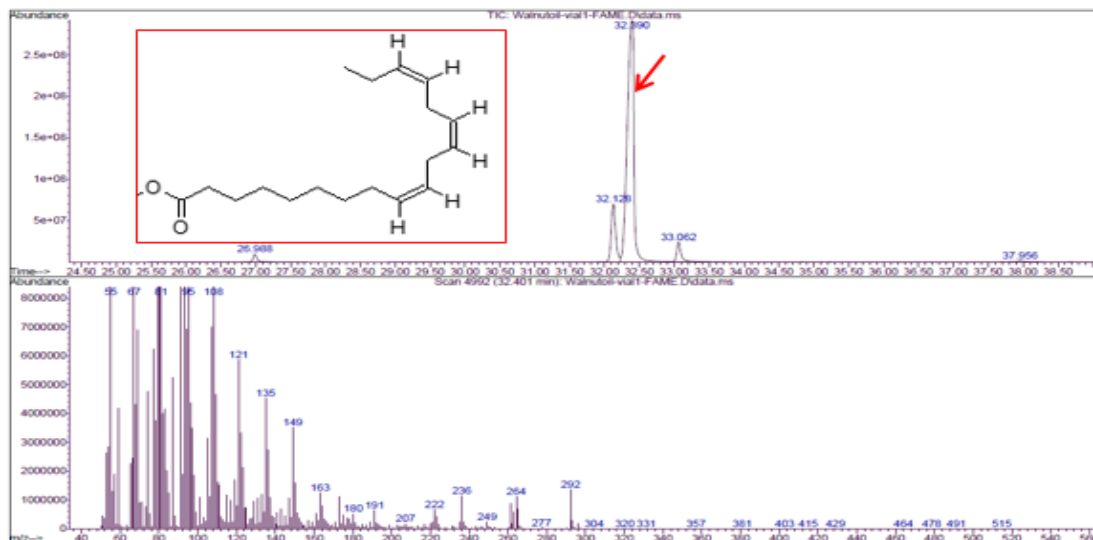


Figure 128. Mass spectrum of linolenic acid methyl ester (C18:3) identified in African walnut oil with a retention time of 32.39 min and an m/z of 292 corresponding to its molecular weight.

### Mass fragmentation of peak 26.98 min, (C16:0)



Figure 129. Mass spectrum of palmitic acid methyl esters (C16:0) identified in African walnut oil with retention times 26.98 min and an m/z =270 corresponding to its molecular weight.

### Mass fragmentation of peak 32.12 min, (C18:2)

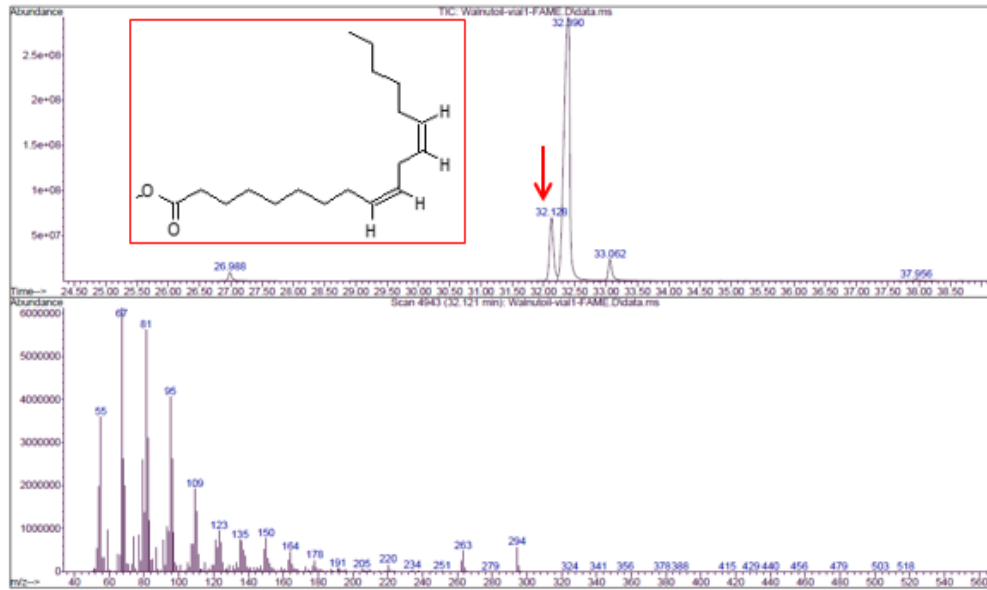


Figure 130. Mass spectrum of linoleic acid methyl esters (C18:2) identified in African walnut oil with retention time of 32.12 min and  $m/z = 294$

### Mass fragmentation of peak 33.06 min, (C18:0)

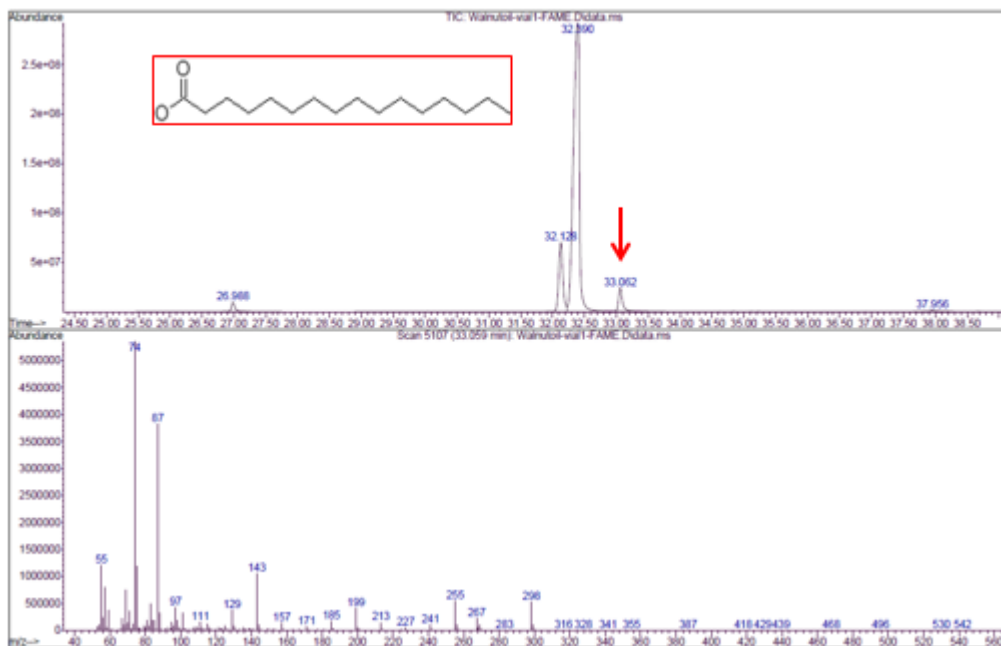


Figure 131. Mass spectrum of stearic acid methyl esters (C18:0) identified in African walnut oil with retention time of 33.06 and  $m/z = 298$ . The x-axis represents the M/Z ratios.

### Mass fragmentation of peak 37.95 min, (C20:1)

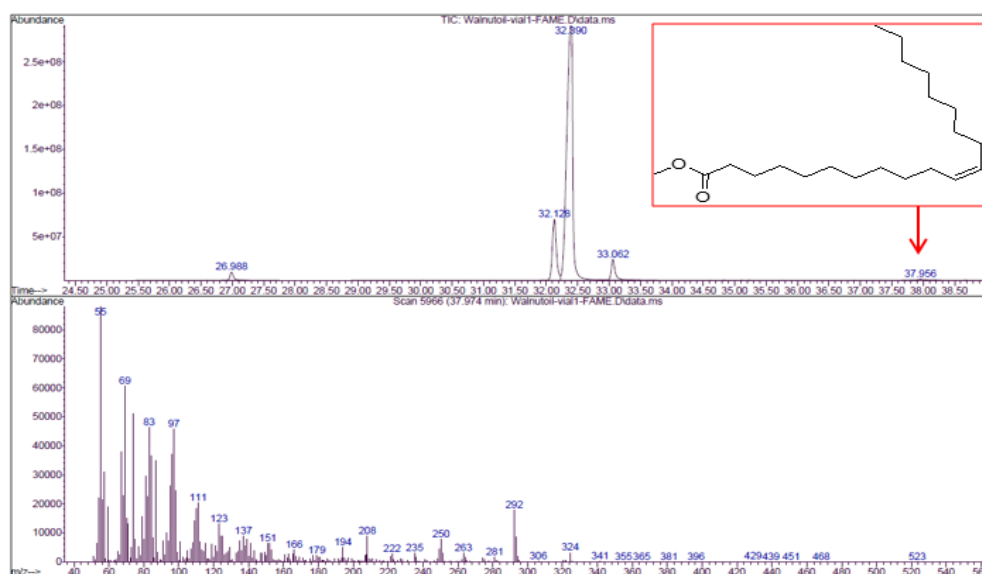


Figure 132. GC-MS chromatogram and spectrum of eicosenoic acid methyl esters (C20:1) identified in African walnut oil with retention time of 37.95 min and  $m/z = 292$ .

## 8.2.3 Chemical and antimicrobial investigation of the active fractions of African walnut oil

### 8.2.3.1 Separation and purification of African walnut oil

Fraction distillation was used to separate and purify cold pressed African walnut oil into different fractions. The cold pressed extraction method of African walnut oil yielded (69 g). 100 mL of the oil was distilled, and the vapour yielded 4 (four) fractions as presented in Table 44. This distillation process was based on the difference in boiling point among all compounds in the mixture of fatty acids. Generally, the boiling point of fatty acids such as linoleic acid was 230 °C, linolenic acid (230 °C), palmitic acid (351 °C), stearic acid (361 °C) and eicosanoic acid (328 °C) (Bono, Pin & Jiun 2010). However, because of their high boiling temperature, vacuum distillation helped to reduce temperature and separation into four distinct fractions were obtained.

**Table 44. Data of fractions temperature range and the yield of each African walnut oil fraction**

Fractions	Temperature (°C)	Volume (mL)
A. 1	80-115	14.3
B. 2	115-125	23.0
C. 3	125-135	17.9
D. 4	135-145	9.7

Table 44 presents the yield of each fraction, with fraction 2 and 3 having the largest quantity indicated by its largest volume among the four fractions. The collected fractions appeared in different colours, as a yellow viscous liquid (Figure 133). Bioassay guided fractionation of African walnut oil was used to identify the most active fraction in the oil.

#### **8.2.3.2 Bioassay-guided fraction and antimicrobial activity of African walnut oil fractions.**

The fractional separation of walnut oil was performed in a vacuum distillation column and several fractions of oil distillate were collected and their antimicrobial property was analyzed. The four fractions were tested for antimicrobial activity against MRSA 252 and *S. aureus* ATCC 6538. The various fractions were tested for antimicrobial activity using Kirby bauer well diffusion assay Figure 133.

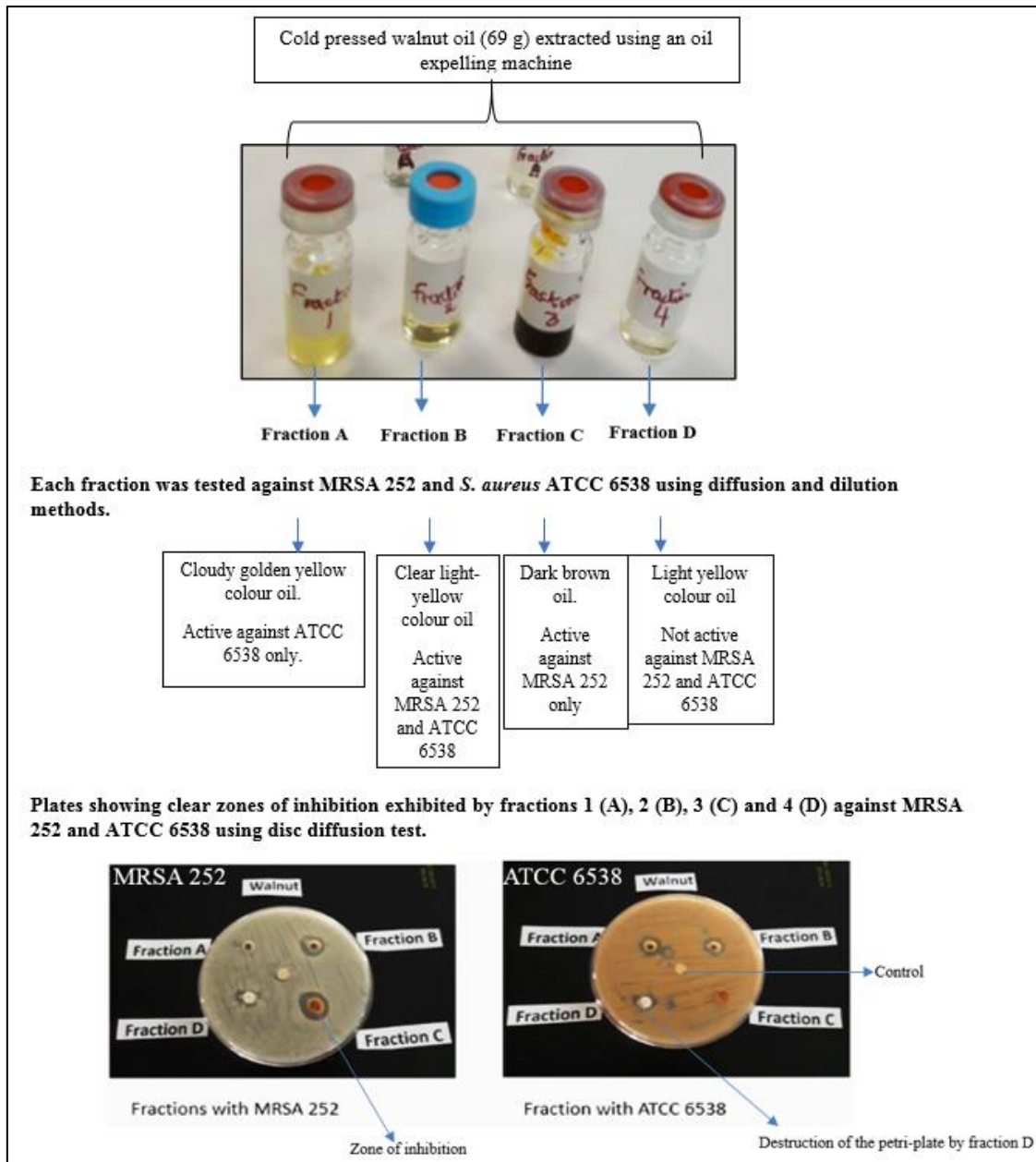


**Figure 133. Scheme of bioassay guided-fractionation of African walnut oil and antimicrobial activity of the four fractions.**

Disc diffusion assay showing zones of each fraction tested on MRSA 252 and ATCC 6538. (A) Fraction A activity on MRSA 252 and ATCC 6538. (B) Fraction B activity on MRSA 252 and ATCC 6538. (C) Fraction C activity on MRSA 252 and ATCC 6538. (D) Fraction D activity on MRSA 252 and ATCC 6538.

**Table 45. Diameter of inhibitory zones produced by the four fractions**

Fractions	Diameter of the zones (mm)	
	MRSA 252	ATCC 6538
A. 1	No growth (no clear zone)	12 mm
B. 2	13 mm	12 mm
C. 3	16 mm	No growth (no clear zone)
D. 4	No growth (no clear zone)	No growth (no clear zone)

Figure 133 shows the zones of diameter obtained from the activity of the different fractions on MRSA 252 and *S. aureus* ATCC 6538. The zones of diameter were obtained from agar wells filled with 15  $\mu$ L of the 100 % pure fraction and incubated for 24-48 h at 37 °C. The antimicrobial activity of each fraction was evaluated by measuring the diameter of the clear zone of inhibition of growth against the test organisms (MRSA 252 and ATCC 6538) in comparison to a control (no fraction added, just 6 mm diameter disc filled with 0.5% DMSO (15  $\mu$ L).

According to the results, there was variation in the activity of the different fractions against MRSA 252 and ATCC 6538. As observed in the diameter of zones, MRSA 252 was resistant to fractions A and D (was not active), while fractions B and C was active (clear zones). For ATCC 6538, surprisingly fraction A became active as well as fraction B. However, the strain was resistant to C and D as no clear zones were observed on the plate in these areas.

## 8.2.4 Molecular structure identification

### 8.2.4.1 Fourier transform infra-red spectroscopy of African walnut oil fractions

FTIR spectra of African walnut oil fractions (Fractions A, B and C) obtained via fractional distillation, were collected between numbers of 4000 and 600  $\text{cm}^{-1}$  and results are presented in figures 134 to 136. In the FTIR spectra quite intensive bands which may be attributed to specific functional groups of fatty acids were obtained. Peaks in the spectra are similar since the studied vegetable oil is mainly composed from triglyceride with certain fatty acids. However, the spectra of studied oil fractions reveal a bit differences in terms of band intensities and the exact frequencies at which the maximum absorbance are generated in each fraction. In

the presented absorption spectra of the three fractionated oil samples, they exhibited a broad band in the region from 3400 – 2800  $\text{cm}^{-1}$ . Bands identified in FTIR spectra of the fractions as listed in Tables 46 – 48 confirms the presence of volatile compounds at varying bending and stretching such as aldehydes, alkanes, alcohols, esters and derivatives of carboxylic acid.

### Fraction A

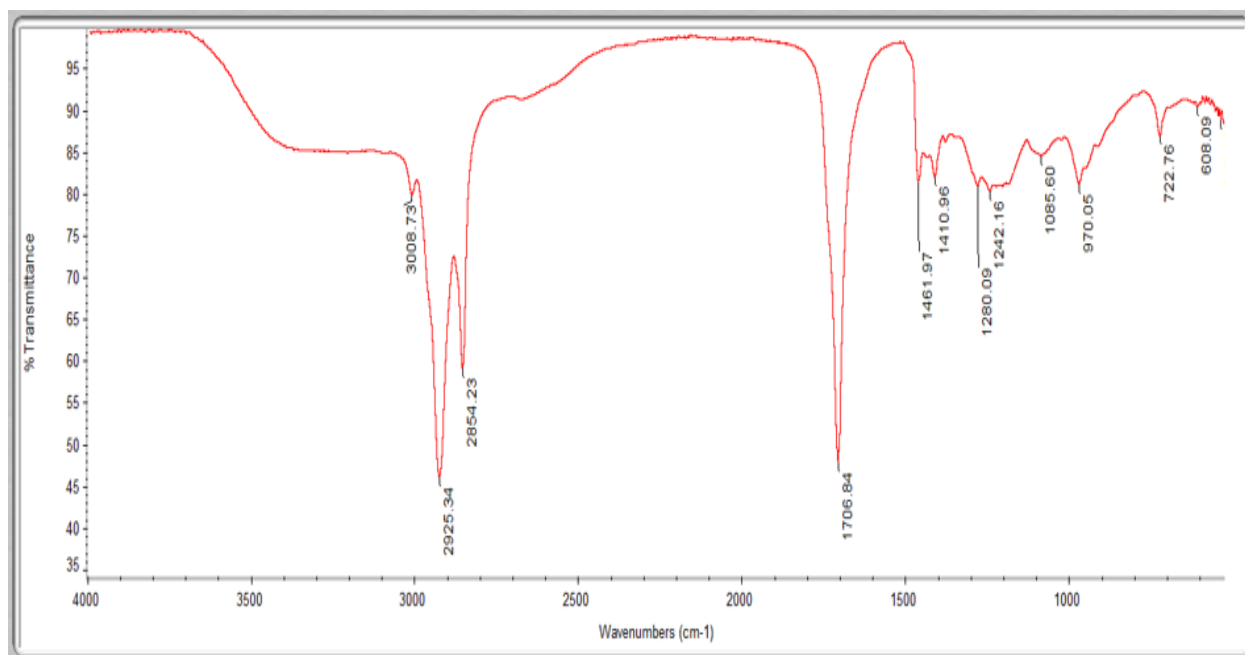


Figure 134. FTIR spectrum of fraction A obtained from fractional distillation of African walnut oil.

Table 46. Infrared absorption of fraction 1 (A) of African walnut oil

Frequency $\text{cm}^{-1}$	Peak assignment
3008	= C-H (cis) stretch Fatty acid back bone
2924	C-H methyl stretch asymmetrical or $\text{CH}_2$
2854	C-H methyl stretch symmetrical Aliphatic group of triglycerides or $\text{CH}_2$ .
1704	-C=O stretch bends
1481	C-H methylene scissoring
1410	C-H methylene scissoring
1280	-C-O stretch
1242	-C-O stretch
1085	-C-O stretch
970	=CH (trans)
722	=C-H (cis) bending out of plane conjugated

FTIR frequencies in this study were assignment according to Rohman and Man, (2011) and Liang *et al.*, (2012). Results presented in table 46 shows the position of absorption bands with the appropriate vibration in spectral range from 4000 to 600  $\text{cm}^{-1}$  for fraction A of African walnut oil.

### Fraction B

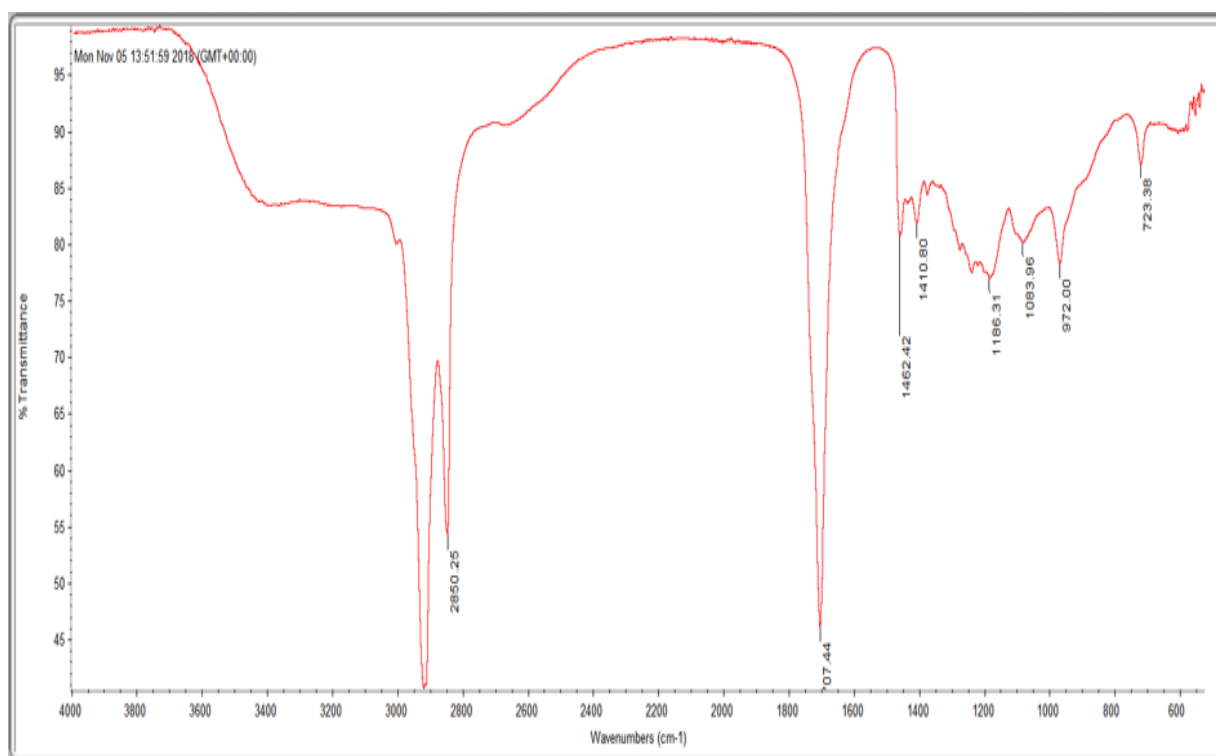


Figure 135. FTIR spectrum of fraction B obtained from fractional distillation of African walnut oil

Table 47. Infrared absorption of fraction 2 (B) of African walnut oil

Frequency $\text{cm}^{-1}$	Peak assignment
2924	C-H methyl stretch asymmetrical or $\text{CH}_2$
2850	C-H methyl stretch symmetrical Aliphatic group of triglycerides or $\text{CH}_2$
1707	C=O stretch
1462	C-H methylene scissoring bends
1410	C-H methylene scissoring bends
1186	-C-O stretch; - $\text{CH}_2$ weak bending
1083	-C-O stretch; - $\text{CH}_2$ weak bending
972	=CH (trans)
723	=C-H (cis) bending out of plane conjugated

FTIR frequencies in this study were assignment according to Rohman and Man, (2011) and Liang *et al.*, (2012). Results presented in table 47 shows the position of absorption bands with the appropriate vibration in spectral range from 4000 to 600  $\text{cm}^{-1}$  for fraction B of African walnut oil.

### Fraction C

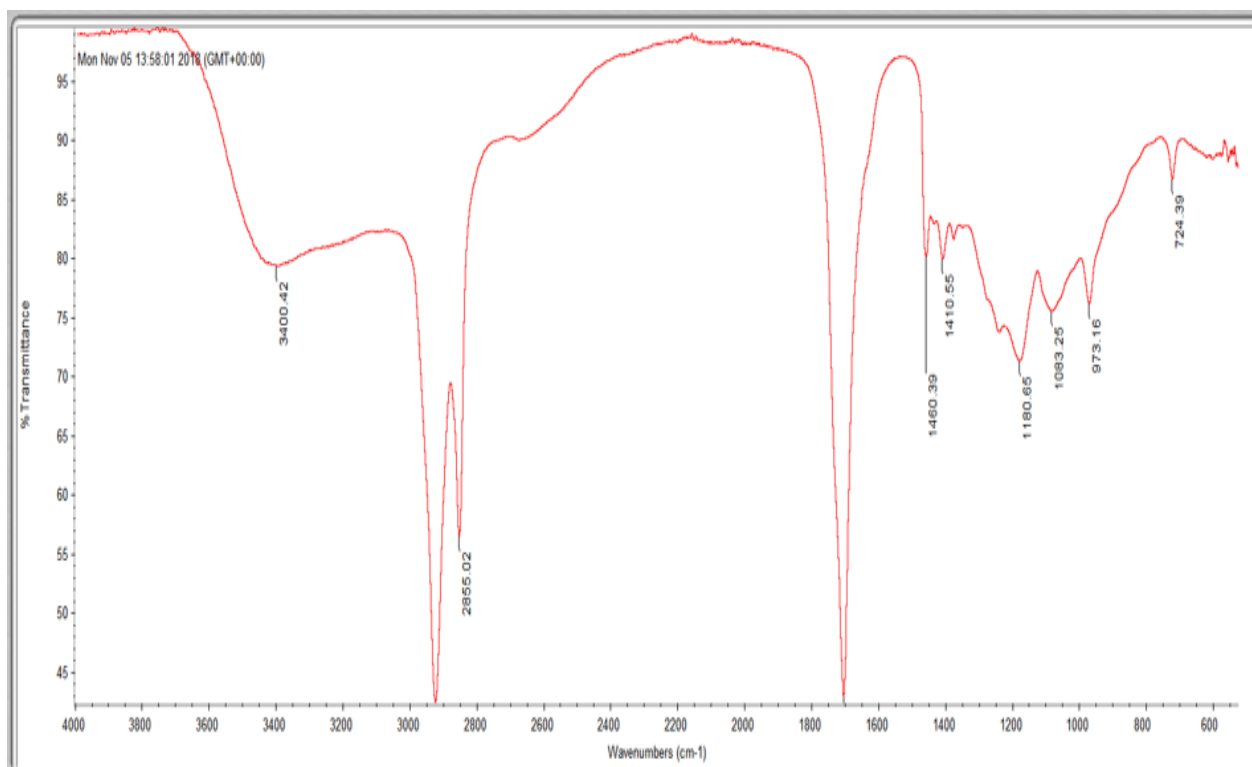


Figure 136. FTIR spectrum of fraction C obtained from fractional distillation of African walnut oil.

Table 48. Infrared absorption of fraction C of African walnut oil

Frequency $\text{cm}^{-1}$	Peak assignment
3400	Bending out of plane.
2924	C-H methyl stretch asymmetrical or $\text{CH}_2$
2855	C-H methyl stretch symmetrical Aliphatic group of triglycerides or $\text{CH}_2$
1700	-C=O stretch
1480	C-H methylene scissoring
1083	-C-O stretch
973	-C-H (trans)
724	=C-H (cis) bending out of plane conjugated

FTIR frequencies in this study were assignment according to Rohman and Man, (2011) and Liang *et al.*, (2012). Results presented in table 48 shows the position of absorption bands with the appropriate vibration in spectral range from 4000 to 600  $\text{cm}^{-1}$  for fraction C of walnut oil.

#### **8.2.4.2 Nuclear magnetic resonance of African walnut oil fractions obtained from fractional distillation**

Based on the result obtained from the antimicrobial analysis (diameter of zones) of each fraction tested, fractions 2 and 3 were further examined to determine their active component.

#### **Proton NMR ( $^1\text{H}$ -NMR), Carbon NMR ( $^{13}\text{C}$ NMR) and $^{13}\text{C}$ APT results of fractions of African walnut oil**

Proton NMR classifies the presence of a hydrogen functional group.  $^1\text{H}$  NMR spectrum of fractions 1(A) - 3 (C) of African walnut oil is shown in tables 49-52. The presence of alkanes, carbonyl, and alkene groups with proton shifts are observed and it is detailed in Table 49-52. Varying signal characteristics for the shifts were observed in the fractions which includes doublets, triplet, quartet and multiplets. In addition,  $^{13}\text{C}$  NMR was performed to allow the identification of carbon atoms in each fraction of African walnut oil. Further-more,  $^{13}\text{C}$  Carbon APT test provides information about the protons attached to carbon atoms in each fraction.

#### **Fraction 2 (B)**

The  $^1\text{H}$  NMR spectrum of fraction 2 is shown in Appendix 1. The hydrogen proton of the major functional groups present in the fraction were assigned according to literature (Cipriani *et al.*, 2009) and are shown in Table 49.  $^1\text{H}$  NMR spectra of fraction 2 show some characteristic chemical shifts corresponding to different functional groups in the fraction. Chemical shifts for hydrogen protons peaks were recorded between 0.85-5.3 ppm. Chemical shift at 0.85 ppm show a  $\text{CH}_3$  methyl group saturated with  $\text{CH}_2$  groups but the  $\text{CH}_3$  appears to be overlapping with another  $\text{CH}_3$ . Chemical shift at 0.98 ppm shows linolenic acid. At 1.3 and 1.6 ppm  $\text{CH}_2$  groups are observed. At shift of 2.35 ppm a  $\text{CH}_2$  attached to a carbonyl is apparent. Chemical shift at 2.07 ppm and 2.8 ppm, alkane and alkene type hydrogen were observed. The olefinic protons was observed at shift 5.3 ppm. However, a strong peak at chemical shift 5.37 ppm ensures the presence of esters in major composition (Hariram *et al.*, 2016). In addition, the proton shifts obtained in fraction 2 at a chemical shift of 0.85 and 0.98 ppm which indicates the presence of  $\text{CH}_3$ s with linoleic and oleic as well as linolenic protons were also identified in  $^1\text{H}$  NMR spectra

of linolenic acid. This peak corresponds to CH<sub>3</sub> group harboured by both linoleic and oleic acid, which provides the terminal methyl backbone of fatty acid structure (Cipriani *et al.*, 2009). However, a comparative assessment of fraction 2 and linolenic <sup>1</sup>H NMR spectra showed clearly that fraction 2 strongly exhibited very similar shifts (apart from those observed at 0.85 and 0.98) as linolenic acid (Table 49). Therefore, the spectra of fraction 2 is in a very good agreement with the standard chromatogram of linolenic acid, thus it can be certainly concluded that these spectra represent linolenic acid which collected as fraction 2 of reduced pressure distillation at 115-125°C (See Appendix 1). Furthermore, different signal characteristics were observed at the various chemical shifts identified in <sup>1</sup>H NMR spectrum of fractions 2 (Table 49). In the <sup>1</sup>H NMR spectrum of fractions 2, the CH<sub>3</sub> signal is a triplet, the CH<sub>2</sub> signals are multiplets, carbonyl (-OCO-CH<sub>2</sub>-) signals are triplets and quartet. Proton NMR for fraction 2 and linolenic acid are presented below. The spectra of linolenic acid are provided as evidence of great similarity between fraction 2 and linolenic acid (Appendix 4).

### **Carbon NMR (<sup>13</sup>C-NMR)**

<sup>13</sup>C-NMR technique spectrum for fraction 2 is shown in Appendix 2 and Table 50 shows the complete inferences of the spectral data. On analysing the <sup>13</sup>C NMR spectrum of fraction 2, signal was found between 14.05-14.09 ppm and this indicates the presence of methyl carbon region (CH<sub>3</sub>), signal between 20.53-34.04 ppm indicates the presence of CH<sub>2</sub> (alkane), another alkene carbon region (127.11 – 131.94 ppm) and carbonyl region (179.86 ppm). Hybridizations sp<sup>3</sup> for CH<sub>3</sub> and CH<sub>2</sub>, sp<sup>2</sup> for C=C and sp for C=O are observed. CDCl<sub>3</sub> deuterated chloroform was observed in 76.72-77.36 ppm which is peculiar to all <sup>13</sup>C-NMR spectra. No quaternary carbon was observed in the spectra. Furthermore, the linolenic acid <sup>13</sup>C NMR spectrum also showed similar result (Appendix 5).

### **<sup>13</sup>C Attached-Proton Test (APT)**

Fraction 2 Spectra obtained for APT showed signal of methyl carbon region (CH<sub>3</sub>) at 9.73-14.11 ppm, olefinic (127.73-130.20 ppm) (Table 50 and Appendix 3). CH<sub>2</sub> signal was present between 22.67-43.81 ppm and carbonyl region (179.5 ppm). CH<sub>3</sub> signals are pointing upward because the carbon has odd number of hydrogen atoms and all the CH<sub>2</sub> pointed downwards because the carbon has even number of hydrogen atoms. CDCl<sub>3</sub> deuterated chloroform was observed in 76.73-77.37 ppm. This result was also not too different from signals observed on the spectra of linolenic acid (Appendix 6).

### **Proton NMR (<sup>1</sup>H-NMR), Carbon NMR (<sup>13</sup>CNMR) and APT results of fractions 3**

<sup>1</sup>H NMR spectrum classifies the presence of hydrogen functional group at various places of carbon chain of fraction 3. <sup>1</sup>H NMR spectrum of fractions 3 shows the presence of alkanes, carbonyl, alkene and glyceric group. This is detailed and presented in Table 51. Varying signal characteristics for the shifts were observed in the fractions which includes doublets, triplet, quartet and multiplets. Carbon NMR (<sup>13</sup>C NMR) and APT are also provided in Table 52.

<sup>1</sup>H NMR spectra of fraction 3 show some characteristic chemical shifts corresponding to different functional groups in the fraction. Chemical shifts for hydrogen protons peaks were recorded between 0.80-5.3 ppm. Chemical shift at 0.80 ppm show a CH<sub>3</sub> methyl group next to a CH<sub>2</sub> group but with another CH<sub>3</sub> group next to a CH<sub>2</sub>. At 1.3 and 1.5 ppm CH<sub>2</sub> (alkanes) were observed. At shift of 2.0 and 2.3 ppm alkane type hydrogen and most likely an ester type hydrogen was observed. Chemical shift at 2.7 ppm shows CH<sub>2</sub> an alkane type hydrogen observed. At 4.0-4.2 ppm, glycerol hydrogens are observed and lastly at 5.3 ppm an alkane type hydrogen which represent the olefinic protons were observed. The chemical shift observed between 4.0-4.2 ppm confirms the presence of glyceric group (Cipriani *et al.*, 2009). However, a comparative assessment of fraction 2, 3 and linolenic <sup>1</sup>H NMR spectra showed clearly that fraction 2 strongly exhibited very similar shifts (apart from those observed at 0.8-0.9 and 4.0-4.2 ppm) as linolenic acid. Therefore, the spectra of fraction 3 is in a very good agreement with the standard chromatogram of linolenic acid, thus it can be certainly concluded that these spectra represent linolenic acid but contains glycerol group that may be responsible for the fraction prominent antimicrobial activity as observed on MRSA 252 (appendix 10 and appendix 11). This is the fraction which was collected as fraction 3 of reduced pressure distillation at 125-135°C (See Appendix 7).

### **Carbon NMR (<sup>13</sup>C NMR)**

<sup>13</sup>C NMR spectrum for fraction 3 is shown in Appendix 8 and Table 52. On analysing the <sup>13</sup>C NMR spectrum of fraction 3, signal was found between 13.70-14.14 ppm and this indicates the presence of methyl carbon region (CH<sub>3</sub>), signal between 20.42-32.76 ppm indicates the presence of CH<sub>2</sub> (alkane), another carbon region (126.96 – 131.51 ppm) and carbonyl region (172.21-172.56 ppm). No quaternary carbon was observed in the spectra. Furthermore, the linolenic acid <sup>13</sup>C NMR spectrum also showed similar result.

### Attached-Proton Test (APT)

Spectra obtained for APT showed signal of methyl carbon region (CH<sub>3</sub>) at 14.11 ppm, CH<sub>3</sub> (129.73-130.03 ppm). CH<sub>2</sub> signal was present between 21.96-33.95 ppm and carbonyl region (179.42-179.70 ppm). CH<sub>3</sub> signals are pointing upward because the carbon has odd number of hydrogen atoms and all the CH<sub>2</sub> pointed downwards because the carbon has even number of hydrogen atoms. CDCl<sub>3</sub> deuterated chloroform was observed in 76.71-77.34 ppm. This result was also not too different from signals observed on the spectra of linolenic acid (Appendix 9).

From the results, 33 fatty acid methyl esters out of Supelco 37 FAME standards mix were identified and a few of them compare favourably well in terms of their retention times with the compounds identified in walnut oil FAME. FAME sample of walnut oil showed the presence of five (5) compounds and this also compare favourably well with previous results. Through fractional distillation, four fractions were obtained in walnut oil and their antimicrobial activity against MRSA 252 and ATCC 6538 strains showed that the strains were both susceptible to the fractions although they exhibited strong resistance to fractions A. Analysis of FAME sample of walnut oil also showed not much of the sample is required to inhibit the growth of the strains. In structure elucidation, the FTIR spectra show quite intensive bands which may be attributed to specific functional groups of fatty acids and both the Proton NMR (<sup>1</sup>H NMR), Carbon NMR (<sup>13</sup>C NMR) and APT results of fractions 2 and 3 of walnut oil show clearly that the active component in walnut oil is linolenic acid and the presence of a glyceric group observed in fraction 3.

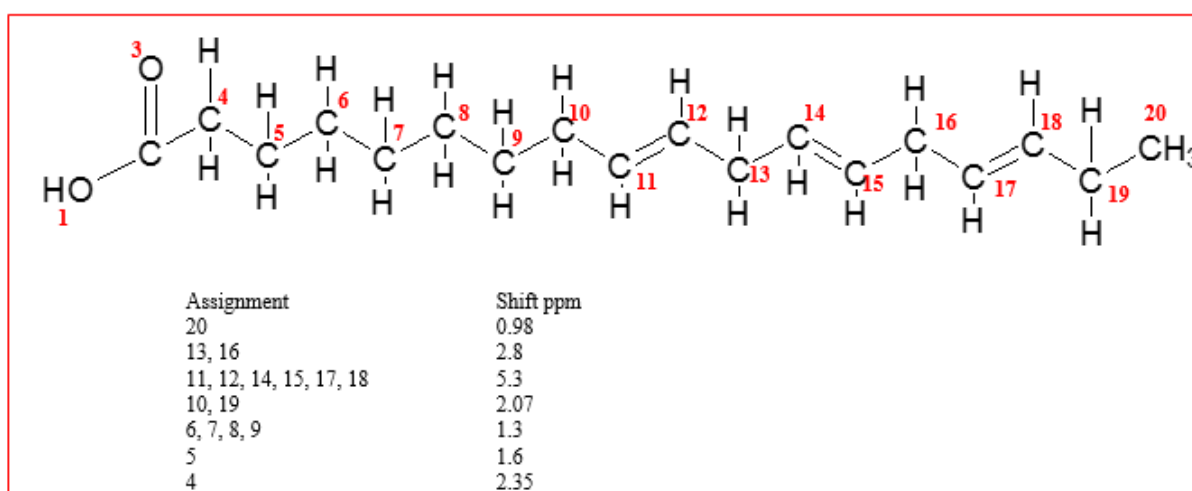


Figure 137: Linolenic acid showing protons and assigned peak

**Table 49. Chemical shifts and assignments of the characteristic resonances in the <sup>1</sup>H NMR spectra of fraction 2 (A) of African walnut oil and linolenic acid standard.**

<b>Fraction 2 of African walnut oil</b>		
<b>δ (ppm)</b>	<b>Inferences of <sup>1</sup>H NMR</b>	<b>Signal characteristics</b>
0.85	CH <sub>3</sub> (Terminal, saturated, oleic and linoleic chain)	Triplet
0.98	CH <sub>3</sub> (Terminal linolenic chains)	Triplet
1.3	-(CH <sub>2</sub> ) n- (Methyl group - Alkane)	Multiplets
1.6	-OCO-CH <sub>2</sub> -CH <sub>2</sub> -	Quartet
2.07	-HC=CH=CH <sub>2</sub>	Multiplet
2.35	-OCO-CH <sub>2</sub> -	Triplet
2.8	-HC=CH-CH <sub>2</sub> -CH=CH- (Alkane)	Multiplets
5.3	-CH=CH- (Alkene, Olefinic region all unsaturated fatty acids)	Multiplets
<b>Linolenic acid standard</b>		
<b>δ (ppm)</b>	<b>Inferences of <sup>1</sup>H NMR</b>	<b>Signal characteristics</b>
0.98	CH <sub>3</sub> (Terminal linolenic chains)	Triplet
1.3	-(CH <sub>2</sub> ) n- (Methyl group - Alkane)	Multiplets
1.6	-OCO-CH <sub>2</sub> -CH <sub>2</sub> - (Esters)	Quartet
2.07	-HC=CH=CH <sub>2</sub>	Multiplets
2.35	-OCO-CH <sub>2</sub> - (Ester)	Triplet
2.8	-HC=CH-CH <sub>2</sub> -CH=CH- (Alkane)	Multiplets
5.3	-CH=CH- (Alkene, Olefinic region all unsaturated fatty acids)	Multiplets

**Table 50. Chemical shifts and assignments of the characteristic resonances in fraction 2 of African walnut oil**

<b>Fraction 2 of walnut oil <sup>13</sup>C NMR</b>		
<b>Chemical shift (ppm)</b>	<b>Carbon type</b>	<b>Signal characteristics</b>
20.53-34.04	C sp <sup>3</sup> (likely CH <sub>2</sub> ) bonded to CH <sub>3</sub>	Multiplets
76.72, 77.04, 77.36	---	CDCl <sub>3</sub>
127.11-131.94	C sp <sup>2</sup> (likely CH) bonded to carbonyl C sp <sup>2</sup>	Singlet and doublet
179.86	C sp <sup>2</sup> (likely C=O) carbonyl C sp <sup>2</sup>	Singlet
14.05, 14.09, 14.25	C sp <sup>3</sup> (likely CH <sub>3</sub> )	
<b>APT Shift</b>		
21.94-43.81	C sp <sup>3</sup> (likely CH <sub>2</sub> ) bonded. Even numbers point downward	Singlet, doublet, triplet
179.42, 179.51, 179.70	C sp <sup>2</sup> (likely CH) bonded to carbonyl C.	Triplet
9.73, 14.11	C sp <sup>3</sup> CH <sub>3</sub> (Odd numbers point up).	Singlet
127.73-130.20	C sp <sup>2</sup> CH <sub>3</sub> . (up)	Triplet, quadruplet
Quaternary carbon	-----	
<b>Linolenic acid standard <sup>13</sup>C NMR</b>		
<b>Chemical shift (ppm)</b>	<b>Carbon type</b>	<b>Signal characteristics</b>
20.55-34.09	C sp <sup>3</sup> (likely CH <sub>2</sub> ) bonded to CH <sub>3</sub>	Singlets, triplets
76.35, 77.03, 76.72	----	CDCl <sub>3</sub>
127.11-131.95	C sp <sup>2</sup> (likely CH) bonded to carbonyl C sp <sup>2</sup>	Singlet and doublet
180.39	C sp <sup>2</sup> (likely C=O) carbonyl C sp <sup>2</sup>	Singlet
14.27	C sp <sup>3</sup> (likely CH <sub>3</sub> )	
<b>APT Shift</b>		
20.55-34.09	C sp <sup>3</sup> (likely CH <sub>2</sub> ) bonded. Even numbers point downward.	Doublet, quadruplets
76.72, 77.03, 77.36		
14.27	CH <sub>3</sub> (pointing up)	Singlet
127.11-131.95	CH <sub>3</sub> (pointing up)	

<sup>13</sup>C NMR and APT spectra of Fraction 2 (100 MHz in CDCl<sub>3</sub> + TMS)

**Table 51. Chemical shifts and assignments of the characteristic resonances in the  $^1\text{H}$  NMR spectra of fraction 3 of African walnut oil**

$\delta$ (ppm)	Fraction 3 Inferences of $^1\text{H}$ -NMR	Signal characteristics
0.80	$\text{CH}_3$	Doublet
0.90	$\text{CH}_3$	Triplet
1.3	$\text{CH}_2$ (Methyl group - Alkane)	Multiplet
1.5	$\text{CH}_2$	Multiplet
1.9	$-\text{CH}_2-\text{CH}=\text{CH}$ (All allylic all unsaturated fatty acids)	Multiplet
2.2	$-\text{CH}_2-\text{C}=\text{C}$	Multiplet
2.7	$\text{CH}_2-\text{C}=\text{O}$	Doublet
4.0	$\text{CH}_2\text{OCOR}$ (Glyceric region all unsaturated fatty acids)	Doublet
4.2	$\text{CH}_2\text{OCOR}$ (Glyceric region all unsaturated fatty acids)	Quadruplet
5.3	$\text{CH}=\text{CH}$ (Alkene, Olefinic region all unsaturated fatty acids).	Triplet

**Table 52. Chemical shifts and assignments of the characteristic resonances in the  $^{13}\text{C}$  NMR and APT spectra of Fraction 3 (100 MHz in  $\text{CDCl}_3$  + TMS)**

Fraction 3 of walnut oil $^{13}\text{C}$ NMR		
Chemical shift (ppm)	Carbon type	Signal characteristics
20.42-33.93	C $\text{sp}^3$ (likely $\text{CH}_2$ ) bonded to $\text{CH}_3$	Quadruplet and triplet
126.96-131.55	C $\text{sp}^2$ (likely CH) bonded to carbonyl C $\text{sp}^2$	Quadruplet and triplet
172.21, 172.56	C $\text{sp}^2$ (likely $\text{C}=\text{O}$ ) carbonyl C $\text{sp}^2$	Doublet
13.70, 13.94, 13.98, 14.14,	C $\text{sp}^3$ (likely $\text{CH}_3$ )	Quadruplet
APT Shift C13APT		
21.96-33.95	C $\text{sp}^3$ (likely $\text{CH}_2$ ) bonded. Even numbers point downward	Multiplets
76.71, 77.03, 77.71	$\text{CDCl}_3$	Triplets
180	C $\text{sp}^2$ (likely CH) bonded to carbonyl C or $\text{C}=\text{O}$ .	Singlet
14.12	C $\text{sp}^3$ $\text{CH}_3$ (Odd numbers point up).	Singlet
129.73, 130.03	C $\text{sp}^2$ CH. (up)	Doublet,
Quaternary carbon	-----	

### 8.3 Discussion

To date, this is the first study to give detailed fatty acid composition of African walnut screw press oil fractions from Nigeria. In a previous study on the fatty acids of African walnut oil, it was established that palmitic (C16:0),  $\alpha$ -linolenic (C18:3), linoleic (C18:2) were the main components of the oil (Nkwonta, 2015). Tchiegang, Kapseu & Parmentier (2001) also reported same types of saturated and polyunsaturated fatty acids in walnut cultivars grown in Cameroon. Although different capillary columns were used by both authors, they still noted that the most abundant fatty acid was the conjugated C18:3 - linolenic acid (70 %) followed by C18:2 (linoleic acid), and C18:0 (palmitic acid) fatty acids. These findings are in good correlation with the results obtained in this present study and suggest a strong similarity between the oil of African walnuts grown in Nigeria and Cameroon despite different ecological factors that possibly influence the growth of the plants. In this present study, polyunsaturated fatty acids were observed as major components with strong indication of linolenic acids (C18:3) as the major fatty acid component of walnut oil. In previous studies no glyceric group has been reported (Ajayi, 2009; Bello, and Anjorin 2012). Whereas, in this study, the presence of glyceric groups at chemical shifts between 4.2-4.3 ppm in fraction 3 was observed in addition to other groups. According to our finding, African walnut oil may be a good source of glyceric acid.

According to Harwood (1980) the major fatty acids in seed oils are palmitic, linoleic and linolenic acids. Linolenic acid is the most usual polyunsaturated fatty acids found in seed fats. Linolenic acid is the most usual form of triethenoid C18 acid found in seed oils. It forms 50% or more of the mixed fatty acids in linseed oil, and occurs in other seed oils (Harwood, 1980). In this study linolenic acid was the predominant fatty acid found in walnut oil and its fractions. Ohta *et al.*, (1995) investigated the activity of ten different fatty acids and their methyl esters against *S. aureus* and MRSA. They found that palmitic acid (C16:0), stearic acid (C18:0) and oleic acid (C18:1) had no activity, but fatty acids with two or more double bonds (starting with C18:2) were more active. Of the polyunsaturated fatty acids tested, the activity of  $\gamma$ -linolenic acid (C18:3) and  $\alpha$ -linolenic acid (C18:3) was the highest, eicosapentaenoic acid (C20:5), and docosahexaenoic acid (C22:6) also had strong activity. The methyl esters were either inactive or much less active than the other acidic form. In this study polyunsaturated acid particularly, linolenic acid, (C18:3) is a carboxylic acid with 18 carbon chain and three cis double bonds was found to be active causing bactericidal activity on MRSA 252 and ATCC 6538. In addition,

pure linolenic acid was observed to inhibit biofilm formation in MRSA 252 and ATCC 6538 at varying concentrations of 7.8 and 15.6 mg/mL respectively which was not different from the FAME sample. This value seems lower than the MBIC values obtained for African walnut oil and indicate that a lower concentration is needed to inhibit the growth of MRSA 252 and ATCC 6538. However overall, FAME sample of walnut oil fraction 2 as well as fraction 3 showed promising activity against methicillin susceptible and resistant strains. Therefore, in contrast to the findings of Ohta *et al.*, (1995) FAME sample of walnut oil was active. Orhan *et al.*, (2011) reported that Linolenic acid possesses additional interesting antibacterial activity. Orhan and his co-workers (2011) investigated the antibacterial activity of  $\alpha$ -linolenic on a pathogenic MRSA strain in an hospital in Japan and demonstrated that  $\alpha$ -linolenic was able to significantly inhibit the growth of MRSA in the growth medium. In this study, disc diffusion assay was able to show that fractions 2 and 3 appeared to be bactericidal on the growth of MRSA 252 and ATCC 6538 since this was observed by the clear zones obtained on Mueller Hinton agar after 24-48 h). Surprisingly fraction 4 appeared too acidic by its ability to destroy the petri-plates. The findings obtained in this study correlates with those of other authors who suggested that inhibitory activity of walnut oil on *S. aureus* is associated with the presence of linolenic acid. Yoon *et al.*, (2018) reported that linolenic acid present in walnut oil play crucial role in inhibiting the growth of *S. aureus*. Its inhibitory activity is associated with an increase in the permeability of the bacterial membrane. The interaction of linolenic acid in plant oils with bacterial cell membranes can destabilize the membrane and increase membrane permeability, thereby inducing leakage of cytosolic contents. In extreme cases, the increased permeability and corresponding membrane destabilization can eventually lead to cell lysis. Similarly, Greenway and Dyke (1979) reported that linolenic acid caused the damage of *S. aureus* cell membranes. Membrane leakage after linolenic acid treatment was detected by measuring the release of biomolecules (e.g., glutamic acid) from bacteria.

African walnut oil, with its very high proportion of linoleic and linolenic acid, contributes to a balanced diet and helps prevent cardiovascular diseases (Saxenaa *et al.*, 2009; Ros, 2010; Alasalvar and Bolling 2015). In this study, the presence of linolenic acid found as major fatty acid of walnut oil show clinical potentials of walnut oil in reducing the risk factors of cardiovascular and coronary heard diseases as well as type 2 diabetes. In a study conducted by Ohta *et al.* (1995)  $\alpha$ -Linolenic acid is considered to have low toxicity and may be used clinically to treat patients infected with MRSA. It is naturally occurring, and hence unfavourable reactions would not be anticipated, it should not destroy the commensal flora, resistance to it

would not develop, and there would apparently be no risk of resistance to antibiotics developing during its use.

## Chapter 9. General Discussion and Future Research

### 9.1 Summary of main findings

*S. aureus* is a human pathogenic strain responsible for numerous infections (Gordon and Lowy, 2008). Its pathogenicity is aided by its ability to form biofilms and the wide range of virulence factors produced by it (Morell and Balkin, 2010). Its ability to form biofilms makes the infections very difficult to treat thus causing high rates of morbidity and mortality in many countries of the world (Hall-Stoodley, Costerton & Stoodley 2004). The biofilm forming ability of *S. aureus* catalysed mainly by the presence of its biofilm formation genes plays a key role in protecting the pathogen from antibiotics in the sessile state and contribute immensely to the manifestation of antibiotic resistances exhibited by the strain (Silva *et al.*, 2016) which makes treatment of *S. aureus* infections very difficult to treat (Hall-Stoodley, Costerton & Stoodley 2004). On the other hand, production of other virulence genes such as the adhesion genes and antibiotic resistance genes, accompanied by its biofilm forming potential contributes to the emergence and prevalence of MRSA infections in various health-care settings world-wide (Gill *et al.*, 2005; Davies and Davies, 2010).

One of the greatest problems of solving an infection is when the pathogenic organism is resistant to antibiotics (Davies and Davies, 2010). This is the case of MRSA. MRSA is of concern when it comes to treatment because it is resistant to numerous drugs. The pathogen is now resistant to antibiotics belonging to different classes such as penicillins, cephalosporins, aminoglycosides, tetracyclines, macrolides and fluoroquinolones (Levy and Marshall, 2004; O'neil, 2008). However, some strains of *S. aureus* still remain susceptible to just two antibiotics such as clindamycin and gentamicin (Marston *et al.*, 2016). Most worrisome is the fact that this pathogenic strain now resides in many health-care systems including intensive care units across the world especially in under-developed countries and everyone visiting the hospital is at risk, since majority of MRSA clinical infections occur in patients who have been in the hospital for long period, patients who have been admitted during MRSA era, patients with cuts, lesions, or wounds, patients with inserted medical device such as catheters and patients placed on antibiotics (Bhat and Tenguria, 2014). Despite tremendous efforts by the medical system in establishing measures such as the institution of standard treatment guidelines to check antibiotic prescriptions and usage, infection control measures such as hand hygiene and good professional practice in hospitals, limited achievements have been made in curbing the menace of MRSA (Abdullahi and Iregbu, 2018). This is the current situation in Nigeria and other

African countries that are under-developed. In Nigeria, drug prescription of antibiotics can be given to patients for treatment of mild infections without due procedure, there is lack of uniformity in drug prescription despite treatment guidelines, and high cost of healthcare facilities which does not allow proper routine infection control (David and Daum, 2010; Abdullahi and Iregbu, 2018). All these three factors hinder the successful reduction of MRSA in the country.

Again, a major concern is the increase in the incidence of multidrug-resistant MRSA staphylococcal organisms and the development of new clones of MRSA in both developed and underdeveloped countries. In Nigeria, recent research studies have found that the prevalence of MRSA in Nigeria is between 28% and 30% with an increase in toxic clonal lineages which include CC80, CC30, CC152 and CC5 in hospitals and environment (Abdulgader *et al.*, 2015). Therefore, substantial measures to curb the emergence of sophisticated MRSA in both the hospitals and community is necessary especially in ensuring strict application of treatment guidelines and provision of infection control facilities (Abdulgader *et al.*, 2015; Abdullahi and Iregbu, 2018).

While many studies have been carried out in search of novel active plant antimicrobials with a special focus on the plant extracts from leaves, root and barks of plants due to their active secondary metabolites against MRSA recent studies about treating MRSA infections have focussed on deriving natural antimicrobials from plants and combination with antibiotics (Lewis, 2013; Fair and Tor, 2014; Gupta and Birdi, 2017). Thus, in a continuing search for natural products with antibacterial activity against MRSA, the aim of this study was to identify novel oils from walnut (*Tetracarpidium conophorum*), Fluted pumpkin (*Telfairia occidentalis*), Cashew (*Anacardium occidentale*). Walnut, cashew and pumpkin were first identified as nuts and seeds that likely harbour oils with antimicrobial potential, possess phytochemical constituents and unobserved potentials in treating *S. aureus* infections using a collection of different methodologies such as mechanical and chemical, phytochemical, biochemical and microbiological.

In this thesis, walnut, cashew and pumpkin oils were extracted using mechanical extraction method and their various extracts were obtained using chemical methods. Mechanical extraction was done using screw press and a combination of best extraction solvents with good polarities described in previous studies (Akpuaka and Nwankwor, 2000; Ajaiyeoba and Fadare, 2006; Maduabuchi and Onyebuchi, 2016). For the first time, this thesis is producing detailed

comparison of both expelled oils and solvent extracted oils. The mechanical method produced expelled oils while the chemical method was the solvent extraction method in which three main solvents namely, n-hexane, chloroform and petroleum ether were used to obtain extracts. So far, results presented in chapter 3 of this thesis showed that a total of three different extracts were obtained for walnut, cashew and pumpkin, making a total of 9 extracts examined. Both the expelled pressed oils and their respective extracts were of good quality and colour varied from brown to shades of yellow. Although the solvent extracted method particularly n-hexane gave high yield more than the other extracts.

In addition, with preliminary phytochemical screening, we identified individual groups of phytochemicals in the oils and extracts using ultra violet absorption. The different groups obtained are identified in literature has important secondary metabolites that could be active components responsible for curative purposes of human infections. In the expelled oils, this study identified similar groups of phytochemicals such as flavonoids, alkaloids, saponins, tannins and terpenoids present in walnut and pumpkin oil, flavonoids, alkaloids and tannins were found in cashew oil. Their respective extracts were mainly found to contain flavonoids, saponins and tannins with variations in alkaloids and terpenoids. The different groups were concluded to be bioactive agents that could be responsible for the antibacterial activity of the oils and extracts against methicillin resistant and susceptible *S. aureus* strains; MRSA 252 and ATCC 6538 tested in this thesis. However, previous reports have showed that walnut oil contain the same phytochemicals identified in this study indicating that the medicinal role of the oil could be associated with the classes of phytochemicals identified in the oil. In addition, the presence of varied combination of phytochemicals in the solvent extracts particularly in n-hexane extracts is an indication that the solubility of phytochemicals in various solvents depends on the polarity of the solvents. In this study, we established that n-hexane produced the highest yield of oil with more classes of phytochemicals a similar observation made by (Maduabuchi and Onyebuchi, 2016). This could be related to its effectiveness against MRSA 252 and ATCC 6538 compared to other extracts. Because numerous studies have reported the antifungal, anti-inflammatory, analgesic and antibacterial potentials of alkaloids and flavonoids in walnut (Ajaiyeoba and Fadare, 2006; Zakavi *et al.*, 2013), therefore the result of this present study may also suggest that walnut oil could also have an anaesthetic potential, wound healing potential and possibly anti-inflammatory activity. In all, results presented in chapter 3 of this thesis showed that oils could be extracted from walnut, cashew and pumpkin using both mechanical and solvent extraction methods producing different yields and that both

the oils and extracts possessed different classes of phytochemicals that could be responsible for their antibacterial properties.

Microbiological tests to confirm *S. aureus* strains were used in this study. These include morphological appearances such as colonial appearances on general purpose media were assessed. This simple test confirmed their colonial appearances on agar media as golden yellow, creamy with trypticase soy agar and Columbia blood base agar as appropriate media suitable for their growth. Biochemical tests such as catalase test and lysostaphin tests were used in this thesis to further also confirm and characterise MRSA 252 and *S. aureus* ATCC 6538 used in this study. Both strains were catalase positive and lysostaphin positive. This confirmatory result led to the investigation of their biofilm forming capacity. The aggregation phase of biofilm formation of bacteria is linked to the secretion of extracellular polysaccharides referred to as slime which play a key role in bacterial adhesion to surfaces (Torlak *et al.*, 2017). In this study we established the biofilm forming potentials of MRSA 252 and *S. aureus* ATCC 6538 using a simple phenotypic test method such as Congo red to detect their slime production. Appearances of black colonies on Congo red agar plates revealed that the *S. aureus* strains used in this study has the ability to form biofilm. Similar approach to determine biofilm forming ability of *S. aureus* strains have been reported in previous studies (Atshan *et al.*, 2012; Atshan *et al.*, 2013). Thus, in this thesis, MRSA 252 was identified as a biofilm former and a strong one while *S. aureus* ATCC 6538 was also a biofilm former but weak. Quantification of their biofilms were assessed using the microtiter plate method. This made it clearer that biofilm formed by both strains was either strong or weak. The results presented in chapter 4 of this thesis showed that MRSA 252 and *S. aureus* ATCC 6538 were *S. aureus* strains exhibiting different colonial morphologies, are biofilm formers and classified into different categories based on their degree of biofilm formation.

Various potentials of each oil sample and extract was determined on MRSA 252 and ATCC 6538 biofilms. These includes the ability of the oils to kill the strains, inhibit the growth of the strains, eradication of the strains and possible synergism with antibiotics. Due to the identification and classification of the biofilm forming capacity of MRSA 252 and *S. aureus* ATCC 6538 biofilms, their susceptibility to different concentrations of walnut, cashew and pumpkin oils were determined using standard methods such as disk diffusion agar, minimum inhibitory concentration, minimum biofilm inhibitory concentration and minimum biofilm eradication concentration. In this study, both the agar well diffusion and disk diffusion tests used in some previous reports (Magaldi *et al.*, 2004; Ajaiyeoba and Fadare, 2006) were used

to determine whether the oils could kill MRSA 252 and ATCC 6538 in biofilms. This was investigated by determining the susceptibility of MRSA 252 and ATCC 6538 biofilms to walnut, cashew and pumpkin oils. In the results, walnut oil exhibited the highest activity with the strains tested compared to cashew and pumpkin oils. At 1000 mg/mL, it had an activity of  $(23.04 \pm 0.21)$  and  $(19.00 \pm 0.22)$  mm with MRSA 252 and ATCC 6538 biofilms. Furthermore, the antibacterial activity of walnut, cashew and pumpkin extracts displayed poor antibacterial activities at 1000 mg/mL. Although the n-hexane extract of walnut oil produced the highest activity.

On the other hand, possible synergism of walnut, cashew and pumpkin oil with varying concentration of antibiotics in different classes (already listed in paragraph 2 of this chapter) were determined. The concept of combining walnut extract with commercial antibiotics have been previously described by Ogbolu and Alli, (2012) although this thesis has elaborated the research on biofilms. This test was carried to determine whether the oils could serve as better antibacterial agents in the treatment of *S. aureus* infections. The activities of the oils in combination with the antibiotics were tested against MRSA 252 and *S. aureus* ATCC 6538 biofilms. Interestingly results obtained which are shown in chapter 5 of this thesis, showed that firstly, the oils alone (single treatment with oils only) showed varying susceptibility indicating antibacterial activity against the strains, secondly that the oils in combination with some antibiotics resulted in varying degrees of drug interactions such synergism, potentiation effect, antagonism which are the four groups of drug interactions identified in literature and thirdly that drugs that produced small zones in diameter (low activity) that their activity enhanced by combination with oils. In the result obtained for this analysis, walnut oil was found to produce profound combination effects with drugs such as gentamicin, carbenicillin, streptomycin, vancomycin, trimethoprim and oxacillin. This result shows a successful trial of plant oil in combination with antibiotics. To this end, this analysis is the first to be carried out on a collection of these expelled oil samples and it suggests that the oil samples particularly walnut oil could be serve as antibacterial agent with therapeutic purposes in disease treatment against methicillin resistant and susceptible *S. aureus* strains.

Similarly, all the individual extracts of walnut, cashew and pumpkin except chloroform showed activity with the *S. aureus* strains. Only the n-hexane extract of walnut showed the highest activity with MRSA 252 and ATCC 6538. In addition, this study showed that both the expelled oils and extracts displayed concentration-dependent antibacterial activities in a concentration range of 0.98 mg/mL-500 mg/mL. This activity was determined when MICs, MBICs and

MBECs of the oils and extracts were investigated. Using the micro-broth dilution method, our result showed for the first time, that walnut, cashew and pumpkin oils showed antibacterial activities against MRSA 252 and ATCC 6538 biofilms. Walnut oil exhibited the highest inhibitory effect on planktonic and 24 h preformed biofilms of MRSA 252 and ATCC 6538. The growth of MRSA 252 and ATCC 6538 biofilms were significantly decreased in planktonic cells faster than in biofilms (probably because of the presence of slime covering which is responsible for the resistant nature of biofilms). However, this study, showed promising antibacterial potential of walnut oil against MRSA 252 and ATCC 6538 biofilms than cashew and pumpkin oils. The potential of the oils to eradicate MRSA 252 and ATCC 6538 biofilms was determined. This was by using the high throughput screening assay to obtain the eradication concentration of each oils sample. Their ability to eradicate the strains was determined over a period of 6 h, 12 h, 24 h and 48 h. This study was undertaken to determine the effect of walnut, cashew and pumpkin oil on 48 h preformed biofilms of MRSA 252 and ATCC 6538. In this study, we present the log-reductions of viable counts of both strains at the different time points. Furthermore, to our knowledge, this is also the first-time log-reductions of viable counts of *S. aureus* strains are determined after treatment with these types of oils. To this end, concentration dependent reduction of both strains was observed, and walnut oil had the capacity to eradicate the biofilms of MRSA 252 and ATCC 6538 compared to cashew and pumpkin. The microbiological analysis presented in chapter 5 of this thesis suggests that walnut oil may be useful as natural antimicrobial agent in the treatment of *S. aureus* infections. Our findings in this study showed that walnut oil possess the potential to kill, inhibit and eradicate the growth of planktonic cells of MRSA 252 and ATCC 6538 as well as the preformed biofilms of the strains. These potentials could no otherwise be related to the presence of phytochemicals observed in chapter 3 of this thesis.

The combinational test results presented for antibiotic synergy with walnut and pumpkin oil in chapter 6 indicated that both oils could be used in single treatment against MRSA and ATCC 6538 as well in combination with antibiotics. Using fractional inhibitory concentration, the synergistic activity of walnut and pumpkin oil with selected antibiotics against MRSA and ATCC 6538 was determined to ascertain whether the drug reactions observed on the disc plates were real. This study found that the best combination of walnut oil was with vancomycin, streptomycin and trimethoprim which showed lowest FIC index value (FIC Index  $\leq 0.5$ ). This combination was able to work effectively well on both MRSA 252 and ATCC 6538. While for pumpkin oil, combination with gentamicin alone produced synergy. Thus, in thesis we show

for the first time that walnut oil may effectively be combined with antibiotics for maximum results in treatment of *S. aureus* infections when used in minimally low concentrations. Furthermore, biofilm kinetic time assay in Chapter 6 of this thesis showed that walnut, cashew and pumpkin oils exhibit the potential of killing MRSA 252 and ATCC 6538 strains with time. This was performed by growing the biofilms first on 96-well plates and then treated each well of the plate with different concentration of walnut and pumpkin oil. Based on the results, findings in this thesis showed that walnut and pumpkin oils can reduce the viable counts of MRSA 252 and ATCC 6538 strains in biofilm with time. Viable counts in MRSA 252 and ATCC 6538 biofilms were recorded in log reduction forms. However, walnut oil showed the highest log reduction in 2 hours after which the count became zero. In this chapter, using *G. mellonella* to mimic the human infection model, the efficacy of using plant oil particularly walnut oil in treating *S. aureus* infections were tested. *G. mellonella*, is used in this thesis because it exhibits similar immunological responses to infection as in human. Recently, this has been widely used in many studies in determining the pathogenicity of pathogenic strains (Pollitt *et al.*, 2018; Yang *et al.*, 2017). This study showed that MRSA 252 exhibited stronger pathogenicity characterized by the forming of thick pellicles called melanin compared to ATCC 6538. This was observed when  $10^0$  of MRSA 252 and ATCC 6538 inoculums were injected into the worm. However,  $10^{-5}$  –  $10^{-4}$  of the same inoculums resulted in reduced number of deaths. Treatment of *G. mellonella* infected with  $10^0$  inoculums of MRSA 252 and ATCC 6538 and treated with 31.25 mg/mL and 15.6 mg/mL concentrations of walnut oil (which was the eradication concentrations), showed that waxworms survived for some days even though they developed another form of pellicle which appears different to the blackish melanin.

The investigation of gene regulation of walnut and pumpkin oil against MRSA and ATCC 6538 strains is described in chapter 7. This was carried out using standard molecular method such as reverse transcriptase polymerase chain reaction (RT-PCR) and quantitative real time PCR (qRT-PCR). In this analysis, virulence genes involved in biofilm formation, adhesion, quorum sensing, and antibiotic resistance were tested in MRSA 252 and ATCC 6538 biofilms were identified. In this study, only genes confirmed to be present in the biofilms of *S. aureus* strains tested had their expression levels determined. This thesis showed the expression of the virulence genes in MRSA 252 and ATCC 6538 biofilms before and after treatment with walnut and pumpkin oils which makes the findings of the thesis the second and quite different from that of Atshan *et al.*, (2013) who was the first to study the expression of adhesion and biofilm genes of *S. aureus* cultures at different growth time points without treatment. Our study showed

in chapter 7 of this thesis that without treatment, generally adhesion genes were downregulated at 12 h in *S. aureus* strains, up-regulated at 24 h and down-regulated at 48 h. However, treatment with oil further down-regulated the genes. A few biofilm genes like *fnbA*, *fnbB*, *clfB* and *eno*, were up-regulated at 12 h, 24 h and 48 h. Although exceptional cases of up-regulation were observed at 24 h for *fnbB* and *icaC*. Interestingly in this study we show that walnut and pumpkin oils significantly inhibited the expression of all the biofilm and adhesion genes as well as the regulatory gene and antibiotic resistance genes such as *agrA*, *blaZ*, and *mecA* genes. *AgrA*, *blaZ*, and *mecA* genes tested are responsible for the regulation of gene expressional levels at exponential and post exponential phases of growth, penicillin and methicillin resistance in *S. aureus*.

Lastly, results presented in chapter 8 of this thesis showed the preliminary investigation of fatty acid components present in walnut oil. Attempts to identify the fatty acid components of walnut oil was carried out because it was found to be the most active oil. This attempt made it possible for vital fatty acids in walnut oil to be identified. This study showed that five (5) fatty acid compounds were observed in walnut oil with some minor ones. This was obtained using GC-MS technique. However, linolenic acid was found to be the most predominant fatty acid in the oil. This same compound has been reported in previous report of Tchiegang, Kapseu & Parmentier (2001) and Nkwonta, (2015). Other identification procedures such as FTIR showed the presence of different functional groups such as aldehydes, alkanes, alcohols, esters and derivatives of carboxylic acid. This was found in walnut oil and its fractions. Furthermore, NMRs including proton NMR, carbon NMR spectrums confirmed the presence of linolenic acid and a combination with linoleic acid a compound found to be peculiar to the oil. From the walnut spectra, the presence of glyceric acid as seen in the spectra of walnut fraction makes this study the second to be reported. A simple bioassay guided-fractionation procedure applied in the study helped to confirm the fractions that were active before further analysis were performed on them. Similarly, in chapter three of this thesis, FTIR results showed the functional groups present in pumpkin and cashew oil although no further study was conducted on them.

In summary, this thesis has made significant and multiple contributions to knowledge: firstly, the that oils from walnut, cashew and pumpkin could be extracted by mechanical and chemical means, secondly that the expelled press oils contain 3-5 main classes of phytochemicals that may be responsible for their activity particularly walnut oil. Thirdly, resistant and susceptible strains of *S. aureus* are biofilm formers that can form varying quantity of biofilm; fourthly that

biofilms of MRSA 252 and ATCC 6538 are susceptible to walnut, cashew and pumpkin and their extracts; that the expelled oils in combination with antibiotics could be used in the treatment of *S. aureus* infections; that biofilm formation in MRSA 252 and ATCC 6538 could be inhibited and eradicated by African walnut, cashew and pumpkin oils. That the expression levels of most genes associated with virulence of *S. aureus* can be controlled by plant oils particularly walnut oil. Lastly, that significant amount of fatty acids is present in African walnut oil and is responsible for its activity.

## **9.2 Future Research**

In this study only two *S. aureus* strains were used throughout the research study. Future work should involve the use of more strains which could include reference strains and clinical isolates from skin infections and infected wounds.

Preliminary investigation and identification of fatty acid components of African walnut oil was done through fractional distillation, GC-MS, NMR and FTIR. In this study, separation of African walnut oil into fractions was really challenging because no favourable result was obtained from the column chromatographic technique that was first tried. Although the fractional distillation process yielded 4 fractions with some showing slight mixture of compounds a better means of separation could be used to obtain maximum separation for optimum results.

Phytochemical analysis was performed to confirm the presence of phytochemicals in African walnut, cashew and pumpkin oils. Although standard procedures were used, better confirmation process could be coupled with mass spectrometry that will help to quantify them. In order to quantify trace amounts of phytochemicals present in the oils and extracts, Raman and surface enhanced Raman spectroscopy could be used since not all the pigmental ranges were observed by UV-visible and ATR FTIR analysis in this study.

## References

- Abdulgader, S. M., Shittu, A. O., Nicol, M. P., & Kaba, M. (2015). Molecular epidemiology of Methicillin-resistant *Staphylococcus aureus* in Africa: a systematic review. *Frontiers in microbiology*, 6, 348.
- Abdullahi, N., & Iregbu, K. C. (2018). Methicillin-Resistant *Staphylococcus aureus* in a Central Nigeria Tertiary Hospital. *Annals of Tropical Pathology*, 9(1), 6.
- Adeel, A., Sohail, A., & Masud, T. (2014). Characterization and antibacterial study of pumpkin seed oil (*Cucurbita pepo*). *Life Sciences Leaflets*, 49.
- Adeigbe, O. O., Olasupo, F. O., Adewale, B. D., & Muyiwa, A. A. (2015). A review on cashew research and production in Nigeria in the last four decades. *Scientific Research and Essays*, 10(5), 196-209.
- Agarwal, A., Singh, K. P., & Jain, A. (2010) Medical significance and management of staphylococcal biofilm. *FEMS Immunology & Medical Microbiology*, 58(2), 147-160.
- Ajaiyeoba, E. O., & Fadare, D. A. (2006). Antimicrobial potential of extracts and fractions of the African walnut–*Tetracarpidium conophorum*. *African Journal of Biotechnology*, 5(22), 123-125
- Ajayi, C. (2018). Determinants of *Staphylococcus aureus* Colonization and Infection. “Exploring the Role of Cell Wall Anchored Proteins in Adhesion and Immune Evasion”.
- Ajileye, O. O., Obuotor, E. M., Akinkunmi, E. O., & Aderogba, M. A. (2015). Isolation and characterization of antioxidant and antimicrobial compounds from *Anacardium occidentale* L.(Anacardiaceae) leaf extract. *Journal of King Saud University-Science*, 27(3), 244-252.
- Akinhanmi, T. F., Atasie, V. N., & Akintokun, P. O. (2008). Chemical composition and physicochemical properties of cashew nut (*Anacardium occidentale*) oil and cashew nut shell liquid. *Journal of Agricultural, Food and Environmental Sciences*, 2(1), 1-10.
- Akpuaka, M. U., & Nwankwor, E. (2000). Extraction, analysis and utilization of a drying-oil from *Tetracarpidium conophorum*. *Bioresource Technology*, 73(2), 195-196.
- Akujobi, C., Anyanwu, B. N., Onyeze, C., & Ibekwe, V. I. (2004). Antibacterial activities and preliminary phytochemical screening of four medicinal plants. *J. Appl. Sci*, 7(3), 4328-4338.
- Albertson, J., McDanel, J. S., Carnahan, R., Chrischilles, E., Perencevich, E. N., Goto, M., . . . Schweizer, M. L. (2015). Determination of Risk Factors for Recurrent Methicillin-Resistant *Staphylococcus aureus* Bacteremia in a Veterans Affairs Healthcare System Population. *Infection Control & Hospital Epidemiology*, 36(05), 543-549.
- Alexander-Lindo, R. L., Morrison, E. S. A., & Nair, M. G. (2004). Hypoglycaemic effect of stigmast-4-en-3-one and its corresponding alcohol from the bark of *Anacardium occidentale* (cashew). *Phytotherapy Research: An International Journal Devoted to Pharmacological and Toxicological Evaluation of Natural Product Derivatives*, 18(5), 403-407.

- Aliyu, O. M., & Awopetu, J. A. (2007). Chromosome studies in cashew (*Anacardium occidentale* L.). *African Journal of Biotechnology*, 6(2), 131-136
- Al-Okbi, S. Y., Mohamed, D. A., Kandil, E., Abo-Zeid, M. A., Mohammed, S. E., & Ahmed, E. K. (2017). Anti-inflammatory activity of two varieties of pumpkin seed oil in an adjuvant arthritis model in rats. *Grasas y Aceites*, 68(1), 180.
- Al-Shuneigat, J. M., Al-Tarawneh, I. N., Al-Qudah, M. A., Al-Sarayreh, S. A., Al-Saraireh, Y. M., & Alsharafa, K. Y. (2015). The chemical composition and the antibacterial properties of *Ruta graveolens* L. essential oil grown in Northern Jordan. *Jordan Journal of Biological Sciences*, 8(2), 139-143.
- Altemimi, A., Lakhssassi, N., Baharlouei, A., Watson, D., & Lightfoot, D. (2017). Phytochemicals: Extraction, isolation, and identification of bioactive compounds from plant extracts. *Plants*, 6(4), 42.
- Aniekwe, N. L., & Mbah, M. C. (2015). Influence of Seed Location in the Fruit Pod of Fluted Pumpkin (*Telfairia Occidentalis* Hook. F.) and Poultry Wastes on Plant Sex Ratio. *Review of Catalysts*, 2(2), 26-33.
- Aparna, M. S., & Yadav, S. (2008). Biofilms: microbes and disease. *Brazilian Journal of Infectious Diseases*, 12(6), 526-530
- Archer, N. K., Mazaitis, M. J., Costerton, J. W., Leid, J. G., Powers, M. E., & Shirtliff, M. E. (2011). *Staphylococcus aureus* biofilms: properties, regulation, and roles in human disease. *Virulence*, 2(5), 445-459.
- Aregheore, E. M. (2012). Nutritive value and inherent anti-nutritive factors in four indigenous edible leafy vegetables in human nutrition in Nigeria: a review. *J. Food Res. Sci*, 1, 1-14.
- Aremu, M. O., Ibrahim, H., & Bamidele, T. O. (2015). Physicochemical characteristics of the oils extracted from some Nigerian plant foods—a review. *Chem. Proc. Eng. Res*, 7, 36-52.
- Arslan, S., & Özkardes, F. (2007). Slime production and antibiotic susceptibility in staphylococci isolated from clinical samples. *Memórias do Instituto Oswaldo Cruz*, 102(1), 29-33.
- Askari, E., Soleymani, F., Arianpoor, A., Tabatabai, S. M., Amini, A., & NaderiNasab, M. (2012). Epidemiology of mecA-methicillin resistant *Staphylococcus aureus* (MRSA) in Iran: a systematic review and meta-analysis. *Iranian journal of basic medical sciences*, 15(5), 1010.
- Atshan, S. S., Shamsudin, M. N., Karunanidhi, A., van Belkum, A., Lung, L. T. T., Sekawi, Z., ... & Abduljaleel, S. A. (2013) Quantitative PCR analysis of genes expressed during biofilm development of methicillin resistant *Staphylococcus aureus* (MRSA). *Infection, Genetics and Evolution*, 18, 106-112.
- Atshan, S. S., Shamsudin, M. N., Lung, T., Than, L., Sekawi, Z., Ghaznavi-Rad, E., & Pei Pei, C. (2012) Comparative characterisation of genotypically different clones of MRSA in the production of biofilms. *BioMed Research International*, 2012.

- Ayoola, P. B., Onawumi, O. O., & Faboya, O. O. P. (2011) Chemical evaluation and nutritive values of *Tetracarpidium conophorum* (Nigerian walnut) seeds. *Journal of Pharmaceutical and Biomedical Sciences (JPBMS)*, *11*(15).
- Azam-Ali, S. H., & Judge, E. C. (2001). Small scale cashew nut processing. A Report to Food and Agricultural Organisation of the United Nation. 86p.
- Bardaa, S., Halima, N. B., Aloui, F., Mansour, R. B., Jabeur, H., Bouaziz, M., & Sahnoun, Z. (2016). Oil from pumpkin (*Cucurbita pepo* L.) seeds: evaluation of its functional properties on wound healing in rats. *Lipids in health and disease*, *15*(1), 73.
- Batabyal, B., Kundu, G., & Biswas, S. (2012). Methicillin-resistant *Staphylococcus aureus*: a brief review. *International Research Journal of Biological Sciences*, *1*(7), 65-71.
- Batista, A. H., Moreira, A. C., de Carvalho, R. M., Sales, G. W., Nogueira, P. C., Grangeiro, T. B., ... & Nogueira, N. A. (2017). Antimicrobial effects of violacein against planktonic cells and biofilms of *Staphylococcus aureus*. *Molecules*, *22*(10), 1534.
- Bayles, K. W. (2007). The biological role of death and lysis in biofilm development. *Nature Reviews Microbiology*, *5*(9), 721.
- Belbase, A., Pant, N. D., Nepal, K., Neupane, B., Baidhya, R., Baidya, R., & Lekhak, B. (2017). Antibiotic resistance and biofilm production among the strains of *Staphylococcus aureus* isolated from pus/wound swab samples in a tertiary care hospital in Nepal. *Annals of clinical microbiology and antimicrobials*, *16*(1), 15.
- Benson, H.J. (2001) Appendix A. In: Microbiological applications: laboratory manual in general microbiology, McGraw Hill, Boston, Massachusetts. 8, 432
- Bien, J., Sokolova, O., & Bozko, P. (2011). Characterization of virulence factors of *Staphylococcus aureus*: novel function of known virulence factors that are implicated in activation of airway epithelial proinflammatory response. *Journal of pathogens*, 2011.
- Blair, J.M., Webber, M.A., Baylay, A.J., Ogbolu, D.O., & Piddock, L.J. 2015. Molecular mechanisms of antibiotic resistance. *Nature reviews microbiology*, *13*(1), p.42.
- Borg, M. A., De Kraker, M., Scicluna, E., van de Sande-Bruinsma, N., Tiemersma, E., Monen, J., & Grundmann, H. (2007). Prevalence of methicillin-resistant *Staphylococcus aureus* (MRSA) in invasive isolates from southern and eastern Mediterranean countries. *Journal of Antimicrobial Chemotherapy*, *60*(6), 1310-1315.
- Boswihi, S. S., & Udo, E. E. (2018). Methicillin-resistant *Staphylococcus aureus*: An update on the epidemiology, treatment options and infection control. *Current Medicine Research and Practice*, *8*(1), 18-24.
- Bruins, M. J., Juffer, P., Wolfhagen, M. J., & Ruijs, G. J. (2007). Salt tolerance of methicillin-resistant and methicillin-susceptible *Staphylococcus aureus*. *Journal of clinical microbiology*, *45*(2), 682-683.
- Burke, F. M., McCormack, N., Rindi, S., Speziale, P., & Foster, T. J. (2010). Fibronectin-binding protein B variation in *Staphylococcus aureus*. *BMC microbiology*, *10*(1), 1.

- Caiazza, N. C., & O'toole, G. A. (2003). Alpha-toxin is required for biofilm formation by *Staphylococcus aureus*. *Journal of bacteriology*, 185(10), 3214-3217.
- Carr, G. B., Schwartz, R. S., Schaudinn, C., Gorur, A., & Costerton, J. W. (2009). Ultrastructural examination of failed molar retreatment with secondary apical periodontitis: an examination of endodontic biofilms in an endodontic retreatment failure. *Journal of endodontics*, 35(9), 1303-1309.
- Chambers, H. F. (2001). The changing epidemiology of *Staphylococcus aureus*? *Emerging infectious diseases*, 7(2), 178.
- Chambers, H. F., & DeLeo, F. R. (2009). Waves of resistance: *Staphylococcus aureus* in the antibiotic era. *Nature Reviews Microbiology*, 7(9), 629.
- Chamdit, S., & Siripermpool, P. (2012). Antimicrobial effect of clove and lemongrass oils against planktonic cells and biofilms of *Staphylococcus aureus*. *Mahidol Univ J Pharm Sci*, 39(2), 28-36.
- Cheesman, M. J., Ilanko, A., Blonk, B., & Cock, I. E. (2017). Developing new antimicrobial therapies: Are synergistic combinations of plant extracts/compounds with conventional antibiotics the solution?. *Pharmacognosy reviews*, 11(22), 57.
- Chen, C. J., & Huang, Y. C. (2014). New epidemiology of *Staphylococcus aureus* infection in Asia. *Clinical Microbiology and Infection*, 20(7), 605-623.
- Cho, S. H., Strickland, I., Boguniewicz, M., & Leung, D. Y. (2001). Fibronectin and fibrinogen contribute to the enhanced binding of *Staphylococcus aureus* to atopic skin. *Journal of Allergy and Clinical Immunology*, 108(2), 269-274.
- Chonoko, U. G., & Rufai, A. B. (2011). Phytochemical screening and antibacterial activity of *Cucurbita pepo* (Pumpkin) against *Staphylococcus aureus* and *Salmonella typhi*. *Bayero Journal of Pure and Applied Sciences*, 4(1), 145-147.
- Christy, A. A., Kasemsumran, S., Du, Y., & Ozaki, Y. (2004). The detection and quantification of adulteration in olive oil by near-infrared spectroscopy and chemometrics. *Analytical Sciences*, 20(6), 935-940.
- Chuang, Y. Y., & Huang, Y. C. (2013). Molecular epidemiology of community-associated methicillin-resistant *Staphylococcus aureus* in Asia. *The Lancet infectious diseases*, 13(8), 698-708.
- CLSI, 2012. Performance standards for antimicrobial susceptibility testing; approved standard M02-11. Clinical and laboratory Standards Institute, Waynes, PA.
- Cohen, B., Hyman, S., Rosenberg, L., & Larson, E. (2012). Frequency of patient contact with health care personnel and visitors: implications for infection prevention. *Joint Commission journal on quality and patient safety/Joint Commission Resources*, 38(12), 560.
- Cohn, L. A., & Middleton, J. R. (2010). A veterinary perspective on methicillin-resistant staphylococci. *Journal of veterinary emergency and critical care*, 20(1), 31-45.
- Corbella, X., Domínguez, M. A., Pujol, M., Ayats, J., Sendra, M., Pallares, R., ... & Gudiol, F. (1997). *Staphylococcus aureus* nasal carriage as a marker for subsequent staphylococcal

- infections in intensive care unit patients. *European Journal of Clinical Microbiology and Infectious Diseases*, 16(5), 351-357.
- Corey, G. R. (2009). *Staphylococcus aureus* bloodstream infections: definitions and treatment. *Clinical Infectious Diseases*, 48(Supplement\_4), S254-S259.
- Correia, S., Poeta, P., Hébraud, M., Capelo, J. L., & Igrejas, G. (2017). Mechanisms of quinolone action and resistance: where do we stand?. *Journal of medical microbiology*, 66(5), 551-559.
- Crawford, E. C., Singh, A., Metcalf, D., Gibson, T. W., & Weese, S. J. (2014). Identification of appropriate reference genes for qPCR studies in *Staphylococcus pseudintermedius* and preliminary assessment of *icaA* gene expression in biofilm-embedded bacteria. *BMC research notes*, 7(1), 451.
- Cuny, C., Friedrich, A., Kozytska, S., Layer, F., Nübel, U., Ohlsen, K., ... & Witte, W. (2010). Emergence of methicillin-resistant *Staphylococcus aureus* (MRSA) in different animal species. *International Journal of Medical Microbiology*, 300(2-3), 109-117.
- da Silva, R. A., Liberio, S. A., do Amaral, F. M., do Nascimento, F. R. F., Torres, L. M. B., Neto, V. M., & Guerra, R. N. M. (2016). Antimicrobial and Antioxidant Activity of *Anacardium occidentale* L. Flowers in Comparison to Bark and Leaves Extracts. *Journal of Biosciences and Medicines*, 4(04), 87.
- Dada, A. A. (2015). Use of fluted pumpkin (*Telfairia occidentalis*) leaf powder as feed additive in African food. *International Journal of Biological and Chemical Sciences*, 9(1), 301-307.
- Dakheel, K. H., Abdul Rahim, R., Neela, V. K., Al-Obaidi, J. R., Hun, T. G., & Yusoff, K. (2016). Methicillin-resistant *Staphylococcus aureus* biofilms and their influence on bacterial adhesion and cohesion. *BioMed research international*, 2016.
- Datta, R., Shah, A., Huang, S. S., Cui, E., Nguyen, V., Welbourne, S. J., ... & Thrupp, L. (2013). High nasal burden of methicillin-resistant *Staphylococcus aureus* increases risk for invasive disease. *Journal of clinical microbiology*, JCM-01606.
- Davey, M. E., & O'toole, G. A. (2000). Microbial biofilms: from ecology to molecular genetics. *Microbiology and molecular biology reviews*, 64(4), 847-867.
- David, M. Z., & Daum, R. S. (2010). Community-associated methicillin-resistant *Staphylococcus aureus*: epidemiology and clinical consequences of an emerging epidemic. *Clinical microbiology reviews*, 23(3), 616-687.
- Davies, J., & Davies, D. (2010). Origins and evolution of antibiotic resistance. *Microbiology and molecular biology reviews*, 74(3), 417-433.
- Deivanayagam, C. C., Rich, R. L., Carson, M., Owens, R. T., Danthuluri, S., Bice, T., ... & Narayana, S. V. (2000). Novel fold and assembly of the repetitive B region of the *Staphylococcus aureus* collagen-binding surface protein. *Structure*, 8(1), 67-78.
- Deivanayagam, C. C., Wann, E. R., Chen, W., Carson, M., Rajashankar, K. R., Höök, M., & Narayana, S. V. (2002). A novel variant of the immunoglobulin fold in surface adhesins of

- Staphylococcus aureus*: crystal structure of the fibrinogen-binding MSCRAMM, clumping factor A. *The EMBO journal*, 21(24), 6660-6672.
- del Giudice, P., Hübiche, T., & Étienne, J. (2012). Long-term use of tetracycline and *Staphylococcus aureus* tetracycline resistance: not only a problem of acne. *Archives of dermatology*, 148(3), 402-402.
- DeLeo, F. R., Kennedy, A. D., Chen, L., Wardenburg, J. B., Kobayashi, S. D., Mathema, B., ... & Porcella, S. F. (2011). Molecular differentiation of historic phage-type 80/81 and contemporary epidemic *Staphylococcus aureus*. *Proceedings of the National Academy of Sciences*, 108(44), 18091-18096.
- Derycke, L., Pérez-Novo, C., Van Crombruggen, K., Corriveau, M. N., & Bachert, C. (2010). *Staphylococcus aureus* and chronic airway disease. *World Allergy Organization Journal*, 3(8), 223.
- Deurenberg, R. H., Vink, C., Kalenic, S., Friedrich, A. W., Bruggeman, C. A., & Stobberingh, E. E. (2007). The molecular evolution of methicillin-resistant *Staphylococcus aureus*. *Clinical Microbiology and Infection*, 13(3), 222-235.
- Dezfulian, A., Salehian, M. T., Amini, V., Dabiri, H., Azimirad, M., Aslani, M. M., ... & Fazel, I. (2010). Catalase-negative *Staphylococcus aureus* isolated from a diabetic foot ulcer. *Iranian journal of microbiology*, 2(3), 165.
- Didier, J. P., Villet, R., Huggler, E., Lew, D. P., Hooper, D. C., Kelley, W. L., & Vaudaux, P. (2011). Impact of ciprofloxacin exposure on *Staphylococcus aureus* genomic alterations linked with emergence of rifampin resistance. *Antimicrobial agents and chemotherapy*.
- Dinges, M. M., Orwin, P. M., & Schlievert, P. M. (2000). Exotoxins of *Staphylococcus aureus*. *Clinical microbiology reviews*, 13(1), 16-34.
- Dobie, D., & Gray, J. (2004). Fusidic acid resistance in *Staphylococcus aureus*. *Archives of disease in childhood*, 89(1), 74-77.
- Dorathy S., Jebapritha, S., Karpagam, I. (2017) Phytochemical Content and Antimicrobial Activity of Cashew Nut Shell Oil. *Journal of Pharmacy and Biological Sciences*. 12(4) 61-64.
- DuMont, A. L., Yoong, P., Surewaard, B. G., Benson, M. A., Nijland, R., van Strijp, J. A., & Torres, V. J. (2013). *Staphylococcus aureus* elaborates leukocidin AB to mediate escape from within human neutrophils. *Infection and immunity*, 81(5), 1830-1841.
- Ekor, M. (2014). The growing use of herbal medicines: issues relating to adverse reactions and challenges in monitoring safety. *Frontiers in pharmacology*, 4, 177.
- Ekwe, C. C., & Ihemeje, A. (2013). Evaluation of physiochemical properties and preservation of African walnut (*Tetracarpidium conophorum*). *Academic Research International*, 4(6), 501.
- El-Bashiti, T. A., Abou Elkhair, E., & Abu Draz, W. S. (2017). The antibacterial and synergistic potential of some Palestinian plant extracts against multidrug resistant *Staphylococcus aureus*. *J. Med. Plants Stud*, 5(2), 54-65.

- Elder, D. P., Kuentz, M., & Holm, R. (2016). Antibiotic resistance: the need for a global strategy. *Journal of pharmaceutical sciences*, 105(8), 2278-2287.
- Fair, R. J., & Tor, Y. (2014). Antibiotics and bacterial resistance in the 21st century. *Perspectives in medicinal chemistry*, 6, PMC-S14459.
- Falagas, M. E., Karageorgopoulos, D. E., Leptidis, J., & Korbila, I. P. (2013). MRSA in Africa: filling the global map of antimicrobial resistance. *PloS one*, 8(7), e68024.
- Faria, N. A., Oliveira, D. C., Westh, H., Monnet, D. L., Larsen, A. R., Skov, R., & de Lencastre, H. (2005). Epidemiology of emerging methicillin-resistant *Staphylococcus aureus* (MRSA) in Denmark: a nationwide study in a country with low prevalence of MRSA infection. *Journal of clinical microbiology*, 43(4), 1836-1842.
- Faron, M. L., Ledebøer, N. A., & Buchan, B. W. (2016). Resistance Mechanisms, Epidemiology, and Approaches to Screening for Vancomycin Resistant Enterococcus (VRE) in the Health Care Setting. *Journal of clinical microbiology*, JCM-00211.
- Fishovitz, J., Hermoso, J. A., Chang, M., & Mobashery, S. (2014). Penicillin-binding protein 2a of methicillin-resistant *Staphylococcus aureus*. *IUBMB life*, 66(8), 572-577.
- Flemming, H. C., & Wingender, J. (2010). The biofilm matrix. *Nature reviews microbiology*, 8(9), 623.
- Foster, T. (2016). The remarkably multifunctional fibronectin binding proteins of *Staphylococcus aureus*. *European Journal of Clinical Microbiology & Infectious Diseases*, 1-9.
- Foster, T. J. (2017). Antibiotic resistance in *Staphylococcus aureus*. Current status and future prospects. *Fems microbiology reviews*, 41(3), 430-449.
- Foulston, L., Elsholz, A. K., DeFrancesco, A. S., & Losick, R. (2014). The extracellular matrix of *Staphylococcus aureus* biofilms comprises cytoplasmic proteins that associate with the cell surface in response to decreasing pH. *MBio*, 5(5), e01667-14.
- Fowler, T., Wann, E. R., Joh, D., Johansson, S., Foster, T. J., & Höök, M. (2000). Cellular invasion by *Staphylococcus aureus* involves a fibronectin bridge between the bacterial fibronectin-binding MSCRAMMs and host cell  $\beta 1$  integrins. *European journal of cell biology*, 79(10), 672-679.
- Frau, T. & Frau, S.-R. (2010). Separation of Fatty Acid Methyl Esters (FAME) on an Agilent J & W Select CP-Sil 88 for FAME GC Column. Agilent Technologies UK, p. 1-3.
- Fraune, S., & Bosch, T. C. (2010). Why bacteria matter in animal development and evolution. *Bioessays*, 32(7), 571-580.
- French, G. L. (2010). The continuing crisis in antibiotic resistance. *International journal of antimicrobial agents*, 36, S3-S7.
- Fuda, C., Suvorov, M., Vakulenko, S. B., & Mobashery, S. (2004). The basis for resistance to  $\beta$ -lactam antibiotics by penicillin-binding protein 2a of methicillin-resistant *Staphylococcus aureus*. *Journal of Biological Chemistry*, 279(39), 40802-40806.

- Fuqua, C., Parsek, M. R., & Greenberg, E. P. (2001). Regulation of gene expression by cell-to-cell communication: acyl-homoserine lactone quorum sensing. *Annual review of genetics*, 35(1), 439-468.
- Ganesh, V. K., Barbu, E. M., Deivanayagam, C. C., Le, B., Anderson, A. S., Matsuka, Y. V., . . . Höök, M. (2011). Structural and biochemical characterization of *Staphylococcus aureus* clumping factor B/ligand interactions. *Journal of Biological Chemistry*, 286(29), 25963-25972.
- Gardete, S., & Tomasz, A. (2014). Mechanisms of vancomycin resistance in *Staphylococcus aureus*. *The Journal of clinical investigation*, 124(7), 2836-2840.
- Garrett, T. R., Bhakoo, M., & Zhang, Z. (2008). Bacterial adhesion and biofilms on surfaces. *Progress in Natural Science*, 18(9), 1049-1056.
- Geisinger, E., Adhikari, R. P., Jin, R., Ross, H. F., & Novick, R. P. (2006). Inhibition of rot translation by RNAIII, a key feature of agr function. *Molecular microbiology*, 61(4), 1038-1048.
- Gill, S. R., Fouts, D. E., Archer, G. L., Mongodin, E. F., DeBoy, R. T., Ravel, J., ... & Dodson, R. J. (2011). Insights on evolution of virulence and resistance from the complete genome analysis of an early methicillin-resistant *Staphylococcus aureus* strain and a biofilm-producing methicillin-resistant *Staphylococcus epidermidis* strain. *Journal of bacteriology*, 187(7), 2426-2438.
- Goossens, H., Ferech, M., Vander Stichele, R., Elseviers, M., & ESAC Project Group. (2005). Outpatient antibiotic use in Europe and association with resistance: a cross-national database study. *The Lancet*, 365(9459), 579-587.
- Gordon, R. J., & Lowy, F. D. (2008). Pathogenesis of methicillin-resistant *Staphylococcus aureus* infection. *Clinical infectious diseases*, 46(Supplement\_5), S350-S359.
- Gowrishankar, S., Kamaladevi, A., Balamurugan, K., & Pandian, S. K. (2016). In vitro and in vivo biofilm characterization of methicillin-resistant *Staphylococcus aureus* from patients associated with pharyngitis infection. *BioMed research international*, 2016.
- Greenway, D. L. A., & Dyke, K. G. H. (1979). Mechanism of the inhibitory action of linoleic acid on the growth of *Staphylococcus aureus*. *Microbiology*, 115(1), 233-245.
- Gross, M., Cramton, S. E., Götz, F., & Peschel, A. (2001) Key role of teichoic acid net charge in *Staphylococcus aureus* colonization of artificial surfaces. *Infection and Immunity*, 69(5), 3423-3426.
- Grosset-Janin, A., Nicolas, X., & Saraux, A. (2012). Sport and infectious risk: a systematic review of the literature over 20 years. *Médecine et maladies infectieuses*, 42(11), 533-544.
- Grounta, A., Harizanis, P., Mylonakis, E., Nychas, G. J. E., & Panagou, E. Z. (2016). Investigating the effect of different treatments with lactic acid bacteria on the fate of *Listeria monocytogenes* and *Staphylococcus aureus* infection in *Galleria mellonella* larvae. *PloS one*, 11(9), e0161263.

- Hair, P. S., Echague, C. G., Sholl, A. M., Watkins, J. A., Geoghegan, J. A., Foster, T. J., & Cunnion, K. M. (2010). Clumping factor A interaction with complement factor I increases C3b cleavage on the bacterial surface of *Staphylococcus aureus* and decreases complement-mediated phagocytosis. *Infection and immunity*, 78(4), 1717-1727.
- Hammadi, K. M., & Yousif, A. A. (2014). Detection of slime material in *Staphylococcus aureus* bacteria from ovine mastitis by transmission electron microscope and Congo red agar method. *Int. J. Curr. Microbiol. App. Sci*, 3(4), 304-309.
- Harbarth, S., Balkhy, H. H., Goossens, H., Jarlier, V., Kluytmans, J., Laxminarayan, R., ... & Pittet, D. (2015). Antimicrobial resistance: one world, one fight!. *Antimicrobial Resistance and Infection Control* 4:49.
- Harborne, J. 1998. *Phytochemical Methods, A guide to modern Techniques of plant analysis*. Science.
- Harraghy, N., Hussain, M., Hagggar, A., Chavakis, T., Sinha, B., Herrmann, M., & Flock, J.-I. (2003). The adhesive and immunomodulating properties of the multifunctional *Staphylococcus aureus* protein Eap. *Microbiology*, 149(10), 2701-2707.
- Hartleib, J., Köhler, N., Dickinson, R. B., Chhatwal, G. S., Sixma, J. J., Hartford, O. M., ... & Herrmann, M. (2000). Protein A is the von Willebrand factor binding protein on *Staphylococcus aureus*. *Blood*, 96(6), 2149-2156.
- Hassan, N. A. A. A., Ali, M. S. M., & Mirad, R. (2016). Antimicrobial potency of essential oil from cashew (*Anacardium occidentale* Linn.) clones. *Journal of Tropical Agriculture and Food Science*, 44(1), 73-80.
- Hassoun, A., Linden, P. K., & Friedman, B. (2017). Incidence, prevalence, and management of MRSA bacteremia across patient populations—a review of recent developments in MRSA management and treatment. *Critical Care*, 21(1), 211.
- Hayes, D., Angove, M. J., Tucci, J., & Dennis, C. (2016). Walnuts (*Juglans regia*) chemical composition and research in human health. *Critical reviews in food science and nutrition*, 56(8), 1231-1241.
- Heilmann, C. (2011). Adhesion mechanisms of staphylococci. In *Bacterial adhesion* (pp. 105-123). Springer, Dordrecht.
- Henderson, B., Nair, S., Pallas, J., & Williams, M. A. (2011). Fibronectin: a multidomain host adhesin targeted by bacterial fibronectin-binding proteins. *FEMS microbiology reviews*, 35(1), 147-200.
- Hienz, S. A., Schennings, T., Heimdahl, A., & Flock, J. I. (1996). Collagen binding of *Staphylococcus aureus* is a virulence factor in experimental endocarditis. *Journal of Infectious Diseases*, 174(1), 83-88.
- Honda, H., Krauss, M. J., Coopersmith, C. M., Kollef, M. H., Richmond, A. M., Fraser, V. J., & Warren, D. K. (2010). *Staphylococcus aureus* nasal colonization and subsequent infection in intensive care unit patients: does methicillin resistance matter?. *Infection Control & Hospital Epidemiology*, 31(6), 584-591.

- Hughes, S., Heard, K., & Moore, L.S., 2018. Antimicrobial therapies for Gram-positive infections. *Lung cancer*, 15, p.05.
- Ige, O. K., Adesanmi, A. A., & Asuzu, M. C. (2011). Hospital-acquired infections in a Nigerian tertiary health facility: An audit of surveillance reports. *Nigerian medical journal: journal of the Nigeria Medical Association*, 52(4), 239.
- Ionesu, M., Vladut, V., Ungureanu, N., Dinca, M., Zabava, B. S., & Stefan, M. (2017). methods for oil obtaining from oleaginous materials. *Annals of the University of Craiova-Agriculture, Montanology, Cadastre Series*, 46(2), 411-417.
- Iyekowa, O., Owolabi, B. J., & Cole, O. (2016). Gas Chromatography (GC)–Mass Spectrometry (MS) analysis of the isolated oil of *Tetracarpidium conophorum* (walnut). Mull (Arg) root bark. *Scientia Africana*, 15(1).
- Jain, V., Garg, A., Parascandola, M., Chaturvedi, P., Khariwala, S. S., & Stepanov, I. (2017). Analysis of Alkaloids in Areca Nut-Containing Products by Liquid Chromatography–Tandem Mass Spectrometry. *Journal of agricultural and food chemistry*, 65(9), 1977-1983.
- Jensen, A. G., Wachmann, C. H., Poulsen, K. B., Espersen, F., Scheibel, J., Skinhøj, P., & Frimodt-Møller, N. (1999). Risk factors for hospital-acquired *Staphylococcus aureus* bacteremia. *Archives of internal medicine*, 159(13), 1437-1444.
- Jokić, S., Moslavac, T., Bošnjak, A., Aladić, K., Rajić, M., & Bilić, M. (2014). Optimization of walnut oil production. *Croatian journal of food science and technology*, 6(1), 27-35.
- Kalmeijer, M. D., van Nieuwland-Bollen, E., Bogaers-Hofman, D., de Baere, G. A., & Kluytmans, J. A. (2000). Nasal carriage of *Staphylococcus aureus*: Is a major risk factor for surgical-site infections in orthopedic surgery. *Infection Control & Hospital Epidemiology*, 21(5), 319-323.
- Kannan, V. R., Sumathi, C. S., Balasubramanian, V., & Ramesh, N. (2009). Elementary chemical profiling and antifungal properties of cashew (*Anacardium occidentale* L.) nuts. *Botany Research International*, 2(4), 253-257.
- Kavanaugh, N. L., & Ribbeck, K. (2012). Selected antimicrobial essential oils eradicate *Pseudomonas* spp. and *Staphylococcus aureus* biofilms. *Applied and environmental microbiology*, AEM-07499.
- Kayode, A. A. A., & Kayode, O. T. (2011). Some medicinal values of *Telfairia occidentalis*: A review. *Am J Biochem Mol Biol*, 1(1), 30-38.
- Keene, A., Vavagiakis, P., Lee, M. H., Finnerty, K., Nicolls, D., Cespedes, C., ... & Lowy, F. D. (2005). *Staphylococcus aureus* colonization and the risk of infection in critically ill patients. *Infection Control & Hospital Epidemiology*, 26(7), 622-628.
- Kerrigan, S. W., Kaw, G., Hogan, M., Penadés, J., Litt, D., Fitzgerald, D. J., . . . Cox, D. (2002). Multiple mechanisms for the activation of human platelet aggregation by *Staphylococcus aureus*: roles for the clumping factors ClfA and ClfB, the serine–aspartate repeat protein SdrE and protein A. *Molecular microbiology*, 44(4), 1033-1044.

- Kielty, C. M., Sherratt, M. J., & Shuttleworth, C. A. (2002). Elastic fibres. *Journal of cell science*, 115(14), 2817-2828.
- Kim, S. Y., Kim, J., Jeong, S. I., Jahng, K. Y., & Yu, K. Y. (2015). Antimicrobial effects and resistant regulation of magnolol and honokiol on methicillin-resistant *Staphylococcus aureus*. *BioMed research international*, doi: [10.1155/2015/283630](https://doi.org/10.1155/2015/283630).
- Kluytmans, J., Van Belkum, A., & Verbrugh, H. (1997). Nasal carriage of *Staphylococcus aureus*: epidemiology, underlying mechanisms, and associated risks. *Clinical microbiology reviews*, 10(3), 505-520.
- Kohanski, M. A., Dwyer, D. J., & Collins, J. J. (2010). How antibiotics kill bacteria: from targets to networks. *Nature Reviews Microbiology*, 8(6), 423.
- Kok, E. T., Jong, M. J., Gravendeel, B., van Leeuwen, W. B., & Baars, E. W. (2015). Resistance to antibiotics and antifungal medicinal products: Can complementary and alternative medicine help solve the problem in infection diseases? The introduction of a Dutch research consortium. *European Journal of Integrative Medicine*, (7), 43.
- Krakauer, T., & Stiles, B. G. (2013). The staphylococcal enterotoxin (SE) family: SEB and siblings. *Virulence*, 4(8), 759-773.
- Krismer, B., & Peschel, A. (2011). Does *Staphylococcus aureus* nasal colonization involve biofilm formation? *Future microbiology*, 6(5), 489-493.
- Kuehnert, M. J., Kruszon-Moran, D., Hill, H. A., McQuillan, G., McAllister, S. K., Fosheim, G., . . . Fridkin, S. K. (2006). Prevalence of *Staphylococcus aureus* nasal colonization in the United States, 2001–2002. *Journal of Infectious Diseases*, 193(2), 172-179.
- Kuroda, M., Ohta, T., Uchiyama, I., Baba, T., Yuzawa, H., Kobayashi, I., ... & Lian, J. (2001). Whole genome sequencing of methicillin-resistant *Staphylococcus aureus*. *The Lancet*, 357(9264), 1225-1240.
- Labro, M. T., & Bryskier, J. M. (2014). Antibacterial resistance: an emerging ‘zoonosis’?. *Expert review of anti-infective therapy*, 12(12), 1441-1461.
- Lacey, K. A., Geoghegan, J. A., & McLoughlin, R. M. (2016). The Role of *Staphylococcus aureus* Virulence Factors in Skin Infection and Their Potential as Vaccine Antigens. *Pathogens*, 5(1), 22.
- Lai, C. F., Liao, C. H., Pai, M. F., Chu, F. Y., Hsu, S. P., Chen, H. Y., ... & Hung, K. Y. (2011). Nasal carriage of methicillin-resistant *Staphylococcus aureus* is associated with higher all-cause mortality in hemodialysis patients. *Clinical Journal of the American Society of Nephrology*, 6(1), 167-174.
- Larsen, A. R., Stegger, M., Böcher, S., Sørum, M., Monnet, D. L., & Skov, R. L. (2009). Emergence and characterization of community-associated methicillin-resistant *Staphylococcus aureus* infections in Denmark, 1999 to 2006. *Journal of clinical microbiology*, 47(1), 73-78.
- Levy, S. B., & Marshall, B. (2004). Antibacterial resistance worldwide: causes, challenges and responses. *Nature medicine*, 10(12s), S122.

- Li, B., & Webster, T. J. (2018). Bacteria antibiotic resistance: New challenges and opportunities for implant-associated orthopedic infections. *Journal of Orthopaedic Research*, 36(1), 22-32.
- Liang, P., Wang, H., Chen, C., Ge, F., Liu, D., Li, S., ... & Zhao, S. (2012). The use of fourier transform infrared spectroscopy for quantification of adulteration in virgin walnut oil. *Journal of Spectroscopy*, 2013.
- Lindsay, D., & Von Holy, A. (2006). Bacterial biofilms within the clinical setting: what healthcare professionals should know. *Journal of Hospital Infection*, 64(4), 313-325.
- Lister, J. L., & Horswill, A. R. (2014). *Staphylococcus aureus* biofilms: recent developments in biofilm dispersal. *Frontiers in cellular and infection microbiology*, 4, 178.
- Liu, Y., & Breukink, E. (2016). The membrane steps of bacterial cell wall synthesis as antibiotic targets. *Antibiotics*, 5(3), 28.
- Llarrull, L. I., Fisher, J. F., & Mobashery, S. (2009). Molecular basis and phenotype of methicillin resistance in *Staphylococcus aureus* and insights into new  $\beta$ -lactams that meet the challenge. *Antimicrobial agents and chemotherapy*, 53(10), 4051-4063.
- Lomovskaya, O., & Watkins, W. (2001). Inhibition of efflux pumps as a novel approach to combat drug resistance in bacteria. *Journal of molecular microbiology and biotechnology*, 3(2), 225-236.
- López, D., Vlamakis, H., & Kolter, R. (2010). Biofilms. *Cold Spring Harbor perspectives in biology*, a000398.
- Luzar, M. A., Coles, G. A., Faller, B., Slingeneyer, A., Dah, G. D., Briat, C., ... & Peluso, F. (1990). *Staphylococcus aureus* nasal carriage and infection in patients on continuous ambulatory peritoneal dialysis. *New England Journal of Medicine*, 322(8), 505-509.
- Lye, W. C., Leong, S. O., & Lee, E. J. C. (1993). Methicillin-resistant *Staphylococcus aureus* nasal carriage and infections in CAPD. *Kidney international*, 43(6), 1357-1362.
- Maduabuchi, E. K., & Onyebuchi, A. M. (2016). Phytochemical analysis of N-Hexane nut extract of *Tetracarpidium conophorum* (Euphorbiaceae) using Ultraviolet-Visible, fourier transform infrared and gas chromatography mass spectrometry techniques. *Journal of Pharmacognosy and Phytochemistry*, 5(6), 332-336.
- Magiorakos, A. P., Srinivasan, A., Carey, R. B., Carmeli, Y., Falagas, M. E., Giske, C. G., ... & Paterson, D. L. (2012). Multidrug-resistant, extensively drug-resistant and pandrug-resistant bacteria: an international expert proposal for interim standard definitions for acquired resistance. *Clinical microbiology and infection*, 18(3), 268-281.
- Mahboubi, M., Kazempour, N., & Taghizadeh, M. (2014). The antibacterial activity of some essential oils against clinical isolates of *Acinetobacter baumannii*. *Songklanakarin Journal of Science & Technology*, 36(5).

- Mahmood, K., Tahir, M., Jameel, T., Ziauddin, A., & Aslam, H. F. (2010). Incidence of Methicillin-resistant *Staphylococcus aureus* (MRSA) causing nosocomial infection in a Tertiary Care Hospital. *Annals of King Edward Medical University*, 16(2), 91-91.
- Mancl, K. A., Kirsner, R. S., & Ajdic, D. (2013). Wound biofilms: lessons learned from oral biofilms. *Wound repair and regeneration*, 21(3), 352-362.
- Mangili, A., Bica, I., Snyderman, D. R., & Hamer, D. H. (2005). Daptomycin-resistant, methicillin-resistant *Staphylococcus aureus* bacteremia. *Clinical infectious diseases*, 40(7), 1058-1060.
- Manna, Adhar C, & Cheung, Ambrose L. (2001). Expression of SarX, a negative regulator of agr and exoprotein synthesis, is activated by agrA in *Staphylococcus aureus*. *Journal of bacteriology*, 188(12), 4288-4299.
- Marston, H. D., Dixon, D. M., Knisely, J. M., Palmore, T. N., & Fauci, A. S. (2016). Antimicrobial resistance. *Jama*, 316(11), 1193-1204.
- Masignani, V., Pizza, M., & Rappuoli, R. (2013). Bacterial Toxins *the Prokaryotes* (pp. 499-554): Springer.
- Massey, R. C., Kantzanou, M. N., Fowler, T., Day, N. P., Schofield, K., Wann, E. R., ... & Peacock, S. J. (2001). Fibronectin-binding protein A of *Staphylococcus aureus* has multiple, substituting, binding regions that mediate adherence to fibronectin and invasion of endothelial cells. *Cellular microbiology*, 3(12), 839-851.
- Mazmanian, S. K., Liu, G., Ton-That, H., & Schneewind, O. (1999). *Staphylococcus aureus* sortase, an enzyme that anchors surface proteins to the cell wall. *Science*, 285(5428), 760-763.
- Mbatchou, V. C., & Kosoono, I. (2011). Aphrodisiac activity of oils from *Anacardium occidentale* L seeds and seed shells. *Phytopharmacology*, 2(1), 81-91.
- Mbim, E. N., Mboto, C. I., & Agbo, B. E. (2016). A review of nosocomial infections in Sub-Saharan Africa. *British Microbiology Research Journal*, 15(1), 1-11.
- McCann, M. T., Gilmore, B. F., & Gorman, S. P. (2008) *Staphylococcus epidermidis* device-related infections: pathogenesis and clinical management. *Journal of Pharmacy and Pharmacology*, 60(12), 1551.
- Miljković-Selimović, B., Dinić, M., Orlović, J., & Babić, T. (2015). *Staphylococcus aureus*: Immunopathogenesis and Human Immunity. *Acta facultatis medicae Naissensis*, 32(4), 243-257.
- Miller, L. G., & Diep, B. A. (2008). Colonization, fomites, and virulence: rethinking the pathogenesis of community-associated methicillin-resistant *Staphylococcus aureus* infection. *Clinical infectious diseases*, 46(5), 752-760.
- Molin, S., & Tolker-Nielsen, T. (2003). Gene transfer occurs with enhanced efficiency in biofilms and induces enhanced stabilisation of the biofilm structure. *Current Opinion in Biotechnology*, 14(3), 255-261.

- Montgomery, C. P., David, M. Z., & Daum, R. S. (2015). Host factors that contribute to recurrent staphylococcal skin infection. *Current opinion in infectious diseases*, 28(3), 253.
- Moreillon, P., Que, Y., & Glauser, M. P. (2005). *Staphylococcus aureus. Principles and Practice of Infectious Diseases, 6a ed.* Philadelphia: Churchill-Livingston, 2321-2351.
- Mukherji, R., Patil, A., & Prabhune, A. (2015). Role of extracellular proteases in biofilm disruption of gram positive bacteria with special emphasis on *Staphylococcus aureus* biofilms. *Enz Eng*, 4, 126.
- Nair, S., Desai, S., Poonacha, N., Vipra, A., & Sharma, U. (2016). Antibiofilm activity and synergistic inhibition of *Staphylococcus aureus* biofilms by bactericidal protein P128 in combination with antibiotics. *Antimicrobial agents and chemotherapy*, AAC-01118.
- Nallapareddy, S. R., Weinstock, G. M., & Murray, B. E. (2003). Clinical isolates of *Enterococcus faecium* exhibit strain-specific collagen binding mediated by Acm, a new member of the MSCRAMM family. *Molecular microbiology*, 47(6), 1733-1747.
- National Committee for Clinical Laboratory standards [NCCLS], *Reference method for antifungal disk diffusion susceptibility testing of yeasts; approved guideline. NCCLS document M44-A.* Wayne: National Committee for Clinical Laboratory standards, 2004.
- Ndie, E. C., Nnamani, C. V., & Oselebe, H. O. (2010). Some physicochemical characteristics of defatted flours derived from African walnut (*Tetracarpidium conophorum*): An underutilized legume. *Pakistan Journal of Nutrition*, 9(9), 909-911.
- Newell, D. G., Koopmans, M., Verhoef, L., Duizer, E., Aidara-Kane, A., Sprong, H., ... & van der Giessen, J. (2010). Food-borne diseases—the challenges of 20 years ago still persist while new ones continue to emerge. *International journal of food microbiology*, 139, S3-S15.
- Nguyen, M. H., Kauffman, C. A., Goodman, R. P., Squier, C., Arbeit, R. D., Singh, N., ... & Victor, L. Y. (1999). Nasal carriage of and infection with *Staphylococcus aureus* in HIV-infected patients. *Annals of internal medicine*, 130(3), 221-225.
- Nickerson, E. K., West, T. E., Day, N. P., & Peacock, S. J. (2012). *Staphylococcus aureus* disease and drug resistance in resource-limited countries in south and east Asia. *The Lancet infectious diseases*, 9(2), 130-135.
- Nielsen, J., Ladefoged, S. D., & Kolmos, H. J. (1998). Dialysis catheter-related septicaemia--focus on *Staphylococcus aureus* septicaemia. *Nephrology, dialysis, transplantation: official publication of the European Dialysis and Transplant Association-European Renal Association*, 13(11), 2847-2852.
- Nordmann, P., Cuzon, G., & Naas, T. (2009). The real threat of *Klebsiella pneumoniae* carbapenemase-producing bacteria. *The Lancet infectious diseases*, 9(4), 228-236.
- Nostro, A., Roccaro, A. S., Bisignano, G., Marino, A., Cannatelli, M. A., Pizzimenti, F. C., ... & Blanco, A. R. (2007). Effects of oregano, carvacrol and thymol on *Staphylococcus aureus* and *Staphylococcus epidermidis* biofilms. *Journal of medical microbiology*, 56(4), 519-523.

- Nouwen, J., Boelens, H., Van Belkum, A., & Verbrugh, H. (2004). Human factor in *Staphylococcus aureus* nasal carriage. *Infection and immunity*, 72(11), 6685-6688.
- Novick, R. P. (2003). Autoinduction and signal transduction in the regulation of staphylococcal virulence. *Molecular microbiology*, 48(6), 1429-1449.
- Nuryastuti, T., van der Mei, H. C., Busscher, H. J., Iravati, S., Aman, A. T., & Krom, B. P. (2009). Effect of cinnamon oil on icaA expression and biofilm formation by *Staphylococcus epidermidis*. *Applied and environmental microbiology*, 75(21), 6850-6855.
- Nuryastuti, T., van der Mei, H. C., Busscher, H. J., Iravati, S., Aman, A. T., & Krom, B. P. (2009). Effect of cinnamon oil on icaA expression and biofilm formation by *Staphylococcus epidermidis*. *Applied and environmental microbiology*, 75(21), 6850-6855.
- Nyong, B. E., Edem, C. A., Obochi, G. O., & Malu, S. P. (2009). Effect of methods of extraction on phytochemical constituents and antibacterial properties of *Tetracarpidium conophorum* seeds. *Global journal of pure and applied sciences*, 15(3-4).
- O'Brien, L., Kerrigan, S. W., Kaw, G., Hogan, M., Penadés, J., Litt, D., ... & Cox, D. (2002). Multiple mechanisms for the activation of human platelet aggregation by *Staphylococcus aureus*: roles for the clumping factors ClfA and ClfB, the serine-aspartate repeat protein SdrE and protein A. *Molecular microbiology*, 44(4), 1033-1044.
- Obboh, G., Nwanna, E. E., & Elusiyan, C. A. (2010). Antioxidant and Antimicrobial Properties of *Telfairia occidentalis* (Fluted pumpkin) Leaf Extracts. *Journal of Pharmacology & Toxicology*, 5(8), 539-547.
- O'Brien, L. M., Walsh, E. J., Massey, R. C., Peacock, S. J., & Foster, T. J. (2002). *Staphylococcus aureus* clumping factor B (ClfB) promotes adherence to human type I cytokeratin 10: implications for nasal colonization. *Cellular microbiology*, 4(11), 759-770.
- Odiaka, N. I., Akoroda, M. O., & Odiaka, E. C. (2008). Diversity and production methods of fluted pumpkin (*Telfairia occidentalis* Hook F.); Experience with vegetable farmers in Makurdi, Nigeria. *African Journal of Biotechnology*, 7(8). 944-954.
- Odewole, M. M., & Sunmonu, O. I. O. (2015). extraction of oil from fluted pumpkin seed (*Telfairia occidentalis*) by solvent extraction method. *J Technol Dev*, 121: 12-17.
- Ogbolu, D. O., & Alli, A. T. (2012). In-vitro antimicrobial activity of aqueous and methanol extracts of *Tetracarpidium conophorum* on some susceptible and multiresistant bacteria. *African Journal of Microbiology Research*, 6(13), 3354-3359.
- Okafor, N. (2011). Taxonomy, Physiology, and Ecology of Aquatic Microorganisms *Environmental Microbiology of Aquatic and Waste Systems* (pp. 47-107): Springer.
- Okeke, I. N., Aboderin, O. A., Byarugaba, D. K., Ojo, K. K., & Opintan, J. A. (2007). Growing problem of multidrug-resistant enteric pathogens in Africa. *Emerging infectious diseases*, 13(11), 1640.
- Okeke, I. N., Lamikanra, A., & Edelman, R. (1999). Socioeconomic and behavioral factors leading to acquired bacterial resistance to antibiotics in developing countries. *Emerging infectious diseases*, 5(1), 18.

- Okpashi, V. E., Ogugua, V. N., Ugian, E. A., & Njoku, O. U. (2013). Physico-chemical properties of fluted pumpkin (*Telfiaria occidentalis* Hook F) seeds. *The International Journal of Engineering and Science*, 2(9), 36-38.
- Olajide, O. A., Aderogba, M. A., Adedapo, A. D., & Makinde, J. M. (2004). Effects of *Anacardium occidentale* stem bark extract on in vivo inflammatory models. *Journal of ethnopharmacology*, 95(2-3), 139-142.
- Olife, I. C., Jolaoso, M. A., & Onwualu, A. P. (2013). Cashew processing for economic development in Nigeria. *Agricultural Journal*, 8(1), 45-50.
- Onanuga, A., & Awhowho, G. O. (2012). Antimicrobial resistance of *Staphylococcus aureus* strains from patients with urinary tract infections in Yenagoa, Nigeria. *Journal of pharmacy & bioallied sciences*, 4(3), 226.
- Onanuga, A., & Temedie, T. C. (2011). Nasal carriage of multi-drug resistant *Staphylococcus aureus* in healthy inhabitants of Amassoma in Niger delta region of Nigeria. *African health sciences*, 11(2).
- Orhan, İ. E., Özçelik, B., & Şener, B. (2011). Evaluation of antibacterial, antifungal, antiviral, and antioxidant potentials of some edible oils and their fatty acid profiles. *Turkish Journal of Biology*, 35(2), 251-258.
- O'Riordan, K., & Lee, J. C. (2004). *Staphylococcus aureus* capsular polysaccharides. *Clinical microbiology reviews*, 17(1), 218-234.
- Orwin, P. M., Leung, D. Y., Donahue, H. L., Novick, R. P., & Schlievert, P. M. (2001). Biochemical and biological properties of staphylococcal enterotoxin K. *Infection and immunity*, 69(1), 360-366.
- Otto, M. (2008). Staphylococcal biofilms *Bacterial biofilms* (pp. 207-228): Springer.
- Oyewole, O. A., & Abalaka, M. E. (2012). Antimicrobial activities of *Telfairia occidentalis* (fluted pumpkins) leaf extract against selected intestinal pathogens. *Journal of Health Science*, 2(2), 1-4.
- Pan, S. Y., Litscher, G., Gao, S. H., Zhou, S. F., Yu, Z. L., Chen, H. Q., ... & Ko, K. M. (2014). Historical perspective of traditional indigenous medical practices: the current renaissance and conservation of herbal resources. *Evidence-Based Complementary and Alternative Medicine*, 2014.
- Paraje, M. G. (2011). Antimicrobial resistance in biofilms. *Science against microbial pathogens: communicating current research and technological advances*, 736-744.
- Parasa, L. S., Tumati, S. R., Kumar, L. C. A., Chigurupati, S. P., & Rao, G. S. (2011). In vitro antimicrobial activity of cashew (*Anacardium occidentale*, L.) nuts shell liquid against methicillin resistant *Staphylococcus aureus* (MRSA) clinical isolates. *Int J Pharm Pharm Sci*, 3(4), 436-40.
- Peacock, S. J., de Silva, I., & Lowy, F. D. (2001). What determines nasal carriage of *Staphylococcus aureus*?. *Trends in microbiology*, 9(12), 605-610.

- Peacock, S. J., Moore, C. E., Justice, A., Kantzanou, M., Story, L., Mackie, K., ... & Day, N. P. (2002). Virulent combinations of adhesin and toxin genes in natural populations of *Staphylococcus aureus*. *Infection and immunity*, 70(9), 4987-4996.
- Percival, S. L., Suleman, L., Vuotto, C., & Donelli, G. (2015). Healthcare-associated infections, medical devices and biofilms: risk, tolerance and control. *Journal of medical microbiology*, 64(4), 323-334.
- Petinaki, E., & Spiliopoulou, I. (2012). Methicillin-resistant *Staphylococcus aureus* among companion and food-chain animals: impact of human contacts. *Clinical Microbiology and Infection*, 18(7), 626-634.
- Petrovska, B.B., 2012. Historical review of medicinal plants' usage. *Pharmacognosy reviews*, 6(11), p.1.
- Piątkowska, E., Piątkowski, J., & Przondo-Mordarska, A. (2012). The strongest resistance of *Staphylococcus aureus* to erythromycin is caused by decreasing uptake of the antibiotic into the cells. *Cellular & molecular biology letters*, 17(4), 633.
- Piątkowska, E., Piątkowski, J., & Przondo-Mordarska, A. (2012). The strongest resistance of *Staphylococcus aureus* to erythromycin is caused by decreasing uptake of the antibiotic into the cells. *Cellular & molecular biology letters*, 17(4), 633.
- Pinho, M. G., Filipe, S. R., de Lencastre, H., & Tomasz, A. (2001). Complementation of the essential peptidoglycan transpeptidase function of penicillin-binding protein 2 (PBP2) by the drug resistance protein PBP2A in *Staphylococcus aureus*. *Journal of bacteriology*, 183(22), 6525-6531.
- Plata, K., Rosato, A. E., & Wegrzyn, G. (2009). *Staphylococcus aureus* as an infectious agent: overview of biochemistry and molecular genetics of its pathogenicity. *Acta Biochimica Polonica*, 56(4), 597.
- Pollitt, E. J., Szkuta, P. T., Burns, N., & Foster, S. J. (2018). *Staphylococcus aureus* infection dynamics. *PLoS pathogens*, 14(6), e1007112.
- Pollitt, E. J., Szkuta, P. T., Burns, N., & Foster, S. J. (2018). *Staphylococcus aureus* infection dynamics. *PLoS pathogens*, 14(6), e1007112.
- Potashman, M. H., Stokes, M., Liu, J., Lawrence, R., & Harris, L. (2016). Examination of hospital length of stay in Canada among patients with acute bacterial skin and skin structure infection caused by methicillin-resistant *Staphylococcus aureus*. *Infection and drug resistance*, 9, 19.
- PrabhuDas, M., Adkins, B., Gans, H., King, C., Levy, O., Ramilo, O., & Siegrist, C.-A. (2011). Challenges in infant immunity: implications for responses to infection and vaccines. *Nature immunology*, 12(3), 189.
- Pujol, M., Peña, C., Pallares, R., Ariza, J., Ayats, J., Dominguez, M. A., & Gudiol, F. (1996). Nosocomial *Staphylococcus aureus* bacteremia among nasal carriers of methicillin-resistant and methicillin-susceptible strains. *The American journal of medicine*, 100(5), 509-516.

- Puspita, N. A. (2015). *Isolation and characterisation of medicinal compounds from Phyllanthus Niruri L* (Doctoral dissertation, University of Salford).
- Qiu, J., Zhang, X., Luo, M., Li, H., Dong, J., Wang, J., ... & Deng, X. (2011). Subinhibitory concentrations of perilla oil affect the expression of secreted virulence factor genes in *Staphylococcus aureus*. *PLoS One*, 6(1), e16160.
- Quinn, R. (2013). Rethinking antibiotic research and development: World War II and the penicillin collaborative. *American journal of public health*, 103(3), 426-434.
- Rahimi, F. (2016). Characterization of resistance to aminoglycosides in methicillin-resistant *Staphylococcus aureus* strains isolated from a tertiary care hospital in Tehran, Iran. *Jundishapur journal of microbiology*, 9(1).
- Rathi, P., Ahmad, M., & Tomar, A. (2014). Study on antimicrobial and antioxidant properties of walnut (*Juglans nigra*) oil. *Int J Curr Res Chem Pharm Sci*, 1(7), 51-55.
- Rayner, C., & Munckhof, W. J. (2005). Antibiotics currently used in the treatment of infections caused by *Staphylococcus aureus*. *Internal medicine journal*, 35, S3-16.
- Rayner, C., & Munckhof, W. J. (2005). Antibiotics currently used in the treatment of infections caused by *Staphylococcus aureus*. *Internal medicine journal*, 35, S3-16.
- Reffuveille, F., Josse, J., Vallé, Q., Mongaret, C., & Gangloff, S. C. (2017). *Staphylococcus aureus* Biofilms and their Impact on the Medical Field. In *The Rise of Virulence and Antibiotic Resistance in Staphylococcus aureus*. InTech.
- Renner, L. D., & Weibel, D. B. (2011). Physicochemical regulation of biofilm formation. *MRS bulletin*, 36(5), 347-355.
- Ribet, D., & Cossart, P. (2015). How bacterial pathogens colonize their hosts and invade deeper tissues. *Microbes and Infection*, 17(3), 173-183.
- Ricciardi-Castagnoli, P., & Granucci, F. (2002). Interpretation of the complexity of innate immune responses by functional genomics. *Nature Reviews Immunology*, 2(11), 881-889.
- Rice, L.B. 2006. Antimicrobial resistance in gram-positive bacteria. *American journal of infection control*, 34(5),S11-S19.
- Richardson, L. A. (2017). Understanding and overcoming antibiotic resistance. *PLoS biology*, 15(8), e2003775.
- Rohman, A., & Man, Y. C. (2010). Fourier transform infrared (FTIR) spectroscopy for analysis of extra virgin olive oil adulterated with palm oil. *Food research international*, 43(3), 886-892.
- Rossolini, G. M., Arena, F., Pecile, P., & Pollini, S. (2014). Update on the antibiotic resistance crisis. *Current opinion in pharmacology*, 18, 56-60.
- Salam, A. M., & Quave, C. L. (2018). Targeting virulence in *Staphylococcus aureus* by chemical inhibition of the accessory gene regulator system in vivo. *MSphere*, 3(1), e00500-17.

- Samuel, S., Kayode, O., Musa, O., Nwigwe, G., Aboderin, A., Salami, T., & Taiwo, S. (2010). Nosocomial infections and the challenges of control in developing countries. *African journal of clinical and experimental microbiology*, *11*(2).
- Samyuktha, S., & Mahajan, S. N. (2016). Isolation and identification of pigment producing bacteria and characterization of extracted pigments. *IJAR*, *2*(7), 657-664.
- Savoia, D., 2012. Plant-derived antimicrobial compounds: alternatives to antibiotics. *Future microbiology*, *7*(8), pp.979-990.
- Saxenaa, R., Joshib, D. D., & Singhc, R. (2009). Chemical composition and antimicrobial activity of walnut oil. *benefits*, *5*, 6.
- Schaumburg, F., Alabi, A. S., Peters, G., & Becker, K. (2014). New epidemiology of *Staphylococcus aureus* infection in Africa. *Clinical Microbiology and Infection*, *20*(7), 589-596.
- Shittu, A. O., Okon, K., Adesida, S., Oyedara, O., Witte, W., Strommenger, B., ... & Nübel, U. (2011). Antibiotic resistance and molecular epidemiology of *Staphylococcus aureus* in Nigeria. *BMC microbiology*, *11*(1), 92.
- Shittu, A. O., Okon, K., Adesida, S., Oyedara, O., Witte, W., Strommenger, B., ... & Nübel, U. (2011). Antibiotic resistance and molecular epidemiology of *Staphylococcus aureus* in Nigeria. *BMC microbiology*, *11*(1), 92.
- Siboo, I. R., Cheung, A. L., Bayer, A. S., & Sullam, P. M. (2001). Clumping Factor A Mediates Binding of *Staphylococcus aureus* to Human Platelets. *Infection and immunity*, *69*(5), 3120-3127.
- Silvestre, W. P., Agostini, F., Muniz, L. A. R., & Pauletti, G. F. (2016). Fractionating of green mandarin (*Citrus deliciosa Tenore*) essential oil by vacuum fractional distillation. *Journal of Food Engineering*, *178*, 90-94.
- Smith, R. D., & Coast, J. (2002). Antimicrobial resistance: a global response. *Bulletin of the World Health Organization*, *80*, 126-133.
- Snodgrass, J. L., Mohamed, N., Ross, J. M., Sau, S., Lee, C. Y., & Smeltzer, M. S. (1999). Functional analysis of the *Staphylococcus aureus* collagen adhesin B domain. *Infection and immunity*, *67*(8), 3952-3959.
- Souza, N. C., de Oliveira, J. M., Morrone, M. D. S., Albanus, R. D. O., Amarante, M. D. S. M., Camillo, C. D. S., ... & Pasquali, M. A. D. B. (2017). Antioxidant and anti-inflammatory properties of *Anacardium occidentale* leaf extract. *Evidence-Based Complementary and Alternative Medicine*, 2017.
- Spaulding, A. R., Salgado-Pabón, W., Kohler, P. L., Horswill, A. R., Leung, D. Y., & Schlievert, P. M. (2013). Staphylococcal and streptococcal superantigen exotoxins. *Clinical microbiology reviews*, *26*(3), 422-447.
- Stegeman, C. A., Tervaert, J. W. C., Sluiter, W. J., Manson, W. L., de Jong, P. E., & Kallenberg, C. G. (1994). Association of chronic nasal carriage of *Staphylococcus aureus* and higher relapse rates in Wegener granulomatosis. *Annals of Internal Medicine*, *120*(1), 12-17.

- Stepanović, S., Vuković, D., Hola, V., BoONAVENTURA, G. D., Djukić, S., Ćirković, I., & Ruzicka, F. (2007). Quantification of biofilm in microtiter plates: overview of testing conditions and practical recommendations for assessment of biofilm production by staphylococci. *Apmis*, *115*(8), 891-899.
- Stone, R. B. (2013) Epidemiology of Hospital Acquired Methicillin Resistant *Staphylococcus aureus* in A Veterans Affairs Medical Center Spinal Cord Injury Unit: Fiscal Years 2008-2011.
- Stoodley, P., Sauer, K., Davies, D. G., & Costerton, J. W. (2002). Biofilms as complex differentiated communities. *Annual Reviews in Microbiology*, *56*(1), 187-209.
- Stryjewski, M. E., & Corey, G. R. (2014) Methicillin-resistant *Staphylococcus aureus*: an evolving pathogen. *Clinical Infectious Diseases*, *58*(suppl 1), S10-S19.
- Tabassum, N., & Vidyasagar, G. M. (2014). In vitro antimicrobial activity of edible oils against human pathogens causing skin infections. *International Journal of Pharmaceutical Sciences and Research*, *5*(10), 4493.
- Tadesse, B. T., Ashley, E. A., Ongarello, S., Havumaki, J., Wijegoonewardena, M., González, I. J., & Dittrich, S. (2017). Antimicrobial resistance in Africa: a systematic review. *BMC infectious diseases*, *17*(1), 616.
- Talay, S. R. (2004). Gram—Positive Adhesins *Concepts in bacterial virulence* (Vol. 12, pp. 90-113): Karger Publishers.
- Tavares, A. L. (2014). Community-associated methicillin-resistant *Staphylococcus aureus* (CA-MRSA) in Portugal: Origin, epidemiology and virulence. *Ann Arbor*, *1001*, 48106-1346.
- Tay, A., Singh, R. K., Krishnan, S. S., & Gore, J. P. (2002). Authentication of olive oil adulterated with vegetable oils using Fourier transform infrared spectroscopy. *LWT-Food Science and Technology*, *35*(1), 99-103.
- Tenover, F. C., McDougal, L. K., Goering, R. V., Killgore, G., Projan, S. J., Patel, J. B., & Dunman, P. M. (2006). Characterization of a strain of community-associated methicillin-resistant *Staphylococcus aureus* widely disseminated in the United States. *Journal of clinical microbiology*, *44*(1), 108-118.
- Thwaites, G. E., & United Kingdom Clinical Infection Research Group. (2010). The management of *Staphylococcus aureus* bacteremia in the United Kingdom and Vietnam: a multi-centre evaluation. *PLoS One*, *5*(12), e14170.
- Torres, F. C., Lucas, A. M., Ribeiro, V. L. S., Martins, J. R., Poser, G. V., Guala, M. S., ... & Cassel, E. (2012). Influence of essential oil fractionation by vacuum distillation on acaricidal activity against the cattle tick. *Brazilian Archives of Biology and Technology*, *55*(4), 613-621.
- Trüper, H. G., & Schleifer, K. H. (2006). Prokaryote characterization and identification. In *The prokaryotes* (pp. 58-79). Springer, New York, NY.

- Trzcinski, K., Cooper, B. S., Hryniewicz, W., & Dowson, C. G. (2000). Expression of resistance to tetracyclines in strains of methicillin-resistant *Staphylococcus aureus*. *Journal of Antimicrobial Chemotherapy*, 45(6), 763-770.
- Tsai, C. J. Y., Loh, J. M. S., & Proft, T. (2016). *Galleria mellonella* infection models for the study of bacterial diseases and for antimicrobial drug testing. *Virulence*, 7(3), 214-229.
- Tsiodras, S., Gold, H. S., Sakoulas, G., Eliopoulos, G. M., Wennersten, C., Venkataraman, L., ... & Ferraro, M. J. (2001). Linezolid resistance in a clinical isolate of *Staphylococcus aureus*. *The Lancet*, 358(9277), 207-208.
- Tsompanidou, E., Denham, E. L., Sibbald, M. J., Yang, X.-m., Seinen, J., Friedrich, A. W., . . . van Dijl, J. M. (2012). The sortase A substrates FnbpA, FnbpB, ClfA and ClfB antagonize colony spreading of *Staphylococcus aureus*.
- Udobi, C. E., Obajuluwa, A. F., & Onaolapo, J. A. (2013). Prevalence and antibiotic resistance pattern of methicillin-resistant *Staphylococcus aureus* from an orthopaedic hospital in Nigeria. *BioMed research international*, 2013.
- Upadhyay, A., Upadhyaya, I., Kollanoor-Johny, A., & Venkitanarayanan, K. (2014). Combating pathogenic microorganisms using plant-derived antimicrobials: a minireview of the mechanistic basis. *BioMed research international*, 2014.
- Uzunova, G., Perifanova-Nemska, M., Stojanova, M., & Gandev, S. (2015). Chemical composition of walnut oil from fruits on different years old branches. *Bulgarian Journal of Agricultural Science*, 21(3), 494-497.
- Vasconcelos, N. G., & de Souza, M. D. L. R. (2010). Staphylococcal enterotoxins: molecular aspects and detection methods. *Journal of Public Health and Epidemiology*, 2(3), 29-42.
- Ventola, C. L. (2015). The antibiotic resistance crisis: part 1: causes and threats. *Pharmacy and Therapeutics*, 40(4), 277.
- Ventola, C. L. (2015). The antibiotic resistance crisis: part 1: causes and threats. *Pharmacy and Therapeutics*, 40(4), 277.
- Verhoeven, P. O., Gagnaire, J., Botelho-Nevers, E., Grattard, F., Carricajo, A., Lucht, F., . . . Berthelot, P. (2014). Detection and clinical relevance of *Staphylococcus aureus* nasal carriage: an update. *Expert review of anti-infective therapy*, 12(1), 75-89.
- Vertes, A., Hitchins, V., & Phillips, K. S. (2012). Analytical challenges of microbial biofilms on medical devices.
- Villegas-Estrada, A., Lee, M., Hesek, D., Vakulenko, S. B., & Mobashery, S. (2008). Co-opting the cell wall in fighting methicillin-resistant *Staphylococcus aureus*: potent inhibition of PBP 2a by two anti-MRSA  $\beta$ -lactam antibiotics. *Journal of the American Chemical Society*, 130(29), 9212-9213.
- Vitko, N. P., & Richardson, A. R. (2013). Laboratory Maintenance of Methicillin-Resistant *Staphylococcus aureus* (MRSA). *Current protocols in microbiology*, 28(1), 9C-2.
- Wang, L., & Ruan, S. (2017). Modeling nosocomial infections of methicillin-resistant *Staphylococcus aureus* with environment contamination. *Scientific Reports*, 7(1), 580.

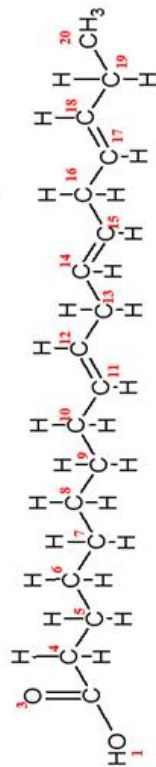
- Wann, E. R., Gurusiddappa, S., & Höök, M. (2000). The Fibronectin-binding MSCRAMM FnbpA of *Staphylococcus aureus* Is a Bifunctional Protein That Also Binds to Fibrinogen. *Journal of Biological Chemistry*, 275(18), 13863-13871.
- Wanten, G. J., van Oost, P., Schneeberger, P. M., & Koolen, M. I. (1996). Nasal carriage and peritonitis by *Staphylococcus aureus* in patients on continuous ambulatory peritoneal dialysis: a prospective study. *Peritoneal dialysis international*, 16(4), 352-356.
- Weinke, T., Schiller, R., Fehrenbach, F. J., & Pohle, H. D. (1992). Association between *Staphylococcus aureus* nasopharyngeal colonization and septicemia in patients infected with the human immunodeficiency virus. *European Journal of Clinical Microbiology and Infectious Diseases*, 11(11), 985-989.
- Wertheim, H. F., Melles, D. C., Vos, M. C., van Leeuwen, W., van Belkum, A., Verbrugh, H. A., & Nouwen, J. L. (2005). The role of nasal carriage in *Staphylococcus aureus* infections. *The Lancet infectious diseases*, 5(12), 751-762.
- Wright, J. S., Traber, K. E., Corrigan, R., Benson, S. A., Musser, J. M., & Novick, R. P. (2005). The agr radiation: an early event in the evolution of staphylococci. *Journal of bacteriology*, 187(16), 5585-5594.
- Yang, H. F., Pan, A. J., Hu, L. F., Liu, Y. Y., Cheng, J., Ye, Y., & Li, J. B. (2017). *Galleria mellonella* as an in vivo model for assessing the efficacy of antimicrobial agents against *Enterobacter cloacae* infection. *Journal of Microbiology, Immunology and Infection*, 50(1), 55-61.
- Yap, P. S. X., Yiap, B. C., Ping, H. C., & Lim, S. H. E. (2014). Essential oils, a new horizon in combating bacterial antibiotic resistance. *The open microbiology journal*, 8, 6.
- Yarwood, J. M., & Schlievert, P. M. (2003). Quorum sensing in Staphylococcus infections. *The Journal of clinical investigation*, 112(11), 1620-1625.
- Yarwood, J. M., Bartels, D. J., Volper, E. M., & Greenberg, E. P. (2004) Quorum sensing in *Staphylococcus aureus* biofilms. *Journal of Bacteriology*, 186(6), 1838-1850.
- Yilmaz, E. Ş., & Aslantaş, Ö. (2017). Antimicrobial resistance and underlying mechanisms in *Staphylococcus aureus* isolates. *Asian Pacific journal of tropical medicine*, 10(11), 1059-1064.
- Yoon, B., Jackman, J., Valle-González, E., & Cho, N. J. (2018). Antibacterial free fatty acids and monoglycerides: biological activities, experimental testing, and therapeutic applications. *International journal of molecular sciences*, 19(4), 1114.
- Yousefi, M., Pourmand, M. R., Fallah, F., Hashemi, A., Mashhadi, R., & Nazari-Alam, A. (2016). Characterization of *Staphylococcus aureus* biofilm formation in urinary tract infection. *Iranian journal of public health*, 45(4), 485.
- Zakavi, F., Golpasand Hagh, L., Daraeighadikolaei, A., Farajzadeh Sheikh, A., Daraeighadikolaei, A., & Leilavi Shooshtari, Z. (2013). Antibacterial effect of Juglans regia bark against oral pathologic bacteria. *International journal of dentistry*, 2013.

- Zimakoff, J., Pedersen, F. B., Bergen, L., Baagø-Nielsen, J., Daldorph, B., Espersen, F., ... & Kolmos, H. J. (1996). *Staphylococcus aureus* carriage and infections among patients in four haemo-and peritoneal-dialysis centres in Denmark. *Journal of Hospital Infection*, 33(4), 289-300.
- Zong, Y., Xu, Y., Liang, X., Keene, D. R., Höök, A., Gurusiddappa, S., . . . Narayana, S. V. (2005). A 'Collagen Hug' model for *Staphylococcus aureus* CNA binding to collagen. *The EMBO journal*, 24(24), 4224-4236.
- Zycinska, K., Wardyn, K. A., Zielonka, T. M., Demkow, U., & Traburzynski, M. S. (2008). Chronic crusting, nasal carriage of *Staphylococcus aureus* and relapse rate in pulmonary Wegener's granulomatosis. *J Physiol Pharmacol*, 59(Suppl 6), 825-831.

## Appendix 1 - 3

**$^1\text{H}$  NMR,  $^{13}\text{C}$  NMR and APT of fraction 2 of African walnut oil**

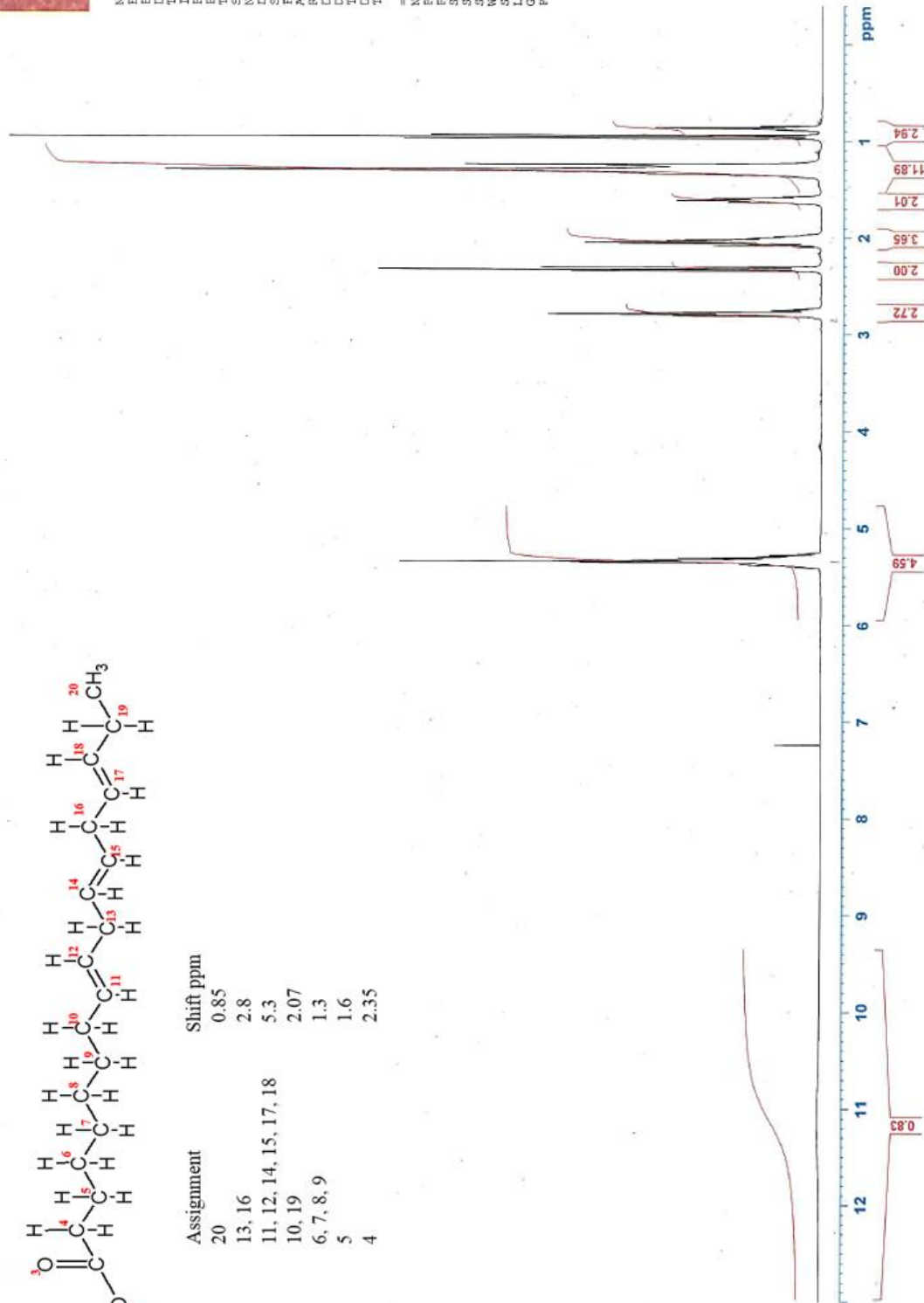
H1 NMR Spectrum of Fr 2 from Walnut oil distillation in CDCl<sub>3</sub>+TMS



Assignment	Shift ppm
20	0.85
13, 16	2.8
11, 12, 14, 15, 17, 18	5.3
10, 19	2.07
6, 7, 8, 9	1.3
5	1.6
4	2.35

```

NAME          FAN
EXPNO         71
PROCNO        1
Date_         20180910
Time         11.24
PROBHD        Spect
PULPROG       5 mm BBO B2-16
TD            65536
AQ            20.2
RG            20.2
DN            56.800 usec
DE            6.50 usec
TE            300.0 K
TD0           2.59999999 sec
===== CHANNEL f1 =====
NUC1          1H
P1            10.05 usec
PL1           -2.00 dB
SFO1         400.1333626 MHz
SI           32768
SF           400.1300175 MHz
WDW          EM
SSB          0
LB           0.30 Hz
GB           0
PC           1.00
    
```



BB H1 Decoupled C13 NMR Spectrum of Fraction 2 of Walnut Oil in CDCL3+TMS



```

NAME          PAM
EXPNO         21
PROCNO        1
Date_         20130905
Time          14.52
INSTRUM       spect
PROBHD        5 mm BBO BB-1H
PULPROG       zgpg30
TD            65536
SOLVENT       CDCl3
NS            16384
DS            4
SWH           23980.814 Hz
FIDRES        0.365916 Hz
AQ            1.3664756 sec
RG            38390.4
DK            20.850 usec
DE            6.50 usec
TE            300.0 K
D1            2.00000000 sec
D11           0.03000000 sec
TD0           1
===== CHANNEL f1 =====
NUC1          13C
PI            9.00 usec
PL1           6.60 dB
SFO1         100.628298 MHz
===== CHANNEL f2 =====
CQDPRG2       waltz16
NUC2          1H
NUC22         50.00 usec
PCPDZ         12.00 dB
PL2           13.75 dB
PL3           13.75 dB
SFO2         400.1316000 MHz
SI            32768
SF           100.6127630 MHz
WDW           EM
SSB           0
LB            1.00 Hz
GB            0
PC            1.00
    
```



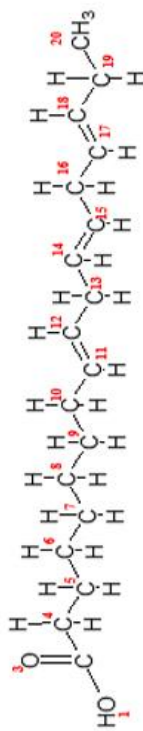
Assignment	ppm
1	179.86
2-11	131.94 to 127.11
12	34.04-31.91
13-16	29.56 to 20.53
17	14.27



## Appendix 4 - 6

**$^1\text{H}$  NMR,  $^{13}\text{C}$  NMR and APT of linolenic acid**

H1 NMR Spectrum of Linolenic Acid in CDCl<sub>3</sub>+TMS  
 PROTON64 CDCl<sub>3</sub> (C:\Bruker\TOPSPIN) MSP 20

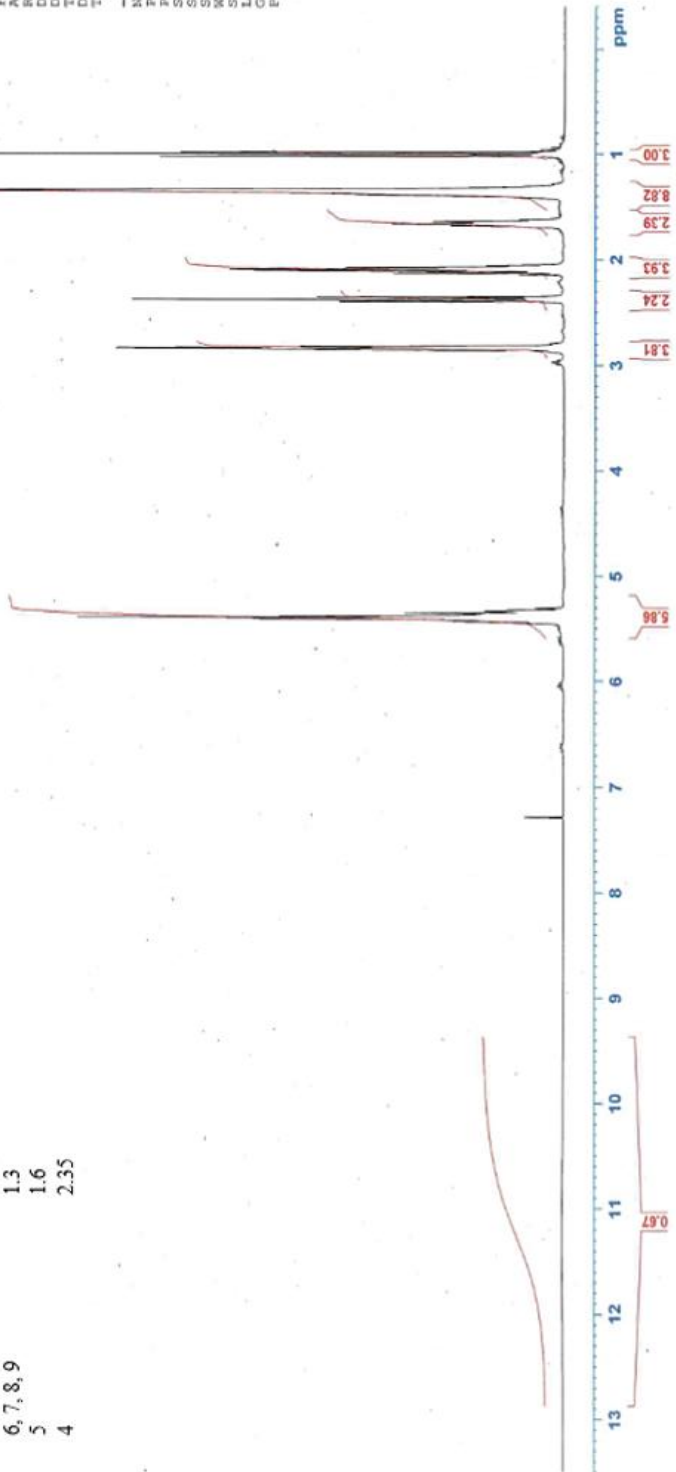


Assignment	Shift ppm
20	0.98
13, 16	2.8
11, 12, 14, 15, 17, 18	5.3
10, 19	2.07
6, 7, 8, 9	1.3
5	1.6
4	2.35

```

NAME          PAM
EXPNO         90
PROCNO        1
Date_         20181114
Time          12.25
INSTRUM       spect
PROBHD        5 mm BBO BB-1H
PULPROG       zgpg30
TD            56290
SOLVENT       CDCl3
NS            64
DS            0
SWH           8802.817 Hz
FIDRES        0.156383 Hz
AQ            3.1973219 sec
RG            56
OR            4.00 usec
DE            296.3 K sec
TE            296.3 K sec
D1            2.5995990 sec
TD0           1

----- CHANNEL f1 -----
NUC1          13C
P1            10.05 usec
PL1           -2.00 dB
SFO1         400.1333626 MHz
SI           32768
SF           400.1300000 MHz
RG           655
WDW           EM
SSB           0.30 Hz
GB           1.00
PC           1.00
  
```



BB H1 Decoupled C13 NMR Spectrum of Linolenic Acid in CDCL3+TMS  
 c13org CDC13 (C:Bruker(ATOPSPIN) MSP 20



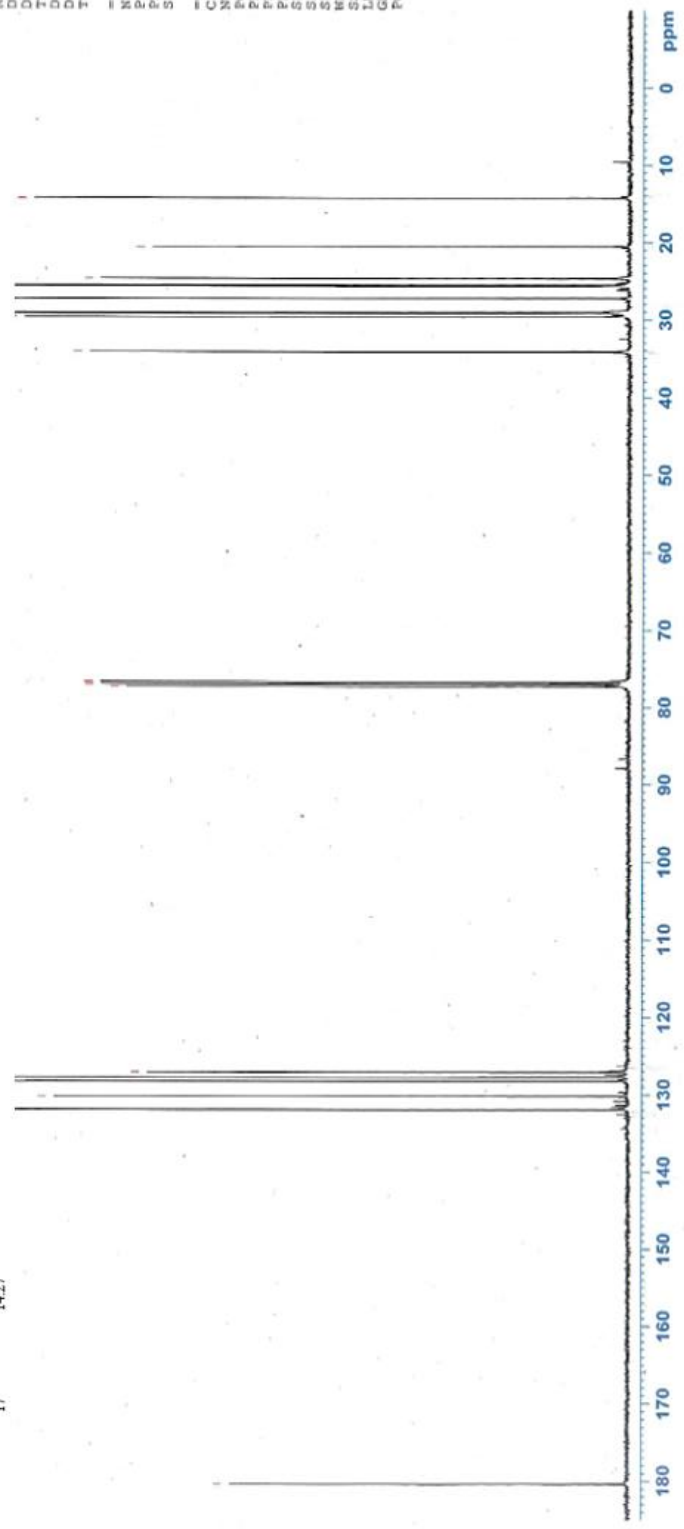
Assignment	ppm
1	180.39
2-6	131.95 to 127.11
7	34.09
8-16	29.56 to 20.55
17	14.27

```

NAME          PAM
EXPNO         91
PROCNO        1
Date_         20181111
Time          22.07
INSTRUM       spect
PROBHD        5 mm BBO BB-1H
PULPROG       zgpg30
TD            65536
SOLVENT       CDCl3
NS            3072
DS            4
SWH           23980.814 Hz
AQ           0.162756 Hz
RG            18390.4
AQ           1.183904 sec
DM            20.850 usec
DE            6.50 usec
TE            296.6 K
D1            2.00000000 sec
D11           0.03000000 sec
TDO           1

===== CHANNEL f1 =====
NUC1          13C
P1            9.00 usec
PL1           6.60 dB
SFO1         100.6228298 MHz

===== CHANNEL f2 =====
CPDPRG2      wait16
NUC2          1H
P2            80.18 usec
PL2           22.00 dB
SFO2         400.1464015 MHz
PL12         15.98 dB
PL13         19.50 dB
SFO2         400.1316005 MHz
SI            32768
SF           100.6127690 MHz
WDW           EM
SSB           0
GB            0
PC            8.00
  
```





## Appendix 7- 9

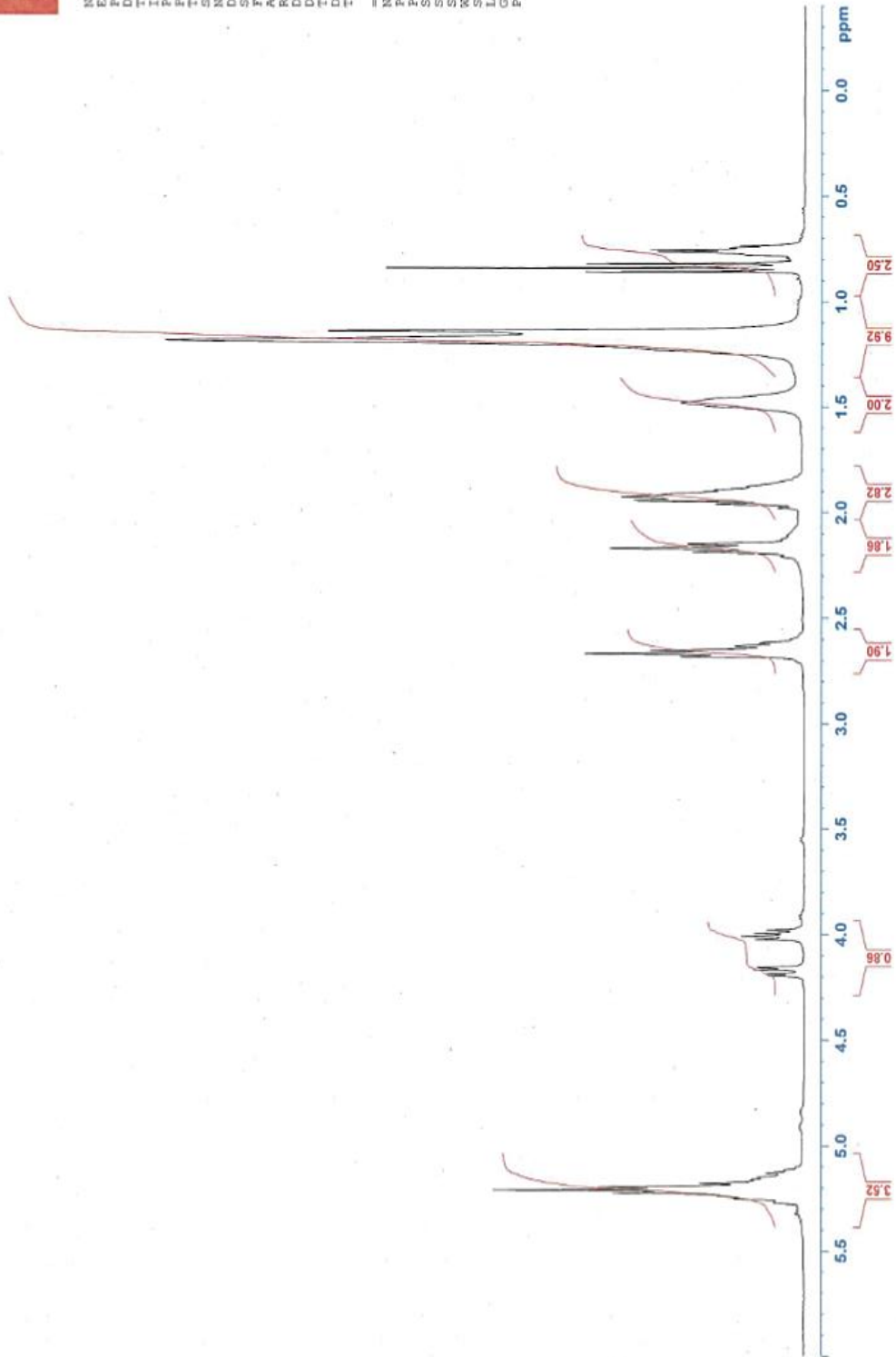
**$^1\text{H}$  NMR,  $^{13}\text{C}$  NMR and APT of fraction 3 of African walnut oil**

NMR Spectrum of Fr 3 from Walnut oil distillation in CDCl<sub>3</sub>+



NAME PAM  
EXPNO 72  
PROCNO 1  
Date\_ 20180910  
Time 11.35  
INSTRUM 5 mm BBO BBP1C  
PROBHD 5 mm BBO BBP1C  
PULPROG zg30  
TD 56290  
SOLVENT CDCl<sub>3</sub>  
NS 24  
DS 0  
SWH 8802.817 Hz  
FIDRES 0.156383 Hz  
AQ 3.197219 sec  
RG 2048  
DM 56.900 usec  
DE 6.50 usec  
TE 300.0 K  
D1 2.5999990 sec  
TD0 1

----- CHANNEL f1 -----  
NUC1 1H  
P1 10.05 usec  
PL 0.00 dB  
SFO1 400.133526 MHz  
SI 32768  
SF 400.1300175 MHz  
WDW EM  
SSB 0  
LB 0.30 Hz  
GB 0  
PC 1.00





Carbon\_K\_CDC13\_{C:\Users\PAR\data\ PAR 3



Current Data Parameters  
 NAME RHA FD3  
 EXPNO 11  
 PROCNO 1

F2 - Acquisition Parameters

Date\_ 20181004  
 Time 19.54 h  
 INSTRUM spect  
 PROBD 2108618\_1016 ( zppg30  
 PULPROG zgpg30  
 TD 65536  
 SOLVENT CDC13  
 NS 1024  
 DS 0  
 SWH 24038.461 Hz  
 FIDRES 0.733596 Hz  
 AQ 1.3631488 sec  
 RG 211.41  
 DW 20.800 usec  
 DE 10.10 usec  
 TE 296.0 K  
 D1 1.70000005 sec  
 D11 0.03000000 sec  
 TD0 1  
 SFO1 100.647973 MHz  
 NUC1 13C  
 P0 3.33 usec  
 F1 10.00 usec  
 PLW1 50.67499924 W  
 SFO2 400.2316009 MHz  
 NUC2 1H  
 CPDPRG[2] waltz65  
 FCFD2 90.00 usec  
 PLW2 12.30500031 W  
 PLW12 0.29776001 W  
 PLW13 0.14977001 W

F2 - Processing parameters

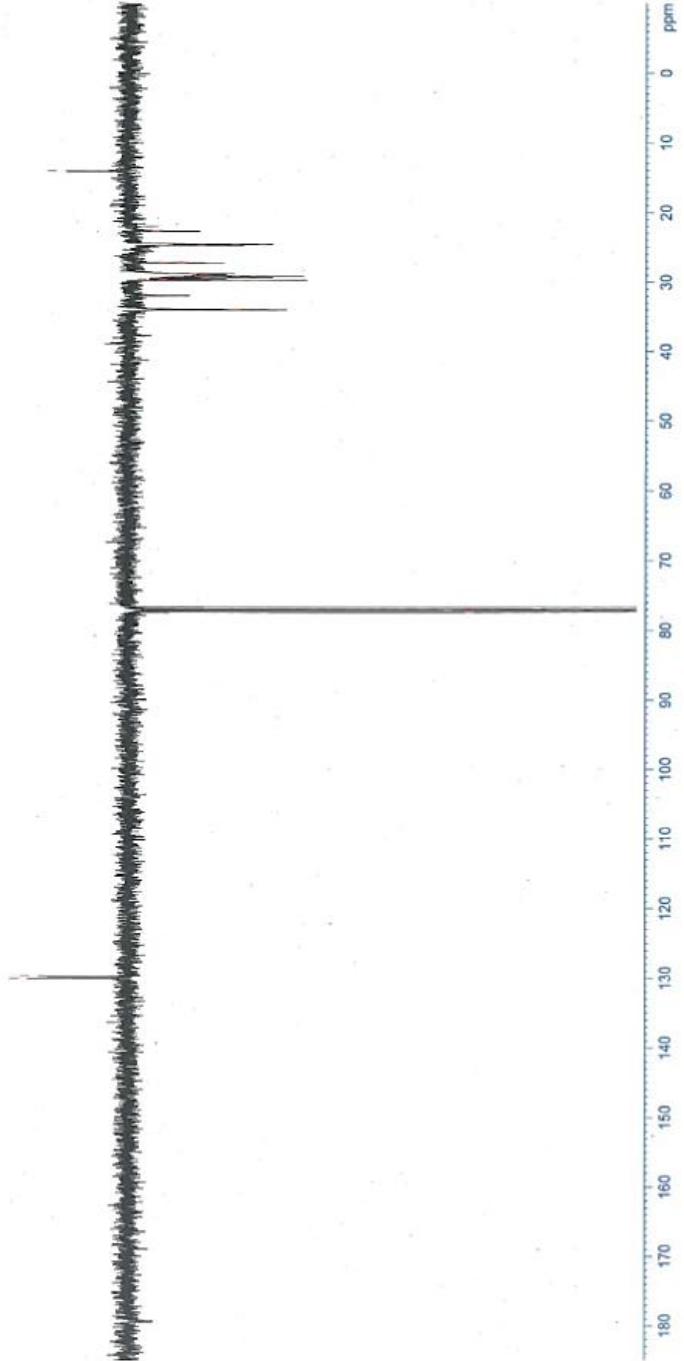
SI 65536  
 SF 100.6379135 MHz  
 EM  
 WDW 0  
 SSB 0  
 LB 0.70 Hz  
 GB 0  
 PC 1.40

JMOD C13 NMR Spectrum of Fraction 3 from Walnut Oil in CDCL3+TMS  
 C13APT CDC13 (C:\Bruker\TOPSPIN) JAH 34

129.73  
 130.03  
 76.71  
 77.34  
 77.03  
 33.95  
 33.80  
 31.51  
 29.77  
 29.70  
 29.60  
 29.52  
 29.45  
 29.37  
 29.32  
 29.18  
 28.77  
 28.07  
 29.04  
 28.91  
 27.22  
 27.15  
 24.68  
 24.56  
 22.60  
 21.96  
 14.12

```

NAME          pom fract_3
EXPNO         1
PROCNO        1
Date_         20181117
Time          21.55
INSTRUM       spect
PROBHD        5 mm BBO BB-1H
PULPROG       jmod
TD            65536
SOLVENT       CDC13
NS            2048
DS            4
SWH           23980.814 Hz
FIDRES        0.289716 Hz
AQ            1.368716 sec
RG            16384
DW            20.850 usec
DE            6.50 usec
TE            296.3 K
CHSTZ         145.0000000
CHST11        1.0000000
D1            2.0000000 sec
D20           0.00689655 sec
TD0           1
===== CHANNEL f1 =====
NUC1          13C
P1            8.70 usec
P2            16.80 usec
PL1           7.00 dB
PL2           7.00 dB
SFO1          100.6282898 MHz
===== CHANNEL f2 =====
CFPRG2        waltz16
NUC2          1H
PCPD2         80.00 usec
PL2           2.00 dB
SFO2          400.1317650 MHz
ST02          32768
SF            100.6127630 MHz
NSM           0
S2B           0
LB            1.00 Hz
GB            0
PC            1.40
  
```



## Appendix 10 – 11

$^1\text{H}$ , NMR of fraction 2 showing the position of the  $\text{CH}_3$  group of linolenic acid

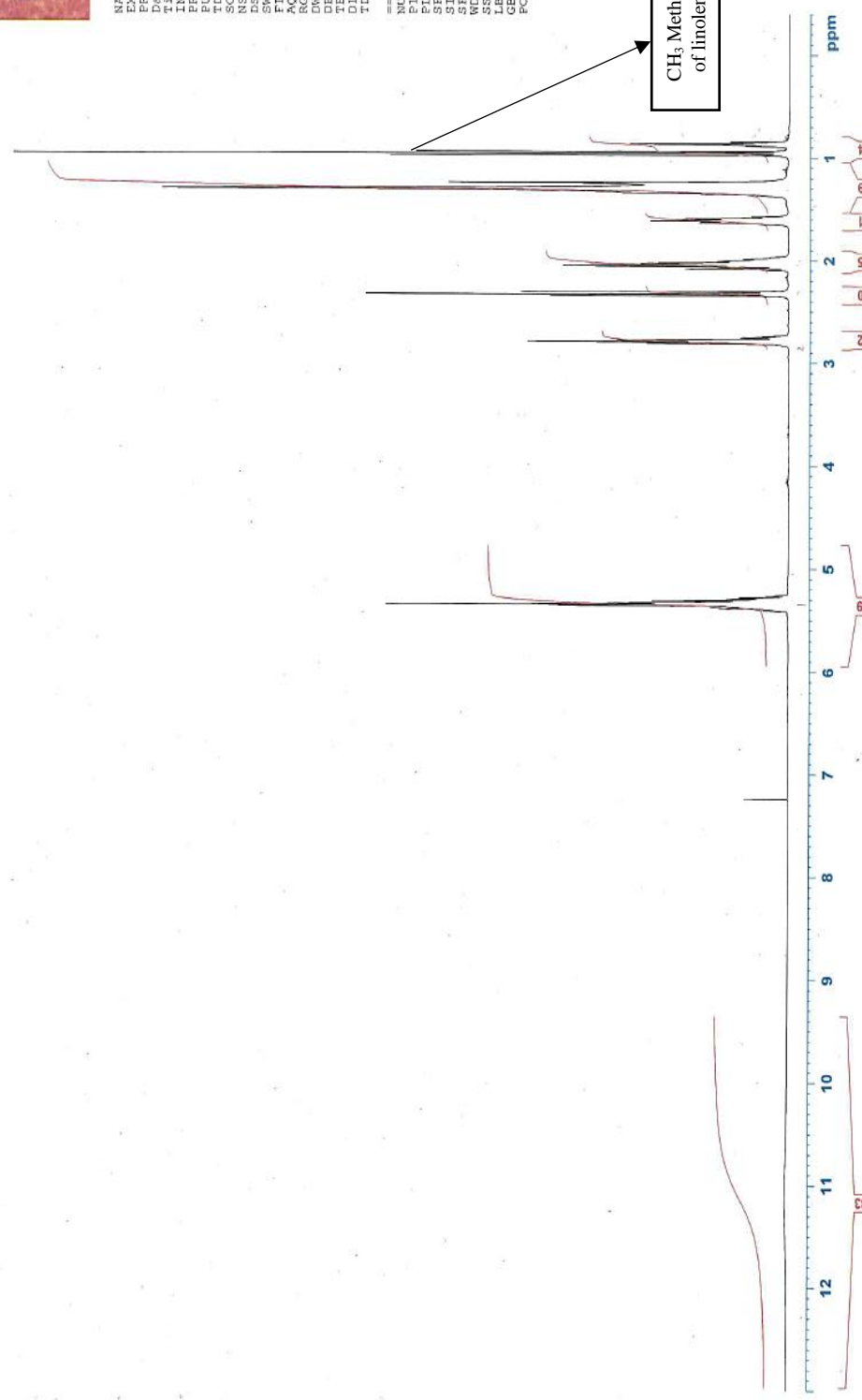
$^1\text{H}$ , NMR of fraction 2 showing the position of the  $\text{CH}_3$  group of linolenic acid and glyceric group

1H NMR Spectrum of Fr 2 from Walnut oil distillation in CDCl3+TMS



NAME  
EXPNO 71  
PROCNO 1  
Date\_ 20180910  
Time 11.24  
INSTRUM spect  
PULPROG zgpg30  
TD 56290  
SOLVENT CDCl3  
NS 48  
SFR 8802.817 Hz  
AQ 0.156383 Hz  
FIDRES 3.1973219 sec  
RG 20.2  
DW 56.800 usec  
TE 300.0 K  
DE 300.0 K  
DI 2.59899990 sec  
TD0 1

===== CHANNEL f1 =====  
NUC1 1H  
P1 10.05 usec  
PL1 -2.00 dB  
SFO1 400.1333626 MHz  
SI 32768  
WDW EM  
SSB 0  
LB 0.30 Hz  
GB 0  
PC 1.00



NMR Spectrum of Fr 3 from Walnut oil distillation in CDCl<sub>3</sub>+



```

NAME          PAM
EXPNO         72
PROCNO        1
Date_         20180910
Time          11.35
INSTRUM       spect
PROBHD        5 mm BBO BBH4
PULPROG       zgpg30
TD            5240
SOLVENT       CDCl3
NS            24
DS            0
SWH           8802.817 Hz
FIDRES        0.156383 Hz
AQ            3.1973219 sec
RG            204.2
DS           562.0 usec
DE           6.50 usec
TE            300.0 K
TE           2.5999990 sec
TD0           1

===== CHANNEL f1 =====
NUC1          1H
P1            10.05 usec
PL            0.00 dB
SFO1          400.1334520 MHz
SI            32768
SF            400.1300175 MHz
XDR          EM
SSB           0
LB            0.30 Hz
GB            0
PC            1.00
    
```

